

DISSERTATION

THE DEVELOPMENT AND APPLICATION
OF METAL-CATALYZED DIAMINATION REACTIONS

Submitted by

Richard G. Cornwall

Department of Chemistry

In partial fulfillment of the requirements

For the Degree of Doctor of Philosophy

Colorado State University

Fort Collins, Colorado

Fall 2014

Doctoral Committee:

Advisor: Yian Shi

Alan Kennan

Brian McNaughton

Charles Henry

Delphi Chatterjee

Copyright by Richard G. Cornwall 2014

All Rights Reserved

ABSTRACT

THE DEVELOPMENT AND APPLICATION OF METAL-CATALYZED DIAMINATION REACTIONS

Nitrogen-rich molecules are of great interest in chemistry and incorporation of nitrogen into molecules is an on-going active field of study. In particular, vicinal diamines are important functional moieties that are found throughout biologically active molecules and natural products as well as highly effective chiral control agents in organic synthesis. There has been much effort directed toward the efficient synthesis of vicinal diamines; however the development of a direct route has proven to be challenging. This dissertation discusses the application of diamination products from existing methods to synthesize biologically active motifs, as well as the development of new metal-catalyzed diamination methods for the synthesis of biologically interesting motifs from readily available starting materials.

The β,γ -diamino acid motif is an area of active research because of its prevalence in biologically active molecules and its use in peptide library syntheses. Cyclization of β,γ -diamino acids give the closely related 4-aminopyrrolidinones. These five-membered amino lactams have been reported to potentiate insulin activity when incorporated into hypoglycemic peptide analogues and made the analogues more stable towards physiological degradation. Current methods for the synthesis of these compounds require multi-step procedures and rely heavily on commercially available amino acids as starting materials, thus limiting the structural variability

for biological studies. Using a diamination method discovered in our lab, 4-aminopyrrolidinones were efficiently synthesized in 40% overall yield, over five steps from readily available terminal olefins or conjugated dienes, providing a comparable process in the synthesis of these compounds.

As part of our ongoing efforts to study the mechanism of metal-catalyzed diaminations using diaziridinone as nitrogen source, it was found that regioselectivity in the diamination of conjugated dienes could be controlled using Cu(I) as catalyst and varying reaction conditions. An alternative nitrogen source, thiadiaziridine 1,1-dioxide, which has shown to display interesting reactivity, was chosen to further investigate the Cu(I)-catalyzed regioselective diamination. Upon varying reaction conditions with Cu(I) catalysts, regioselective diamination occurred for various conjugated dienes and allowed direct access to a range of diverse cyclic sulfamides which have interesting biological potential.

With the racemic synthesis of cyclic sulfamides, it was of interest to obtain these compounds asymmetrically, as their biological properties are of value and current methods for their asymmetric synthesis do not allow much variation in substitution patterns. Using Pd₂(dba)₃ and a chiral phosphoramidite ligand, a variety of chiral cyclic sulfamides were synthesized in moderate to high yields and with ee's greater than 90%, providing direct access to these valuable compounds in one step from readily available conjugated diene substrates.

Lastly, *N,N*-Di-*tert*-butyl thiadiaziridine 1,1-dioxide has been found to be a versatile reagent for interesting reactivity. Other uses of this reagent include the Pd(II)-catalyzed terminal diamination of conjugated dienes, diamination of allenes, and the Pd-catalyzed oxidation of alcohols to form α,β -unsaturated compounds.

TABLE OF CONTENTS

ABSTRACT.....	ii
CHAPTER 1.0: VICINAL DIAMINE FUNCTIONALITY	1
1.1 GENERAL INTRODUCTION.....	1
1.2 METHODS TO SYNTHESIZE VICINAL DIAMINES.....	2
1.2.1 Stoichiometric Diamination.....	2
1.2.2 Catalytic Diamination	9
1.2.3 Methods Inspired by Inherent Ring Strain.....	18
1.2.3.1 Pd-Catalyzed.....	18
1.2.3.2 Cu-Catalyzed.....	25
1.3 REFERENCES	29
CHAPTER 2.0: β,γ -DIAMINO ACIDS and 4-AMINOPYRROLIDINONES	34
2.1 GENERAL INTRODUCTION.....	34
2.1.1 Methods to Synthesize β,γ -Diamino Acids and 4-Aminopyrrolidinones	35
2.2 RESULTS AND DISCUSSION	44
2.2.1 Retrosynthetic Analysis	44
2.2.2 Hydroboration	45
2.2.3 Oxidation to Carboxylic Acid.....	48
2.2.4 Lactamization.....	50
2.3 CONCLUSION.....	52

2.4 EXPERIMENTAL	53
2.5 REFERENCES	62
CHAPTER 3.0: Cu(I)-CATALYZED REGIOSELECTIVE DIAMINATION	64
3.1 GENERAL INTRODUCTION.....	64
3.1.1 Regioselective Diamination Using Diaziridinone	64
3.1.2 Alternative Nitrogen Source and Interesting Reactivity	65
3.2 RESULTS AND DISCUSSION	69
3.2.1 Reaction Conditions and Substrate Scope	69
3.2.2 Mechanistic Hypothesis.....	75
3.3 CONCLUSION.....	77
3.4 EXPERIMENTAL	78
3.5 REFERENCES	90
CHAPTER 4.0: CATALYTIC ASYMMETRIC SYNTHESIS OF CYCLIC SULFAMIDES	92
4.1 GENERAL INTRODUCTION.....	92
4.2 CURRENT METHODS TO SYNTHESIZE CHIRAL CYCLIC SULFAMIDES	92
4.3 RESULTS AND DISCUSSION	95
4.3.1 Reaction Conditions and Substrate Scope	95
4.3.2 Mechanistic Hypothesis.....	103
4.3.3 Attempt at Asymmetric Terminal Diamination	104
4.4 CONCLUSION.....	106
4.5 EXPERIMENTAL	107

4.6 REFERENCES	119
CHAPTER 5.0 OTHER THIADIAZIRIDINE USES	121
5.1 Pd(II)-CATALYZED TERMINAL DIAMINATION.....	121
5.1.1 Background.....	121
5.1.2 Results and Discussion	121
5.1.3 Mechanistic Hypothesis.....	123
5.2 METAL-CATALYZED DIAMINATION OF ALLENES	124
5.2.1 Results and Discussion	124
5.3 OXIDATION OF ALCOHOLS.....	125
5.3.1 Background.....	125
5.3.2 Results and Discussion	126
5.4 CONCLUSION.....	130
5.5 REFERENCES	131
SUPPLEMENTAL	132
Appendix 1 Spectra for Chapter 2	132
Appendix 2 Spectra for Chapter 3	168
Appendix 3 Spectra for Chapter 4	228

1.1 GENERAL INTRODUCTION

Nitrogen-rich molecules are of great interest in chemistry and incorporation of nitrogen into molecules is an ongoing active field of study. In particular, vicinal diamines are important functional moieties that are found throughout biologically active molecules and natural products.¹ Such examples include antiarrhythmics, antihypertensives, antipsychotics, analgesics, anticonvulsants, anticancer and antiparasitic compounds (Figure 1.1). Vicinal diamines are also used as highly effective chiral control agents in organic synthesis (Figure 1.2).^{1,2}

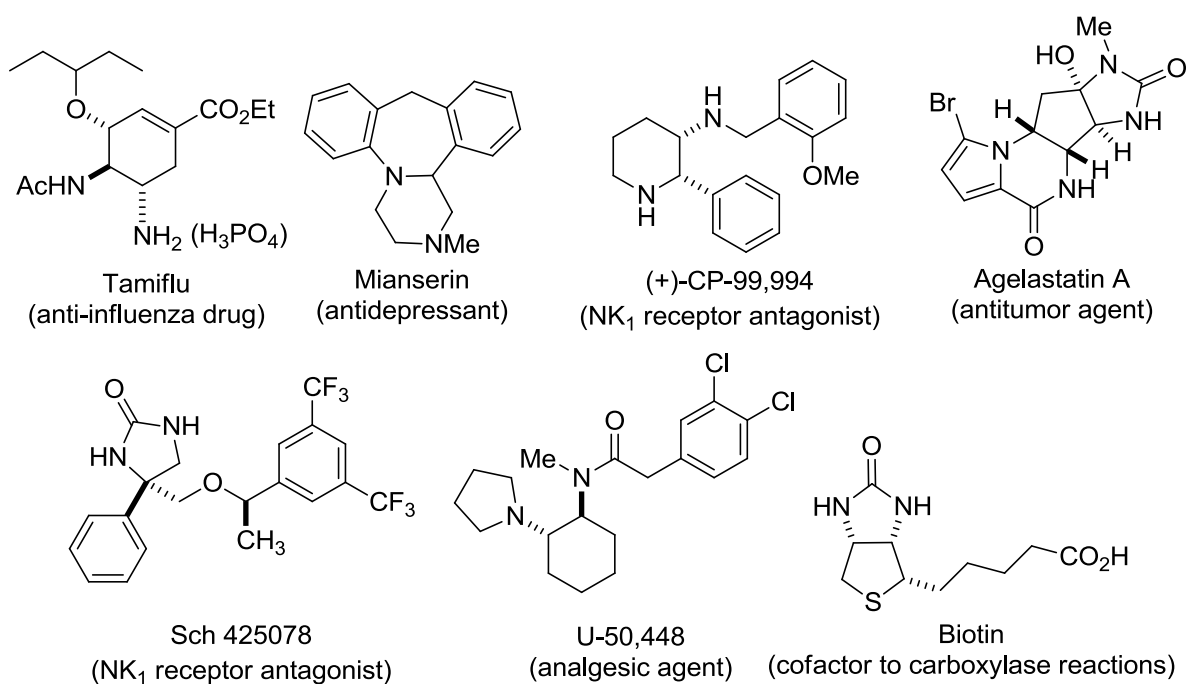


Figure 1.1 Examples of Vicinal Diamines in Biologically Active Molecules

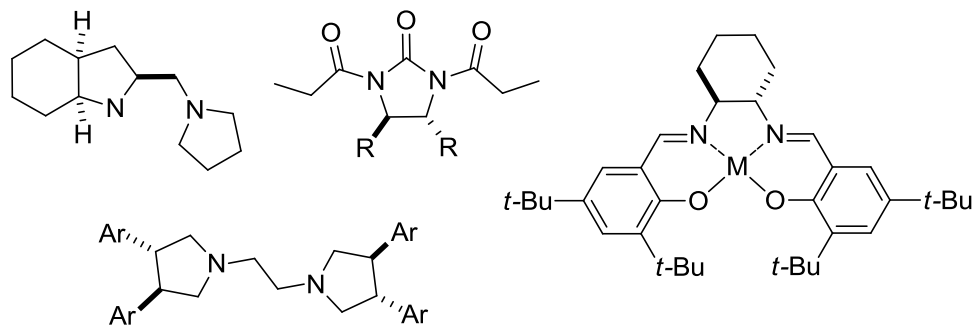


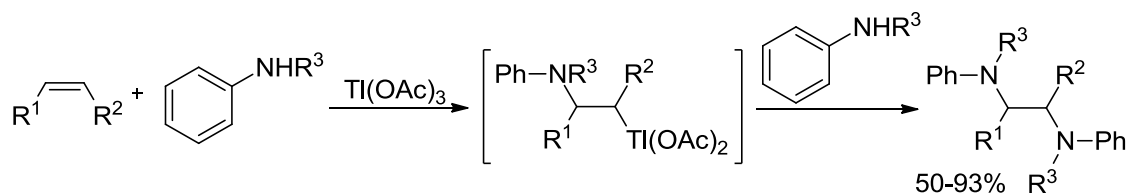
Figure 1.2 Examples of Chiral Diamine Ligands and Auxiliaries

1.2 METHODS TO SYNTHESIZE VICINAL DIAMINES

The introduction of dual functionality within the confines of close proximity is of importance in complex organic synthesis, especially when done in a stereocontrolled manner. There has been much effort directed toward the efficient synthesis of vicinal diamines; however the development of a direct route has proven to be challenging. An expedient approach to install vicinal diamines comes from the direct diamination of olefins, in a manner similar to that of the dihydroxylation reaction of alkenes using OsO_4 .^{1,3} Various processes to access vicinal diamines from olefins have been reported including metal-mediated, metal-catalyzed, as well as metal-free methods. The following chapter will highlight advances in both stoichiometric as well as catalytic diamination methods.

1.2.1 Stoichiometric Diamination

In 1974, Barluenga and coworkers reported the addition of anilines to various alkenes in the presence of thallium(III) acetate to give aromatic vicinal diamines in good yields (Scheme 1.1).⁴ Mercury salts were later employed to expand the substrate scope of the reaction.⁵



Scheme 1.1

Sharpless and Singer reported imido selenium compounds for the diamination of conjugated dienes.⁶ When cyclohexadiene was used as substrate, the nitrogens were introduced *cis* to each other (Figure 1.3). Nosyl-protected imido selenium reagent was also reported.^{6b} In the following year, Sharpless and coworkers reported the stereoselective syn-addition of two nitrogen atoms to mono- and di-substituted trans alkenes using bis- and tris-imidoosmium complexes (Scheme 1.2).⁷ Muñiz and coworkers have reported many studies on the structure and electronic nature of imidoosmium complexes⁸ and have reported moderate diastereoselectivity for substrates bearing attached chiral auxiliaries⁹ as well as additional chiral catalysts.¹⁰

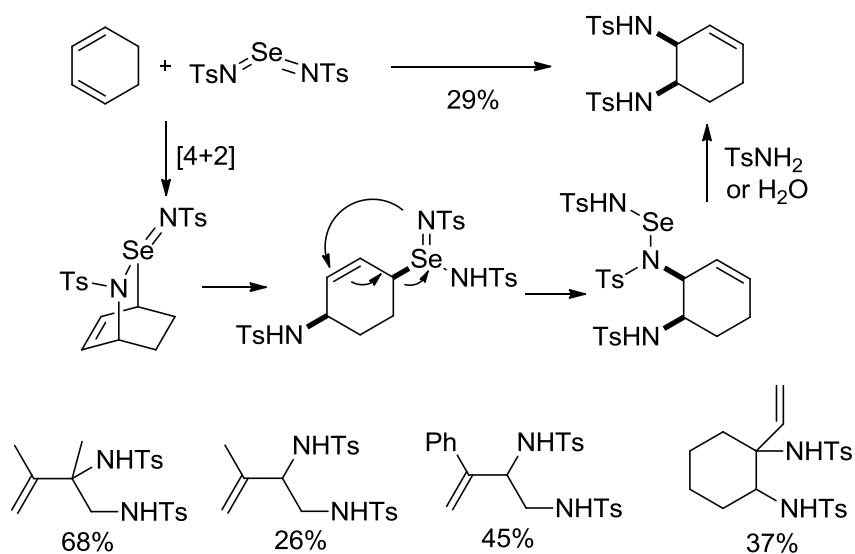
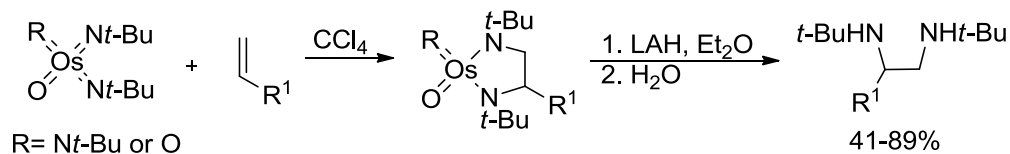


Figure 1.3



Scheme 1.2

In 1978, Bäckvall reported an *aza*-Wacker-type amino-palladation process, followed by stoichiometric oxidation of the Pd and nucleophilic displacement by an amine source (Figure 1.4).¹¹ Although limited to secondary amine sources, Bäckvall's report was nevertheless a pioneering publication which forged the way into transition metal-mediated diamination.

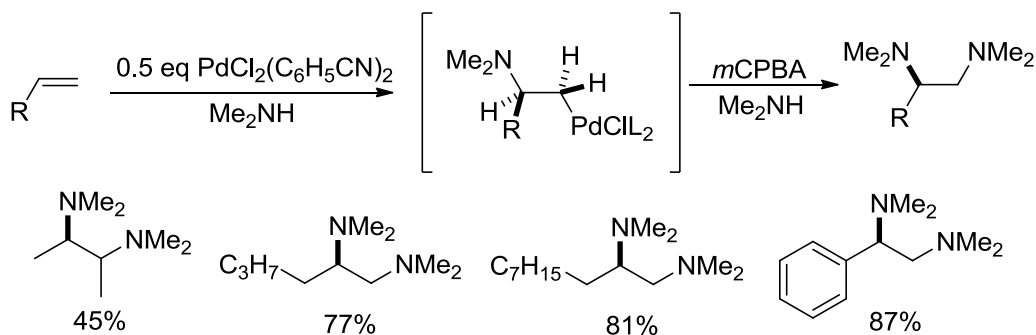
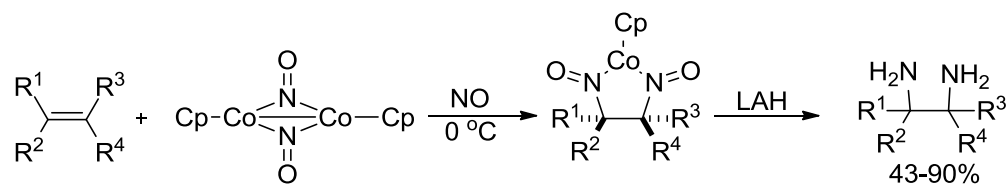


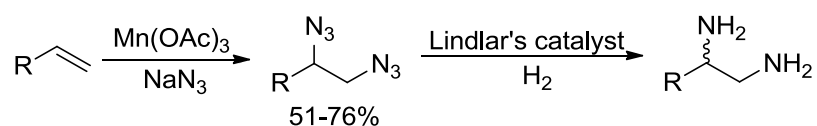
Figure 1.4

Bergman and coworkers described the diamination of a variety of *cis*, *trans*, *tri*- and *tetra*substituted alkenes using a cyclopentadienylnitrosylcobalt dimer and nitric oxide (Scheme 1.3).¹² It was proposed that addition of the nitrogen groups occurs stereoselectively, however epimerization was observed upon reduction to the free diamine using LAH.



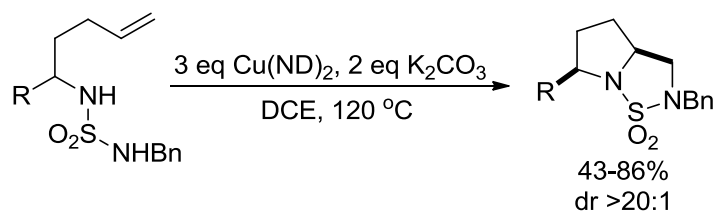
Scheme 1.3

Fristad and coworkers showed in 1985 that Mn(III) species can functionalize terminal, di- and trisubstituted alkenes to give 1,2-diazides (Scheme 1.4).¹³ These were then reduced to yield vicinal diamines in a two-step process. It was proposed that N₃ addition proceeded via a radical process and therefore stereoselectivity was low.



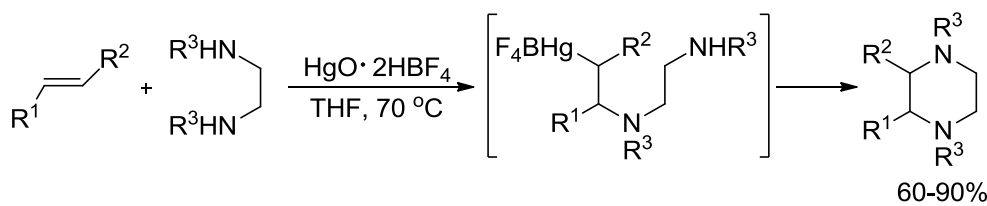
Scheme 1.4

A report from Chemler and coworkers used stoichiometric amounts of copper(II) neodecanoate [Cu(ND)₂] and a tethered sulfamide source of nitrogen to synthesize cyclic sulfamides in an intramolecular diamination reaction (Scheme 1.5).¹⁴ The reaction provides the cyclic sulfamides in good yields and high levels of diastereoselectivity.



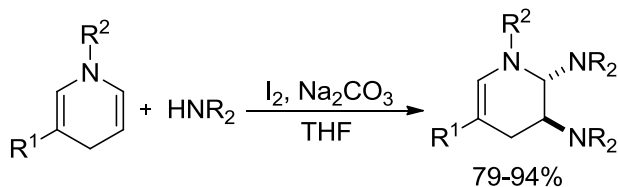
Scheme 1.5

Recently, a series of styrenes were efficiently diaminated using $\text{HgO}\cdot 2\text{HBF}_4$ and *N*-protected ethylenediamine. The resulting piperazines were obtained in moderate to good yields.¹⁵ Activation of the double bond by the mercury salt and attack of one nitrogen gives a β -aminomercury(II)tetrafluoroborate intermediate (Scheme 1.6). Subsequent intramolecular cyclization generates the piperazine products.



Scheme 1.6

Electrophilic iodine has shown to facilitate the diamination of olefins. Lavilla and coworkers reported the diamination of 1,4-dihydropyridines using I_2 and Na_2CO_3 (Scheme 1.7).¹⁶ Electrophilic interaction of the iodine with the alkene allows addition of secondary amines *trans* to each other in good yields. Iodide has also been used in conjunction with chloramine-T for the diamination of glycals in moderate yields.¹⁷



Scheme 1.7

Muñiz and coworkers diaminated styrenes, in an enantioselective fashion, employing stoichiometric amounts of chiral iodine reagent **1-1**.¹⁸ HNMs_2 was selected as a suitable nitrogen source and provided good yields and enantioselectivities ranged from 74-95% (Figure 1.5).

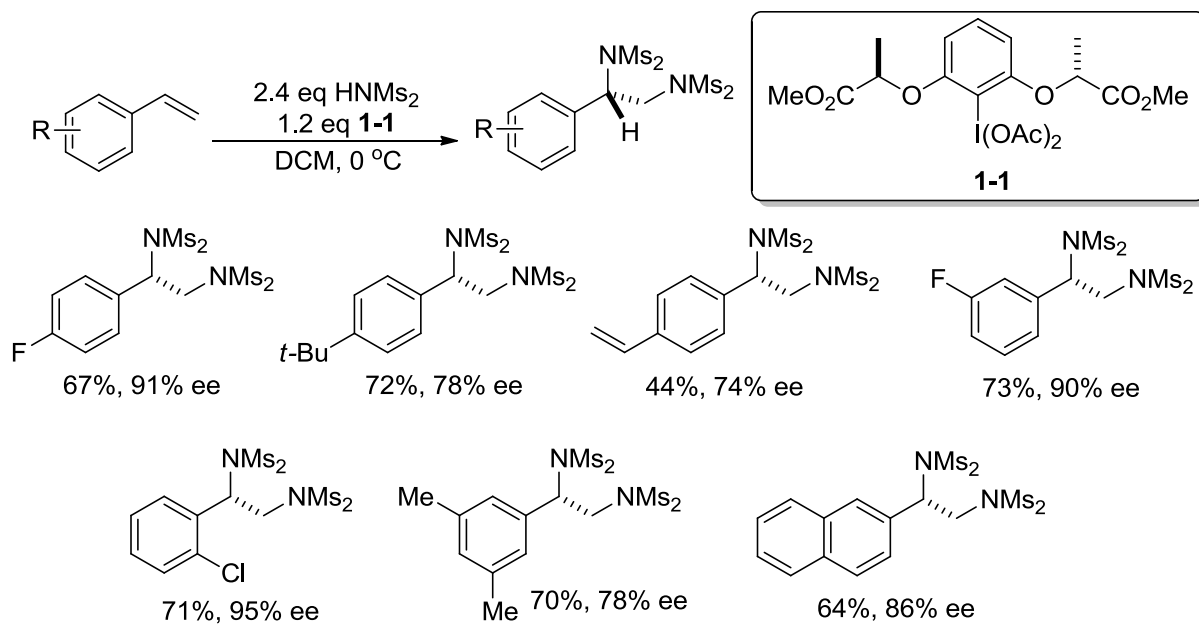
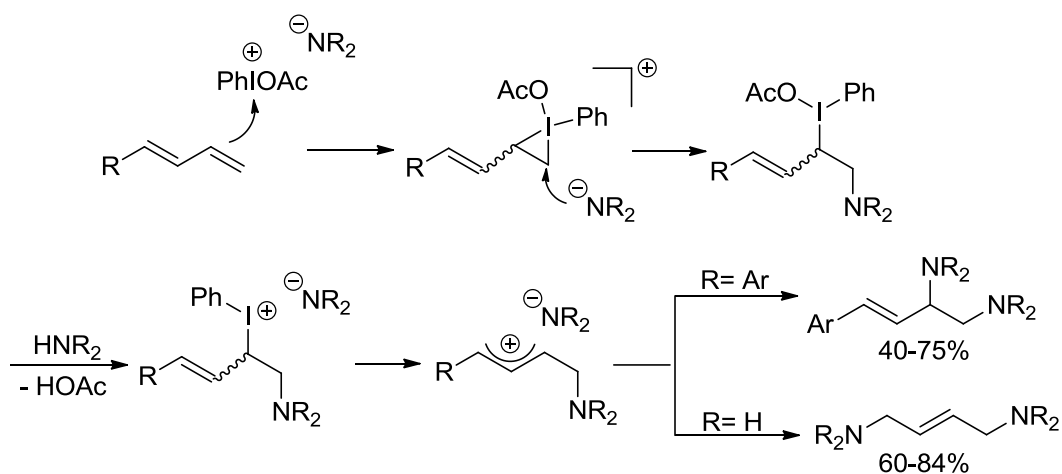


Figure 1.5

Muñiz and coworkers also reported the diamination of conjugated dienes and trienes using $\text{PhI}(\text{OAc})_2$ and either NHTs_2 or NHMs_2 as nitrogen source.¹⁹ Yields were good and the diamination of aryl-substituted dienes resulted in 1,2-diamination, whereas alkyl-substituted dienes gave 1,4-diamination (Scheme 1.8).



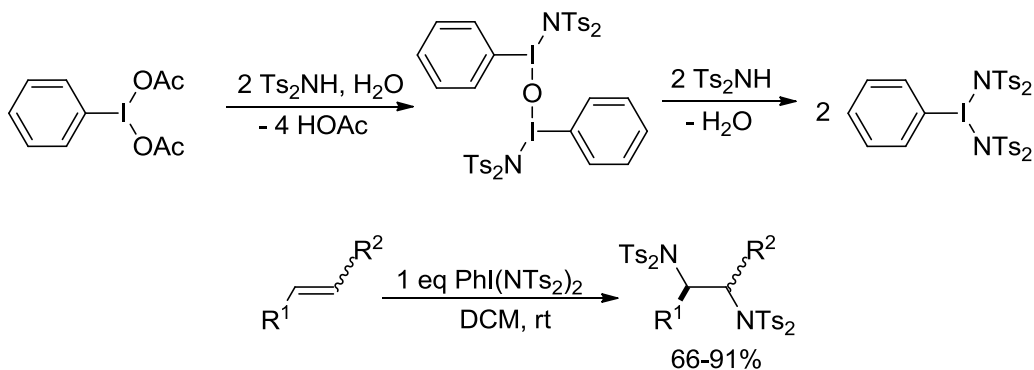
Scheme 1.8

Another electrophilic iodine source, *N*-iodosuccinimide (NIS), has also been used to promote diamination.²⁰ Chiral 2,2'-bipyrrolidines were efficiently constructed using NIS via intramolecular diamination by Hennecke and coworkers (Scheme 1.9).²¹ The bicyclic amines were synthesized in good yields and proved to be an efficient route to *trans*-bpbp ligands.



Scheme 1.9

An in situ-generated iodine source with incorporated transferable nitrogen groups was reported by Muñiz and coworkers. Preformed reagent $\text{PhI}(\text{NTs}_2)_2$ is synthesized from $\text{PhI}(\text{OAc})_2$ and 4 equivalents of Ts_2NH (Scheme 1.10). Diamination was complete within minutes, providing high yields (Scheme 1.10).²² A catalytic variation using dinuclear iodine reagents was also reported with comparable yields.²³



Scheme 1.10

A report from Jeffrey and coworkers employs a chlorourea for the 1,4-diamination of cyclic dienes via a [4+3] cycloaddition (Figure 1.6).²⁴ The choice of base was crucial and the sodium alkoxide of 2,2,3,3-tetrafluoropropanol (TFP-Na) provided optimal yields. High yields were obtained for 12 examples and the resulting bicyclic diamines are valuable synthetic intermediates.

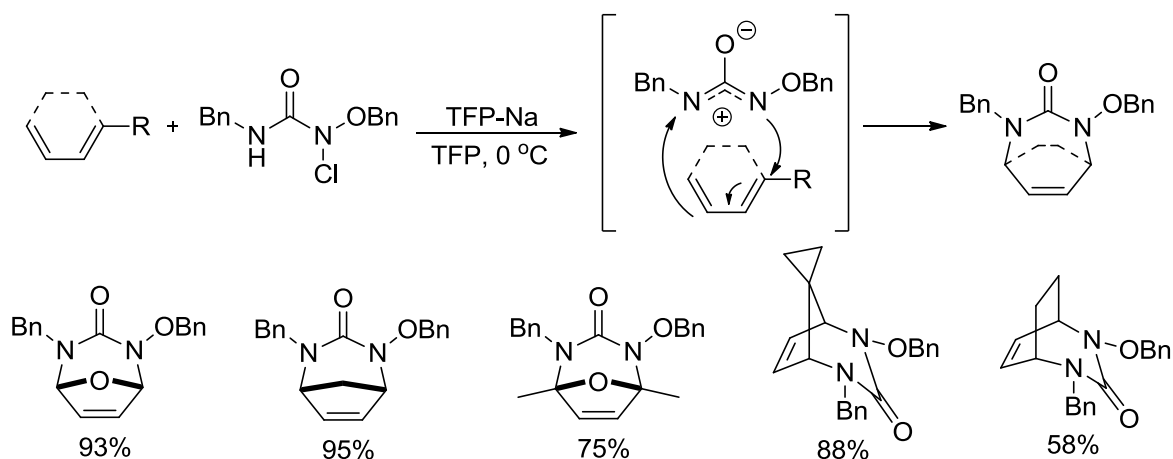


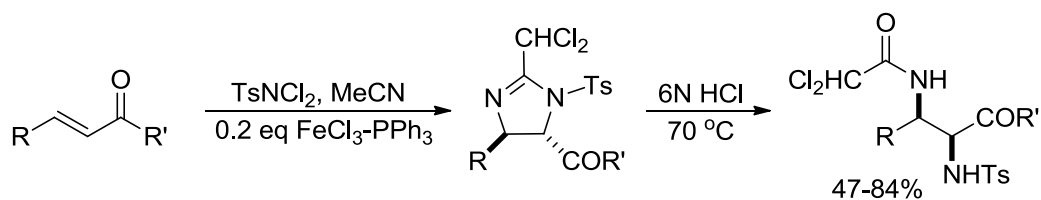
Figure 1.6

A number of additional intra- and intermolecular diamination methods have been reported including the use of other electrophilic iodine reagents²⁵ and HOAc²⁶ to facilitate diamination. A Ritter-type reaction of *N*-chlorosaccharin with terminal alkenes was also reported.²⁷

1.2.2 Catalytic Diamination

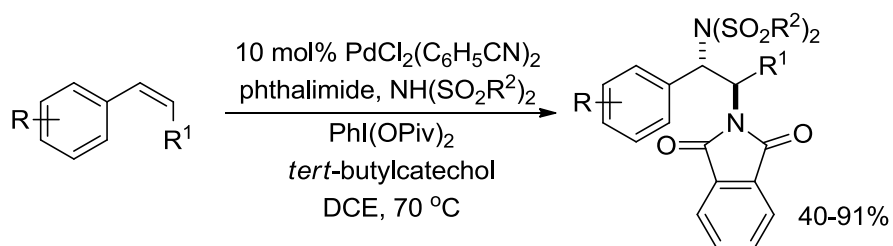
The above metal-mediated processes demonstrate useful approaches to obtain diamines but are limited by the fact that they still require stoichiometric amounts, or high loads of sub-stoichiometric amounts of metal. Many of these methods have a limited scope and have not been developed enantioselectively. Metal-catalyzed diamination of olefins has seen significant progress in the past decade and presents a viable pathway to vicinal diamines.^{1-3,28} In 2001, Li

and coworkers reported the catalytic, electrophilic diamination of α,β -unsaturated ketones and esters using catalytic Rh dimer, FeCl_3 or MnO_2 as catalyst and TsNCl_2 as nitrogen source (Scheme 1.11).²⁹ The resulting imidazoline products can then be opened using acid to yield the protected vicinal diamines. They have also been able to execute this reaction without metal when using nucleophilic nitriles as nitrogen sources.³⁰



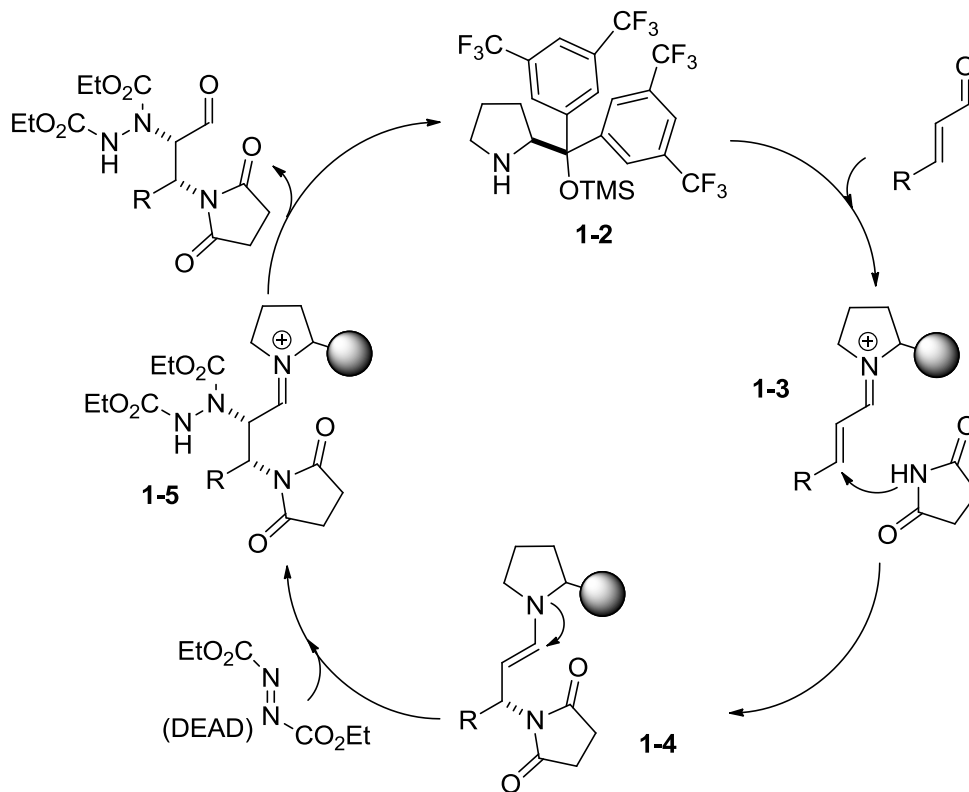
Scheme 1.11

Palladium(II) salts have been used as effective catalysts for the intermolecular diamination of conjugated dienes (Figure 1.7),³¹ unactivated olefins³² and allylic ethers (Scheme 1.12),³³ and β -substituted styrenes (Scheme 1.13). These processes proceed through aminopalladation via initial π -allyl complex formation and subsequent displacement of the palladium by another nitrogen source.³⁴ High diastereoselectivity in the case of internal alkenes supports an aminopalladation mechanism.



Scheme 1.13

Jørgensen and coworkers reported their efforts on the enantioselective diamination of α,β -unsaturated aldehydes via iminium/enamine catalysis.³⁵ As an extension, an electrophilic nitrogen source (DEAD) was used to facilitate the enantioselective diamination of α,β -unsaturated aldehydes. As shown in Scheme 1.14, upon iminium-ion activation of the aldehyde, succinimide adds at the β -position (**1-3**). DEAD attacks at the α -position of enamine **1-4** to form iminium **1-5** which generates the diamination product and regenerates the prolinol-derived catalyst (**1-2**). Two examples were given and *E*-dec-2-enal was effectively diaminated in 39% yield, 80:20 dr and 99% ee.



Scheme 1.14

Intramolecular diamination in which the two nitrogen atoms are tethered to a terminal olefin was reported by Muñiz and coworkers in 2005 using Pd(II) as catalyst.^{36,37} *Syn*-aminopalladation occurs initially, followed by oxidation and nucleophilic replacement of the palladium by the second nitrogen (Figure 1.8). A variety of bicyclic ureas can be obtained in good to high yields. Extensions of this reaction include the synthesis of bisindolines, bispyrrolidines³⁸ and diamine carboxylic esters with high diastereoselectivity.³⁹ A Au(I)-catalyzed variation⁴⁰ as well as a Ni(II)-catalyzed variation via sulfamide transfer have also been reported.⁴¹ Along with PhI(OAc)₂ as oxidant, CuBr₂ and CuCl have also been reported to be effective oxidants to regenerate the active catalyst.⁴² Interestingly, a metal-free Br-catalyzed intramolecular diamination of terminal alkenes and acrylates was reported by Muñiz and

coworkers in 2012.⁴³ KBr is used as catalyst and the economical NaClO₂ as terminal oxidant. Both terminal alkenes and acrylates are efficiently diaminated in high yields and in up to 4:1 dr where applicable (Figure 1.9).

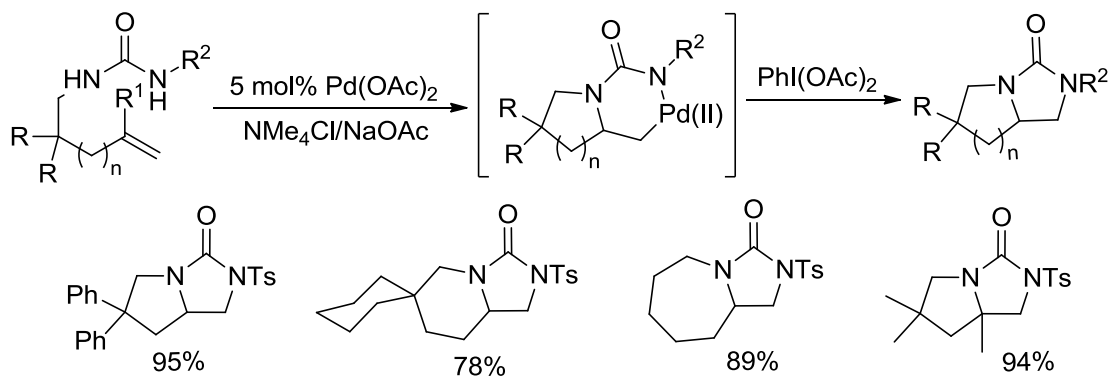


Figure 1.8

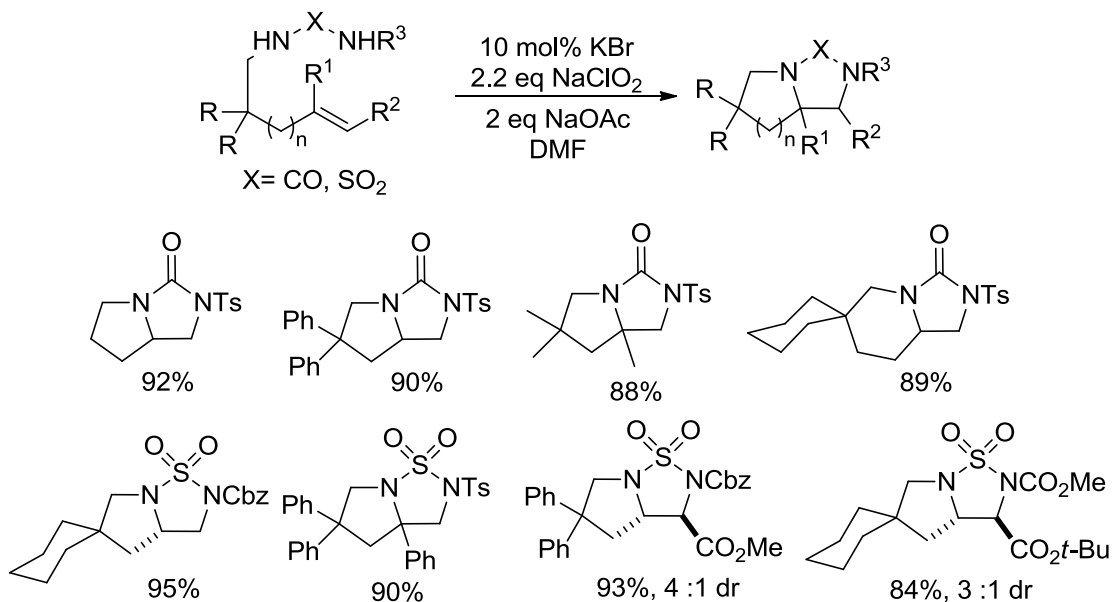
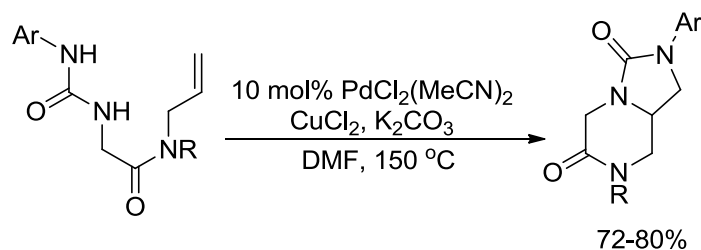


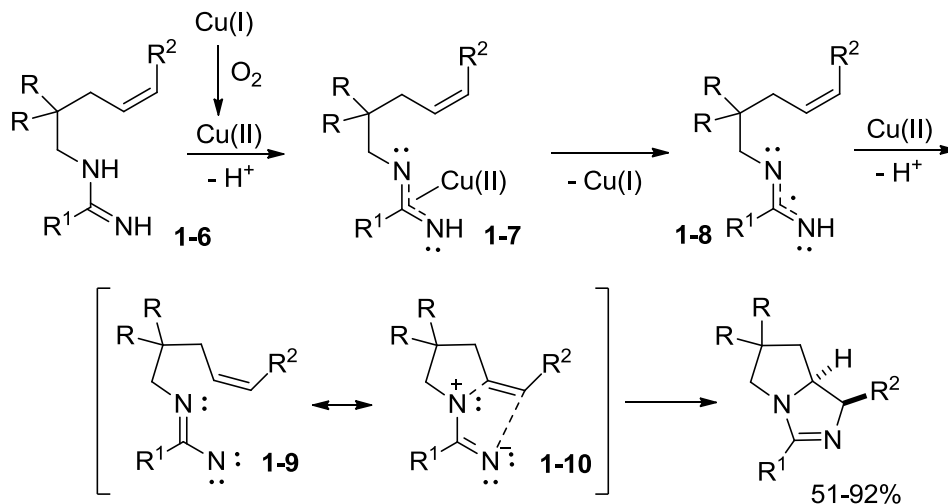
Figure 1.9

Broggini and coworkers recently reported a mechanistically similar reaction of Pd(II)-catalyzed diamination of alkenylureas to form bicyclic piperazinones (Scheme 1.15).⁴⁴ Variation on the nitrogen protecting groups tolerated electron-rich and electron-poor groups and the resulting bicyclic piperazinones were obtained in good yields.



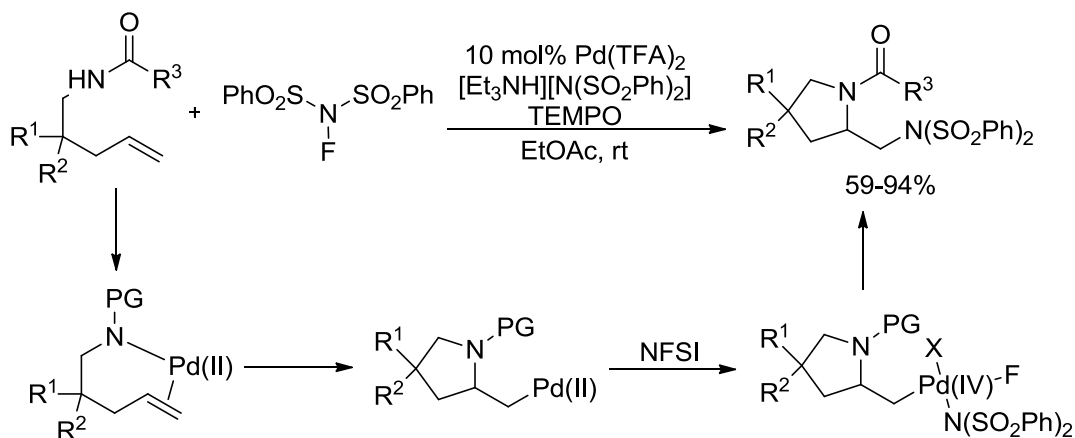
Scheme 1.15

Through an interesting mechanism, Chiba and coworkers reported intramolecular Cu(I)-catalyzed aerobic [3+2]-annulation of *N*-alkenyl amidines for an overall diamination of tethered alkenes (Scheme 1.16).⁴⁵ One-electron oxidation of amidine **1-6** via diazaenolate **1-7** gives radical **1-8**; which upon further oxidation generates nitrene intermediate **1-9**. The authors propose the alternative resonance form **1-10** then undergoes concerted [3+2]-annulation. The resulting bicyclic amidines were obtained in moderate to high yield, retaining the geometry of the starting alkene.



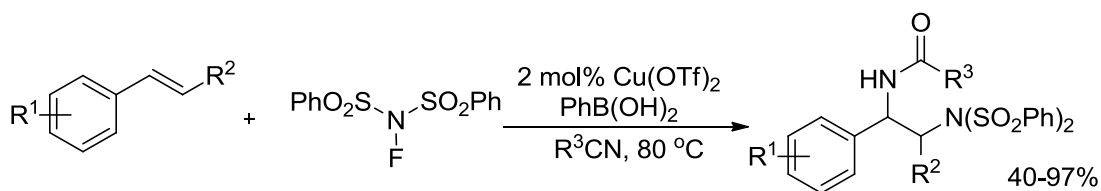
Scheme 1.16

Michael and coworkers reported a related diamination of amide-tethered terminal alkenes using *N*-fluorobenzenesulfonimide (NFSI) as an electrophilic nitrogen source (Scheme 1.17).⁴⁶ Aminopalladation followed by oxidative addition of NFSI gives a Pd(IV) intermediate whereupon reductive elimination, yields the diamine product.^{46b} This process has been made enantioselective using a chiral Ph-quinox ligand and ee's have reached >99%.⁴⁷



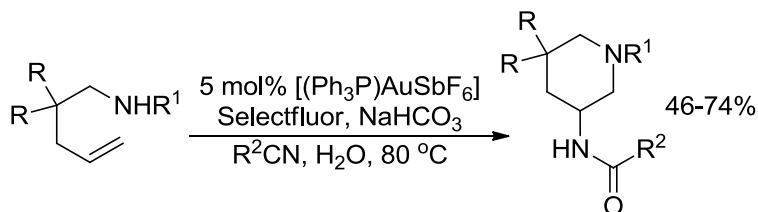
Scheme 1.17

Xiong, Li, Zhang and coworkers developed an intermolecular diamination of substituted styrenes using NFSI as oxidant, Cu(OTf)₂ as catalyst and a second nitrogen source (Scheme 1.18).⁴⁸ Electron-poor styrenes proved most reactive and yields were mostly above 80%.



Scheme 1.18

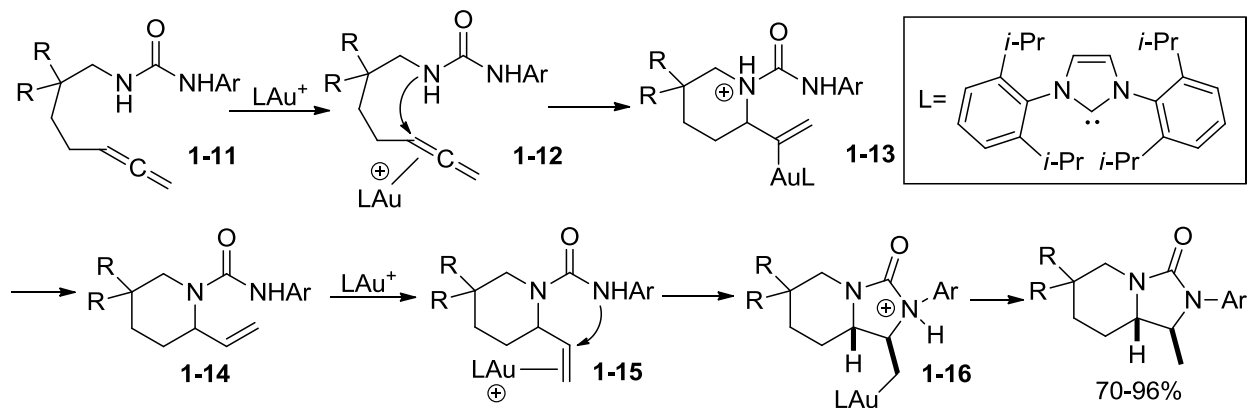
Nevado and de Haro reported in 2011 the oxidative difunctionalization of unactivated alkenes wherein gold catalyzed the diamination of terminal alkenes.⁴⁹ Amine-tethered terminal olefins underwent an aminoamidation reaction to yield the diamine products in good yields (Scheme 1.19). Six-membered rings were the favored formation and the authors' findings propose that multiple mechanisms coexist.



Scheme 1.19

Intramolecular dihydroamination of allenes was reported by Widenhoefer and coworker using 5 mol% Au-carbene complex and AgPF₆ (Scheme 1.20).⁵⁰ Activation of the allene by gold (**1-12**) and intramolecular attack of the first nitrogen closes the ring which upon proton transfer/protodeauration and subsequent attack of the second nitrogen (**1-15**) yields alkyl gold species **1-16**. Proton transfer yielded the diamination products in good to high yields.

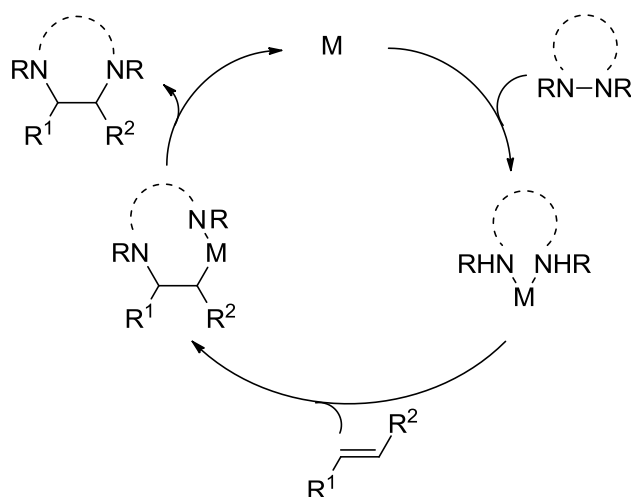
Diamination of internal as well as terminal alkynes has been reported using Cu(II)/Fe(III),⁵¹ Pd(II)⁵² and Cu(II)⁵³ catalysts via intra- and intermolecular processes with promising yields.



1.2.3 Methods Inspired by Inherent Ring Strain

1.2.3.1 Pd-Catalyzed

Small rings bear attractive reactive capabilities, as they inherently possess potential energy which could be harnessed for a variety of chemical reactions and transformations. Shi and coworkers envisioned employing a strained dinitrogen-containing ring as a nitrogen source and utilizing a metal to insert into the N-N bond to relieve the ring strain. This complex could then coordinate to an unsaturated double bond, allowing insertion of the first nitrogen followed by reductive elimination to give diamination and regeneration of the metal catalyst (Scheme 1.21).



Scheme 1.21

This was in fact realized when Shi and coworkers reported in 2007 the regio- and stereoselective diamination of conjugated dienes and trienes using di-*tert*-butyldiaziridinone (**1-17**) as nitrogen source.⁵⁴ Using $Pd(PPh_3)_4$ as catalyst, the intermolecular diamination is highly effective for a variety of conjugated dienes including *trans*, trisubstituted, electron deficient and electron-rich dienes in high yields and short reaction times (Figure 1.10). It was shown that the diamination occurred regioselectively at the internal *trans* double bond and was highly diastereoselective, with both nitrogens adding syn to the olefin, yielding the *trans* diamination product. When a mixture of *E* and *Z* isomers were subjected to the reaction conditions, only the *E* isomer was consumed and the *Z* isomer was left enriched. The nitrogen source di-*tert*-butyldiaziridinone (**1-17**), a protected form of urea, is easily synthesized in three steps in multi-gram quantities. (Scheme 1.22).⁵⁵

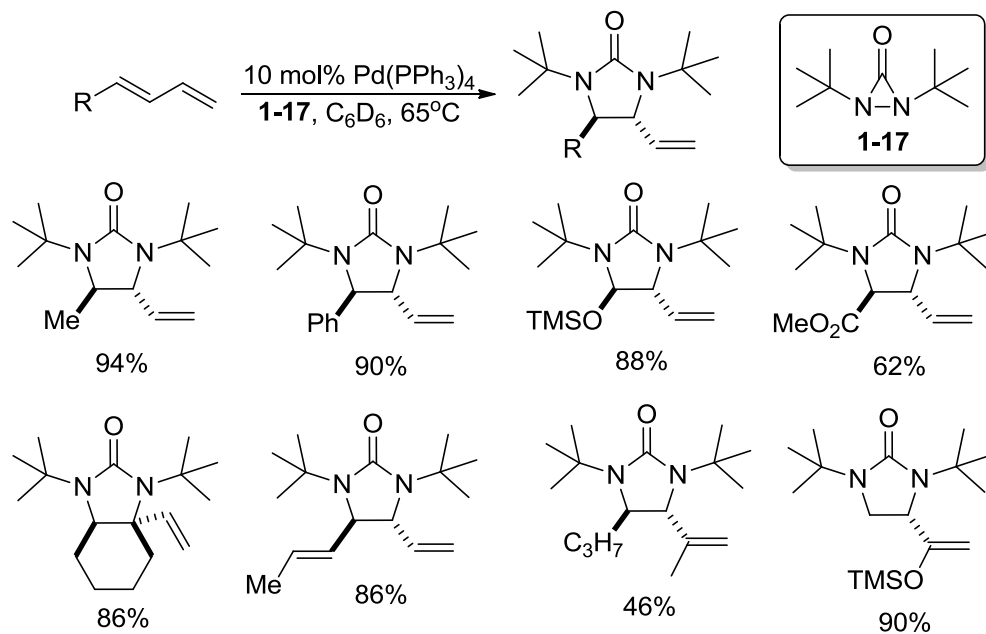
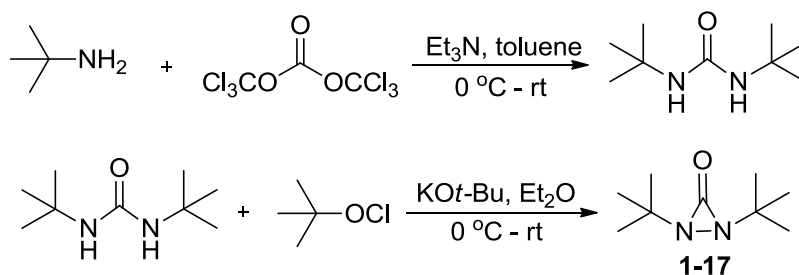
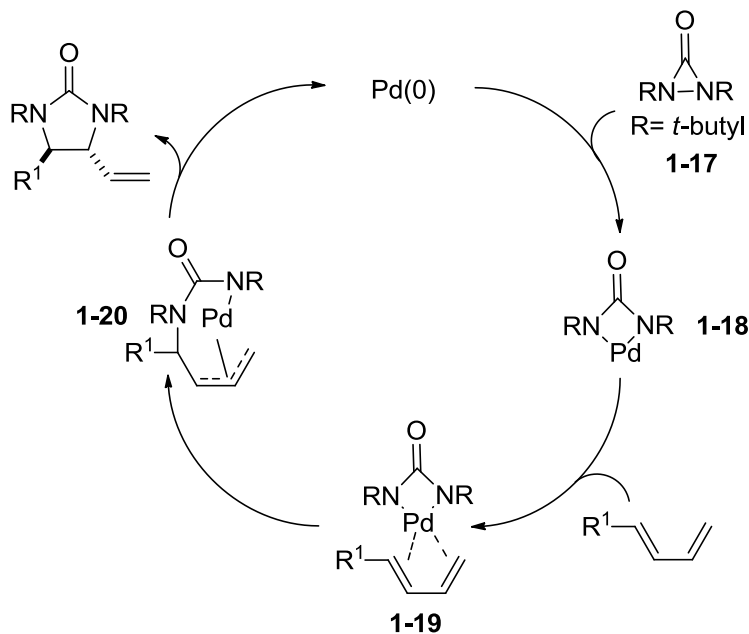


Figure 1.10



Scheme 1.22

It was proposed that oxidative insertion of Pd(0) into the N-N bond of diaziridinone **1-17** formed the four-membered Pd(II) complex **1-18** (Scheme 1.23). Complex **1-18** coordinates with the diene and after migratory insertion of one nitrogen, the π -allyl Pd complex **1-20** is generated. Reductive elimination yields the diamination product and regenerates the Pd(0) catalyst (Scheme 1.23).^{54,56}



Scheme 1.23

In the same year, this reaction was expanded to effectively diaminate the allylic and homoallylic carbons of terminal olefins under solvent-free conditions (Figure 1.11).⁵⁷ It was proposed that this reaction proceeded through a C-H activation mechanism (Scheme 1.24). Coordination of the terminal olefin **1-21** to the four-membered Pd(II) complex (**1-18**) gives **1-22**. Removal of an allylic hydrogen results in π -allyl Pd complex **1-23**. It is proposed that after β -H elimination the reactive diene **1-24** is formed *in situ* and is subsequently diaminated at the internal trans double bond according to the mechanism described for conjugated diene substrates. The diene **1-24** was able to be detected by ¹H NMR but was not isolated.

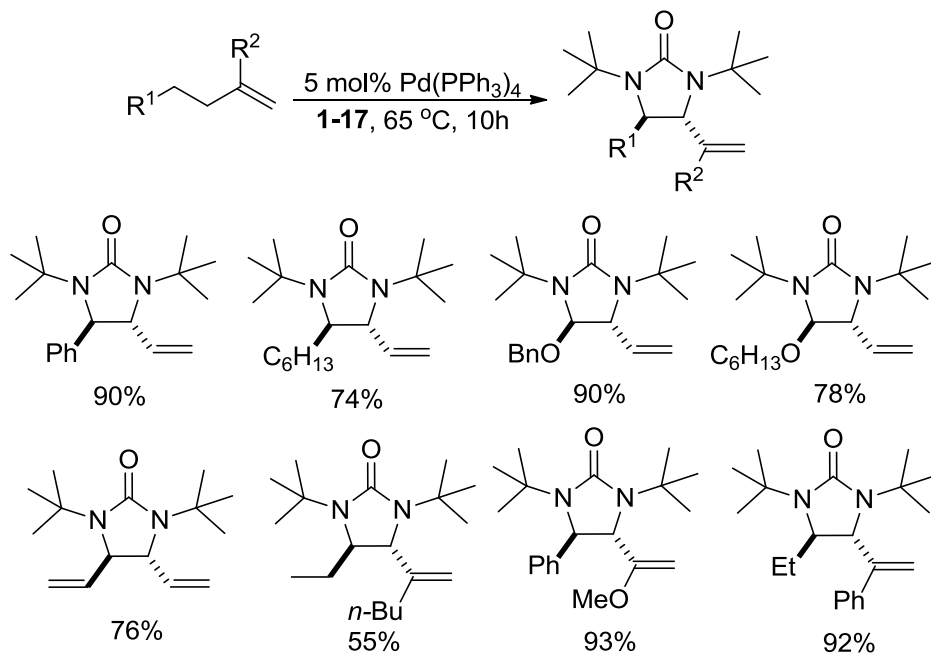
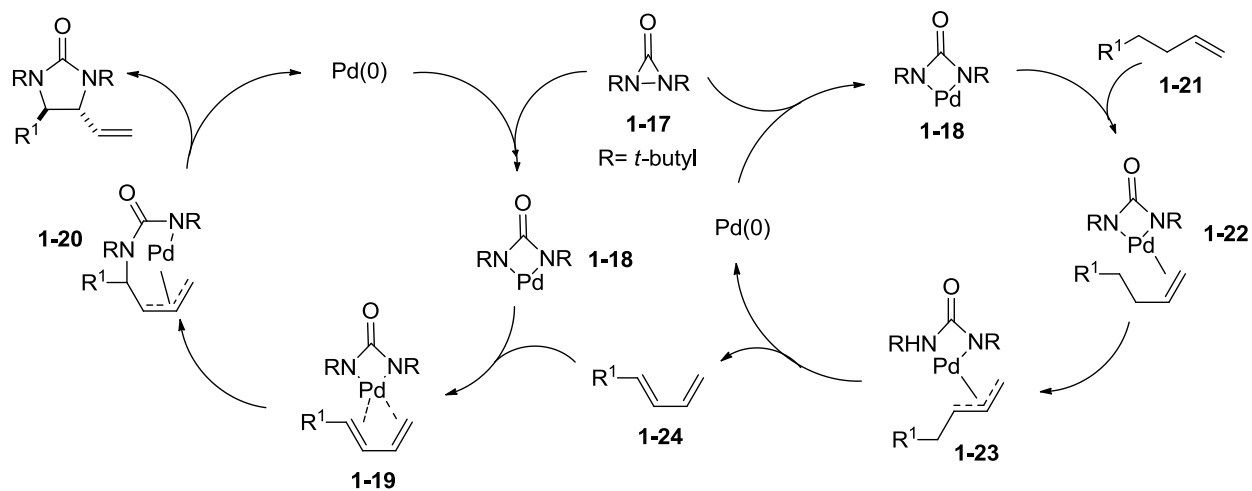


Figure 1.11



Scheme 1.24

Both of the aforementioned diamination systems have been developed asymmetrically using chiral ligands **1-25**⁵⁸ and **1-26**⁵⁹ respectively (Figure 1.12).⁶⁰ The steric bulkiness of the

amine substituent played a large role in reactivity and enantioselectivity of the diamination. Enantioselectivities ranged from 87-95% for a variety of acyclic and cyclic *trans* dienes and terminal olefins.

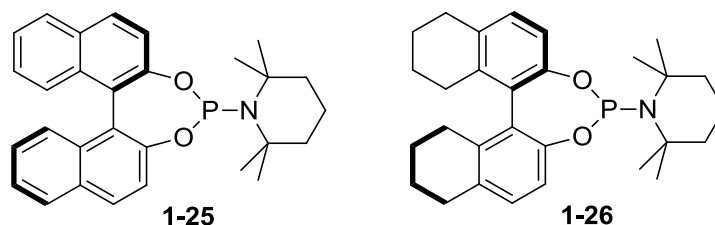
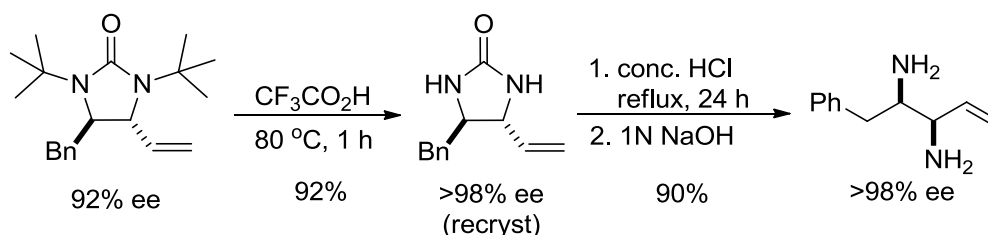


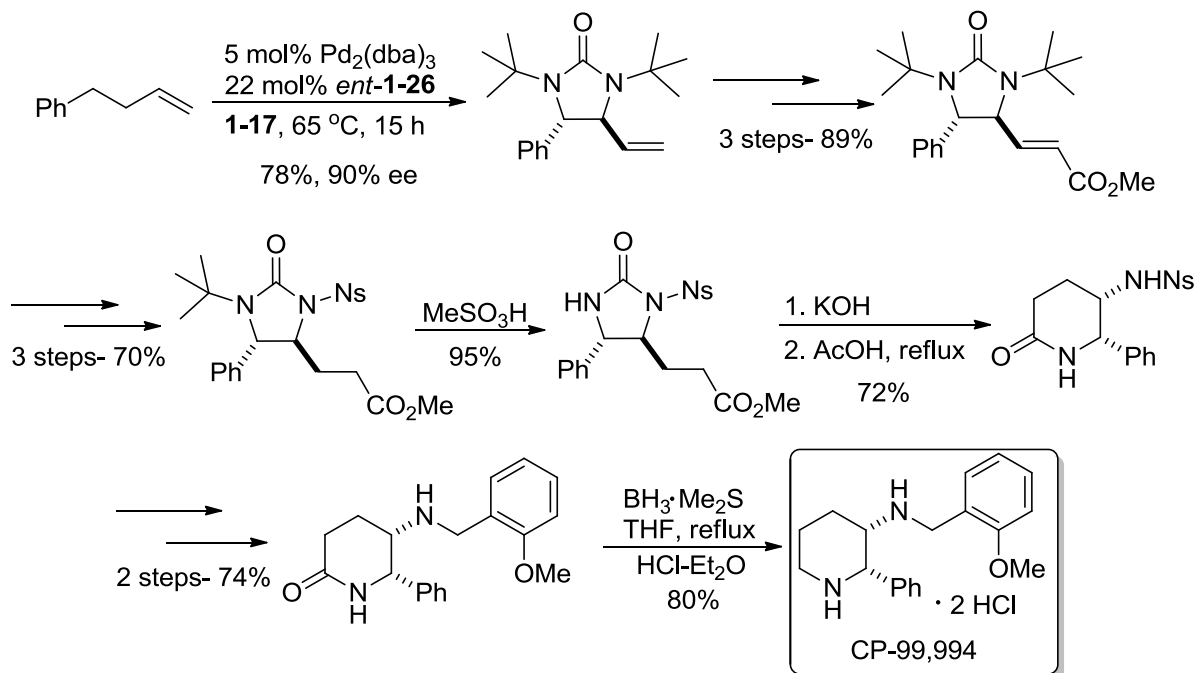
Figure 1.12

Removal of the *tert*-butyl groups from the cyclic urea products could be accomplished upon stirring in trifluoroacetic acid at 80 °C for 1 hour (Scheme 1.25). Further deprotection via removal of the carbonyl was performed in concentrated HCl at reflux for 24 hours (Scheme 1.25). The free diamine was obtained in high yield and optical purity.



Scheme 1.25

The asymmetric diamination via C-H bond activation and employing ligand *ent*-**1-26**, has been applied in the total synthesis of substance P receptor antagonist (+)-CP-99,994 (Scheme 1.26).⁶¹ Diamination of 1,5-hexadiene employing C-H activation diamination conditions and ligand **1-26** yielded cyclic urea **1-27** which was employed as a chiral ligand for asymmetric conjugate addition reactions to cyclic enones (Figure 1.13).⁶²



Scheme 1.26

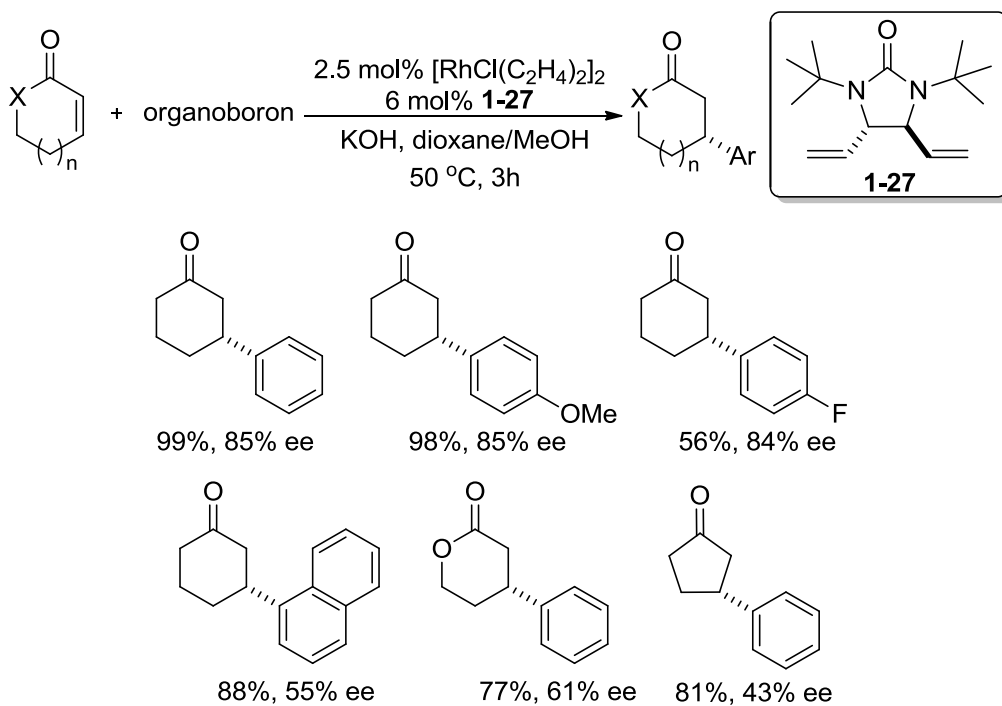


Figure 1.13

Shi and coworkers have also reported the diamination of conjugated dienes using *N*-heterocyclic carbene-Pd(0) complexes as catalysts.⁶³ Recently, Pd(PPh₃)₄ was used as catalyst for sequential C-N bond formation via allylic and aromatic C-H amination of α -methylstyrenes.⁶⁴ Four C-N bonds are formed in one step and yields were good for a variety of substitutions (Figure 1.14).

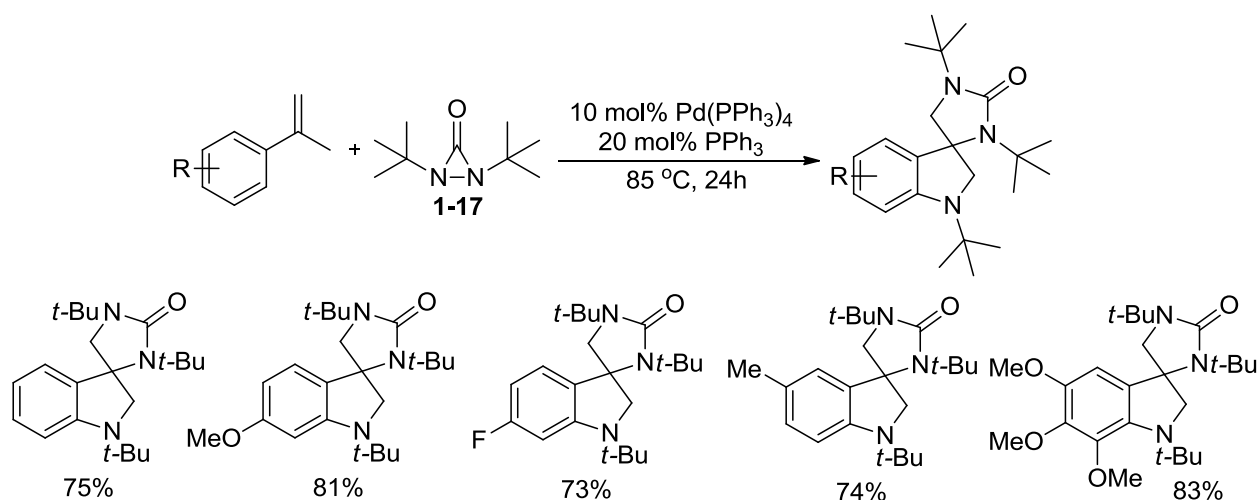


Figure 1.14

1.2.3.2 Cu-Catalyzed

Shi and coworkers have also developed a Cu-catalyzed diamination process for conjugated diene substrates which is complementary in regioselectivity to that of the Pd-catalyzed processes. Using CuCl-P(OPh)₃ as catalyst and **1-17** as nitrogen source, the terminal double bond of conjugated dienes were diaminated with high regioselectivity (Figure 1.15).⁶⁵ One exception to the high terminal selectivity was the diamination of *trans*-1,3-pentadiene which gave a 1 : 1.3 ratio of terminal to internal products. It was proposed that the reaction proceeded through a radical mechanism (Scheme 1.27). The copper catalyst reductively cleaves the N-N bond of the diaziridinone to give radical species **1-28**. Terminal addition of **1-28** into the diene

yields π -allyl radical species **1-29** which upon radical recombination, or formation of Cu(III) species **1-30** and successive reductive elimination, gives the diamination product and recycles the Cu(I) catalyst.

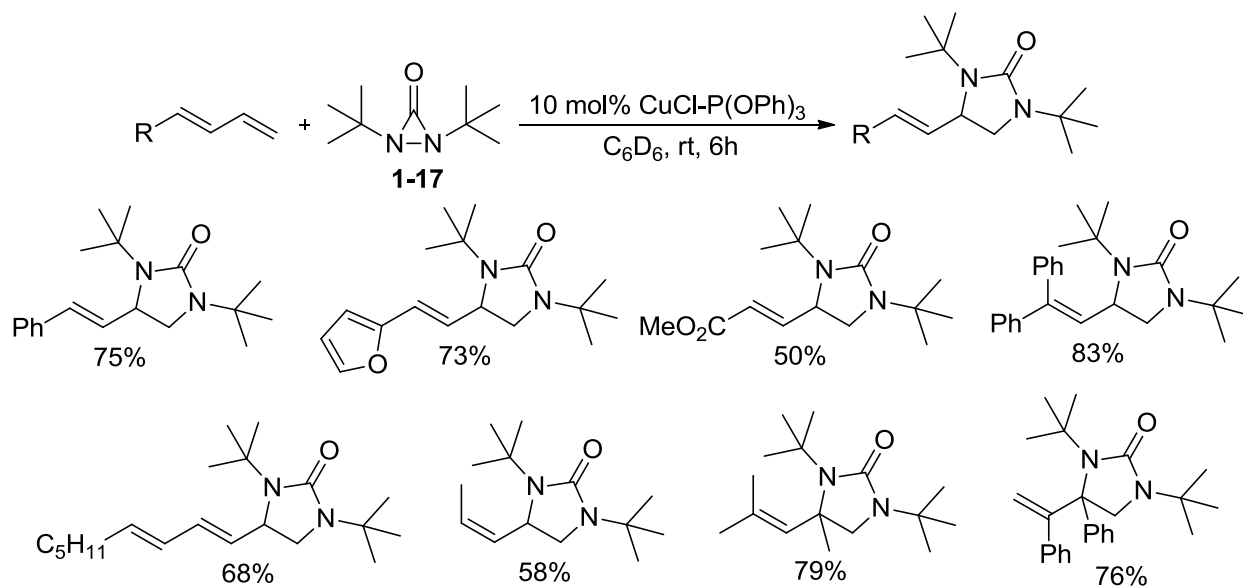
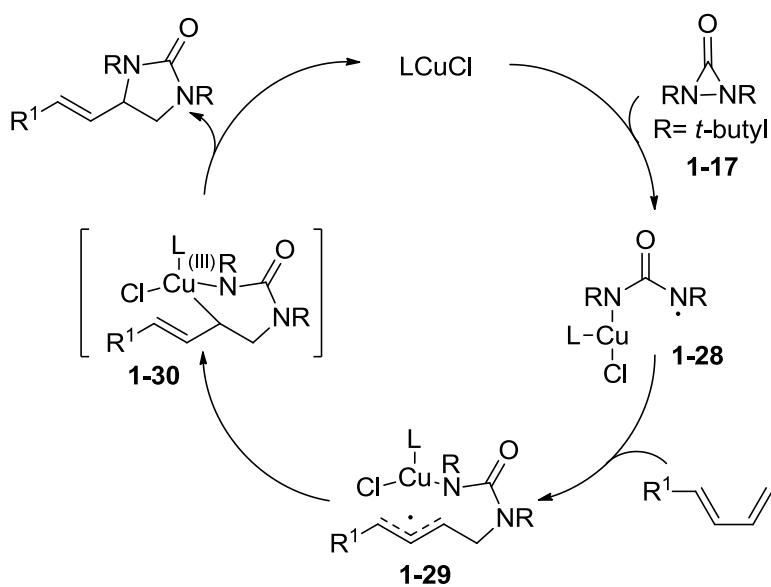


Figure 1.15



Scheme 1.27

Due to the proposed radical pathway, an asymmetric variant proved to be challenging however enantioselectivities for terminal diamination could be obtained using ligand **1-31** or copper catalysts with chiral counteranions (**1-32**) (Figure 1.16). Diamination using (*R*)-DTBM-SEGPHOS (**1-31**) provided encouraging ee's ranging from 23-74% for a variety of conjugated dienes and a triene.⁶⁶ Chiral copper catalyst **1-32** also effectively induced asymmetry with 49-61% ee for conjugated dienes and a triene.⁶⁷

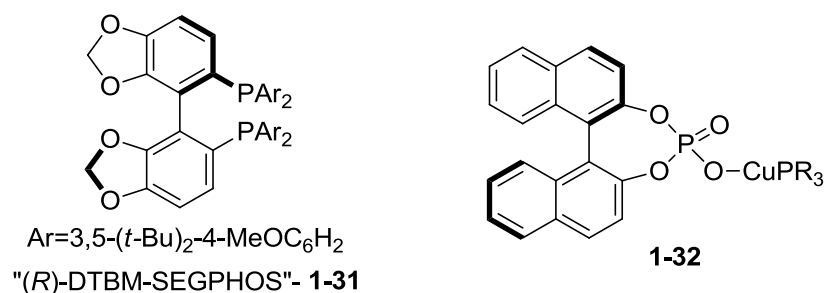


Figure 1.16

1,1-Disubstituted terminal olefins were also found to be good substrates for Cu(I)-catalyzed diamination using nitrogen source **1-17**. A variety of 1,1-disubstituted olefins including substituted α -methylstyrenes were efficiently diaminated in moderate to good yields (Figure 1.17) and the method was employed for the synthesis of a potent NK₁ antagonist (Scheme 1.28).⁶⁸ Other related methods employing diaziridinone **1-17** include the Cu-catalyzed C-H α -amination of esters⁶⁹ and aryl ketones⁷⁰ to synthesize hydantoins and imidazolinones respectively. An alternative nitrogen source (**1-33**) has also been reported for the cycloguanidination of terminal olefins (Figure 1.18).⁷¹ Conjugated dienes, trienes, enynes and aryl-substituted olefins were cycloguanidinated in moderate to good yields using CuCl-PPh₃ as catalyst.

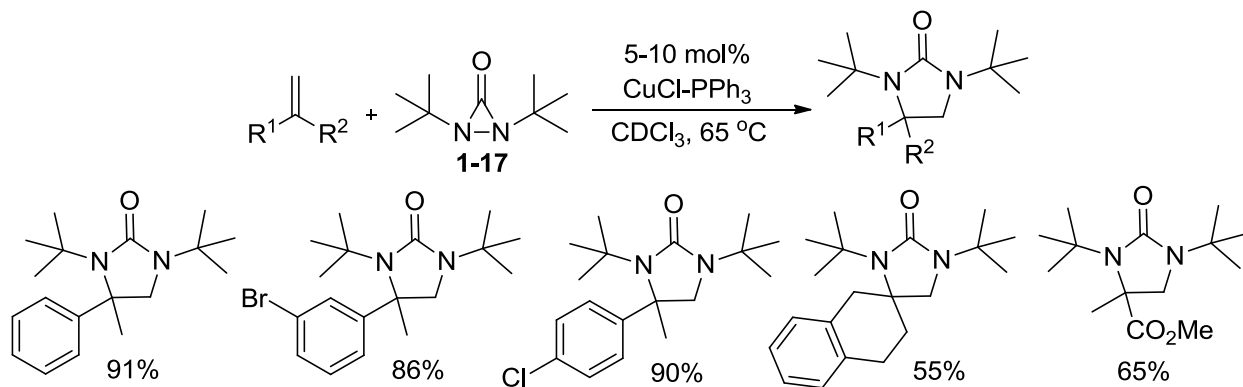
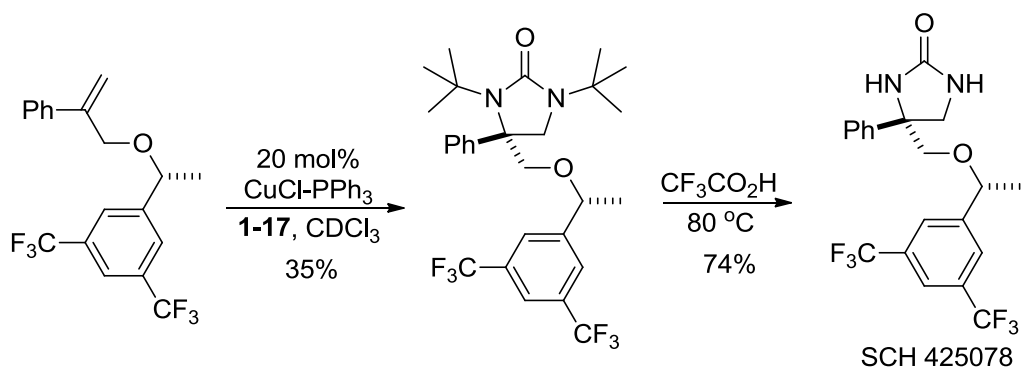


Figure 1.17



Scheme 1.28

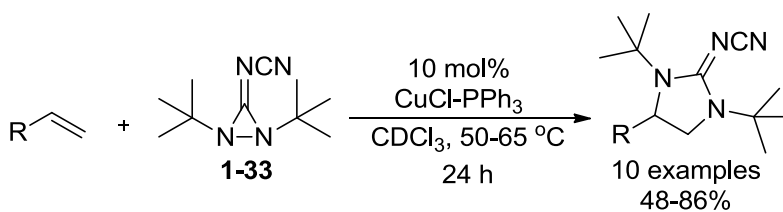


Figure 1.18

1.3 REFERENCES

- ¹ For leading reviews, see: (a) Lucet, D.; Le Gall, T.; Mioskowski, C. *Angew. Chem. Int. Ed.* **1998**, *37*, 2580 (b) Kotti, S.R.S.S.; Timmons, C.; Li, G. *Chem Biol. Drug Des.* **2006**, *67*, 101 (c) De Jong, S.; Nosal, D.G.; Wardrop, D.J. *Tetrahedron* **2012**, *68*, 4067.
- ² For leading reviews, see: (a) Kizirian, J.-C. *Chem. Rev.* **2008**, *108*, 140 (b) Lin, G.-Q.; Xu, M.-H.; Zhong, Y.-W.; Sun, X.-W. *Acc. Chem. Res.* **2008**, *41*, 831.
- ³ For leading reviews, see: (a) Mortensen, M.S.; O'Doherty, G.A. *Chemtracts: Org. Chem.* **2005**, *18*, 555 (b) Jensen, K.H.; Sigman, M.S. *Org. Biomol. Chem.* **2008**, *6*, 4083 (c) de Figueirido, R.M. *Angew. Chem. Int. Ed.* **2009**, *48*, 1190 (d) Cardona, F.; Goti, A. *Nat. Chem.* **2009**, *1*, 269.
- ⁴ Aranda, V.G.; Barluenga, J.; Aznar, F. *Synthesis* **1974**, 504.
- ⁵ Barluenga, J.; Alonso-Cires, L.; Asensio, G. *Synthesis* **1979**, 962.
- ⁶ (a) Sharpless, K.B.; Singer, S.P. *J. Org. Chem.* **1976**, *41*, 2504 (b) Bruncko, M.; Khuong, T.-A.V.; Sharpless, K.B. *Angew. Chem. Int. Ed.* **1996**, *35*, 454.
- ⁷ Chong, A.O.; Oshima, K.; Sharpless, K.B. *J. Am. Chem. Soc.* **1977**, *99*, 3420
- ⁸ (a) Muñiz, K.; Iesato, A.; Nieger, M. *Chem. Eur. J.* **2003**, *9*, 5581 (b) Deubel, D.V.; Muñiz, K. *Chem. Eur. J.* **2004**, *10*, 2475 (c) Muñiz, K. *Chem. Soc. Rev.* **2004**, *33*, 166 (d) Muñiz, K. *Eur. J. Org. Chem.* **2004**, 2243.
- ⁹ (a) Muñiz, K.; Nieger, M. *Synlett* **2003**, 211 (b) Muñiz, K.; Nieger, M.; Mansikkamäki, H. *Angew. Chem. Int. Ed.* **2003**, *42*, 5958 (c) Muñiz, K. *New J. Chem.* **2005**, *29*, 1371.
- ¹⁰ (a) Muñiz, K.; Nieger, M. *Chem. Commun.* **2005**, 2729 (b) Almodovar, I.; Hövelmann, C.H.; Streuff, J.; Nieger, M.; Muñiz, K. *Eur. J. Org. Chem.* **2006**, 704.
- ¹¹ Bäckvall, J.-E. *Tetrahedron Lett.* **1978**, 163.
- ¹² (a) Becker, P.N.; White, M.A.; Bergman, R.G. *J. Am. Chem. Soc.* **1980**, *102*, 5676 (b) Becker, P.N.; Bergman, R.G. *Organometallics* **1983**, *2*, 787.
- ¹³ Fristad, W.E.; Brandvold, T.A.; Peterson, J.R.; Thompson, S.R. *J. Org. Chem.* **1985**, *50*, 3647.
- ¹⁴ (a) Zabawa, T.P.; Kasi, D.; Chemler, S.R. *J. Am. Chem. Soc.* **2005**, *127*, 11250 (b) Zabawa, T.P.; Chemler, S.R. *Org. Lett.* **2007**, *9*, 2035 (c) Sequeira, F.C.; Turnpenney, B.W.; Chemler, S.R. *Angew. Chem. Int. Ed.* **2010**, *49*, 6365.
- ¹⁵ Kour, H.; Paul, S.; Singh, P.P.; Gupta, M.; Gupta, R. *Tetrahedron Lett.* **2013**, *54*, 761.

- ¹⁶ (a) Lavilla, R.; Kumar, R.; Coll, O.; Masdeu, C.; Bosch, J. *Chem. Commun.* **1998**, 2715 (b) Lavilla, R.; Kumar, R.; Coll, O.; Masdeu, C.; Spada, A.; Bosch, J.; Espinosa, E.; Molins, E. *Chem. Eur. J.* **2000**, *6*, 1763.
- ¹⁷ Kumar, V.; Ramesh, N.G. *Chem. Commun.* **2006**, 4952.
- ¹⁸ Röben, C.; Souto, J.A.; González, Y.; Lischchynskyi, A.; Muñiz, K. *Angew. Chem. Int. Ed.* **2011**, *50*, 9478.
- ¹⁹ Lischchynskyi, A.; Muñiz, K. *Chem. Eur. J.* **2012**, *18*, 2212.
- ²⁰ Li, H.; Widenhoefer, R.A. *Tetrahedron* **2010**, *66*, 4827.
- ²¹ Müller, C.H.; Fröhlich, R.; Daniliuc, C.G.; Hennecke, U. *Org. Lett.* **2012**, *14*, 5944.
- ²² (a) Souto, J.A.; González, Y.; Iglesias, A.; Zian, D.; Lischchynski, A.; Muñiz, K. *Chem. Asian J.* **2012**, *7*, 1103 (b) Souto, J.A.; Martínez, C.; Velilla, I.; Muñiz, K. *Angew. Chem. Int. Ed.* **2013**, *52*, 1324.
- ²³ Röben, C.; Souto, J.A.; Escudero-Adán, E.C.; Muñiz, K. *Org. Lett.* **2013**, *15*, 1008.
- ²⁴ Jeffrey, C.S.; Anumandla, D.; Carson, C.R. *Org. Lett.* **2012**, *14*, 5764.
- ²⁵ For additional examples employing electrophilic iodine reagents for diamination, see: (a) Kong, A.; Blakey, S.B. *Synthesis* **2012**, *44*, 1190 (b) Kim, H.J.; Cho, S.H.; Chang, S. *Org. Lett.* **2012**, *14*, 1424.
- ²⁶ Zhu, M.-K.; Chen, Y.-C.; Loh, T.-P. *Chem. Eur. J.* **2013**, *19*, 5250.
- ²⁷ Booker-Milburn, K.I.; Guly, D.J.; Cox, B.; Procopiou, P.A. *Org. Lett.* **2003**, *5*, 3313.
- ²⁸ Muñiz, K.; Martínez, C. *J. Org. Chem.* **2013**, *78*, 2168.
- ²⁹ (a) Li, G.; Wei, H.-X.; Kim, S.H.; Carducci, M.D. *Angew. Chem. Int. Ed.* **2001**, *40*, 4277 (b) Wei, W.-X.; Kim, S.H.; Li, G. *J. Org. Chem.* **2002**, *67*, 4777 (c) Wei, H.-X.; Siruta, S.; Li, G. *Tetrahedron Lett.* **2002**, *43*, 3809 (d) Timmons, C.; Mcpherson, L.M.; Chen, D.; Wei, H.-X.; Li, G. *J. Peptide Res.* **2005**, *66*, 249 (e) Han, J.; Li, T.; Pan, Y.; Kattuboina, A.; Li, G. *Chem. Biol. Drug Des.* **2008**, *71*, 71.
- ³⁰ (a) Li, G.; Kim, S.H.; Wei, H.-X. *Tetrahedron Lett.* **2000**, *41*, 8699 (b) Chen, D.; Timmons, C.; Wei, H.-X.; Li, G. *J. Org. Chem.* **2003**, *68*, 5742 (c) Pei, W.; Wei, H.-X.; Chen, D.; Headley, A.D.; Li, G. *J. Org. Chem.* **2003**, *68*, 8404 (d) Timmons, C.; Chen, D.; Xu, X.; Li, G. *Eur. J. Org. Chem.* **2003**, 3850 (e) Timmons, C.; Chen, D.; Barney, E.; Kirtane, S.; Li, G. *Tetrahedron* **2004**, *60*, 12095 (f) Wu, H.; Ji, X.; Sun, H.; An, G.; Han, J.; Li, G.; Pan, Y. *Tetrahedron* **2010**, *66*, 4555.

- ³¹ Bar, G.L.J.; Lloyd-Jones, G.C.; Booker-Milburn, K.I. *J. Am. Chem. Soc.* **2005**, *127*, 7308.
- ³² Iglesias, Á.; Pérez, E.G.; Muñiz, K. *Angew. Chem. Int. Ed.* **2010**, *49*, 8109.
- ³³ Muñiz, K.; Kirsch, J.; Chávez, P. *Adv. Synth. Catal.* **2011**, *353*, 689.
- ³⁴ For mechanistic studies on Pd(II)-catalyzed intermolecular diamination, see: Yu, Y.; Shen, W.; Zhang, J.; He, R.; Li, M. *J. Phys. Org. Chem.* **2008**, *21*, 979.
- ³⁵ Jiang, H.; Nielsen, J.B.; Nielsen, M.; Jørgensen, K.A. *Chem. Eur. J.* **2007**, *13*, 9068.
- ³⁶ (a) Streuff, J.; Hövelmann, C.H.; Nieger, M.; Muñiz, K. *J. Am. Chem. Soc.* **2005**, *127*, 14586
(b) Muñiz, K.; Hövelmann, C.H.; Nieger, M.; Muñiz, K. *J. Am. Chem. Soc.* **2008**, *130*, 763.
- ³⁷ For mechanistic studies on Pd(II)-catalyzed intramolecular diamination, see: Yu, H.; Fu, Y.; Guo, Q.; Lin, Z. *Organometallics* **2009**, *28*, 4507.
- ³⁸ Muñiz, K. *J. Am. Chem. Soc.* **2007**, *129*, 14542.
- ³⁹ (a) Muñiz, K.; Streuff, J.; Chávez, P.; Hövelmann, C.H. *Chem. Asian J.* **2008**, *3*, 1248 (b) Chávez, P.; Kirsch, J.; Streuff, J.; Muñiz, K. *J. Org. Chem.* **2012**, *77*, 1922.
- ⁴⁰ Iglesias, A.; Muñiz, K. *Chem. Eur. J.* **2009**, *15*, 10563.
- ⁴¹ (a) Muñiz, K.; Streuff, J.; Hövelmann, C.H.; Núñez, A.; *Angew. Chem. Int. Ed.* **2007**, *46*, 7125
(b) Muñiz, K.; Hövelmann, C.H.; Streuff, J.; Campos-Gómez, E. *Pure Appl. Chem.* **2008**, *80*, 1089.
- ⁴² (a) Muñiz, K.; Hövelmann, C.H.; Campos-Gómez, E.; Barluenga, J.; González, J.M.; Streuff, J.; Nieger, M. *Chem. Asian J.* **2008**, *3*, 776 (b) Hövelmann, C.H.; Streuff, J.; Brelot, L.; Muñiz, K. *Chem. Commun.* **2008**, 2334.
- ⁴³ (a) Chávez, P.; Kirsch, J.; Hövelmann, C.H.; Streuff, J.; Martínez-Belmonte, M.; Escudero-Adán, E.C.; Martín, E.; Muñiz, K. *Chem. Sci.* **2012**, *3*, 2375 (b) Muñiz, K. *Pure Appl. Chem.* **2013**, *85*, 755.
- ⁴⁴ Brogini, G.; Barbera, V.; Beccalli, E.M.; Chiacchio, U.; Fasana, A.; Galli, S.; Gazzola, S. *Adv. Synth. Catal.* **2013**, *355*, 1640.
- ⁴⁵ Wang, Y.-F.; Zhu, X.; Chiba, S. *J. Am. Chem. Soc.* **2012**, *134*, 3679.
- ⁴⁶ (a) Sibbald, P.A.; Michael, F.E. *Org. Lett.* **2009**, *11*, 1147 (b) Sibbald, P.A.; Rosewall, C.F.; Swartz, R.D.; Michael, F.E. *J. Am. Chem. Soc.* **2009**, *131*, 15945.
- ⁴⁷ Ingalls, E.L.; Sibbald, P.A.; Kaminsky, W.; Michael, F.E. *J. Am. Chem. Soc.* **2013**, *135*, 8854.

- ⁴⁸ Zhang, H.; Pu, W.; Xiong, T.; Li, Y.; Zhou, X.; Sun, K.; Liu, Q.; Zhang, Q. *Angew. Chem. Int. Ed.* **2013**, *52*, 2529.
- ⁴⁹ de Haro, T.; Nevado, C. *Angew. Chem. Int. Ed.* **2011**, *50*, 906.
- ⁵⁰ Li, H.; Widenhofer, R.A. *Org. Lett.* **2009**, *11*, 2671.
- ⁵¹ Zeng, J.; Tan, Y.J.; Leow, M.L.; Liu, X.-W. *Org. Lett.* **2012**, *14*, 4386.
- ⁵² Yao, B.; Wang, Q.; Zhu, J. *Angew. Chem. Int. Ed.* **2012**, *51*, 5170.
- ⁵³ Li, J.; Neuville, L. *Org. Lett.* **2013**, *15*, 1752.
- ⁵⁴ Du, H.; Zhao, B.; Shi, Y. *J. Am. Chem. Soc.* **2007**, *129*, 762.
- ⁵⁵ (a) Greene, F.D.; Stowell, J.C.; Bergmark, W.R. *J. Org. Chem.* **1969**, *34*, 2254 (b) Du, H.; Zhao, B.; Shi, Y. *Org. Synth.* **2009**, *86*, 315.
- ⁵⁶ Zhao, B.; Du, H.; Cui, S.; Shi, Y. *J. Am. Chem. Soc.* **2010**, *132*, 3523.
- ⁵⁷ Du, H.; Yuan, W.; Zhao, B.; Shi, Y. *J. Am. Chem. Soc.* **2007**, *129*, 7496.
- ⁵⁸ Du, H.; Yuan, W.; Zhao, B.; Shi, Y. *J. Am. Chem. Soc.* **2007**, *129*, 11688.
- ⁵⁹ (a) Du, H.; Zhao, B.; Shi, Y. *J. Am. Chem. Soc.* **2008**, *130*, 8590 (b) Zhao, B.; Du, H.; Fu, R.; Shi, Y. *Org. Synth.* **2010**, *87*, 263.
- ⁶⁰ For mechanistic studies on asymmetric diamination using ligand **1-25**, see: Jindal, G; Sunoj, R.B. *Chem. Eur. J.* **2012**, *18*, 7045.
- ⁶¹ Fu, R.; Zhao, B.; Shi, Y. *J. Org. Chem.* **2009**, *74*, 7577.
- ⁶² Hu, X.; Cao, Z.; Liu, Z.; Wang, Y.; Du, H. *Adv. Synth. Catal.* **2010**, *352*, 651.
- ⁶³ (a) Xu, L.; Du, H.; Shi, Y. *J. Org. Chem.* **2007**, *72*, 7038 (b) Xu, L.; Shi, Y. *J. Org. Chem.* **2008**, *73*, 749.
- ⁶⁴ Ramirez, T.A.; Wang, Q.; Zhu, Y.; Zheng, H.; Peng, X.; Cornwall, R.G.; Shi, Y. *Org. Lett.* **2013**, *15*, 4210.
- ⁶⁵ Yuan, W.; Du, H.; Zhao, B.; Shi, Y. *Org. Lett.* **2007**, *9*, 2589.
- ⁶⁶ Du, H.; Zhao, B.; Yuan, W.; Shi, Y. *Org. Lett.* **2008**, *10*, 4231.
- ⁶⁷ Zhao, B.; Du, H.; Shi, Y. *J. Org. Chem.* **2009**, *74*, 8392.
- ⁶⁸ Wen, Y.; Zhao, B.; Shi, Y. *Org. Lett.* **2009**, *11*, 2365.

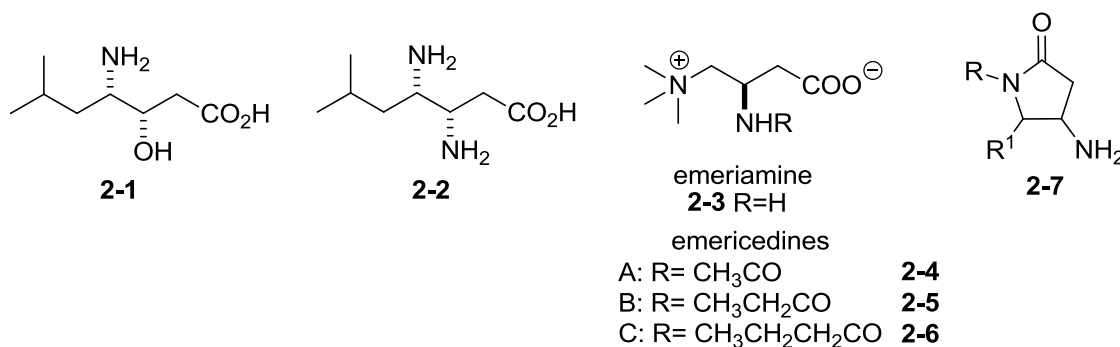
⁶⁹ Zhao, B.; Du, H.; Shi, Y. *J. Am. Chem. Soc.* **2008**, *130*, 7220.

⁷⁰ Zhao, B.; Du, H.; Shi, Y. *J. Org. Chem.* **2009**, *74*, 4411.

⁷¹ Zhao, B.; Du, H.; Shi, Y. *Org. Lett.* **2008**, *10*, 1087.

2.1 GENERAL INTRODUCTION

The β,γ -diamino acid motif is an area of active research because of its prevalence in biologically active molecules and its use in peptide library syntheses.¹ Statine [(3*S*,4*S*)-4-amino-3-hydroxy-6-methylheptanoic acid, Sta] (**2-1**) (Figure 2.1) is an integral component of the aspartyl proteinase inhibitor pepstatin A. Incorporation of statine into structural analogues has led to the discovery of a variety of potent inhibitors of renin, an aspartyl proteinase that plays a role in hypertension. One such derivative is 3-aminodeoxystatine (Asta) (**2-2**) (Figure 2.1).² (*S,S*)-**2-2** has displayed similar IC₅₀ values for renin inhibition as (*S,S*)-**2-1** while improved potencies of (*S,R*)-**2-2** were noticed compared to (*S,R*)-**2-1**.^{2a} Another example of the β,γ -diamino acid motif is emeriamine (**2-3**) and the emericedine family of betaines (**2-4**, **2-5** and **2-6**), which have shown to be effective inhibitors of fatty acid-oxidation (Figure 2.1).³

**Figure 2.1**

Cyclization of β,γ -diamino acids gives the closely related 4-aminopyrrolidinones **2-7** (Figure 2.1). These five-membered amino lactams have been reported to potentiate insulin activity when incorporated into hypoglycaemic peptide analogues and make the analogues more stable towards

physiological degradation.⁴ The 4-aminopyrrolidinone motif was also incorporated into the CCK-A tetrapeptide, which plays a role in the regulation of food intake in animals. The aminopyrrolidinone moiety provided a conformationally constrained environment which displayed beneficial agonist activity *in vitro*.⁵ 4-Aminopyrrolidinones have also been observed in biologically active natural products such as the macrocyclic Microsclerodermins⁶ and Koshikamide B⁷ (Figure 2.2).

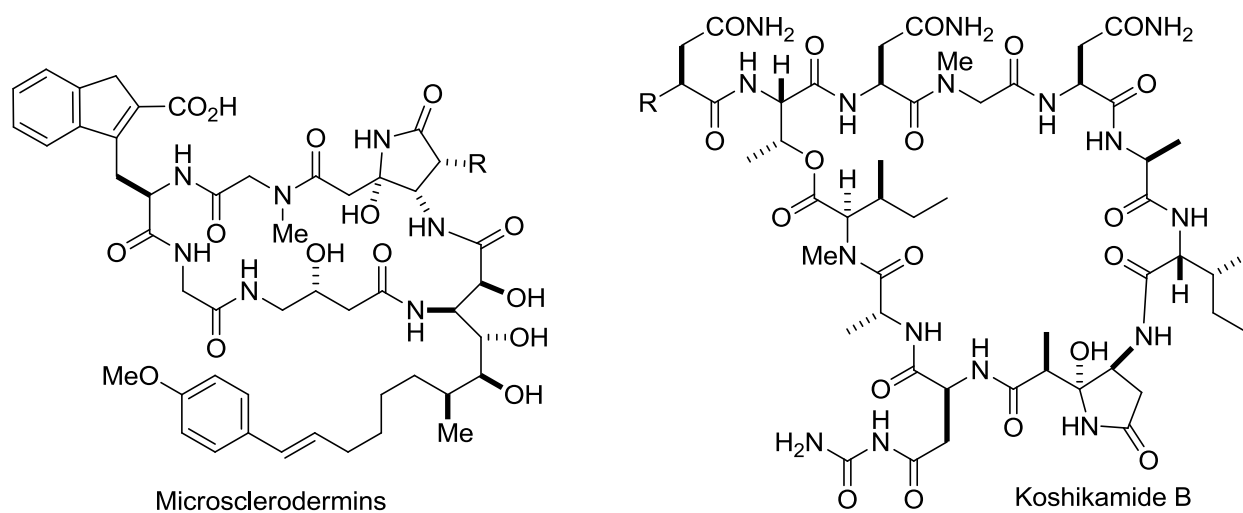


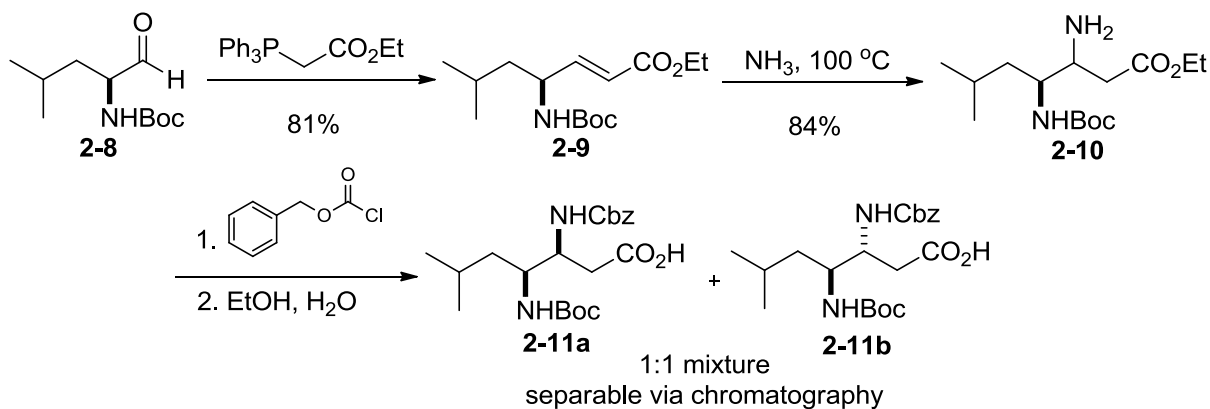
Figure 2.2

2.1.1 Methods to Synthesize β,γ -Diamino Acids and 4-Aminopyrrolidinones

Various methods have been reported for the synthesis of β,γ -diamino acids and related 4-aminopyrrolidinones. Although functionally quite simple, a direct route to synthesize these motifs require multi-step procedures and rely heavily on commercially available amino acids as starting materials, thus limiting the structural variability for biological studies. The following section will highlight the currently available routes to synthesize these compounds.

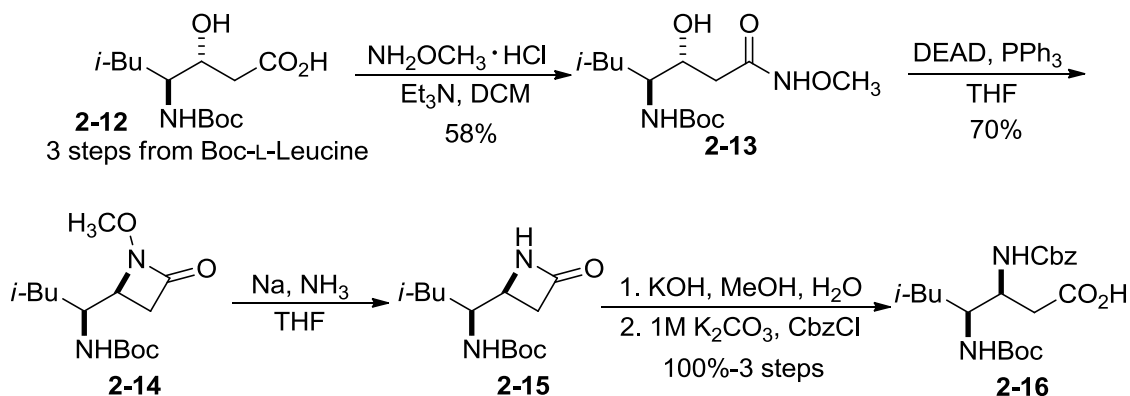
In 1986, Harris and coworkers reported the first synthesis of protected 3-aminodeoxystatine from (*S*)-Boc-leucinal (Scheme 2.1).^{2a,8} Wittig reaction of aldehyde **2-8** and

conjugate addition of ammonia gave β,γ -diamino ester **2-10**. Protection of the free amine with benzyl chloroformate and hydrolysis of the ester furnished a 1:1 mixture of diastereomeric isomers. The yield for the last step was not reported but the diastereomers could be separated by column chromatography.



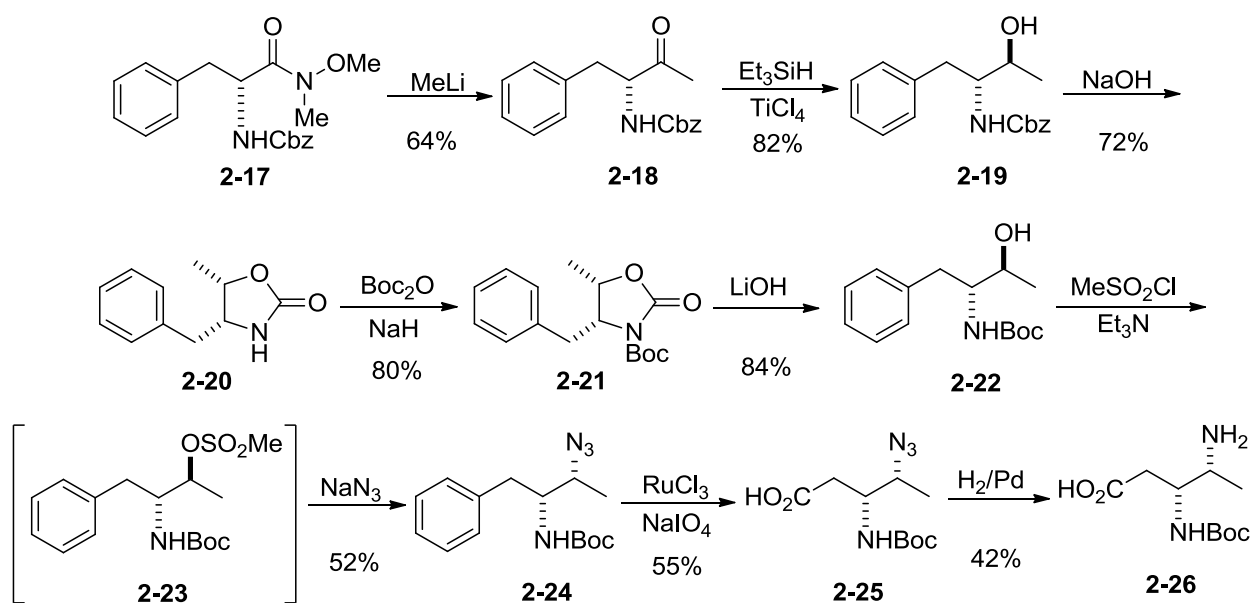
Scheme 2.1

Schostarez synthesized 3-aminodeoxystatine starting from *N*-Boc-L-Leucine, establishing diastereoselectivity and thus eliminating the need for diastereomeric separations (Scheme 2.2).⁹ A stereoselective intramolecular Mitsunobu reaction of **2-13** established the desired stereochemistry of the amine followed by reductive removal of the amide methoxy to give **2-15**. Aqueous KOH was used to cleave the amide and yield the suitably protected aminodeoxystatine derivative **2-16** in 8 steps overall.



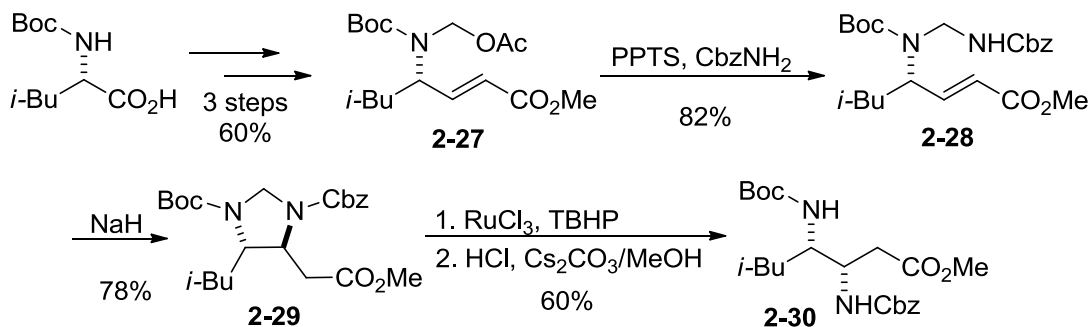
Scheme 2.2

Kano and coworkers reported the synthesis of diamino acid **2-26** using the aminoalcohol derived from D-phenylalanine (Scheme 2.3).¹⁰ Methylation of amide **2-17** was accomplished using MeLi and reduction of the ketone was accomplished using Et₃SiH and TiCl₄ in high diastereoselectivity. Cyclization of amino alcohol **2-19** using NaOH yielded oxazolidinone **2-20**. The amide nitrogen was Boc protected and ring opening yielded Boc-protected amino alcohol **2-22**. Replacement of the alcohol with azide was performed using methanesulfonyl chloride and cleavage of the phenyl group was accomplished using ruthenium chloride-sodium metaperiodate to give **2-25**. Catalytic hydrogenation of azide **2-25** over Pd black yielded Boc-protected diaminoacid **2-26** in 8 or 9 steps and in 3% overall yield.



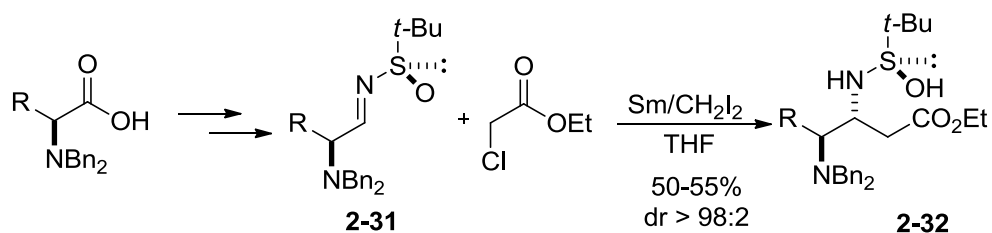
Scheme 2.3

In 2005, Kim and coworkers reported an intramolecular conjugate addition of carbamate to α,β -unsaturated esters as a viable route to synthesize 3-aminodeoxystatine derivatives (Scheme 2.4).¹¹ Starting from *N*-Boc-L-Leucine, benzyl carbamate was used to give the unsaturated ester containing a methylamido group (**2-28**). Treatment with NaH induced conjugate addition to the ester and catalytic oxidation using RuCl₃ yielded the diamine ester of 3-aminodeoxystatine (**2-30**) in 23% overall yield.



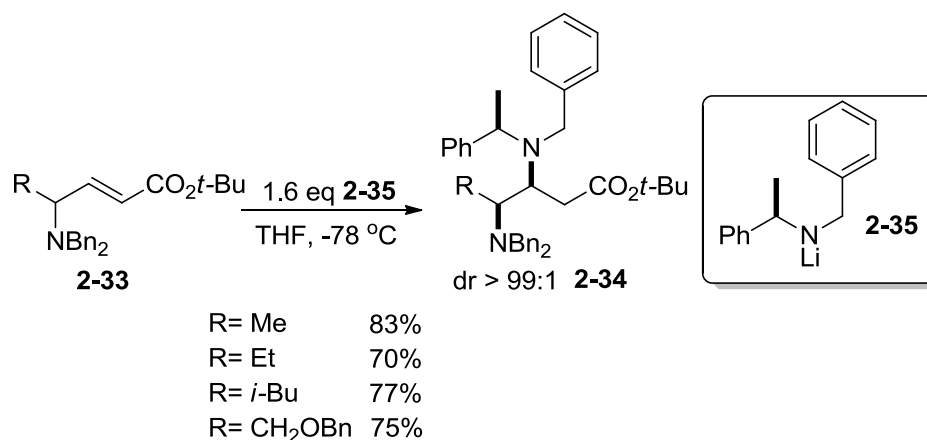
Scheme 2.4

In 2009, Concellón and coworkers reported the addition of samarium enolates, derived from esters and amides, to imines to yield β,γ -diamino esters and amides (Scheme 2.5).¹² Imines **2-31** were synthesized from protected amino acids and the enantiopure 3,4-diamino esters (**2-32**) were obtained in moderate yields upon treatment with samarium. Deprotection of the sulfoxide group was accomplished using HCl.

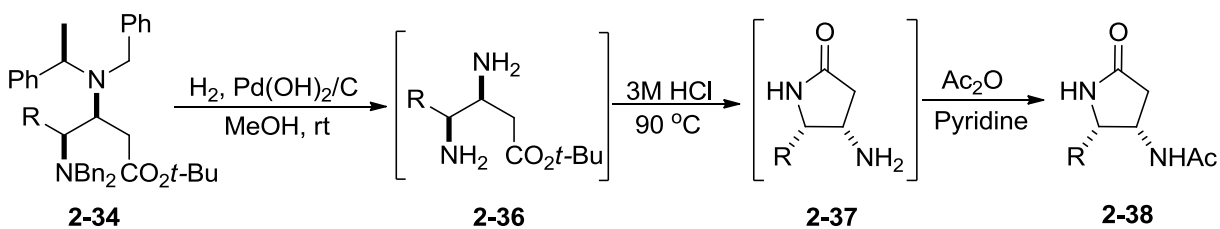


Scheme 2.5

Conjugate addition of lithium amides to α,β -unsaturated esters has shown to be a direct route to diamino acids¹³ and a stereoselective synthesis via kinetic resolution has also been used for the synthesis of diamino acids and 4-aminopyrrolidinones. Davies and coworkers used chiral lithium amides for the kinetic resolution of racemic γ -amino- α,β -unsaturated esters (**2-33**), giving good yields and excellent diastereoselectivities (Scheme 2.6).¹⁴ The resulting diamines were cyclized upon reduction and treatment with acid to yield 4-aminopyrrolidinones **2-38** (Scheme 2.7).



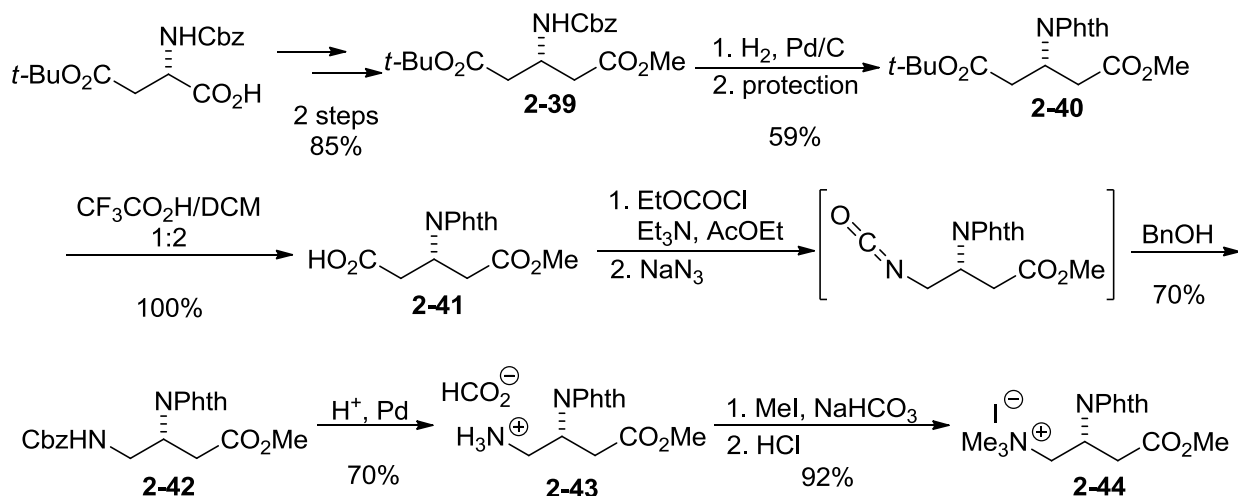
Scheme 2.6



Scheme 2.7

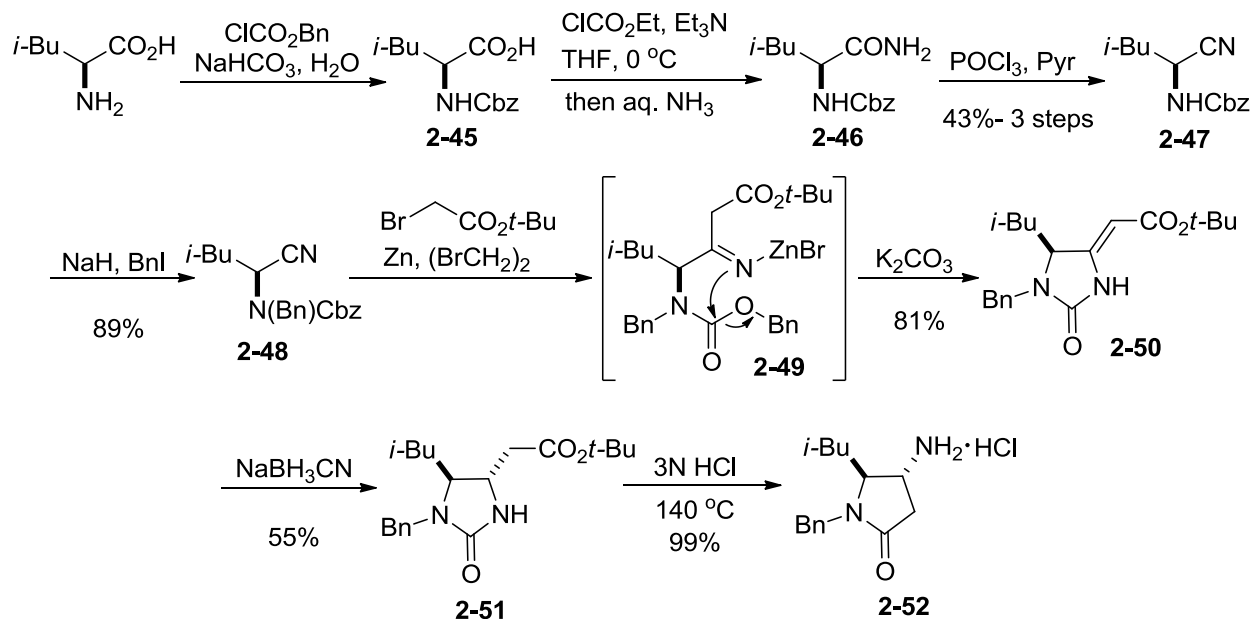
Misiti and coworkers employed a Curtius rearrangement in their synthesis of both enantiomers of emeramine from commercially available *N*-Cbz-*L*-aspartic acid 4-*tert*-butyl ester (Scheme 2.8).¹⁵ Phthalimido protection (**2-40**) of the amine was necessary to avoid imidazolidinone formation during the Curtius rearrangement. Selective conversion of the *t*-butyl ester to the carboxylic acid **2-41** and subsequent Curtius rearrangement followed by quenching with benzyl alcohol yielded diamino ester **2-42** in good yield. Removal of Cbz and subsequent methylation proceeded smoothly to give protected (*R*)-emeramine (**2-44**) in 22% overall yield

over 10 steps. Additional syntheses of emeriamine have been reported from (*R*)-carnitine through double inversion of configuration¹⁶ and also from D-aspartic acid.¹⁷

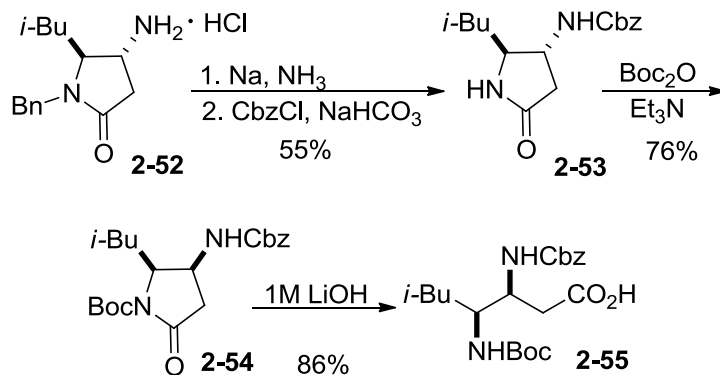


Scheme 2.8

Kouklovsky, Alezra and coworkers have utilized a tandem zinc-mediated homologation/Blaise reaction to synthesize 4-aminopyrrolidinones (Scheme 2.9) and β,γ -diamino acids (Scheme 2.10) from readily available α -amino acids.¹⁸ Starting from L-leucine, Cbz protection and conversion of the acid to the amide furnished **2-46**. Dehydration of the amide to nitrile **2-47** finished the 3 step sequence in 43% yield.^{18a} A second protection of the amine was necessary for the following Blaise reaction to proceed which yielded the cyclic urea **2-50** in 81% yield. Reduction using NaBH_3CN gave the diastereomer shown as the major product (**2-51**). Addition of acid and elevated temperature gave the 4-aminopyrrolidinone hydrochloride salt **2-52**. Further protecting group manipulations and opening of the five-membered ring with LiOH gave the protected 3-aminodeoxystatine **2-55** (Scheme 2.10).



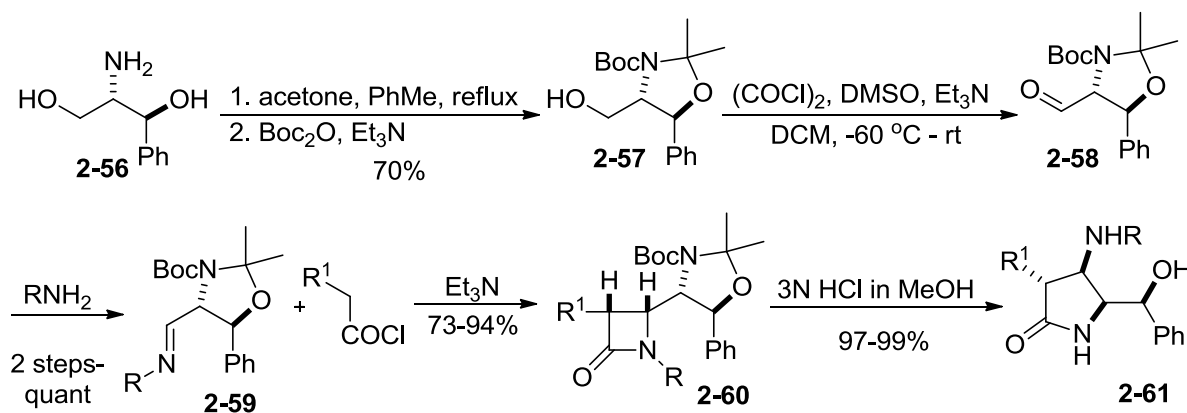
Scheme 2.9



Scheme 2.10

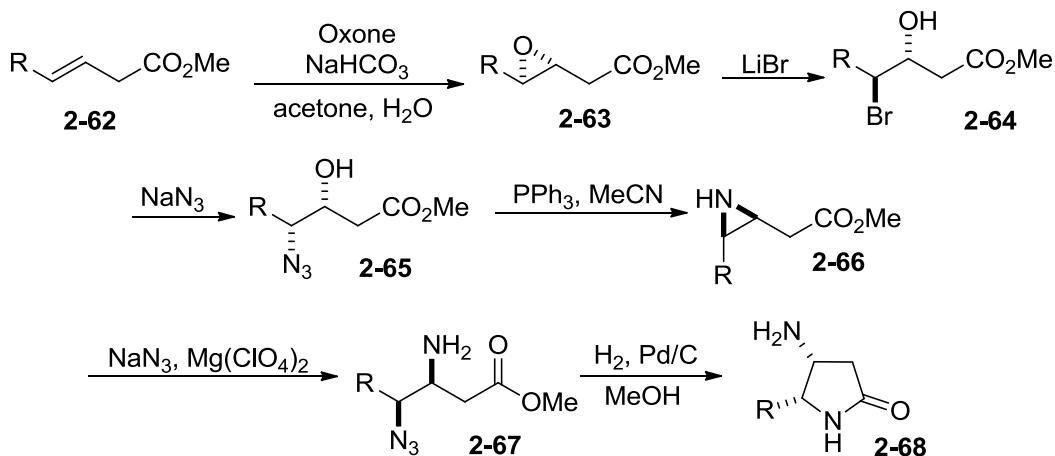
Jayaraman, Bhawal and coworkers used β -lactams as key intermediates for the synthesis of aminopyrrolidinones (Scheme 2.11).^{19,20} Acetonide formation of amino alcohol **2-56** and subsequent Boc protection yielded primary alcohol **2-57** in 70% yield. Swern oxidation and imine formation gave the cycloaddition precursors **2-59**. In the presence of triethylamine,

cyclization occurred and provided β -lactams **2-60** in 73-94% yield. Treatment of these β -lactams with acid at 60 °C afforded the rearranged 4-aminopyrrolidinones **2-61** in almost quantitative yields.



Scheme 2.11

In 2011, Sá and coworkers reported the nucleophilic ring-opening of aziridines for the racemic synthesis of aminopyrrolidinones (Scheme 2.12).²¹ Epoxidation of **2-62** followed by ring opening with lithium bromide set the required stereochemistry for displacement with azide (**2-64**). Aziridine formation is accomplished using triphenylphosphine and the second nitrogen is added as azide to give the β,γ -diamino ester **2-67**. Reduction of the azide and concomitant cyclization gave the aminopyrrolidinone **2-68**. Additional procedures for the synthesis of aminopyrrolidinones include the derivatization of natural asparagine,²² radical addition-cyclization of oxime ethers²³ and reductive amination of tetramic acids.²⁴



Scheme 2.12

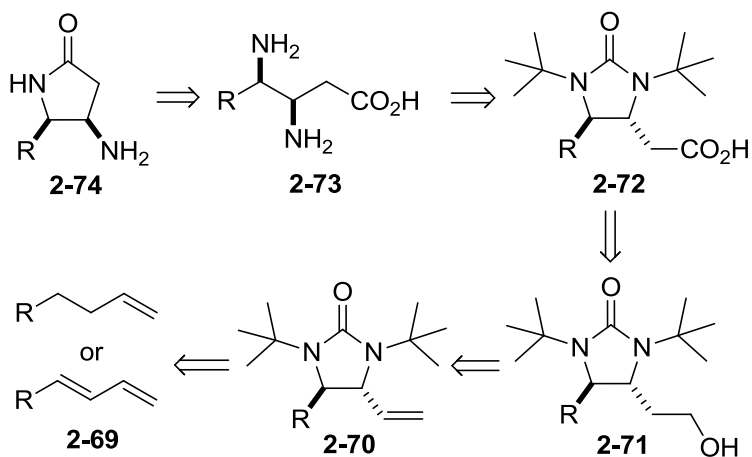
The methods presented above illustrate the currently available routes to β,γ -diamino acids and 4-aminopyrrolidinones. Although the core of these functional motifs is structurally simple, high step counts, low yields, and substrate scope limitations plague the abovementioned routes. It was envisioned that these motifs could be readily synthesized via the diamination protocols developed in our lab in a direct and efficient manner. This chapter will describe the preliminary results on the synthesis of both β,γ -diamino acids and 4-aminopyrrolidinones.

2.2 RESULTS and DISCUSSION

2.2.1 Retrosynthetic Analysis

It was proposed that the common limitations in current routes could be greatly minimized by using the diamination method developed in our group and a retrosynthetic plan was formulated to access these compounds in five to six steps from simple terminal olefins or conjugated dienes (Scheme 2.13). Employing Pd-catalyzed diamination of readily available terminal olefins or dienes (**2-69**) installs both nitrogen moieties in one step followed by anti-Markovnikov hydration of the terminal double bond (**2-71**). Oxidation of the alcohol to the

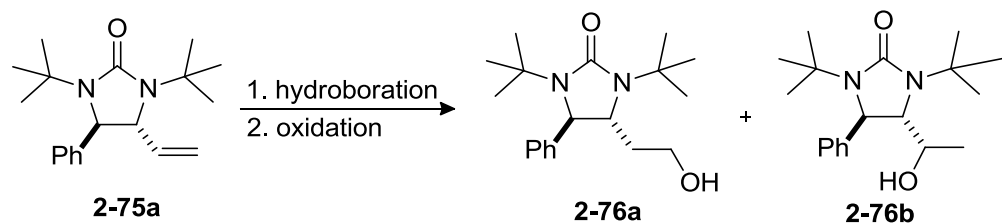
carboxylic acid would give **2-72**. Deprotection would yield β,γ -diamino acids **2-73**, which could then be cyclized to yield corresponding 4-aminopyrrolidinones **2-74**. Because the diamination of **2-69** can be carried out in an asymmetric fashion, this route is also amenable for the chiral synthesis of these compounds.



Scheme 2.13

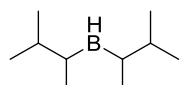
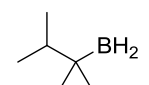
2.2.2 Hydroboration

Diamination product **2-75a** was chosen for screening with racemic material, and the hydroboration and oxidation of the terminal double bond was pursued (Scheme 2.14). It was found that steric hindrance between the hydroborating reagent and the nitrogen *tert*-butyl groups of the substrate played a factor in the selectivity of the hydroboration. Smaller reagents resulted in a mixture of regioisomers (Table 2.1, entries 1-3, 6), whereas the bulky 9-BBN (Table 2.1, entry 5) gave no reaction. Cy_2BH (Table 2.1, entry 4) provided the highest selectivity for the primary alcohol and did so in better yield than hexylborane (Table 2.1, entry 7).



Scheme 2.14

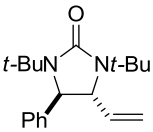
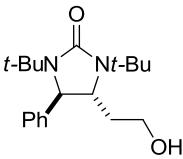
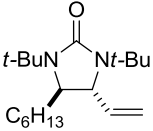
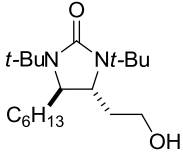
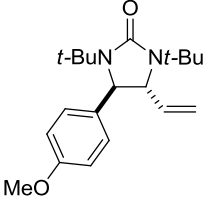
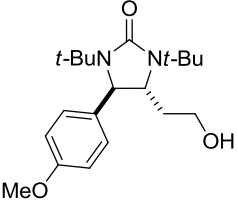
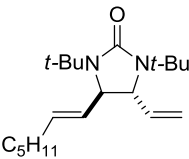
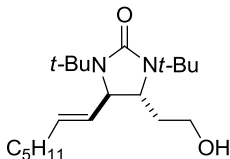
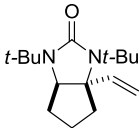
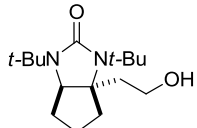
Table 2.1 Screening Conditions for Hydroboration and Oxidation of Cyclic Ureas

Entry	Reagent	2-76a : 2-76b ^a	Yield (%)
1	BH ₃ -THF	1.3 : 1	36
2	BH ₃ -SMe ₂	1 : 1.2	34
3	BH ₂ Cl-SMe ₂	2.8 : 1	66
4	Cy ₂ BH	1 : 0	70
5	9-BBN	NR	-
6		1.2 : 1	58
7		1 : 0	35

^a Selectivity determined by crude ¹H NMR

Optimization of the reaction conditions started with the *in-situ* formation of Cy₂BH. It was found that 1.5 eq of 1M BH₃-THF to 3 eq cyclohexene formed this intermediate, by monitoring the disappearance of starting material by TLC. Reaction conditions including solvent, NaOH loading and reaction time were screened and the optimal conditions are presented in Table 2.2, providing moderate to excellent yields.

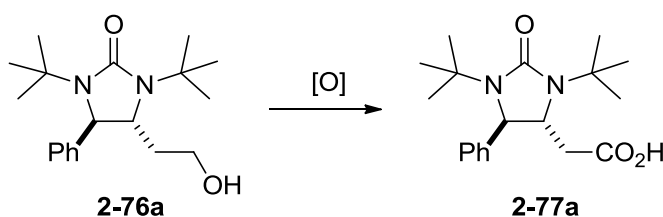
Table 2.2 Hydroboration of Cyclic Ureas^a

Entry	Substrate	Product	Yield (%)
1	 2-75a	 2-76a	78
2	 2-75b	 2-76b	92
3	 2-75c	 2-76c	58
4	 2-75d	 2-76d	66
5 ^b	 2-75e	 2-76e	58

^a All reactions were carried out with **2-75** (0.1 mmol), Cy₂BH (0.15 mmol), 2.5 M NaOH (0.3 mmol), 30% H₂O₂ (1.63 mmol) in THF at 0 °C for 9.5 h unless otherwise stated. Reactions were completely selective for terminal alcohol products ^b Disiamylborane was used.

2.2.3 Oxidation to Carboxylic Acid

Methods for the direct oxidation of the alcohol to the carboxylic acid were subsequently screened (Scheme 2.15). Each reaction resulted in almost complete disappearance of starting material and similar isolated yield (Table 2.3), however purification of the resulting acid proved to be the deciding factor. Whereas the other methods required column purification or resulted in generation of hazardous waste, the TEMPO-catalyzed NaOCl oxidation (Table 2.3, entry 5) provided the acid in sufficiently pure form after acidification and extraction from the reaction mixture, and no further purification was required. After the screening of the compounds shown in Table 2.4, entries 3 and 4 showed interesting reactivity. As determined by crude ^1H NMR, entry 3 was determined to be a mixture of products. The major product was the desired acid and minor product was thought to be a product of possible chlorination, however this was neither isolated nor characterized. It was determined by crude ^1H NMR that the double bond in entry 4 was lost. Oxidation of these substrates was accomplished using PDC as an alternative method.



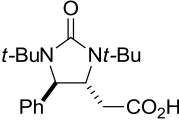
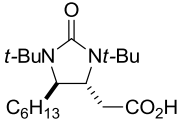
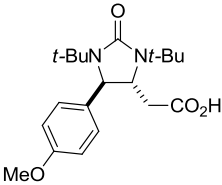
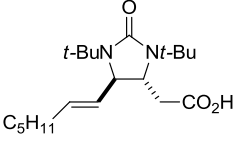
Scheme 2.15

Table 2.3 Screening Conditions for Oxidation to Acid

Entry	Oxidation System	Conversion (%) ^a	Yield of 2-77a (%)
1	RuCl ₃ , NaIO ₄	>90%	56
2	KMnO ₄	100	50
3	PtO ₂ , O ₂	>90%	-
4	PDC	100	60
5	TEMPO, NaOCl	100	65

^a Conversion determined by crude ¹H NMR

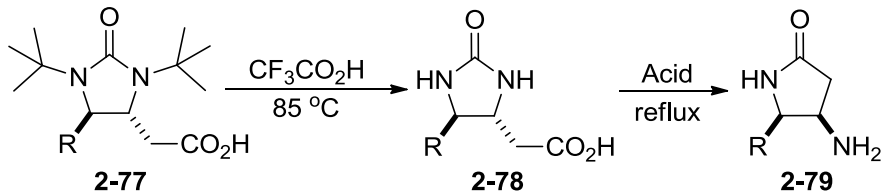
Table 2.4 Oxidation of Cyclic Diamino Alcohols^a

Entry	Product	Method	Yield (%)
1	 2-77a	A	76
2	 2-77b	A	60
3	 2-77c	B	60
4	 2-77d	B	60

^a Method A: Reactions were carried out with **2-76** (0.23 mmol), TEMPO (2.3 x 10⁻³ mmol), NaHCO₃/KBr/TBACl soln. (0.44 mL), NaOCl/NaHCO₃/NaCl (7.2 mmol) in DCM at 0 °C for 18 h unless otherwise stated. For entry 1, reaction was run on 1.2 scale. Method B: Reactions were carried out with **2-76** (0.06 mmol), PDC (0.207 mmol) in DMF at rt unless otherwise stated. For entry 3, reaction was run on 2.3 scale.

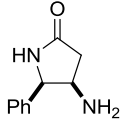
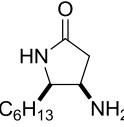
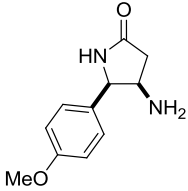
2.2.4 Lactamization

With the hydroboration and oxidation steps optimized, it was envisioned that deprotection of the *t*-butyl groups on the nitrogens followed by decarbonylation would yield the β,γ -diamino acid derivatives. Removal of the *t*-butyl groups proved to be facile as has been previously reported by heating at 80 °C for 2.5 hours in $\text{CF}_3\text{CO}_2\text{H}$. Isolation of the β,γ -diamino acid proved to be much more difficult and presented additional challenges. After refluxing in 2M HCl for 2 hours, it was found that acid-catalyzed cyclization was occurring rapidly, resulting in lactamization to give the corresponding 4-aminopyrrolidinones **2-79** (Scheme 2.16). After optimization of acid concentration, reaction time and temperature, lactamization using 2M HCl at 150 °C for 14 h and subsequent basification with NaOH provided the 4-aminopyrrolidinones in good yield (Table 2.5)



Scheme 2.16

Table 2.5 Lactamization of Carboxylic Acids^a

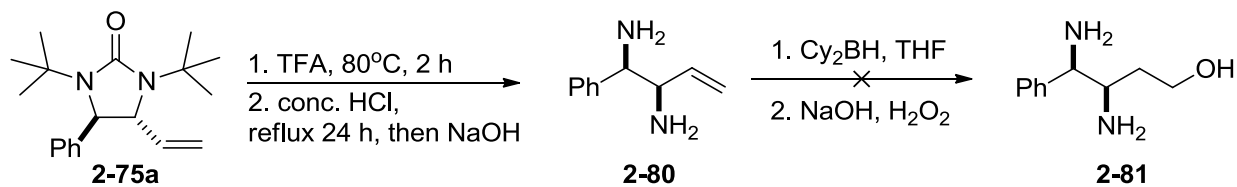
Entry	Product	Yield (%)
1	 2-79a	75
2	 2-79b	80
3	 2-79c	70

^a All reactions were carried out with **2-77** (0.5 mmol), CF₃CO₂H at 80 °C for 3 h, then 2N HCl at 150 °C for 14 h.

It was then of interest to intercept the possible β,γ -diamino acid intermediate before cyclization and it was envisioned that this could be accomplished with milder reaction conditions. However, all efforts via lower temperatures and more dilute acid concentrations failed to stop the cyclization from occurring and mixtures of starting material and lactam were obtained.

Alternate routes were then explored in attempts to isolate the β,γ -diamino acid derivatives. Following diamination of 4-phenyl-1-butene, the *tert*-butyl groups of **2-75a** were removed by stirring in CF₃CO₂H at 80°C for 2 hours (Scheme 2.17). Decarbonylation was then executed using conc. HCl at reflux for 24 hours. After basification and extraction, **2-80** was obtained in 66% yield over three steps from 4-phenyl-1-butene. The hydroboration of **2-80** was then attempted using the conditions described above (Table 2.2). This was unsuccessful

however, most likely due to the basic nature of the free amine groups which deactivated the reactive Cy_2BH reagent.



Scheme 2.17

2.3 CONCLUSION

The efficient and enantioselective synthesis of the β,γ -diamino acid motif still warrants further investigation as it is a useful functional group present in biologically active molecules and serves as a precursor to β - and γ -peptides. It appears that through the current route, these compounds are difficult to isolate. Current procedures to synthesize 4-aminopyrrolidinones require multiple steps, often necessitate protecting group manipulation, and substitution at the 5-position is often limited to alkyl groups originating from natural amino acids. Utilizing the above described method, various substituted 4-aminopyrrolidinones can be synthesized over five steps from readily available dienes or terminal olefins in up to 40% overall yield, providing a competitive process in the synthesis of these compounds. One can also envision that reduction of the 4-aminopyrrolidinone compounds to the corresponding 3-aminopyrrolidines would be of worth, as pyrrolidines are present in numerous natural products and have a wide applicability in organic synthesis.

2.4 EXPERIMENTAL

Representative Diamination of Terminal Olefins (2-75a).²⁵ A 1.5-mL vial charged with Pd(PPh₃)₄ (0.0924 g, 0.08 mmol) was evacuated and then filled with argon followed by addition of 4-phenyl-1-butene (0.211 g, 1.6 mmol). The resulting mixture was immersed into an oil bath (65 °C) with stirring. Di-*t*-butyldiaziridinone (**1-17**) (0.748 g, 4.4 mmol) was added by syringe pump at the rate of 0.4 mmol/h. Upon completion of addition (7 h), the reaction mixture was stirred for another hour and purified by flash chromatography (silica gel, hexane:ethyl acetate = 4:1) to give the product **2-75a** as a colorless oil (0.432 g, 90% yield).

Representative Diamination of Conjugated Dienes (2-75d).²⁶ A 1.5-mL vial charged with Pd(PPh₃)₄ (0.023 g, 0.02 mmol) was evacuated and then filled with argon followed by addition of (3*E*,5*E*)-undeca-1,3,5-triene (0.036 g, 0.24 mmol) and benzene-*d*₆ (0.6 mL). Di-*t*-butyldiaziridinone (**1-17**) (0.034 g, 0.2 mmol) was added and the resulting mixture was immersed into an oil bath (65 °C) with stirring for 30 min. The reaction mixture was purified by flash chromatography (silica gel, hexane:ethyl acetate = 4:1) to give the product **2-75d** as a yellow oil (0.062 g, 81% yield).

Representative Hydroboration of Cyclic Ureas (Table 2.2, entry 2). A 3 mL vial charged with a magnetic stir bar and 1M BH₃-THF (0.15 mL, 0.15 mmol) was cooled to 0 °C followed by addition of cyclohexene (0.03 mL, 0.3 mmol) and stirred for 2.5 h. 1,3-di-*tert*-butyl-4-hexyl-5-vinylimidazolidin-2-one (**2-75b**) (31 mg, 0.1 mmol) in THF (0.1 mL) was added slowly and the mixture was allowed to stir at rt for 5 h. Upon completion of the reaction via monitoring by TLC, the reaction was cooled to 0 °C and 2.5M NaOH (0.12 mL, 0.3 mmol) was added followed by 30% H₂O₂ (0.05 mL, 1.63 mmol). The reaction was stirred for 30 min, whereupon it was diluted

with EtOAc and the aqueous layer was separated from the organic layer. The organic layer was washed with H₂O and brine (3 times), dried over Na₂SO₄ and concentrated. The residue was purified by flash chromatography [silica gel; Hex, then Hexanes:EtOAc 1:15 (50 mL), then Hexanes:EtOAc 1:4] to give the cyclic diamino alcohol **2-76b** as a white solid (30mg, 92% yield).

Representative TEMPO Oxidation of Cyclic Diamino Alcohols, Method A (Table 2.4, entry

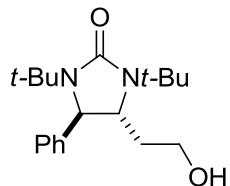
1). To a 3 mL vial equipped with a magnetic stir bar charged with 1,3-di-*tert*-butyl-4-(2-hydroxyethyl)-5-phenylimidazolidin-2-one (**2-76a**) (74 mg, 0.23 mmol) in DCM (0.66 mL) was added TEMPO (0.35 mg, 2.3x10⁻³ mmol) and a solution of sat NaHCO₃/KBr/TBACl (0.44 mL/0.02mmol/0.01mmol). The reaction was cooled to 0 °C followed by addition of a solution of NaOCl/sat NaHCO₃/sat NaCl (7.2 mmol/0.24 mL/0.47 mL) over 35 min. The reaction was allowed to warm to rt and stir overnight. The mixture was diluted with DCM and the aqueous layer was separated from the organic layer. The organic layer was washed with H₂O (3 times), dried over MgSO₄ and concentrated. The white carboxylic acid solid (**2-77a**) was pure by ¹H NMR and used directly without further purification (58.4 mg, 76%).

Representative PDC Oxidation of Cyclic Diamino Alcohols, Method B (Table 2.4, entry 3).

To a 3 mL vial equipped with a magnetic stir bar was added 1,3-di-*tert*-butyl-4-(2-hydroxyethyl)-5-(4-methoxyphenyl)imidazolidin-2-one (**2-76c**) (50 mg, 0.14 mmol) and PDC (189 mg, 0.5 mmol) in DMF (0.75 mL). The reaction was stirred at room temperature overnight. The reaction was diluted with H₂O and extracted with Et₂O eight times. The combined organic layers were washed with H₂O (3 times), dried over MgSO₄ and concentrated. The residue was purified by flash chromatography [silica gel; Hexanes:EtOAc 6:1 1% AcOH] to give the white carboxylic acid solid **2-77c** (74 mg, 60% yield).

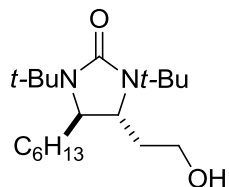
Representative Lactamization (Table 2.5, entry 3). To a 3 mL vial equipped with a magnetic stir bar was added 2-(1,3-di-*tert*-butyl-5-(4-methoxyphenyl)-2-oxoimidazolidin-4-yl)acetic acid (**2-77c**) (20 mg, 0.05 mmol) and CF₃CO₂H (0.7 mL) and stirred at 80 °C for 3 h. Upon concentration, the residue was transferred to a high-pressure vessel and dissolved in 2M HCl (0.5 mL). The reaction was then heated in a sand bath measuring 150 °C and stirred for 14 h after which the vessel was allowed to cool and the water was removed under reduced pressure. The resulting residue was dried under reduced pressure at 150 °C for 3h after which the sample was dissolved in water and made basic using 2.5 M NaOH (pH~14). The product was extracted using CHCl₃ and washed with H₂O (3 times), brine, dried over Na₂SO₄ and concentrated to give 4-aminopyrrolidinone **2-79c** as a dark yellow oil (7.8 mg, 70%)

Table 2.2, entry 1 (rc_b2_40), (rc_b2_44).



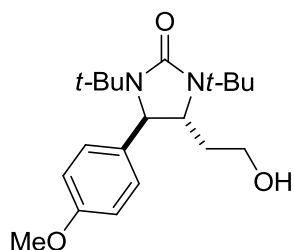
White solid; mp 144 °C; IR (film) 3422, 2961, 1660 cm⁻¹; ¹H NMR (300 MHz, CDCl₃) δ 7.36-7.20 (m, 5H), 4.40 (s, 1H), 3.87 (t, *J* = 6.3 Hz, 2H), 3.36 (dd, *J* = 7.5, 3.6 Hz, 1H), 2.42 (brs, 1H), 2.20-1.82 (m, 2H), 1.36 (s, 9H), 1.29 (s, 9H); ¹³C NMR (75 MHz, CDCl₃) δ 159.0, 144.3, 128.9, 127.7, 125.8, 61.6, 60.0, 59.1, 53.5, 52.9, 38.1, 29.1; HRMS Calcd for C₁₉H₃₀N₂O₂ (M+H)⁺: 319.2380, Found: 319.2382.

Table 2.2, entry 2 (rc_b3_5_1), (rc_b3_38_4).



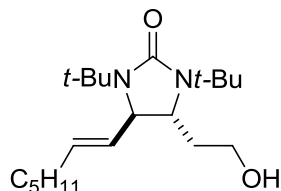
White solid; mp 62 °C; IR (film) 3422, 2958, 2929, 2858, 1660 cm^{-1} ; ^1H NMR (300 MHz, CDCl_3) δ 3.79-3.60 (m, 2H), 3.38 (dd, $J = 8.1, 3.6$ Hz, 1H), 3.22 (dd, $J = 8.1, 3.6$ Hz, 1H), 1.95 (brs, 1H), 1.84-1.72 (m, 2H), 1.54-1.42 (m, 2H), 1.38 (s, 9H), 1.37 (s, 9H), 1.34-1.16 (m, 8H), 0.88 (t, $J = 6.3$ Hz, 3H); ^{13}C NMR (75 MHz, CDCl_3) δ 158.2, 58.9, 58.0, 55.0, 52.6, 52.5, 37.2, 34.3, 31.9, 29.5, 29.2, 24.8, 22.7, 14.2; HRMS Calcd for $\text{C}_{19}\text{H}_{38}\text{N}_2\text{O}_2$ ($\text{M}+\text{H}$) $^+$: 327.3006, Found: 327.3005.

Table 2.2, entry 3 (rc_b2_47_1), (rc_b3_43_1).



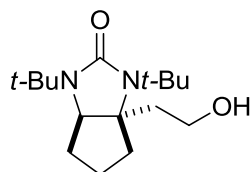
White solid; mp 104-109 °C; IR (film) 3417, 2960, 1660 cm^{-1} ; ^1H NMR (300 MHz, CDCl_3) δ 7.20 (d, $J = 9.0$ Hz, 2H), 6.86 (d, $J = 9.0$ Hz, 2H), 4.34 (s, 1H), 3.88 (t, $J = 6.3$ Hz, 2H), 3.81 (s, 3H), 3.35 (dd, $J = 6.9, 3.9$ Hz, 1H), 1.98-1.85 (m, 2H), 1.38 (s, 9H), 1.29 (s, 9H); ^{13}C NMR (75 MHz, CDCl_3) δ 159.2, 159.0, 136.6, 127.0, 114.2, 61.2, 60.1, 59.3, 55.4, 53.5, 53.0, 38.1, 29.11, 29.08; HRMS Calcd for $\text{C}_{20}\text{H}_{32}\text{N}_2\text{O}_3$ ($\text{M}+\text{H}$) $^+$: 349.2486, Found: 349.2494.

Table 2.2, entry 4 (rc_b2_47_2), (rc_b3_43_3).



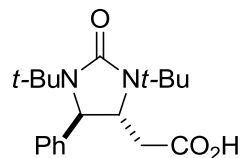
Colorless oil; IR (film) 3422, 2959, 2926, 2871, 1660 cm^{-1} ; ^1H NMR (300 MHz, CDCl_3) δ 5.65-5.40 (m, 2H), 3.79-3.66 (m, 3H), 3.30 (dd, $J = 6.9, 3.6$ Hz, 1H), 2.34 (brs, 1H), 2.06-1.94 (m, 2H), 1.89-1.76 (m, 2H), 1.37 (s, 9H), 1.33 (s, 9H), 1.42-1.18 (m, 6H), 0.87 (t, $J = 6.6$ Hz, 3H); ^{13}C NMR (75 MHz, CDCl_3) δ 158.6, 132.3, 131.5, 60.8, 59.1, 57.6, 53.2, 53.0, 37.0, 32.2, 31.5, 29.1, 28.9, 22.6, 14.2; HRMS Calcd for $\text{C}_{20}\text{H}_{38}\text{N}_2\text{O}_2$ ($\text{M}+\text{H}$) $^+$: 339.3006, Found: 339.3013.

Table 2.2, entry 5 (rc_b3_13_1).



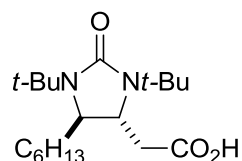
Colorless solid; mp 96-100 $^\circ\text{C}$; IR (film) 3425, 2960, 1656 cm^{-1} ; ^1H NMR (300 MHz, CDCl_3) δ 3.73 (t, $J = 6.9$ Hz, 2H), 3.55 (t, $J = 6.6$ Hz, 1H), 2.27-2.13 (m, 1H), 2.12-1.96 (m, 3H), 1.88-1.77 (m, 1H), 1.76-1.63 (m, 2H), 1.60-1.44 (m, 1H), 1.47 (s, 9H), 1.37 (s, 9H); ^{13}C NMR (100 MHz, CDCl_3) δ 158.5, 67.8, 64.2, 59.3, 54.8, 53.1, 44.1, 42.2, 37.0, 30.0, 29.0, 23.5; HRMS Calcd for $\text{C}_{16}\text{H}_{30}\text{N}_2\text{O}_2$ ($\text{M}+\text{H}$) $^+$: 283.2380, Found: 282.2382.

Table 2.4, entry 1 (rc_b2_27_2), (rc_b2_42), (rc_b3_46_1).



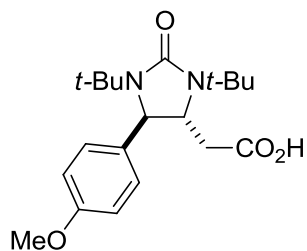
White solid; mp 203-206 °C; IR (film) 2964, 1723, 1626 cm^{-1} ; ^1H NMR (300 MHz, CDCl_3) δ 7.41-7.28 (m, 5H), 4.45 (s, 1H), 3.65 (dd, $J = 7.2$, 1H), 2.82-2.64 (m, 2H), 1.38 (s, 9H), 1.32 (s, 9H); ^{13}C NMR (75 MHz, CDCl_3) δ 175.5, 158.6, 143.0, 128.9, 128.0, 126.1, 61.8, 58.6, 53.7, 53.1, 39.8, 29.10, 29.06; HRMS Calcd for $\text{C}_{19}\text{H}_{28}\text{N}_2\text{O}_3$ ($\text{M}+\text{H}$) $^+$: 333.2173, Found: 333.2178.

Table 2.4, entry 2 (rc_b3_14_1), (rc_b3_46_2).



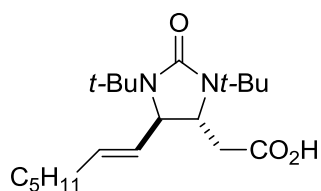
Yellow oil; IR (film) 2959, 2929, 2858, 1733, 1653 cm^{-1} ; ^1H NMR (300 MHz, CDCl_3) δ 3.66 (dd, $J = 7.8, 5.4$ Hz, 1H), 3.27 (t, $J = 6.0$ Hz, 1H), 2.63-2.52 (m, 2H), 1.58-1.45 (m, 2H), 1.39 (s, 9H), 1.38 (s, 9H), 1.46-1.23 (m, 8H), 0.89 (t, $J = 5.7$ Hz, 3H); ^{13}C NMR (100 MHz, CDCl_3) δ 171.4, 157.7, 60.6, 58.6, 52.8, 52.7, 33.8, 32.0, 29.5, 29.3, 29.2, 24.7, 22.8, 21.3, 14.4; HRMS Calcd for $\text{C}_{19}\text{H}_{36}\text{N}_2\text{O}_3$ ($\text{M}+\text{H}$) $^+$: 341.2799, Found: 341.2807.

Table 2.4, entry 3 (rc_b4_19).



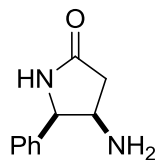
White solid; mp 197-200 °C; IR (film) 2973, 1613, 1512 cm^{-1} ; ^1H NMR (300 MHz, CDCl_3) δ 11.15 (bs, 1H), 7.24 (d, $J = 8.4$ Hz, 2H), 6.86 (d, $J = 8.4$ Hz, 2H), 4.40 (s, 1H), 3.79 (s, 3H), 3.63 (dd, $J = 8.1, 4.2$ Hz, 1H), 2.78-2.63 (m, 2H), 1.37 (s, 9H), 1.30 (s, 9H); ^{13}C NMR (75 MHz, CDCl_3) δ 175.3, 159.3, 158.6, 135.1, 127.2, 114.1, 61.3, 58.8, 55.4, 53.6, 53.0, 39.7, 29.1, 29.0; HRMS Calcd for $\text{C}_{20}\text{H}_{30}\text{N}_2\text{O}_4$ ($\text{M}+\text{H}$) $^+$: 363.2278, Found: 363.2283.

Table 2.4, entry 4 (rc_b3_48).



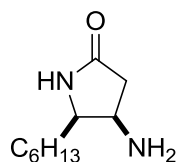
White solid; mp 72 °C; IR (film) 2960, 2927, 2872, 1733, 1692, 1653 cm^{-1} ; ^1H NMR (300 MHz, CDCl_3) δ 5.73-5.58 (m, 1H), 5.57-5.44 (m, 1H), 3.78 (d, $J = 7.5$ Hz, 1H), 3.58 (dd, $J = 9.0, 3.6$ Hz, 1H), 2.72-2.52 (m, 2H), 2.10-1.98 (m, 2H), 1.39 (s, 9H), 1.35 (s, 9H), 1.46-1.22 (m, 6H), 0.89 (t, $J = 6.6$ Hz, 3H); ^{13}C NMR (100 MHz, CDCl_3) δ 175.8, 158.1, 133.2, 130.5, 60.8, 56.7, 53.3, 53.0, 38.4, 32.3, 31.5, 29.2, 28.9, 22.7, 14.3; HRMS Calcd for $\text{C}_{20}\text{H}_{36}\text{N}_2\text{O}_3$ ($\text{M}+\text{H}$) $^+$: 353.2799, Found: 353.2805.

Table 2.5, entry 1 (rc_b4_16).



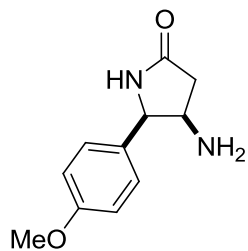
Dark green oil; IR (film) 3263, 2922, 2850, 1691 cm^{-1} ; ^1H NMR (300 MHz, CDCl_3) δ 7.46-7.31 (m, 3H), 7.30-7.23 (m, 2H), 6.27 (brs, 1H), 4.84 (d, $J = 6.0$ Hz, 1H), 3.95-9.85 (m, 1H), 2.72 (dd, $J = 16.8, 7.5$ Hz, 1H), 2.25 (dd, $J = 16.8, 5.4$ Hz, 1H); ^{13}C NMR (100 MHz, CDCl_3) δ 177.1, 136.9, 129.1, 128.6, 127.1, 63.2, 52.2, 39.6; HRMS Calcd for $\text{C}_{10}\text{H}_{12}\text{N}_2\text{O}$ ($\text{M}+\text{H}$)⁺: 177.1022, Found: 177.1018.

Table 2.5, entry 2 (rc_b4_31_2).



Yellow oil; IR (film) 3211, 2927, 2856, 1695 cm^{-1} ; ^1H NMR (400 MHz, CDCl_3) δ 6.05 (brs, 1H), 3.72-3.63 (m, 1H), 3.61-3.52 (m, 1H), 2.61 (dd, $J = 16.4, 7.2$ Hz, 1H), 2.12 (dd, $J = 16.4, 4.4$ Hz, 1H), 1.66-1.54 (m, 1H), 1.54-1.42 (m, 1H), 1.41-1.14 (m, 8H), 0.90 (t, $J = 6.4$ Hz, 3H); ^{13}C NMR (100 MHz, CDCl_3) δ 176.5, 59.0, 50.6, 40.9, 31.9, 29.49, 29.46, 26.5, 22.8, 14.2; HRMS Calcd for $\text{C}_{10}\text{H}_{20}\text{N}_2\text{O}$ ($\text{M}+\text{H}$)⁺: 185.1648, Found: 185.1648.

Table 2.5, entry 3 (rc_b4_31_1).



Orange oil; IR (film) 3264, 2921, 2850, 1691, 1247 cm^{-1} ; ^1H NMR (300 MHz, CDCl_3) δ 7.19 (d, $J = 8.4$ Hz, 2H), 6.94 (d, $J = 8.4$ Hz, 1H), 6.03 (brs, 1H), 4.79 (d, $J = 6.3$ Hz, 1H), 3.92-3.78 (m, 1H), 3.83 (s, 3H), 2.70 (dd, $J = 17.1, 7.5$ Hz, 1H), 2.24 (dd, $J = 17.1, 5.7$ Hz, 1H); ^{13}C NMR (100 MHz, CDCl_3) δ 176.9, 159.9, 128.7, 128.3, 114.5, 62.7, 55.6, 52.1, 39.6; HRMS Calcd for $\text{C}_{11}\text{H}_{14}\text{N}_2\text{O}_2$ ($\text{M}+\text{H}$) $^+$: 206.1128, Found: 207.1126.

2.5 REFERENCES

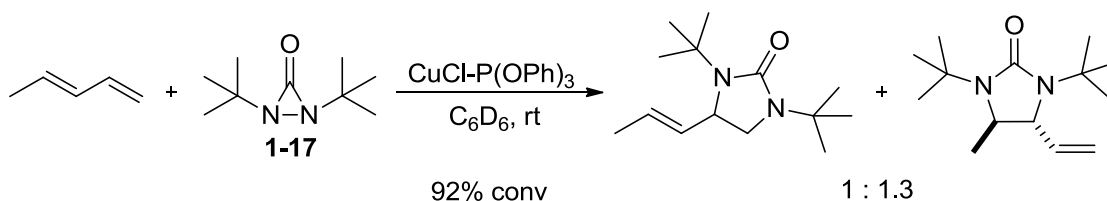
- ¹ For a leading review, see: Viso, A.; de la Pradilla, R.F.; Tortosa, M.; García, A.; Flores, A. *Chem. Rev.* **2011**, *111*, PR1-PR42.
- ² (a) Arrowsmith, R.J.; Carter, K.; Dann, J.G.; Davies, D.E.; Harris, C.J.; Morton, J.A.; Lister, P.; Robinson, J.A.; Williams, D.J. *J. Chem. Soc. Chem. Commun.* **1986**, 755 (b) Thaisrivongs, S.; Schostarez, H.J.; Pals, D.T.; Turner, S.R. *J. Med. Chem.* **1987**, *30*, 1837 (c) Bradbury, R.H.; Rivett, J.E. *J. Med. Chem.* **1991**, *34*, 151 (d) Jones, D.M.; Sueiras-Diaz, J.; Szelke, M.; Leckie, B.J.; Beattie, S.R.; Morton, J.; Neidle, S.; Kuroda, R. *J. Peptide Res.* **1997**, *50*, 109 (e) Thétiot-Laurent, S.; Bouillère, F.; Baltaze, J.-P.; Brisset, F.; Feytens, D.; Kouklovsky, C.; Miclet, E.; Alezra, V. *Org. Biomol. Chem.* **2012**, *10*, 9660.
- ³ (a) Kanamaru, T.; Shinagawa, S.; Asai, M.; Okazaki, H.; Sugiyama, Y.; Fujita, T.; Iwatsuka, Y.; Yoneda, M. *Life Sci.* **1985**, *37*, 217 (b) Shinagawa, S.; Kanamaru, T.; Harada, S.; Asai, M.; Okazaki, H. *J. Med. Chem.* **1987**, *30*, 1458 (c) Maeda, H.; Fujiwara, M.; Fujita, K.; Fukuda, N. *J. Nutr. Sci. Vitaminol.* **1996**, *42*, 111 (d) Maeda, H.; Fujiwara, M.; Miyamoto, K.; Hamamoto, H.; Fukuda, N. *J. Nutr. Sci. Vitaminol.* **1996**, *42*, 469 (e) Fukuda, N.; Fukui, M.; Kai, Y.; Jayasooriya, A.P.; Sakano, M.; Maeda, H.; Ide, T.; Yamamoto, K. *J. Nutr. Sci. Vitaminol.* **1998**, *44*, 525 (f) Del Prete, E.; Lutz, T.A.; Althaus, J.; Scharrer, E. *Physiol. Behav.* **1998**, *63*, 751.
- ⁴ Ede, N.J.; Rae, I.D.; Hearn, M.T.W. *Tetrahedron Lett.* **1990**, *31*, 6071.
- ⁵ Elliot, R.L.; Kopecka, H.; Tufano, M.D.; Shue, Y.-K.; Gauri, A.J.; Lin, C.-W.; Bianchi, B.R.; Miller, T.R.; Witte, D.G.; Stashko, M.A.; Asin, K.E.; Nikkel, A.L.; Bednarz, L.; Nadzan, A.M. *J. Med. Chem.* **1994**, *37*, 1562.
- ⁶ Bewley, C.A.; Debitus, C.; Faulkner, D.J. *J. Am. Chem. Soc.* **1994**, *116*, 7631.
- ⁷ Araki, T.; Matsunaga, S.; Nakao, Y.; Furihata, K.; West, L.; Faulkner, D.J.; Fusetani, N. *J. Org. Chem.* **2008**, *73*, 7889.
- ⁸ For a related synthesis of β,γ -diaminoacid via conjugate addition of NH_3 , see: Doherty, A.M.; Kornberg, B.E.; Reily, M.D. *J. Org. Chem.* **1993**, *58*, 795.
- ⁹ Schostarez, H.J. *J. Org. Chem.* **1988**, *53*, 3628.
- ¹⁰ Kano, S.; Yokomatsu, T.; Iwasawa, H. *Chem. Pharm. Bull.* **1988**, *36*, 3341.
- ¹¹ Yoo, D.; Kwon, S.; Kim, Y.G. *Tetrahedron: Asymmetry* **2005**, *16*, 3762.

- ¹² (a) Concellón, J.M.; Rodríguez-Solla, H.; Simal, C. *Adv. Synth. Catal.* **2009**, *351*, 1238 (b) Concellón, J.M.; Rodríguez-Solla, H.; Simal, C.; del Amo, V.; García-Granda, S.; Díaz, M.R. *Adv. Synth. Catal.* **2009**, *351*, 2991.
- ¹³ Davies, S.G.; Garner, A.C.; Goddard, E.C.; Kruchinin, D.; Roberts, P.M.; Rodriguez-Solla, H.; Smith, A.D. *Chem. Commun.* **2006**, 2664.
- ¹⁴ Davies, S.G.; Lee, J.A.; Roberts, P.M.; Thomson, J.E.; Yin, J. *Org. Lett.* **2012**, *14*, 218.
- ¹⁵ Misiti, D.; Santaniello, M.; Zappia, G. *Bioorg. Med. Chem. Lett.* **1992**, *2*, 1029.
- ¹⁶ Castagnani, R.; De Angelis, F.; De Fusco, E.; Giannessi, F.; Misiti, D.; Meloni, D.; Tinti, M.O. *J. Org. Chem.* **1995**, *60*, 8318.
- ¹⁷ Calvisi, G.; Dell'Uomo, N.; De Angelis, F.; Dejas, R.; Giannessi, F.; Tinti, M.O. *Eur. J. Org. Chem.* **2003**, 4501.
- ¹⁸ (a) Hoang, C.T.; Alezra, V.; Guillot, R.; Kuoklovsky, C. *Org. Lett.* **2007**, *9*, 2521 (b) Hoang, C.T.; Nguyen, V.H.; Alezra, V.; Kuoklovsky, C. *J. Org. Chem.* **2008**, *73*, 1162 (c) Hoang, C.T.; Bouillère, F.; Johannesen, S.; Zulauf, A.; Panel, C.; Pouilhès, A.; Gori, D.; Alezra, V.; Kouklovsky, C. *J. Org. Chem.* **2009**, *74*, 4711 (d) Bouillère, F.; Guillot, R.; Kouklovsky, C.; Alezra, V. *Org. Biomol. Chem.* **2011**, *9*, 394.
- ¹⁹ (a) Jayaraman, M.; Deshmukh, A.R.; Bhawal, B.M. *Tetrahedron* **1996**, *52*, 8989 (b) Jayaraman, M.; Puranik, V.G.; Bhawal, B.M. *Tetrahedron* **1996**, *52*, 9005
- ²⁰ For another example of the synthesis of 4-aminopyrrolidinones from β -lactams, see: Palomo, C.; Cossío, F.P.; Cuevas, C.; Odriozola, J.M.; Ontoria, J.M. *Tetrahedron Lett.* **1992**, *33*, 4827.
- ²¹ Bisol, T.B.; Bortoluzzi, A.J.; Sá, M.M. *J. Org. Chem.* **2011**, *76*, 948.
- ²² Lehman, T.; Michel, D.; Glänzel, M.; Waibel, R.; Gmeiner, P. *Heterocycles* **1999**, *51*, 1389.
- ²³ Miyabe, H.; Ueda, M.; Fujii, K.; Nishimura, A.; Naito, T. *J. Org. Chem.* **2003**, *68*, 5618.
- ²⁴ Pinheiro, S.; da Silva Júnior, R.C.; de Souza, A.S.; del M. Carneiro, J.W.; Muri, E.M.F.; Antunes, O.A.C. *Tetrahedron Lett.* **2009**, *50*, 2402.
- ²⁵ Du, H.; Yuan, W.; Zhao, B.; Shi, Y. *J. Am. Chem. Soc.* **2007**, *129*, 7496.
- ²⁶ Du, H.; Zhao, B.; Shi, Y. *J. Am. Chem. Soc.* **2007**, *129*, 762.

3.1 GENERAL INTRODUCTION

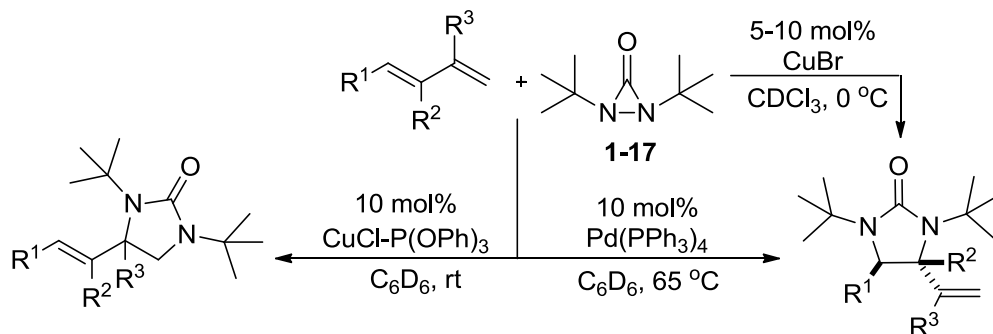
3.1.1 Regioselective Diamination Using Diaziridinone

As part of the ongoing efforts in our lab to study the mechanism of metal-catalyzed diaminations using diaziridinone as nitrogen source, the study of the terminal diamination mechanism was further investigated. It was initially reported that a mixture of diamination products was observed when (*E*)-penta-1,3-diene was subjected to the reaction conditions (Scheme 3.1).¹



Scheme 3.1

Upon closer inspection, it was found that reaction conditions played a very influential role in the observed selectivity of diamination. Varying reaction conditions such as Cu(I) salt, addition of ligand, temperature and concentration, the regioselectivity of diamination could be tuned to favor internal diamination (Scheme 3.2).² The reaction proved to be very efficient and a wide variety of substitution on the dienes could be tolerated (Figure 3.1). The use of CuBr instead of Pd(0) provided an economical alternative to synthesize the internal regioisomer and the reaction could be scaled up to give 38g of product.



Scheme 3.2

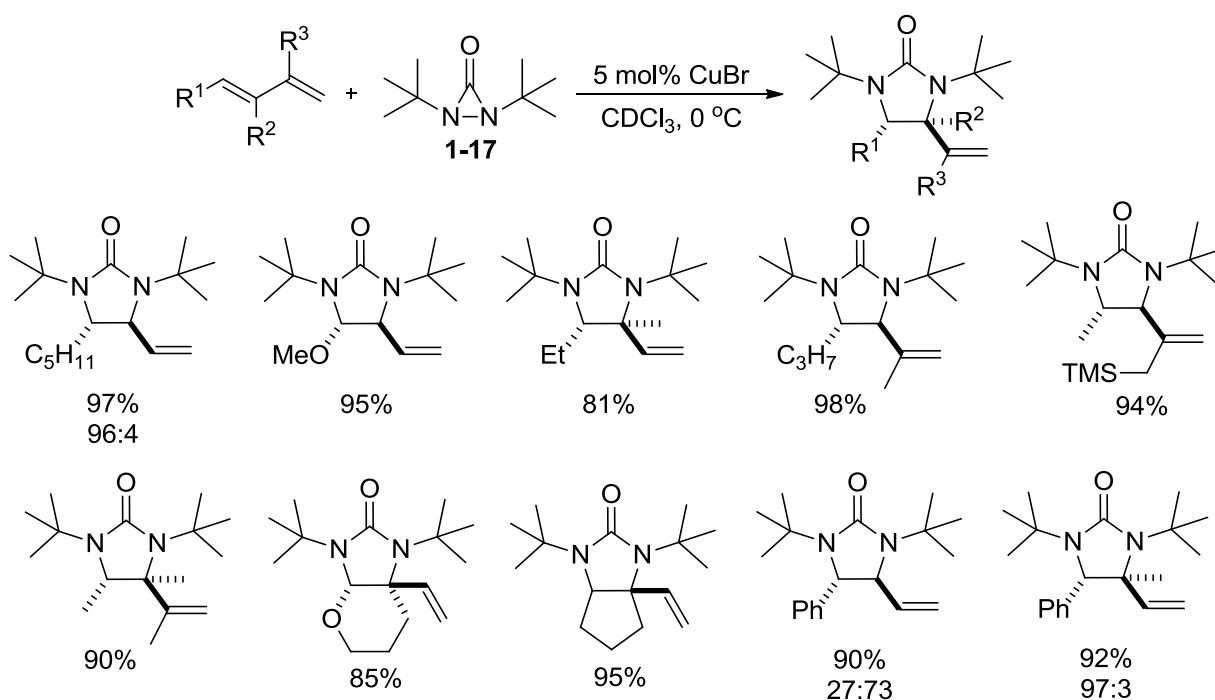


Figure 3.1

3.1.2 Alternative Nitrogen Source and Interesting Reactivity

Additionally, alternative nitrogen sources have been reported to be effective nitrogen transfer reagents. In 2007, Shi and coworkers reported *N,N*-di-*tert*-butylthiadiaziridine 1,1-dioxide (**3-1**) as nitrogen source for the diamination of terminal olefins (Figure 3.2).³ Using CuCl as catalyst with P(*n*-Bu)₃ as ligand, various substituted styrenes, terminal olefins and an enyne

were diaminated in good yields. The sulfone moiety could also be removed to provide free diamines using HCl/BaCO₃. The nitrogen source, *N,N*-di-*tert*-butylthiadiaziridine 1,1-dioxide (**3-1**), is easily synthesized in three steps and is obtained pure as a white solid at room temperature (Scheme 3.3).⁴

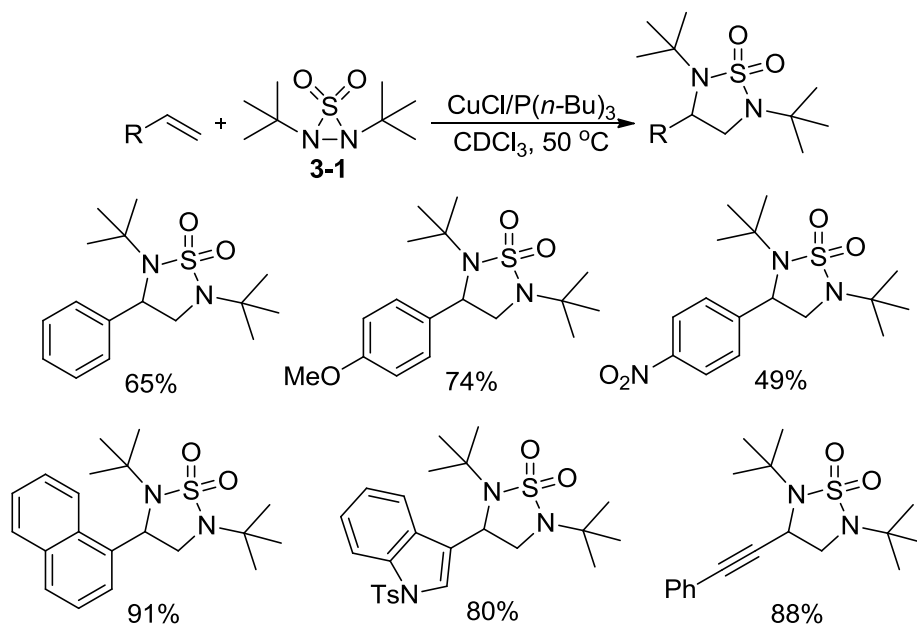
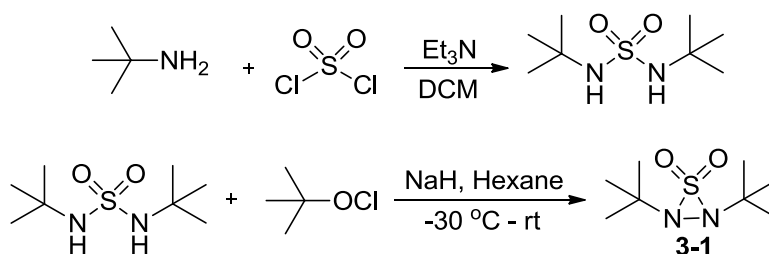


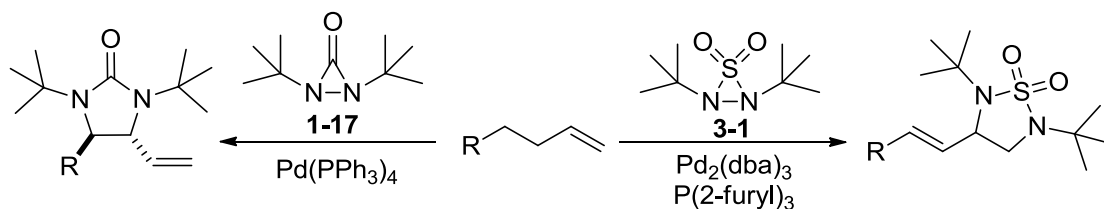
Figure 3.2



Scheme 3.3

It was also found that nitrogen source **3-1** exhibited interesting reactivity when applied to the diamination of terminal olefins. Whereas Pd-catalyzed diamination of terminal olefins using diaziridinone **1-17** resulted in diamination at the allylic and homoallylic carbons via a C-H

activation mechanism, employing thiadiaziridine **3-1** resulted in an overall dehydrogenative diamination (Scheme 3.4).⁵ A variety of terminal olefins with aryl and alkyl substitution as well as internal spectator double bonds were efficiently diaminated in moderate to good yields (Figure 3.3).



Scheme 3.4

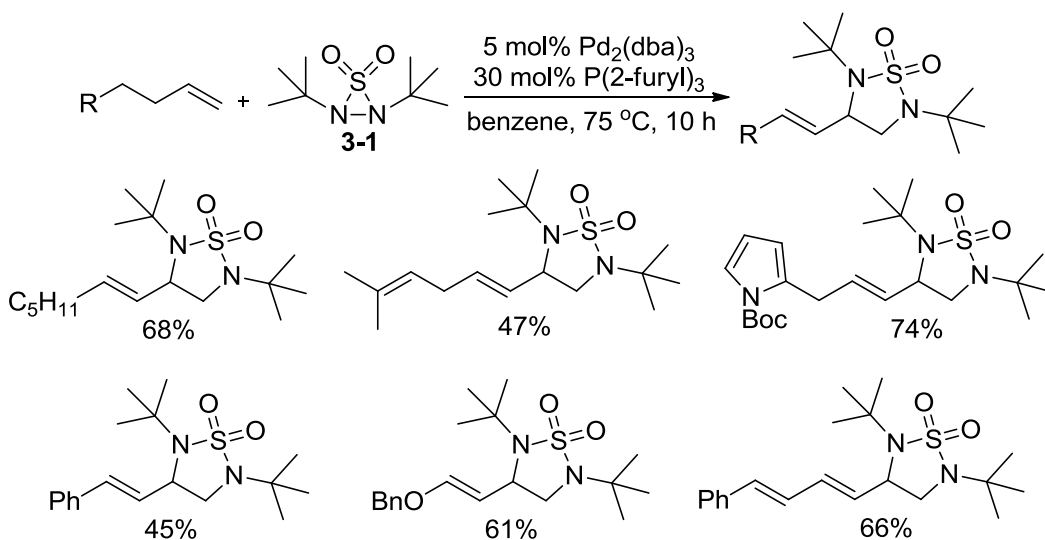
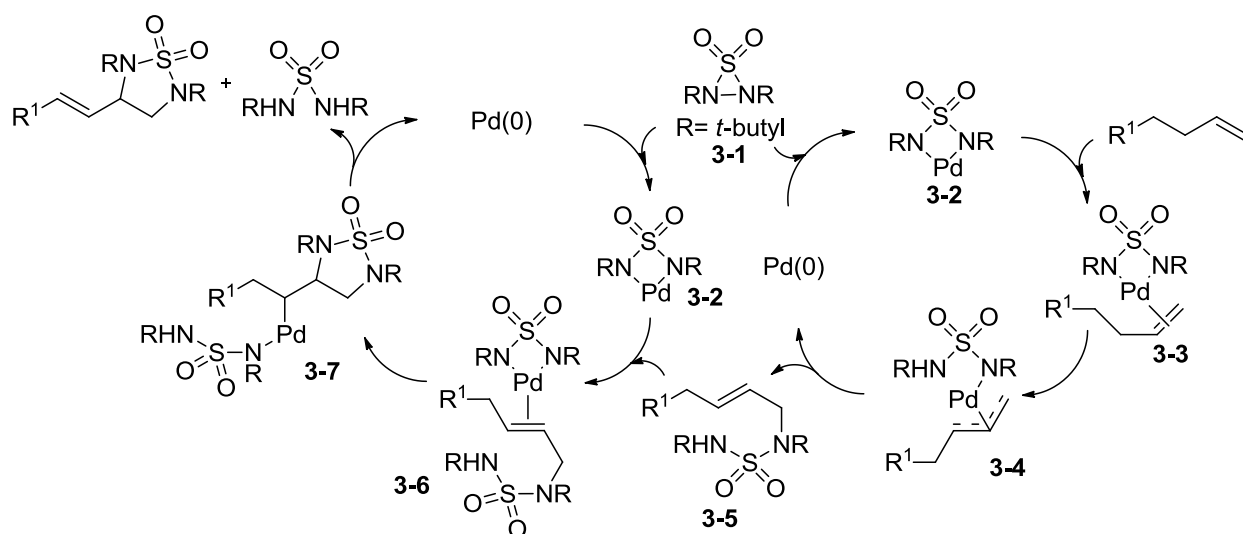


Figure 3.3

The unexpected dehydrogenative diamination is proposed to proceed via the mechanism shown in Scheme 3.5. The palladium catalyst inserts into the N-N bond of thiadiaziridine **3-1** to form four-membered Pd complex **3-2** which coordinates to the terminal olefin to give complex **3-3**. Upon removal of an allylic hydrogen, (π -allyl)Pd complex **3-4** provides allylic sulfamidate **3-5**

via reductive elimination and regenerates the Pd(0) catalyst. Coordination of another equivalent of four-membered complex **3-2** undergoes Pd(II)-catalyzed cyclization to give **3-7**. β -Hydride elimination yields the dehydrogenative diamination product and *tert*-butyl sulfamide as byproduct.



Scheme 3.5

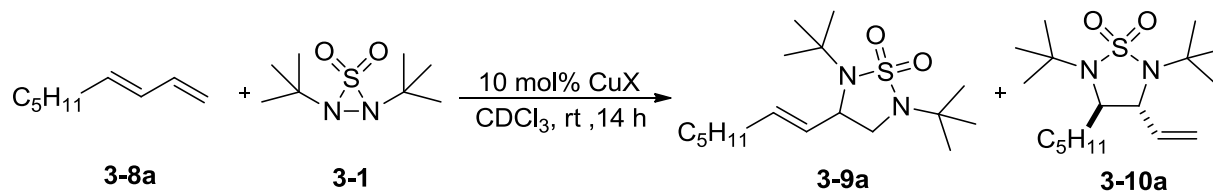
The above methods to install vicinal diamine functionality using thiadiaziridine **3-1** allow facile introduction of nitrogen into readily available starting materials. Also of importance are the resulting cyclic sulfamide motifs themselves. Cyclic sulfamides are promising functional moieties present in many medicinal and biologically active molecules⁶ and have also been used as chiral control agents.⁷ The interesting diamination reactivity observed with Cu(I) salts as catalysts and **1-17** (Scheme 3.2), prompted us to study the possible unique reactivity using nitrogen source **3-1** and to develop a concise route to the synthetically valuable cyclic sulfamide motif from readily available conjugated dienes. The following chapter describes our studies on the Cu(I)-catalyzed regioselective diamination of conjugated dienes to form cyclic sulfamides.

3.2 RESULTS AND DISCUSSION

3.2.1 Reaction Conditions and Substrate Scope

Investigation began using (*E*)-nona-1,3-diene as test substrate and studying the effect of reaction conditions. As shown in Table 3.1, both regioisomers can be formed and the regioselectivity can be heavily influenced by the reactions parameters. After screening various Cu(I) and Cu(II) salts as catalysts, CuCl and CuBr were found to give the best reactivity (Table 3.1, entries 6 and 7). CuCl displayed a slight preference for the internal diamination **3-10a**, whereas CuBr gave a much higher preference for internal product **3-10a**. Addition of ligand proved to be a major factor influencing regioselectivity. CuCl with added phosphine ligand improved the reactivity as well as regioselectivity and shifted the ratio in favor of terminal product **3-9a** (Table 3.1, entries 1-5). Both P(Cy)₃ and P(*n*-Bu)₃ were found to effectively promote terminal diamination (Table 3.1, entries 1 and 2). Likewise, addition of phosphine ligand to CuBr also reversed regioselectivity from internal product **3-10a** to terminal **3-9a**, but lowered the reactivity of the catalyst (Table 3.1, entry 9). Concentration also proved to be an integral parameter for high regioselectivity. Reactivity as well as terminal regioselectivity was further favored using CuCl-P(*n*-Bu)₃ when a more concentrated reaction mixture was used (Table 3.1, entry 3). Conversely, internal regioselectivity was further increased using CuBr without ligand when a more dilute reaction mixture was used (Table 3.1, entry 8).

Table 3.1 Effect of Reaction Conditions on Regioselectivity
of Cu(I)-Catalyzed Diamination of Dienes.^a

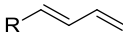
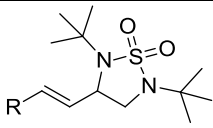
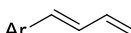
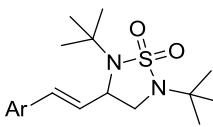
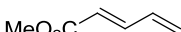
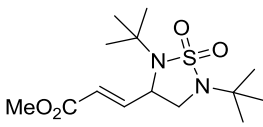
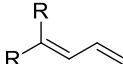
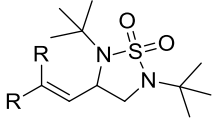
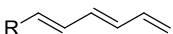
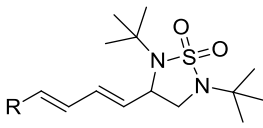


Entry	Conditions	Conv (%)	3-9a:3-10a
1	CuCl-P(Cy) ₃ (1:1)	44	14:1 ^d
2	CuCl-P(<i>n</i> -Bu) ₃ (1:1)	47	14:1 ^d
3 ^b	CuCl-P(<i>n</i>-Bu)₃ (1:1)	65	>25:1^d
4	CuCl-P(PPh) ₃ (1:1)	40	1:1 ^e
5	CuCl-dppe (1:1)	23	2:1 ^e
6	CuCl	39	1:3 ^e
7	CuBr	70	1:10 ^d
8 ^c	CuBr	76	1:19^d
9	CuBr-P(<i>n</i> -Bu) ₃ (1:1)	24	1.7:1 ^e

^a All reactions were carried out with olefin **3-8a** (0.20 mmol), **3-1** (0.24 mmol), and Cu(I) catalyst (0.020 mmol) in CDCl₃ (0.3 mL) under Ar at rt for 14 h unless otherwise stated. ^b 0.1 mL of CDCl₃ was used. ^c 0.6 mL of CDCl₃ was used. ^d When the selectivity is high, an accurate ratio of **3-9a** to **3-10a** was difficult to obtain by ¹H NMR analysis of the crude reaction mixture due to baseline noise interference. The ratio was then obtained by ¹H NMR analysis after flash chromatography (**3-9a** and **3-10a** were nearly inseparable). ^e When the selectivity is low, the ratio of **3-9a** to **3-10a** was determined by ¹H NMR analysis of the crude reaction mixture.

With optimal reaction conditions in hand, investigation into the substrate scope for both terminal and internal diamination was pursued.⁸ CuCl/P(*n*-Bu)₃-catalyzed terminal diamination was effective for a variety of conjugated dienes and trienes in good to high yield (Table 3.2). Electron-rich (Table 3.2, entries 4 and 6) and electron-deficient dienes (Table 3.2, entries 5 and 7) were smoothly diaminated at room temperature.

Table 3.2 CuCl-catalyzed Regioselective Diamination^a

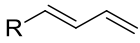
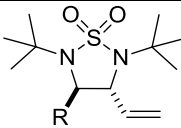
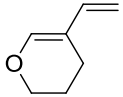
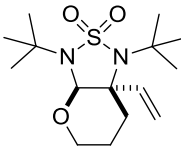
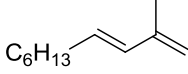
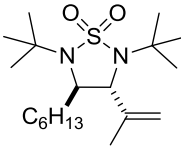
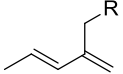
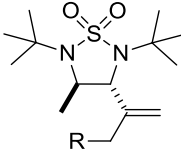
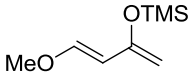
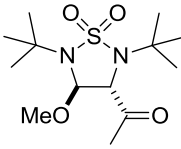
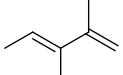
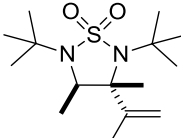
Entry	Substrate (3-8)	Product (3-9)	Yield (%) ^g
1 ^b	 3-8a , R = C ₅ H ₁₁	 3-9a	61
2 ^c	3-8b , R = Me	3-9b	65
3	 3-8c , Ar = Ph	 3-9c	97
4	3-8d , Ar = <i>p</i> -MeOC ₆ H ₄	3-9d	93
5	3-8e , Ar = <i>p</i> -NO ₂ C ₆ H ₄	3-9e	94
6	3-8f , Ar = 2-furyl	3-9f	80
7 ^d	 3-8g	 3-9g	67
8	 3-8h , R = Ph	 3-9h	95
9 ^e	3-8i , R = Me	3-9i	89
10	 3-8j , R = Me	 3-9j	74
11 ^f	3-8k , R = C ₅ H ₁₁	3-9k	83

^a All reactions were carried out with olefin **3-8** (0.40 mmol), CuCl/P(*n*-Bu)₃ (1:1) complex (0.020 mmol), and **3-1** (0.48 mmol) in CDCl₃ (0.1 mL) under Ar at rt unless otherwise stated. Reaction times: For entry 1, 24 h; entry 2, 48 h; entry 3, 3.5 h; entry 4, 8 h; entry 5, 12 h; entry 6, 20 h; entry 7, 48 h; entry 8, 12 h; entry 9, 24 h; entry 10, 36 h; entry 11, 8h. ^b Olefin **3-8a** (0.20 mmol), CuCl/P(*n*-Bu)₃ (1:1) complex (0.040 mmol), and **3-1** (0.24 mmol). ^c CuCl/P(*n*-Bu)₃ (1:1) complex (0.080 mmol), and **3-1** (0.80 mmol). ^d CuCl/P(*n*-Bu)₃ (1:1) complex (0.080 mmol), and **3-1** (0.60 mmol). ^e CuCl/P(*n*-Bu)₃ (1:1) complex (0.040 mmol), and **3-1** (0.60 mmol). ^f **3-1** (0.6 mmol). ^g Isolated yield.

Although alkyl dienes (Table 3.2, entries 1-2) were efficiently diaminated, aryl dienes and trienes (Table 3.2, entries 3-6, 8, 10, 11) proved superior and catalyst loading could be reduced to 5 mol%. All reactions were highly regioselective for terminal diamination and no internal regioisomer was detectable by ^1H NMR.

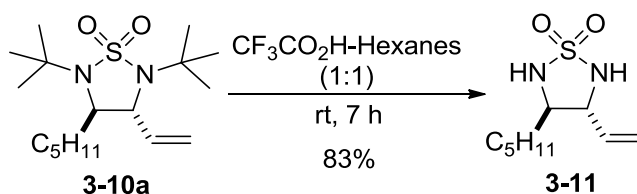
CuBr-catalyzed internal diamination was examined next. Various *trans* alkyl dienes were readily diaminated at the internal double bond with only one regioisomer being present most of the time as judged by ^1H NMR (Table 3.3). 1-Monosubstituted (Table 3, entries 1, 2), 1,2- (Table 3, entry 3), and 1,3-disubstituted (Table 3, entries 4-7), and 1,2,3-trisubstituted (Table 3, entry 8) dienes were smoothly diaminated with high regioselectivity and in good yield. Danishefsky's diene was subjected to CuBr conditions to give internal diamination followed by desilylation upon purification with silica gel to yield ketone **3-10p** (Table 3.3, entry 7). When *cis*-pentadiene was subjected to CuBr-catalyzed conditions, no diamination product was obtained and starting material was returned. The internal diamination can also be carried out on gram scale (Table 3.3, entry 1). Removal of the *tert*-butyl groups from the resulting internal cyclic sulfamides can be accomplished by stirring in a mixture of $\text{CF}_3\text{CO}_2\text{H}$ -hexanes (1:1) at room temperature for 7 hours (Scheme 3.6).

Table 3.3 CuBr-Catalyzed Regioselective Diamination^a

Entry	Substrate (3-8)	Product (3-10)	Yield (%) ^c
1	 3-8a , R = C ₅ H ₁₁	 3-10a	70 (75) ^d (1:19) ^e
2	3-8b , R = Me	3-10b	75
3	 3-8l	 3-10l	62
4	 3-8m	 3-10m	63
5	 3-8n , R = TMS	 3-10n	74
6	3-8o , R = Me	3-10o	81
7	 3-8p	 3-10p	75
8 ^b	 3-8q	 3-10q	65

^a All reactions were carried out with olefin **3-8** (0.20 mmol), CuBr (0.030 mmol), and **3-1** (0.24 mmol) in CDCl₃ (0.6 mL) under Ar at rt for 24 h, unless otherwise stated. For entry 1, 0.040 mmol of CuBr was used. For entry 8, the reaction was carried out on double scale. ^b Diamination product **3-10q** is acid sensitive and was obtained by crystallization from hexanes. ^c

Isolated yield. ^d The reaction was carried out with 8 mmol of olefin **3-8a**. ^e The ratio of **3-9a** to **3-10a** was determined by ¹H NMR analysis after flash chromatography.



Scheme 3.6

Substrates shown in Figure 3.4 were subjected to internal diamination conditions using CuBr but displayed very low conversion or polymerization as judged by ¹H NMR of the crude reaction mixtures. Radical-stabilizing dienes, such as trienes, gave mixtures of internal and terminal diamination products when reacted under CuBr conditions (Figure 3.5). Trisubstituted diene substrates generally gave high conversion but presented difficulty when purified on acidic silica gel. Attempts at recrystallization in lieu of silica gel chromatography yielded product **7q** (Table 3.3, entry 8) in good yield but purification of other diamination products proved very challenging and decomposition prevailed (Figure 3.6).

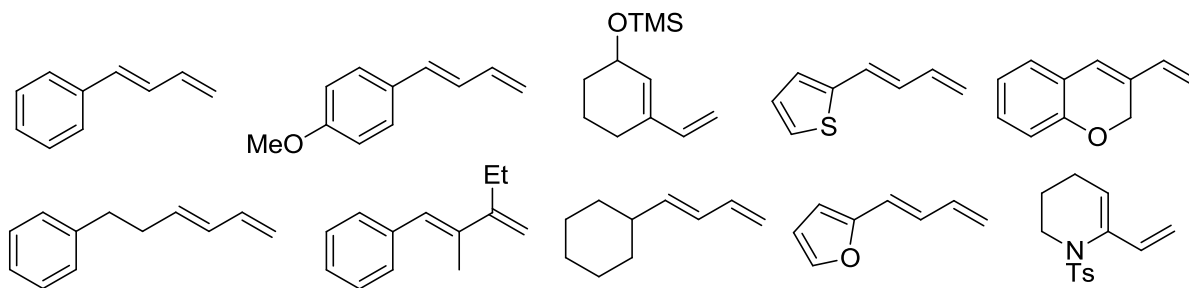


Figure 3.4

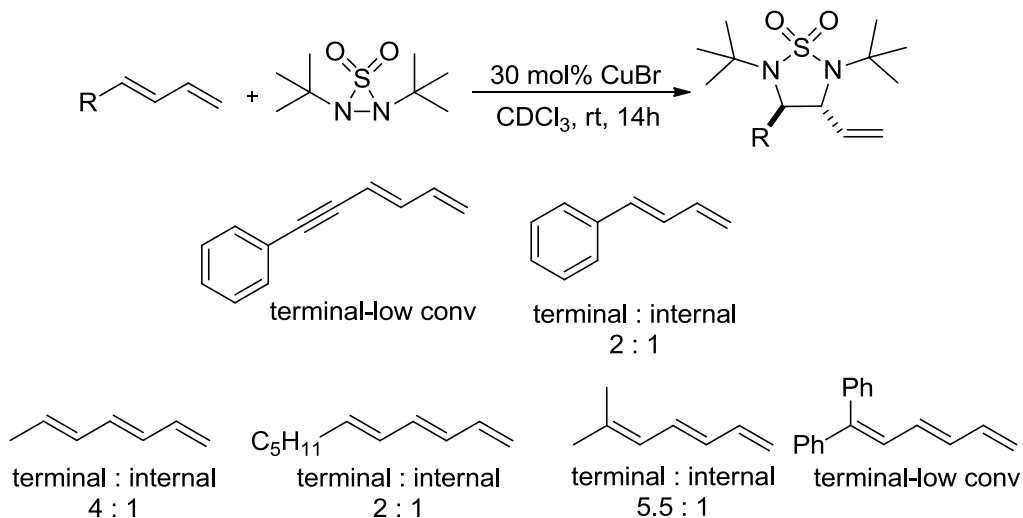


Figure 3.5

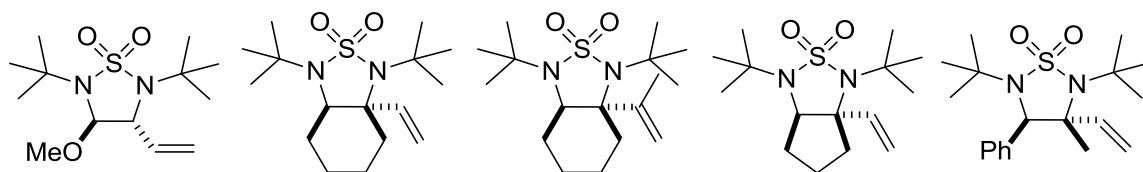
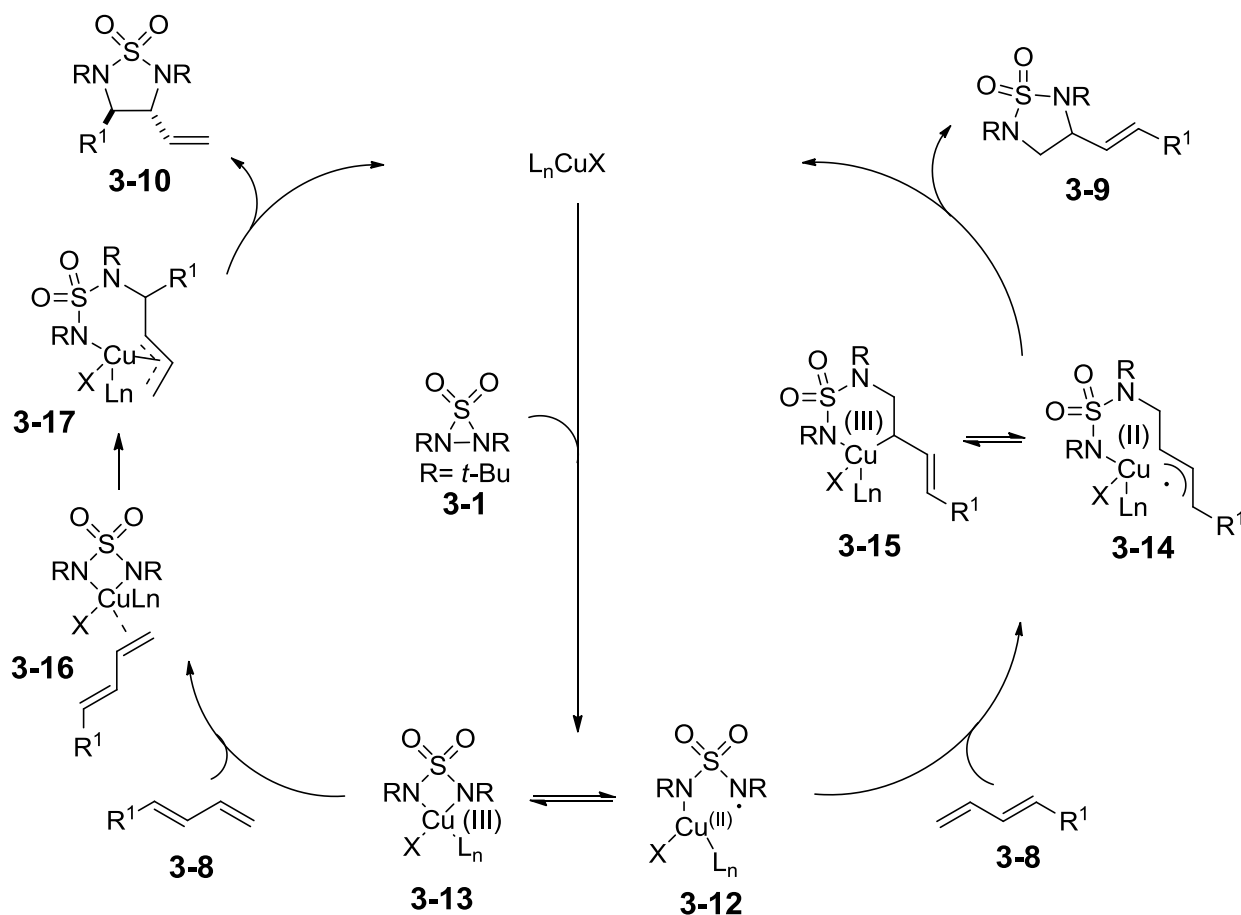


Figure 3.6

3.2.2 Mechanistic Hypothesis

Although a precise reaction mechanism awaits further study, it is proposed that the regioselective diamination of conjugated dienes using **3-1** is analogous to the Cu-catalyzed reaction employing **1-17**.² As shown in Scheme 3.7, the Cu(I) catalyst inserts into the N-N bond of thiadiaziridine **3-1** to form an equilibrium between Cu(II) radical species **3-12** and Cu(III) species **3-13**. Terminal diamination is proposed to proceed via a radical pathway. Terminal attack of species **3-12** onto the conjugated diene yields another equilibrium of Cu(II) radical species **3-14** and Cu(III) species **3-15**. Either through radical recombination or reductive

elimination, terminal diamination product **3-9** is formed and the Cu(I) catalyst is regenerated. Internal diamination is proposed to stem from Cu(III) species **3-13** and resemble a more concerted process, similar to that of Pd-catalyzed diene diamination. Coordination of Cu(III) species **3-13** to the diene substrate and migratory insertion of the first nitrogen forms (π -allyl)Cu species **3-17**. Reductive elimination yields the internal diamination product and regenerates the Cu(I) catalyst.



Scheme 3.7

Addition of ligand promotes terminal diamination through coordination of the ligand to the Cu center which in turn hinders coordination of the diene to Cu(III) species **3-13**, retarding

internal diamination. With respect to reaction concentration, a more dilute reaction mixture favors internal diamination as it facilitates the intermolecular coordination of species **3-13** with the diene substrate. Along with reaction conditions, type of diene also influences regioselectivity. Alkyl dienes present a class of dienes that are suitable for either terminal or internal diamination and regioselectivity can be tuned based upon reaction conditions. Dienes which possess radical stabilizing groups such as aryl groups and trienes are particularly reactive for terminal diamination. Electron-rich dienes, such as polysubstituted dienes, display high reactivity and regioselectivity towards internal diamination, analogous to the Pd-catalyzed diamination of dienes. Substitution of the terminal olefins of entries 4-8 (Table 3.3) could also play a role in favoring internal selectivity over terminal.

3.3 CONCLUSION

In summary, a variety of conjugated dienes have been regioselectively diaminated employing Cu(I) as catalysts and thiadiaziridine **3-1** as nitrogen source. Reaction conditions as well as substrate type influence the resulting regioselectivity of diamination with CuCl-P(*n*-Bu)₃ as catalyst favoring terminal diamination and CuBr as catalyst for internal diamination. Two distinct and competing mechanistic pathways are proposed to be responsible for the observed regioselectivity with terminal diamination resulting from a radical process and internal diamination resulting from a concerted pathway involving a Cu(III) species. The resulting cyclic sulfamides are interesting synthetic intermediates as well as desirable targets for medicinal and biological studies. This method presents a direct approach to synthesize these compounds from readily available dienes and uses inexpensive Cu(I) as catalyst.

3.4 EXPERIMENTAL

Representative terminal diamination using CuCl (Table 3.2, entry 3): To a 1.5 mL vial equipped with a magnetic stir bar was added CuCl (0.0020 g, 0.020 mmol). The sealed vial was evacuated and filled with argon three times, followed by addition of *d*-chloroform (0.1 mL) and tri-*n*-butylphosphine (0.005 mL, 0.020 mmol). After the mixture was stirred at room temperature for 30 min, (*E*)-4-phenylbuta-1,3-diene (**3-8c**) (0.052 g, 0.40 mmol) was added followed by *N,N*-di-*tert*-butylthiadiaziridine 1,1-dioxide (**3-1**) (0.099 g, 0.48 mmol). The reaction mixture was stirred at room temperature for 3.5 h and then purified by flash chromatography (silica gel, ethyl acetate:hexanes = 1:10) to give terminal cyclic sulfamide **3-9c** as a white solid (0.130 g, 97%).

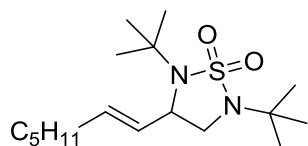
Representative internal diamination using CuBr (Table 3.3, entry 6): To a 1.5 mL vial equipped with a magnetic stir bar was added CuBr (0.0043 g, 0.030 mmol). The sealed vial was evacuated and filled with argon three times, followed by addition of *d*-chloroform (0.6 mL) and (*E*)-2-ethylpenta-1,3-diene (**3-8o**) (0.019 g, 0.20 mmol). *N,N*-di-*tert*-butylthiadiaziridine 1,1-dioxide (**3-1**) (0.050 g, 0.24 mmol) was then added and the reaction mixture was stirred at room temperature for 24 h and purified by flash chromatography (silica gel, hexanes, 1:25 ethyl acetate:hexanes) to give internal cyclic sulfamide **3-10o** as a colorless oil (0.049 g, 81%).

Representative internal diamination using CuBr on gram scale (Table 3.3, entry 1): To a 50 mL round bottom flask equipped with a magnetic stir bar was added CuBr (0.171 g, 1.20 mmol). The sealed flask was evacuated and filled with argon three times, followed by addition of chloroform (24 mL) and (*E*)-2-ethylpenta-1,3-diene (**3-8a**) (1.0 g, 8.0 mmol). *N,N*-di-*tert*-

butylthiadiaziridine 1,1-dioxide (**3-1**) (1.97 g, 9.6 mmol) was then added and the reaction mixture was stirred at room temperature for 24 h and purified by flash chromatography (silica gel, hexanes, 1:25 ethyl acetate:hexanes) to give internal cyclic sulfamide **3-10a** as a colorless oil (1.99 g, 75%).

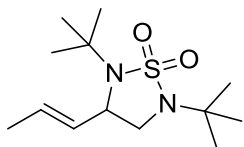
Deprotection of 3-10a (Scheme 3.6). A mixture of **3-10a** (0.040 g, 0.12 mmol) in CF₃CO₂H-hexanes (1:1, 1.2 mL) was stirred at room temperature for 7 h and then purified by flash chromatography (silica gel, hexanes, 1:4 ethyl acetate:hexanes) to give compound **3-11** as a yellow oil (0.022 g, 83%).

Table 3.2, entry 1 (rc_b5_1)



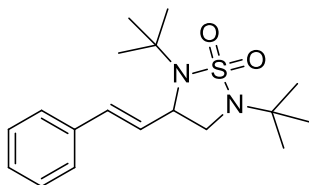
Pale yellow oil; IR (film) 1726, 1481, 1397 cm⁻¹; ¹H NMR (400 MHz, CDCl₃) δ 5.75-5.60 (m, 2H), 4.00-3.95 (m, 1H), 3.42 (dd, *J* = 8.8, 6.4 Hz, 1H), 2.96 (dd, *J* = 8.8, 3.6 Hz, 1H), 2.07-2.0 (m, 2H), 1.41 (s, 9H), 1.38 (s, 9H), 1.42-1.22 (m, 6H), 0.88 (t, *J* = 6.8, 3H); ¹³C NMR (100 MHz, CDCl₃) δ 133.4, 131.2, 57.7, 56.3, 55.6, 47.7, 32.1, 31.6, 28.8, 27.5, 22.6, 14.2; Anal. calcd. for C₁₇H₃₁N₂O₂S: C 61.77, H 10.37, N 8.48; found: C 61.82, H 10.19, N 8.31.

Table 3.2, entry 2 (zbg0330B)



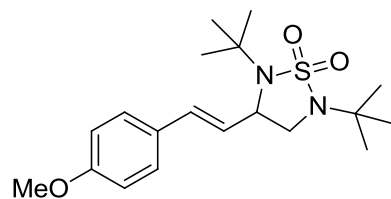
Colorless oil; IR (film) 1481, 1370, 1291, 1198, 1143, 1038 cm^{-1} ; ^1H NMR (300 MHz, CDCl_3) 5.78-5.62 (m, 2H), 4.01-3.94 (m, 1H), 3.42 (dd, $J = 8.7, 6.3$ Hz, 1H), 2.96 (dd, $J = 8.7, 4.2$ Hz, 1H), 1.71 (d, $J = 4.8$ Hz, 3H), 1.41 (s, 9H), 1.38 (s, 9H); ^{13}C NMR (75 MHz, CDCl_3) 132.3, 127.9, 57.7, 56.3, 55.4, 47.5, 28.7, 27.5, 17.7; Anal. calcd. for $\text{C}_{13}\text{H}_{26}\text{N}_2\text{O}_2\text{S}$: C 56.90, H 9.55, N 10.21; found: C 56.76, H 9.40, N 9.96.

Table 3.2, entry 3 (zbg0327A)



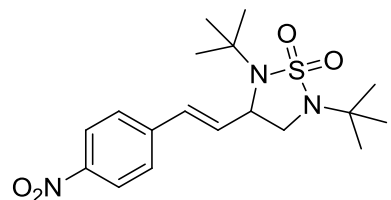
White solid, mp 164-166 $^\circ\text{C}$; IR (film) 1284, 1196, 1139 cm^{-1} ; ^1H NMR (300 MHz, CDCl_3) δ 7.46-7.22 (m, 5H), 6.59 (d, $J = 16.2$ Hz, 1H), 6.44 (dd, $J = 16.2, 8.4$ Hz, 1H), 4.20 (ddd, $J = 8.4, 6.3, 3.6$ Hz, 1H), 3.54 (dd, $J = 8.7, 6.3$ Hz, 1H), 3.09 (dd, $J = 8.7, 3.6$ Hz, 1H), 1.45 (s, 9H), 1.41 (s, 9H); ^{13}C NMR (100 MHz, CDCl_3) δ 136.2, 131.6, 130.5, 128.8, 128.2, 126.7, 57.7, 56.4, 55.6, 47.4, 28.7, 27.5; Anal. calcd. for $\text{C}_{18}\text{H}_{28}\text{N}_2\text{O}_2\text{S}$: C 64.25, H 8.39, N 8.33; found: C 64.14, H 8.54, N 8.11.

Table 3.2, entry 4 (zbg0343H)



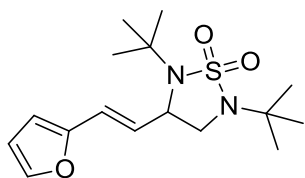
White solid, mp 112-116 °C; IR (film) 1607, 1512, 1370, 1291, 1249, 1143, 1035 cm^{-1} ; ^1H NMR (300 MHz, CDCl_3) δ 7.33 (d, $J = 8.7$ Hz, 2H), 6.87 (d, $J = 8.7$ Hz, 2H), 6.50 (d, $J = 15.6$ Hz, 1H), 6.28 (dd, $J = 15.6, 8.4$ Hz, 1H), 4.21-4.13 (m, 1H), 3.81 (s, 3H), 3.52 (dd, $J = 8.7, 6.0$ Hz, 1H), 3.07 (dd, $J = 8.7, 3.6$ Hz, 1H), 1.44 (s, 9H), 1.40 (s, 9H); ^{13}C NMR (75 MHz, CDCl_3) δ 159.7, 131.1, 128.9, 128.2, 127.9, 114.3, 57.7, 56.4, 55.9, 55.5, 47.5, 28.8, 27.5; Anal. calcd. for $\text{C}_{19}\text{H}_{30}\text{N}_2\text{O}_3\text{S}$: C 62.26, H 8.25, N 7.64; found: C 62.27, H 8.40, N 7.53.

Table 3.2, entry 5 (zbg0424B)



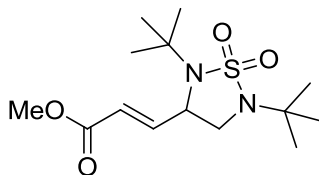
Yellow solid, mp 119-120 °C; IR (film) 1597, 1518, 1370, 1343, 1291, 1198, 1143, 1037 cm^{-1} ; ^1H NMR (300 MHz, CDCl_3) δ 8.17 (d, $J = 8.7$ Hz, 2H), 7.52 (d, $J = 8.7$ Hz, 2H), 6.71 (d, $J = 15.6$ Hz, 1H), 6.62 (dd, $J = 15.6, 6.9$ Hz, 1H), 4.23 (ddd, $J = 6.9, 6.6, 3.0$ Hz, 1H), 3.58 (dd, $J = 9.0, 6.6$ Hz, 1H), 3.10 (dd, $J = 9.0, 3.0$ Hz, 1H), 1.43 (s, 9H), 1.39 (s, 9H); ^{13}C NMR (75 MHz, CDCl_3) δ 147.3, 142.7, 135.4, 129.6, 127.3, 124.2, 57.9, 56.6, 54.9, 47.1, 28.6, 27.5; Anal. calcd. for $\text{C}_{18}\text{H}_{27}\text{N}_3\text{O}_4\text{S}$: C 56.67, H 7.13, N 11.01; found: C 56.58, H 7.40, N 10.90.

Table 3.2, entry 6 (zbg0424A)



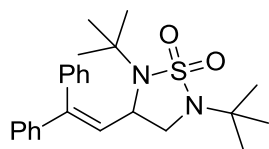
White solid, mp 160-162 °C; IR (film) 3133, 1464, 1396, 1370, 1282, 1201, 1140, 1031 cm^{-1} ; ^1H NMR (300 MHz, CDCl_3) δ 7.35 (d, $J = 1.8$ Hz, 1H), 6.49-6.28 (m, 4H), 4.17-4.09 (m, 1H), 3.50 (dd, $J = 8.7, 6.3$ Hz, 1H), 3.07 (dd, $J = 8.7, 3.6$ Hz, 1H), 1.43 (s, 9H), 1.39 (s, 9H); ^{13}C NMR (75 MHz, CDCl_3) δ 152.0, 142.5, 128.8, 120.1, 111.6, 108.8, 57.8, 56.4, 55.0, 47.4, 28.7, 27.6; Anal. calcd. for $\text{C}_{16}\text{H}_{26}\text{N}_2\text{O}_3\text{S}$: C 58.87, H 8.03, N 8.58; found: C 59.01, H 7.70, N 8.28.

Table 3.2, entry 7 (zbg0424E)



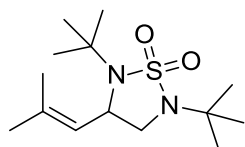
White solid, mp 81-82 °C; IR (film) 1725, 1661, 1372, 1299, 1195, 1143, 1038, 678 cm^{-1} ; ^1H NMR (300 MHz, CDCl_3) δ 7.06 (dd, $J = 15.3, 6.9$ Hz, 1H), 6.13 (d, $J = 15.3$ Hz, 1H), 4.17-4.09 (m, 1H), 3.75 (s, 3H), 3.51 (dd, $J = 9.3, 6.9$ Hz, 1H), 3.03 (dd, $J = 9.3, 3.6$ Hz, 1H), 1.38 (s, 9H), 1.36 (s, 9H); ^{13}C NMR (75 MHz, CDCl_3) δ 166.5, 147.9, 122.8, 57.9, 56.6, 53.2, 51.9, 46.2, 28.4, 27.6; Anal. calcd. for $\text{C}_{14}\text{H}_{26}\text{N}_2\text{O}_4\text{S}$: C 52.81, H 8.23, N 8.80; found: C 53.01, H 8.21, N 8.77.

Table 3.2, entry 8 (zbg0424C)



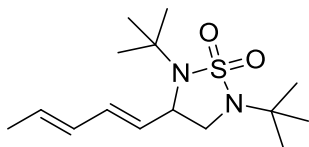
Colorless oil; IR (film) 1598, 1576, 1397, 1370, 1294, 1197, 1144, 1032, 911 cm^{-1} ; ^1H NMR (300 MHz, CDCl_3) δ 7.46-7.36 (m, 3H), 7.33-7.22 (m, 5H), 7.14-7.10 (m, 2H), 6.46 (d, $J = 9.6$ Hz, 1H), 4.08 (ddd, $J = 9.6, 6.6, 3.6$ Hz, 1H), 3.49 (dd, $J = 8.7, 6.6$ Hz, 1H), 3.19 (dd, $J = 8.7, 3.6$ Hz, 1H), 1.41 (s, 9H), 1.32 (s, 9H); ^{13}C NMR (75 MHz, CDCl_3) δ 142.2, 141.0, 138.7, 129.7, 129.5, 128.8, 128.5, 128.1, 128.0, 127.5, 57.5, 56.5, 51.7, 47.4, 28.7, 27.5; Anal. calcd. for $\text{C}_{24}\text{H}_{32}\text{N}_2\text{O}_4\text{S}$: C 69.87, H 7.82, N 6.79; found: C 69.67, H 7.62, N 6.65.

Table 3.2, entry 9 (zbg0330C)



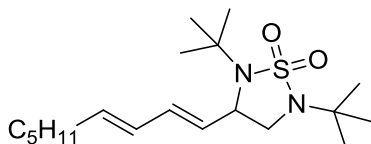
White solid, mp 58-60 $^{\circ}\text{C}$; IR (film) 1481, 1397, 1144 cm^{-1} ; ^1H NMR (300 MHz, CDCl_3) δ 5.46-5.40 (m, 1H), 4.26-4.18 (m, 1H), 3.35 (dd, $J = 8.4, 6.3$ Hz, 1H), 2.88 (dd, $J = 8.4, 5.1$ Hz, 1H), 1.70 (d, $J = 0.9$ Hz, 3H), 1.66 (d, $J = 1.2$ Hz, 3H), 1.37 (s, 9H), 1.36 (s, 9H); ^{13}C NMR (75 MHz, CDCl_3) δ 133.4, 126.5, 57.4, 56.3, 51.3, 47.2, 28.7, 27.4, 25.9, 18.0; Anal. calcd. for $\text{C}_{14}\text{H}_{28}\text{N}_2\text{O}_2\text{S}$: C 58.29, H 9.78, N 9.71; found: C 58.20, H 9.90, N 9.56.

Table 3.2, entry 10 (zbg0331A)



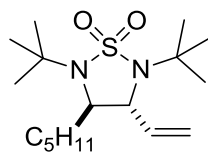
White solid, mp 126-128 °C; IR (film) 1367, 1280, 1199, 1141, 998 cm^{-1} ; ^1H NMR (300 MHz, CDCl_3) δ 6.21-6.00 (m, 2H), 5.82-5.68 (m, 2H), 4.05-3.97 (m, 1H), 3.44 (dd, $J = 9.0, 6.0$ Hz, 1H), 2.98 (dd, $J = 9.0, 4.2$ Hz, 1H), 1.76 (d, $J = 6.9$ Hz, 3H), 1.41 (s, 9H), 1.38 (s, 9H); ^{13}C NMR (75 MHz, CDCl_3) δ 132.1, 131.2, 131.1, 130.5, 57.7, 56.4, 55.4, 47.5, 28.7, 27.5, 18.3; Anal. calcd. for $\text{C}_{15}\text{H}_{28}\text{N}_2\text{O}_2\text{S}$: C 59.96, H 9.39, N 9.32; found: C 59.76, H 9.18, N 9.15.

Table 3.2, entry 11 (zbg0314)



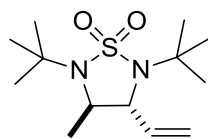
Colorless oil; IR (film) 1397, 1294, 1143 cm^{-1} ; ^1H NMR (300 MHz, CDCl_3) δ 6.25-5.94 (m, 2H), 5.82-5.65 (m, 2H), 4.05-3.97 (m, 1H), 3.44 (dd, $J = 8.4, 6.3$ Hz, 1H), 2.98 (dd, $J = 8.4, 3.6$ Hz, 1H), 2.07 (q, $J = 6.9$ Hz, 2H), 1.40 (s, 9H), 1.37 (s, 9H), 1.41-1.22 (m, 6H), 0.88 (t, $J = 6.9$ Hz, 3H); ^{13}C NMR (75 MHz, CDCl_3) δ 136.7, 132.2, 131.2, 128.9, 57.7, 56.3, 55.4, 47.5, 32.8, 31.6, 29.0, 28.7, 27.5, 22.7, 14.2; HRMS calcd. For $\text{C}_{19}\text{H}_{37}\text{N}_2\text{O}_2\text{S}$ ($\text{M}+\text{H}^+$): 357.2576, found 357.2577.

Table 3.3, entry 1 (rc_b5_5_0)



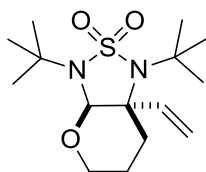
Pale yellow oil; IR (film) 1467, 1290, 1196, 1143 cm⁻¹; ¹H NMR (300 MHz, CDCl₃) δ 6.13-5.98 (ddd, *J* = 17.1, 10.5, 6.6 Hz, 1H), 5.34 (d, *J* = 17.1 Hz, 1H), 5.19 (d, *J* = 10.5 Hz, 1H), 3.74 (d, *J* = 6.6 Hz, 1H), 3.06 (dd, *J* = 11.4, 3.0 Hz, 1H), 1.95-1.79 (m, 1H), 1.65-1.52 (m, 1H), 1.39 (s, 9H), 1.37 (s, 9H), 1.41-1.25 (m, 6H), 0.93-0.84 (m, 3H); ¹³C NMR (100 MHz, CDCl₃) δ 139.7, 116.5, 60.4, 60.1, 57.0, 56.9, 36.1, 31.7, 28.9, 25.9, 22.7, 14.1; Anal. calcd. for C₁₇H₃₄N₂O₂S: C 61.77, H 10.37, N 8.48; found: C 61.61, H 10.24, N 8.11.

Table 3.3, entry 2 (rc_b5_5_16)



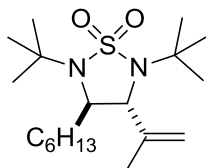
White solid, mp 78-80 °C; IR (film) 1370, 1280, 1252, 1139 cm⁻¹; ¹H NMR (300 MHz, CDCl₃) δ 6.13-6.01 (ddd, *J* = 17.1, 10.2, 6.9 Hz, 1H), 5.37 (dd, *J* = 17.1, 0.6 Hz, 1H), 5.21 (dd, *J* = 10.2, 0.6 Hz, 1H), 3.61 (d, *J* = 6.9 Hz, 1H), 3.33 (q, *J* = 6.6 Hz, 1H), 1.42 (d, *J* = 6.6 Hz, 3H), 1.41 (s, 9H), 1.39 (s, 9H); ¹³C NMR (100 MHz, CDCl₃) δ 139.1, 116.7, 63.3, 56.9, 55.8, 29.0, 28.9, 22.9; Anal. calcd. for C₁₃H₂₆N₂O₂S: C 56.90, H 9.55, N 10.21; found: C 56.70, H 9.37, N 9.90.

Table 3.3, entry 3 (rc_b5_7)



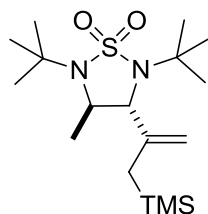
Yellow oil; IR (film) 1364, 1220, 1156 cm^{-1} ; ^1H NMR (300 MHz, CDCl_3) δ 6.24 (dd, $J = 17.4$, 10.8 Hz, 1H), 5.40 (d, $J = 17.4$ Hz, 1H), 5.27 (d, $J = 10.8$ Hz, 1H), 4.93 (s, 1H), 4.08-3.99 (m, 1H), 3.63-3.50 (m, 1H), 2.08-2.00 (m, 1H), 1.88-1.70 (m, 3H), 1.45 (s, 9H), 1.31 (s, 9H); ^{13}C NMR (100 MHz, CDCl_3) δ 139.3, 116.3, 87.7, 81.6, 58.0, 57.3, 55.5, 32.0, 28.7, 28.3, 17.8; HRMS calcd. for $\text{C}_{15}\text{H}_{29}\text{N}_2\text{O}_3\text{S}$ ($\text{M}+\text{H}^+$): 316.1821, found 316.1829.

Table 3.3, entry 4 (rc_b5_24_2d)



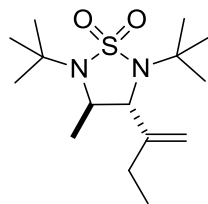
Colorless oil; IR (film) 1371, 1289, 1197, 1144 cm^{-1} ; ^1H NMR (400 MHz, CDCl_3) δ 5.40 (s, 1H), 5.02 (s, 1H), 3.51 (s, 1H), 3.08 (dd, $J = 11.6$, 2.4 Hz, 1H), 1.97-1.83 (m, 1H), 1.75 (s, 3H), 1.69-1.59 (m, 1H), 1.39 (s, 9H), 1.40 (s, 9H), 1.37-1.24 (m, 8H), 0.89 (t, $J = 6.0$ Hz, 3H); ^{13}C NMR (100 MHz, CDCl_3) δ 144.0, 114.0, 62.5, 58.9, 56.9, 56.6, 36.5, 31.9, 29.3, 29.21, 28.19, 26.3, 22.8, 19.4, 14.3; Anal. calcd. for $\text{C}_{19}\text{H}_{38}\text{N}_2\text{O}_2\text{S}$: C 63.64, H 10.68, N 7.81; found: C 63.61, H 10.52, N 7.88.

Table 3.3, entry 5 (rc_b5_5_6)



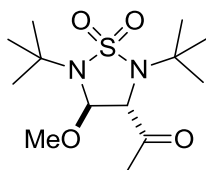
Pale yellow oil; IR (film) 1371, 1289, 1251, 1144 cm^{-1} ; ^1H NMR (300 MHz, CDCl_3) δ 5.40 (s, 1H), 4.87 (s, 1H), 3.45 (q, $J = 6.6$ Hz, 1H), 3.34 (s, 1H), 1.66 (d, $J = 14.7$ Hz, 1H), 1.43 (d, $J = 6.6$ Hz, 3H), 1.41 (s, 9H), 1.35 (s, 9H), 1.22 (d, $J = 14.7$ Hz, 1H), 0.07 (s, 9H); ^{13}C NMR (100 MHz, CDCl_3) δ 144.4, 111.9, 66.1, 56.7, 56.5, 53.9, 29.2, 28.4, 24.1, 23.2, -0.68; Anal. calcd. for $\text{C}_{17}\text{H}_{36}\text{N}_2\text{O}_2\text{SSi}$: C 56.62, H 10.06, N 7.77; found: C 56.79, H 9.97, N 7.54.

Table 3.3, entry 6 (rc_b5_14_19)



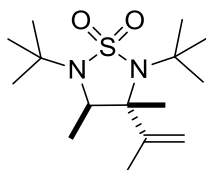
Colorless oil; IR (film) 1398, 1287, 1143 cm^{-1} ; ^1H NMR (300 MHz, CDCl_3) δ 5.44 (s, 1H), 4.99 (s, 1H), 3.44 (s, 1H), 3.32 (q, $J = 6.6$ Hz, 1H), 2.16-1.92 (m, 2H), 1.43 (d, $J = 6.6$ Hz, 3H), 1.38 (s, 9H), 1.35 (s, 9H), 1.10 (t, $J = 7.2$ Hz, 3H); ^{13}C NMR (100 MHz, CDCl_3) δ 149.9, 111.3, 65.0, 56.8, 56.7, 54.7, 29.3, 28.2, 25.6, 24.0, 12.4; Anal. calcd. for $\text{C}_{15}\text{H}_{30}\text{N}_2\text{O}_2\text{S}$: C 59.56, H 10.00, N 9.26; found: C 59.55, H 10.12, N 8.99.

Table 3.3, entry 7 (rc_b5_5_13)



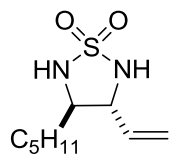
Yellow oil; IR (film) 1715, 1302, 1194, 1151, 1070 cm^{-1} ; ^1H NMR (400 MHz, C_6D_6) δ 4.34 (s, 1H), 3.64 (s, 1H), 2.91 (s, 1H), 2.25 (s, 1H), 1.28 (s, 9H), 1.21 (s, 9H); ^{13}C NMR (100 MHz, C_6D_6) δ 209.4, 87.0, 67.0, 66.9, 58.4, 57.6, 53.0, 52.9, 29.5, 28.2, 26.6; Anal. calcd. for $\text{C}_{13}\text{H}_{26}\text{N}_2\text{O}_4\text{S}$: C 50.96, H 8.55, N 9.14; found: C 51.03, H 8.60, N 8.94.

Table 3.3, entry 8 (rc_b5_18_24)



White solid, mp 84-86 $^{\circ}\text{C}$; IR (film) 1255, 1214, 1104 cm^{-1} ; ^1H NMR (400 MHz, CDCl_3) δ 5.12 (s, 1H), 4.99 (s, 1H), 3.89 (q, $J = 6.4$ Hz, 1H), 1.91 (s, 3H), 1.43 (s, 9H), 1.39 (s, 3H), 1.39 (d, $J = 6.4$ Hz, 3H), 1.32 (s, 9H); ^{13}C NMR (100 MHz, CDCl_3) δ 146.9, 112.2, 87.8, 58.3, 57.3, 55.3, 31.9, 29.2, 23.0, 19.6, 18.9; Anal. calcd. for $\text{C}_{15}\text{H}_{30}\text{N}_2\text{O}_2\text{S}$: C 59.56, H 10.00, N 9.26; found: C 59.39, H 9.91, N 9.12.

Scheme 3.6 (rc_b5_20_1to1)



Yellow oil; IR (film) 3255, 1302, 1168 cm⁻¹; ¹H NMR (300 MHz, CDCl₃) δ 5.80 (ddd, *J* = 16.8, 10.5, 7.5 Hz, 1H), 5.40 (d, *J* = 16.8 Hz, 1H), 5.33 (d, *J* = 10.5 Hz, 1H), 4.61 (d, *J* = 6.0 Hz, 1H), 4.54 (d, *J* = 8.4 Hz, 1H), 3.96-3.80 (m, 1H), 3.52-3.41 (m, 1H), 1.75-1.24 (m, 8H), 0.89 (t, *J* = 6.9 Hz, 3H); ¹³C NMR (100 MHz, CDCl₃) δ 133.8, 120.8, 66.4, 63.0, 32.3, 31.6, 26.4, 22.6, 14.1; Anal. calcd. for C₉H₁₈N₂O₂S: C 49.51, H 8.31, N 12.83; found: C 49.43, H 8.11, N 12.90.

3.5 REFERENCES

- ¹ Yuan, W.; Du, H.; Zhao, B.; Shi, Y. *Org. Lett.* **2007**, *9*, 2589.
- ² (a) Zhao, B.; Peng, X.; Cui, S.; Shi, Y. *J. Am. Chem. Soc.* **2010**, *132*, 11009 (b) Zhao, B.; Peng, X.; Zhu, Y.; Ramirez, T.A.; Cornwall, R.G. *J. Am. Chem. Soc.* **2011**, *133*, 20890.
- ³ Zhao, B.; Yuan, W.; Du, H.; Shi, Y. *Org. Lett.* **2007**, *9*, 4943.
- ⁴ (a) Timberlake, J.W.; Alender, J.; Garner, A.W.; Hodges, M.L.; Özmeral, C.; Szilagy, S.; Jacobus, J.O. *J. Org. Chem.* **1981**, *46*, 2082. (b) Ramirez, T.A.; Zhao, B.; Shi, Y. *Tetrahedron Lett.* **2010**, *51*, 1822.
- ⁵ Wang, B.; Du, H.; Shi, Y. *Angew. Chem. Int. Ed.* **2008**, *47*, 8224.
- ⁶ (a) Rosenberg, S.H.; Dellaria, J.F.; Kempf, D.J.; Hutchins, C.W.; Woods, K.W.; Maki, R.G.; de Lara, E.; Spina, K.P.; Stein, H.H.; Cohen, J.; Baker, W.R.; Plattner, J.J.; Kleinert, H.D.; Perun, T.J. *J. Med. Chem.* **1990**, *33*, 1582 (b) Castro, J.L.; Baker, R.; Guiblin, A.R.; Hobbs, S.C.; Jenkins, M.R.; Russell, M.G.N.; Beer, M.S.; Stanton, J.A.; Scholey, K.; Hargreaves, R.J.; Graham, M.I.; Matassa, V.G. *J. Med. Chem.* **1994**, *37*, 3023 (c) Kim, I.-W.; Jung, S.-H. *Arch. Pharm. Res.* **2002**, *25*, 421 (d) Zhong, J.; Gan, X.; Alliston, K.R.; Groutas, W.C. *Bioorg. Med. Chem.* **2004**, *12*, 589 (e) Zhong, J.; Gan, X.; Alliston, K.R.; Lai, Z.; Yu, H.; Groutas, C.S.; Wong, T.; Groutas, W.C. *J. Comb. Chem.* **2004**, *6*, 556 (f) Bendjeddou, A.; Djeribi, R.; Regainia, Z.; Aouf, N.-E. *Molecules* **2005**, *10*, 1387 (g) Sparey, T.; Beher, D.; Best, J.; Biba, M.; Castro, J. L.; Clarke, E.; Hannam, J.; Harrison, T.; Lewis, H.; Madin, A.; Shearman, M.; Sohal, B.; Tsou, N.; Welch, C.; Wrigley, J. *Bioorg. Med. Chem. Lett.* **2005**, *15*, 4212. (h) Winum, J.-Y.; Scozzafava, A.; Montero, J.-L.; Supuran, C. T. *Med. Res. Rev.* **2006**, *26*, 767. (i) Winum, J.-Y.; Scozzafava, A.; Montero, J.-L.; Supuran, C. T. *Expert Opin. Ther. Patents.* **2006**, *16*, 27. (j) Kim, S. J.; Jung, M.-H.; Yoo, K. H.; Cho, J.-H.; Oh, C.-H. *Bioorg. Med. Chem. Lett.* **2008**, *18*, 5815. (k) Benlifa, M.; Moreno, M. I. G.; Mellet, C. O.; Fernández, J. M. G.; Wadouachi, A. *Bioorg. Med. Chem. Lett.* **2008**, *18*, 2805. (l) Yang, Q.; Li, Y.; Dou, D.; Gan, X.; Mohan, S.; Groutas, C.S.; Stevenson, L.E.; Lai, Z.; Alliston, K.R.; Zhong, J.; Williams, T.D.; Groutas, W.C. *Arch. Biochem. Biophys.* **2008**, *475*, 115 (m) Reitz, A. B.; Smith, G. R.; Parker, M. H. *Expert Opin. Ther. Patents.* **2009**, *19*, 1449 (n) Dou, D.; Tiew, K.-C.; He, G.; Mandadapu, S.R.; Aravapalli, S.; Alliston, K.R.; Kim, Y.; Chang, K.-O.; Groutas, W.C. *Bioorg. Med. Chem.* **2011**, *19*, 5975 (o) Dou, D.; Mandadapu, S.R.; Alliston, K.R.; Kim, Y.; Chang, K.-O.; Groutas, W.C. *Eur. J. Med. Chem.* **2012**, *47*, 59 (p) Brodney, M.A.; Barreiro, G.; Ogilvie, K.; Hajos-Korcsok, E.; Murray, J.; Vajdos, F.; Ambroise, C.; Christoffersen, C.; Fisher, K.; Lanyon, L.; Liu, J.H.; Nolan, C.E.; Withka, J.M.; Borzilleri, K.A.; Efremov, I.; Oborski, C.E.; Varghese, A.; O'Neill, B.T. *J. Med. Chem.* **2012**, *55*, 9224.

⁷ (a) Ahn, K.H.; Yoo, D.J.; Kim, J.S. *Tetrahedron Lett.* **1992**, *33*, 6661 (b) Fécourt, F.; Lopez, G.; Van Der Lee, A.; Martinez, J.; Dewynter, G. *Tetrahedron: Asymmetry.* **2010**, *21*, 2361.

⁸ Cornwall, R.G.; Zhao, B.; Shi, Y. *Org. Lett.* **2011**, *13*, 434.

CHAPTER 4.0: CATALYTIC ASYMMETRIC SYNTHESIS OF CYCLIC SULFAMIDES

4.1 GENERAL INTRODUCTION

The cyclic sulfamide motif is a promising functional group in the area of medicinal chemistry as they have shown to exhibit interesting biological activity as HIV protease inhibitors, anti-inflammatory agents, antibacterials, blood pressure regulators, enzyme inhibitors, and treatments for Alzheimer's disease (Figure 4.1).¹ Cyclic sulfamides have also been used as chiral control agents in asymmetric aldol reactions and alkylations.²

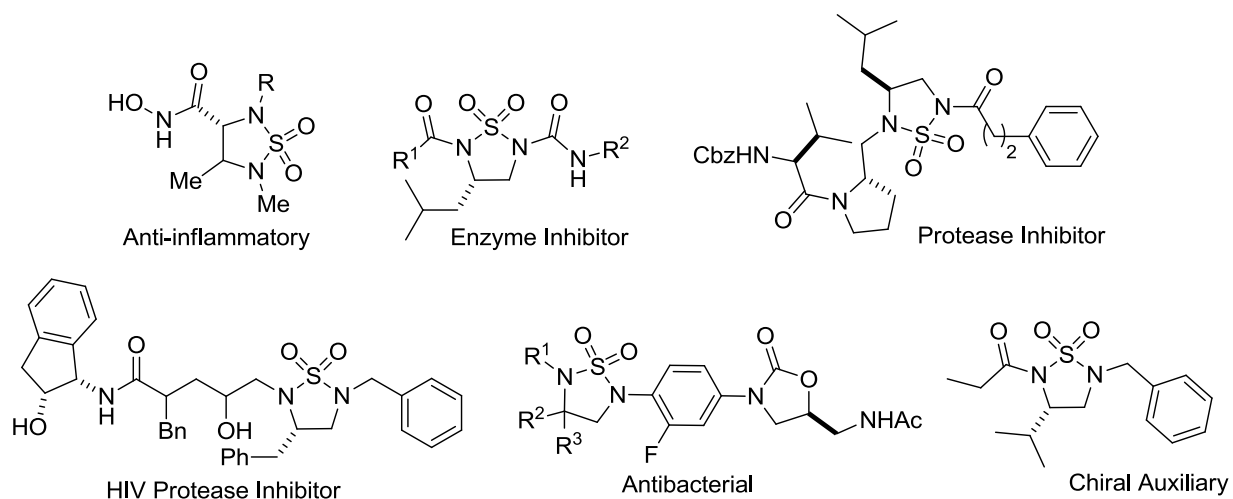
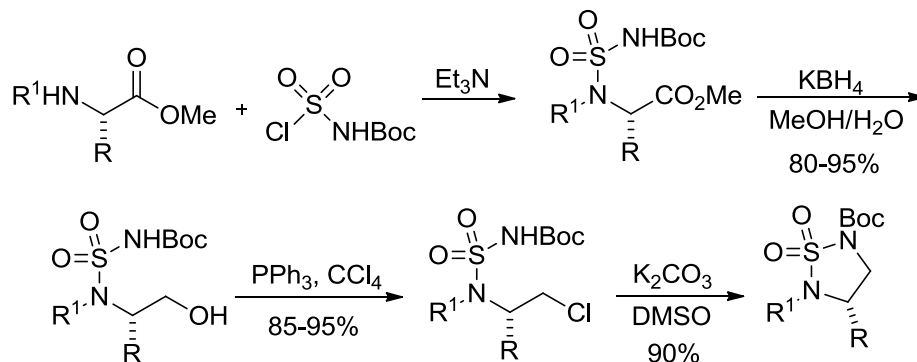


Figure 4.1

4.2 CURRENT METHODS TO SYNTHESIZE CHIRAL CYCLIC SULFAMIDES

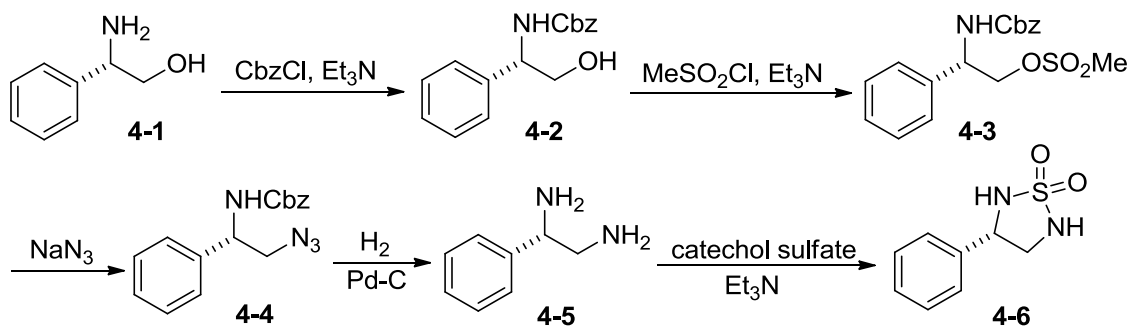
Due to the potential significance that cyclic sulfamides possess for biological studies, methods for their asymmetric synthesis have been reported. Commonly used methods employ multistep syntheses from chiral amino acids.^{1f,3} In 2000, Dewynter and coworkers reported the synthesis of chiral cyclosulfamides from amino acid methyl esters and chlorosulfonyl isocyanate

(Scheme 4.1).^{3a} Good yields were obtained in four steps while maintaining the starting material chirality and providing substitution at the 3-position.



Scheme 4.1

Kim and Jung synthesized cyclic sulfamide **4-6** from (*S*)-(+)-phenylglycinol (**4-1**) (Scheme 4.2). After Cbz protection of the nitrogen and activation of the alcohol with MsCl, the amino azide **4-4** was obtained.⁴ Reduction of the azide and deprotection occurred in one step using H₂/Pd-C to give diamine **4-5**. Catecholsulfate was employed to form cyclic sulfamide **4-6** in five steps overall.



Scheme 4.2

More recently, Lee and coworkers reported a highly enantioselective synthesis of cyclic sulfamides via asymmetric hydrogenation of thiadiazole 1,1-dioxides (Figure 4.2).⁵ Starting from

α -hydroxy aryl ketones, condensation of sulfamide gave the parent thiadiazole 1,1-dioxides **4-8**. Asymmetric hydrogenation using chiral catalyst **4-10** gave the chiral cyclic sulfamides in high yield and mostly high ee's. This process allowed substitution on the sulfamide ring to vary from naturally occurring amino acids, however it was still limited to aryl groups.

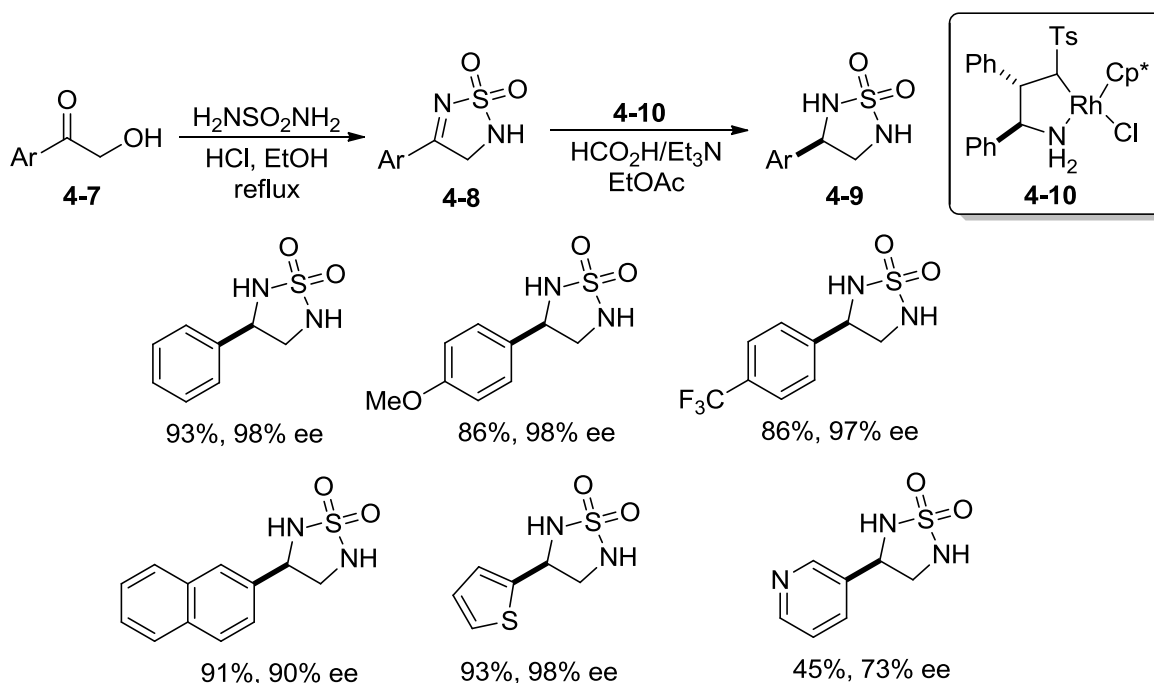


Figure 4.2

Chiral cyclic sulfamides can be obtained through the abovementioned methods, however substrate variability is limited to naturally occurring amino acid side chains or aryl groups and multiple steps are needed in the syntheses. It was envisioned that asymmetric diamination using thiadiaziridine **3-1** (Figure 4.3) could provide a direct and viable route to chiral cyclic sulfamides and greatly expand the substitution possibilities. The following chapter describes the asymmetric synthesis of cyclic sulfamides using **3-1** as nitrogen source.

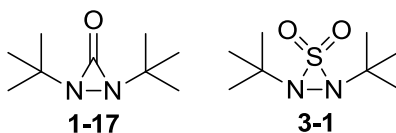
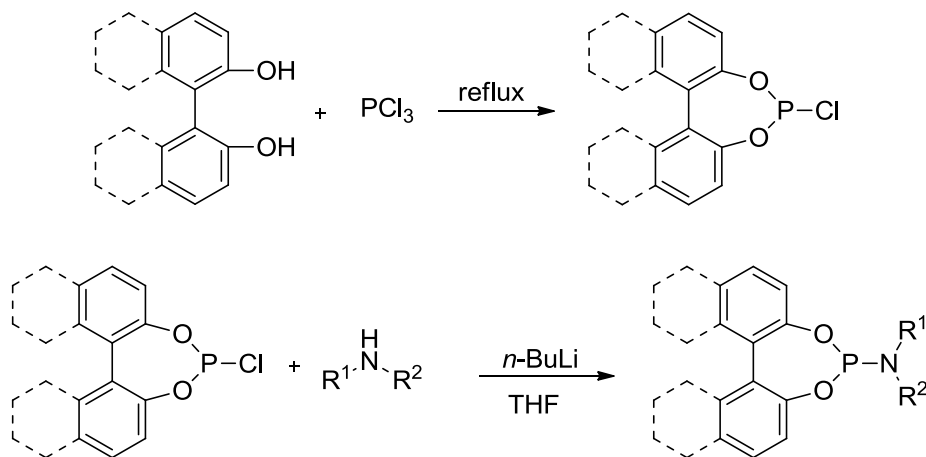


Figure 4.3

4.3 RESULTS AND DISCUSSION

4.3.1 Reaction Conditions and Substrate Scope

(*E*)-nona-1,3-diene was chosen as a test substrate for screening initial asymmetric diamination conditions. Various phosphoramidite and TADDOL-derived ligands were synthesized using known procedures as exemplified in Scheme 4.3.⁶ Catalysts generated from Pd₂(dba)₃ and a chiral ligand were screened for reactivity and selectivity (Figure 4.4).⁷ As shown in Figure 4.4, bidentate ligand *R*-BINAP (**4-11**) displayed no reaction. TADDOL-derived ligand **4-12** gave promising ee, while ligand **4-13** gave good reactivity but low selectivity. BINOL-based phosphoramidite ligands gave the most promising selectivity and diamination occurred exclusively at the internal double bond.



Scheme 4.3

Ligand **4-15** displayed moderate reactivity with good selectivity. Interestingly, ligands **4-16** and **4-17**, which had shown to be optimal for asymmetric diamination of dienes using nitrogen source **1-17**,⁸ displayed diminished selectivity using nitrogen source **3-1**. Ligand **4-18**, having previously been less reactive using **1-17**, gave very promising selectivity and reactivity with **3-1**, providing the cyclic sulfamide **4-22d** in 76% yield and 90% ee. Diastereomeric ligand **4-19** gave comparable yield but selectivity was lower, indicating a matched/mismatched relationship between the BINOL and amine portions of the ligand necessary for high asymmetric induction. Comparison of biphenyl ligand **4-14** with the reactive ligand **4-18** shows that the resulting stereochemistry of the sulfamide products is determined by the BINOL skeleton and not the amine portion. The hydrogenated ligand **4-20**, with the opposite stereochemistry of ligand **4-18**, also displayed high selectivity and provided the opposite enantiomer of the sulfamide product.

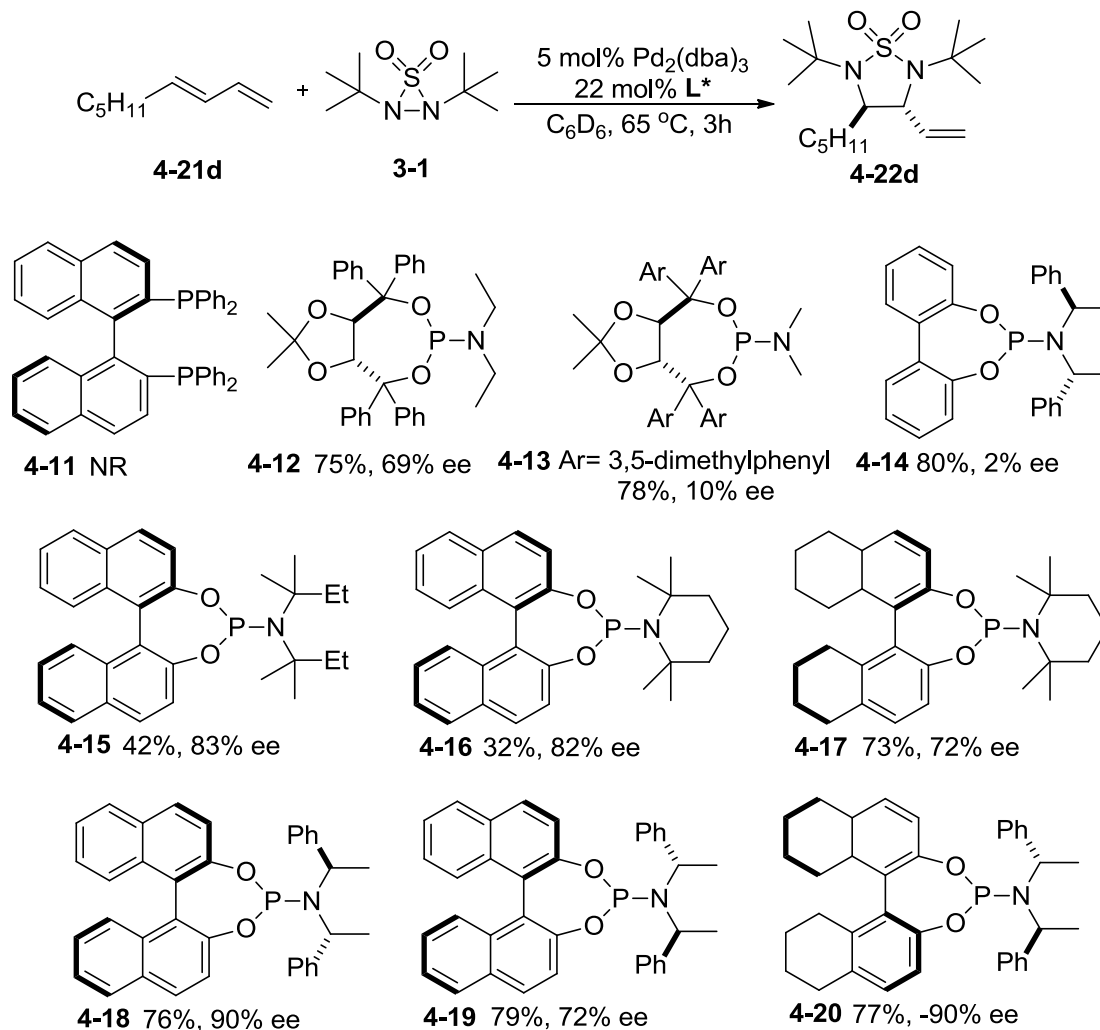
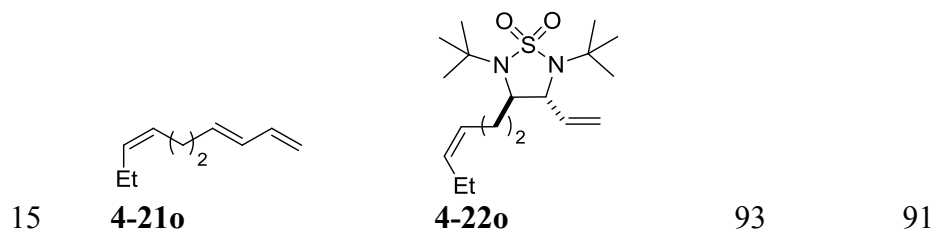


Figure 4.4

Using ligand **4-18** and upon further screening of reaction parameters, investigation into the substrate scope was carried out. A variety of (*E*)-alkyl-substituted conjugated dienes were efficiently diaminated at the internal double bond under the reaction conditions in good to high yield and provided enantioselectivities above 90% (Table 4.1). No diamination product was observed when *cis*-1,3-pentadiene was subjected to the reaction conditions, returning starting material.

Table 4.1 Catalytic Asymmetric Diamination of Conjugated Dienes to Form Cyclic Sulfamides

Entry	Diene (4-21)	Product (4-22) ^b	Yield (%) ^c	ee (%) ^d
1	4-21a , R= Me	4-22a	97	90
2	4-21b , R= <i>n</i> -Pr	4-22b	79	90
3	4-21c , R= <i>i</i> -Bu	4-22c	84	90
4	4-21d , R= <i>n</i> -C ₅ H ₁₁	4-22d	91	91
5	4-21e , R= <i>n</i> -C ₁₀ H ₂₁	4-22e	97	83
6	4-21f , R= (CH ₂) ₂ Cy	4-22f	89	91
7	4-21g , R= (CH ₂) ₂ TMS	4-22g	98	91
8	4-21h	4-22h	90	93 ^e
9 ^f	4-21i , Ar= Ph	4-22i	88	92 ^e
10	4-21j , Ar= 4-MeOPh	4-22j	77	90 ^e
11	4-21k , R= <i>n</i> -C ₆ H ₁₃	4-22k	69	93
12 ^g	4-21l , R= Ph	4-22l	81	93 ^h
13	4-21m	4-22m	66	91
14	4-21n	4-22n	98	91

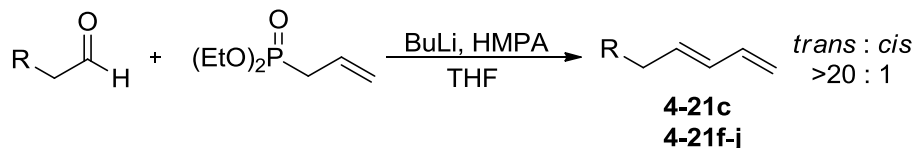


^a All reactions were carried out with diene **4-21** (0.20 mmol), **3-1** (0.30 mmol), Pd₂(dba)₃ (0.005 mmol), and **4-18** (0.02 mmol) in toluene (0.10 mL) under Ar at 65 °C for 3 h, unless otherwise stated. ^b For entries 4 and 8, the absolute configurations (*R,R*) were determined by comparison of the optical rotations with reported ones after complete deprotection to the free diamine (ref. 8a, 9). For all other entries, the absolute configurations were not determined and the stereochemistry indicated represents relative stereochemistry. ^c Isolated yield. ^d The ee was determined by chiral HPLC (Chiralpak IC column) after removal of the *t*-Bu groups, unless otherwise stated. ^e The ee was determined without removal of the *t*-Bu groups. ^f The reaction was carried out with diene **4-21i** (6.96 mmol), **3-1** (9.03 mmol), Pd₂(dba)₃ (0.10 mmol), and **4-18** (0.46 mmol) in toluene (3.5 mL) under Ar at 65 °C for 3 h. ^g Reaction time, 6 h. ^h The ee was determined by chiral HPLC (Chiralpak IA column).

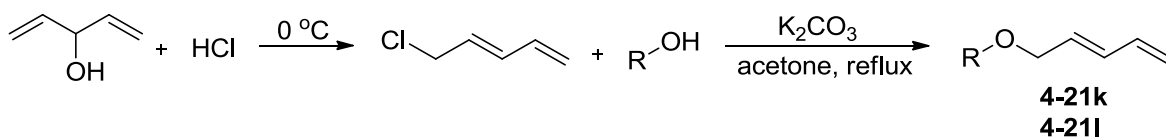
The reaction conditions are suitable for substrates with substitution on the alkyl chains such as silyl (Table 4.1, entry 7) and aryl groups (Table 4.1, entries 8-10) as well as ethers (Table 4.1, entries 11-13). Spectator double bonds were also left unreacted in geometrically pure form (Table 4.1, entries 14-15). The catalytic asymmetric diamination was also run on gram scale with catalyst loading being reduced to 1.4 mol% Pd₂(dba)₃ (Table 4.1, entry 8).

The diene substrates were synthesized from readily available α,β -unsaturated aldehydes and MePPh₃Br. In order to obtain strictly pure *trans*-dienes, other methods were employed to synthesize certain substrates (Schemes 4.4-4.6). Olefins **4-21c** and **4-21f-j** were prepared using preformed diethyl allylphosphonate and the corresponding aldehydes (Scheme 4.4).¹⁰ The resulting selectivity for *trans* and *cis* isomers was >20:1 as judged by ¹H NMR. 1-Chloro-2,4-pentadiene was synthesized with complete *trans* selectivity from 1,4-pentadien-3-ol and conc. HCl (Scheme 4.5). Reaction with the appropriate alcohol and K₂CO₃ gave the corresponding *trans* dienes **4-21k** and **4-21l** in good yield (Scheme 4.5).¹¹ Lastly, olefin **4-21m** was synthesized

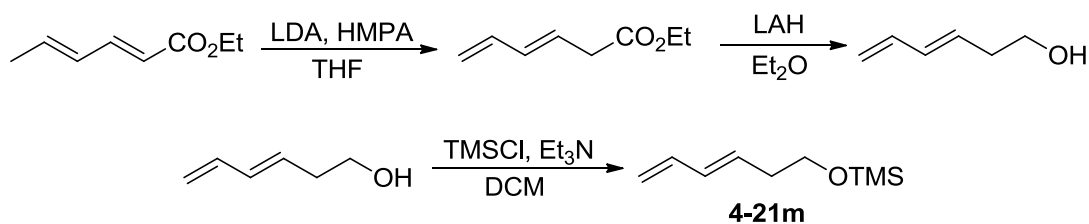
via base-mediated double bond isomerization followed by reduction of the diene ester (Scheme 4.6).¹² TMS protection of the alcohol yielded diene **4-21m**.¹³



Scheme 4.4

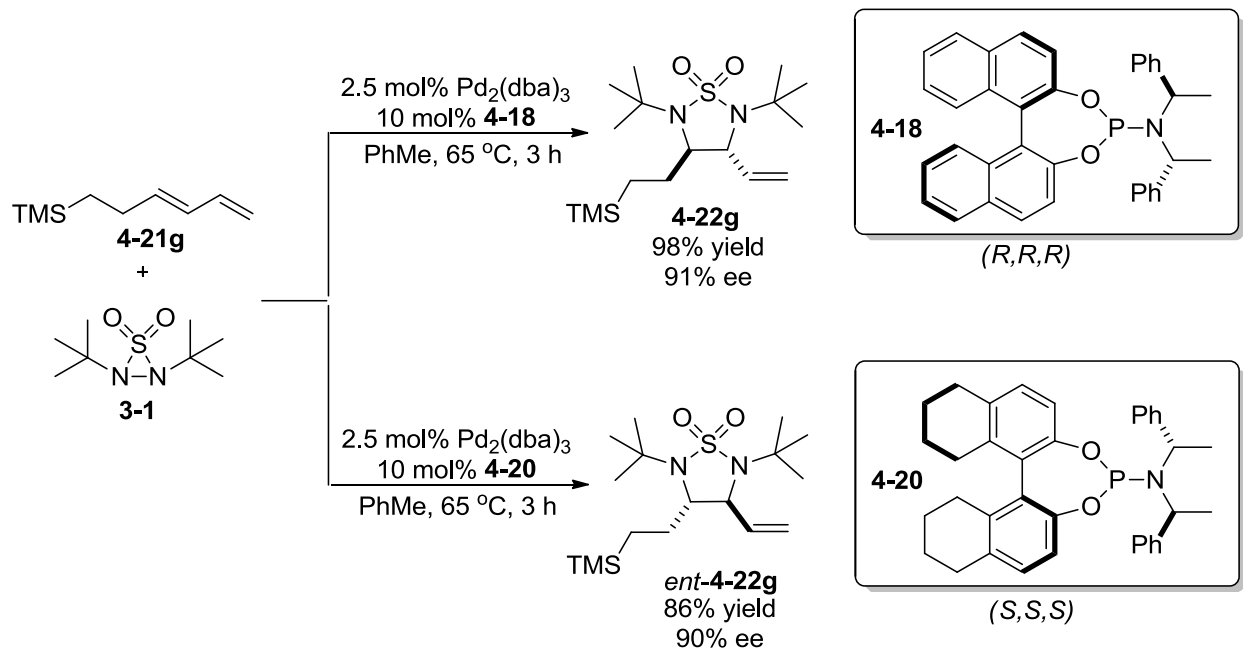


Scheme 4.5



Scheme 4.6

Using ligands **4-18** and **4-20**, diene **4-21g** was diaminated asymmetrically to give both enantiomers of the resulting cyclic sulfamide in good yield and selectivity (Scheme 4.7). The X-ray structure of product **4-22g** was obtained via X-ray diffraction of a single crystal, confirming the relative stereochemistry as *trans* (Figure 4.5).



Scheme 4.7

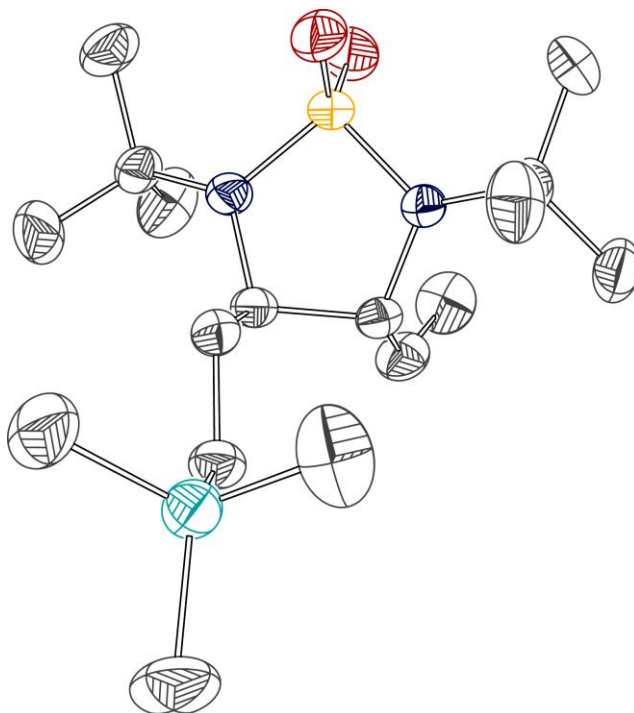


Figure 4.5

Alkyl dienes proved to be the most reactive substrate class. The dienes shown in Figure 4.6 proved reactive, however enantioselectivity was unable to be obtained because the racemic reaction using CuBr gave no racemic diamination product. The dienes shown in Figure 4.7 were also subjected to the reaction conditions but low conversion or no diamination was observed. Even at higher reaction temperatures, conversions remained low.

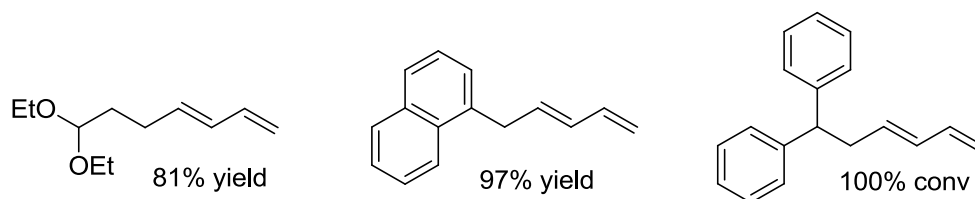


Figure 4.6

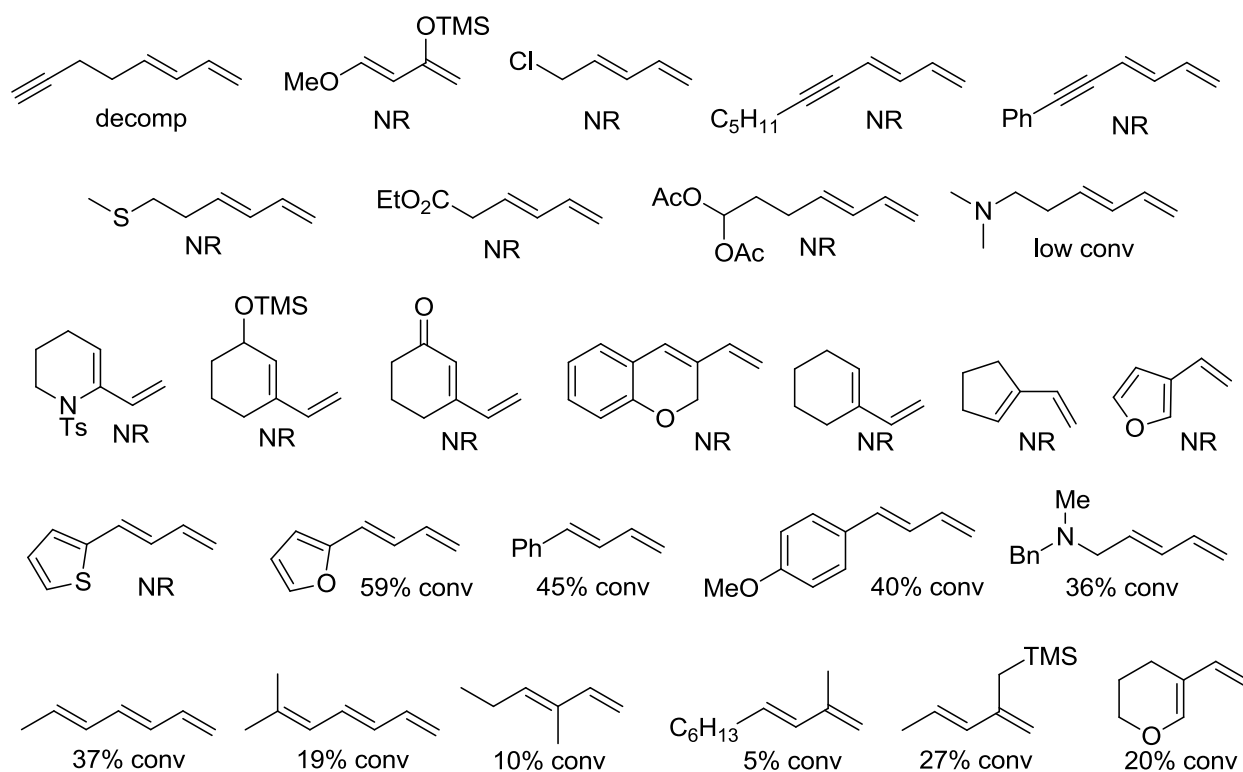
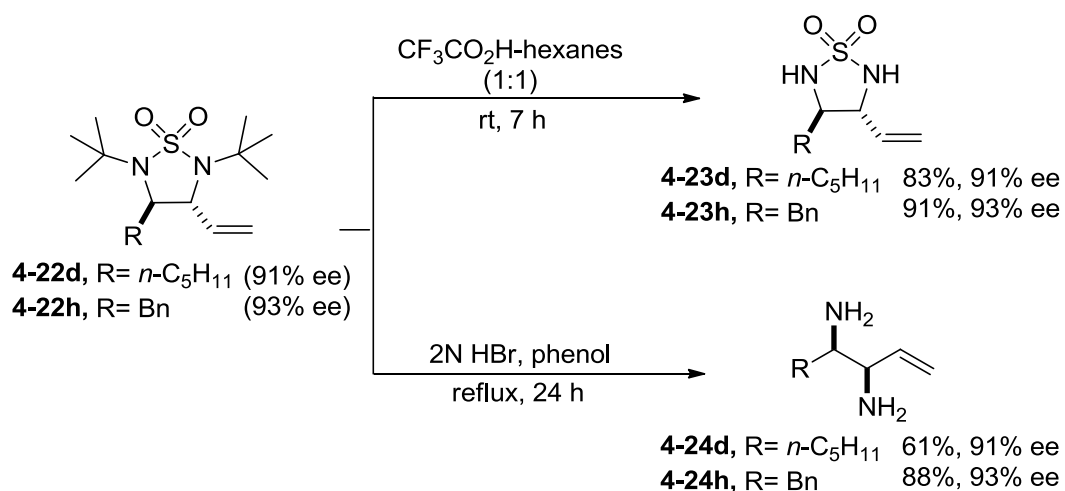


Figure 4.7

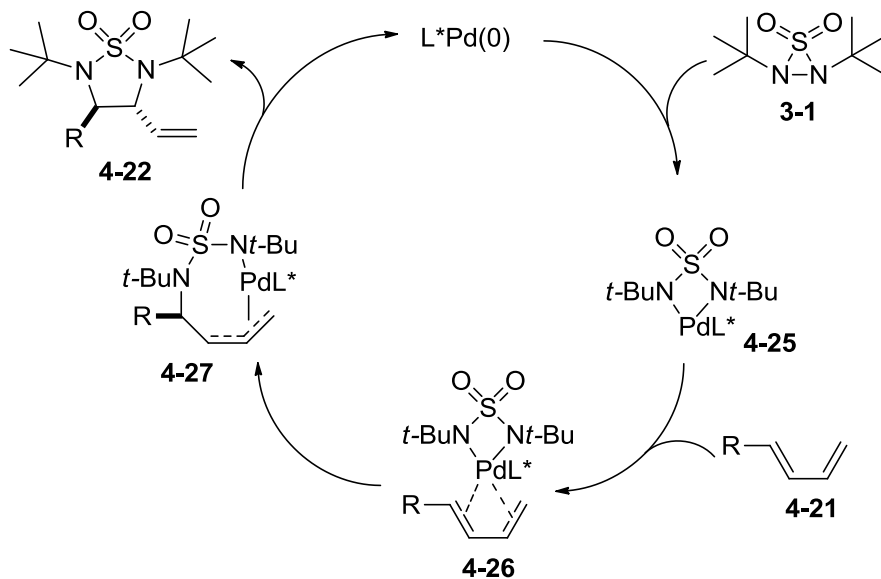
Facile removal of the *tert*-butyl groups from the resulting cyclic sulfamide products was accomplished using a mixture of CF₃CO₂H-hexanes at room temperature (Scheme 4.8). This provided access for possible derivatization of the sulfamide nitrogens. Both *tert*-butyl groups and the sulfone group were removed in one step by refluxing in aqueous HBr to yield the free diamine (Scheme 4.8).¹⁴



Scheme 4.8

4.3.2 Mechanistic Hypothesis

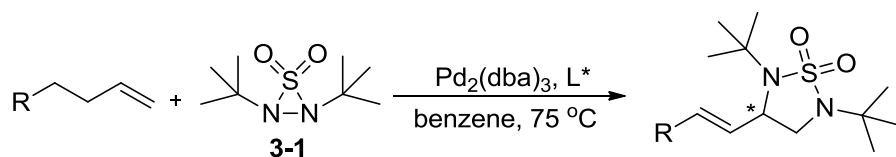
The catalytic asymmetric diamination of conjugated dienes using **3-1** as nitrogen source is proposed to be very similar and analogous to the Pd-catalyzed asymmetric diamination of dienes using **1-17** as nitrogen source (Scheme 4.9). Initially, the Pd(0) complex inserts into the N-N bond of thiadiaziridine **3-1** to give four-membered Pd complex **4-25**. Coordination of this complex with the diene substrate (**4-26**) and migratory insertion of one nitrogen gives π -allyl Pd complex **4-27**. Upon reductive elimination, the cyclic sulfamide is formed and the Pd catalyst is regenerated.



Scheme 4.9

4.3.3 Attempt at Asymmetric Terminal Diamination

Also of interest would be the development of an asymmetric dehydrogenative diamination to give chiral terminal diamination products (Scheme 4.10). 1-Nonene was chosen as test substrate and various chiral phosphoramidite ligands were employed with $Pd_2(dba)_3$ to investigate the terminal diamination (Figure 4.8).¹⁵ No conversion was obtained using ligands **4-28** and **4-29**. Variation of the nitrogen portion of the ligand increased conversion and gave differing ratios for the terminal and internal products. Ligand **4-32** gave moderate conversion with high selectivity for terminal diamination. Diisopropyl amine (**4-33**) and dicyclohexyl amine (**4-35**) further increased conversion but at the cost of selectivity.



Scheme 4.10

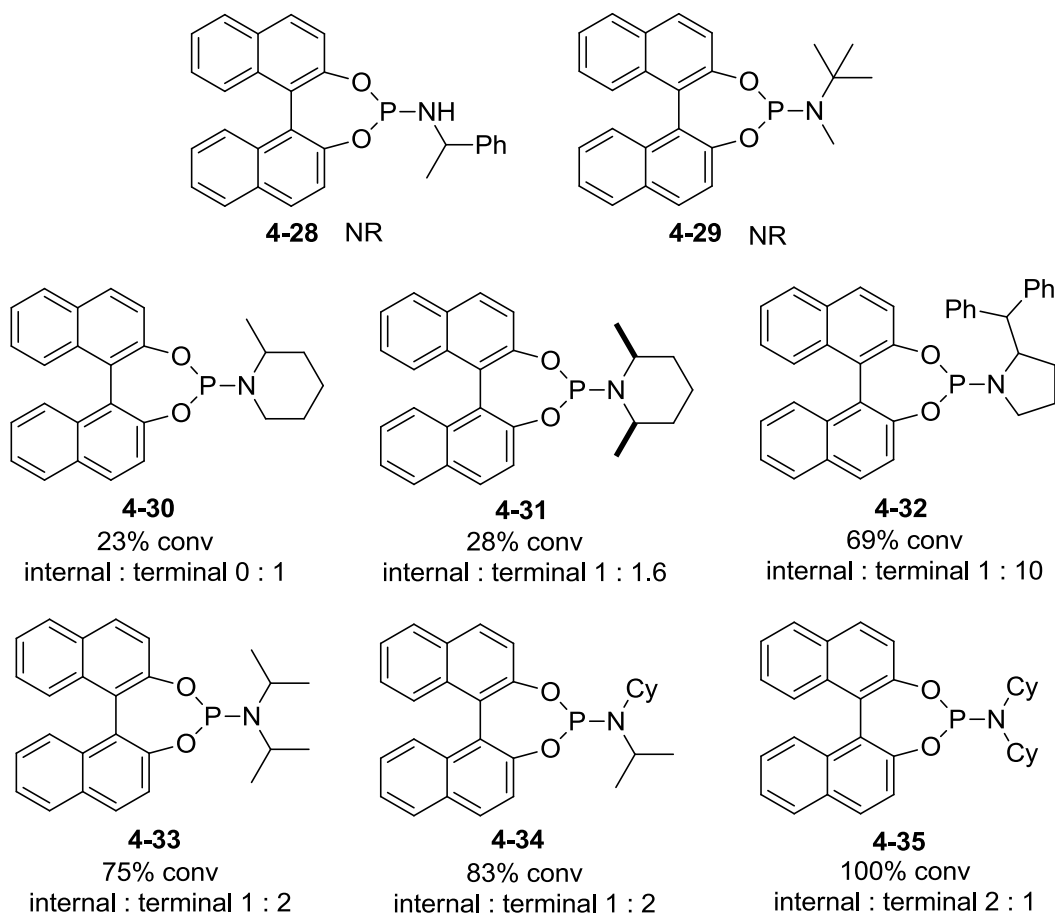
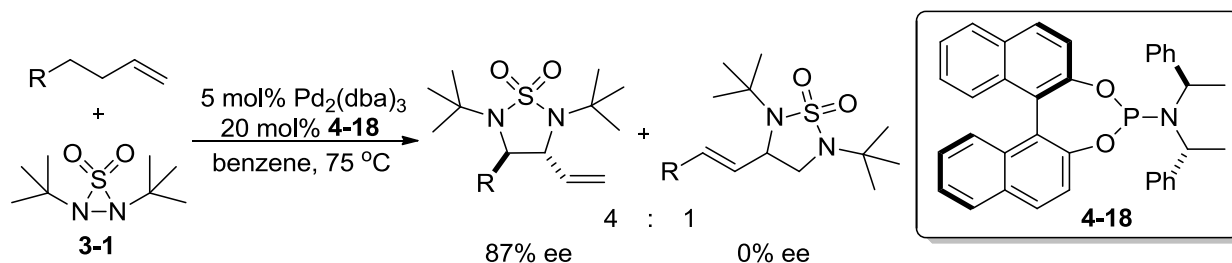


Figure 4.8

Ligand **4-11** gave good conversion and a ratio of 4 : 1, internal to terminal diamination (Scheme 4.11), and careful separation of the two isomers was performed via silica gel chromatography.

Removal of the *tert*-butyl groups in $\text{CF}_3\text{CO}_2\text{H}:\text{hexanes}$ allowed separation via HPLC. It was

found that the internal diamination product was obtained in 87% ee, while the terminal diamination product was racemic (Scheme 4.11). The terminal asymmetric dehydrogenative diamination of dienes remains an interesting and important endeavor and work is ongoing in our lab.



Scheme 4.11

4.4 CONCLUSION

Cyclic sulfamides are important functional motifs which exhibit potentially very useful biological activity when incorporated into peptide scaffolds as well as small molecules. Current routes for their asymmetric synthesis limit substitution on the sulfamide ring to natural amino acid side chains and aryl groups. Using the above route, chiral cyclic sulfamides are synthesized directly in one step from readily available alkyl-substituted dienes using Pd and ligand **4-18** as catalyst, and **3-1** as nitrogen source. The resulting cyclic sulfamides are obtained in good yield and high ee with a variety of substitution and a pendant vinyl group for further manipulation. Using the opposite enantiomer ligand provides complementary enantioselectivity for the cyclic sulfamide products. The resulting cyclic sulfamides can be deprotected to yield the free diamine while maintaining ee. It is proposed that utilization of this method will provide greater access to more structural variety in the synthesis of these chiral compounds and lead to more biological studies.

4.5 EXPERIMENTAL

Representative catalytic asymmetric diamination procedure (Table 4.1, entry 1): To a flame-dried 1.5 mL vial equipped with a magnetic stir bar was added Pd₂(dba)₃ (0.0046 g, 0.005 mmol) and **4-18** (0.0108 g, 0.02 mmol). The sealed vial was evacuated and filled with argon three times, followed by addition of toluene (0.1 mL, distilled from sodium). The mixture was immersed in an oil bath (65 °C) and stirred for 10 min. *trans*-Penta-1,3-diene (**4-21a**) (0.0136 g, 0.20 mmol) was added followed by *N,N'*-di-*tert*-butylthiadiaziridine 1,1-dioxide (**3-1**) (0.062 g, 0.30 mmol) in one portion and the reaction mixture was stirred at 65 °C for 3 h. The crude product was purified by flash chromatography (silica gel, 25:1 hexanes: ethyl acetate). A second column was used to remove excess dba (silica gel, toluene until the yellow color elutes, then 25:1 hexanes: ethyl acetate). Cyclic sulfamide **4-22a** was obtained as a white solid (0.053 g, 97% yield, 90% ee).

Representative diamination on gram scale (Table 4.1, entry 9): To a flame-dried 15 mL vial equipped with a magnetic stir bar was added Pd₂(dba)₃ (0.0915 g, 0.10 mmol) and **4-18** (0.2476 g, 0.46 mmol). The sealed vial was evacuated and filled with argon three times, followed by addition of toluene (3.5 mL, distilled from sodium). The mixture was immersed in an oil bath (65 °C) and stirred for 10 min. *trans*-1-Phenyl-hexa-3,5-diene (**4-21i**) (1.10 g, 6.96 mmol) was added followed by *N,N'*-di-*tert*-butylthiadiaziridine 1,1-dioxide (**3-1**) (1.86 g, 9.03 mmol) in one portion and the reaction mixture was stirred at 65 °C for 3 h. The crude product was purified by flash chromatography (silica gel, 15:1 (v/v) hexanes: ethyl acetate). A second column was used to remove excess dba (silica gel, toluene until the yellow color elutes, then 15:1 (v/v) hexanes: ethyl acetate). Cyclic sulfamide **4-22i** was obtained as a white solid (2.24 g, 88% yield, 92% ee).

Representative procedure for removal of *t*-Butyl groups (Scheme 4.8). A mixture of sulfamide **4-22h** (0.094 g, 0.27 mmol) in CF₃CO₂H-hexanes (1:1 (v/v), 2.4 mL) was stirred at room temperature for 7 h, concentrated, and subsequently purified by flash chromatography (silica gel, 4:1 (v/v) hexanes: ethyl acetate) to give compound **4-23h** as a white solid (0.058 g, 91% yield, 93% ee).

Cornwall, R.G.; Zhao, B.; Shi, Y. *Org. Lett.* **2011**, *13*, 434.

Representative procedure for deprotection to free diamine (Scheme 4.7). To a 25 mL round-bottom flask equipped with a magnetic stir bar and reflux condenser was added sulfamide **4-22h** (0.258 g, 0.736 mmol) and phenol (0.263 g, 2.79 mmol). 2N HBr (8.5 mL) was added and the mixture was vigorously refluxed for 24 h. The reaction was allowed to cool to room temperature and washed with Et₂O to remove excess phenol as monitored by TLC. The acidic aqueous layer was made basic with solid NaOH and extensively extracted with Et₂O as monitored by TLC. The combined organic layers were dried over Na₂SO₄, filtered, and concentrated to yield diamine **4-24h** as a pale yellow oil (0.114 g, 88% yield, 93% ee).

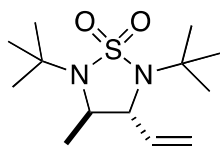
Pansare, S.V.; Rai, A.N.; Kate, S.N. *Synlett* **1998**, 623.

The ee of free diamine 4-24h was determined after derivatization to the di-*m*-toluoyl amide by the following procedure: To a 5 mL vial charged with diamine **4-24h** (0.008 g, 0.045 mmol) was added NaOH solution (2.0 M, 0.27 mL, 0.54 mmol) and CH₂Cl₂ (1.2 mL). Upon stirring at rt for 2 min, *m*-toluoyl chloride (0.015 g, 0.10 mmol) was added via syringe and the resulting mixture was stirred at rt for 10 min. A portion (30 μL) of the organic layer was diluted with

Hex/IPA (1:1) (2 mL) and submitted to HPLC analysis (Chiralpak IC column, Hex:IPA 95:5, 1mL/min).

Zhao, B.; Peng, X.; Cui, S.; Shi, Y. *J. Am. Chem. Soc.* **2010**, *132*, 11009

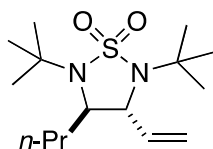
Table 4.1, entry 1 (rc_b8_6_1)



White solid; mp 91-95 °C; $[\alpha]_D^{20} = +39.1$ (c 1.0, CHCl₃) (90% ee); IR (film) 1371, 1275, 1138 cm⁻¹; ¹H NMR (300 MHz, CDCl₃) δ 6.07 (ddd, *J* = 17.1, 10.2, 6.9 Hz, 1H), 5.37 (d, *J* = 17.1 Hz, 1H), 5.21 (d, *J* = 10.2 Hz, 1H), 3.61 (d, *J* = 6.9 Hz, 1H), 3.34 (q, *J* = 6.6 Hz, 1H), 1.42 (d, *J* = 6.6 Hz, 3H), 1.41 (s, 9H), 1.39 (s, 9H); ¹³C NMR (100 MHz, CDCl₃) δ 139.1, 116.7, 63.3, 56.91, 56.89, 55.8, 29.0, 28.9, 22.9; HRMS calcd. for C₁₃H₂₆N₂NaO₂S (M+Na)⁺: 297.1607. Found: 297.1603.

Cornwall, R.G.; Zhao, B.; Shi, Y. *Org. Lett.* **2011**, *13*, 434.

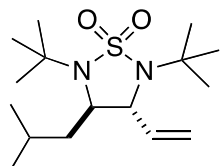
Table 4.1, entry 2 (rc_b8_6_3)



Pale yellow oil; $[\alpha]_D^{20} = +82.4$ (c 0.71, CHCl₃) (90% ee); IR (film) 1644, 1398, 1290 cm⁻¹; ¹H NMR (300 MHz, CDCl₃) δ 6.07 (ddd, *J* = 17.1, 10.2, 6.9 Hz, 1H), 5.34 (dd, *J* = 17.1, 0.6 Hz, 1H), 5.20 (dd, *J* = 10.2, 0.6 Hz, 1H), 3.76 (d, *J* = 6.9 Hz, 1H), 3.10 (dd, *J* = 11.1, 2.7 Hz, 1H), 1.98-1.81 (m, 1H), 1.66-1.51 (m, 1H), 1.44-1.36 (m, 2H), 1.40 (s, 9H), 1.39 (s, 9H), 0.97 (t, *J* = 7.8 Hz, 3H); ¹³C NMR (75 MHz, CDCl₃) δ 139.7, 116.5, 60.1, 57.0, 56.9, 38.2, 28.9, 19.4, 14.0;

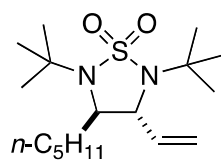
Anal. calcd. for C₁₅H₃₀N₂O₂S: C, 59.56; H, 10.00; N, 9.26. Found: C, 59.33; H, 9.79; N, 9.41.

Table 4.1, entry 3 (rc_b9_32_1)



White solid; mp 51-54 °C; $[\alpha]_{\text{D}}^{20} = +29.7$ (c 0.37, CHCl₃) (90% ee); IR (film) 1469, 1290, 1143 cm⁻¹; ¹H NMR (300 MHz, CDCl₃) δ 6.07 (ddd, *J* = 16.8, 10.2, 6.6 Hz, 1H), 5.34 (d, *J* = 16.8 Hz, 1H), 5.20 (d, *J* = 10.2 Hz, 1H), 3.75 (d, *J* = 6.9 Hz, 1H), 3.20 (dd, *J* = 11.7, 2.4 Hz, 1H), 2.07-1.88 (m, 1H), 1.75-1.57 (m, 2H), 1.39 (s, 9H), 1.38 (s, 9H), 0.97 (d, *J* = 6.6 Hz, 3H), 0.93 (d, *J* = 6.6 Hz, 3H); ¹³C NMR (75 MHz, CDCl₃) δ 139.6, 116.5, 60.0, 58.7, 57.1, 56.8, 44.9, 29.0, 28.8, 25.7, 24.2, 21.3. Anal. calcd. for C₁₆H₃₂N₂O₂S: C, 60.72; H, 10.19; N, 8.85. Found: C, 60.90; H, 9.91; N, 8.86.

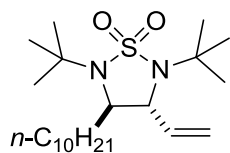
Table 4.1, entry 4 (rc_b8_6_10)



Pale yellow oil; $[\alpha]_{\text{D}}^{20} = +25.6$ (c 0.5, CHCl₃) (91% ee); IR (film) 1468, 1290, 1196, 1143 cm⁻¹; ¹H NMR (300 MHz, CDCl₃) δ 6.07 (ddd, *J* = 17.1, 10.2, 6.6 Hz, 1H), 5.35 (d, *J* = 17.1 Hz, 1H), 5.20 (d, *J* = 10.2 Hz, 1H), 3.75 (d, *J* = 6.6 Hz, 1H), 3.07 (dd, *J* = 11.4, 2.7 Hz, 1H), 1.98-1.80 (m, 1H), 1.66-1.52 (m, 1H), 1.39 (s, 9H), 1.37 (s, 9H), 1.41-1.25 (m, 6H), 0.95-0.84 (m, 3H); ¹³C NMR (75 MHz, CDCl₃) δ 139.7, 116.5, 60.4, 60.1, 57.0, 56.9, 36.1, 31.7, 28.9, 25.9, 22.7, 14.1. Anal. calcd. for C₁₇H₃₄N₂O₂S: C, 61.77; H, 10.37; N, 8.48. Found: C, 61.92; H, 10.17; N, 8.56.

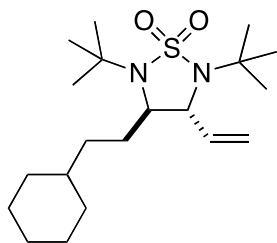
Cornwall, R.G.; Zhao, B.; Shi, Y. *Org. Lett.* **2011**, *13*, 434.

Table 4.1, entry 5 (rc_b8_6_4)



Pale yellow oil; $[\alpha]_{\text{D}}^{20} = +19.3$ (c 7, CHCl₃) (83% ee); IR (film) 2926, 2855, 1293, 1143 cm⁻¹; ¹H NMR (300 MHz, CDCl₃) δ 6.06 (ddd, $J = 17.4, 10.5, 7.2$ Hz, 1H), 5.35 (d, $J = 17.4$ Hz, 1H), 5.20 (d, $J = 10.5$ Hz, 1H), 3.75 (d, $J = 6.6$ Hz, 1H), 3.07 (dd, $J = 11.1, 2.4$ Hz, 1H), 2.00-1.78 (m, 1H), 1.66-1.52 (m, 1H), 1.41 (s, 9H), 1.39 (s, 9H), 1.40-1.20 (m, 11H), 0.88 (t, $J = 6.3$ Hz, 1H); ¹³C NMR (100 MHz, CDCl₃) δ 139.7, 116.5, 60.5, 60.1, 57.0, 56.9, 36.1, 32.1, 29.8, 29.72, 29.70, 29.52, 29.51, 29.0, 26.2, 22.9, 14.3. Anal. calcd. for C₂₂H₄₄N₂O₂S: C, 65.95; H, 11.07; N, 6.99. Found: C, 66.07; H, 10.91; N, 6.89.

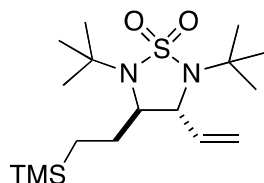
Table 4.1, entry 6 (rc_b9_32_2)



Colorless oil; $[\alpha]_{\text{D}}^{20} = +24.3$ (c 0.75, CHCl₃) (91% ee); IR (film) 1291, 1143 cm⁻¹; ¹H NMR (300 MHz, CDCl₃) δ 6.05 (ddd, $J = 16.8, 10.2, 6.9$ Hz, 1H), 5.36 (dd, $J = 16.8, 0.9$ Hz, 1H), 5.19 (dd, $J = 10.2, 0.9$ Hz, 1H), 3.73 (d, $J = 6.9$ Hz, 1H), 3.02 (dd, $J = 11.1, 2.4$ Hz, 1H), 1.97-1.81 (m, 1H), 1.80-1.54 (m, 6H), 1.40 (s, 9H), 1.38 (s, 9H), 1.28-1.12 (m, 6H), 0.80-0.99 (m, 2H); ¹³C NMR (100 MHz, CDCl₃) δ 139.6, 116.5, 60.9, 60.0, 56.9, 56.8, 37.8, 34.1, 33.8, 33.6, 33.3,

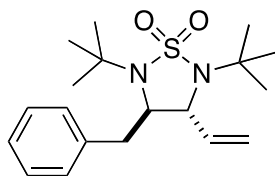
28.91, 28.89, 26.7, 26.5, 26.4; Anal. calcd. for C₂₀H₃₈N₂O₂S: C, 64.82; H, 10.34; N, 7.56.
Found: C, 64.64; H, 10.49; N, 7.28.

Table 4.1, entry 7 (rc_b9_10_3)



White solid; mp 129-131 °C; $[\alpha]_D^{20} = +30.0$ (c 0.83, CHCl₃) (91% ee); IR (film) 1279 cm⁻¹; ¹H NMR (300 MHz, CDCl₃) δ 6.06 (ddd, *J* = 17.1, 10.5, 6.6 Hz, 1H), 5.38 (d, *J* = 17.1 Hz, 1H), 5.21 (d, *J* = 10.5 Hz, 1H), 3.81 (d, *J* = 6.6 Hz, 1H), 2.97 (dd, *J* = 10.8, 2.7 Hz, 1H), 1.87-1.68 (m, 1H), 1.64-1.48 (m, 1H), 1.40 (s, 9H), 1.38 (s, 9H), 0.54 (td, *J* = 13.5, 4.2 Hz, 1H), 0.39 (td, *J* = 13.5, 4.2 Hz, 1H), 0.01 (s, 9H); ¹³C NMR (100 MHz, CDCl₃) δ 139.8, 116.5, 63.4, 59.4, 56.9, 30.5, 28.93, 28.90, 13.4, -1.66; HRMS calcd. for C₁₇H₃₆N₂NaO₂SSi (M+Na)⁺: 383.2159. Found: 383.2153.

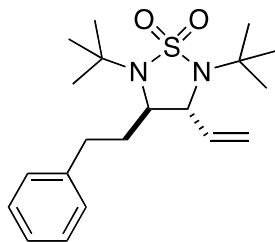
Table 4.1, entry 8 (rc_b9_10_1)



White solid; mp 86-88 °C; $[\alpha]_D^{20} = +23.3$ (c 0.90, CHCl₃) (93% ee); IR (film) 1398, 1292, 1143 cm⁻¹; ¹H NMR (400 MHz, CDCl₃) δ 7.39-7.33 (m, 2H), 7.31-7.25 (m, 1H), 7.24-7.19 (m, 2H), 5.95 (ddd, *J* = 17.2, 10.4, 6.8 Hz, 1H), 5.08 (d, *J* = 10.4 Hz, 1H), 5.04 (d, *J* = 17.2 Hz, 1H), 3.75 (d, *J* = 6.8 Hz, 1H), 3.48 (dd, *J* = 10.8, 4.4 Hz, 1H), 3.10 (dd, *J* = 14.0, 4.4 Hz, 1H) 3.03 (dd, *J* =

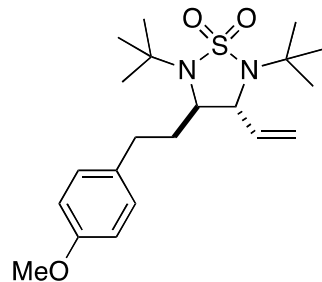
14.0, 10.8 Hz, 1H), 1.46 (s, 9H), 1.44 (s, 9H); ^{13}C NMR (100 MHz, CDCl_3) δ 139.4, 137.8, 129.2, 129.1, 127.2, 116.7, 61.4, 59.3, 57.5, 57.1, 42.0, 29.2, 29.0; HRMS calcd. for $\text{C}_{19}\text{H}_{30}\text{N}_2\text{NaO}_2\text{S}$ ($\text{M}+\text{Na}$) $^+$: 373.1920. Found: 373.1923.

Table 4.1, entry 9 (rc_b9_10_2)



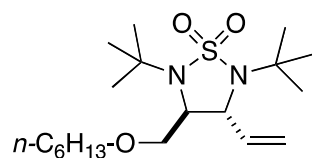
White solid; mp 50-54 °C; $[\alpha]_{\text{D}}^{20} = +20.0$ (c 0.39, CHCl_3) (92% ee); IR (film) 1454, 1286, 1142 cm^{-1} ; ^1H NMR (300 MHz, CDCl_3) δ 7.34-7.12 (m, 5H), 6.03 (ddd, $J = 16.8, 10.2, 6.9$ Hz, 1H), 5.33 (d, $J = 16.8$ Hz, 1H), 5.21 (d, $J = 10.2$ Hz, 1H), 3.75 (d, $J = 6.8$ Hz, 1H), 3.10 (dd, $J = 10.8, 2.4$ Hz, 1H), 2.86-2.72 (m, 1H), 2.70-2.57 (m, 1H), 2.34-2.17 (m, 1H), 2.20-1.86 (m, 1H), 1.40 (s, 9H), 1.31 (s, 9H); ^{13}C NMR (100 MHz, CDCl_3) δ 140.6, 139.2, 128.8, 128.6, 126.5, 116.8, 60.1, 59.5, 57.1, 56.9, 37.4, 32.6, 29.0, 28.8; HRMS calcd. for $\text{C}_{20}\text{H}_{32}\text{N}_2\text{NaO}_2\text{S}$ ($\text{M}+\text{Na}$) $^+$: 387.2077. Found: 387.2080.

Table 4.1, entry 10 (rc_b9_10_5)



Yellow solid; mp 46-50 °C; $[\alpha]_D^{20} = +11.8$ (c 0.60, CHCl₃) (90% ee); IR (film) 1612, 1513, 1466, 1286, 1142 cm⁻¹; ¹H NMR (400 MHz, CDCl₃) δ 7.09 (d, *J* = 8.8 Hz, 2H), 6.85 (d, *J* = 8.8 Hz, 2H), 6.04 (ddd, *J* = 16.8, 10.4, 6.8 Hz, 1H), 5.34 (d, *J* = 16.8 Hz, 1H), 5.21 (d, *J* = 10.4 Hz, 1H), 3.79 (s, 3H), 3.77 (d, *J* = 6.8 Hz, 1H), 3.09 (dd, *J* = 11.2, 2.4 Hz, 1H), 2.80-2.69 (m, 1H), 2.63-2.52 (m, 1H), 2.29-2.17 (m, 1H), 1.98-1.85 (m, 1H), 1.41 (s, 9H), 1.31 (s, 9H); ¹³C NMR (100 MHz, CDCl₃) δ 158.3, 139.2, 132.5, 129.5, 116.7, 114.2, 60.1, 59.4, 57.1, 56.9, 55.5, 37.5, 31.6, 29.0, 28.8; HRMS calcd. for C₂₁H₃₄N₂NaO₃S (M+Na)⁺: 417.2182. Found: 417.2195.

Table 4.1, entry 11 (rc_b8_6_11)

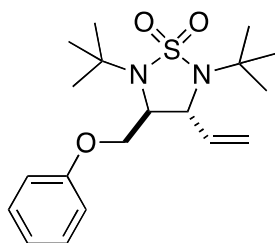


Pale yellow oil; $[\alpha]_D^{20} = +21.7$ (c 0.83, CHCl₃) (93% ee); IR (film) 1468, 1296, 1145 cm⁻¹; ¹H NMR (400 MHz, CDCl₃) δ 6.08 (ddd, *J* = 16.8, 10.4, 6.4 Hz, 1H), 5.44 (d, *J* = 16.8 Hz, 1H), 5.25 (d, *J* = 10.4 Hz, 1H), 4.15 (d, *J* = 6.4 Hz, 1H), 3.61-3.48 (m, 2H), 3.47-3.38 (m, 2H), 3.33 (dd, *J* = 10.8, 4.4 Hz, 1H), 1.65-1.53 (m, 2H), 1.43 (s, 9H), 1.40 (s, 9H), 1.40-1.22 (m, 6H), 0.90 (t, *J* = 6.4 Hz, 3H); ¹³C NMR (75 MHz, CDCl₃) δ 139.0, 117.1, 71.7, 58.8, 58.1, 57.1, 31.8,

29.7, 28.9, 28.8, 26.1, 22.8, 14.2; HRMS calcd. for $C_{19}H_{38}N_2NaO_3S$ ($M+Na$)⁺: 397.2495.

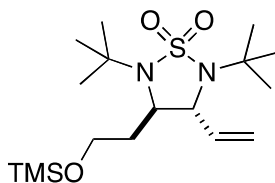
Found: 397.2488.

Table 4.1, entry 12 (rc_b8_28_8)



White solid; mp 80-82 °C; $[\alpha]_D^{20} = +42.6$ (c 0.97, $CHCl_3$) (93% ee); IR (film) 1600, 1498, 1398, 1295, 1144 cm^{-1} ; 1H NMR (300 MHz, $CDCl_3$) δ 7.38-7.25 (m, 2H), 7.03-6.90 (m, 3H), 6.14 (dddd, $J = 16.8, 10.2, 6.3, 0.9$ Hz, 1H), 5.50 (dd, $J = 16.8, 0.9$ Hz, 1H), 5.31 (dd, $J = 10.2, 0.9$ Hz, 1H), 4.21 (d, $J = 6.3$ Hz, 1H), 4.12 (t, $J = 9.6$ Hz, 1H), 3.95 (dd, $J = 9.6, 3.9$ Hz, 1H), 3.57 (dd, $J = 10.2, 3.9$ Hz, 1H), 1.43 (s, 9H), 1.39 (s, 9H); ^{13}C NMR (75 MHz, $CDCl_3$) δ 158.3, 138.5, 129.9, 121.7, 117.6, 114.8, 68.6, 58.6, 58.3, 57.35, 57.30, 28.9, 28.7; Anal. calcd. for $C_{19}H_{30}N_2O_3S$: C, 62.26; H, 8.25; N, 7.64. Found: C, 62.58; H, 8.08; N, 7.67.

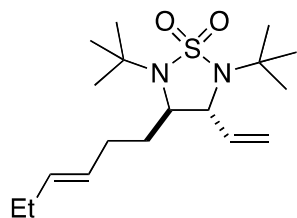
Table 4.1, entry 13 (rc_b8_34_2)



Colorless oil; $[\alpha]_D^{20} = +28.9$ (c 0.61, $CHCl_3$) (91% ee); IR (film) 1644, 1398, 1291 cm^{-1} ; 1H NMR (300 MHz, $CDCl_3$) δ 6.06 (ddd, $J = 17.1, 10.5, 6.9$ Hz, 1H), 5.33 (d, $J = 17.1$ Hz, 1H), 5.18 (d, $J = 10.5$ Hz, 1H), 3.99 (d, $J = 6.9$ Hz, 1H), 3.72-3.61 (m, 2H), 3.31 (dd, $J = 10.5, 2.4$ Hz, 1H), 2.15-2.00 (m, 1H), 1.85-1.72 (m, 1H), 1.37 (s, 9H), 1.35 (s, 9H), 0.08 (s, 9H); ^{13}C NMR

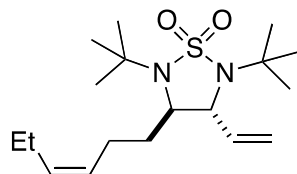
(75 MHz, CDCl₃) δ 139.4, 116.6, 60.7, 59.7, 58.6, 57.1, 56.9, 38.5, 29.0, 28.9, -0.47; Anal. calcd. for C₁₇H₃₆N₂O₃SSi: C, 54.21; H, 9.63; N, 7.44. Found: C, 54.02; H, 9.38; N, 7.55.

Table 4.1, entry 14 (rc_b8_6_6)



Colorless oil; $[\alpha]_D^{20} = +25.0$ (c 0.46, CHCl₃) (91% ee); IR (film) 1644, 1289, 1142 cm⁻¹; ¹H NMR (300 MHz, CDCl₃) δ 6.04 (ddd, $J = 16.8, 9.9, 6.6$ Hz, 1H), 5.57-5.44 (m, 1H), 5.42-5.30 (m, 1H), 5.34 (d, $J = 16.8$ Hz, 1H), 5.19 (d, $J = 10.2$ Hz, 1H), 3.78 (d, $J = 7.2$ Hz, 1H), 3.13 (dd, $J = 11.1, 2.7$ Hz, 1H), 2.22-1.88 (m, 5H), 1.74-1.56 (m, 1H), 1.39 (s, 9H), 1.37 (s, 9H), 0.95 (t, $J = 7.2$ Hz, 3H); ¹³C NMR (75 MHz, CDCl₃) δ 139.4, 134.0, 127.3, 116.5, 59.9, 59.5, 57.1, 56.9, 35.5, 29.2, 28.9, 25.7, 14.0; Anal. calcd. for C₁₈H₃₄N₂O₂S: C, 63.11; H, 10.00; N, 8.18. Found: C, 63.34; H, 9.89; N, 7.93.

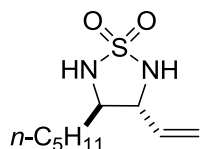
Table 4.1, entry 15 (rc_b8_6_5)



Colorless oil; $[\alpha]_D^{20} = +27.2$ (c 1.2, CHCl₃) (91% ee); IR (film) 1727, 1644, 1398, 1290, 1143 cm⁻¹; ¹H NMR (300 MHz, CDCl₃) δ 6.06 (ddd, $J = 17.1, 10.2, 6.9$ Hz, 1H), 5.52-5.24 (m, 2H), 5.36 (d, $J = 17.1$ Hz, 1H), 5.21 (d, $J = 10.2$ Hz, 1H), 3.79 (d, $J = 6.9$ Hz, 1H), 3.11 (dd, $J = 10.8, 2.4$ Hz, 1H), 2.24-1.90 (m, 5H), 1.74-1.58 (m, 1H), 1.41 (s, 9H), 1.38 (s, 9H), 0.97 (t, $J = 7.8$ Hz,

3H); ^{13}C NMR (75 MHz, CDCl_3) δ 139.4, 133.3, 127.2, 116.7, 60.1, 59.7, 57.1, 56.9, 35.8, 29.0, 28.9, 23.7, 20.8, 14.4; Anal. calcd. for $\text{C}_{18}\text{H}_{34}\text{N}_2\text{O}_2\text{S}$: C, 63.11; H, 10.00; N, 8.18. Found: C, 62.83; H, 9.82; N, 7.96.

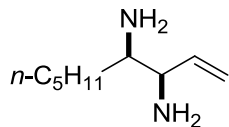
Scheme 4.7 (rc_b9_38_2) 4-23d



Yellow Oil; $[\alpha]_{\text{D}}^{20} = +25.6$ (c 0.5, CHCl_3) (91% ee); IR (film) 3255, 1302, 1168 cm^{-1} ; ^1H NMR (300 MHz, CDCl_3) δ 5.80 (ddd, $J = 16.8, 10.5, 7.5$ Hz, 1H), 5.40 (d, $J = 16.8$ Hz, 1H), 5.33 (d, $J = 10.5$ Hz, 1H), 4.61 (d, $J = 6.0$ Hz, 1H), 4.54 (d, $J = 8.4$ Hz, 1H), 3.96-3.80 (m, 1H), 3.52-3.41 (m, 1H), 1.75-1.24 (m, 8H), 0.89 (t, $J = 6.9$ Hz, 3H); ^{13}C NMR (100 MHz, CDCl_3) δ 133.8, 120.8, 66.4, 63.0, 32.3, 31.6, 26.4, 22.6, 14.1; Anal. calcd. for $\text{C}_9\text{H}_{18}\text{N}_2\text{O}_2\text{S}$: C 49.51, H 8.31, N 12.83; found: C 49.43, H 8.11, N 12.90.

Cornwall, R.G.; Zhao, B.; Shi, Y. *Org. Lett.* **2011**, *13*, 434.

Scheme 4.7 (rc_b9_38) 4-24d

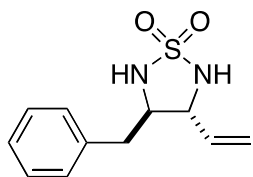


Pale yellow oil; $[\alpha]_{\text{D}}^{20} = +29.5$ (c 0.84, CHCl_3) (91% ee); IR (film) 3369, 3593, 2927, 2857, 1466 cm^{-1} ; ^1H NMR (400 MHz, CDCl_3) δ 5.84 (ddd, $J = 12.6, 7.5, 4.8$, 1H), 5.19 (d, $J = 12.6$ Hz, 1H), 5.12 (d, $J = 7.5$ Hz, 1H), 3.17 (t, $J = 4.8$, 1H), 2.61 (dd, $J = 6.0, 3.3$, 1H), 1.57-1.40 (m, 2H), 1.38-1.16 (m, 10H), 0.90 (t, $J = 4.8$); ^{13}C NMR (100 MHz, CDCl_3) δ 141.7, 115.0, 59.2,

55.7, 34.6, 32.2, 26.4, 22.9, 14.3.

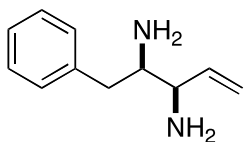
Zhao, B.; Peng, X.; Cui, S.; Shi, Y. *J. Am. Chem. Soc.* **2010**, *132*, 11009.

Scheme 4.7 (rc_b9_38_2) 4-23h



White solid; mp 77-79 °C; $[\alpha]_{\text{D}}^{20} = +24.3$ (c 0.75, CHCl₃) (93% ee); IR (film) 3261, 1497, 1167 cm⁻¹, ¹H NMR (300 MHz, CDCl₃) δ 7.40-7.19 (m, 5H), 5.76 (ddd, $J = 17.1, 9.9, 7.2$ Hz, 1H), 5.38 (d, $J = 17.1$ Hz, 1H), 5.29 (d, $J = 9.9$ Hz, 1H), 4.85 (d, $J = 6.0$ Hz, 1H), 4.67 (d, $J = 7.2$ Hz, 1H), 4.10-3.96 (m, 1H), 3.80-3.65 (m, 1H), 2.99 (dd, $J = 14.1, 4.8$ Hz, 1H), 2.88 (dd, $J = 14.1, 8.7$ Hz, 1H); ¹³C NMR (75 MHz, CDCl₃) δ 136.6, 133.6, 129.3, 129.0, 127.3, 120.7, 64.9, 63.5, 38.4. HRMS calcd. for C₁₁H₁₅N₂O₂S (M+H⁺): 239.0849. Found: 239.0847.

Scheme 4.7 (rc_b9_38) 4-24h



Pale yellow oil; $[\alpha]_{\text{D}}^{20} = +43.7$ (c 0.71, CHCl₃) (93% ee); IR (film) 3374, 3295, 1639, 1602, 1495, 1453 cm⁻¹; ¹H NMR (400 MHz, CDCl₃) δ 7.35-7.28 (m, 2H), 7.25-7.19 (m, 3H), 5.92 (ddd, $J = 17.2, 10.4, 6.4$ Hz, 1H), 5.25 (d, $J = 17.2$ Hz, 1H), 5.18 (d, $J = 10.4$ Hz, 1H), 3.29-3.22 (m, 1H), 2.99-2.89 (m, 2H), 2.50 (dd, $J = 14.4, 10.4$ Hz, 1H), 1.18 (brs, 4H); ¹³C NMR (100 MHz, CDCl₃) δ 141.5, 139.8, 129.4, 128.7, 126.5, 115.4, 58.7, 57.1, 41.2.

Du, H.; Yuan, W.; Zhao, B.; Shi, Y. *J. Am. Chem. Soc.* **2007**, *129*, 11688.

4.6 REFERENCES

¹ (a) Rosenberg, S.H.; Dellaria, J.F.; Kempf, D.J.; Hutchins, C.W.; Woods, K.W.; Maki, R.G.; de Lara, E.; Spina, K.P.; Stein, H.H; Cohen, J.; Baker, W.R.; Plattner, J.J.; Kleinert, H.D.; Perun, T.J. *J. Med. Chem.* **1990**, *33*, 1582. (b) Castro, J.L.; Baker, R.; Guiblin, A.R.; Hobbs, S.C.; Jenkins, M.R.; Russell, M.G.N.; Beer, M.S.; Stanton, J.A.; Scholey, K.; Hargreaves, R.J.; Graham, M.I.; Matassa, V.G. *J. Med. Chem.* **1994**, *37*, 3023. (c) McDonald, I.M.; Dunstone, D.J.; Tozer, M.J. WO-9905141 **1999** [*Chem. Abst.* **1999**, *130*, 168372]. (d) Tung, R.D.; Salituro, F.G.; Deininger, D.D.; Bhisetti, G.R.; Baker, C.T.; Spaltenstein, A. US-5945413 **1999** [*Chem. Abst.* **1999**, *131*, 185247]. (e) Cherney, R.J.; King, B.W. WO-0228846 **2002** [*Chem. Abst.* **2002**, *136*, 309923]. (f) Zhong, J.; Gan, X.; Alliston, K.R.; Groutas, W.C. *Bioorg. Med. Chem.* **2004**, *12*, 589 (g) Zhong, J.; Gan, X.; Alliston, K.R.; Lai, Z.; Yu, H.; Groutas, C.S.; Wong, T.; Groutas, W.C. *J. Comb. Chem.* **2004**, *6*, 556. (h) Bendjeddou, A.; Djeribi, R.; Regainia, Z.; Aouf, N.-E. *Molecules*, **2005**, *10*, 1387. (i) Sparey, T.; Beher, D.; Best, J.; Biba, M.; Castro, J.L.; Clarke, E.; Hannam, J.; Harrison, T.; Lewis, H.; Madin, A.; Shearman, M.; Sohal, B.; Tsou, N.; Welch, C.; Wrigley, J. *Bioorg. Med. Chem. Lett.* **2005**, *15*, 4212. (j) Winum, J.-Y.; Scozzafava, A.; Montero, J.-L.; Supuran, C.T. *Med. Res. Rev.* **2006**, *26*, 767. (k) Winum, J.-Y.; Scozzafava, A.; Montero, J.-L.; Supuran, C.T. *Expert Opin. Ther. Patents* **2006**, *16*, 27. (l) Yang, Q.; Li, Y.; Dou, D.; Gan, X.; Mohan, S.; Groutas, C.S.; Stevenson, L.E.; Lai, Z.; Alliston, K.R.; Zhong, J.; Williams, T.D.; Groutas, W.C. *Arch. Biochem. Biophys.* **2008**, *475*, 115. (m) Benlifa, M.; García Moreno, M.I.; Mellet, C.O.; García Fernández, J.M.; Wadouachi, A. *Bioorg. Med. Chem. Lett.* **2008**, *18*, 2805. (n) Kim, S.J.; Jung, M.-H.; Yoo, K.H.; Cho, J.-H.; Oh, C.-H. *Bioorg. Med. Chem. Lett.* **2008**, *18*, 5815. (o) Dou, D.; Tiew, K.-C.; He, G.; Mandadapu, S.R.; Aravapalli, S.; Alliston, K.R.; Kim, Y.; Chang, K.-O.; Groutas, W.C. *Bioorg. Med. Chem.* **2011**, *19*, 5975. (p) Dou, D.; Mandadapu, S.R.; Alliston, K.R.; Kim, Y.; Chang, K.-O.; Groutas, W.C. *Eur. J. Med. Chem.* **2012**, *47*, 59. (q) Brodney, M.A.; Barreiro, G.; Ogilvie, K.; Hajos-Korcsok, E.; Murray, J.; Vajdos, F.; Ambroise, C.; Christofferson, C.; Fisher, K.; Lanyon, L.; Liu, J.; Nolan, C.E.; Withka, J.W.; Borzilleri, K.A.; Efremov, I.; Oborski, C.E.; Varghese, A.; O'Neill, B.T. *J. Med. Chem.* **2012**, *55*, 9224.

² (a) Ahn, K.H.; Yoo, D.J.; Kim, J.S. *Tetrahedron Lett.* **1992**, *33*, 6661 (b) Fécourt, F.; Lopez, G.; Van Der Lee, A.; Martinez, J.; Dewynter, G. *Tetrahedron: Asymmetry.* **2010**, *21*, 2361.

³ (a) Regainia, Z.; Abdaoui, M.; Aouf, N.-E.; Dewynter, G.; Montero, J.-L. *Tetrahedron* **2000**, *56*, 381 (b) Berredjem, M.; Djebbar, H.; Regainia, Z.; Aouf, N.-E.; Dewynter, G.; Winum, J.-Y.; Montero, J.-L. *Phosphorus, Sulfur Silicon Relat. Elem.* **2003**, *178*, 693 (c)

⁴ Kim, I.-W.; Jung, S.-H. *Arch. Pharm. Res.* **2002**, *25*, 421.

⁵ Lee, S.A.; Kwak, S.H.; Lee, K.-I. *Chem. Commun.* **2011**, *47*, 2372.

⁶ For leading references on the synthesis of phosphoramidite and TADDOL-derived phosphoramidite ligands, see: (a) Seebach, D.; Dahinden, R.; Marti, R.E.; Beck, A.K.; Plattner, D.A.; Kühnle, F.N.M. *J. Org. Chem.* **1995**, *60*, 1788 (b) Beck, A.K.; Bastani, B.; Plattner, D.A.; Petter, W.; Seebach, D.; Braunschweiger, H.; Gysi, P.; La Lecchia, L. *Chimia* **1991**, *45*, 238 (c) Harada, H.; Thalji, R.K.; Bergman, R.G.; Ellman, J.A. *J. Org. Chem.* **2008**, *73*, 6772 (d) Smith, C.R.; Mans, D.J.; Rajanbabu, T.V. *Org. Synth.* **2008**, *85*, 238.

⁷ Cornwall, R.G.; Zhao, B.; Shi, Y. *Org. Lett.* **2013**, *15*, 796.

⁸ (a) Du, H.; Yuan, W.; Zhao, B.; Shi, Y. *J. Am. Chem. Soc.* **2007**, *129*, 11688 (b) Du, H.; Zhao, B.; Shi, Y. *J. Am. Chem. Soc.* **2008**, *130*, 8590 (c) Zhao, B.; Du, H.; Fu, R.; Shi, Y. *Org. Synth.* **2010**, *87*, 263.

⁹ Zhao, B.; Peng, X.; Cui, S.; Shi, Y. *J. Am. Chem. Soc.* **2010**, *132*, 11009.

¹⁰ (a) Fourgeaud, P.; Midrier, C.; Vors, J.-P.; Volle, J.-N.; Pirat, J.-L.; Virieux, D. *Tetrahedron* **2010**, *66*, 758 (b) Krauss, G.A.; Kim, J. *Org. Lett.* **2004**, *6*, 3115.

¹¹ (a) Maruyama, K.; Nagai, N.; Naruta, Y. *J. Org. Chem.* **1986**, *51*, 5083 (b) Kimura, M.; Ezo, A.; Mori, M.; Tamaru, Y. *J. Am. Chem. Soc.* **2005**, *127*, 201.

¹² (a) Stevens, R.V.; Cherpeck, R.E.; Harrison, B.L.; Lai, J.; Lapalme, R. *J. Am. Chem. Soc.* **1976**, *98*, 6317 (b) Miller, C.A.; Batey, R.A. *Org. Lett.* **2004**, *6*, 699.

¹³ Haynes, R.K.; Lam, K.-P.; Wu, K.-Y.; Williams, I.D.; Yeung, L.-L. *Tetrahedron* **1999**, *55*, 89.

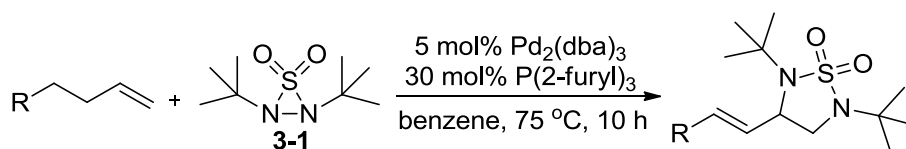
¹⁴ Pansare, S.V.; Rai, A.N.; Kate, S.N. *Synlett* **1998**, 623.

¹⁵ See rc_b9_18 and rc_b9_20.

5.1 Pd(II)-CATALYZED TERMINAL DIAMINATION

5.1.1 Background

As discussed in Chapter 3, diamination of terminal olefins using Pd and thiadiaziridine **3-1** resulted in overall dehydrogenative diamination (Scheme 5.1).¹ In a related reaction, it was also shown that under the same reaction conditions and with a conjugated diene as substrate, a mixture of internal and terminal diamination products was observed. Because Pd was thought to only provide internal diamination of diene substrates, it was of interest to investigate how terminal diamination could be obtained using Pd as catalyst.



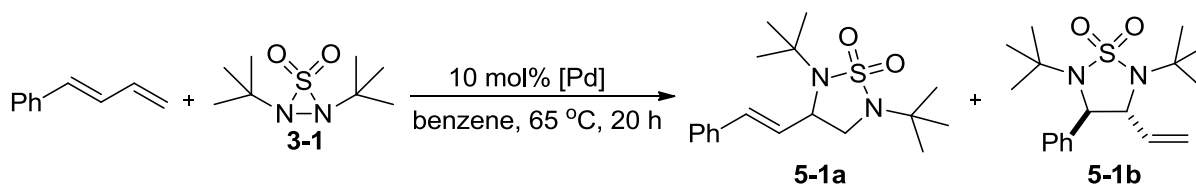
Scheme 5.1

5.1.2 Results and Discussion

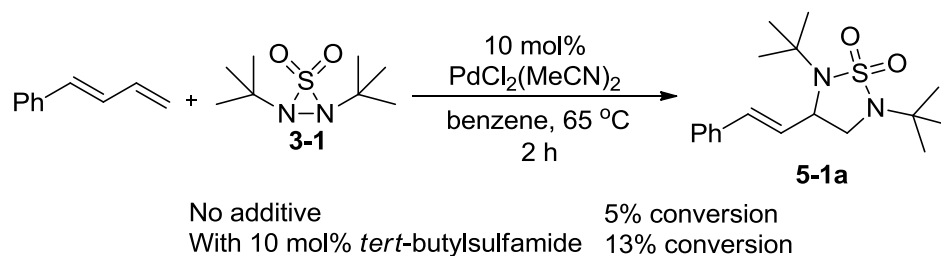
Using 1-phenyl-1,3-butadiene as substrate, various Pd catalysts were screened (Table 5.1). Both Pd(II) (Table 5.1, entries 1-7) as well as Pd(0) (Table 5.1, entries 8-10) gave good conversions but PdCl₂(MeCN)₂ provided the highest conversion and exclusive terminal diamination in 30% yield (Table 5.1, entry 6).² Upon screening ligands for the reaction, conversions were lowered, apparently hindering the reaction. When diisopropyl ethylamine was added, conversion increased to 100%, but yield remained at 30%. It was also noticed that upon

addition of sulfur urea, the reaction sped up (Scheme 5.2). Using only *tert*-butylsulfamide, without thiadiaziridine **3-1**, however resulted in no reaction.

Table 5.1 Pd Screening for Terminal Diamination of Conjugated Dienes



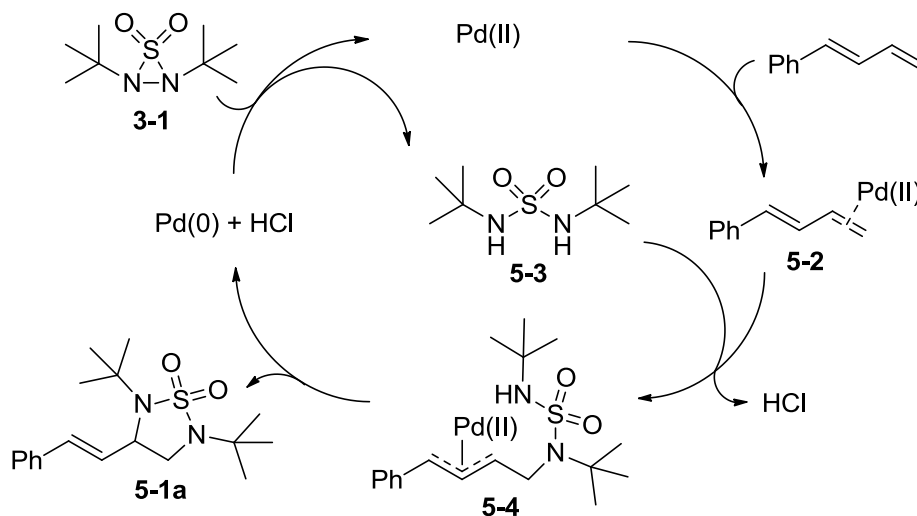
Entry	Catalyst	Conversion	Selectivity (5-1a : 5-1b)
1	PdCl ₂	50	1 : 0
2	Pd(OAc) ₂	18	-
3	PdI ₂	4	-
4	Pd(TFA) ₂	65	1.1 : 1
5	PdCl ₂ (CNPh) ₂	56	1 : 0
6	PdCl ₂ (MeCN) ₂	83 (30% yield)	1 : 0
7	PdCl ₂ (cod)	67	1 : 0
8	Pd(dppe) ₂	0	-
9	Pd ₂ (dba) ₃	28	1 : 0
10	Pd(PPh ₃) ₄	56	1 : 1.6



Scheme 5.2

5.1.3 Mechanistic Hypothesis

Using the above observations, the following mechanism was hypothesized (Scheme 5.3). The Pd(II) catalyst complexes with the conjugated diene to give **5-2** whereupon nucleophilic attack of *tert*-butylsulfamide (**5-3**) gives π -allyl Pd(II) complex **5-4**. Addition of the second nitrogen closes the ring to form product **5-1a** and generates Pd(0) and HCl. Thiadiaziridine **3-1** acts as an oxidant to oxidize Pd(0) back to Pd(II), regenerating the active catalyst. Addition of base (ie. diisopropyl ethylamine) is beneficial to the reaction as it could serve to deprotonate the *tert*-butyl sulfamide **5-3**.



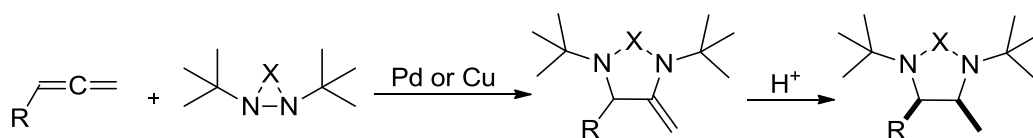
Scheme 5.3

Polymerization was a major problem and attempts to decrease polymerization and increase yield via drop-wise addition of **3-1** and lower reaction temperature, were unsuccessful. Addition of 5 mol% benzoquinone however increased yield to 40%. The reaction parameters screened as well as the proposed mechanism was very similar to those reported by Lloyd-Jones, Booker-Milburn and coworkers³ and therefore, this project was pursued no further.

5.2 METAL-CATALYZED DIAMINATION OF ALLENES

5.2.1 Results and Discussion

Of the many methods to synthesize vicinal diamines, the synthesis of cis-diamines presents an especially unique challenge. It was proposed that cis-diamines could be obtained via the diamination of allenes and subsequent hydrogenation to give the desired stereochemistry (Scheme 5.4).

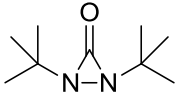
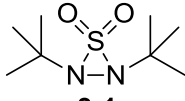
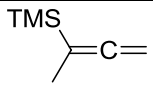
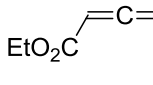
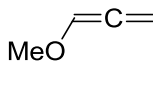
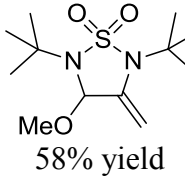


Scheme 5.4

Diamination conditions involving nitrogen sources **1-17** and **3-1**, as well as both Pd and Cu catalysts are summarized in Table 5.2.⁴ Diaziridinone **1-17** showed little to no reactivity with Pd or Cu catalysts. Thiadiaziridine **3-1** also displayed little to no reactivity with electron withdrawing allenes but the electron donating methoxy allene gave 100% conversion under both Pd and Cu catalysis conditions. The internal diamination product was inferred based on ¹H NMR analysis of the purified product. The product was stable enough for purification on silica gel

however, it is likely acid sensitive. Judging from these results, the diamination of allenes is an interesting project but at this time is likely limited in scope/applicability.

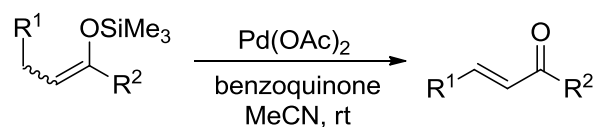
Table 5.2 Diamination of Allenes

	 1-17			 3-1		
	Pd(PPh ₃) ₄	CuCl/P(<i>n</i> -Bu) ₃	CuBr	Pd(PPh ₃) ₄	CuCl/P(<i>n</i> -Bu) ₃	CuBr
	Decomp	NR	NR	Decomp	NR	NR
	NR	NR	NR	NR	NR	NR
	NR	Low conv	Low conv	40% yield	 58% yield	62% yield

5.3 OXIDATION OF ALCOHOLS

5.3.1 Background

The Saegusa oxidation is a well-known organic reaction for the efficient conversion of silyl enol ethers to the corresponding α,β -unsaturated carbonyls and remains a leading method for the synthesis of α,β -unsaturated carbonyls (Scheme 5.5).⁵ Recently, Shi and coworkers have reported alternative uses for diaziridinone **1-17** as an oxidative reagent such as mediating the coupling of anilines to form azo compounds and hydrazines,⁶ as well as the Cu(I)-catalyzed oxidation of alcohols to ketones and aldehydes (Figure 5.1).⁷ A variety of primary and secondary alcohols can be smoothly oxidized using CuBr as catalyst to give the corresponding aldehydes and ketones in high yields.



Scheme 5.5

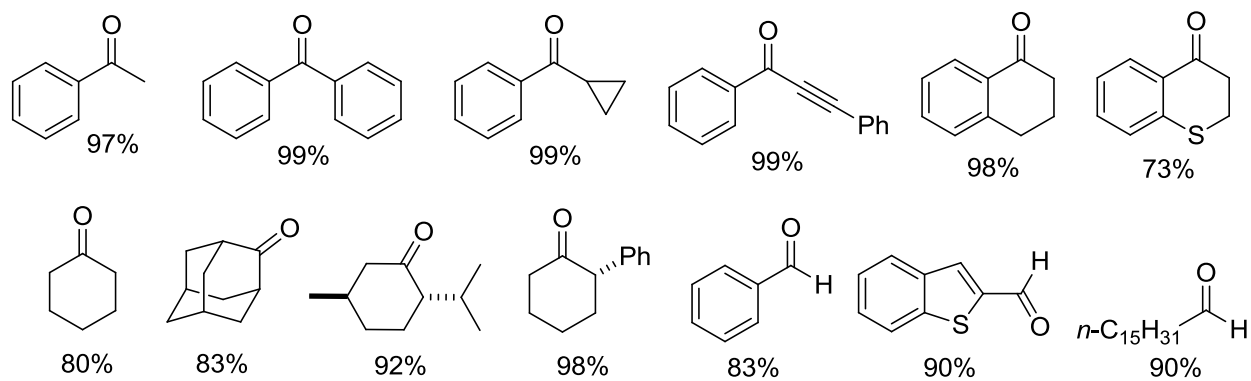
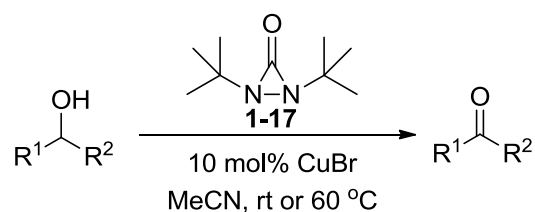
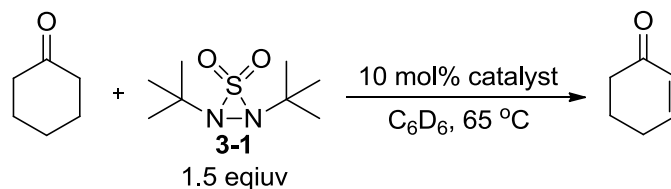


Figure 5.1

5.3.2 Result and Discussion

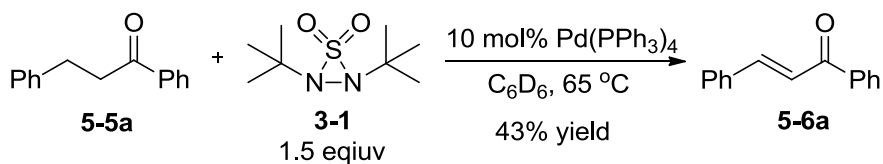
Along the same lines employing diaziridinone and thiadiaziridine as oxidizing reagents, it was envisioned that the dehydrogenation of carbonyls could be accomplished. Cyclohexanone was employed to test this hypothesis (Table 5.3).⁸ Good conversion was obtained using Pd as catalyst with either oxidant; however, separation of the starting material, product and urea byproduct was very difficult by silica gel chromatography. Because of this, an alternate substrate was screened.

Table 5.3 Initial Screening for Oxidation of Cyclohexanone



Entry	Catalyst	Oxidant	Conversion (%)
1	Pd(PPh ₃) ₄		~58
2	CuBr		NR
3	CuCl/P(<i>n</i> -Bu) ₃		NR
4	Pd(PPh ₃) ₄		70

Acyclic ketone 1,3-diphenylpropanone (**5-5a**), was converted to chalcone (**5-6a**) in 67% conversion and separation on silica gel chromatography using Pentane:Et₂O 100:1 gave the pure product in 43% yield as a light yellow solid (Scheme 5.6).

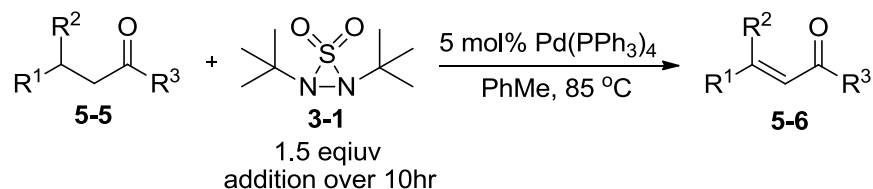


Scheme 5.6

Catalyst loading was investigated next and any lowering from 10 mol% Pd(PPh₃)₄ resulted in diminished conversion. Screening of the addition of various phosphorus ligands also resulted in

diminished reactivity. Slow addition of thiadiaziridine **3-1** produced a noticeable increase in conversion and upon raising the reaction temperature to 85 °C, the catalyst loading could be reduced to 5 mol%. The oxidation of 1,3-diphenylpropanone (**5-5a**) was accomplished in 72% yield (Table 5.4, Entry 1).⁹ Unfortunately, without aryl groups at the R¹ and R³ positions, no reaction took place (Table 5.4, entries 2,3). Sterically bulky **5-5d** was very reactive and oxidation occurred cleanly in 81% yield (Table 5.4, entry 4). Cyclic ketones also provided good conversion, however separation and volatility made purification difficult (Table 5.4, entries 5,6). α -Substitution also diminished reactivity (Table 5.4, entries 8,9). α -Methyl cyclohexanone was selectively oxidized at the least hindered position, albeit in 43% conversion (Table 5.4, entry 9). The oxidation of aldehydes was also investigated (Table 5.4, entries 10-14). 3-Phenylpropanal (**5-5j**) was oxidized in 100% conversion and 5-hexanal (**5-5l**) and isobutyraldehyde (**5-5n**) were oxidized in ~50% conversion, whereas other aldehydes screened gave no conversion. It is known that acyclic ketones and aldehydes are less reactive than their cyclic counterparts and it is hypothesized that optimal conditions exist for each substrate class.

Table 5.4 Oxidation to α,β -Unsaturated Carbonyls^a

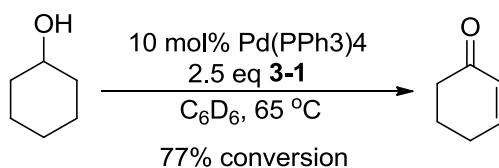


Entry	Substrate (5-5)	Product (5-6)	Conversion (%)
1	5-5a , R ¹ , R ³ = Ph, R ² = H	5-6a	78 (72% yield)
2	5-5b , R ¹ = CH ₃ , R ² = H, R ³ = Ph	5-6b	NR
3	5-5c , R ¹ , R ³ = CH ₃ , R ² = H	5-6c	NR
4	5-5d , R ¹ , R ² , R ³ = Ph	5-6d	81% yield
5	5-5e , X = CH ₂	5-6e	71
6	5-5f , X = O	5-6f	63
7	5-5g , X = CHPh	5-6g	NR
8	5-5h	5-6h	NR
9	5-5i	5-6i	43
10	5-5j , R = Ph	5-6j	100
11	5-5k , R = H	5-6k	NR
12	5-5l , R = Et	5-6l	45
13	5-5m , R = SMe	5-6m	NR
14	5-5n	5-6n	50

^a All reactions were carried out with ketone or aldehyde **5-5** (0.40 mmol), Pd(PPh₃)₄ (0.020 mmol) in toluene (0.1 mL) at 85 °C with slow addition of **3-1** (0.6 mmol) for 24 h, unless

otherwise stated. Entries 5,6,10-14 were carried out at 65 °C. For entries 11-14, **3-1** was added in one portion.

It was also observed that the oxidation from alcohols to α,β -unsaturated carbonyls could be accomplished using 2.5 equivalents of oxidant **3-1** (Scheme 5.7).¹⁰ Employing Pd(PPh₃)₄ as catalyst and 2.5 equivalents of oxidant **3-1** at 65 °C gave cyclohexenone in 77% conversion. 1,3-diphenyl-1-propanol was also oxidized directly to chalcone, but a complex mixture of products was formed.



Scheme 5.7

5.4 CONCLUSION

Thiadiaziridine **3-1** is a highly effective diamination reagent to install vicinal diamine functionality across olefins employing Pd or Cu as catalyst. This versatility is demonstrated by Pd(II)-catalyzed terminal diamination of conjugated dienes and Pd(0) or Cu(I)-catalyzed diamination of electron-rich allenes. The oxidation of alcohols and ketones/aldehydes to the corresponding α,β -unsaturated carbonyls using **3-1** as oxidant demonstrates the untapped potential for the strained three-membered ring as a versatile organic reagent.

5.5 REFERENCES

¹ Wang, B.; Du, H.; Shi, Y. *Angew. Chem. Int. Ed.* **2008**, *47*, 8224.

² See: rc_b5_22, rc_b5_28 and rc_b5_35.

³ Bar, G.L.J.; Lloyd-Jones, G.C.; Booker-Milburn, K.I. *J. Am. Chem. Soc.* **2005**, *127*, 7308.

⁴ See: rc_b10_17, rc_b10_19 and rc_b10_21.

⁵ Ito, Y.; Hirao, T.; Saegusa, T. *J. Org. Chem.* **1978**, *43*, 1011.

⁶ Zhu, Y.; Shi, Y. *Org. Lett.* **2013**, *15*, 1942.

⁷ Zhu, Y.; Zhao, B.; Shi, Y. *Org. Lett.* **2013**, *15*, 992.

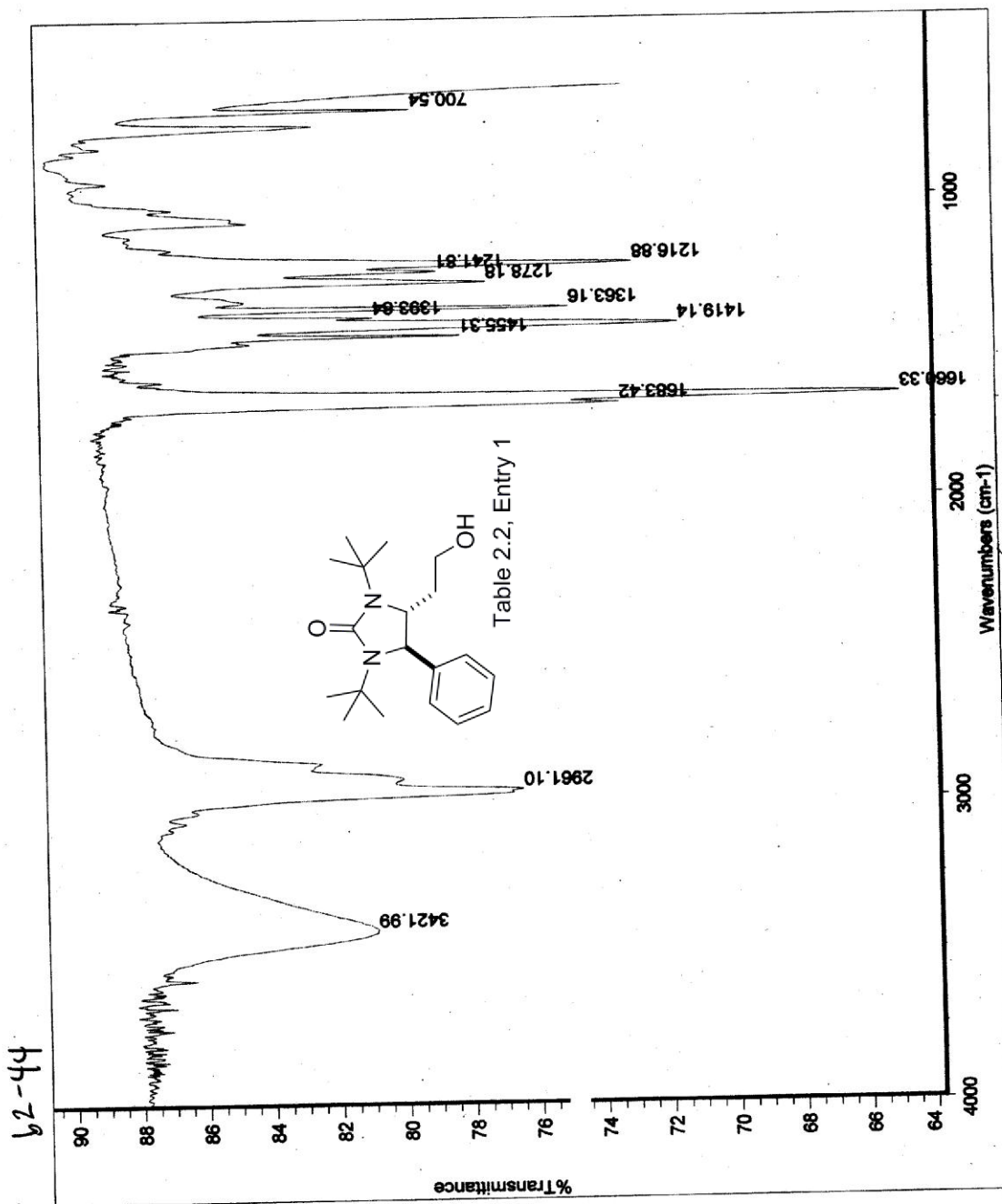
⁸ See: rc_b10_23 and rc_b10_45.

⁹ For substrate screening, see: rc_b11_27 and rc_b11_31.

¹⁰ See: rc_b10_46.

SUPPLEMENTAL

Appendix 1 Spectra for Chapter 2



STANDARD 1H OBSERVE

Pulse Sequence: s2pul

Solvent: CDCl3

Ambient Temperature:

File: rC_b2_d4_mocremat_pure

INDVA-500 "epox148"

Relax. delay 0.000 sec

Pulse 26.0 degrees

Time 2.695 sec

Width 595.2 Hz

4 repetitions

OBSERVE H1, 300.1592196 MHZ

DATA PROCESSING

Gauss apodization 0.896 sec

File size 327.06

Total time 0 min, 16 sec

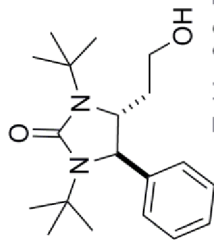
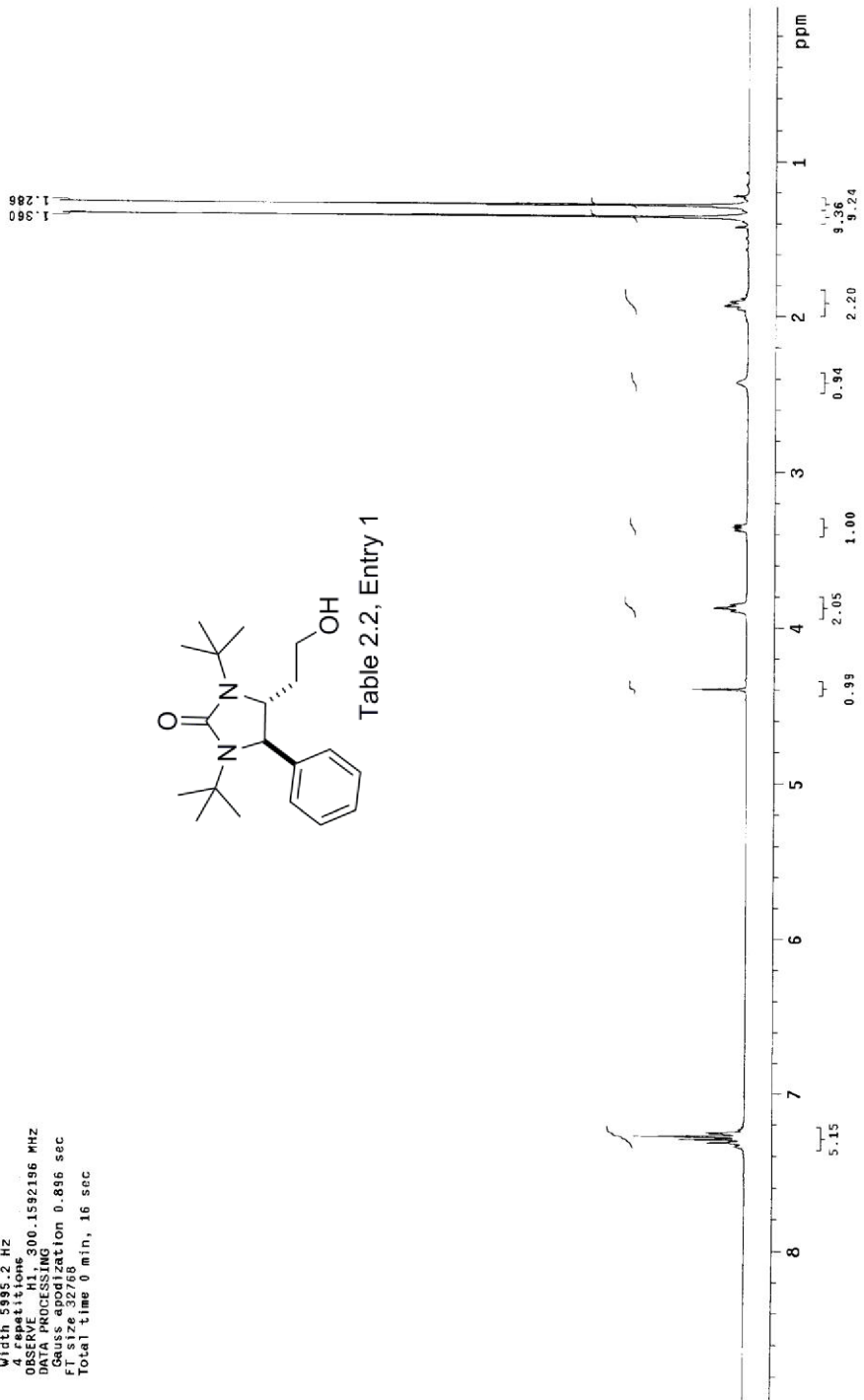


Table 2.2, Entry 1



13C OBSERVE

Pulse Sequence: s2pu1
Solvent: CDCl3
Ambient Temperature
File: r_c_b2_70_carbon
INOVA-500 "epoxide"

Relax. delay 1.000 sec
Pulse prog. 46.3 degrees
Acq. time 0.00000000 sec
Width 22935.8 Hz
175 repetitions
OBSERVE C13, 75.4750832 MHZ
DECUPLE H1, 300.1606799 MHZ
Contingency on
WALTZ-16 modulated
DATA PROCESSING
Line broadening 2.0 Hz
FT size 32788
Total time 473916 hr., 13 min, 52 sec

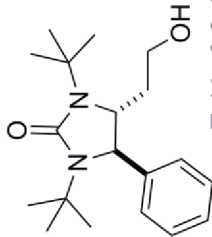
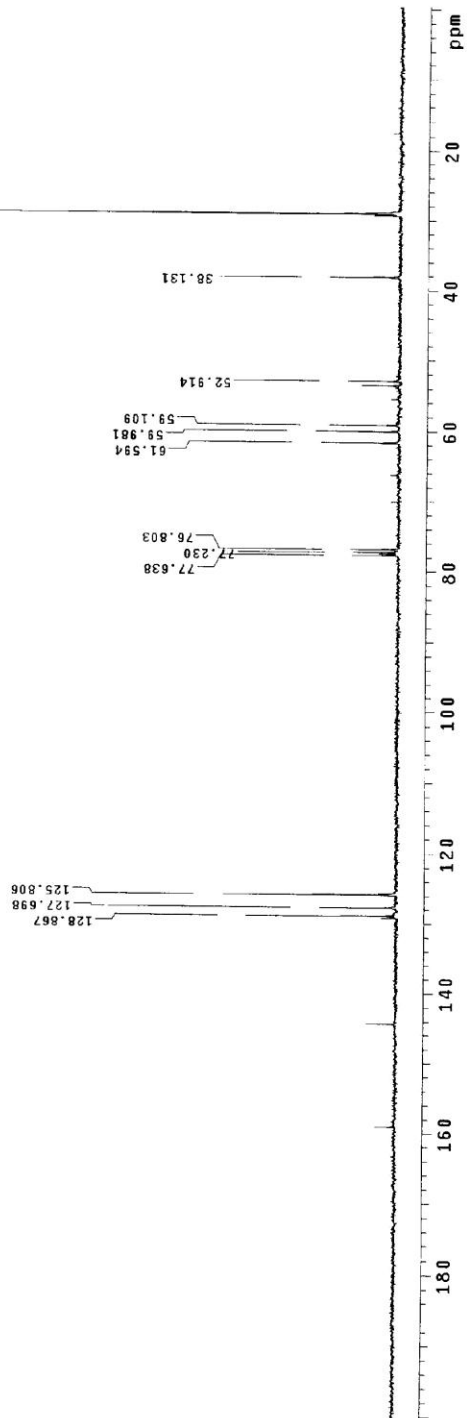
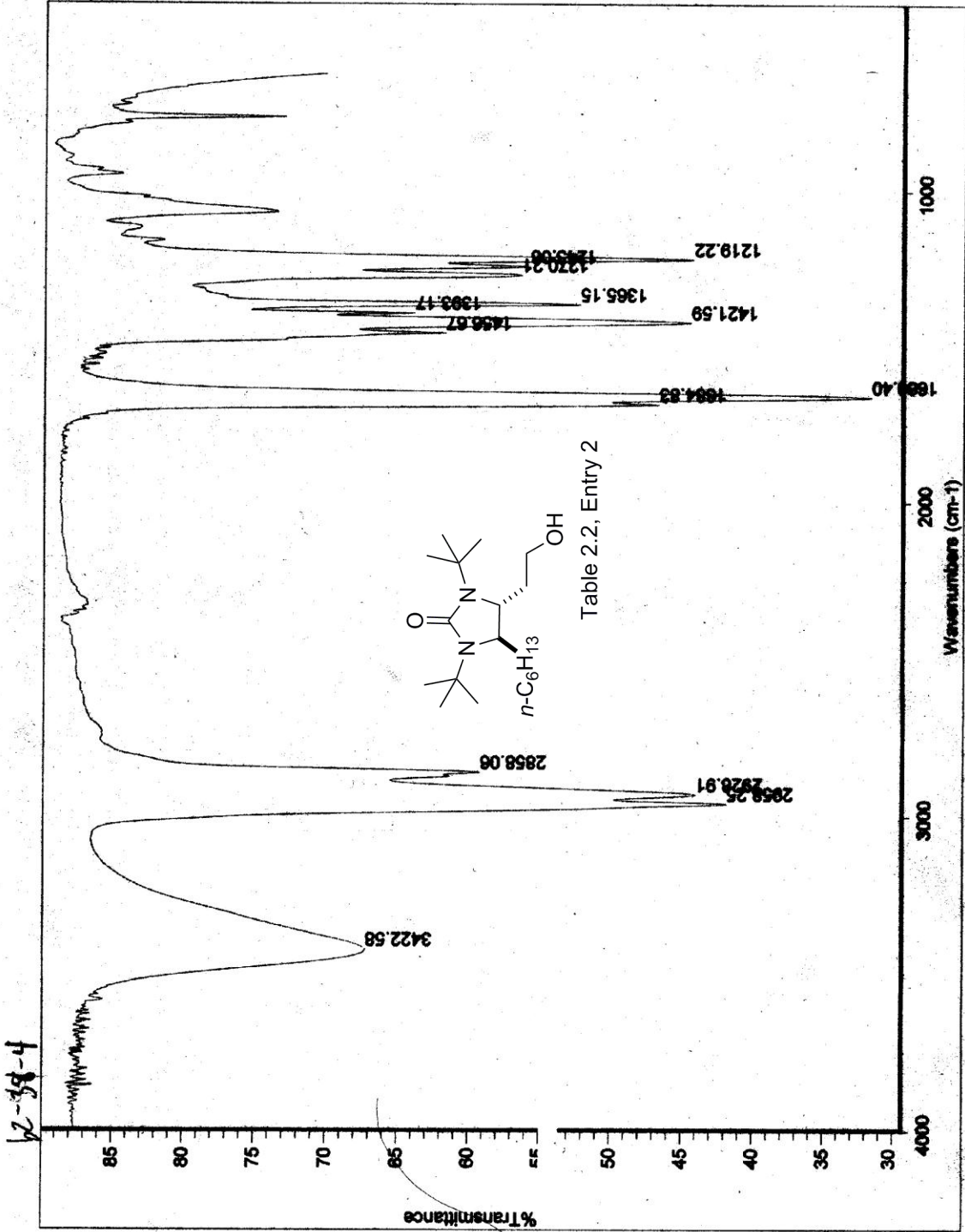


Table 2.2, Entry 1





STANDARD 1H OBSERVE

Pulse Sequence: s2pul
Solvent: CDCl3
Ambient Temperature
File: rc_b3_5_1_pure
INOVA-500 1Hepoxidin

Relax. delay 0.000 sec
Pulse 26.0 degrees
Width 6.000 sec
Width 5995.2 Hz
4 repetitions
OBSERVE H1, 300.1592167 MHz
DATA PROCESSING
Gauss apodization 0.396 sec
F2 size 65536
Total time 0 min, 16 sec

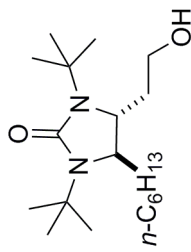
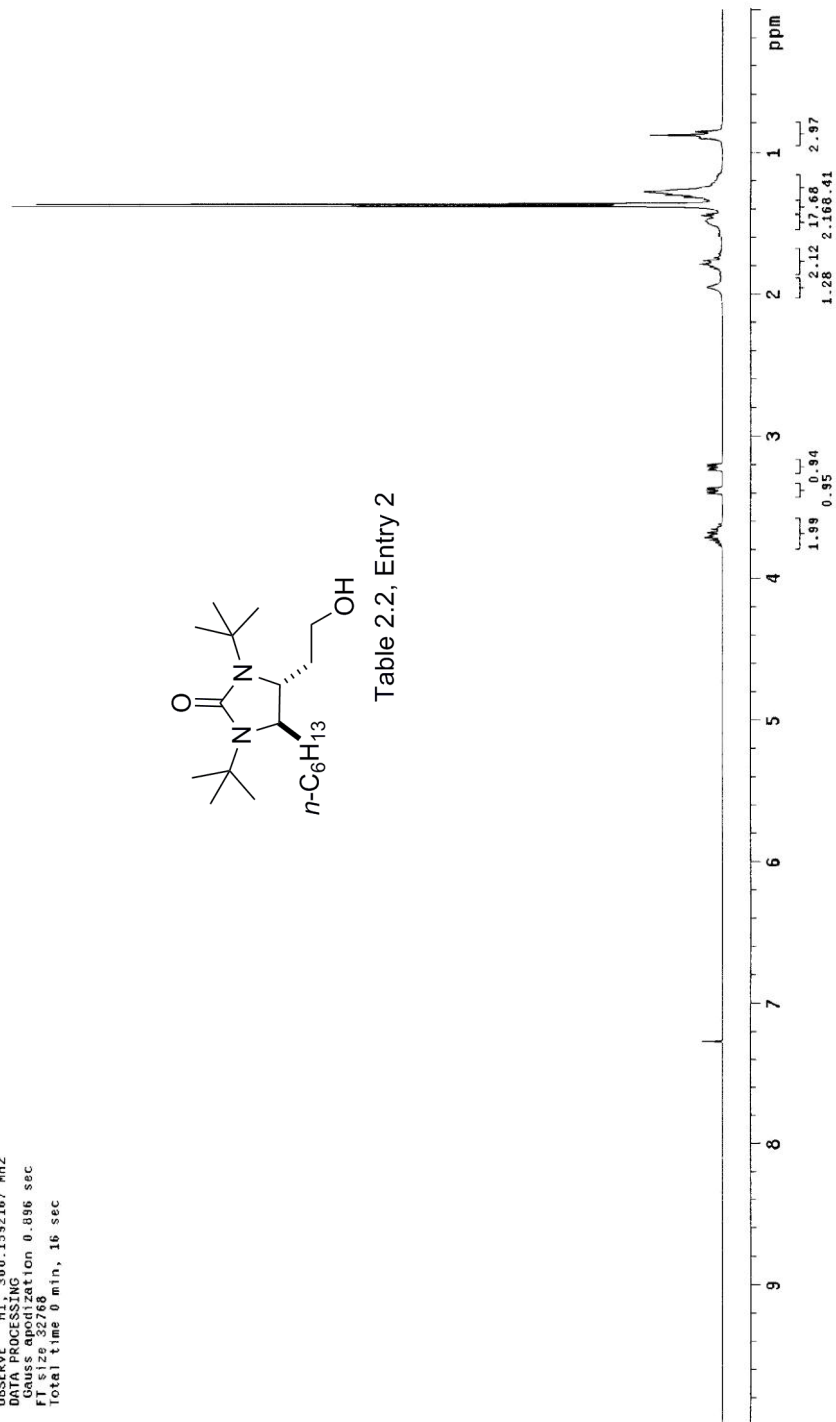


Table 2.2, Entry 2



13C OBSERVE

Pulse Sequence: s2pul

Solvent: CDCl3

Ambient temperature

Frequency: 101.626 MHz

INNOVA-500 "report18"

Relax delay 1.500 sec

Pulse 39.1 degrees

Acq. time 0.800 sec

Width 20000.0 Hz

162 repetitions

Observed C13, 421530 MHz

Observed C11, 299.9518066 MHz

Power 36 dB,

continuously on

WALTZ-16 modulated

DATA PROCESSING

Line broadening 1.0 HZ

File size 1.0 MB

Total time 641343 hr, 30 min, 7 sec

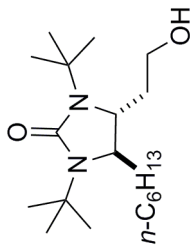
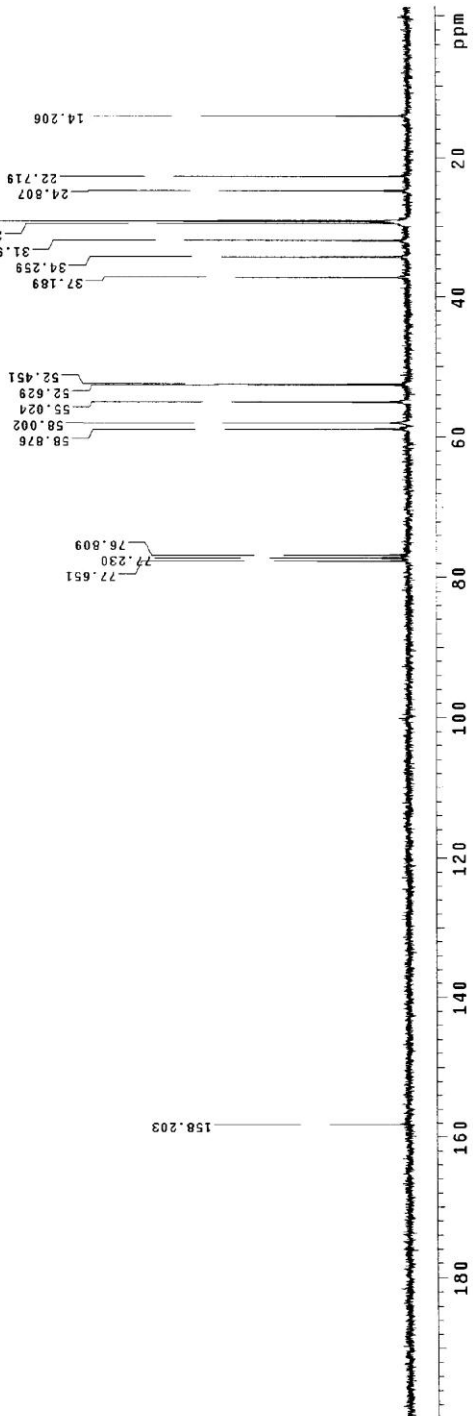
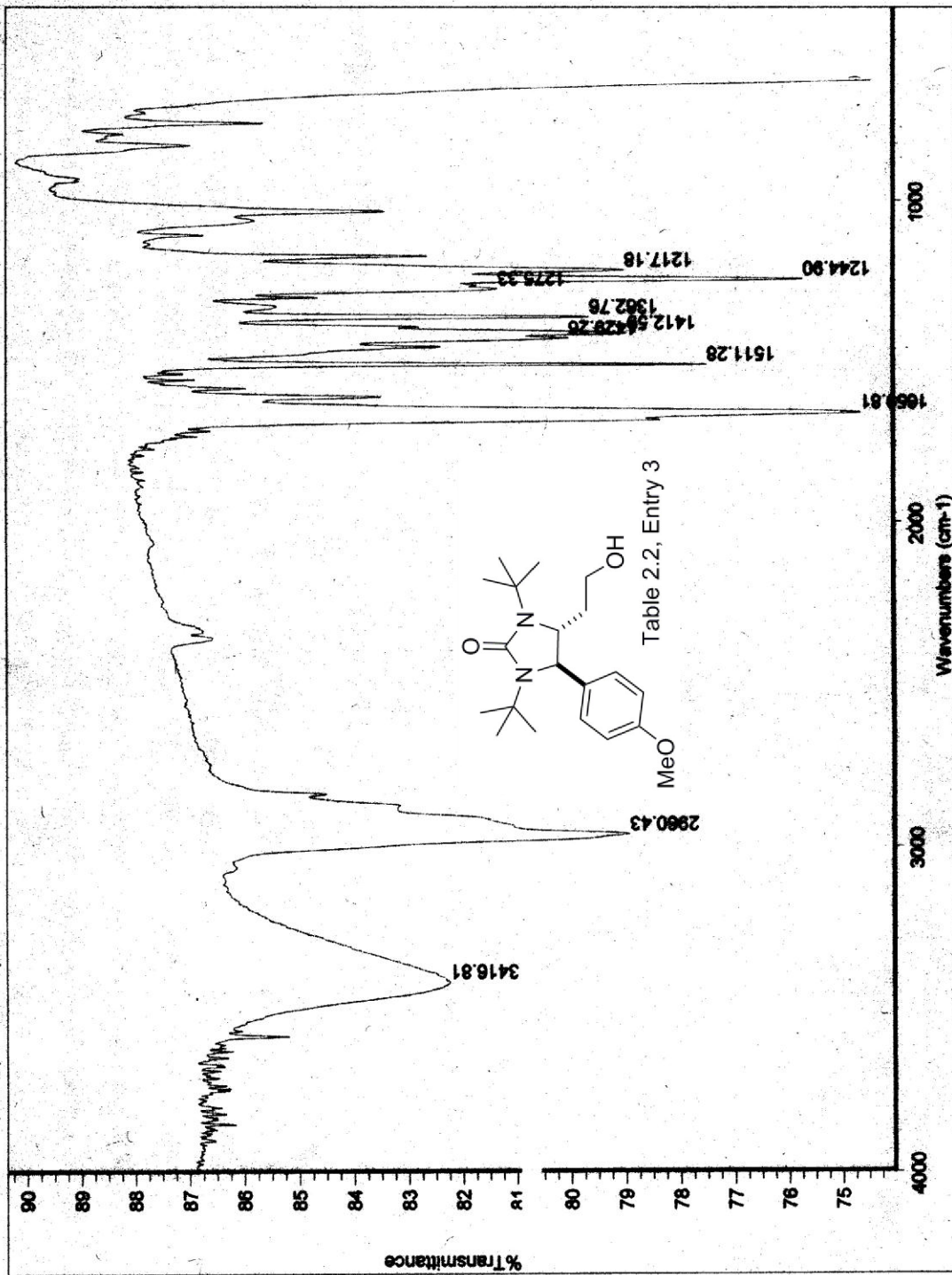


Table 2.2, Entry 2



rc-63-43-1



STANDARD 1H OBSERVE

Pulse Sequence: s2pu1
Solvent: CDCl3
Ambient Temperature:
File: FC_b2_47_1_Check
INDVA-500 "epoxide"

Relax. delay 0.000 sec
Pulse 26.0 degrees
Acq. time 2.998 sec
Width 1562.472
4 Repetitions
OBSERVE H1 300.1592164 MHZ
DATA PROCESSING
Gauss apodization 0.896 sec
F1 size 32768
Total time 0 min, 16 sec

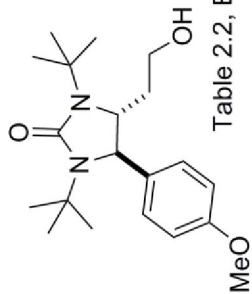
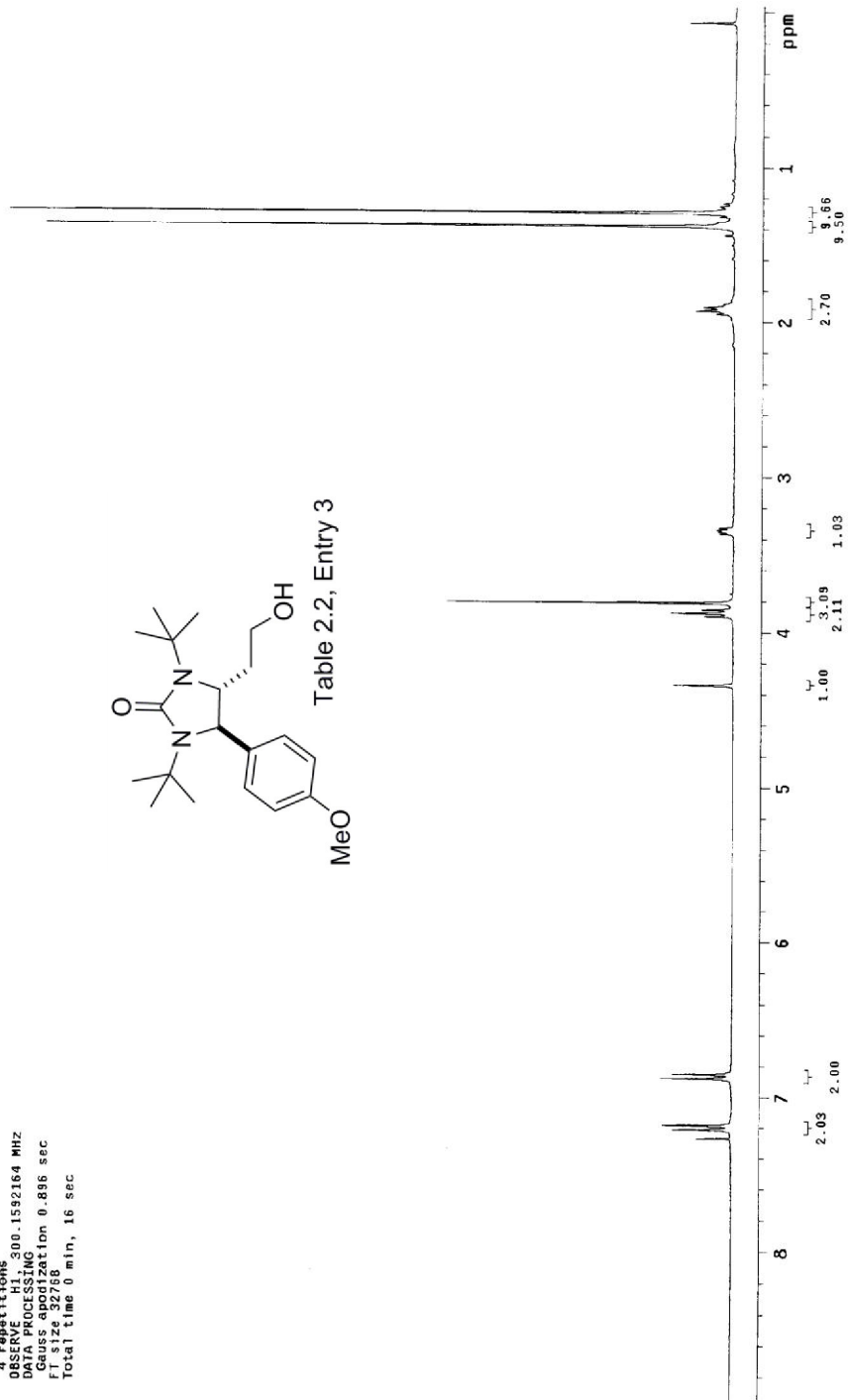


Table 2.2, Entry 3



13C OBSERVE

Pulse Sequence: s2pu1
Solvent: CDCl3
Ambient temperature
INOVA-500

Relax. delay: 1.500 sec
Pulse: 39.1 degrees
Acq. time: 0.800 sec
Width: 20000.0 Hz
F02: 100.625493 MHz
DECUPLE: CH1, 259.9510068 MHz
Power: 36 dB
continuously on
WALTZ-16 modulated
DATA PROCESSING
FT size: 32768
FT time: 30.000 min, 1.0 Hz
Total time: 64.1343 hr, 30 min, 7 sec

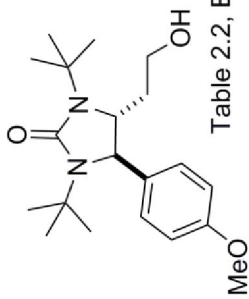
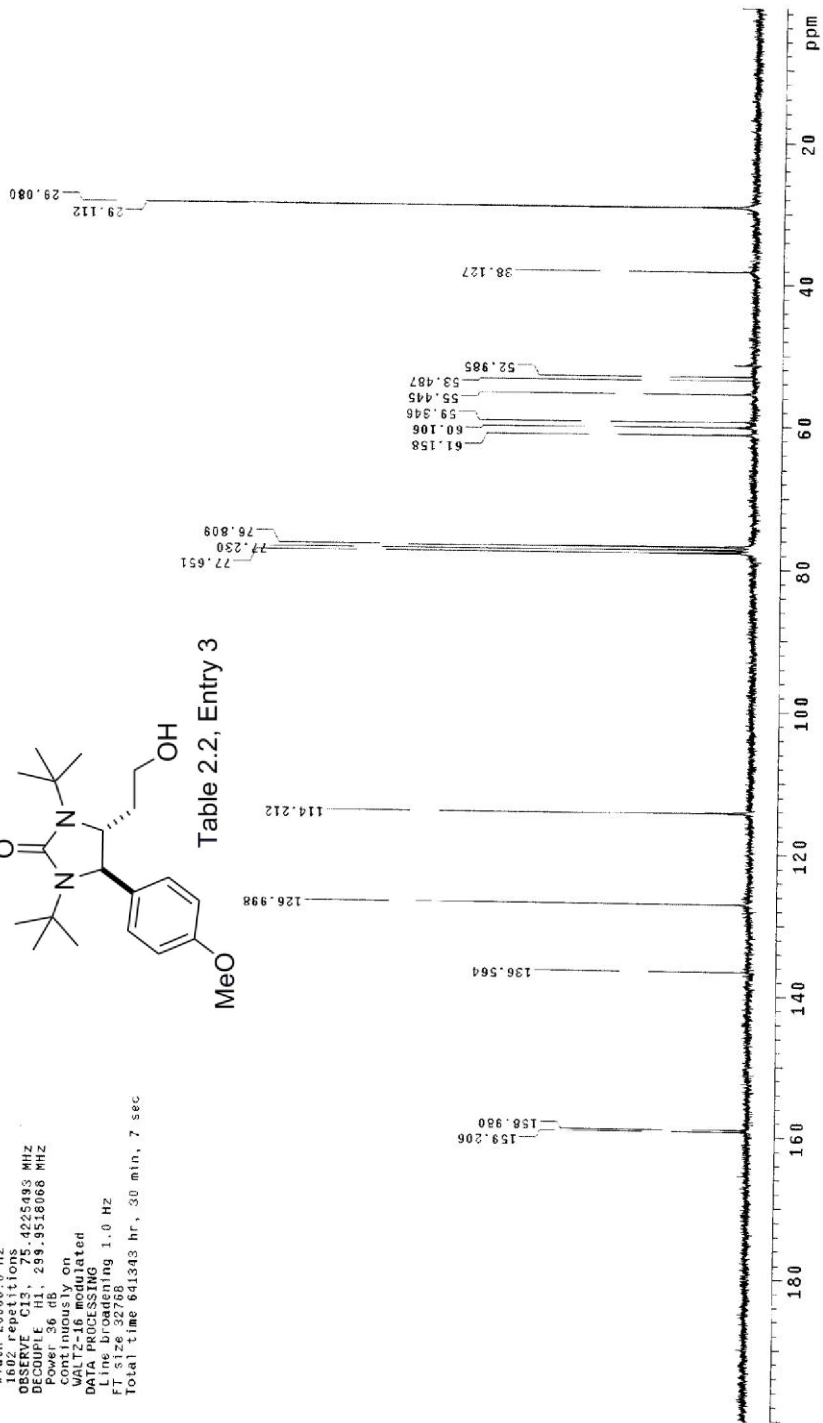
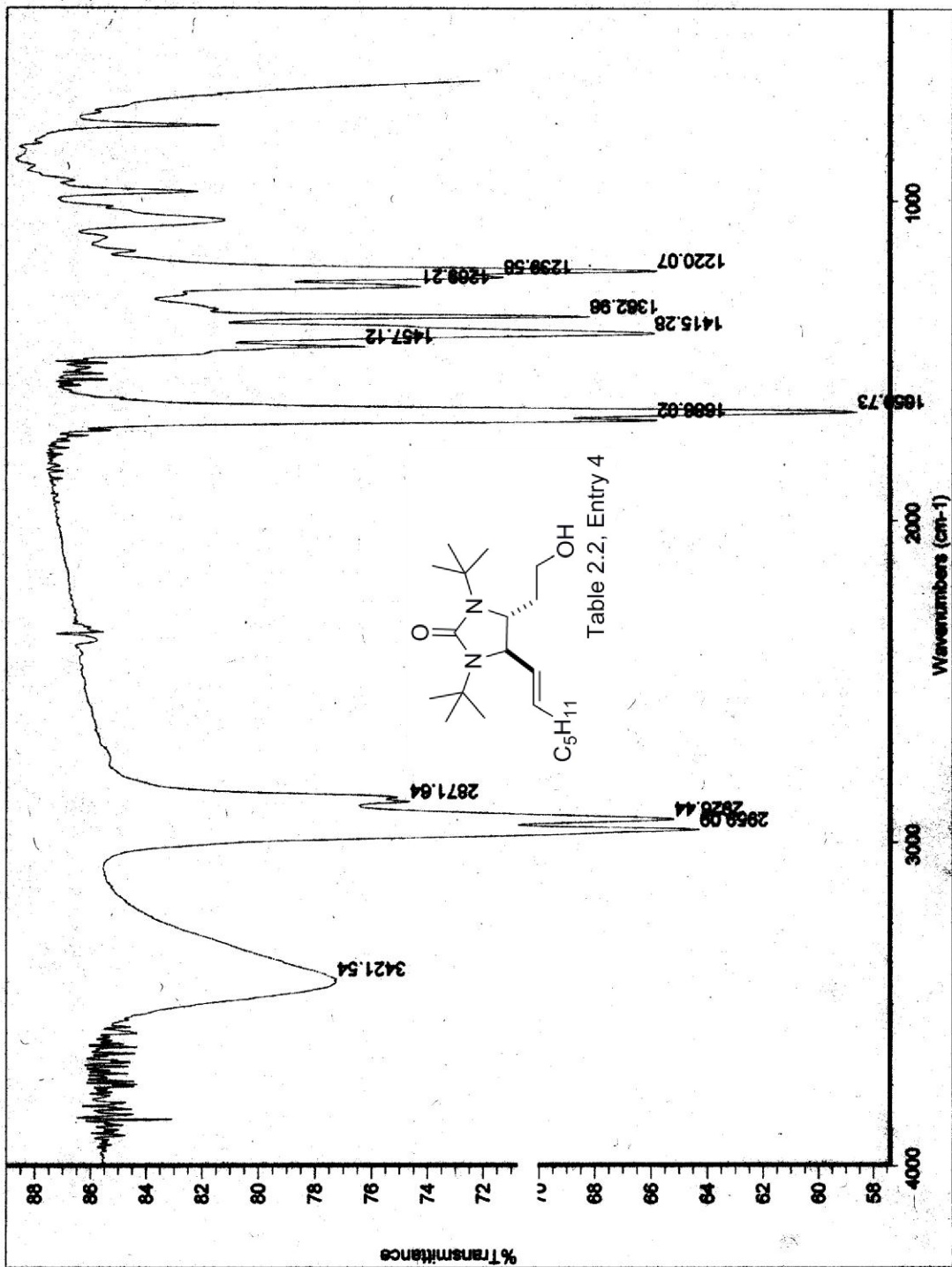


Table 2.2, Entry 3





STANDARD 1H OBSERVE

Pulse Sequence: s2pu1

Solvent: CDCl3

File: rc_b3_43_3_puf8

INOVA-500 "epoxide"

Relax. delay 0.000 sec

Pulse 26.0 degrees

Acq. time 2.668 sec

File name: s2pu1

4 FID011100

OBSERVE H1, 300.1592164 MHZ

DATA PROCESSING

Gauss apodization 0.896 sec

FI size 32788

Total time 0 min, 16 sec

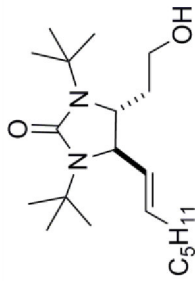
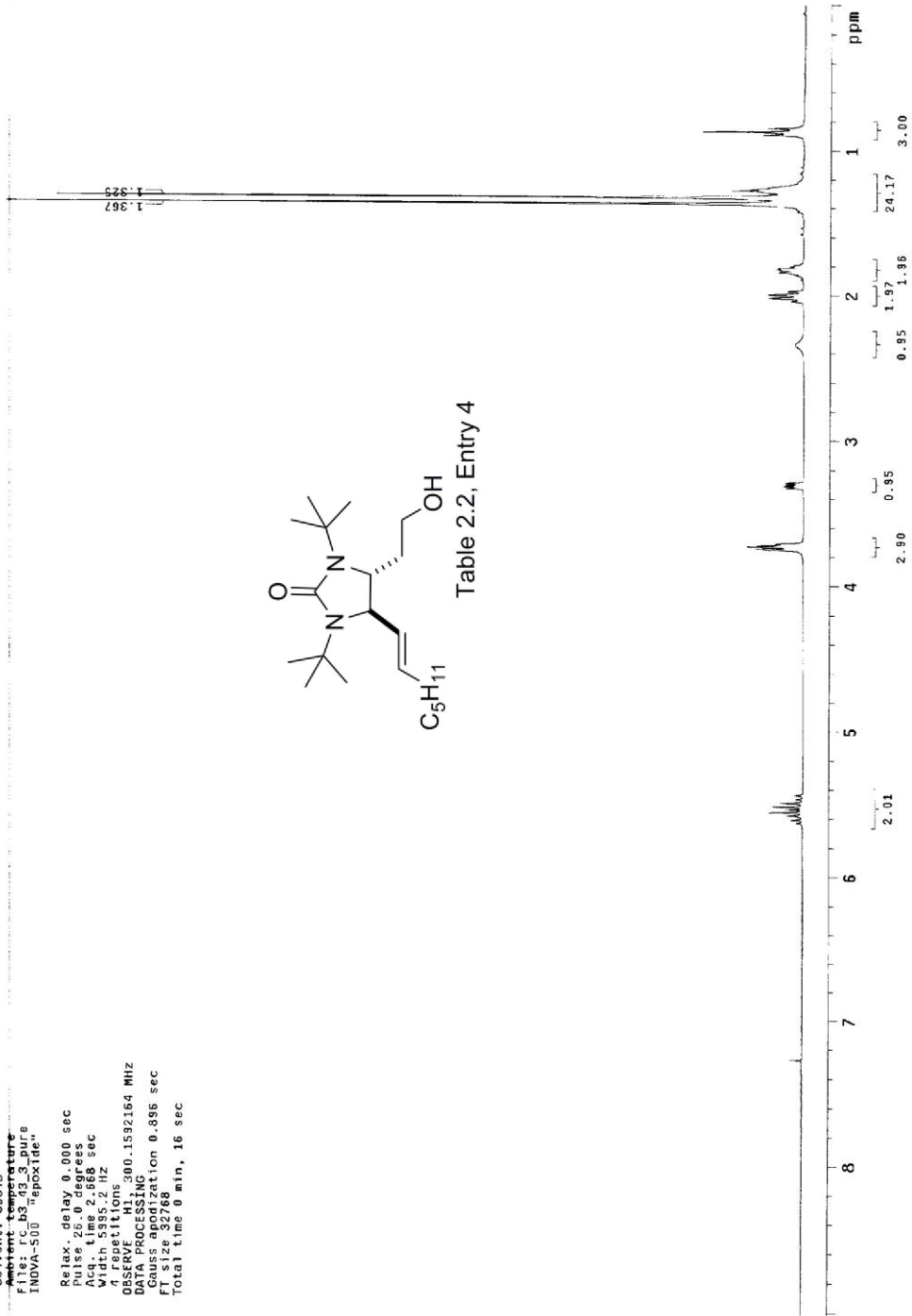


Table 2.2, Entry 4



13C OBSERVE

Pulse Sequence: s2pul
Solvent: CDCl3
Ambient temperature
F116: r6_b3_45_Carbon
INOVA-500 "epoxide"

Relax. delay: 1.000 sec
Acq. time: 0.697 sec
Acq. time: 0.697 sec
Width: 22935.8 Hz
164 repetitions
OBSERVE: C13, 75.4750816 MHz
DECOUPLE: H1, 300.1606799 MHz
CONTINUOUSLY on
WALTZ-16 modulated
DATA PROCESSING
Line broadening: 2.0 Hz
FT size: 32768
Total time: 473916 hr, 13 min, 52 sec

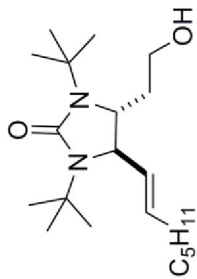
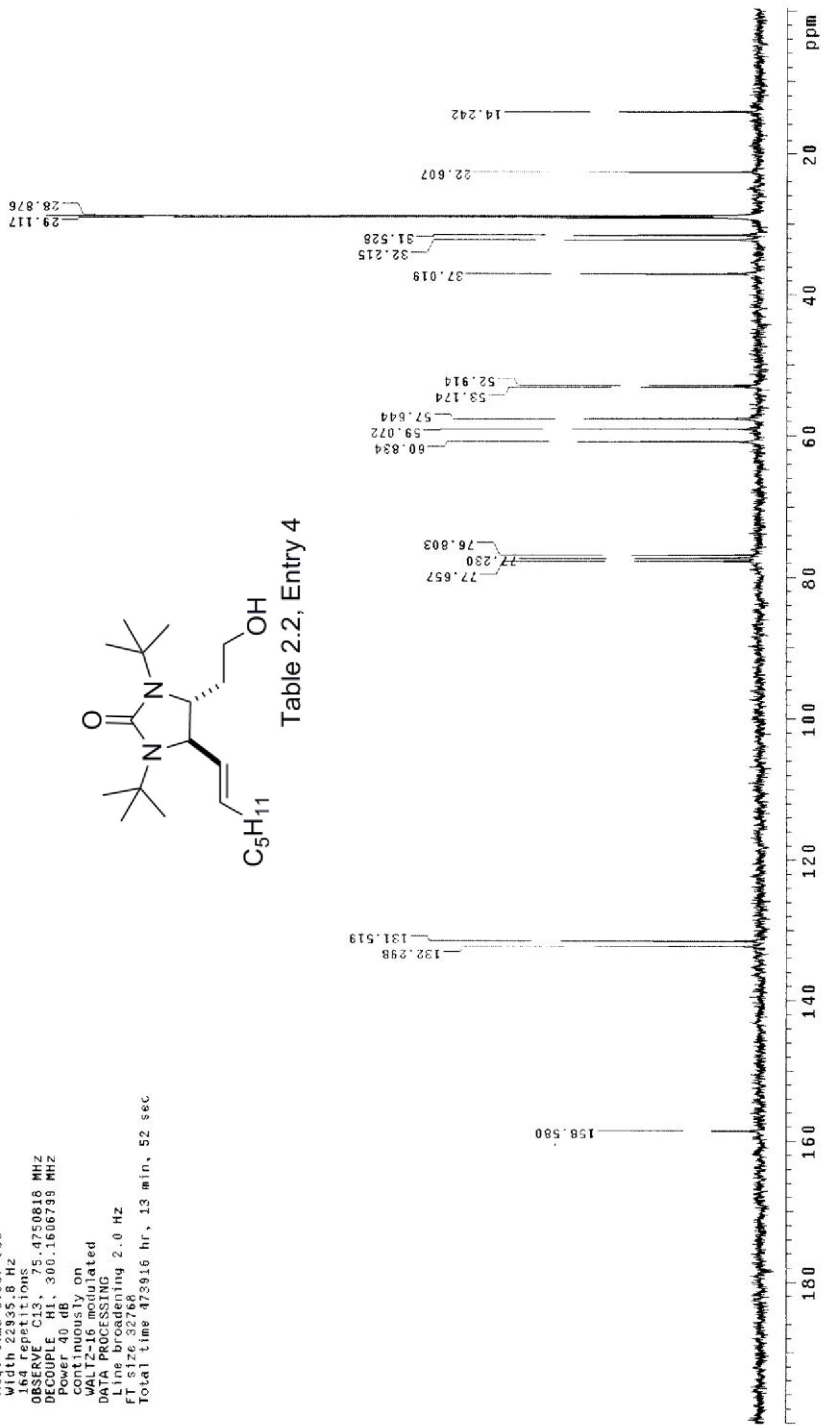
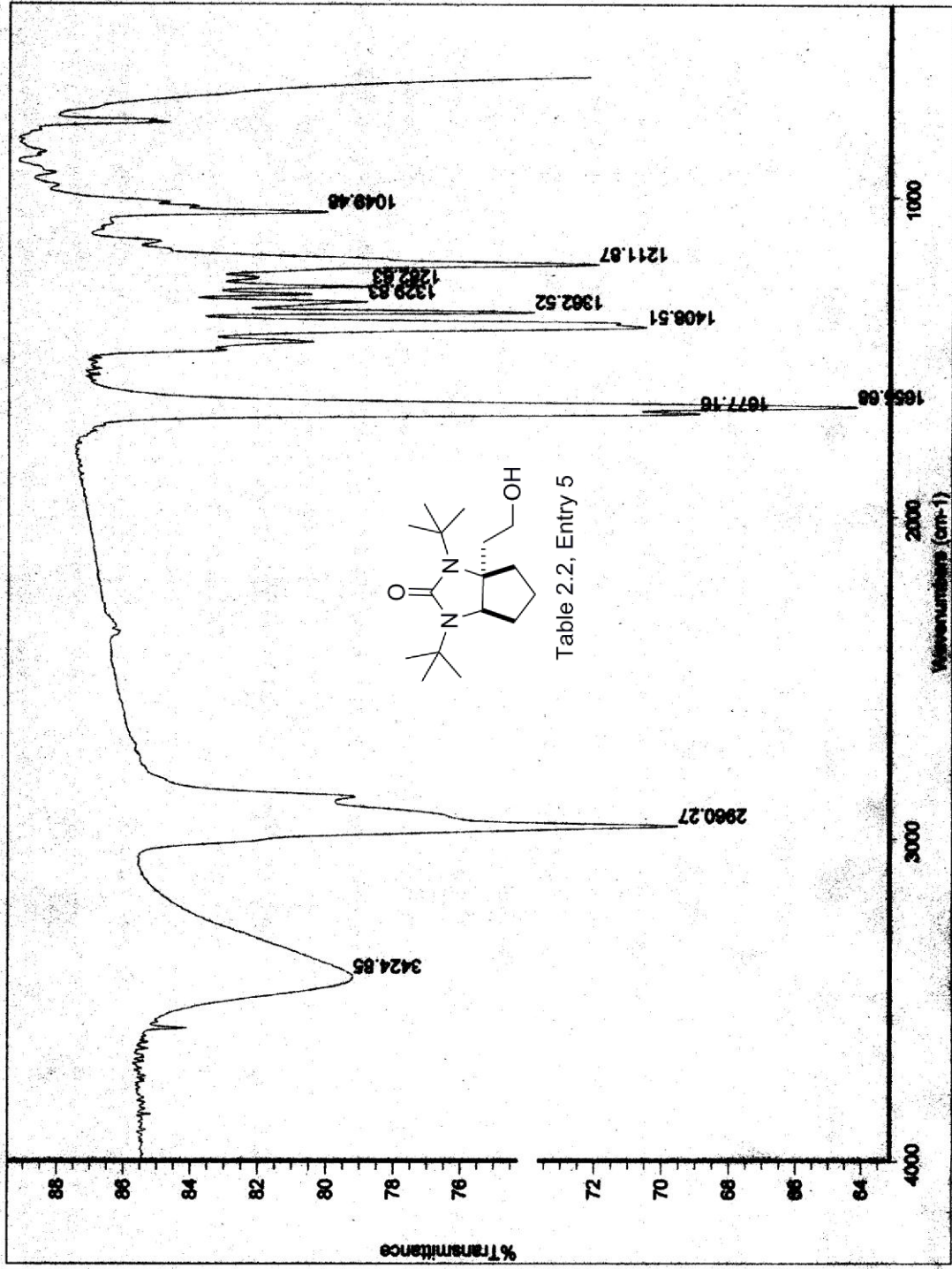


Table 2.2, Entry 4



rc-63-13-1



STANDARD 1H OBSERVE

Pulse Sequence: s2pu1
Solvent: CDCl3
Ambient Temperature
File: FC_0313_1_frac2
INDVA-500 "epoxide"

Relax. delay 0.000 sec
Pulse 26.0 degrees
Acq. time 2.668 sec
Date_ 0313_2172
8 FID031308

OBSERVE H1 300.1592161 MHz
DATA PROCESSING
Gauss apodization 0.896 sec
F1 size 32768
Total time 0 min, 26 sec

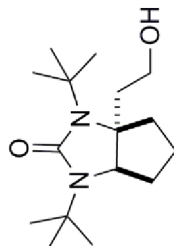
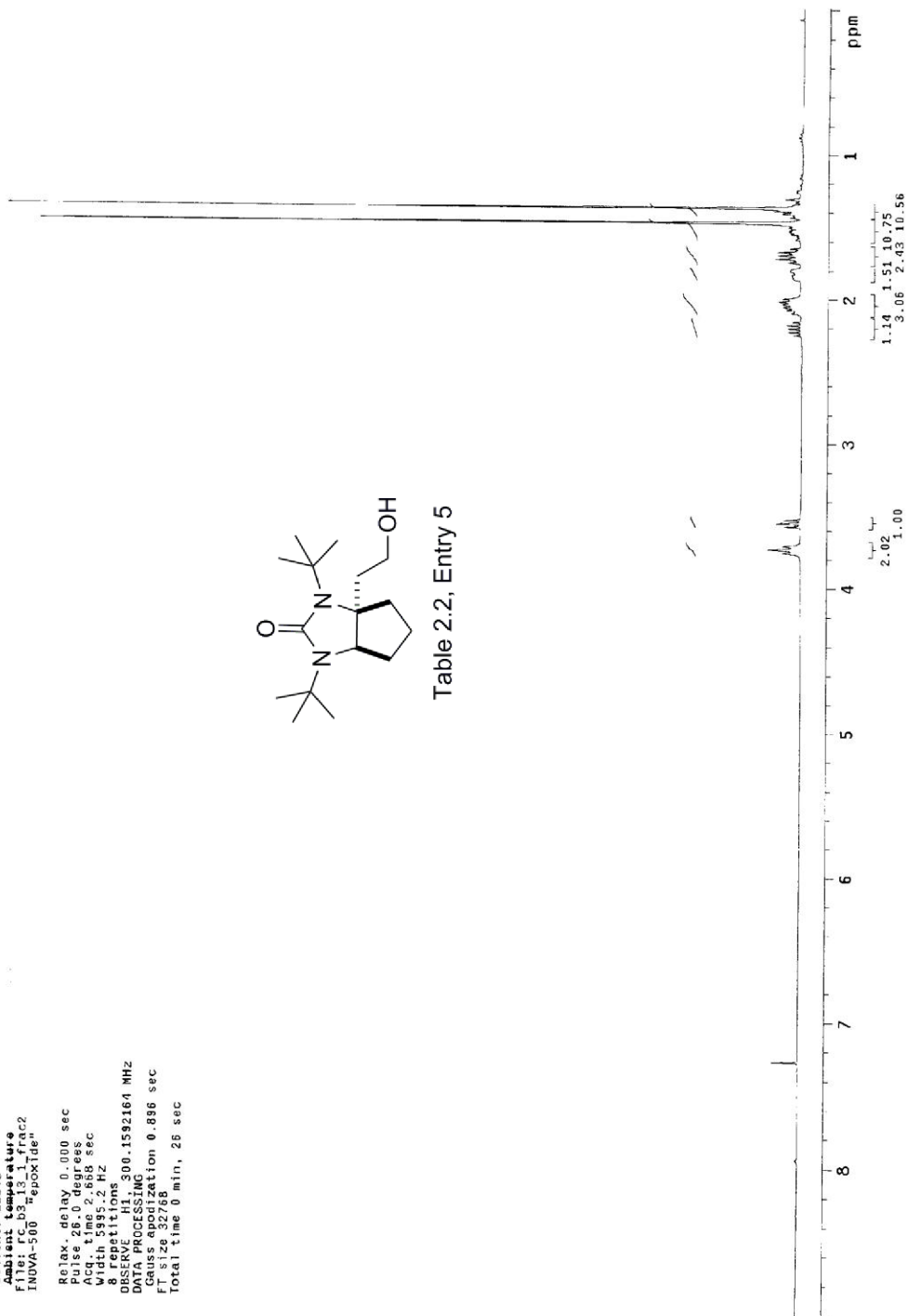


Table 2.2, Entry 5



13C OBSERVE

Pulse Sequence: s2pu1
Solvent: CDCl3
Acq. time: 0.533 sec
File: FC_03_15_1_carbon
INOVA-500 "ReproTide"

Relax. delay: 1.700 sec
Pulse: 44.5 degrees
Acq. time: 0.533 sec
1205.50018.8 Hz

OBSERVE: PC13, 100.6067923 MHz
DECOUPLE: H1, 400.1083268 MHz
Power: 42 dB

continuously on
Acq. time: 0.533 sec

DATA PROCESSING

Line broadening: 2.0 Hz

FT size: 32768

Total time: 622735 hr., 34 min., 7 sec.

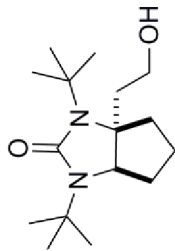
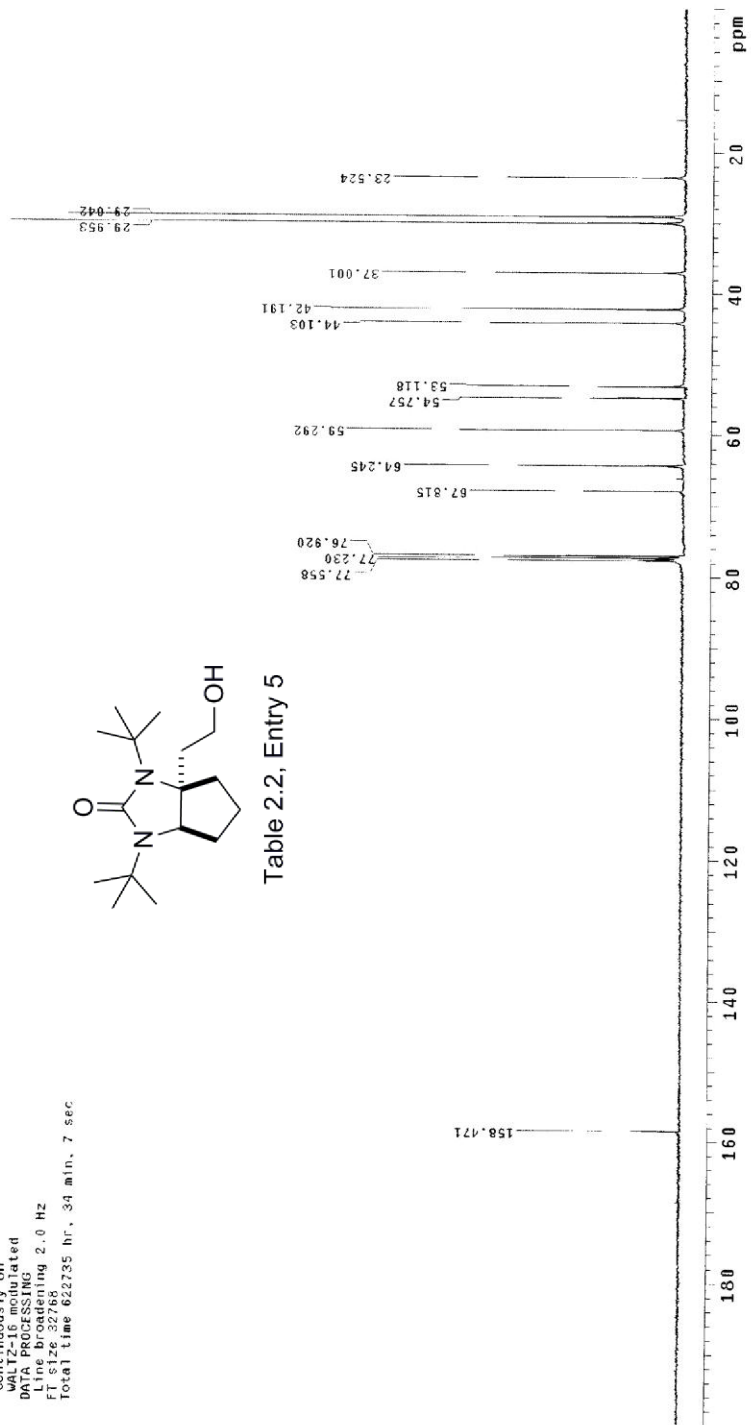
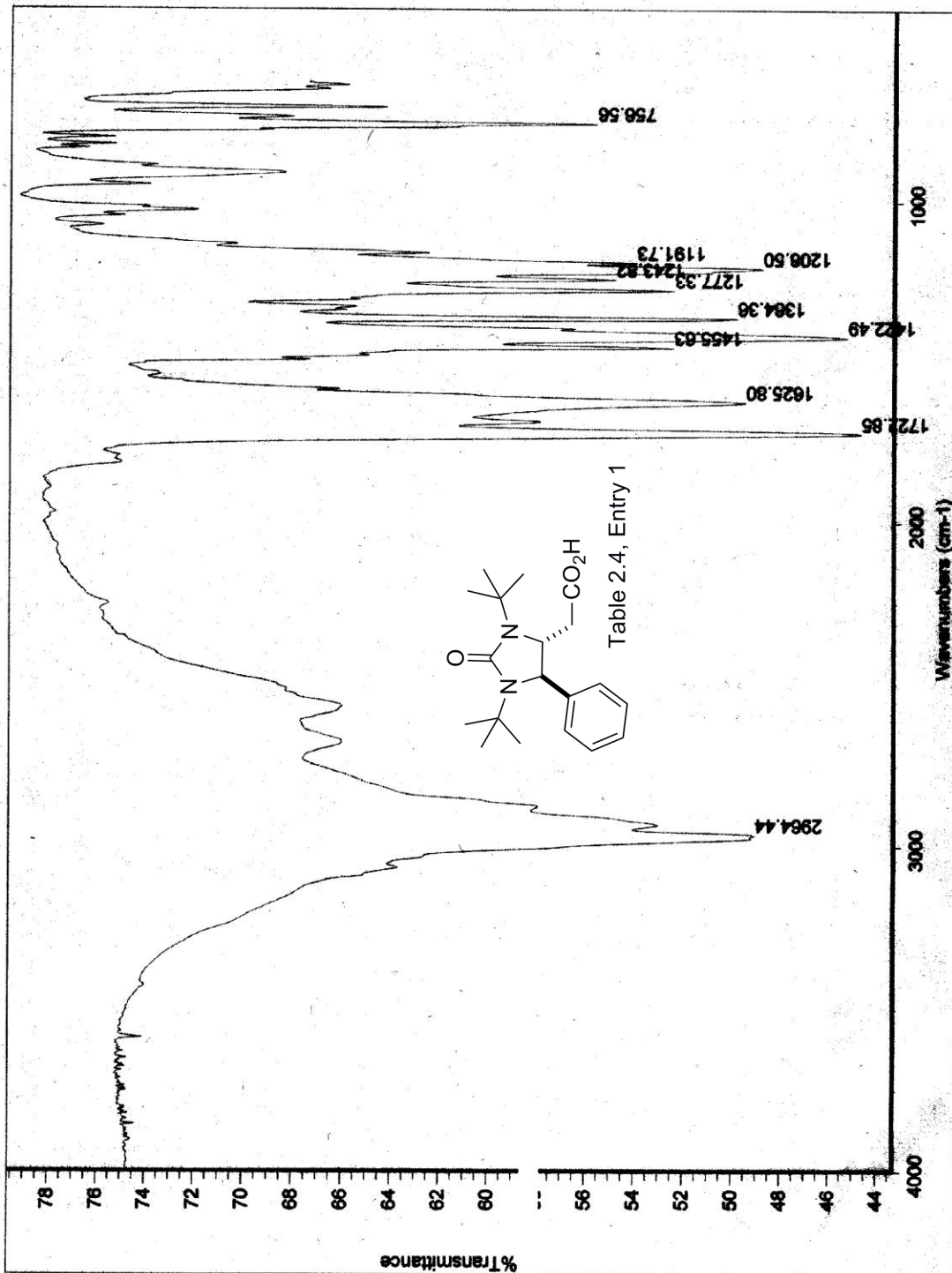


Table 2.2, Entry 5



rc-b3-46-1



STANDARD 1H OBSERVE

Pulse Sequence: s2pu1

Solvent: CDCl3

Temperature:

INOVA-500 "epoxide"

Relax. delay 0.000 sec

Pulse 26.0 degrees

Acq. time 2.668 sec

Width 5995.2 Hz

Observer: jlm

DATE: 01/10/03 00.1592164 MHz

DATA PROCESSING

Gauss apodization 0.896 sec

FT size 32768

Total time 0 min, 16 sec

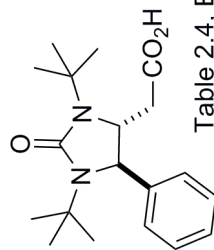
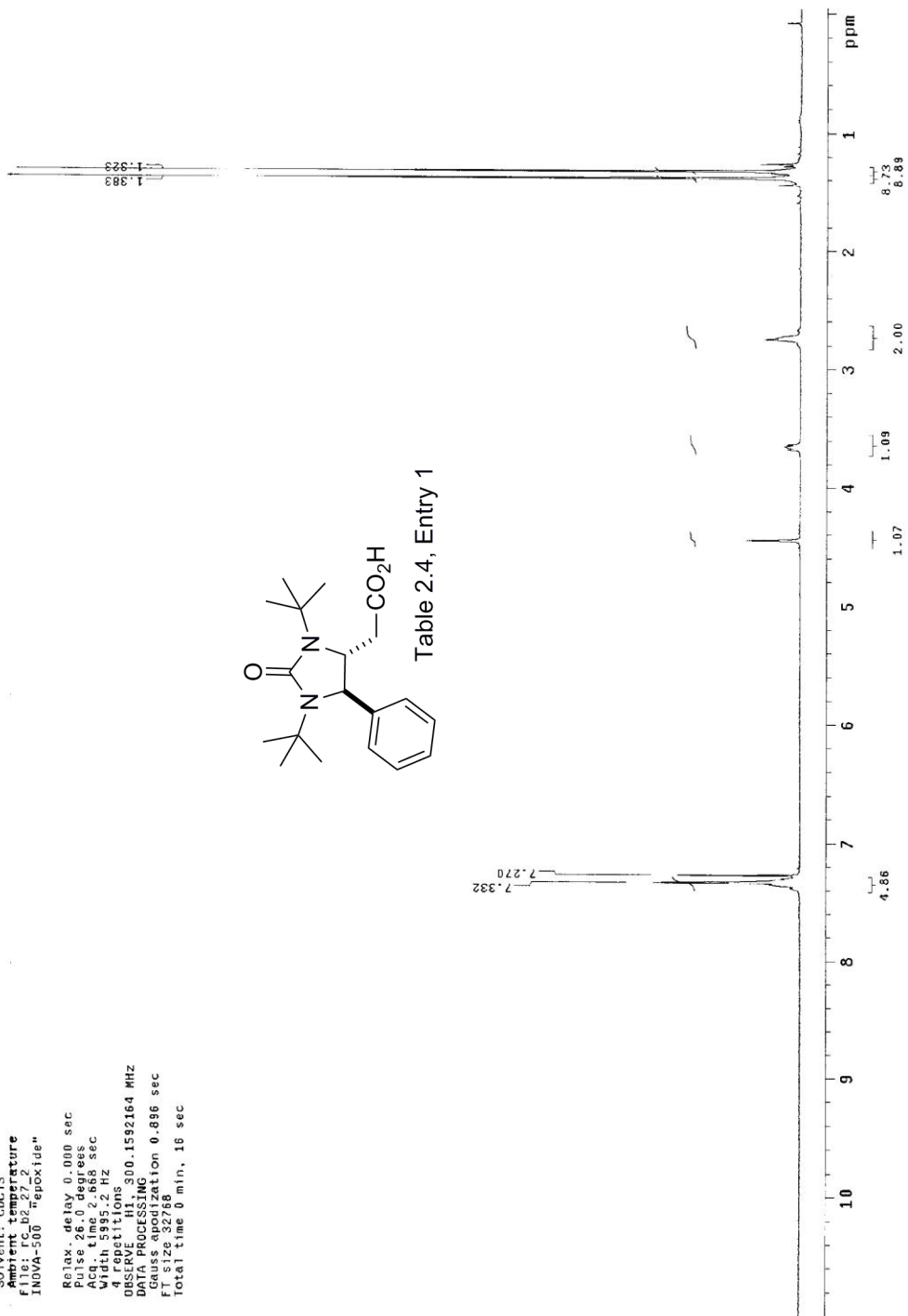


Table 2.4, Entry 1



13C OBSERVE

Pulse Sequence: s2pul1

Solvent: CDCl3

Sample Name: epoxide

File: rc_b2_42_purecarbon2

INOVA-500 "epoxide"

Relax. delay 1.000 sec

Pulse 46.3 degrees

Acq. time 0.697 sec

Width 22835.8 Hz

Observed 13C ions 75.4750790 MHz

OBSERVE CH1, 300.1606799 MHz

DECOUPLE H1, 300.1606799 MHz

Power 40 dB

continuously on

Waltz-16 modulated

D112=16 pulses/4G

D11=16 pulses/4G

D1 line broadening 2.0 Hz

FT size 32768

Total time 473916 hr, 13 min, 52 sec

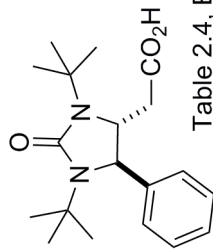
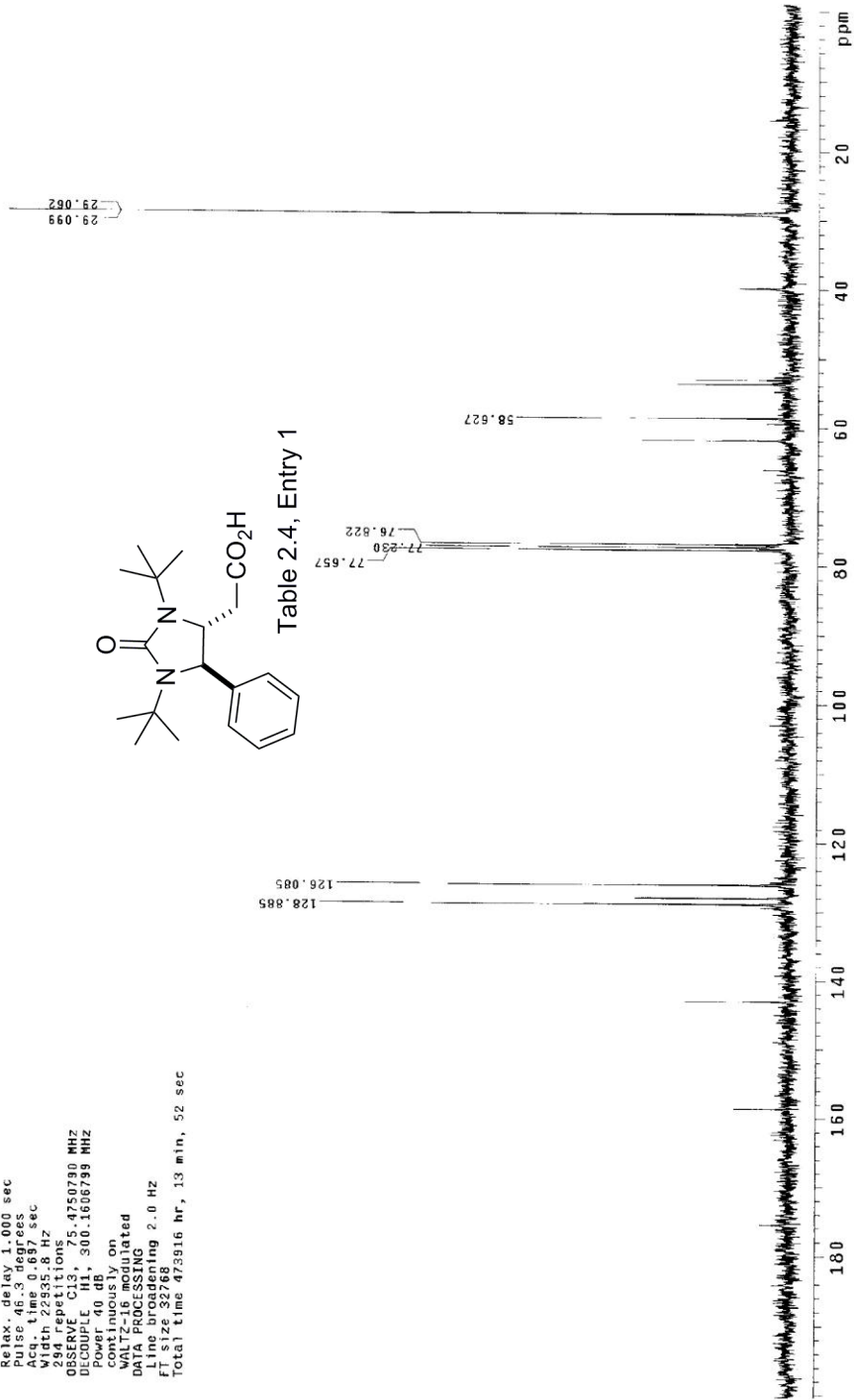
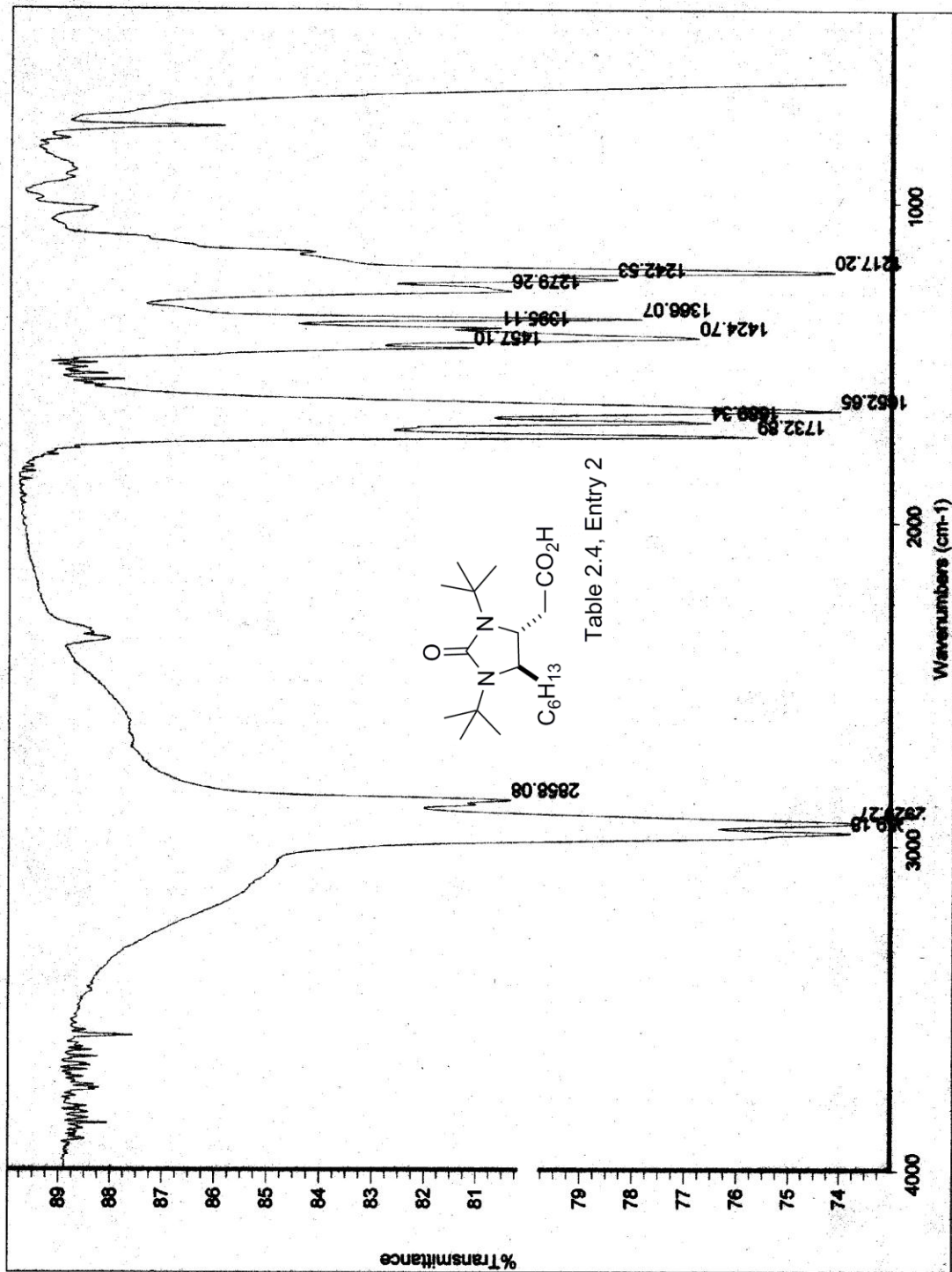


Table 2.4, Entry 1



rc-b3-46-2



STANDARD 1H OBSERVE

Pulse Sequence: s2pul

Solvent: CDCl3

Temperature

File Name: 1592164

INNOVA-500 "epox1de"

Relax. delay 0.000 sec

Pulse 26.0 degrees

Acq. time 2.668 sec

Width 5995.2 Hz

Resolution 0.0001 Hz

OBSERVE: 13C

ORSE: 13C

DATA PROCESSING

Gauss apodization 0.896 sec

FT size 32768

Total time 0 min, 16 sec

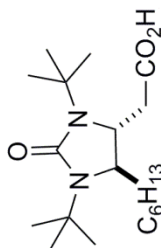
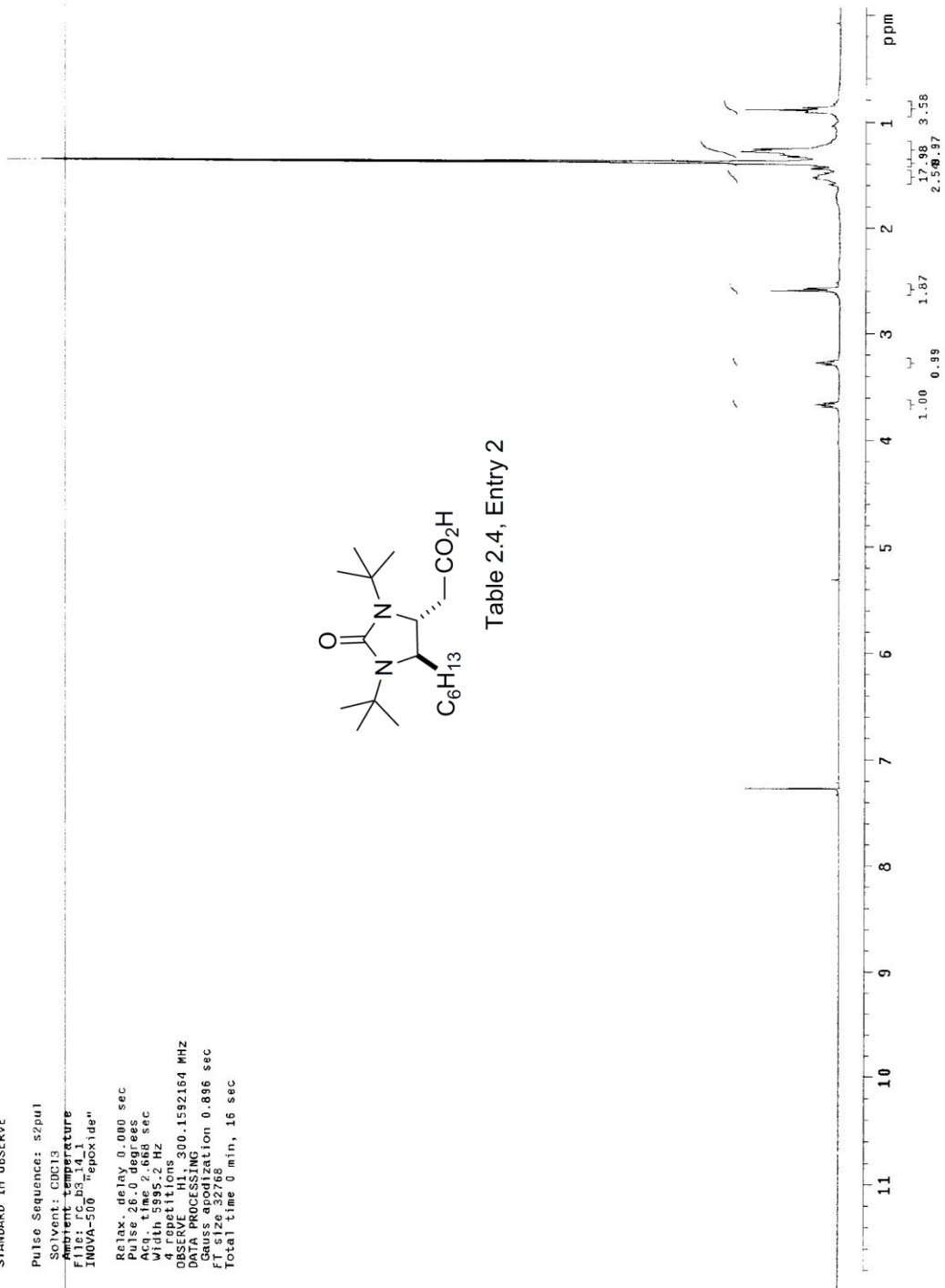


Table 2.4, Entry 2



Archive directory: /home/_data/walkup/cornwall
 Sample directory: rc_b3_46_2_check_2010421_01

Pulse Sequence: s2pu1
 Solvent: cdcl3
 Temp. 26.0 C / 293.1 K
 Sample #23482 check_1SC
 File #35482 check_1SC
 IMOVA-500 "epoxide"

Relax. delay 1.000 sec
 Pulse 45.0 degrees
 Acq. time 1.311 sec
 Width 25000.0 Hz
 Size 1 repetitions
 SIZ 10.5050693 MHZ
 DECOUPL 43.180.5050693 MHZ
 Power 38 dB
 continuously on
 WALTZ-16 modulated
 DATA PROCESSING
 Time averaging 0.5 Hz
 File #35482
 Total time 19 min, 47 sec

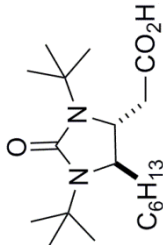
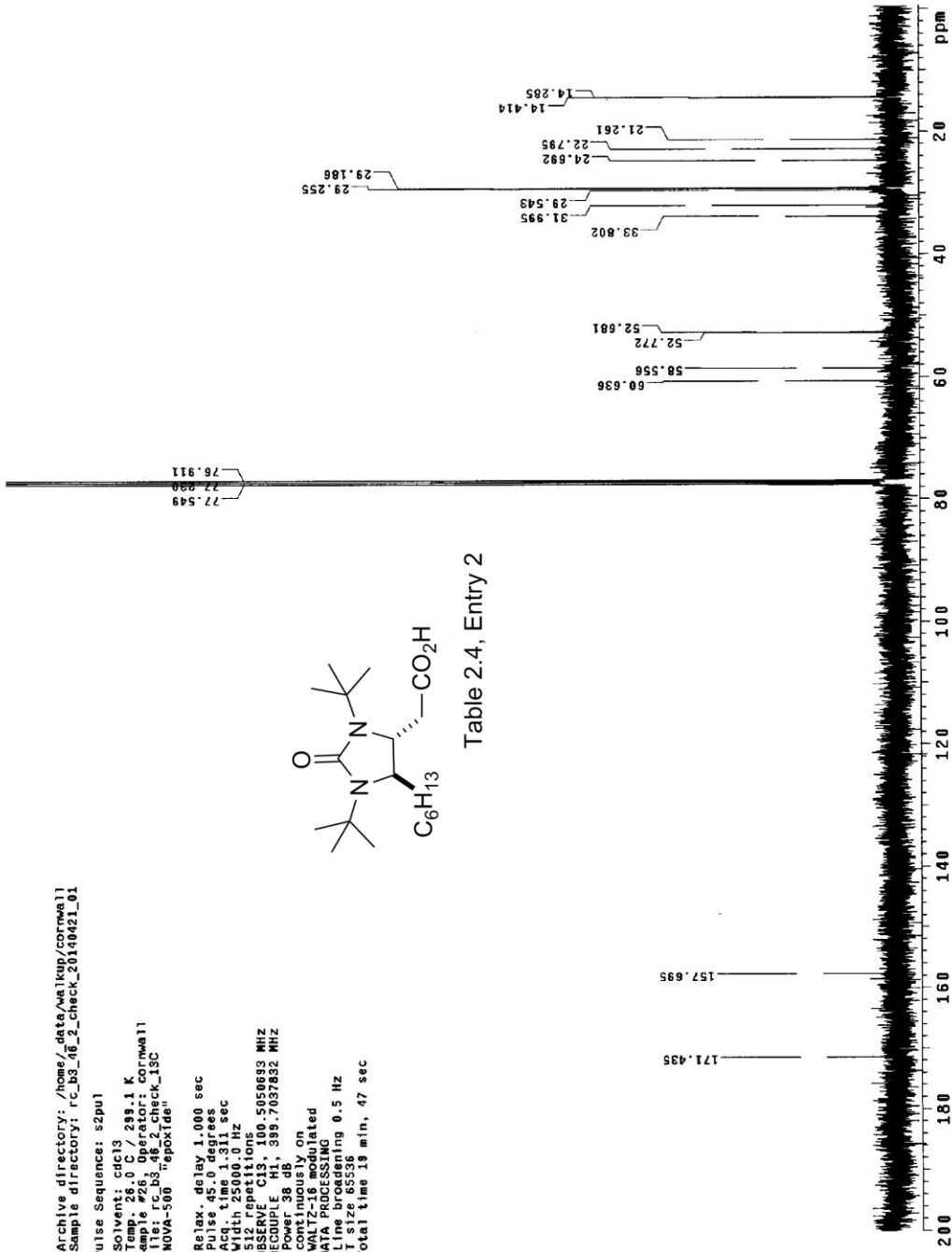
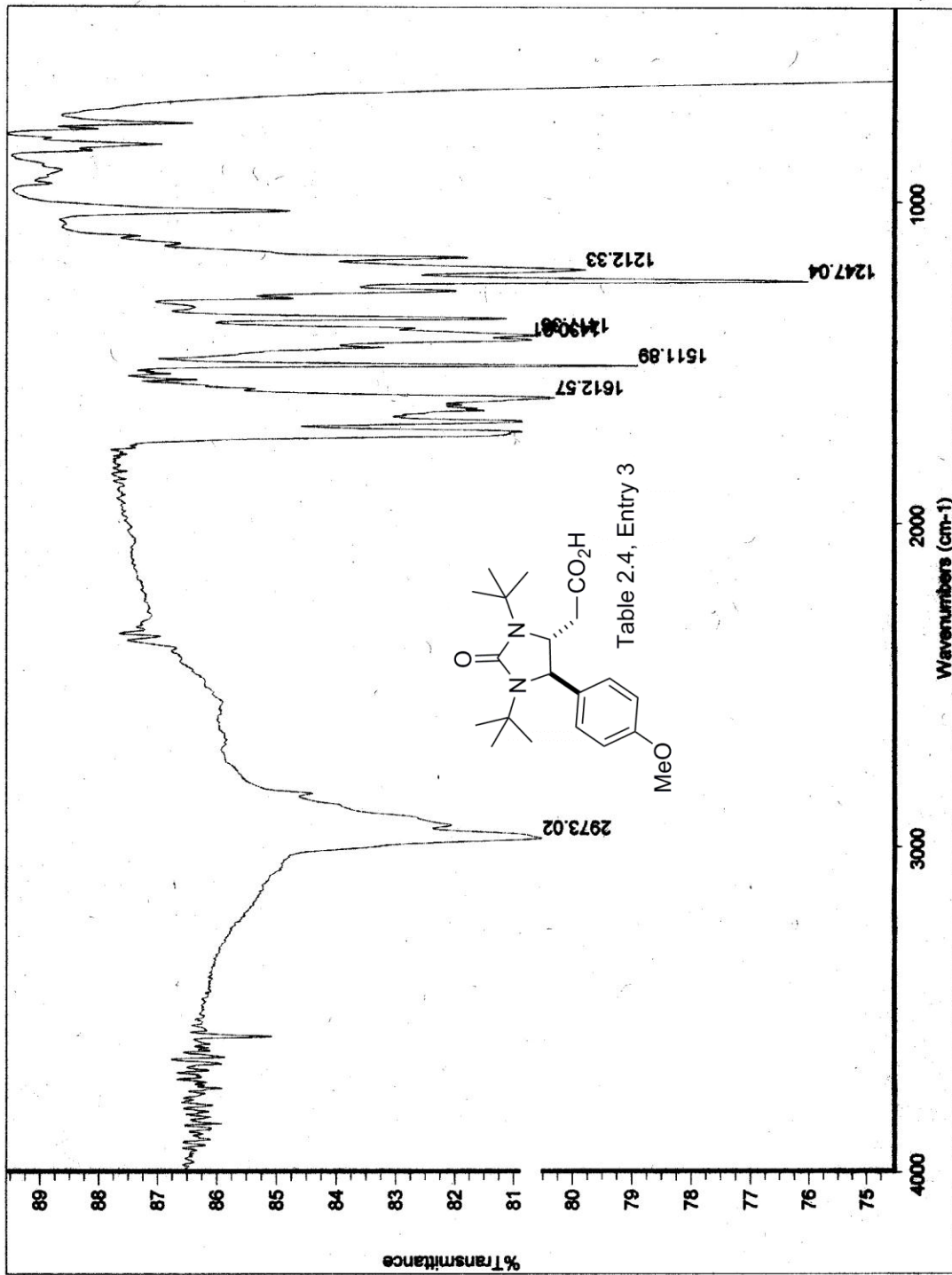


Table 2.4, Entry 2



b4-19



STANDARD 1H OBSERVE

Pulse Sequence: s2pu1

Solvent: CDCl3

Acquisition Date: 11/19/02

File: rc_04_19_pure2

INOVA-500 "epoxide"

Relax. delay 0.000 sec

Pulse 26.0 degrees

Acq. time 2.668 sec

Width 9995.2 Hz

Offset 0.000 Hz

OBSERVE 1H 300.1592196 MHz

DATA PROCESSING

Gauss apodization 0.896 sec

FT size 32768

Total time 0 min, 16 sec

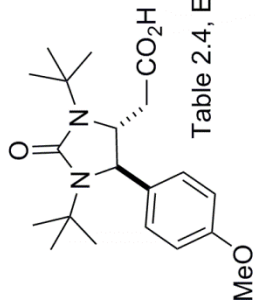
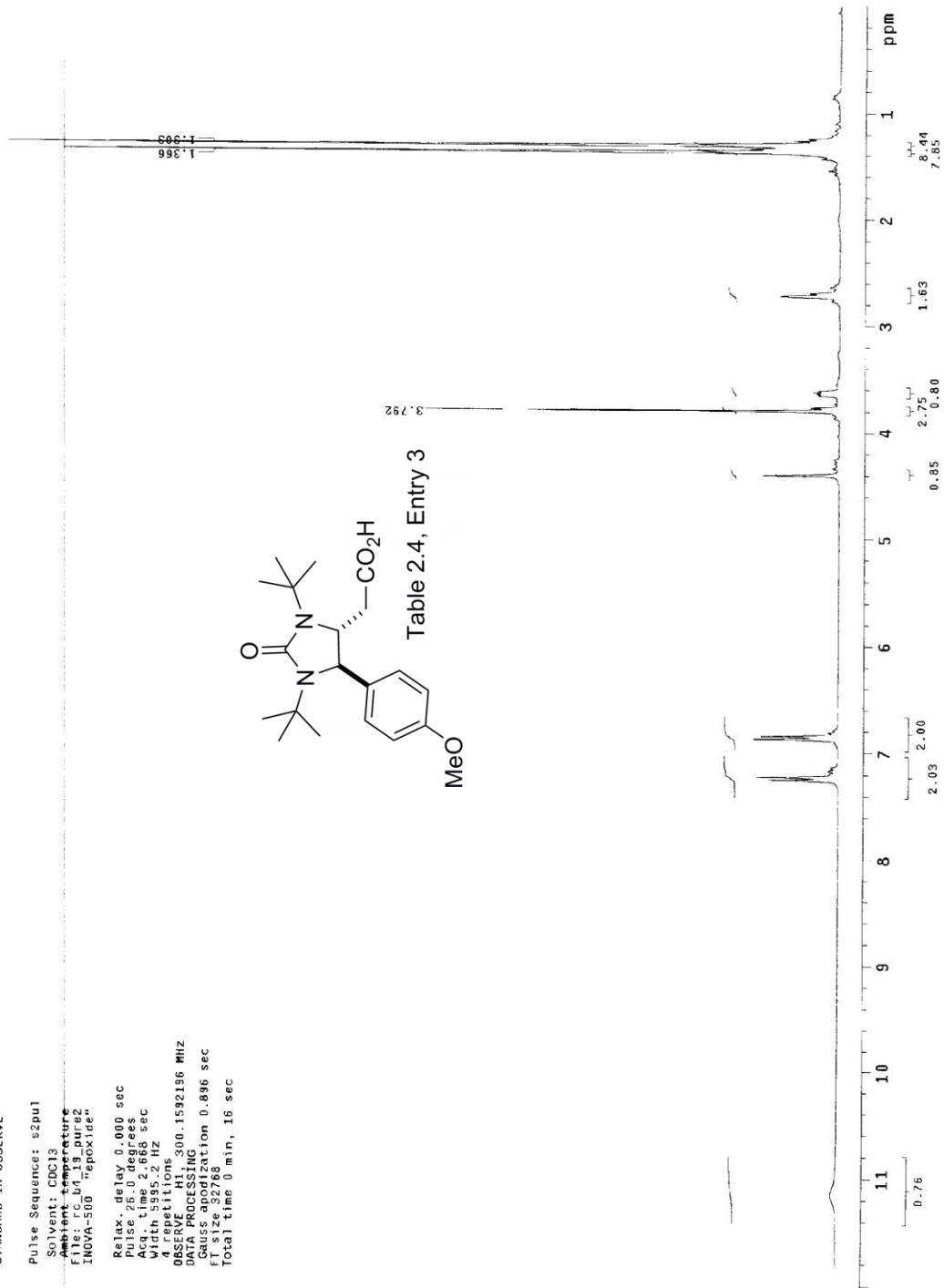


Table 2.4, Entry 3



13C OBSERVE

Pulse Sequence: s2pul
 Solvent: CDCl3
 Solvent Temperature: 30.00°C
 File Name: 13C-13010001
 INOVA-500 90px1d0"

Relax. delay 1.000 sec
 Pulse 40.5 degrees
 Acq. time 0.697 sec
 Width 22935.8 Hz
 Sweep 120.00 MHz
 OBSERVE F1 4750816 MHz
 DECOUPLE F1 300.1606793 MHz
 Power 40 dB
 continuously on
 WALTZ-16 modulated
 DATA PROCESSING
 F1 size 32768
 FT size 32768
 Total time 473916 hr, 13 min, 52 sec

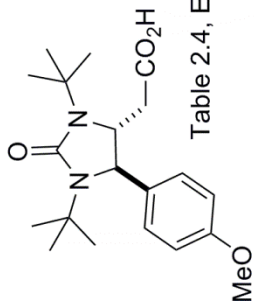
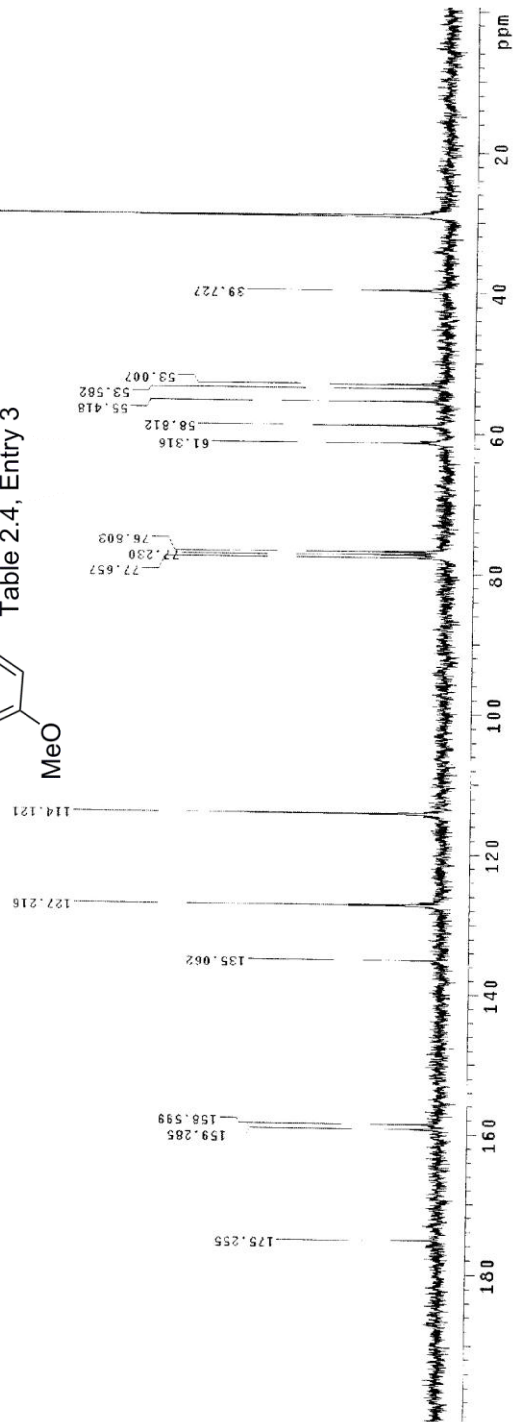
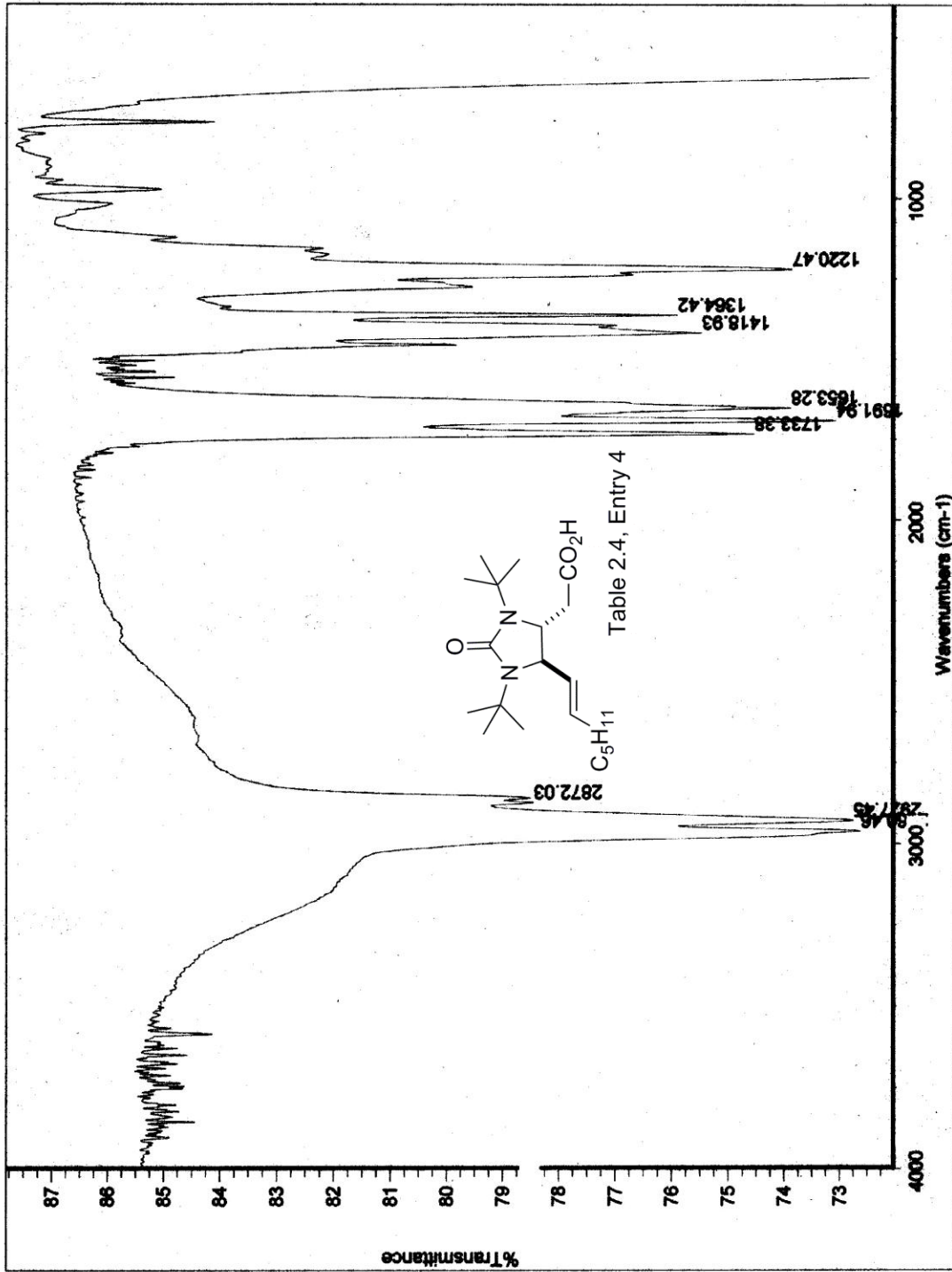


Table 2.4, Entry 3



12-63-48



STANDARD 1H OBSERVE

Pulse Sequence: s2pu1

Solvent: CDCl3

Ambient Temperature

File: rC_b3_18_pure

INDVA-500 "epoxide"

Relax. delay 0.000 sec

Pulse 26.0 degrees

Width 2.668 sec

Width 595.2 Hz

4 repetitions

OBSERVE H1, 300.1592164 MHZ

DATA PROCESSING

Gauss apodization 0.896 sec

File size 32768

Total time 0 min, 16 sec

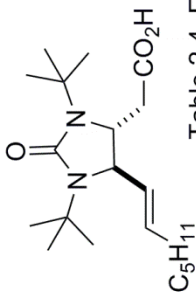
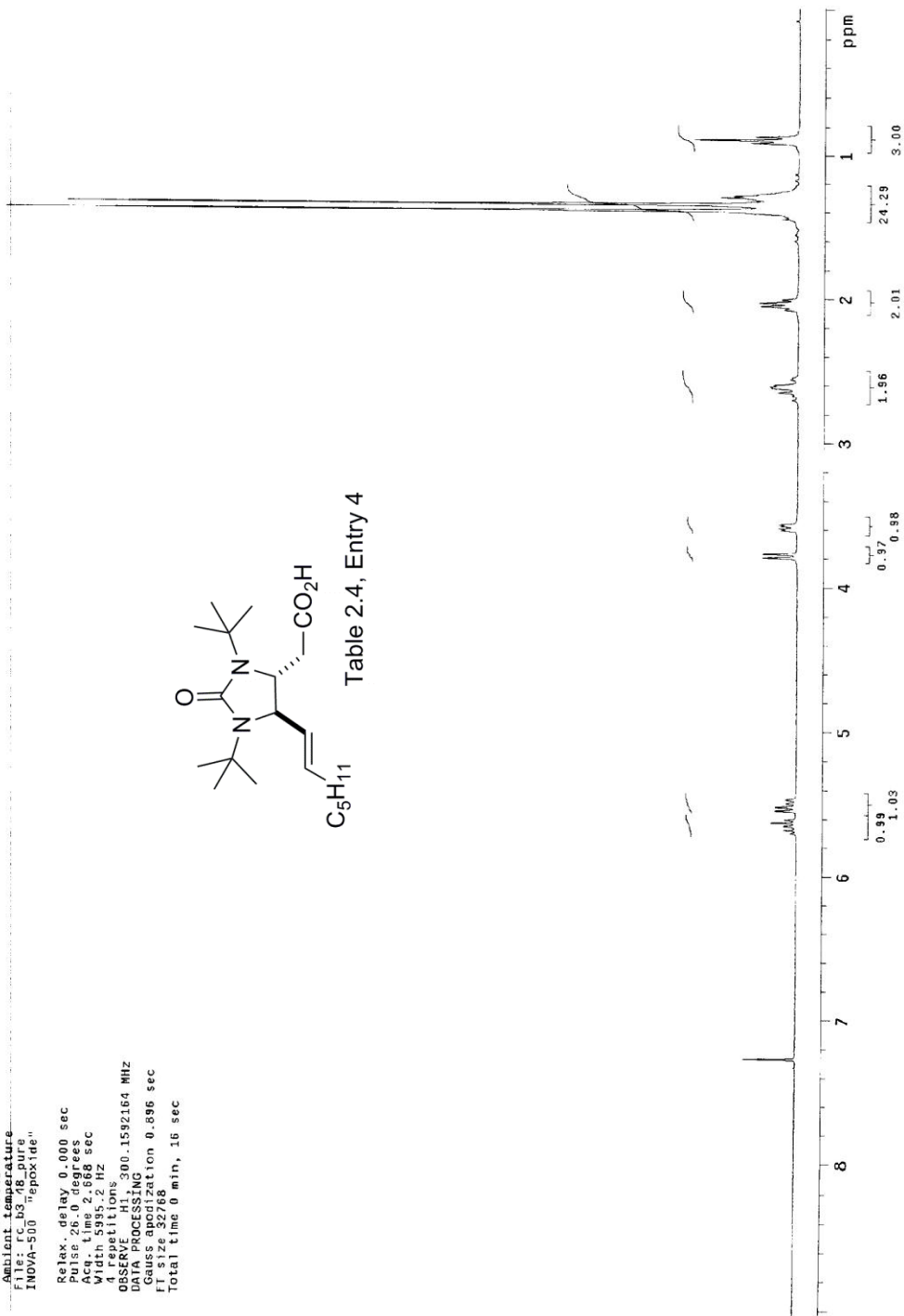


Table 2.4, Entry 4



13C OBSERVE

Pulse Sequence: s2pu1

Solvent: CDCl3

Ambient Temperature

100.625 ppm reference carbon

INOVA-500

400.1053266 MHz

Relax. delay 1.700 sec

Pulse 41.5 degrees

Acq. time 0.533 sec

Width 30018.8 Hz

Observ. repetitions

2

OBSERVE F1

400.1053266 MHz

DECOUPLE H1

Power 42 dB

continuously on

WALTZ-16 modulated

DATA PROCESSING

FT size 32768

Acquiring 2.0 Hz

Total time 622735 hr, 34 min, 7 sec

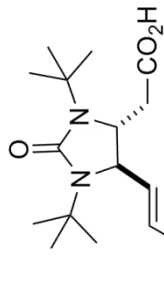
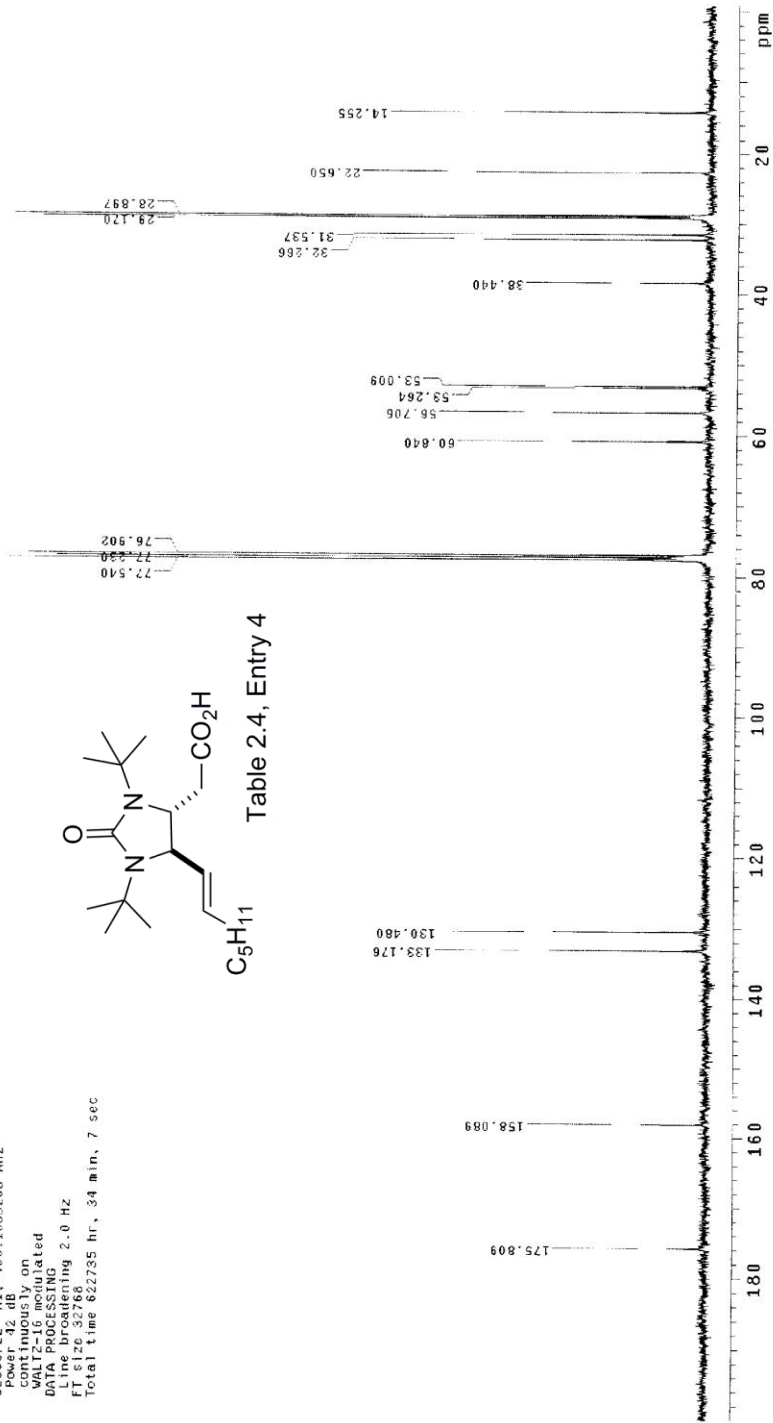
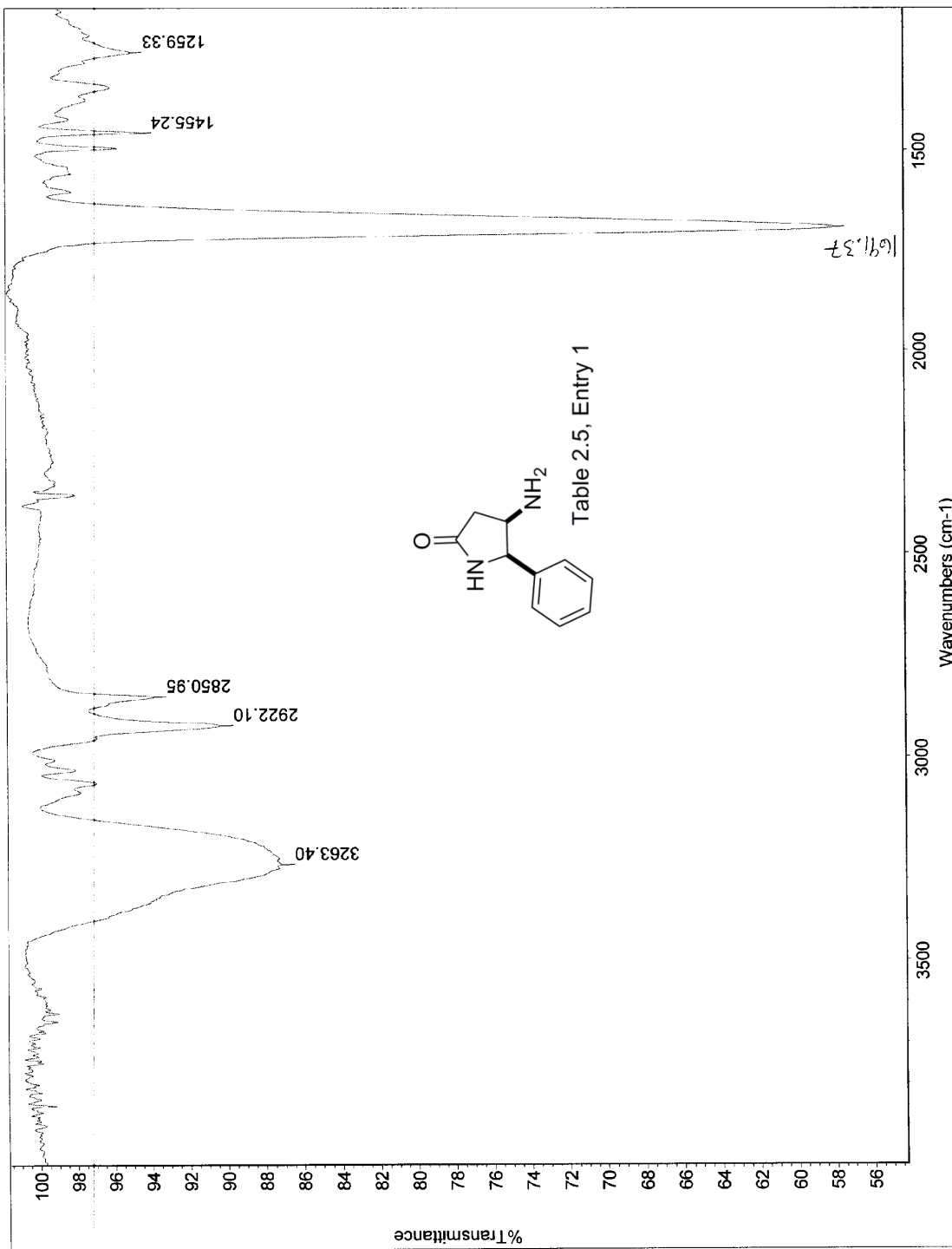


Table 2.4, Entry 4





64-16-ndb

STANDARD 1H OBSERVE

Pulse Sequence: s2pu1
Solvent: CDCl3
Acquisition: 16
File: PC.b4.16.16do.1H
INOVA-500 "1H"epoxide"

Relax. delay 1.000 sec
Pulse 31.5 degrees
Acq. time 1.995 sec
FID ch 4506.5 Hz
M 16
OBSERVE 1H 300.1592166 MHz
DATA PROCESSING
FT size 32768
Total time 0 min, 12 sec

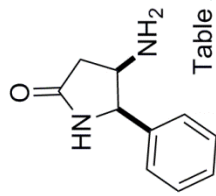
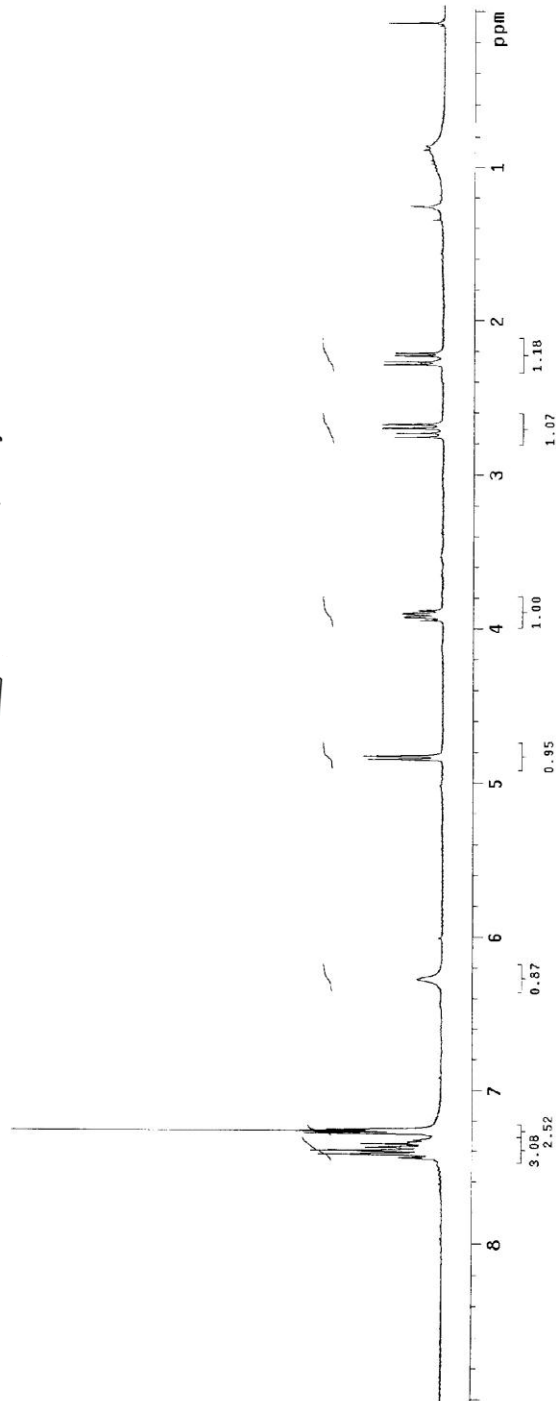


Table 2.5, Entry 1



Archive directory: /home/data/walkup/cornwall
Sample directory: rc_b4_16_20140408_01

Pulse Sequence: g2pu1

Solvent: dcd13

Temp: 299.0 C / 299.1 K

Sample Operator: Cornwall

File: rc_b4_16_20140408_01

INOVA-500 TepeX180

Relax. delay 1.000 sec

Pulse 45.0 degrees

Acq. time 1.311 sec

Width 25000.0 Hz

Observe 13C

OBSERVE F1 5050716 MHz

DECOUPLE H1 399.7037632 MHz

Power 38 dB

continuously on

WALTZ-16 modulated

DATA PROCESSING

Resolution 0.5 Hz

FT size 65536

Total time 1 hr, 17 min, 19 sec

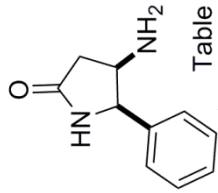
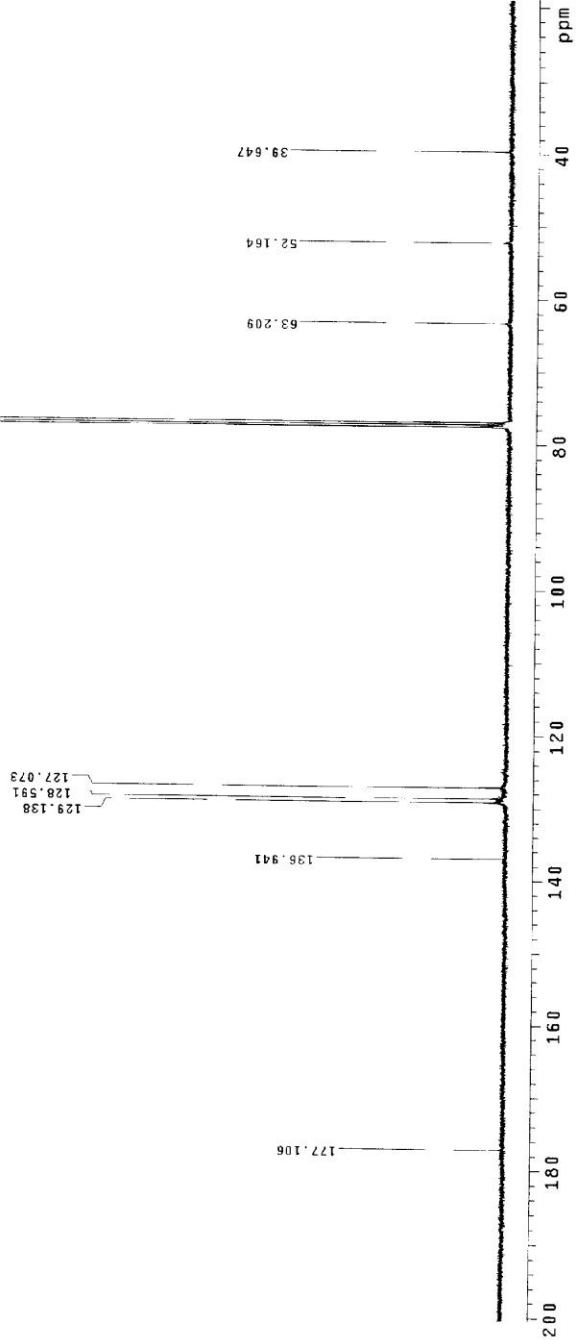
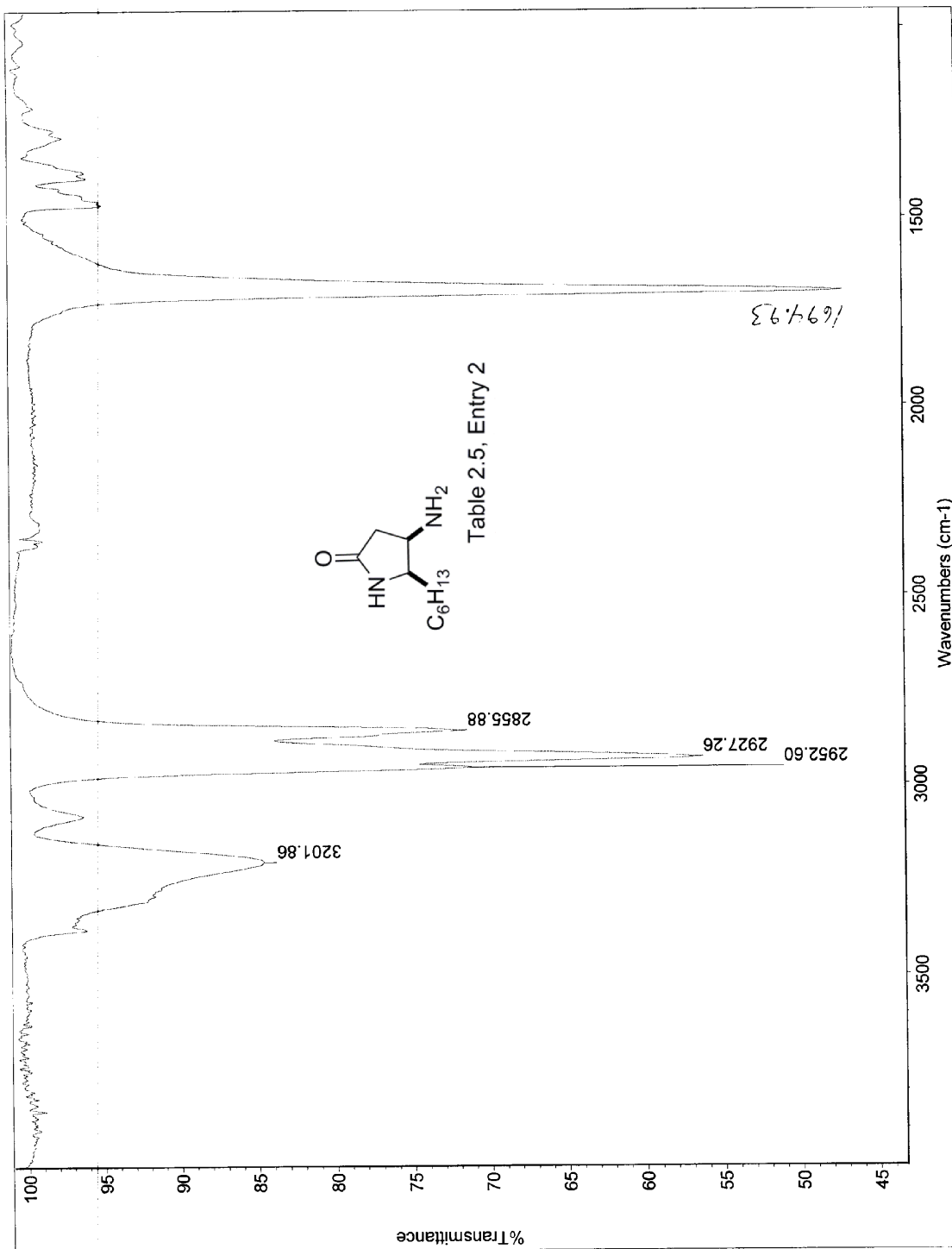


Table 2.5, Entry 1





64-31-2-080

Archive directory: /home_data/walkup/cornwall
Sample directory: rC_b4_31_2_201009_01

Pulse Sequence: s2pul

Solvent: cdcl3
Temp: 25.0 C / 299.1 K
Sample #29, Operator: cornwall
File: rC_b4_31_2_redo_1H
INDVA=500 "epoxide"

Relax. delay 1.000 sec
Pulse 45.0 degrees
Acq. time 2.556 sec
Waltz 60.3 Hz
64 repetitions
OBSERVE H1, 399.7017802 MHz
DATA PROCESSING
FT size 32768
Total time 3 min, 48 sec

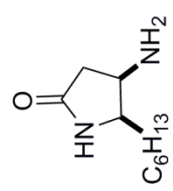
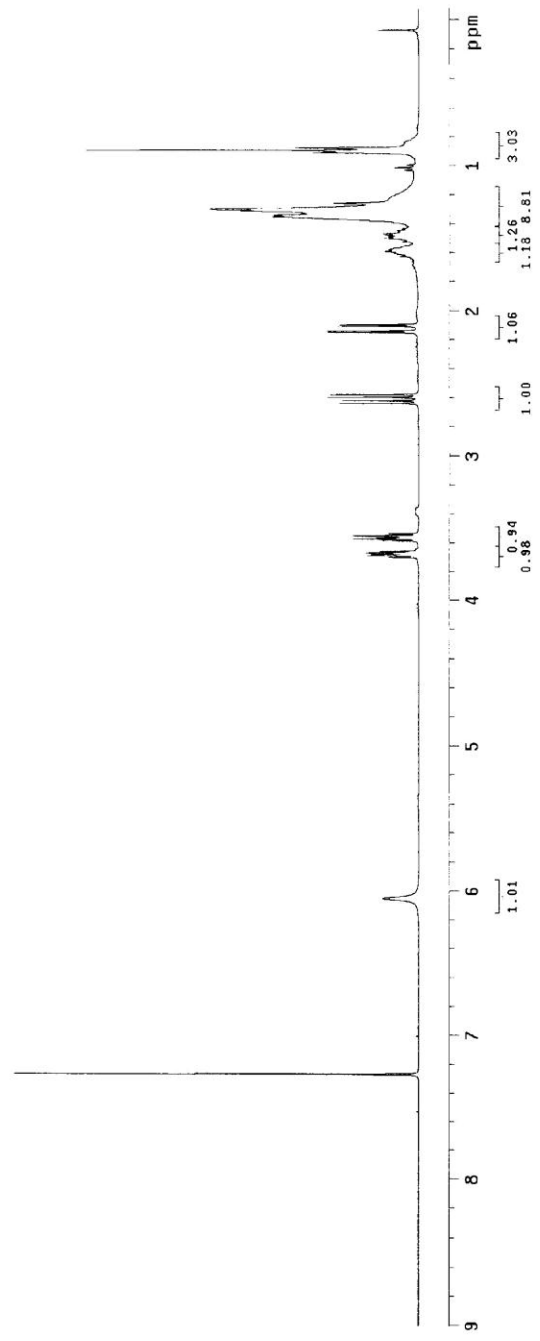


Table 2.5, Entry 2



Archive directory: /home/data/walkup/cormwall
Sample directory: rc_b4_31_2_20160409_01

Pulse Sequence: s2pu1

Solvent: cdcl3

Temp: 29.0 C / 299.1 K

Sample: 425 mg, 0.5000 mol, CORMWALL

File: rc_b4_31_2_Fe00_130

INOVA-500 "epoXtide"

Relax. delay 1.000 sec

Pulse 45.0 degrees

Acq. time 1.311 sec

2400, 25000.0 Hz

2400, 25000.0 Hz

OBSERVE C13 100.5050708 MHz

DECOUPLE H1 399.7037832 MHz

Power 38 dB

continuously on

Waltz16 modulated

DWAVE SSING

Line broadening 0.5 Hz

FT size 65536

Total time 1 hr, 17 min, 19 sec

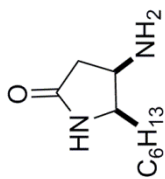
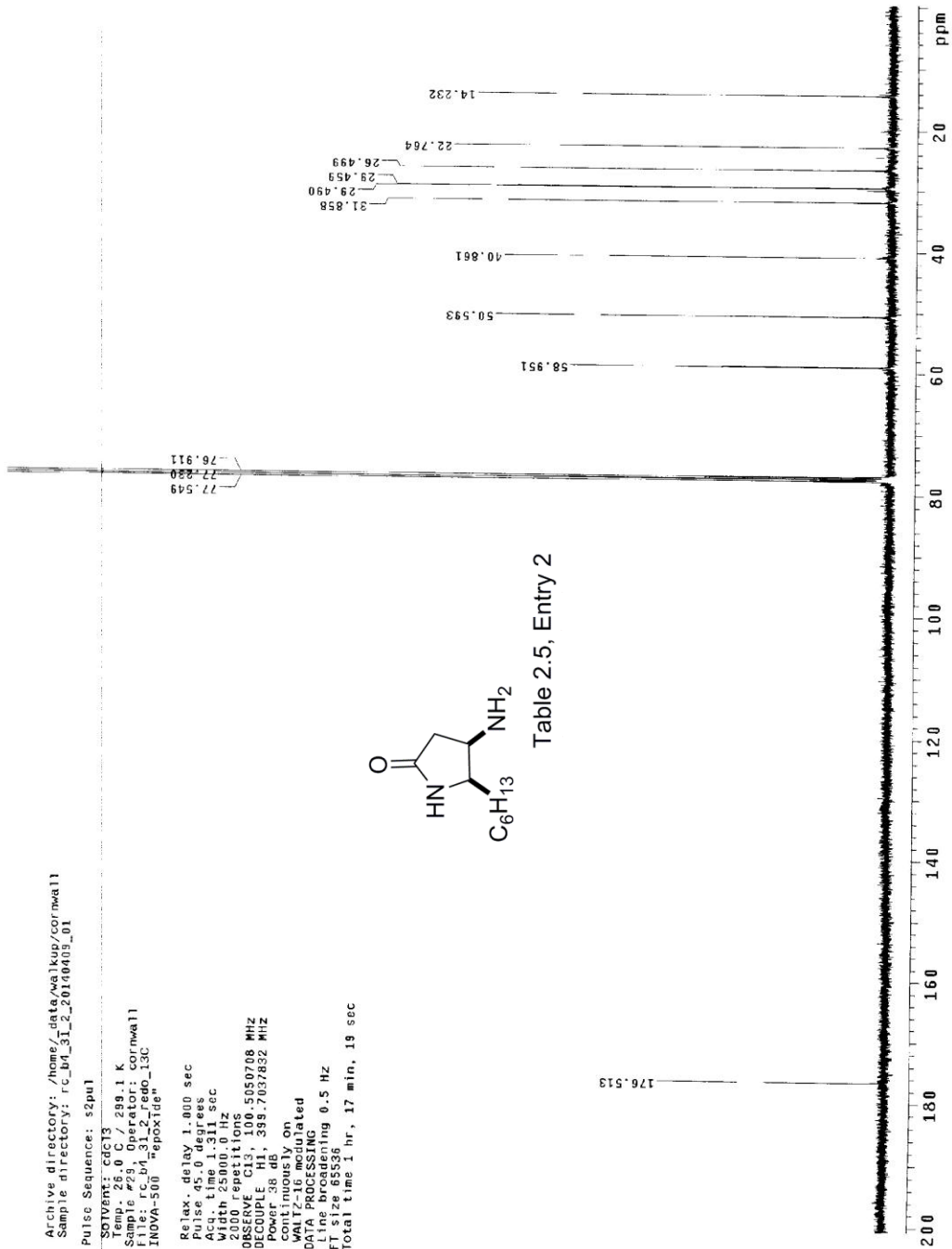
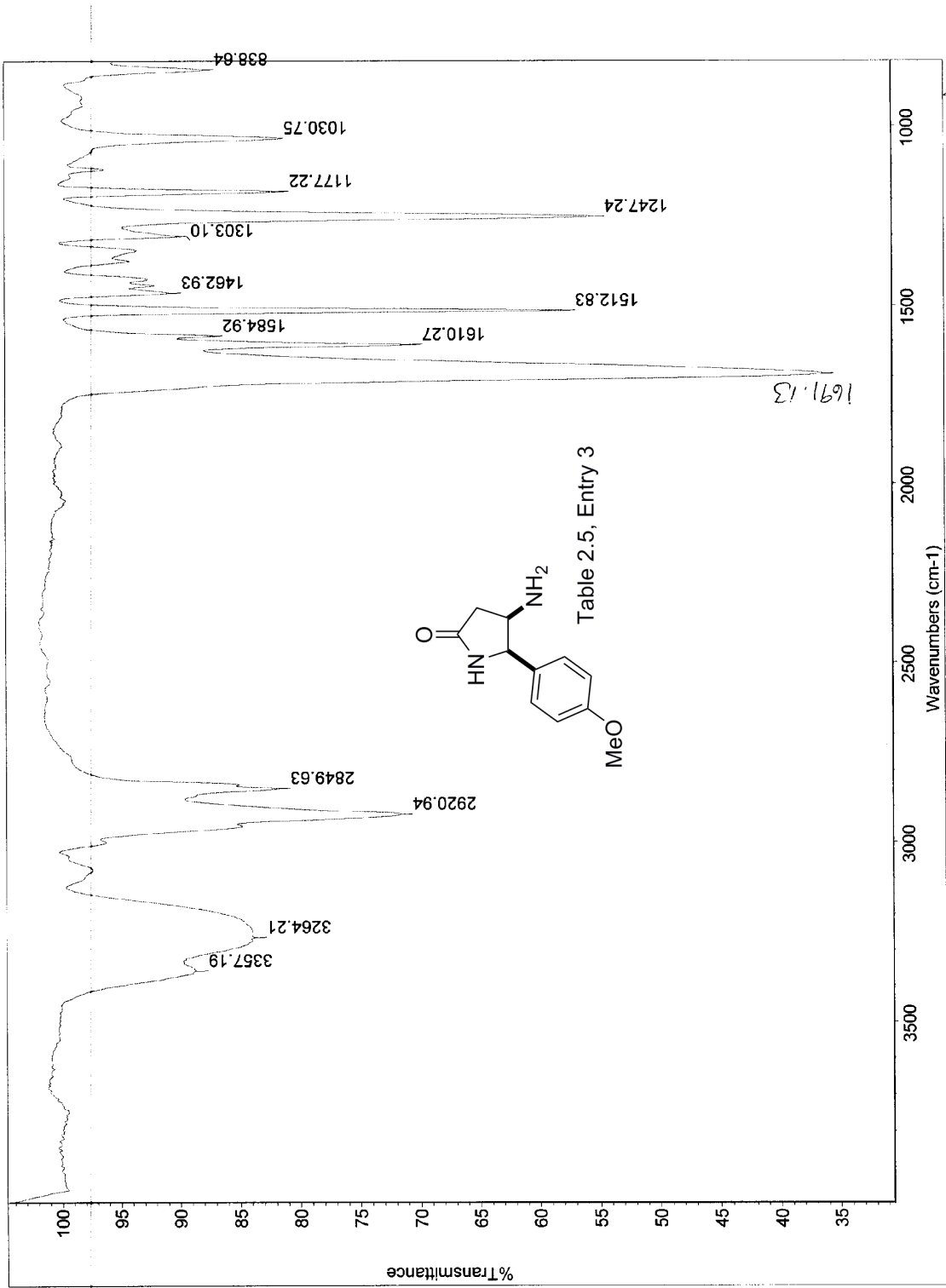


Table 2.5, Entry 2





h4-31-redo

STANDARD 1H OBSERVE

Pulse Sequence: s2pu1

Solvent: CDCl3

Ambient Temperature

File: 31_1_inh_CHCl3extract2

INVA: 500 "epok1db"

Relax. delay 0.000 sec

Pulse: 26.0 degrees

Acq. time 2.668 sec

Width 5895.2 Hz

4 repetitions

QPC: 300.1592164 MHz

DATA PROCESSING

Gauss apodization 0.896 sec

FT size 32768

Total time 0 min, 16 sec

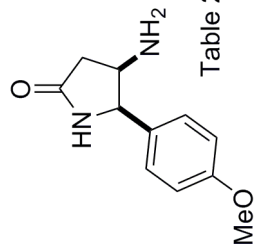
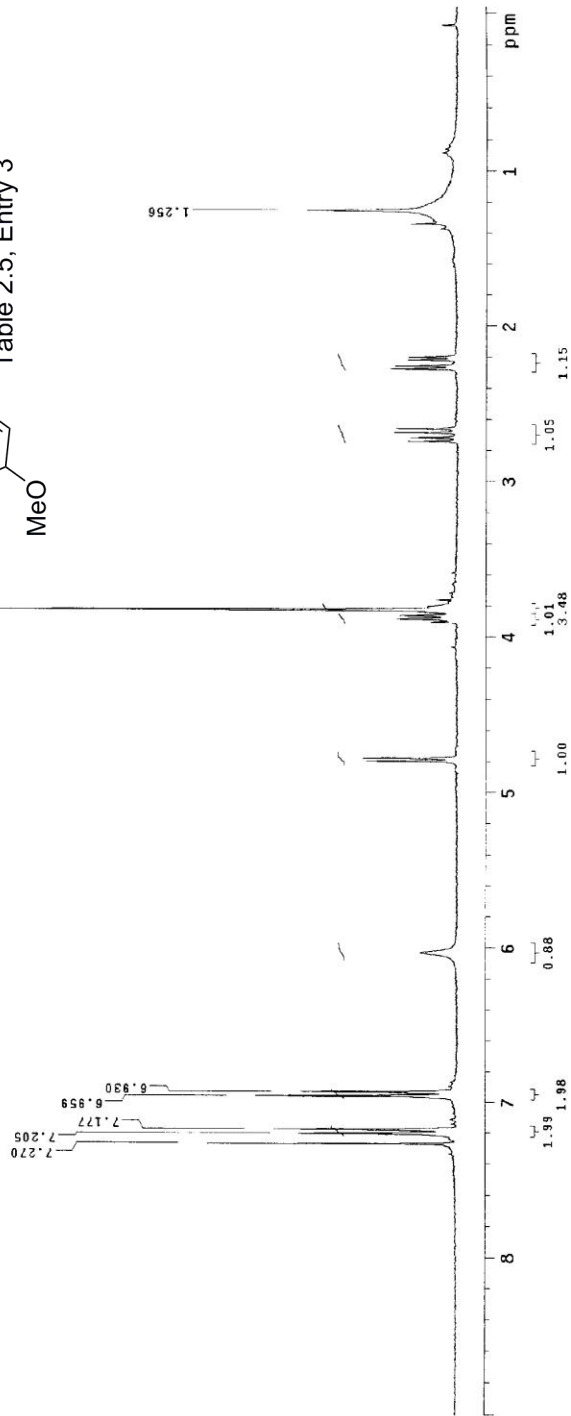


Table 2.5, Entry 3



Archive directory: /home/_data/walkup/cornwall
Sample directory: rc_b4_31_1_20140312_01

Pulsa Sequence: s2pul

Solvent: cdcl3
Temp: 26.0 C / 289.1 K
Sample #38, Operator: cornwall
File: rc_b4_31_1_check_13C
INOVA-500 "epoxide"

Relax. delay 1.000 sec
Pulse 45.0 degrees
Pulse width 12.000 sec
Width 2800.0 Hz
2000 repetitions
OBSERVE C13, 100.5050708 MHz
DECOUPLE H1, 399.7037832 MHz
Power 38 dB
Continuously on
Waltz modulated
DATA PROCESSING
Line broadening 0.5 Hz
FT size 65536
Total time 1 hr, 17 min, 19 sec

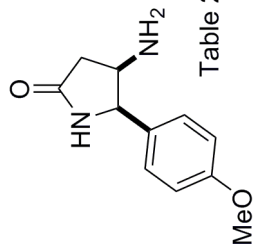
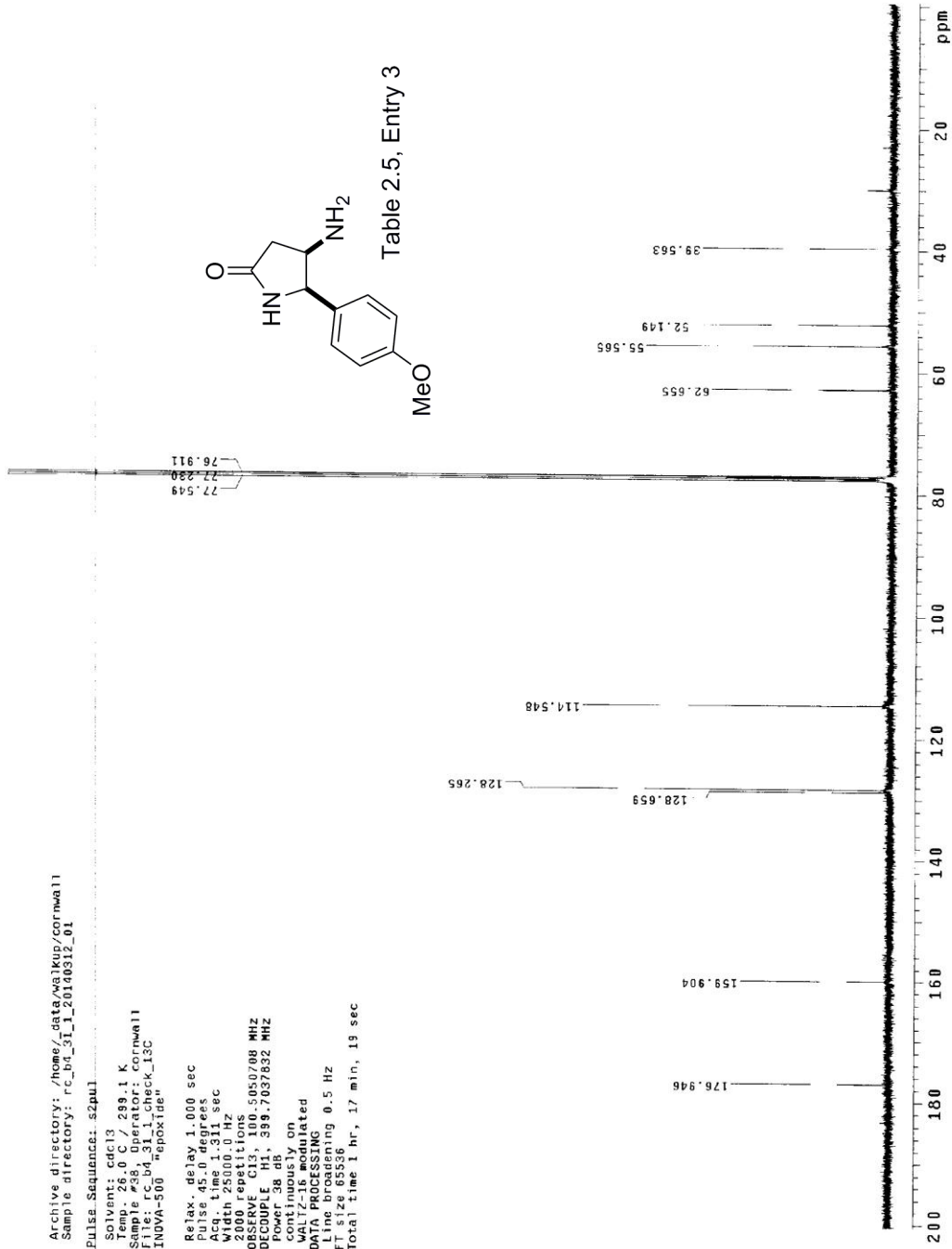
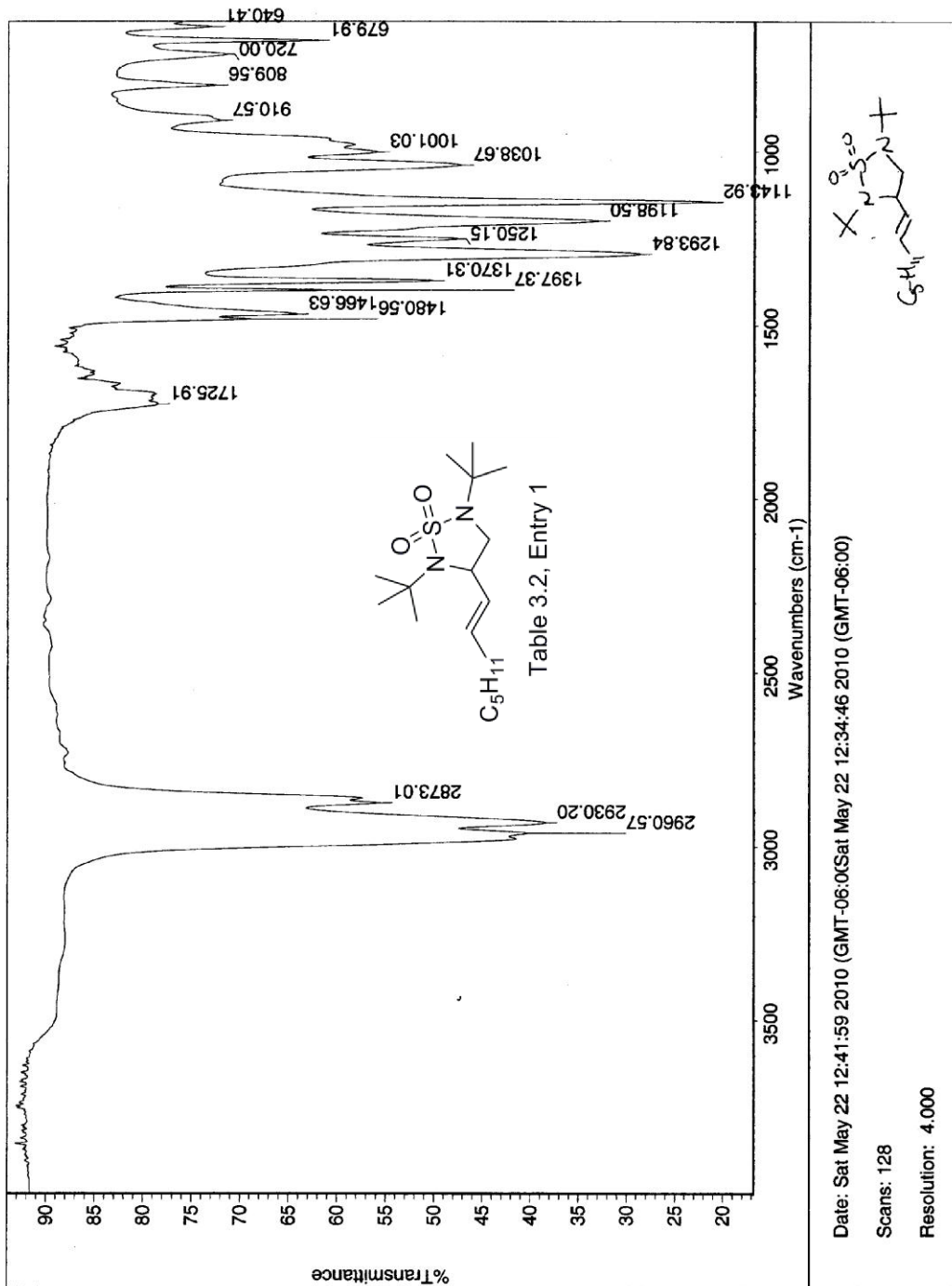


Table 2.5, Entry 3



Appendix 2 Spectra for Chapter 3



STANDARD 1H OBSERVE

Pulse Sequence: s2pul
 Solvent: CDCl3
 Acquisition Mode
 File: FC_500_0016.F
 INOVA-500 1Hproxiide"

Pulse 42.4 degrees
 Acq. time 2.281 sec
 F1 freq 500.136115 MHz
 F2 freq 125.761531 MHz
 4 FID bits
 OBSERVE H1, 400.1063115 MHz
 DATA PROCESSING
 Phase optimization 0.971 sec
 F1 resolution 0.395 Hz
 Total time 0 min, 13 sec

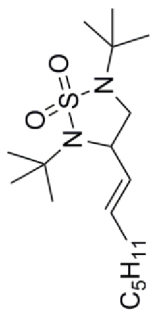
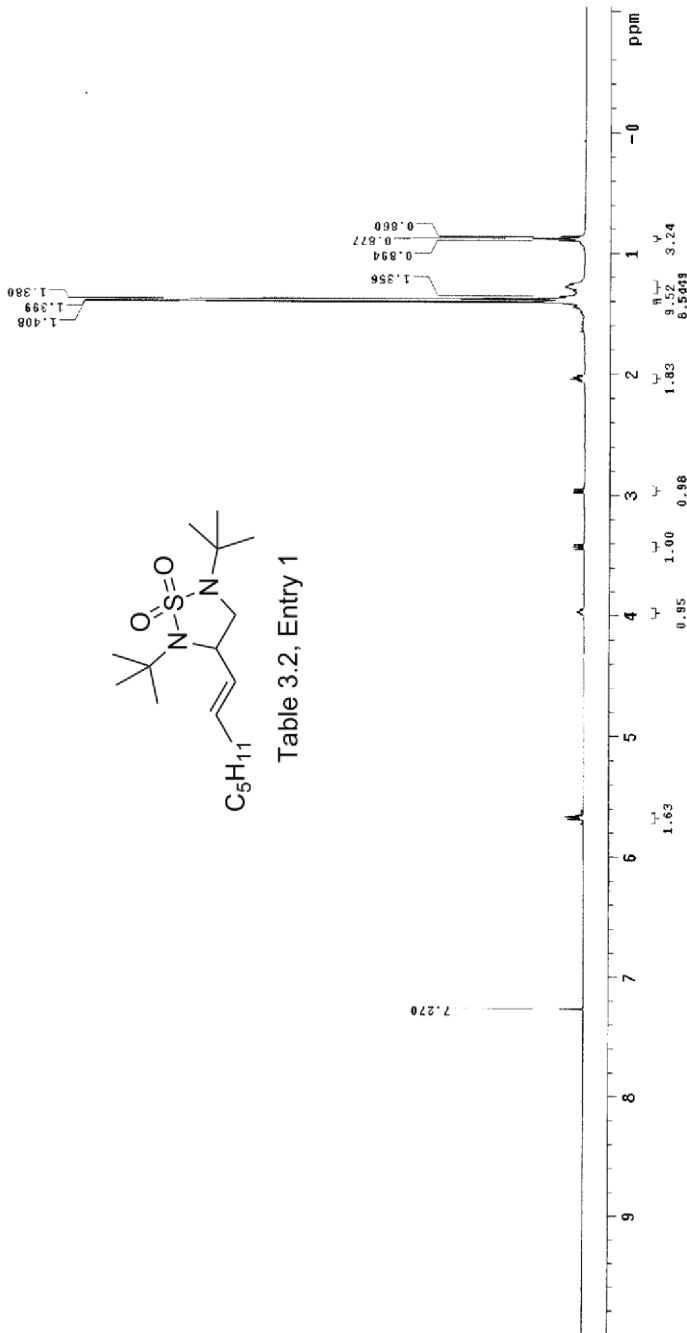


Table 3.2, Entry 1



13C OBSERVE

Pulse Sequence: s2pul1

Solvent: CDCl3

Ambient Temperature

INOR-500

Relax. delay 1.700 sec

Pulse 36.6 degrees

Acq. time 0.583 sec

width 30010.0 Hz

895

OBSERVE C13, 100.6067923 MHz

DECOUPLE H1, 400.1083268 MHz

Power 3b db

WALTZ-16 modulated

DATA PROCESSING

Line broadening 2.0 Hz

Total Time 02:27:35 hr, 34 min, 7 sec

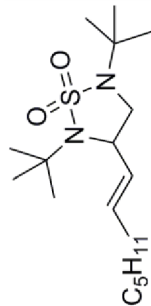
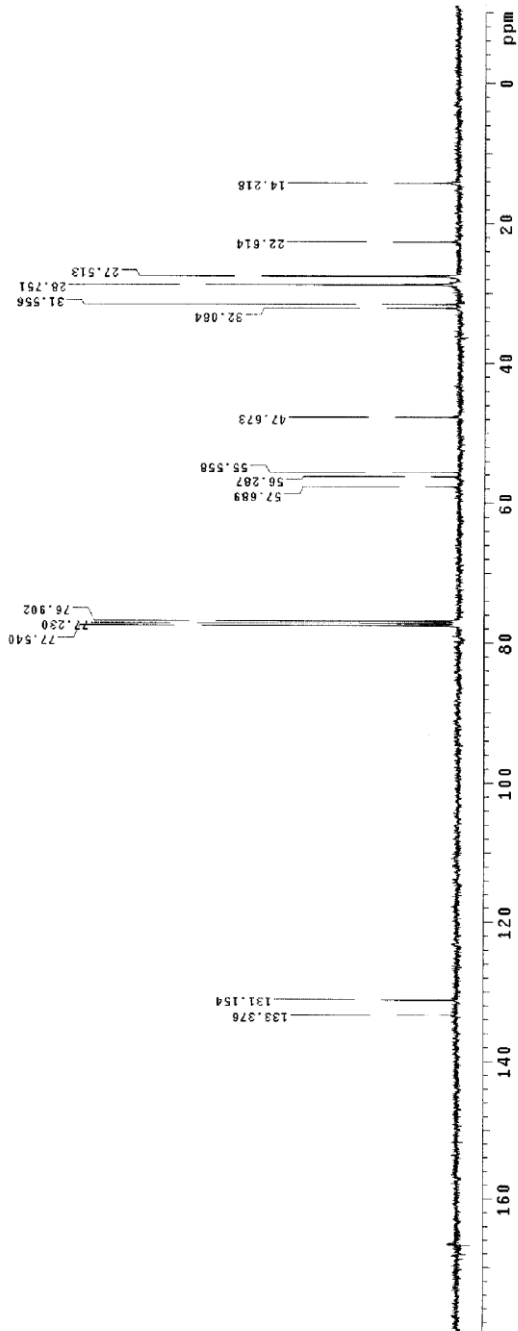


Table 3.2, Entry 1



STANDARD IN OBSERVE

Pulse Sequence: s2pul
Solvent: CDCl3
Ambient temperature
New 0035264
INDWA-500 "report.de"

Relax. delay 0.000 sec
Pulse 26.0 degrees
Acq. time 2.065 sec
F1 300.13102 Hz
F2 75.26130 Hz

OBSERVE F1, 300.1592164 MHz
DATA PROCESSING
Gauss. apodization 0.896 sec
Phase 0.0000000000000000
Total time 0 min, 10 sec

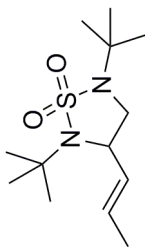
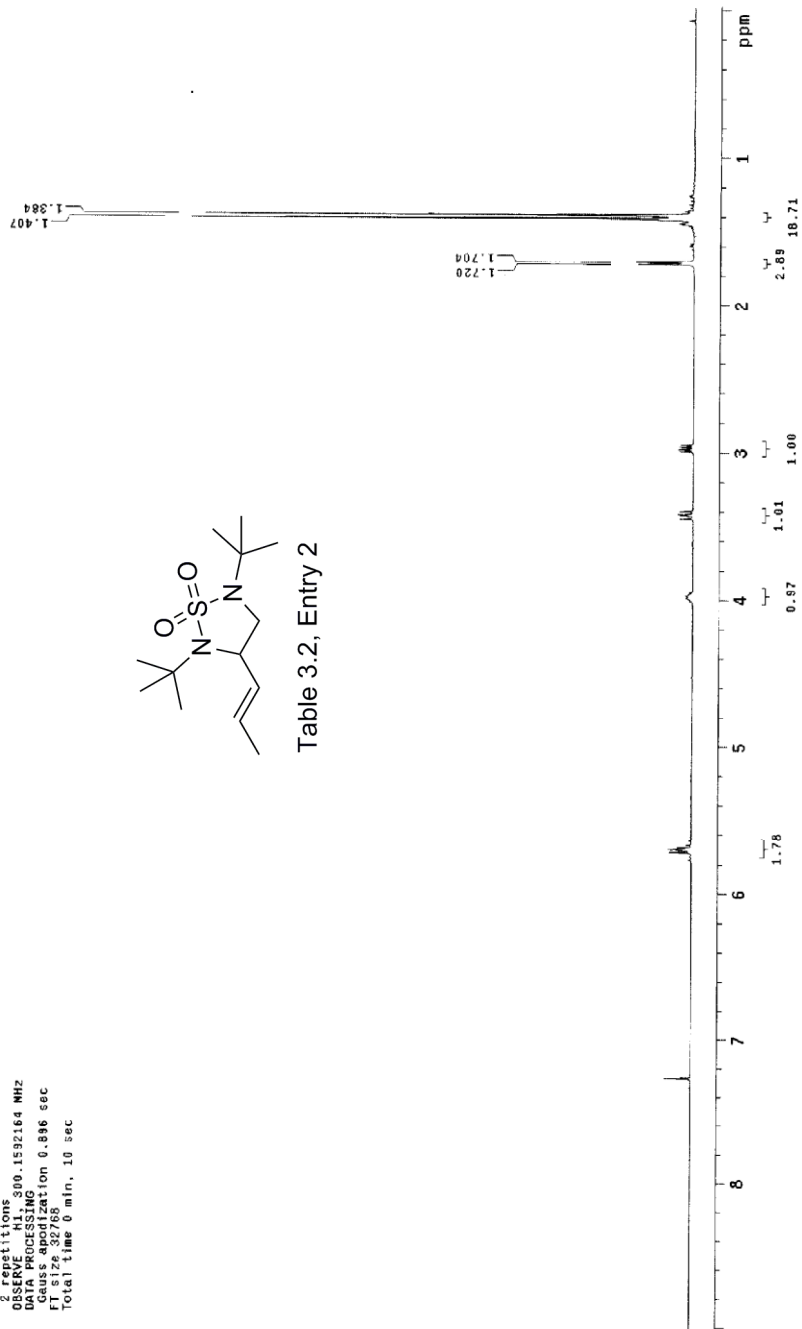


Table 3.2, Entry 2



13C OBSERVE

Pulse Sequence: s2pul

Solvent: CDCl3

Ambient temperature

IN00A-508 "epoxide"

Relax. delay 1.000 sec

Pulse 46.3 degrees

Acq. time 0.697 sec

Relax. delay 2.000 sec

104 repetitions

OBSERVE C13, 75.4750804 MHZ

DECOUPLE H1, 300.1606799 MHZ

Cont. acquire on

WALTZ-16 modulated

DATA PROCESSING

Line broadening 2.0 Hz

Relax. delay 2.000 sec

Total time 28 min, 26 sec

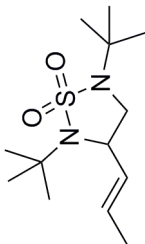
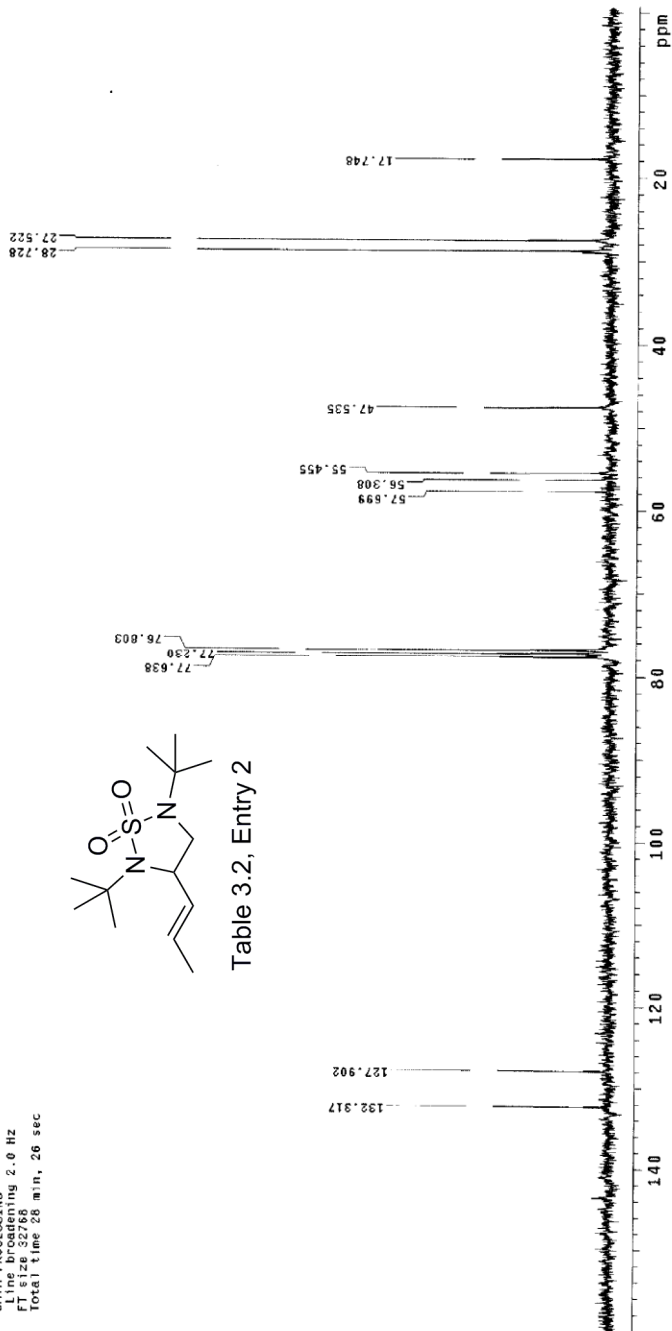
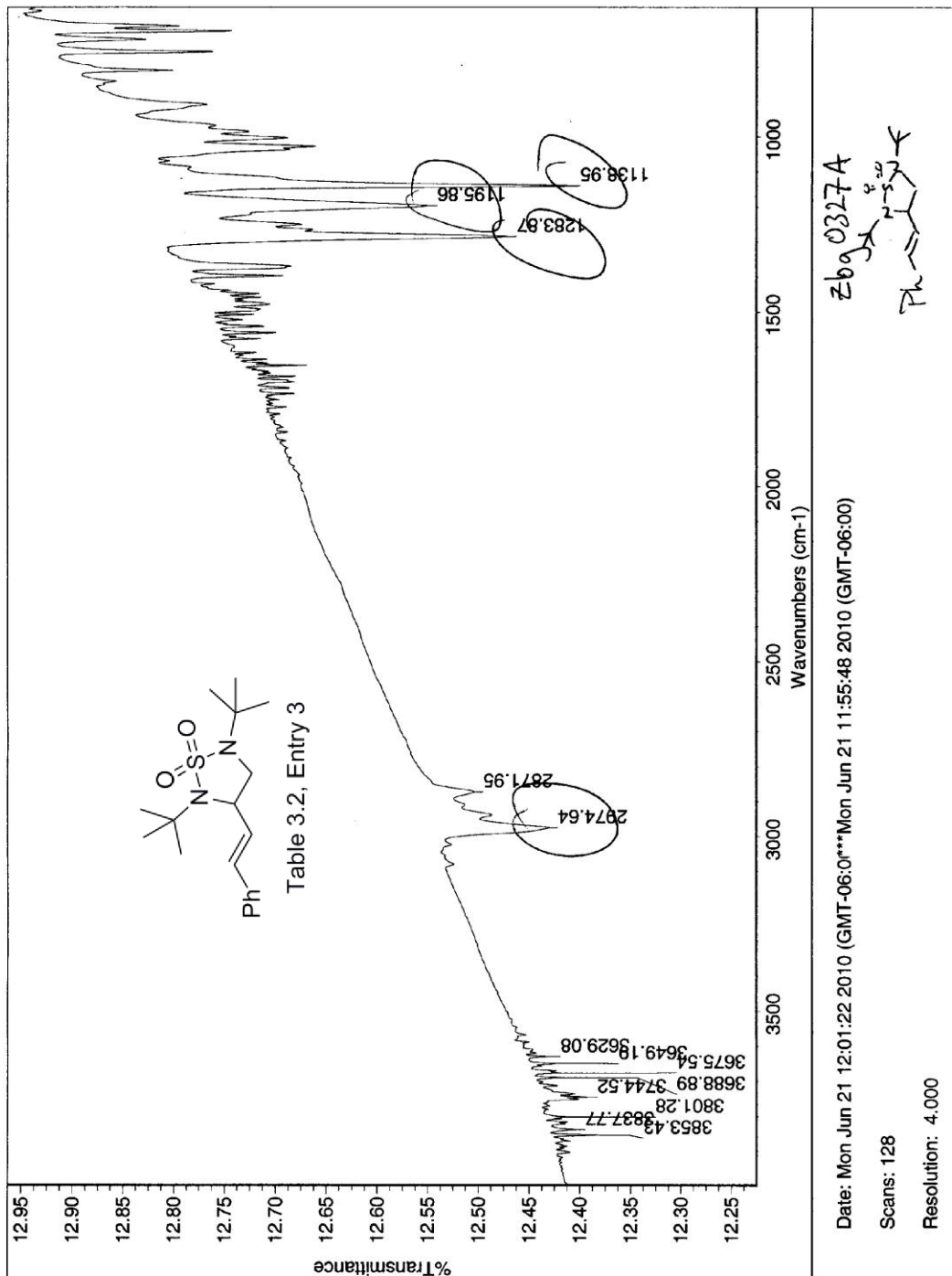


Table 3.2, Entry 2





STANDARD 1H OBSERVE

Pulse Sequence: s2pul

Solvent: CDCl3

Ambient temperature

Pressure: 1013.25 hPa

INVA-500 - epoxide

Relax. delay 1.000 sec

Pulse 34.0 degrees

Acq. time 2.732 sec

Chemical shift

4.1 ppm

4.1 ppm

OBSERVE 1H, 299.8503069 MHZ

DATA PROCESSING

Guess apodization 0.824 sec

Phase shift

Total time 0 min, 22 sec

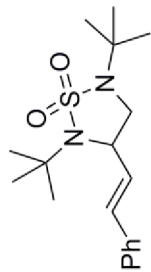
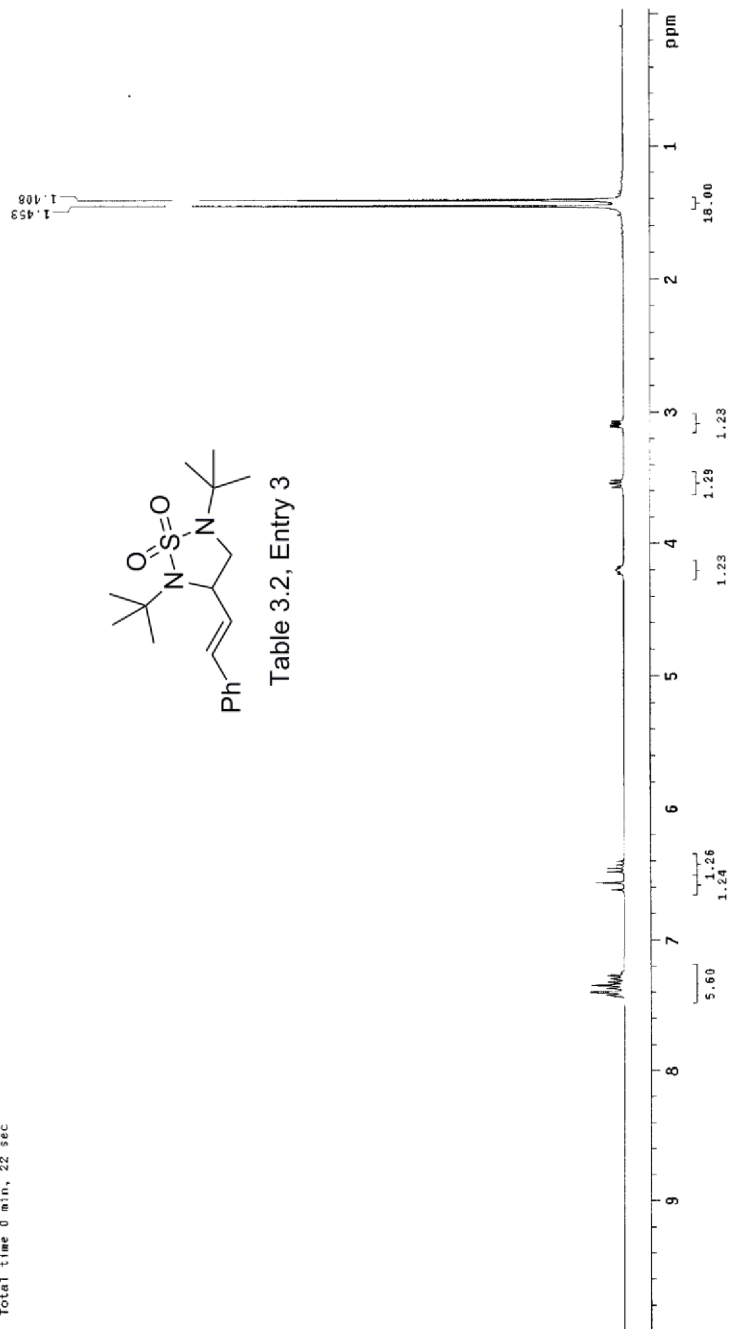


Table 3.2, Entry 3



13C OBSERVE

Pulse Sequence: s2pul
Solvent: CDCl3
Ambient temperature
Relaxation delay: 1.700 sec
INOVA-500 -topoxide

Relax. delay 1.700 sec
Pulse 56.6 degrees
Acq. time 0.535 sec
Mag. 10.000000 Hz
167 repetitions

OBSERVE C13, 100.6068014 MHZ
DECOUPLE H1, 400.1085268 MHZ

CONTINUOUSLY ON
WALTZ-16 modulated

DATA PROCESSING
Line broadening 2.0 Hz

Total time 627.35 hr, 34 min, 7 sec

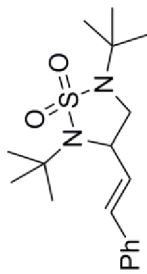
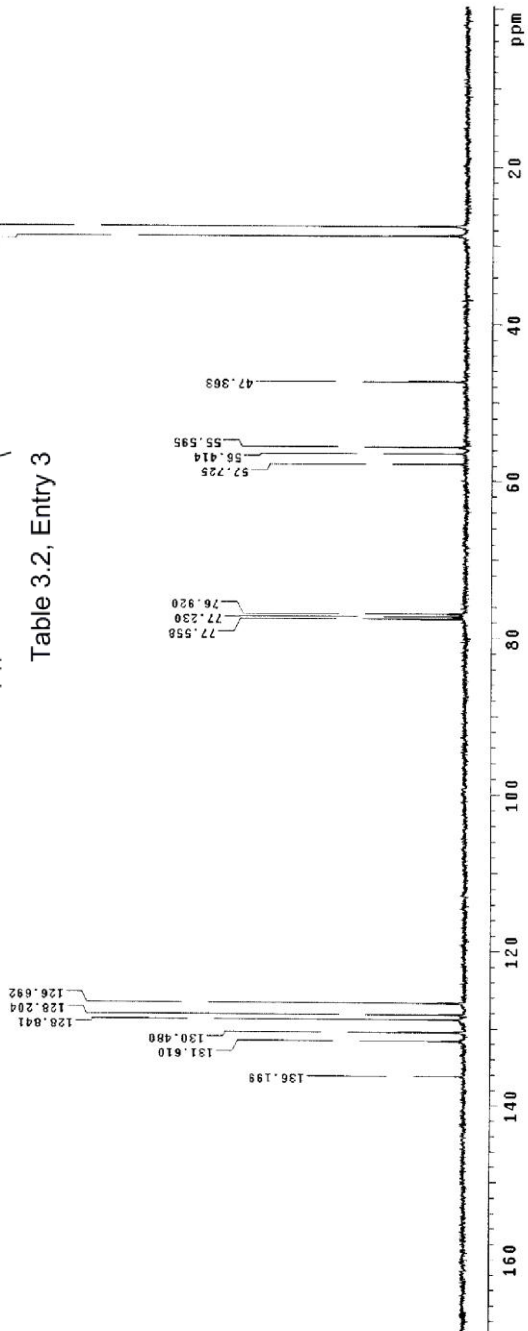
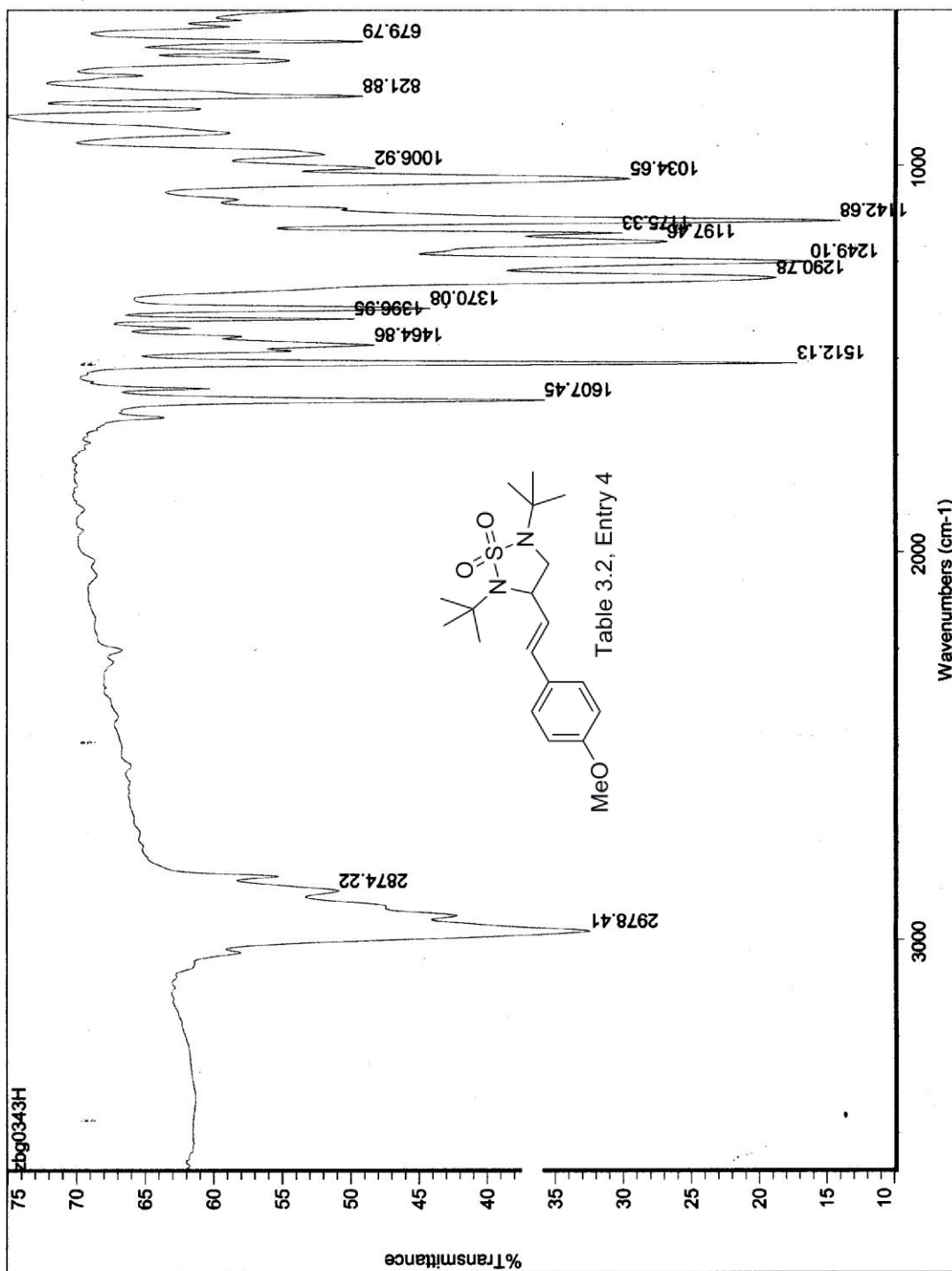


Table 3.2, Entry 3





STANDARD 1H OBSERVE

Pulse Sequence: s2pul
Solvent: CDCl3
Ambient temperature
Reference: 0.05 ppm
INVA: 500 "ppm/ide"

Relax. delay 0.000 sec
Pulse 26.0 degrees
Acq. time 2.665 sec
Width 245.2 Hz
Z-fid 115.2 Hz

OBSERVE F1: 300.1592160 MHz
DATA PROCESSING
Gauss apodization 0.896 sec
F1: 300.1592160 MHz
Total time 0 min, 10 sec

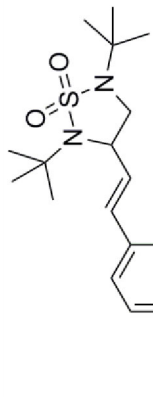
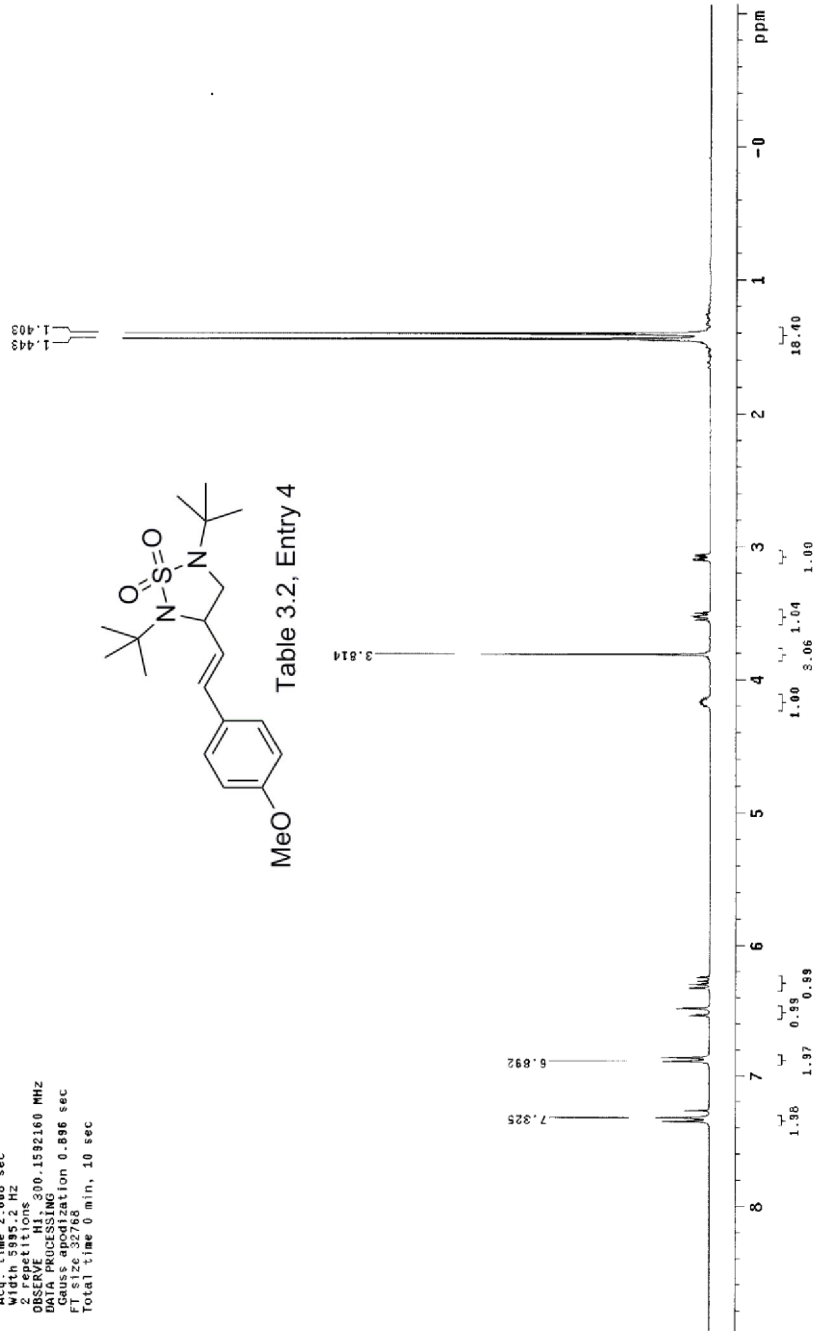


Table 3.2, Entry 4



13C OBSERVE

Pulse Sequence: s2put
Solvent: CDCl3
Ambient temperature
File: 200033H-Cl3
INVA-500 "apocrite"
Relax. delay 1.000 sec
Pulse 46.3 degrees
Acq. time 0.697 sec
Width 2325.8 Hz
SFO 100.625139 MHz
OBSERVE C13 75.4750846 MHz
DECOUPLE H1 300.1602739 MHz
Power 40 dB
SFO 100.625139 MHz
WALTZ-16 modulated
DATA PROCESSING
Line broadening 2.0 Hz
FI size 32768
Total time 28 min, 26 sec

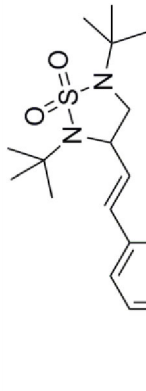
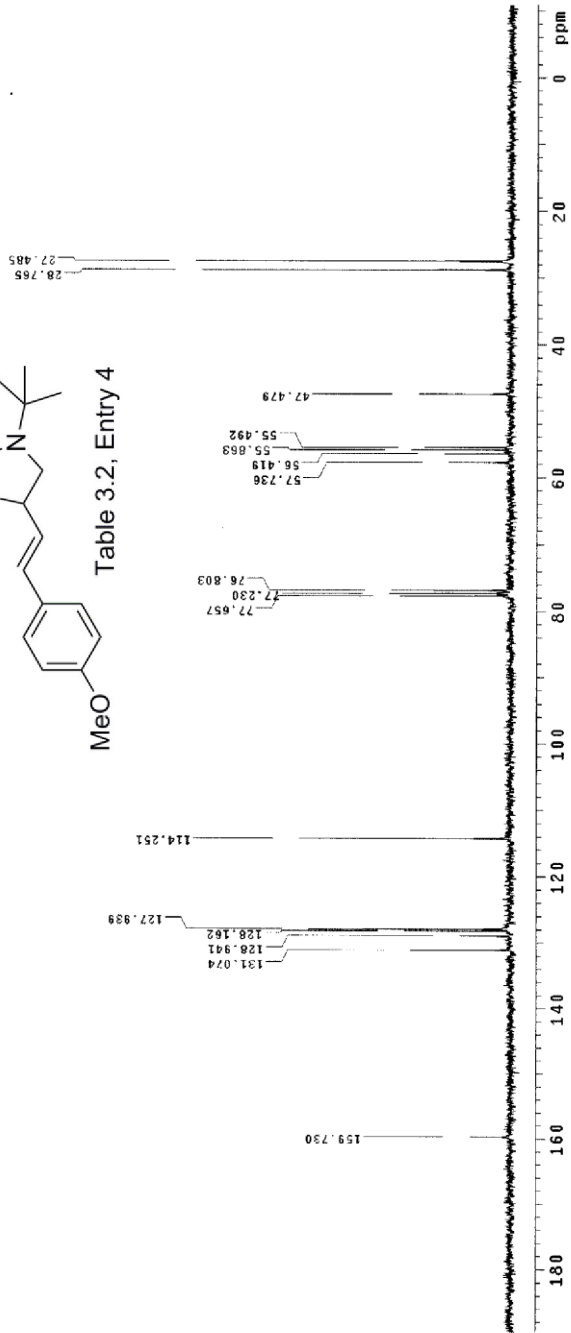
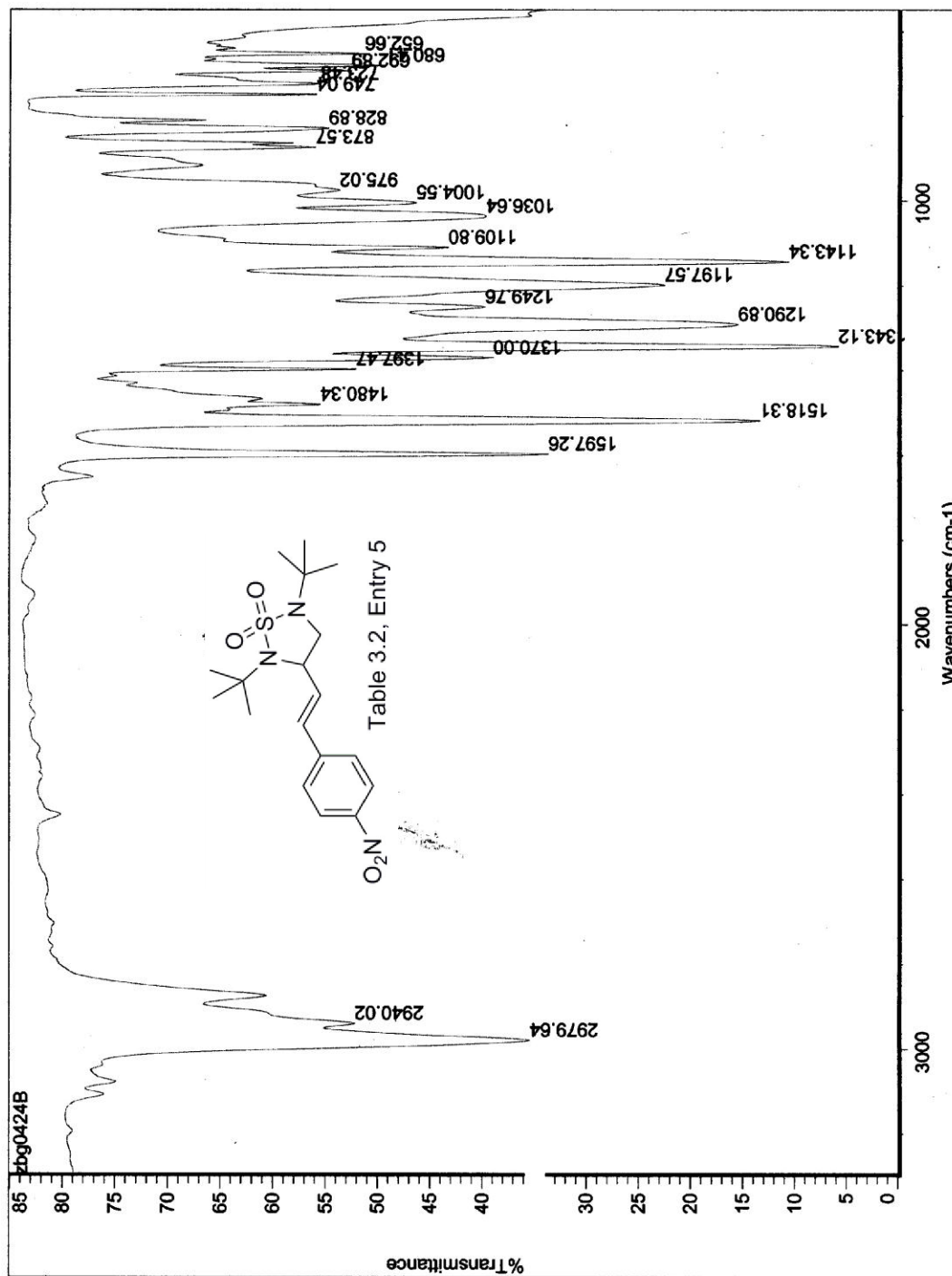


Table 3.2, Entry 4





STANDARD 1H OBSERVE

Pulse Sequence: s2pul

Solvent: CDCl3

Ambient temperature

F100: Z0000248-N

INSTR: 500 "epoxide"

Relax. delay 0.000 sec

Pulse 26.0 degrees

Acq. time 2.666 sec

31.000 MHz

31.000 MHz

OBSERVE F1: 300.1592164 MHZ

DATA PROCESSING

Gauss apodization 0.696 sec

Phase 0.000000

Total time 7 hr, 26 min, 17 sec

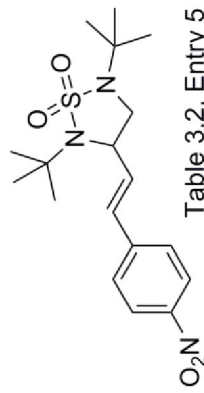
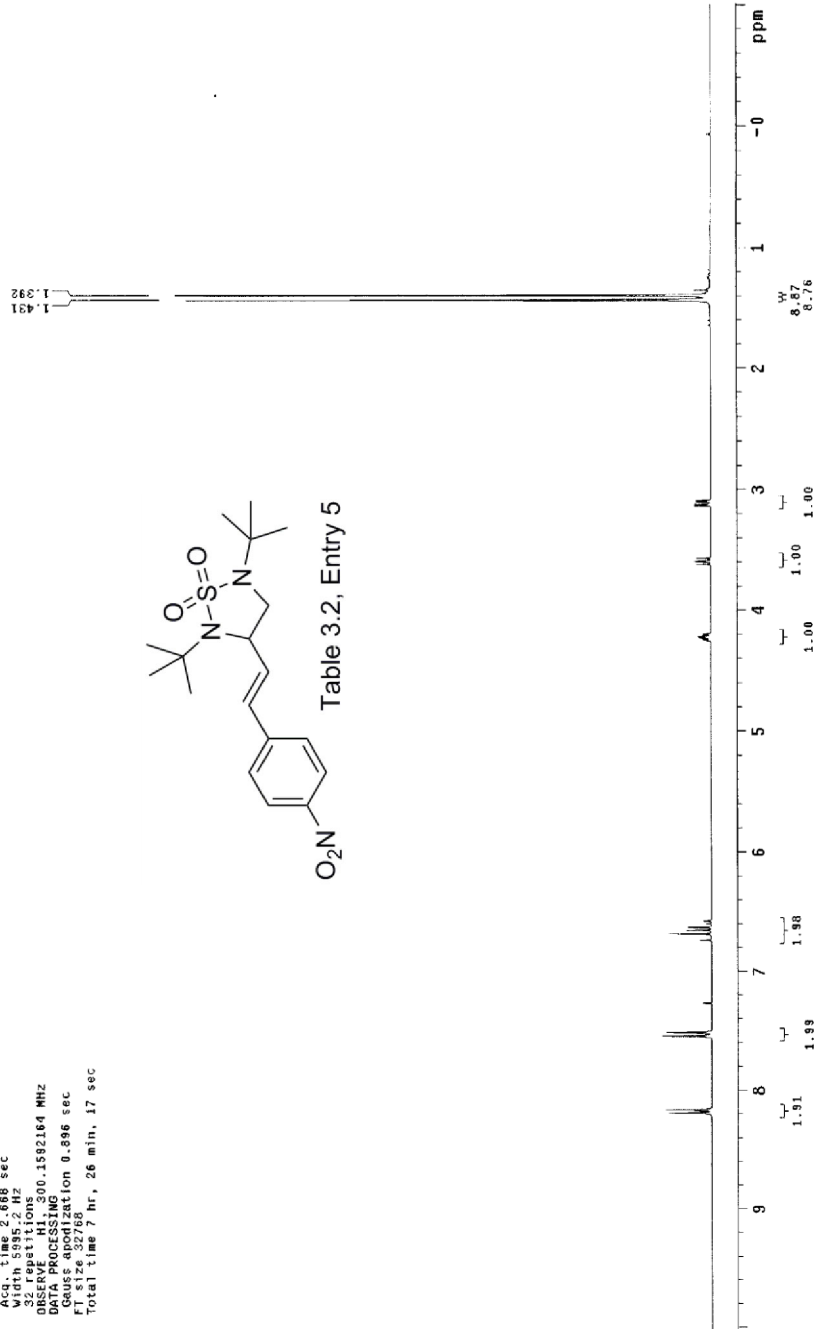


Table 3.2, Entry 5



13C OBSERVE

Pulse Sequence: s2pul
Solvent: CDCl3
Ambient Temperature
File: zbg0424b-c13
IN04A-509 "epoxide"

Relax delay 1.000 sec
Pulse 46.3 degrees
Acq. time 0.657 sec
Width 2235.8 Hz
Observer: C13 75.4750846 MHz
DECOUPLE H1 300.1608738 MHz
Power 40 dB
Continuously on
Data Processing
Line broadening 2.0 Hz
F1 size 32788
Total time 4 hr., 44 min., 20 sec

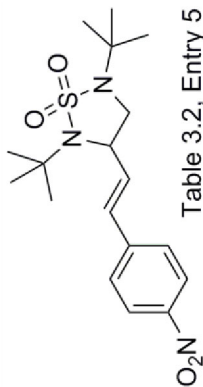
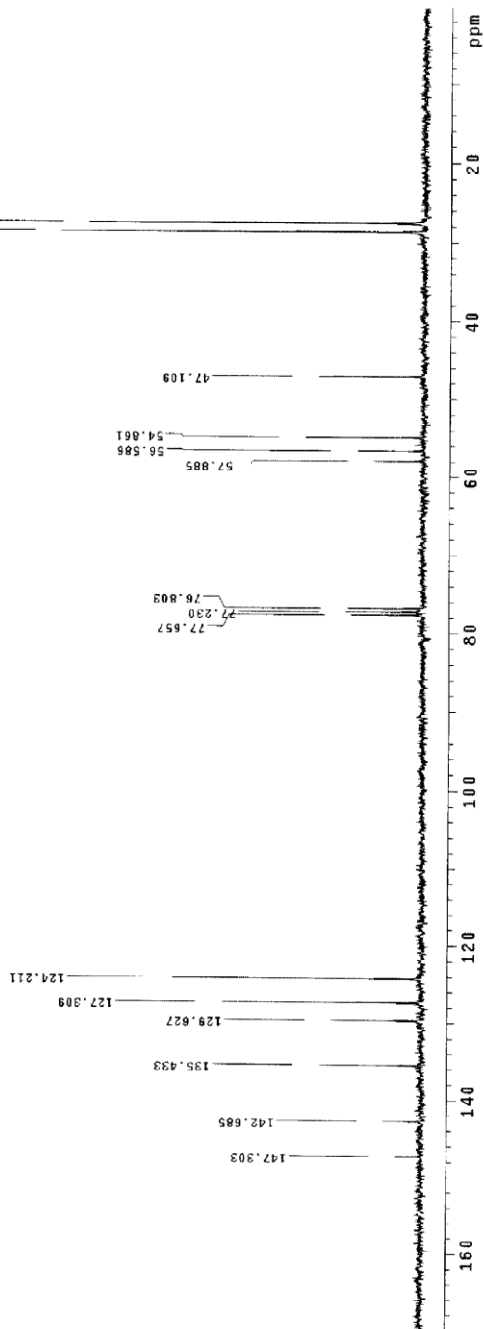
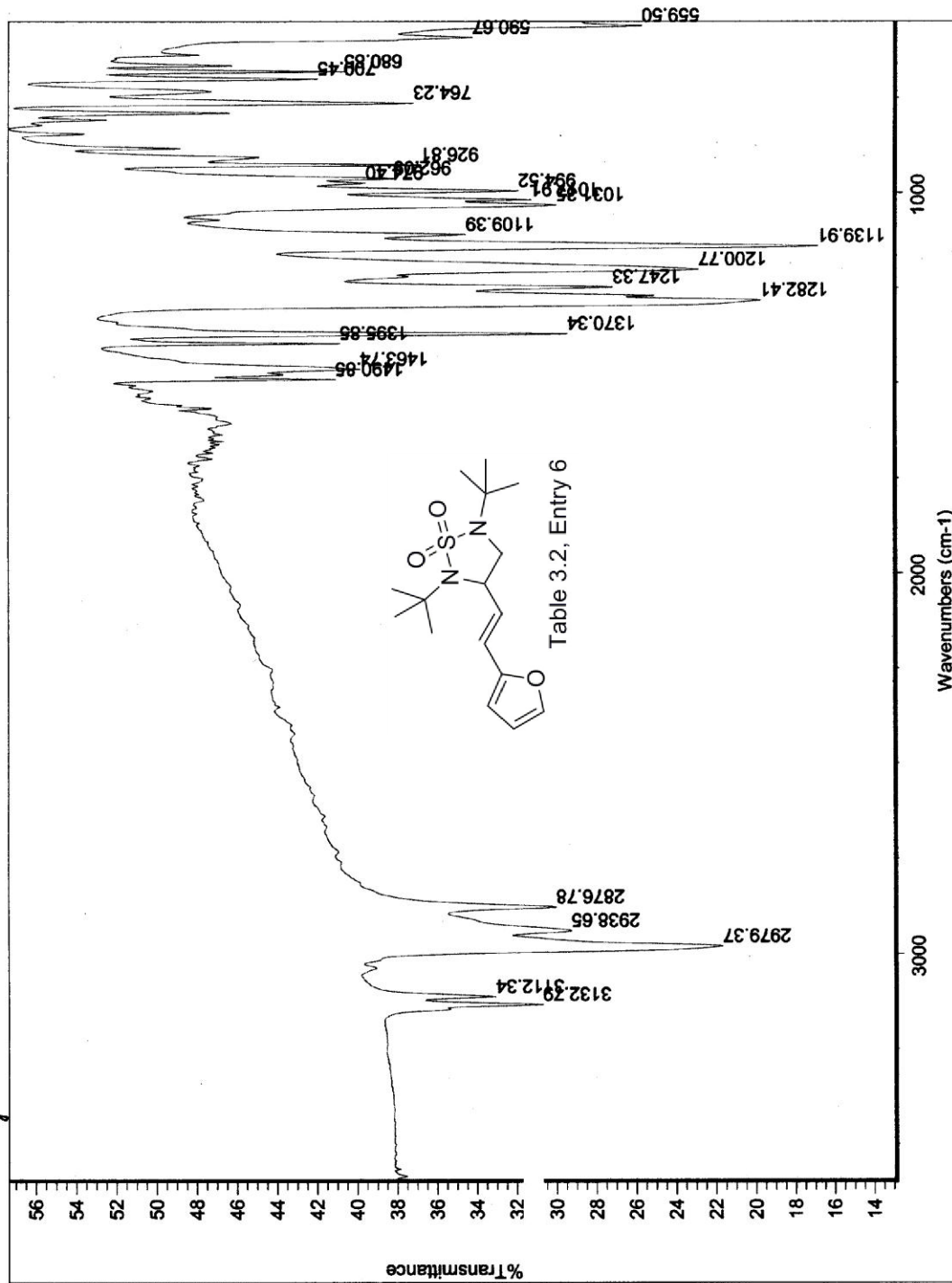


Table 3.2, Entry 5



2469000 A



STANDARD 1H OBSERVE

Pulse Sequence: s2pul
Solvent: CDCl3
Ambient temperature
File: 20040424-A-1
INOVA-500 "epoxide"
Relax. delay 0.000 sec
Pulse 26.0 degrees
Acq. time 2.565 sec
Width 5335.2 Hz
F2 125.760 MHz
OBSERVE 1H 300.1582164 MHz
DATA PROCESSING
Cause apodization 0.998 sec
F2 125.760 MHz
Total time 0 min, 10 sec

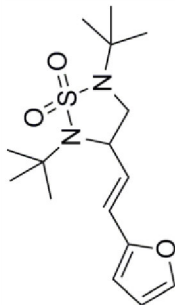
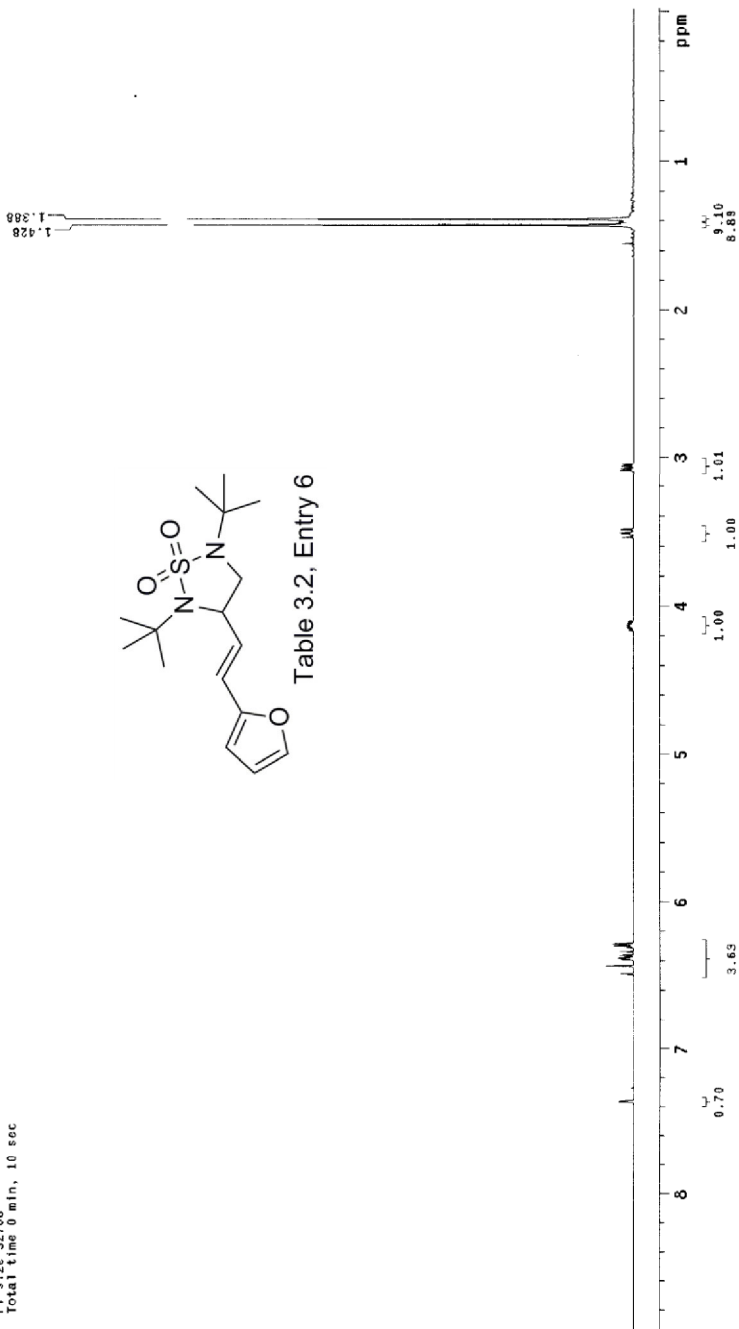


Table 3.2, Entry 6



13C OBSERVE

Pulse Sequence: s2pul
Solvent: CDCl3
Ambient temperature
F1: 100.626313
INVA: 500 "positive"

Relax. delay 1.000 sec
Pulse 46.3 deg/raes
Acq. time 0.597 sec
Width 2833.6 Hz
90 deg 41.30
OBSERVE C13, 75.4750818 MHZ
DECOUPLE H1, 300.1606799 MHZ
Power 40 dB
Pulse delay on
WALTZ-16 modulation
DATA PROCESSING
Line broadening 2.0 Hz
F1 size 32786
Total time 4 hr, 44 min, 20 sec

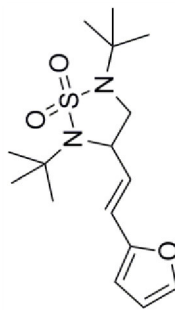
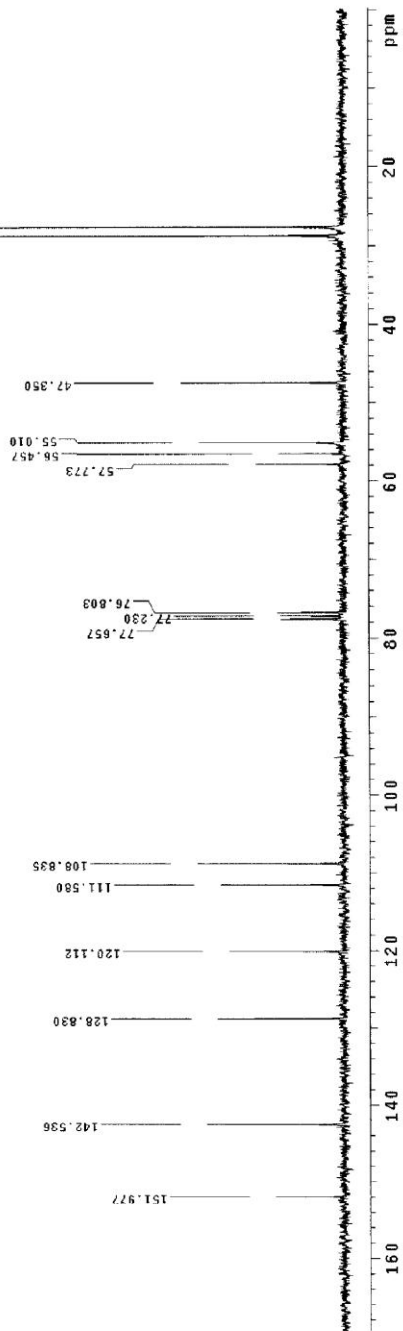
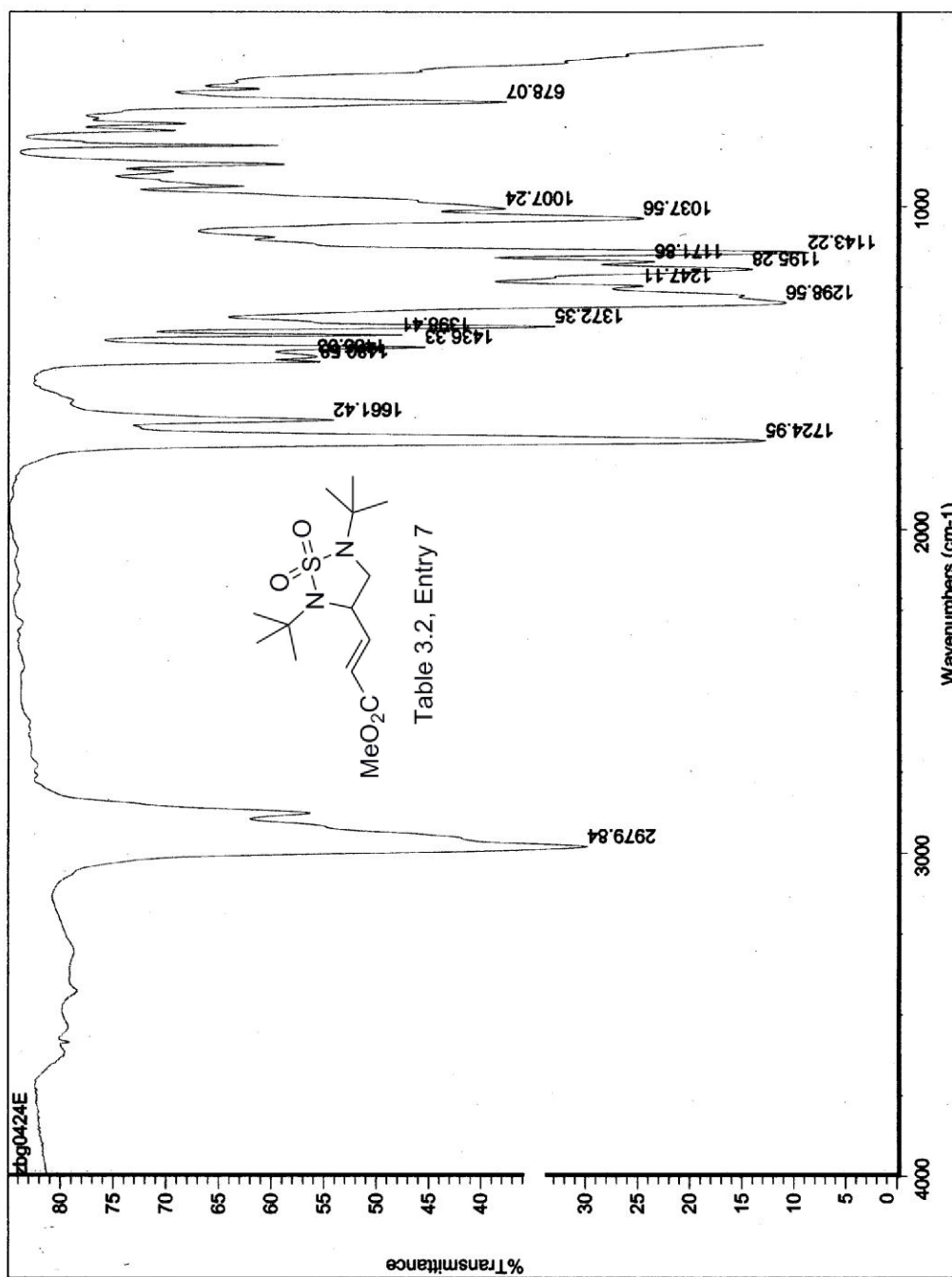


Table 3.2, Entry 6



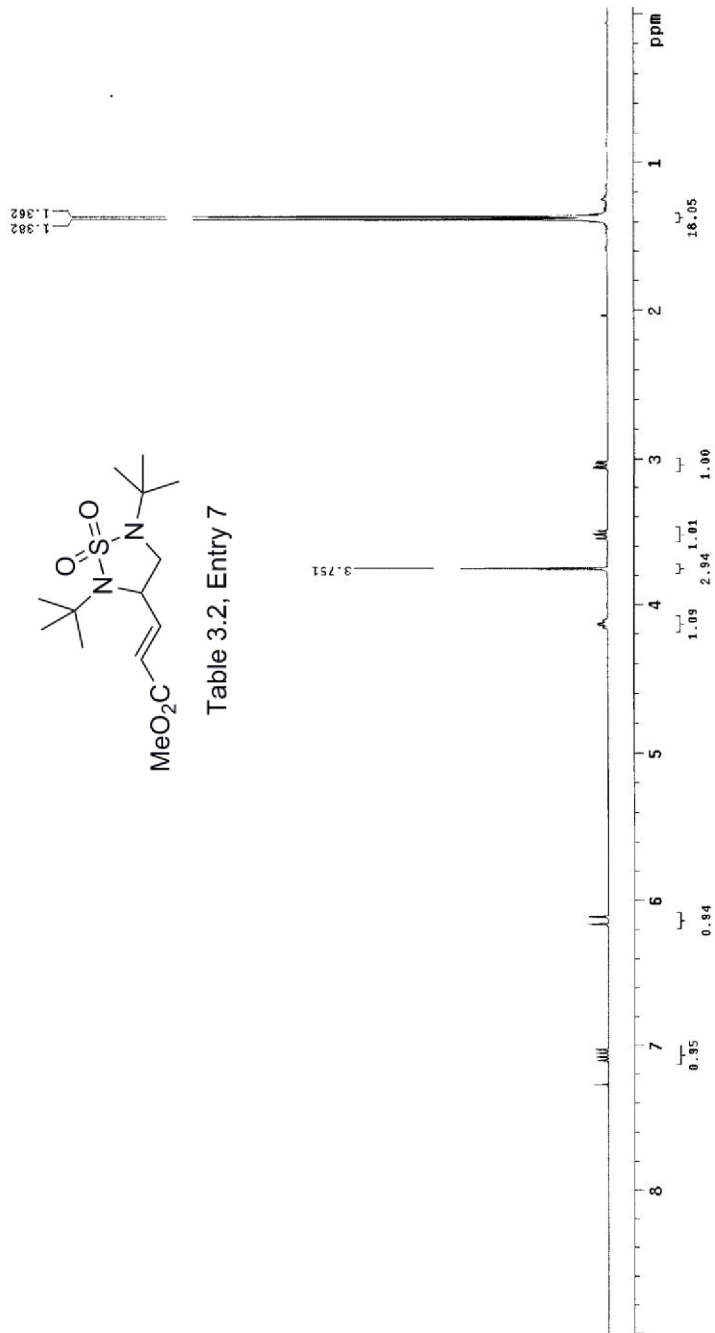


STANDARD 1H OBSERVE

Pulse Sequence: s2pul
Solvent: CDCl3
Ambient temperature
F100: 500.136242 MHz
INVA: 500 "aprox.1de"

Relax. delay 0.400 sec
Pulse 26.0 degrees
Acq. time 2.668 sec
Width 6995.2 Hz

OBSERVE F1 300.1582164 MHz
DATA PROCESSING
Gauss apodization 0.896 sec
F1 500.136242 MHz
Total time 0 min, 10 sec



13C OBSERVE

Pulse Sequence: szpul
Solvent: CDCl3
Ambient temperature
File: zba0424E-C13
INOVA-500 "epoxide"

Relax. delay 1.000 sec
Pulse 45.3 degrees
Acq. time 0.687 sec
Width 22955.8 Hz
Sweep 10000.0 Hz
OBSERVE C13 75.42750818 MHZ
DECOUPLE H1 300.1606799 MHZ
Power 40 dB
Continuously on
Water gated
DATA PROCESSING
Line broadening 2.0 Hz
FT size 32768
Total time 4 hr, 44 min, 20 sec

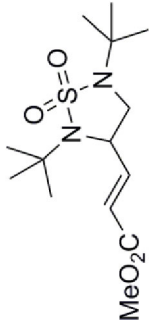
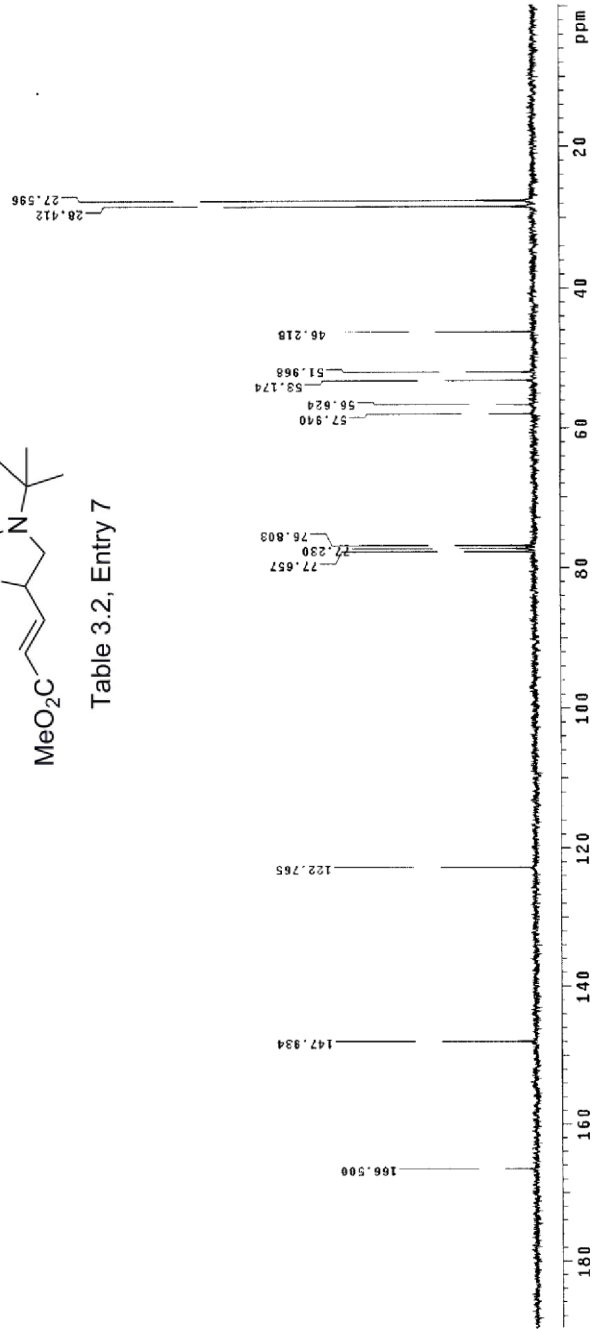
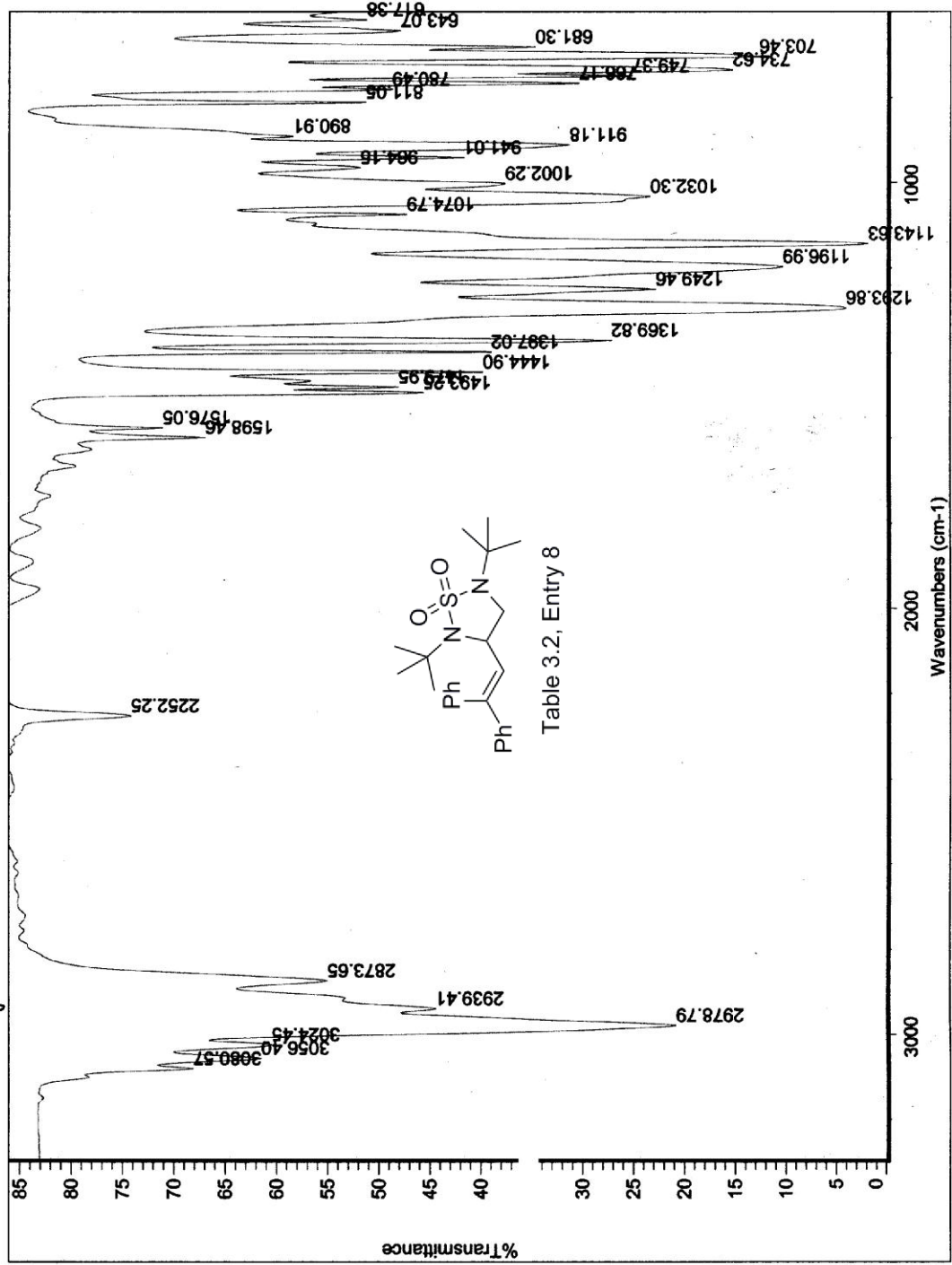


Table 3.2, Entry 7



289424 C



STANDARD 1H OBSERVE

Pulse Sequence: s2pu1
 Solvent: CDCl3
 Temperature: 300.2 K
 File: 200424C-H
 INOVA-500 "epoxide"

Relax. delay 0.000 sec
 Pulse 26.0 degrees
 Width 5.000 sec
 Width 5.000 sec
 Width 5.000 sec
 2 repetitions
 OBSERVE H1, 300.1532196 MHZ
 DATA PROCESSING
 Acquisition time 0.896 sec
 File size 427.88
 Total time 0 min, 10 sec

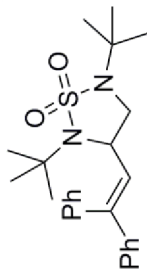
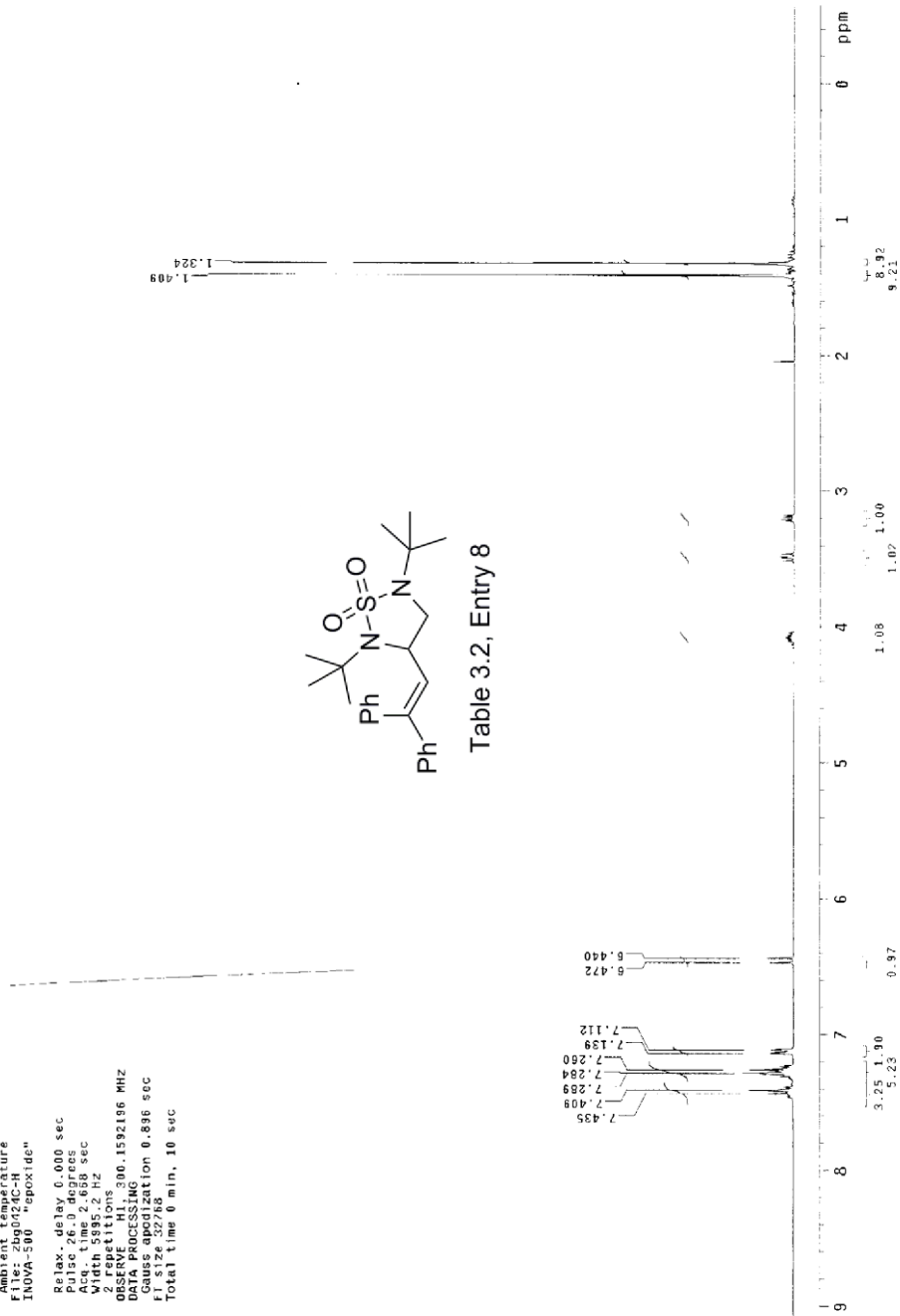


Table 3.2, Entry 8



13C OBSERVE

Pulse Sequence: s2pul

Solvent: CDCl3

Ambient temperature

File: 090740-Cl3

INSTR: 500 "epoc1de"

Relax. delay 1.000 sec

Pulse 46.3 degrees

Acq. time 0.697 sec

Width 24331.8 Hz

Obs 24331.8 Hz

OBSERVE C13, 75.4750860 MHZ

DECOUPLE H1, 300.1605799 MHZ

Power 40 dB

Transmit on

WALTZ-16 modulated

DATA PROCESSING

Line broadening 2.0 Hz

F1: 3128.32768

Total time: 4 hr, 44 min, 20 sec

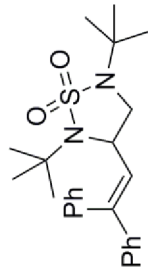
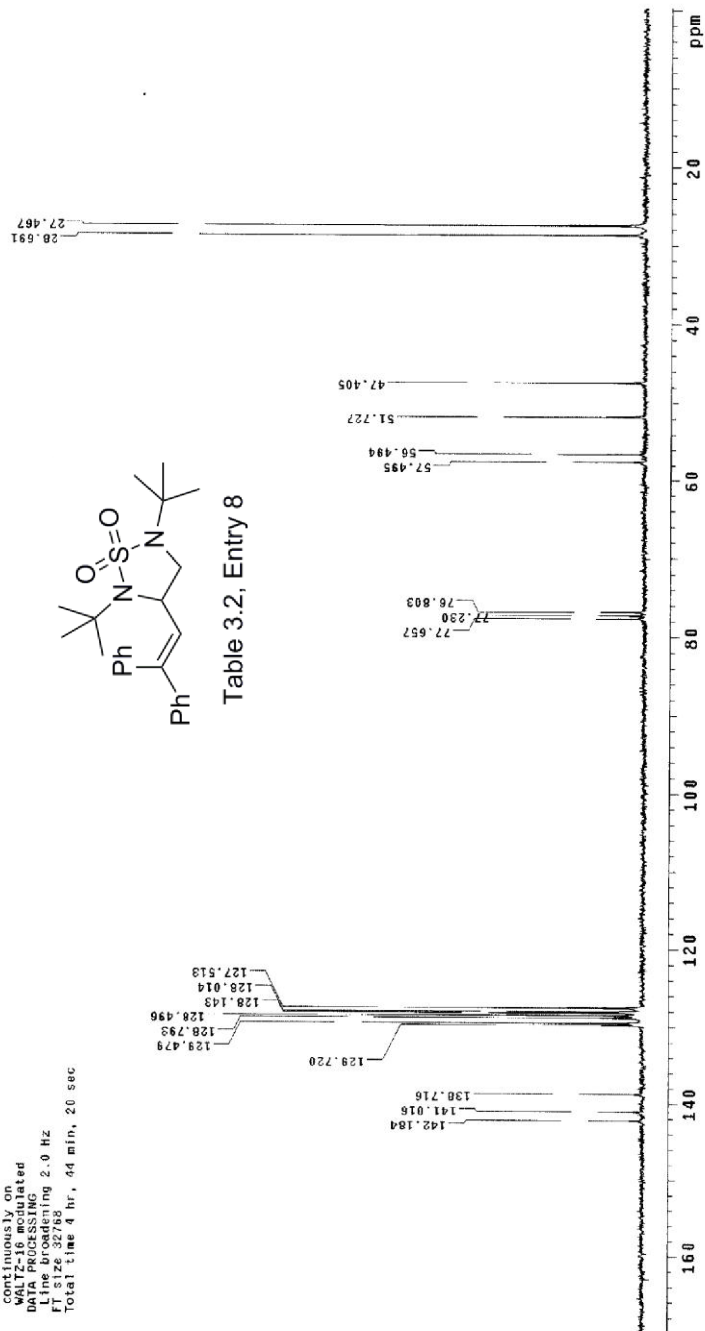
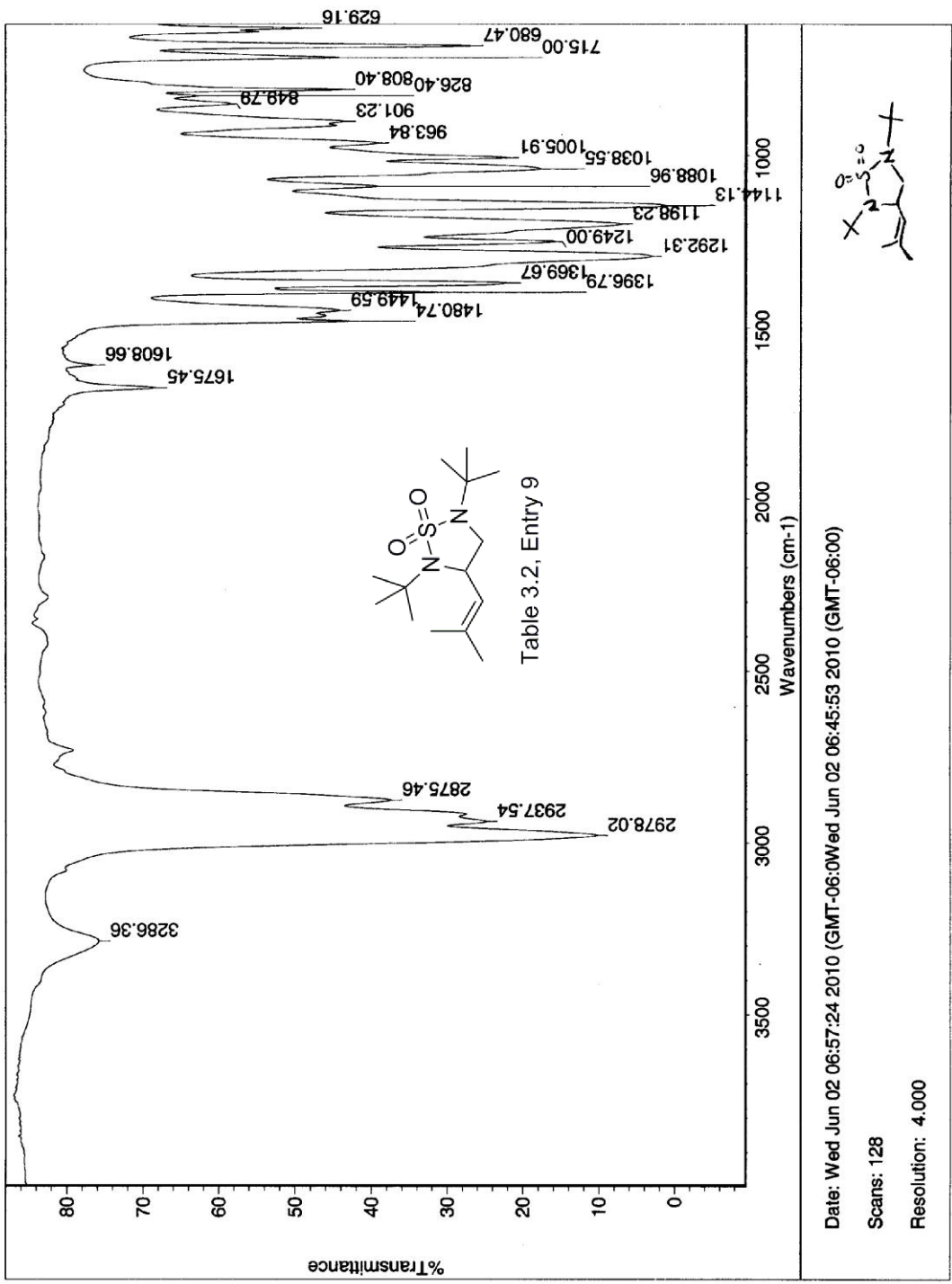


Table 3.2, Entry 8





13C OBSERVE

Pulse Sequence: s2pul
Solvent: CDCl3
Ambient temperature
Experiment: 13C-epoxide
INOVA-500 "epoxide"
Relax. delay 1.000 sec
Pulse 46.3 degrees
Acq. time 0.897 sec
4ft. time 0.897 sec
4ft. time 0.897 sec
42 repetitions
OBSERVE C13, 75.4750818 MHZ
DECUPLE H1, 300.1608799 MHZ
Power 18.000 W
Cont. frequency on
WALTZ-16 modulated
DATA PROCESSING
Line broadening 2.0 Hz
F1 12.222286
Total time 28 min, 26 sec

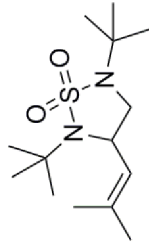
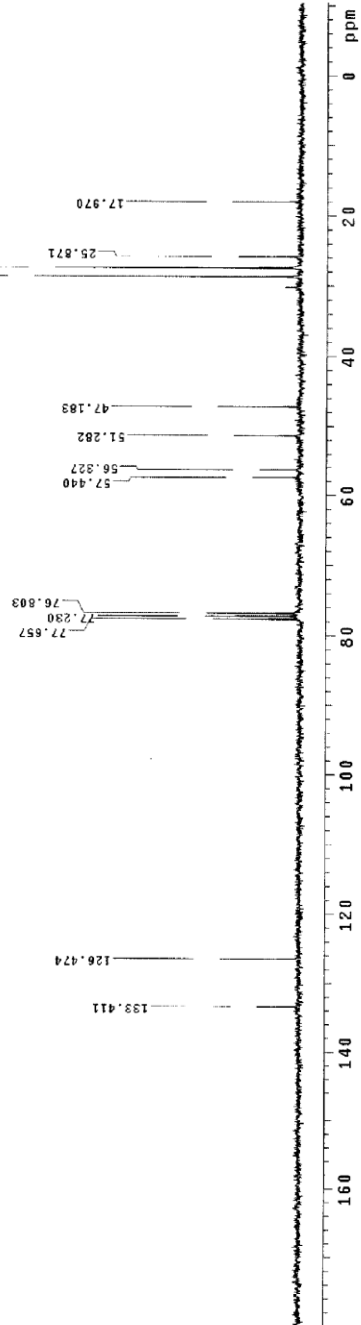
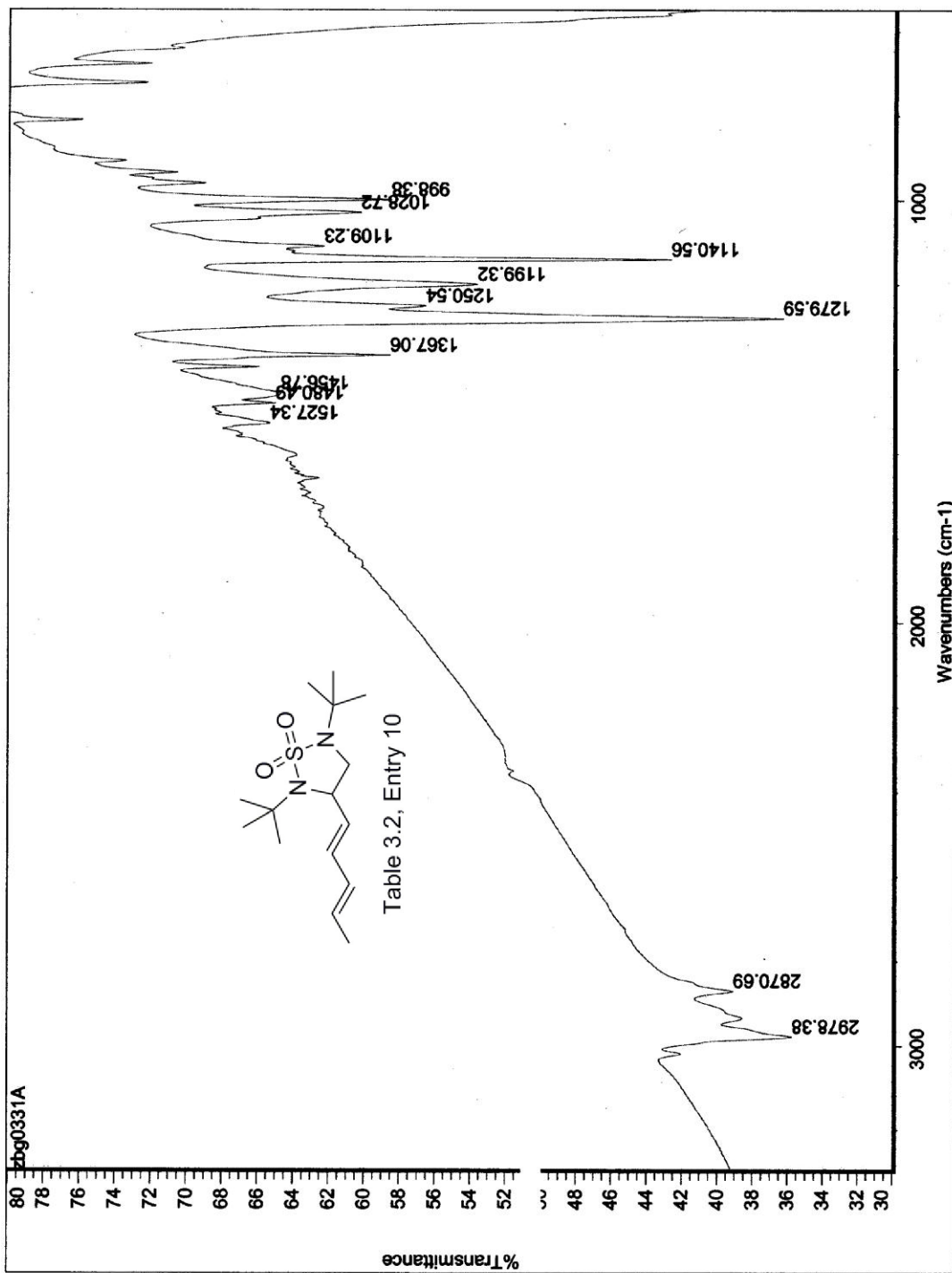


Table 3.2, Entry 9





STANDARD 1H OBSERVE

Pulse Sequence: szpul
Solvent: CDCl3
Ambient temperature
File: 080314A
INOVA-500 -epoxide"

Relax. delay 0.000 sec
Pulse 25.0 degrees
Acq. time 2.669 sec
Width 333.2 Hz

OBSERVE 1H 300.1592164 MHZ
DATA PROCESSING
Gauss apodization 0.896 sec
F1 12.8276
Total time 0 min, 10 sec

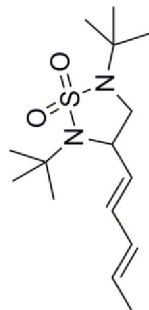
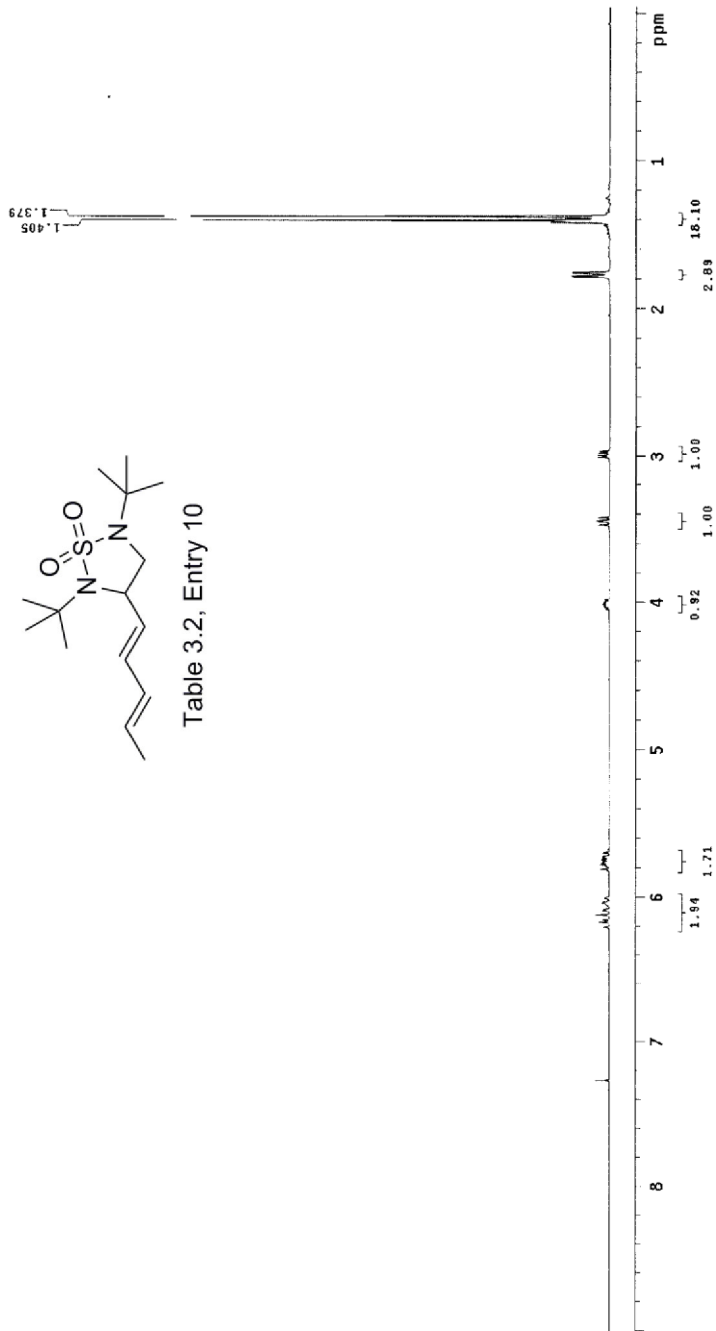


Table 3.2, Entry 10



13C OBSERVE

Pulse Sequence: szpul

Solvent: CDCl3

Ambient temperature

101.32999999999999

INVA=50 "opposite"

Relax. delay 1.000 sec

Pulse 46.3 degrees

Acq. time 0.587 sec

Scch. 2235.8 Hz

Obs. 75.4750804 MHz

OBSERVE C13 300.1606799 MHz

Power 40 dB

Continuously on

MULTI-ROUTED

DATA PROCESSING

Line broadening 2.0 Hz

FI size 32768

Total time 26 min, 26 sec

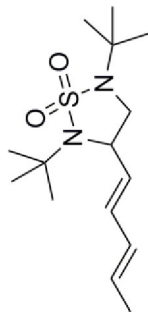
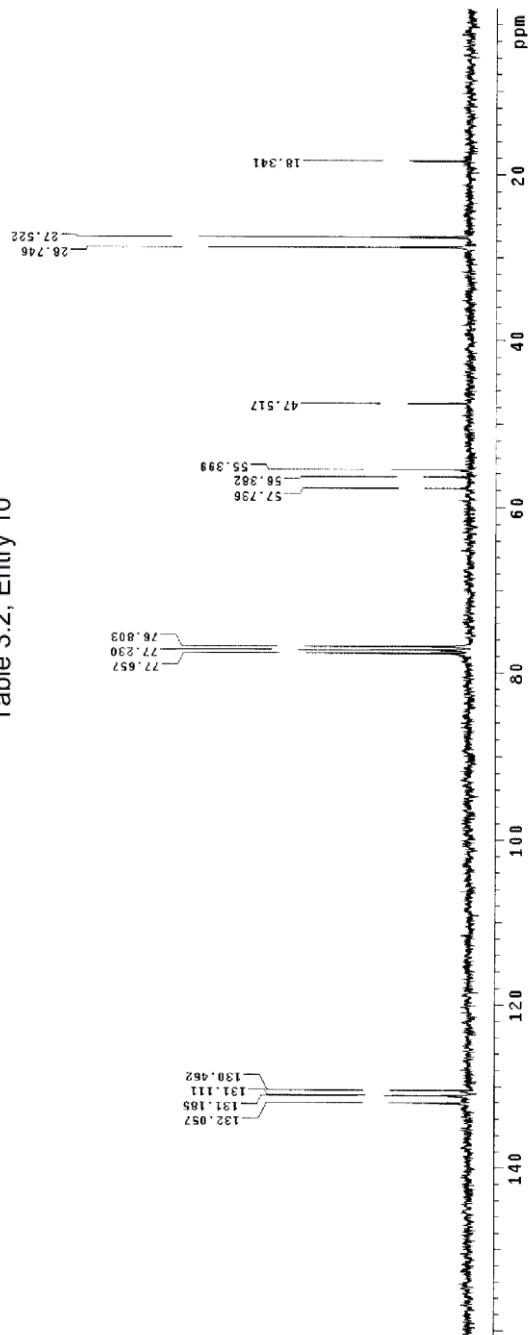
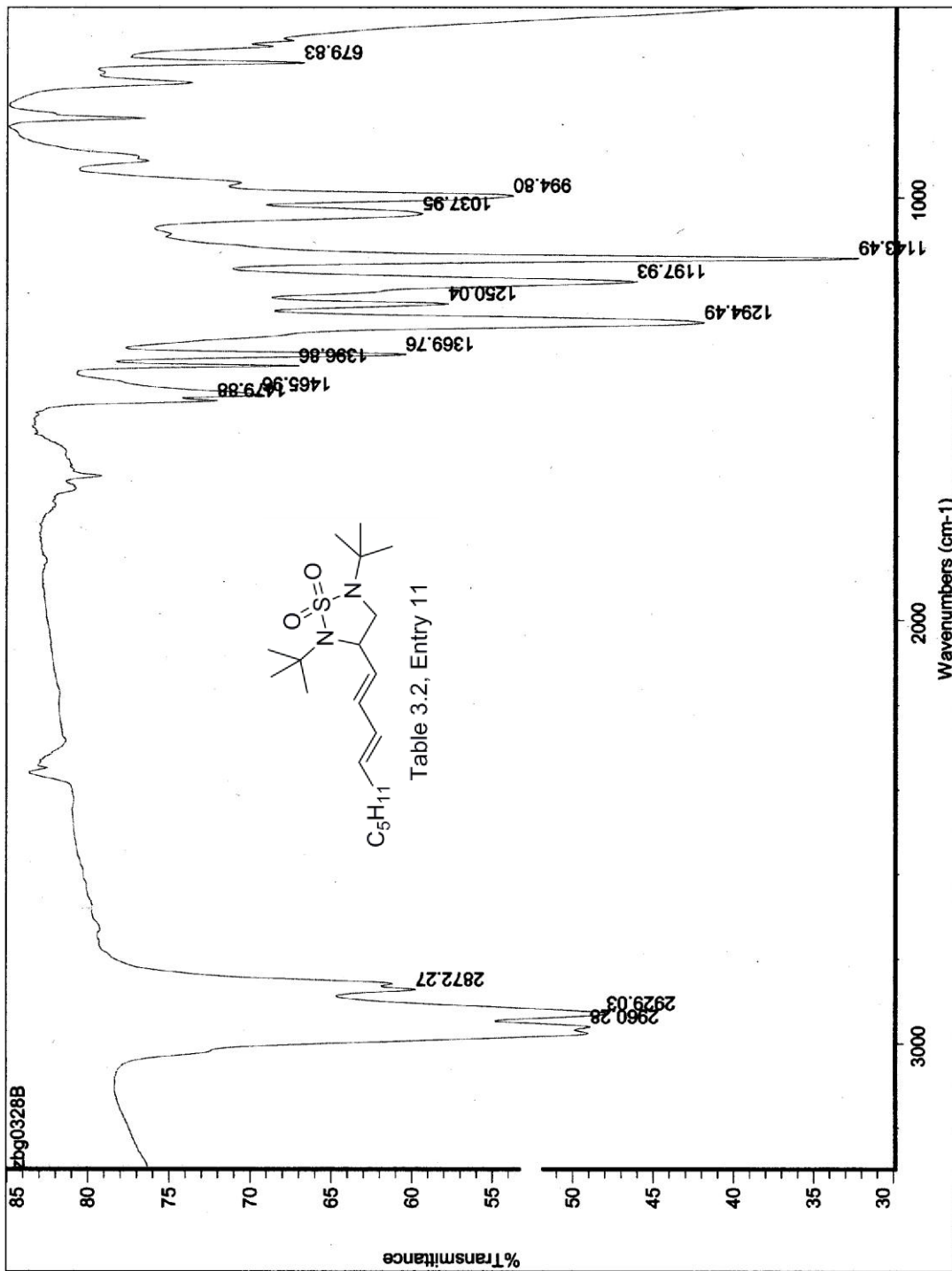


Table 3.2, Entry 10





STANDARD 1H OBSERVE

Pulse Sequence: s2pul
 Solvent: CDCl3
 Ambient temperature
 File: Z09051d-H
 INOVA-500 "epoxide"
 Relax. delay: 0.000 sec
 Pulse: 25.0 degrees
 Acq. time: 2.668 sec
 Width: 5995.2 Hz
 Observed: 110.000
 OBSERVE: H1, 300.1592167 MHZ
 DATA PROCESSING
 Cause apodization: 0.896 sec
 Size: 32768
 Total time: 0 min, 10 sec

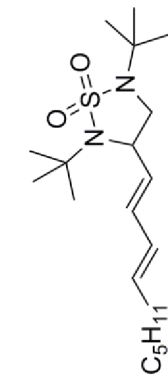
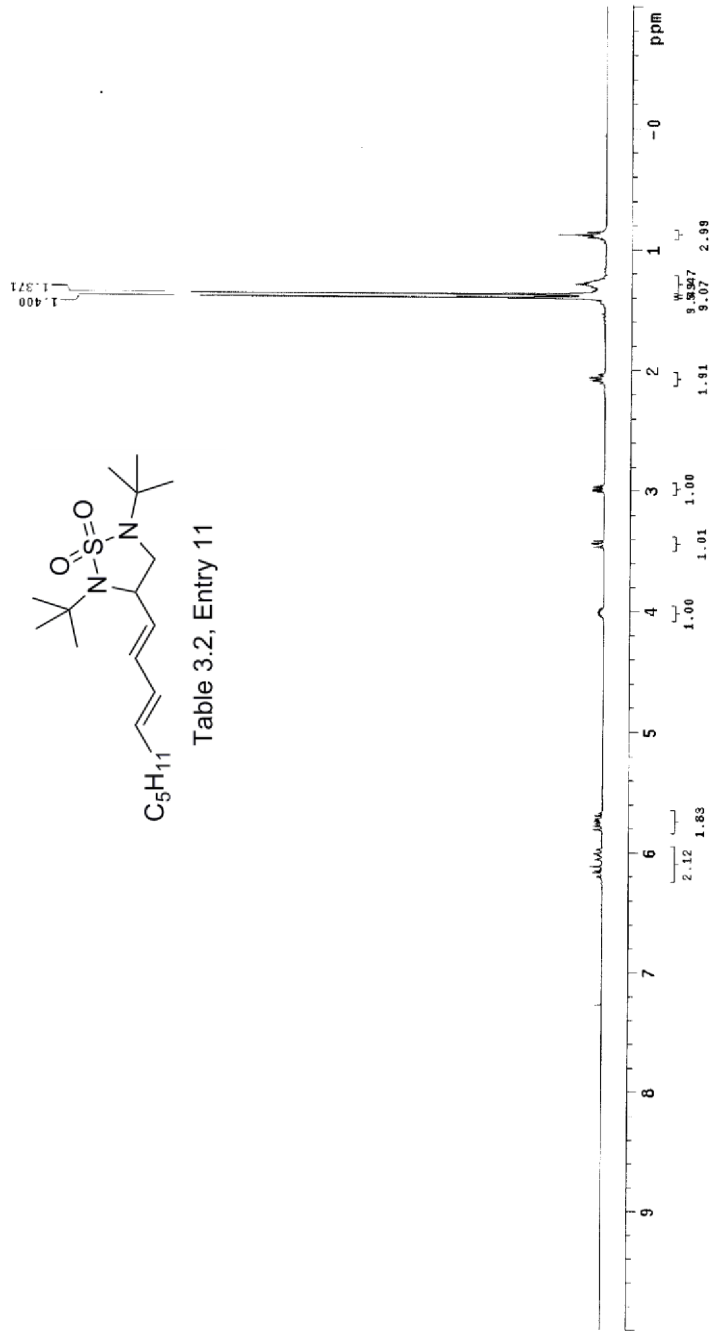


Table 3.2, Entry 11



13C OBSERVE

Pulse Sequence: s2pul
Solvent: CDCl3
Ambient temperature
File: 20g0324-013
INSTR: 500 "epoxide"
Relax. delay 1.000 sec
Pulse 46.3 degrees
Acq. time 0.697 sec
Width 22355.8 Hz
Observer: C13, 75.4750832 MHz
DECOUPLE: H1, 300.1606789 MHz
Power 40 dB
SOLVENT: CDCl3
WALTZ-16 amplitude
DATA PROCESSING
Line broadening 2.0 Hz
F1 size 32768
Total time 14 min, 18 sec

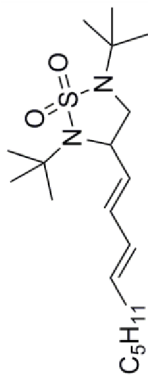
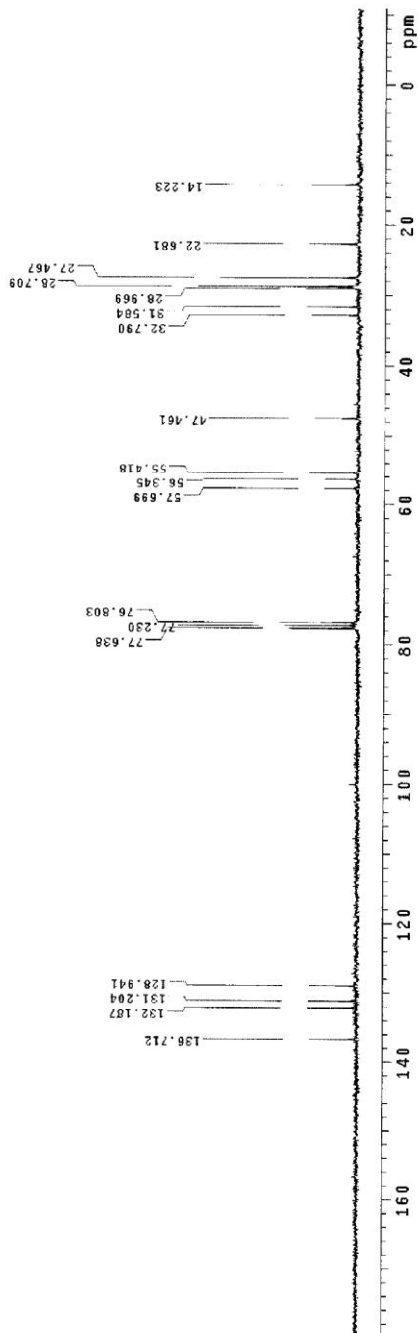
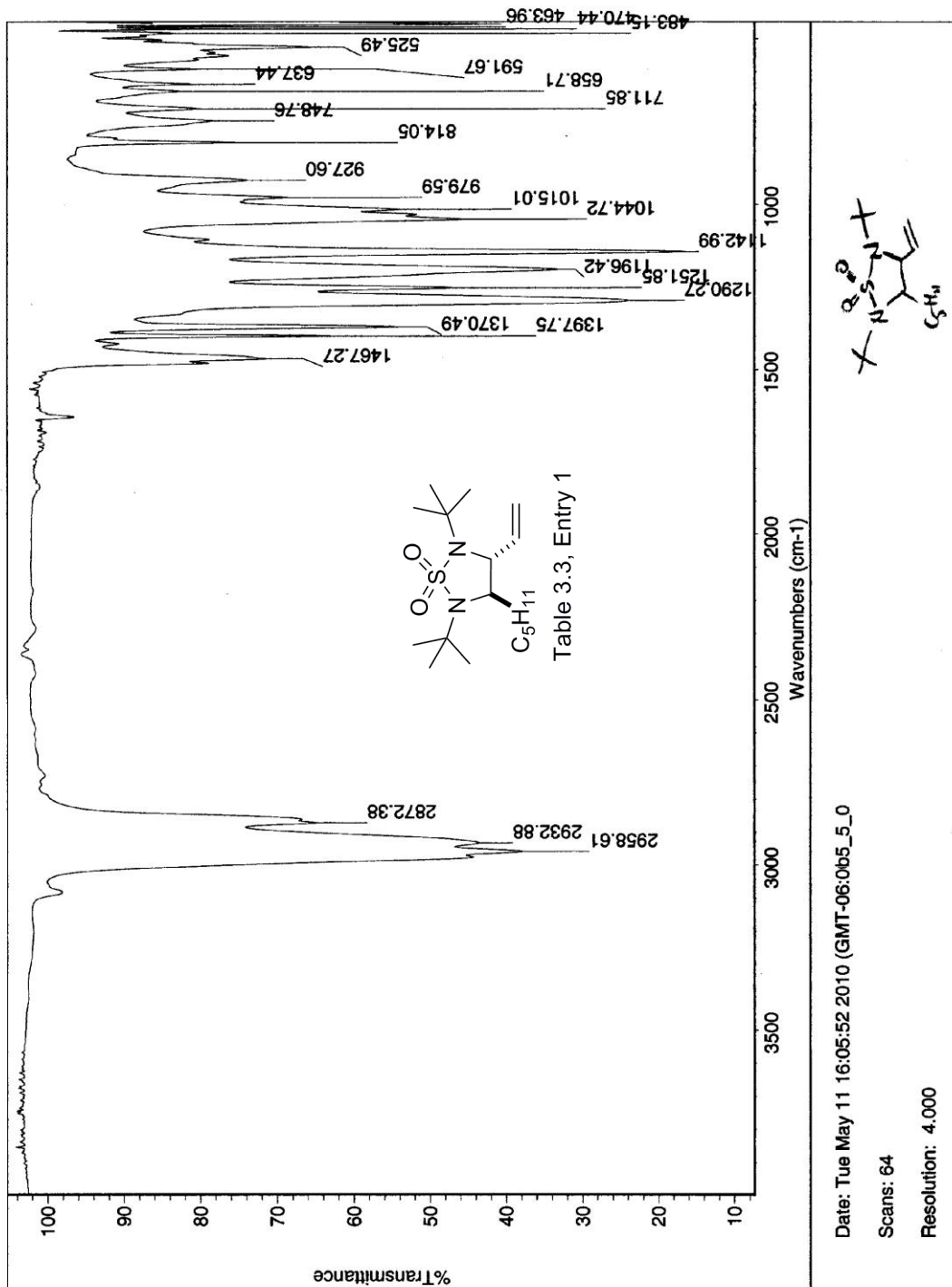


Table 3.2, Entry 11





STANDARD 1H OBSERVE

Pulse Sequence: s2pul
 Solvent: CDCl3
 Temperature: 25.000000
 File: tc_b5_0_Regular_pure
 INOVA-500 "epoxide"
 Relax, delay 0.800 sec
 Pulse 26.0 degrees
 Width 5895.2 Hz
 Height 1.000000 sec
 4 repetitions
 OBSERVE RL, 300.1582196 MHz
 INH, PROCESSING
 Class, Acquisition 0.836 sec
 FT size 32768
 Total time 0 min, 16 sec

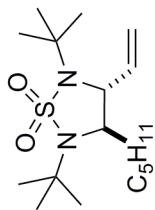
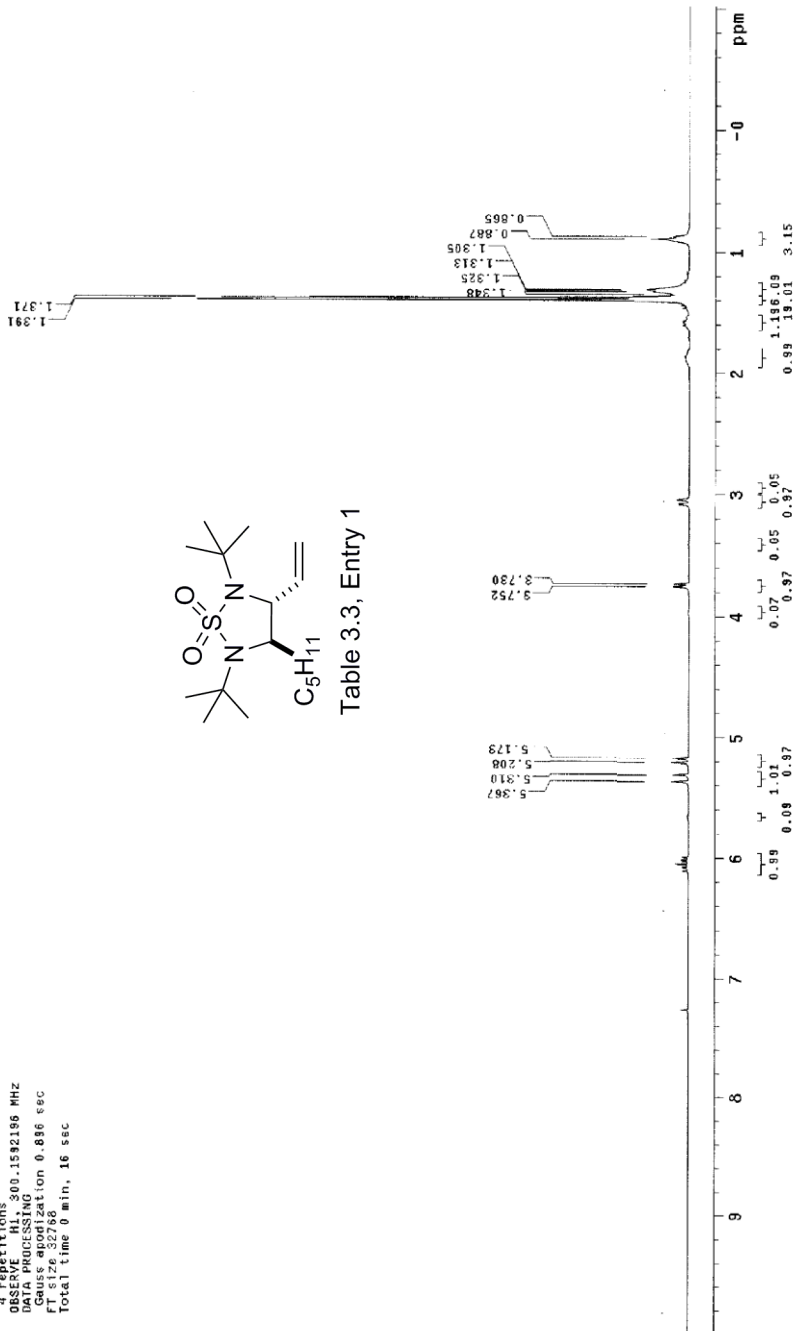


Table 3.3, Entry 1



13C OBSERVE

Pulse Sequence: zgpg30

Solvent: CDCl3

Sample Name: 1

File Name: 13C

INOVA-500 "epoxide"

Relax. delay 1.700 sec

Pulse 56.6 degrees

Time 0.00000000 sec

Width 30018.78 Hz

164 repetitions

OBSERVE C13, 100.6067323 MHz

DCouple 136, 400.1063266 MHz

Continuously on

WALTZ-16 modulated

DATA PROCESSING

Time 0.00000000 sec

FT 132.02086

Total time 6:27:35 hr, 34 min, 7 sec

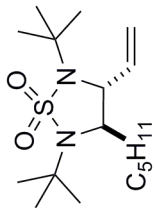
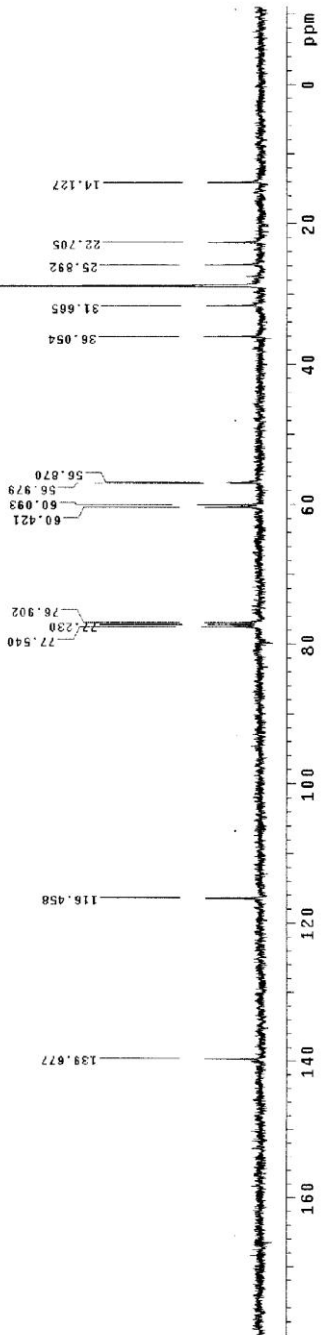
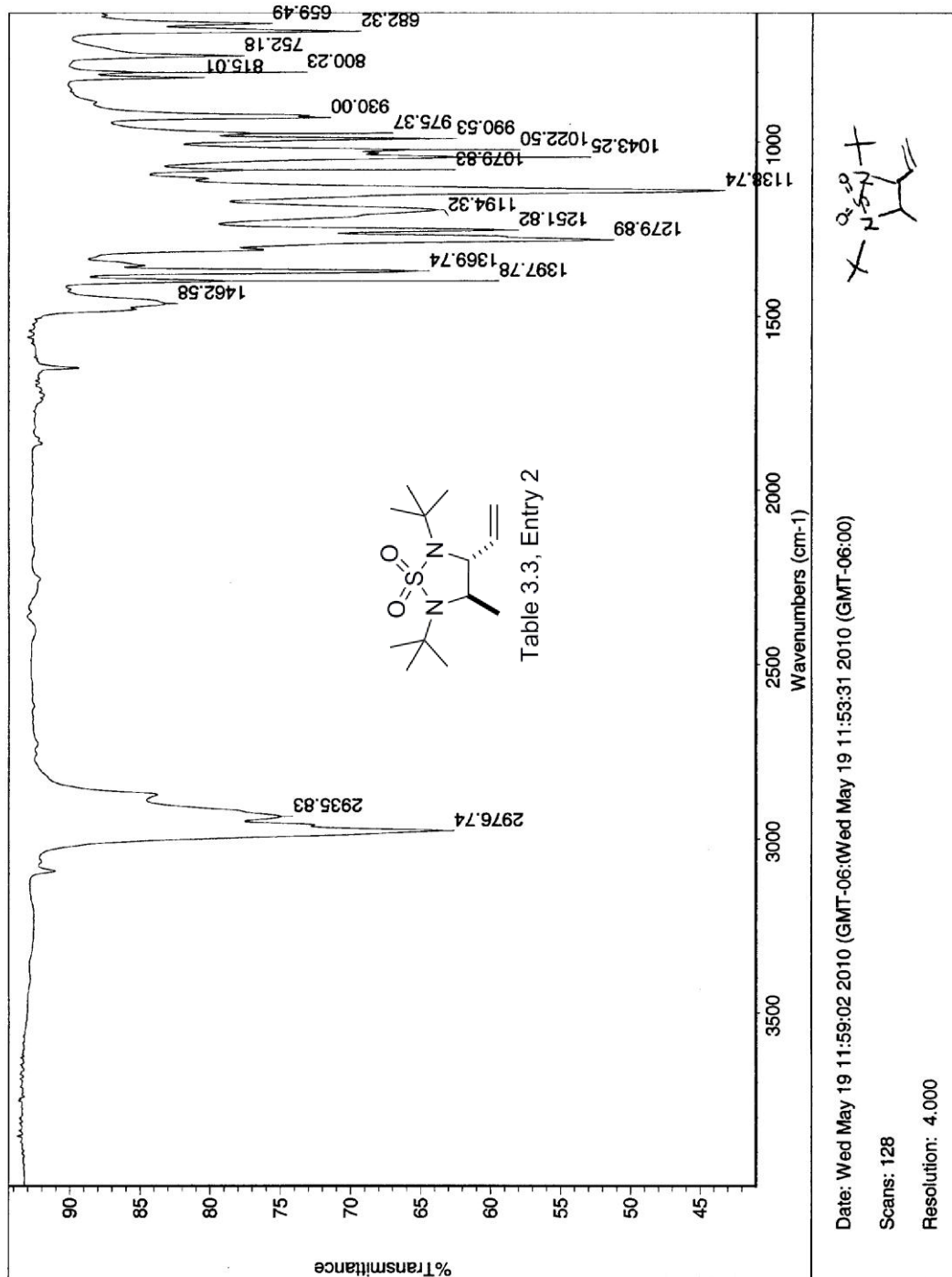


Table 3.3, Entry 1





13C OBSERVE

Pulse Sequence: sZpu1
Solvent: CDCl3
Acquire: 14.2 min
File: r5_05_5_16_carbon
INDVA-500 "epoxide"

Relax. delay: 1.700 sec
Acq: 36.6 degrees
Acq: 0.05 sec
Width: 30018.8 Hz
396 repetitions
OBSERVE C13, 100.6067995 MHz
Power: 56 dB, 400.108286 MHz
continuously on
WALTZ-16 modulated
Data Processing
File: B0551601
FT Size: 32768 intg 2.0 Hz
Total time: 622735 hr, 34 min, 7 sec

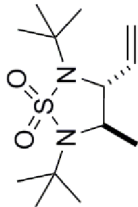
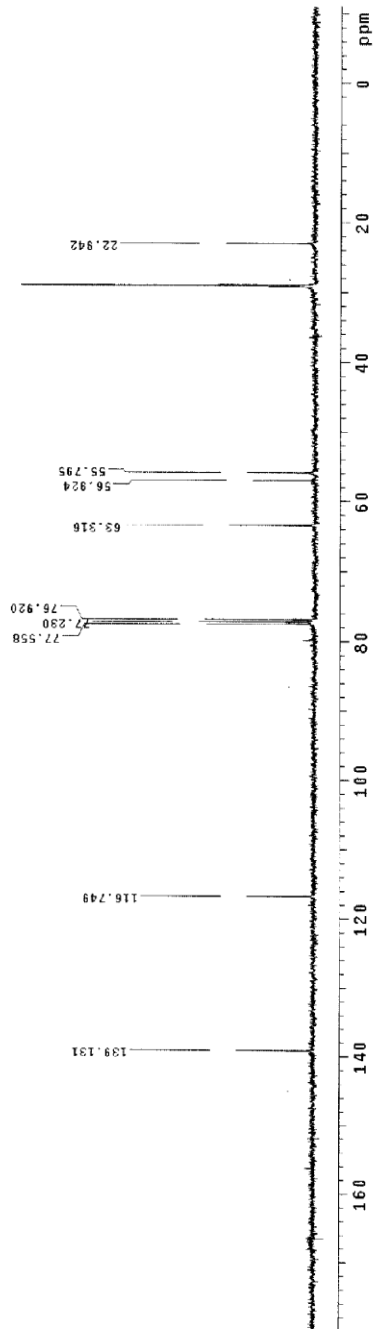
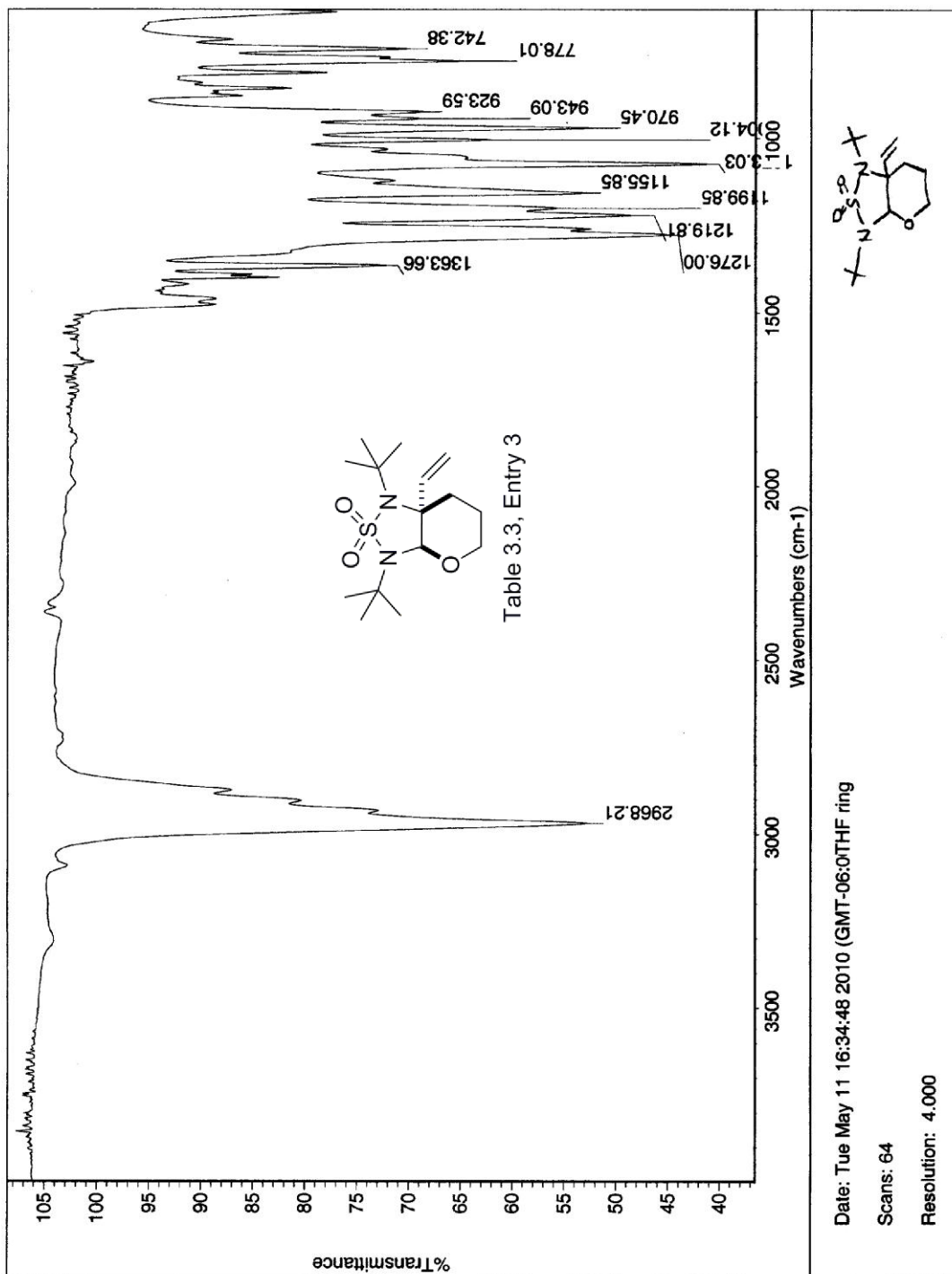


Table 3.3, Entry 2





STANDARD 1H OBSERVE

Pulse Sequence: s2pul

Solvent: CDCl3

File Name: 150717_01

File Path: /home/chem/pure2

INOVA-500 1H-peptide

Relax. delay 0.000 sec

Pulse 26.0 degrees

Width 595.200 sec

4 Repetitions

OBSERVE H1, 300.1592167 MHZ

DATA PROCESSING

Integration 0.896 sec

FT size 32768

Total time 0 min, 16 sec

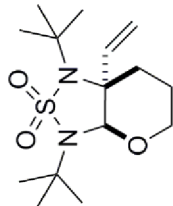
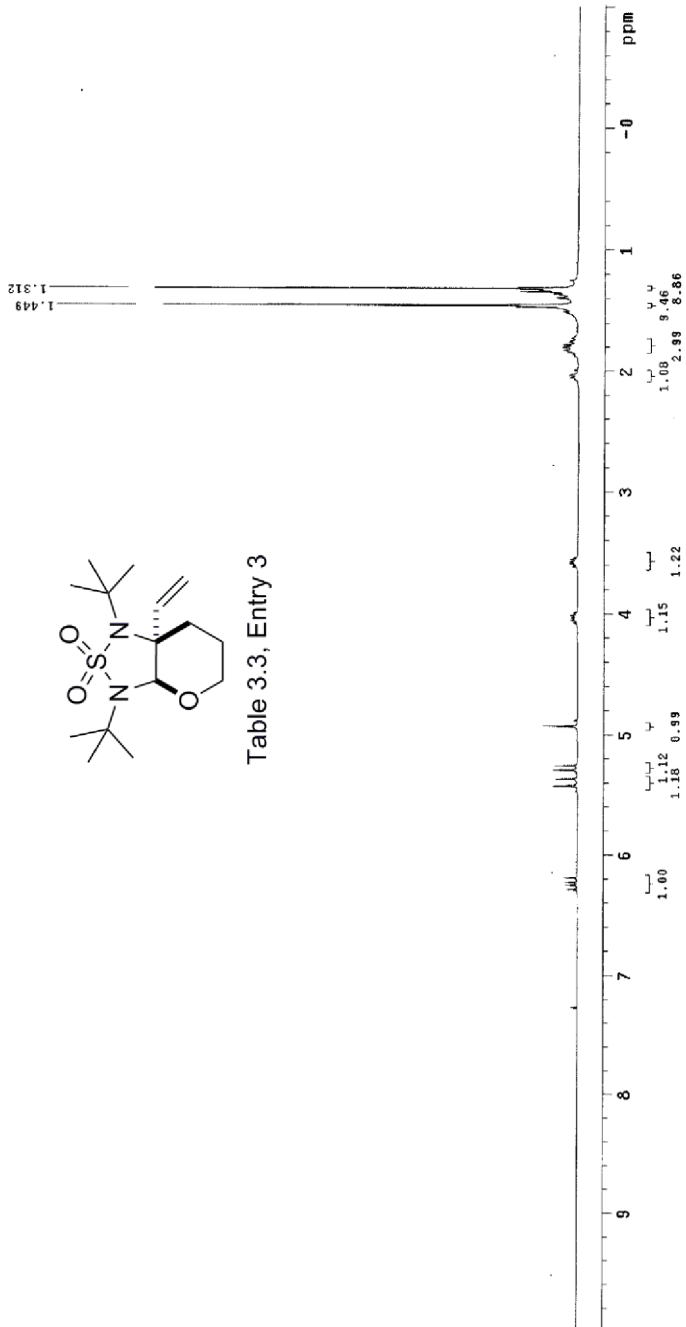


Table 3.3, Entry 3



13C OBSERVE

Pulse Sequence: s2pul
Solvent: CDCl3
Temperature: 25.000000
File: rc_b5_72.ctc@compure
INOVA-500 "epoxide"
Relax. delay 1.700 sec
Pulse 36.6 degrees
Pulse program: zgpg30
Width 3000.8 Hz
1316 repetitions
OBSERVE C13, 100.6067905 MHz
PCOUPL 56.48, 400.1063268 MHz
continuous on
WALTZ-16 modulated
DATA PROCESSING
Line spacing 2.0 Hz
FT size 32768
Total time 622735 hr, 54 min, 7 sec

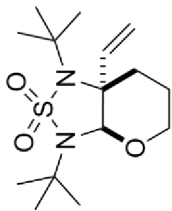
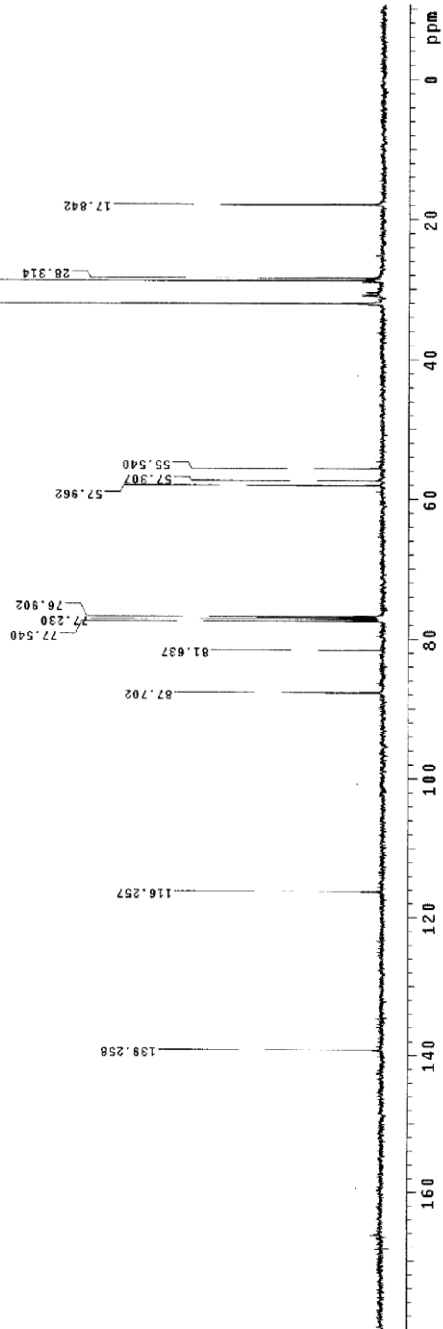
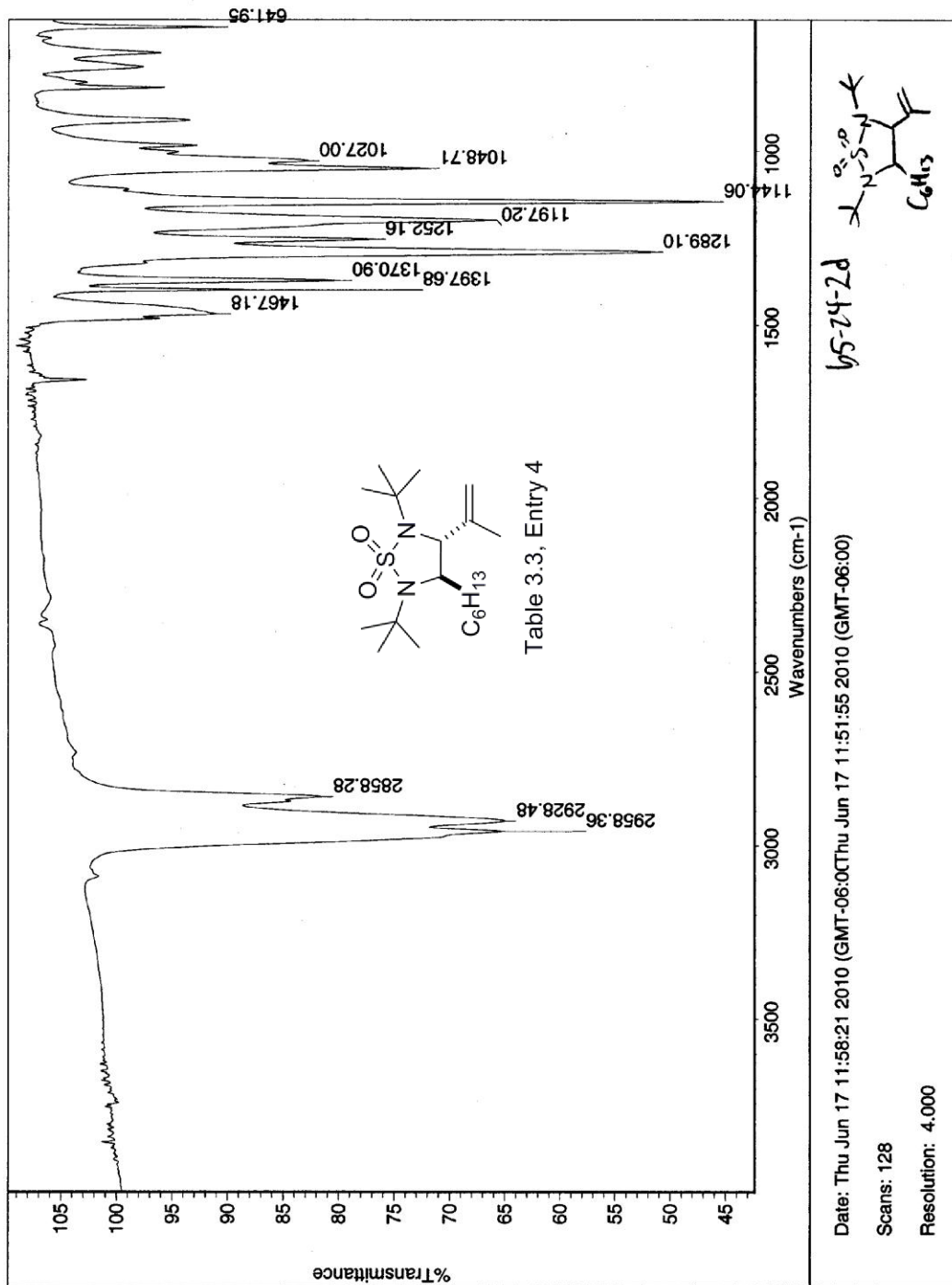


Table 3.3, Entry 3





STANDARD 1H OBSERVE

Pulse Sequence: s2pul
 Solvent: CDCl3
 File: FC_55_24_2d.pure
 INOVA-500 "epox1d"

Pulse 42.4 degrees
 Acq time 2.291 sec
 4 scans
 4 repeats
 OBSERVE f1, 400.1063124 MHZ
 DATA PROCESSING
 Corp. acquisition 0.971 sec
 Processing 0.971 sec
 Total time 0 min, 13 sec

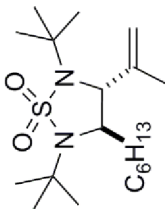
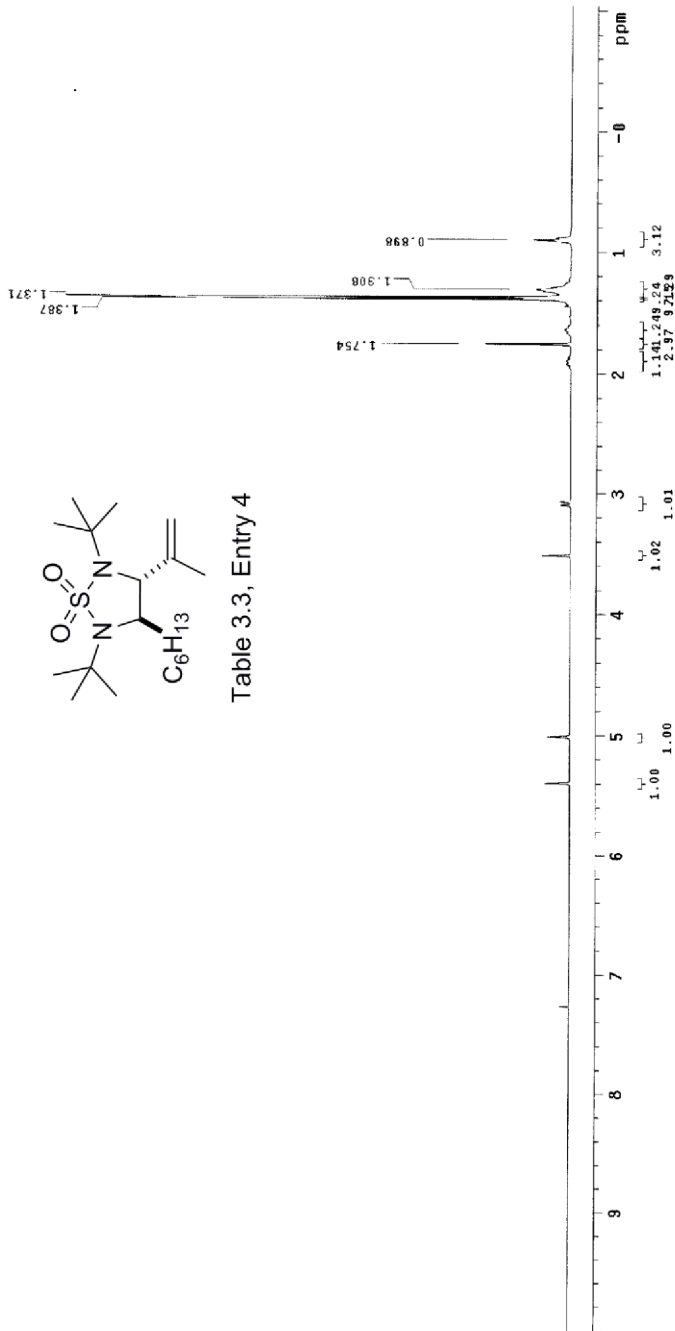


Table 3.3, Entry 4



13C OBSERVE

Pulse Sequence: s2pul
Solvent: CDCl3
Ambient Temperature
Reference: Tetramethylsilane
INVA-500 T-ppm: 160
Relax. delay 1.700 sec
Pulse 36.6 degreeec
Acq. time 0.533 sec
Adapt. time 0.014 sec
Waltz 30014 Hz
1334.50014 MHz
OBSERVE C13, 100.6067917 MHZ
DECUPLE H1, 400.1083268 MHZ
Power 36 dB
Pulse delay on
WALTZ-16 modulated
DATA PROCESSING
Line broadening 2.0 Hz
F1 size 32768
Total time 02:27:35 hr, 34 min, 7 sec

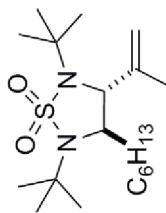
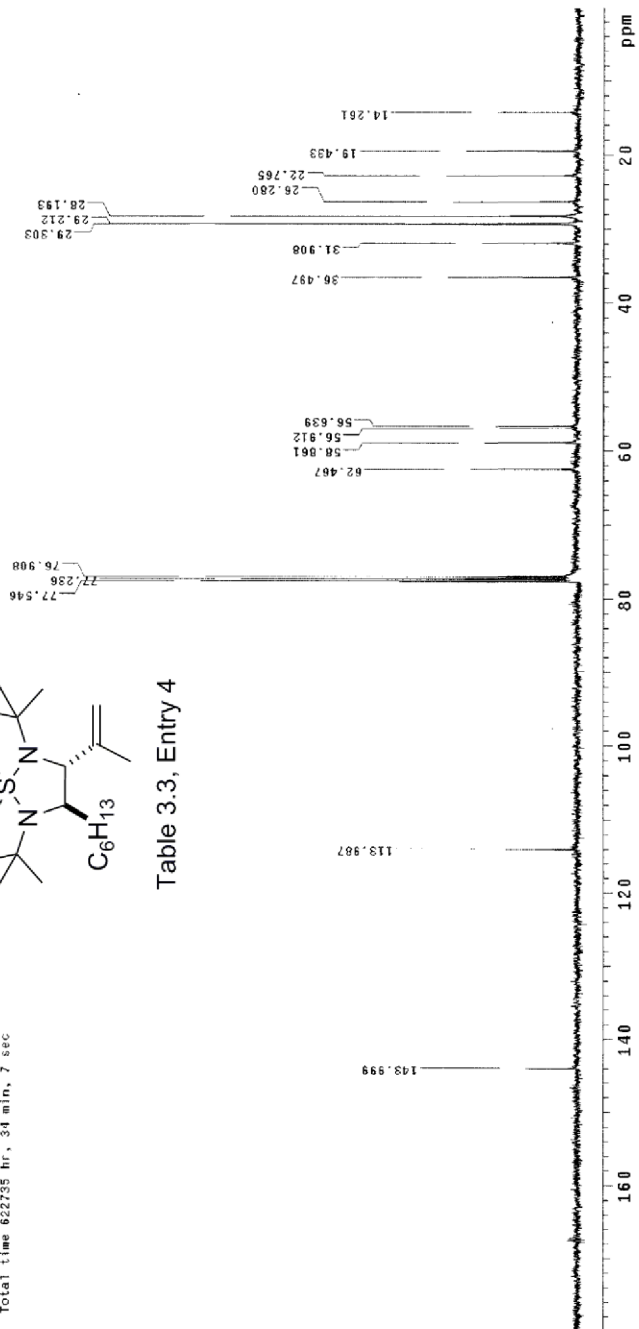
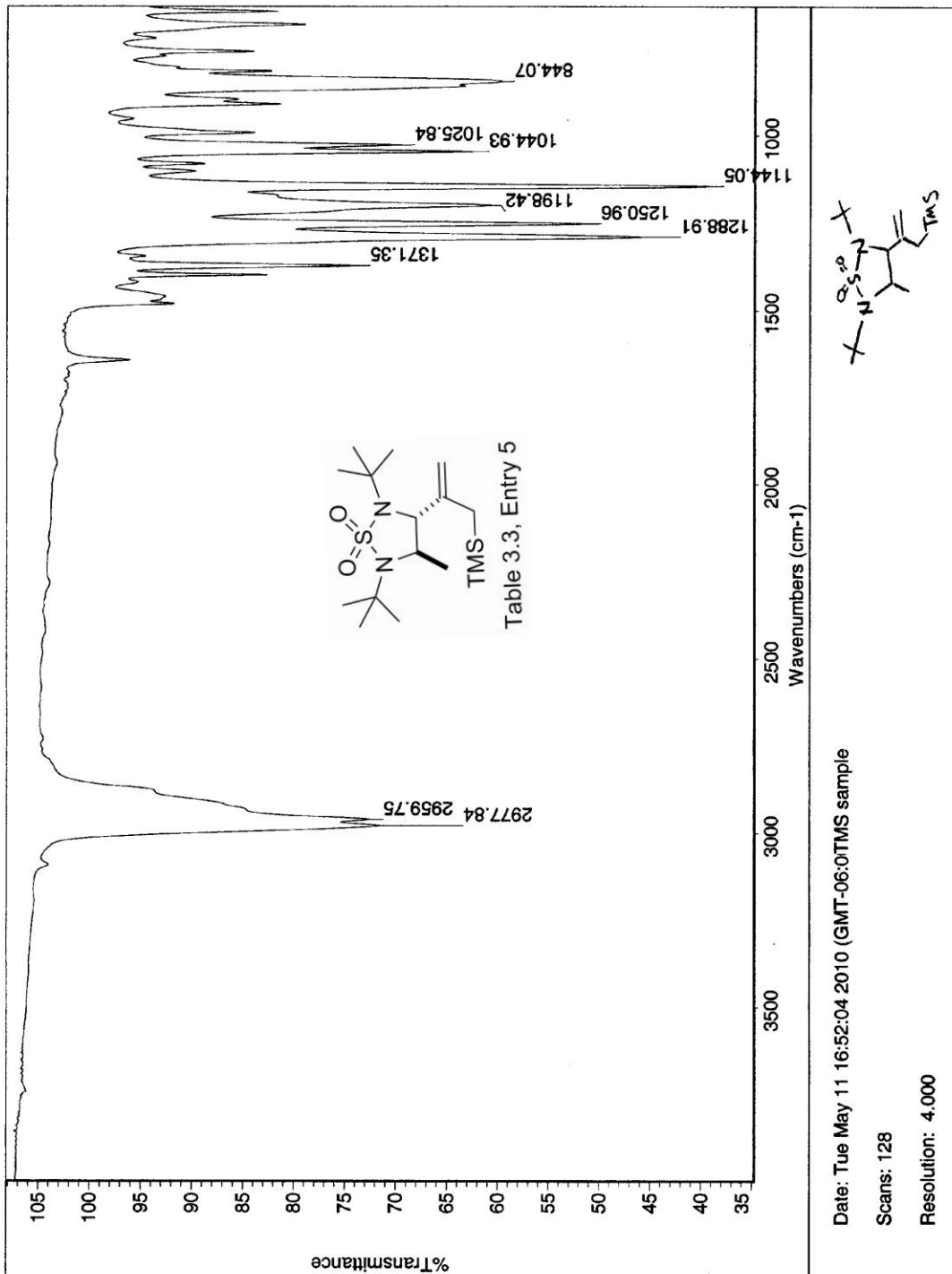


Table 3.3, Entry 4





STANDARD 1H OBSERVE

Pulse Sequence: s2pu1
Solvent: CDCl3
Ambient Temperature
Time: 11:30:11
INOVA-500 "apoxide"
Relax. delay 0.000 sec
Pulse 26.0 degrees
Acq. time 2.666 sec
F1 (nu) 500.136 MHz
repetitions 1
OBSERVE H1, 306.1592160 MHz
DATA PROCESSING
Gauss approximation 0.886 sec
Phase correction 0.000 sec
Total time 0 min, 16 sec

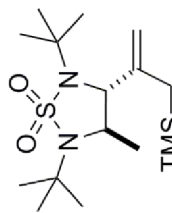
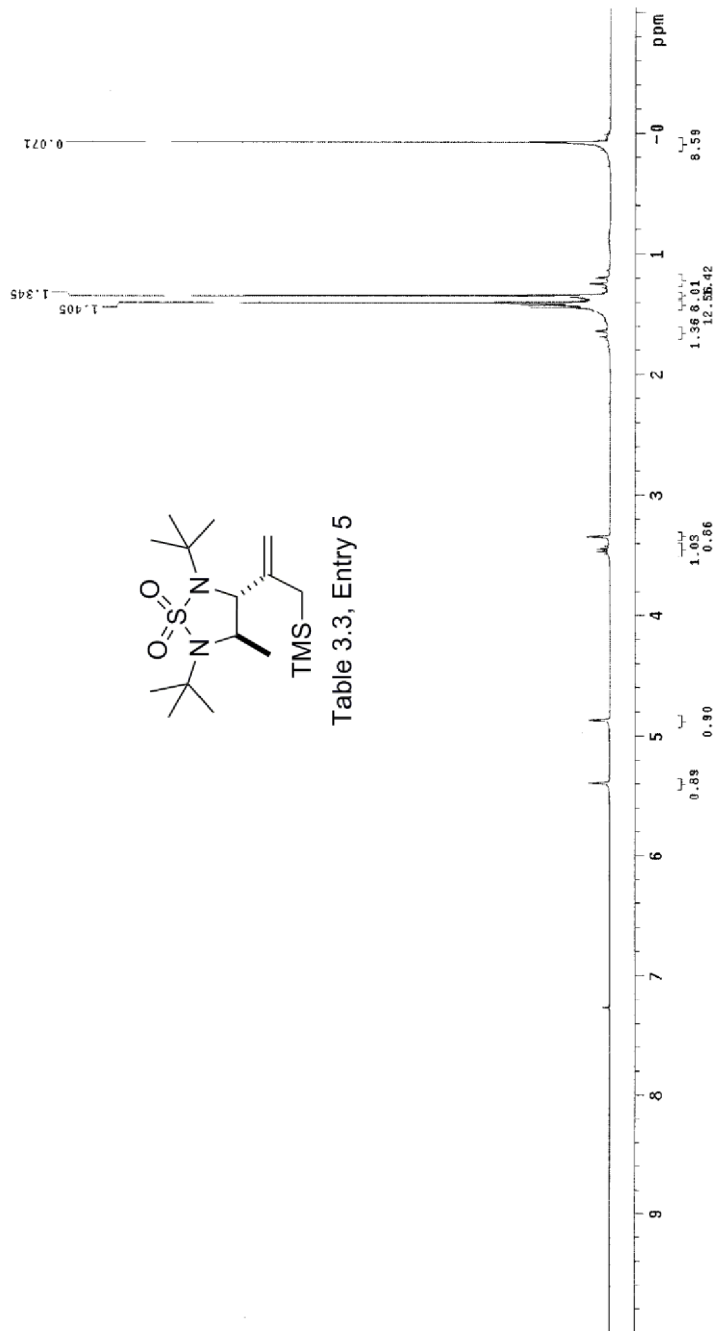


Table 3.3, Entry 5



13C OBSERVE

Pulse Sequence: szpul
Solvent: CDCl3
Ambient temperature
File: F00056_carbon_pure
INVA=500, npt=1024
Relax. delay 1.700 sec
Pulse 36.6 degrees
Acq. time 0.533 sec
Waltz 30013.9 Hz
Waltz 1499.0 Hz
OBSERVE C13, 100.6067323 MHz
DECOUPLE H1, 400.1083268 MHz
Power 36 db
P1 1.000000 sec
WALTZ-16 modulated
DATA PROCESSING
Line broadening 2.0 Hz
File size 32788
Total time 02:27:35 hr, 34 min, 7 sec

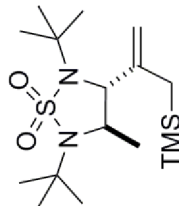
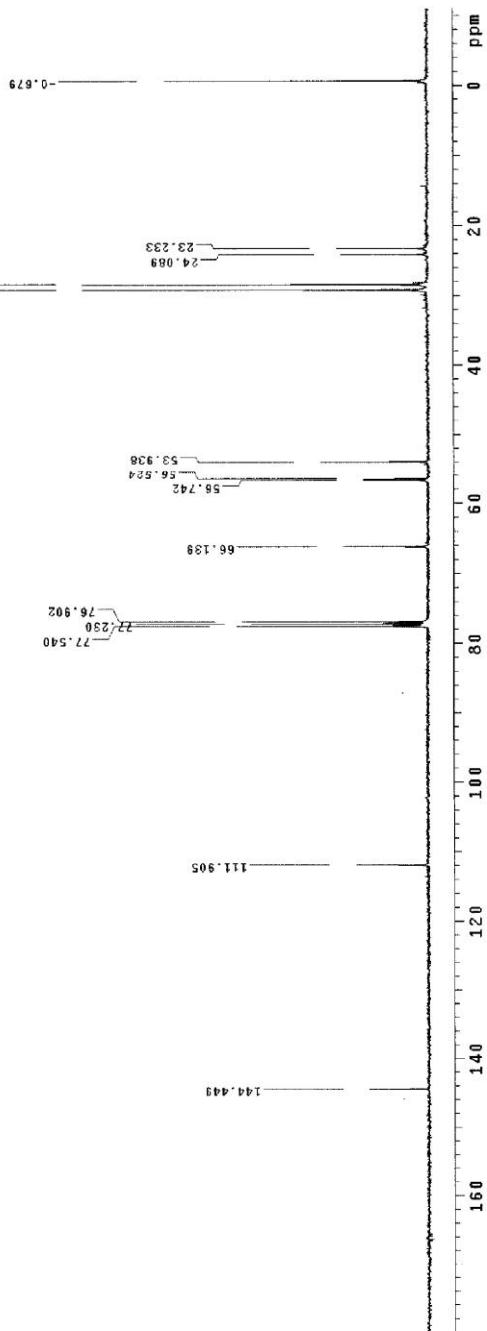
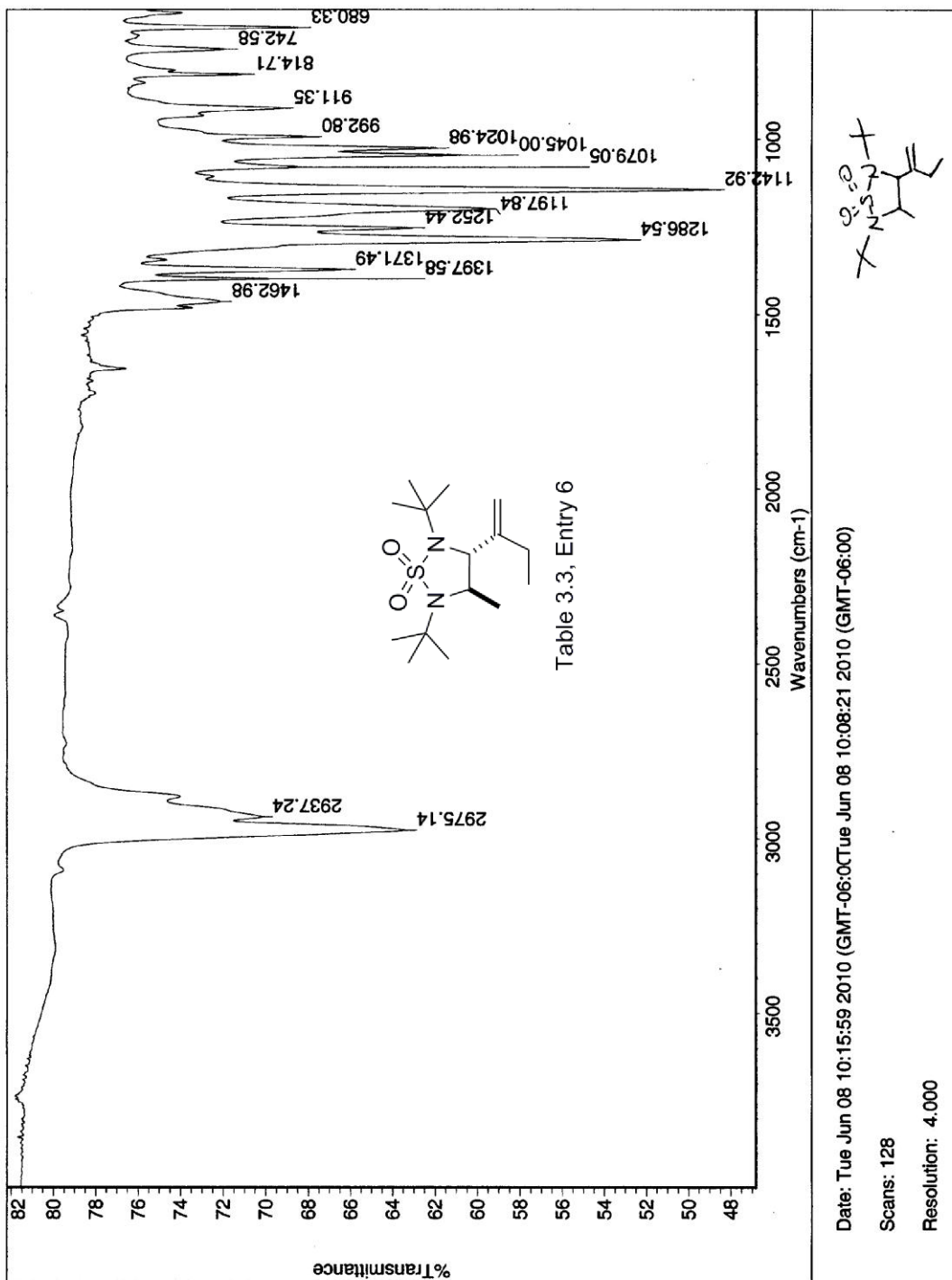


Table 3.3, Entry 5





STANDARD 1H OBSERVE

Pulse Sequence: s2pul
Solvent: CDCl3
Ambient Temperature: 25.00
INOVA-500 "pproxide"
Relax. delay 0.800 sec
Pulse 26.0 degrees
Acq. time 2.668 sec
F1 499.999 MHz
4 FSPET11ions
OBSERVE H1 300.1582164 MHZ
DATA PROCESSING
Sweep rate 120.000 MHz
F2 499.999 MHz
Total time 0 min, 16 sec

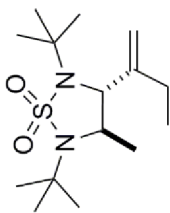
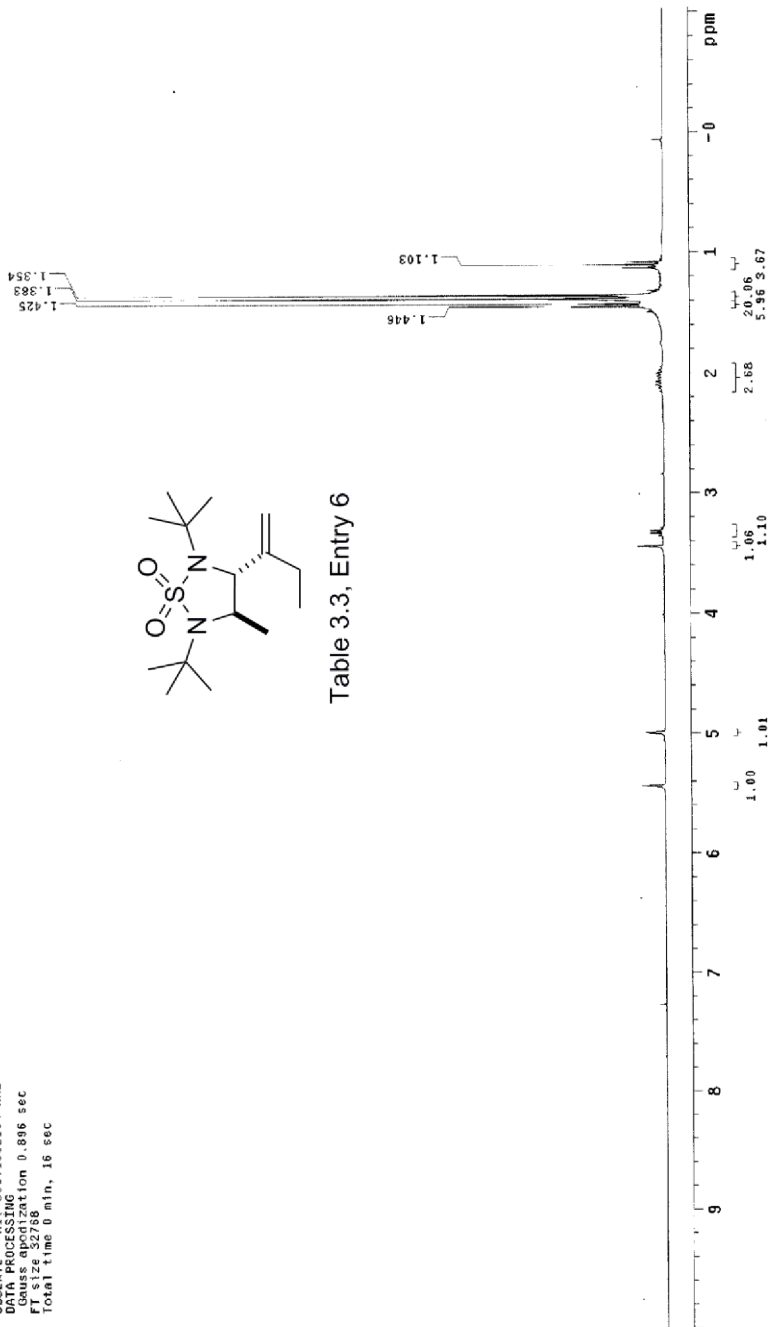
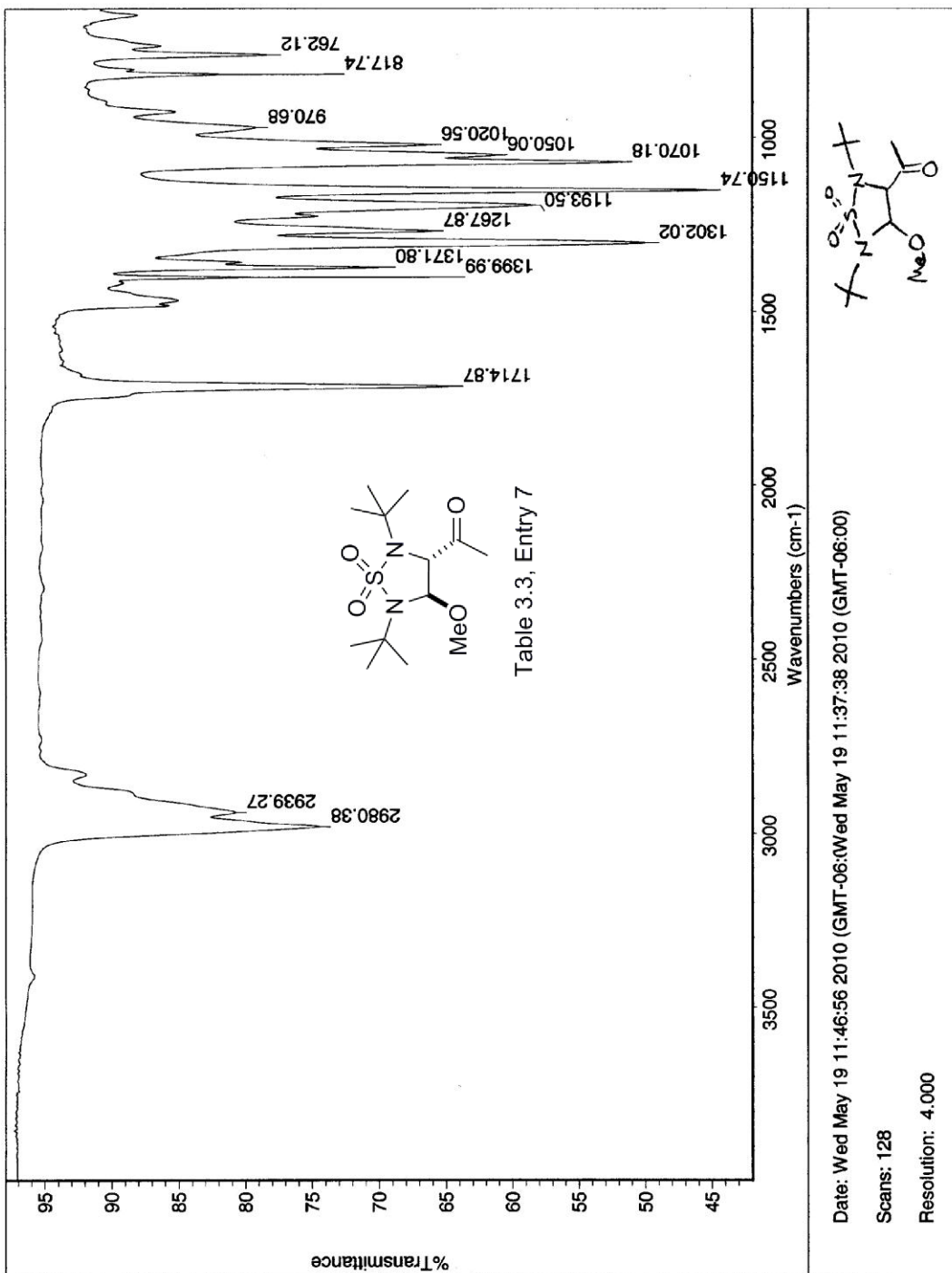


Table 3.3, Entry 6





STANDARD 1H OBSERVE

Pulse Sequence: s2pul
Solvent: Benzene
Ambient Temperature
F1: INOVA-500
F2: EPOX-TD1
Pulse: 42.4 degrees
Acq. time: 2.091 sec
Width: 6982.6 Hz
FID: 4
OBSERVE: H1, 400.1065274 MHz
DATA PROCESSING
Gauss apodization: 0.971 sec
Phase: 0
Total time: 0 min, 13 sec

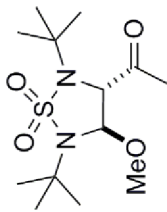
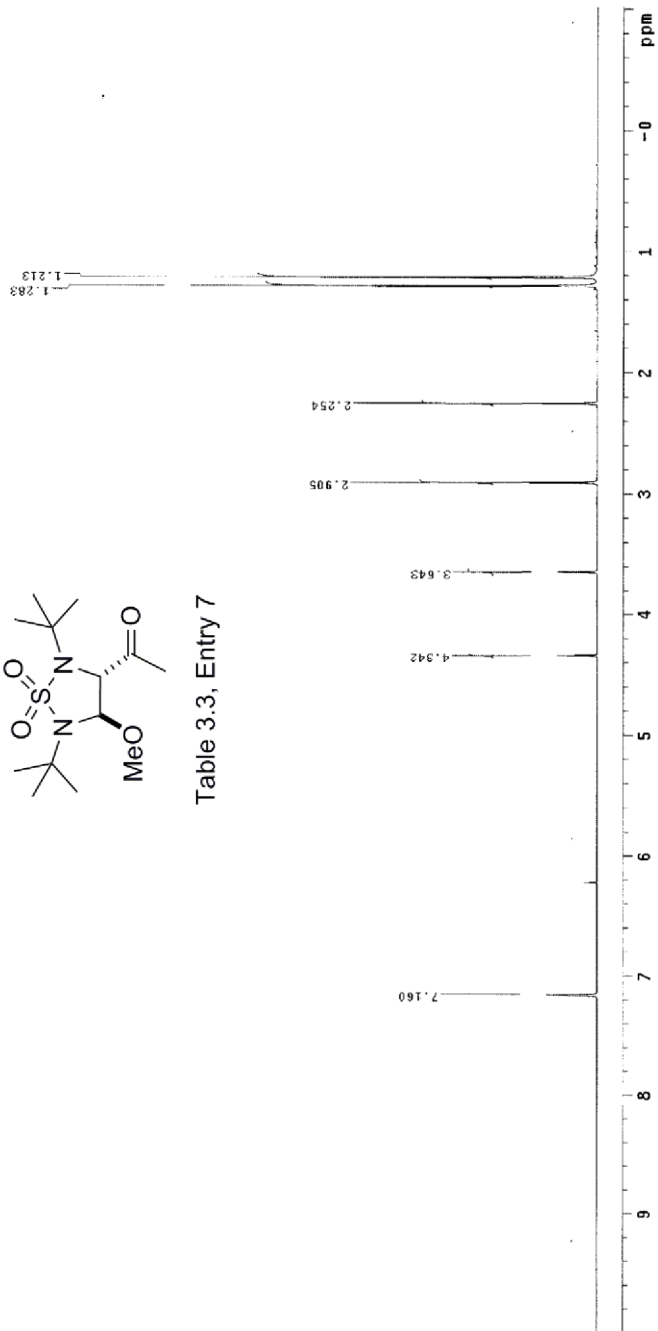


Table 3.3, Entry 7



13C OBSERVE

Pulse Sequence: s2pul
Solvent: Benzene
Acquire: 1.00000000
File: r_c_b5_13_Carbon
INOVA-500 "epoxide"
Relax_delay 1.700 sec
rise_time 0.05000000
width 30016.8 Hz
2796 repetitions
OBSERVE C13, 100.6067473 MHz
Power 56 dB, 400.1065628 MHz
continuously on
WALTZ-16 modulated
DATA PROCESSING
FT size 32768
Total time 622735 hr, 34 min, 7 sec

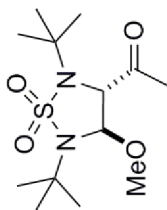
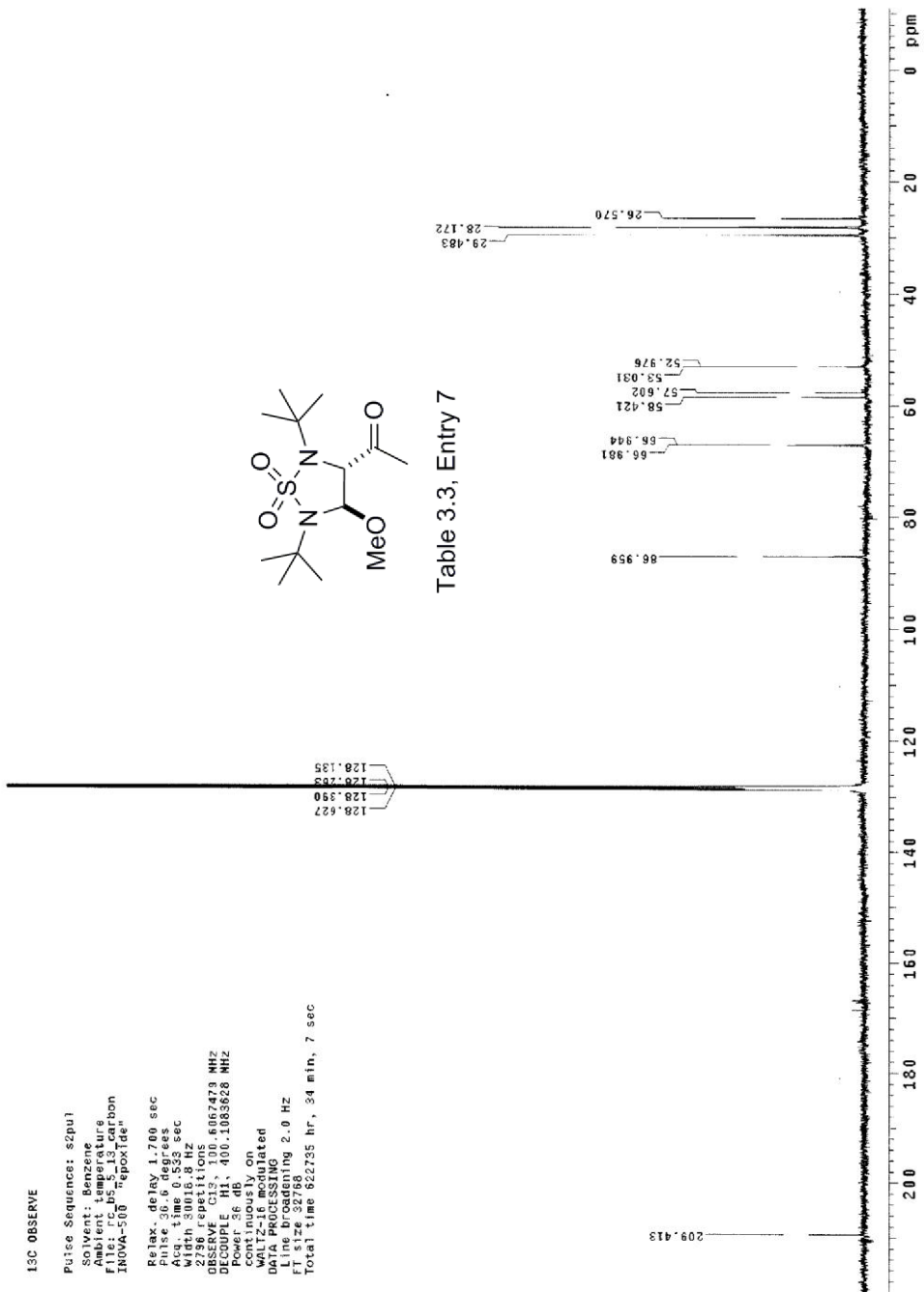
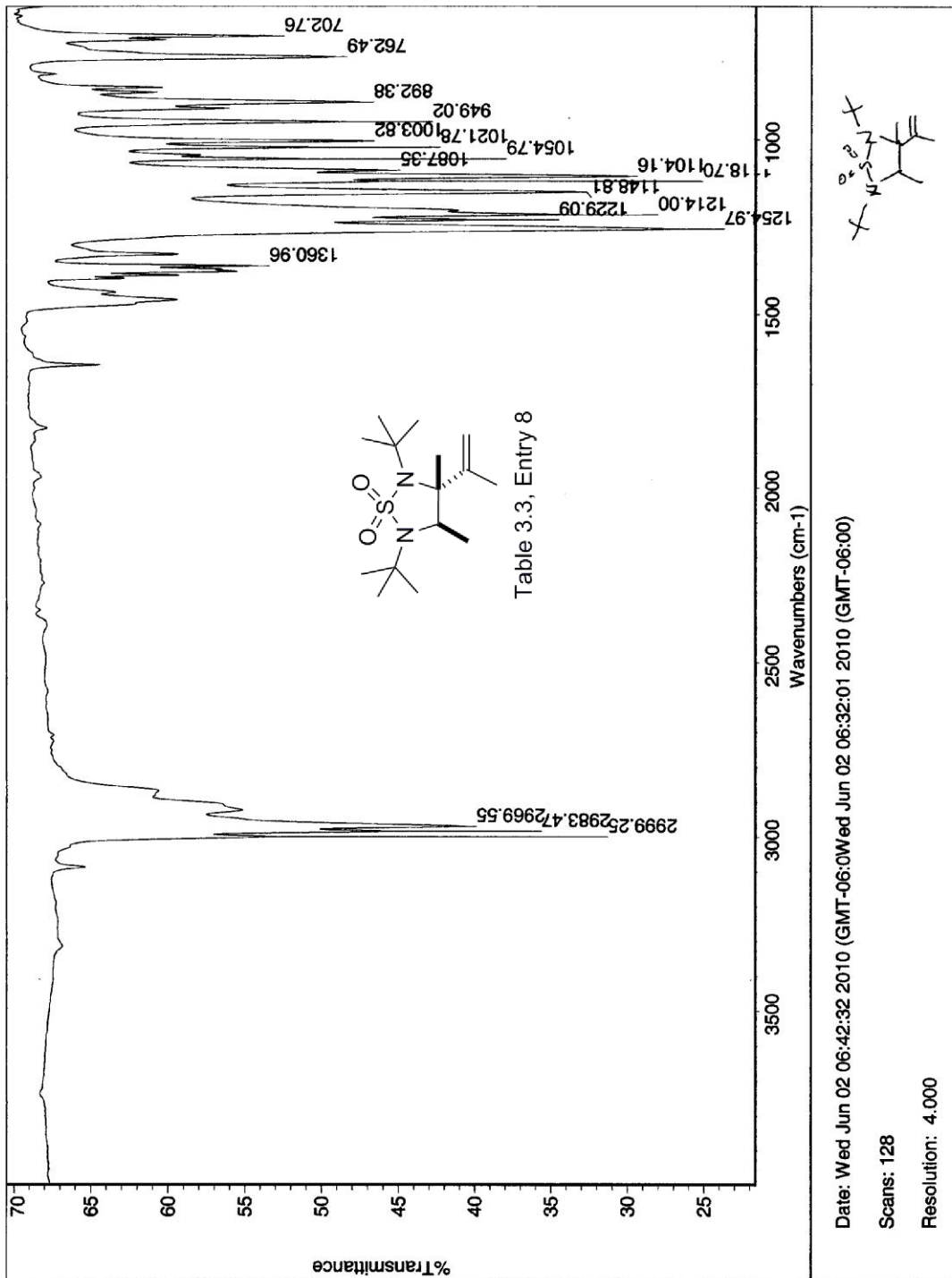


Table 3.3, Entry 7





STANDARD 1H OBSERVE

Pulse Sequence: s2pu1
Solvent: CDCl3
Ambient Temperature: 25.000000
F1: INOVA-500 "690X1d0"
Pulse 42.4 degrees
Acq. time 2.291 sec
Width 6982.6 Hz
SFO: 500.136450 MHz
OBSERVE F1: 500.136450 MHz
DATA PROCESSING
Gauss apodization 0.971 sec
F1: s129 65536
Total time 0 min, 13 sec

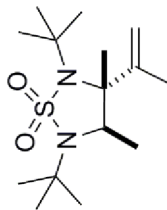
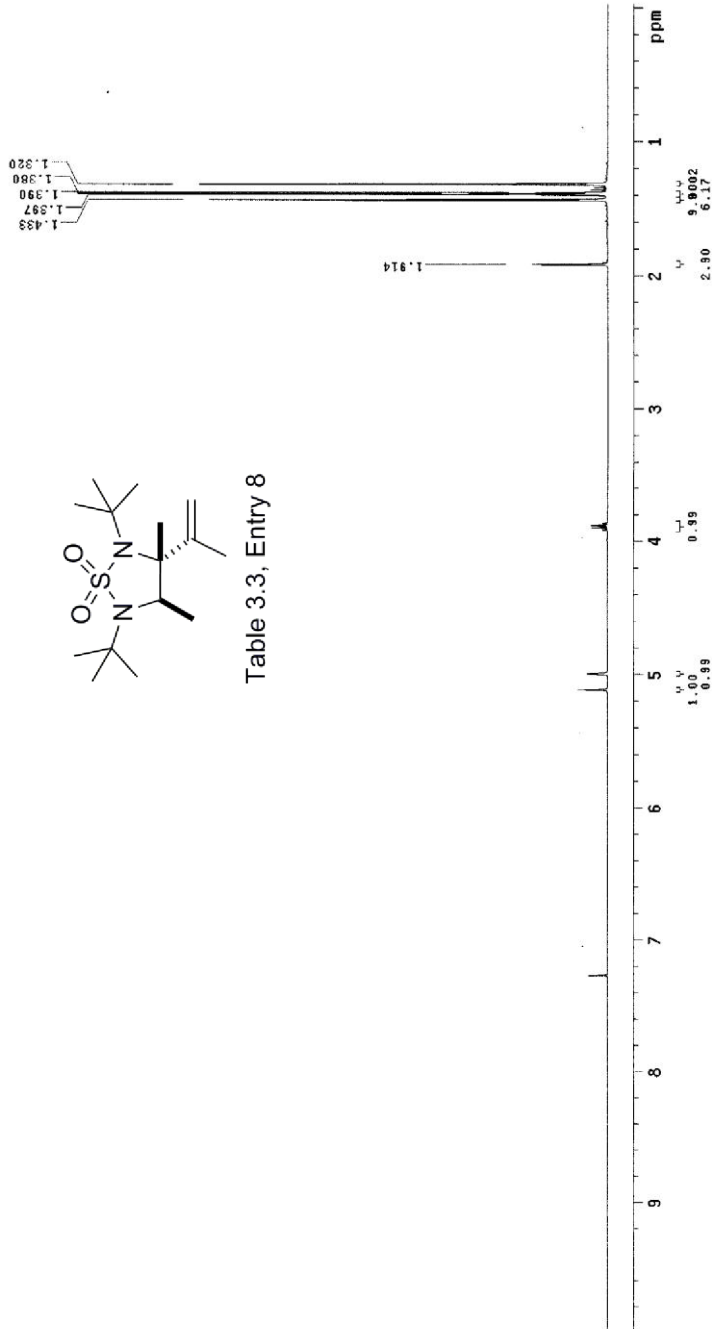


Table 3.3, Entry 8



13C OBSERVE

Pulse Sequence: zgpg30
Solvent: CDCl3
Sample Temperature: 25.00
File: FC_b5_18_24_carbon
INOVA-500 "epoxide"

Relax. delay: 1.700 sec
Pulse: 36.000000 sec
Pulse width: 12.000000 sec
Width: 3000.0 Hz
1050 repetitions
OBSERVE: C13, 100.6067923 MHz
Power: 56 dB, 400.1068268 MHz
continuously on
WALTZ-16 modulated
DATA PROCESSING
FT size: 32768
Total time: 622735 hr, 34 min, 7 sec

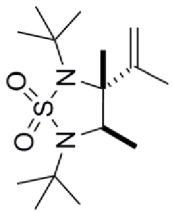
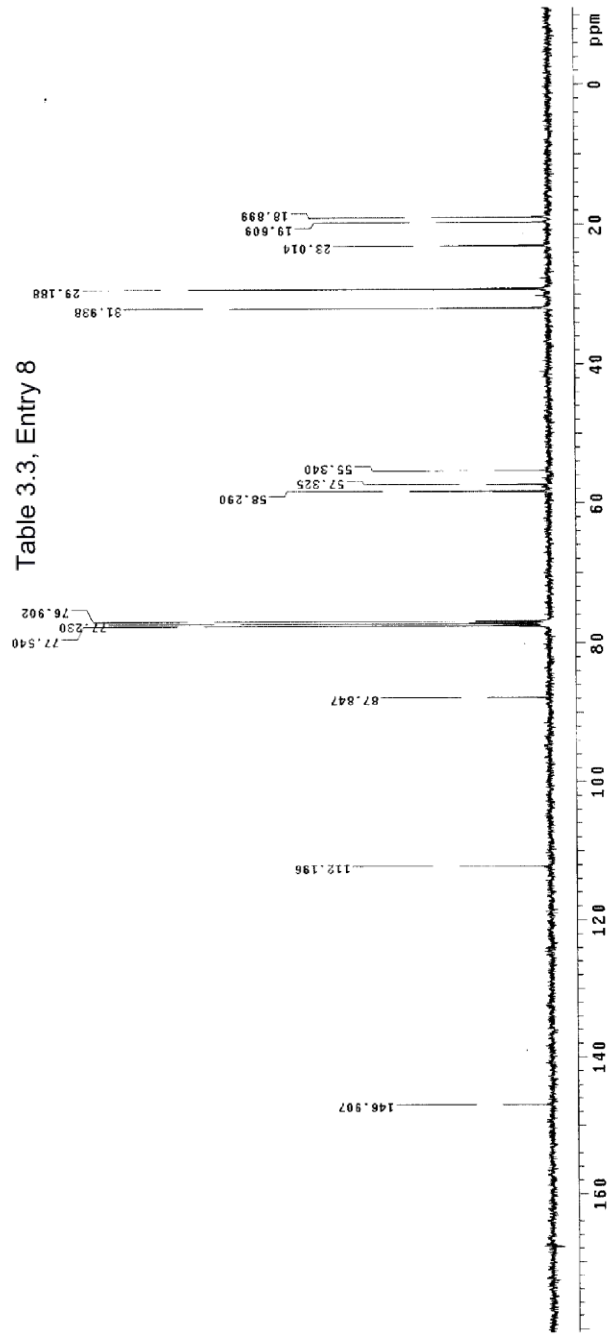
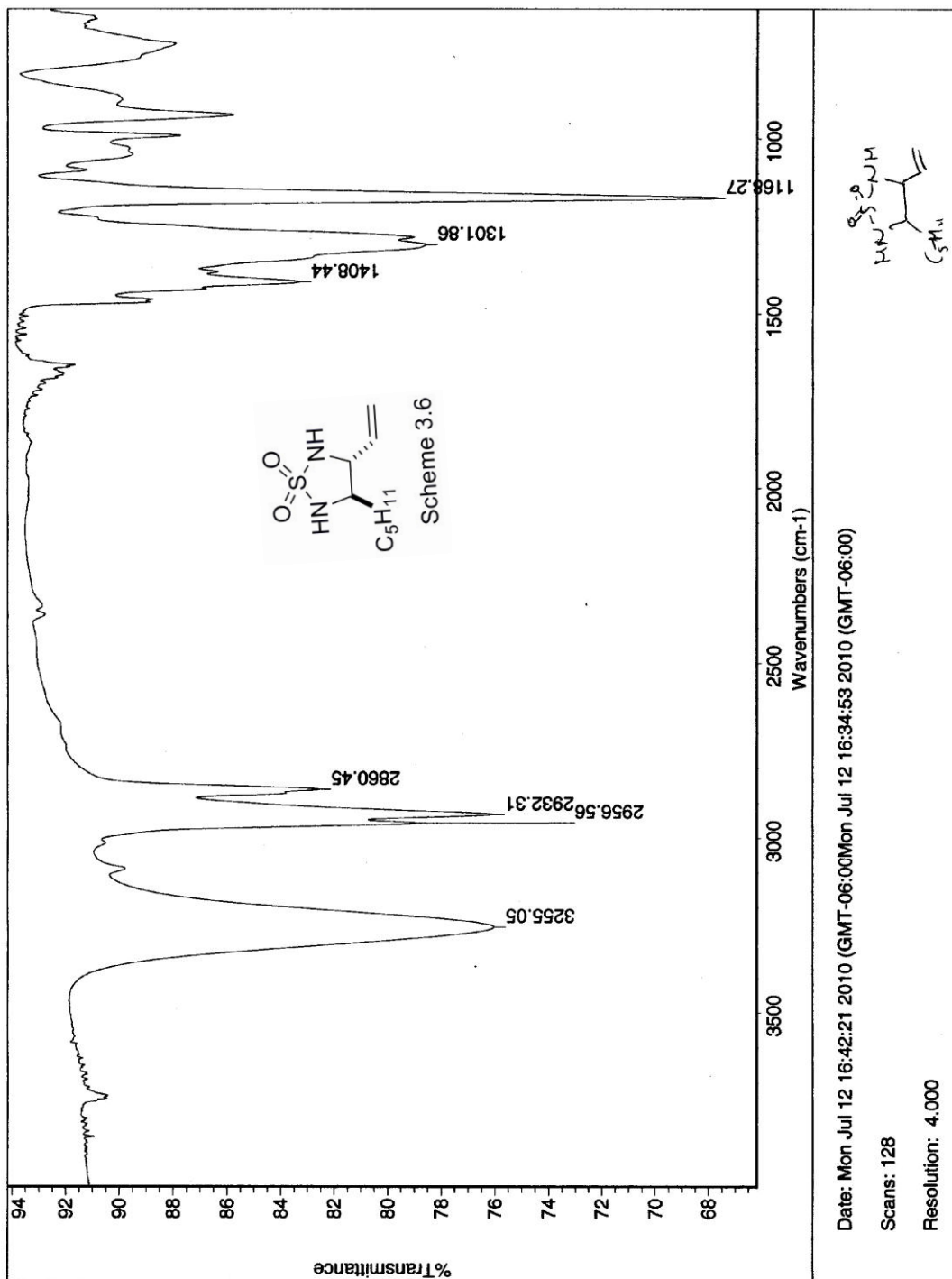


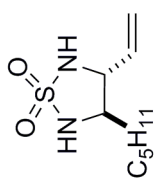
Table 3.3, Entry 8



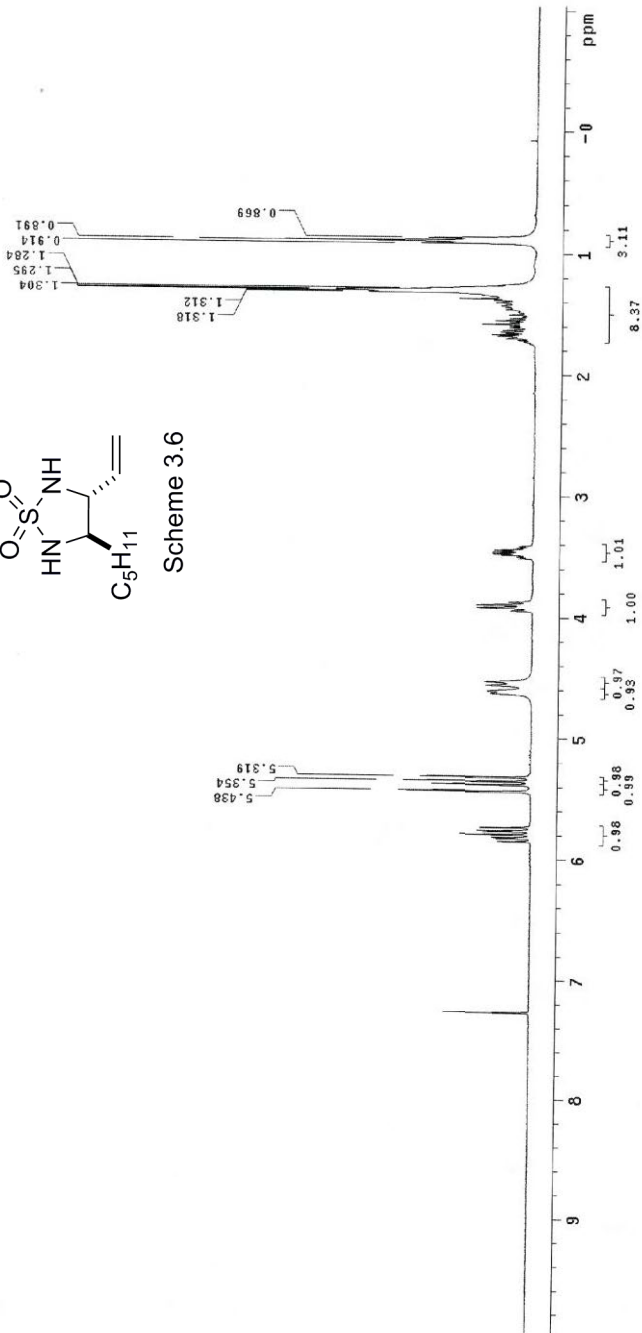


STANDARD 1H OBSERVE

Pulse Sequence: s2pul
 Solvent: CDCl3
 Ambient temperature
 File: C:\95_20_t01_pure_check
 IN004-500_Teppoxide
 Relax. delay 0.000 sec
 Pulse 26.0 degrees
 Acq. time 2.568 sec
 Width 5335.2 Hz
 Frequency 300.1592164 MHz
 OBSERVE 1H
 DATA PROCESSING
 Gauss apodization 0.898 sec
 Filter 12.22716
 Total time 0 min, 16 sec



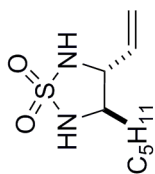
Scheme 3.6



13C OBSERVE

Pulse Sequence: s2pul
Solvent: CDCl3
Ambient temperature
file: rc_hs_26_1to1_carbon
INOVA-500 "epoxide"

Relax. delay 1.700 sec
Pulse program: zgpg30
Acq. time 0.535 sec
Width 30018.6 Hz
2240 repetitions
OBSERVE C13, 100.6087923 MHz
D1 0.50000000 sec
Power 36 dB, 400.1053268 MHz
continuously on
WALTZ-16 modulated
DATA PROCESSING
FT size 32768
Total time 622735 hr, 34 min, 7 sec



Scheme 3.6

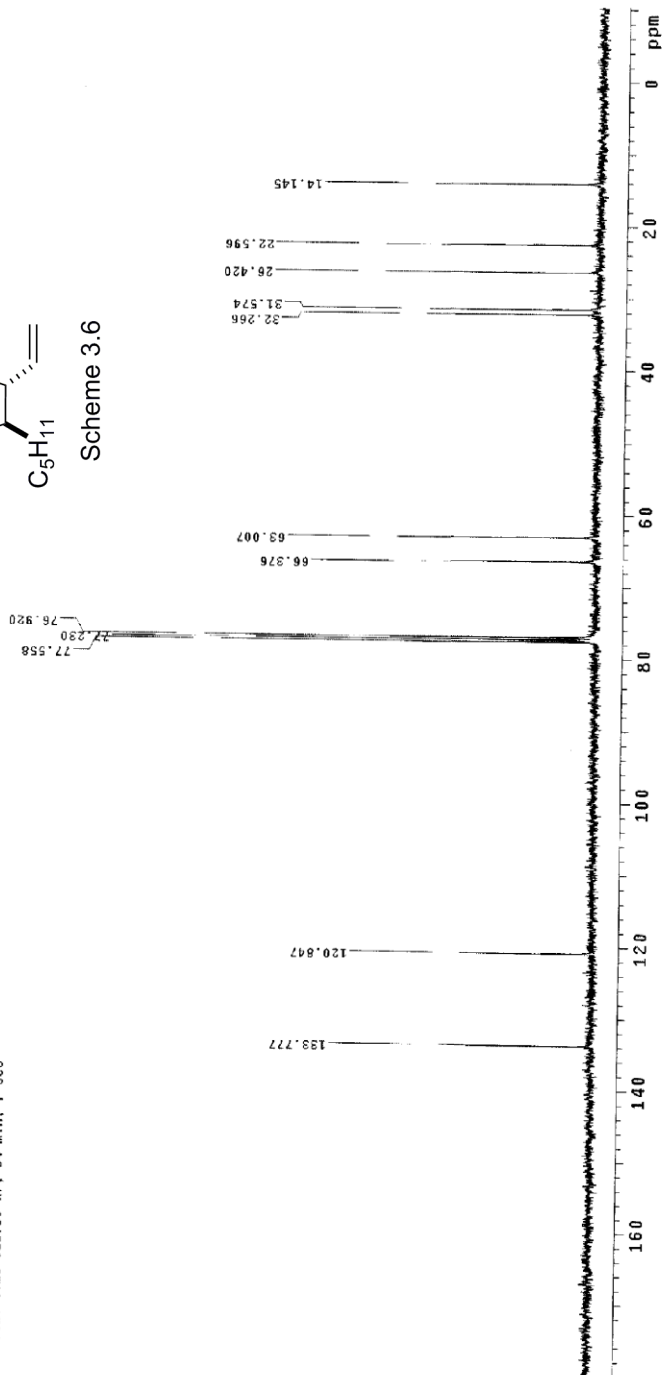
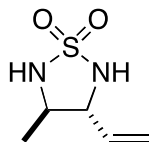
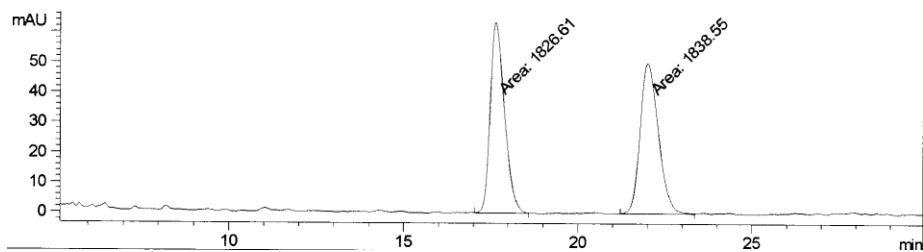


Table 4.1, entry 1



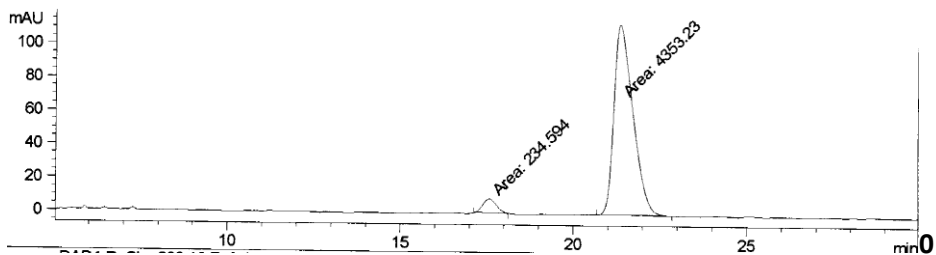
HPLC Conditions: Column: Chiralpak IC (Column No. IC00CE-MJ032), Daicel Chemical Industries, Ltd. Eluent: Hexanes/IPA (70/30); Flow rate: 1.0 mL/min; Detection: UV210

Racemic



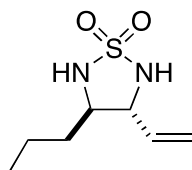
Peak #	RetTime [min]	Type	Width [min]	Area [mAU*s]	Height [mAU]	Area %
1	17.628	MM	0.4810	1826.61499	63.29630	49.8372
2	21.996	MM	0.6136	1838.54614	49.93508	50.1628

Chiral



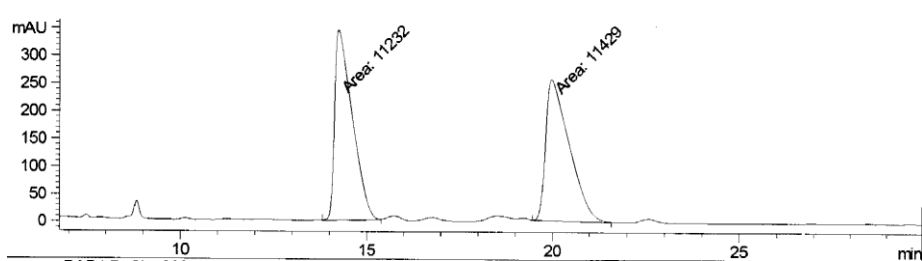
Peak #	RetTime [min]	Type	Width [min]	Area [mAU*s]	Height [mAU]	Area %
1	17.573	MM	0.4612	234.59427	8.47831	5.1134
2	21.313	MM	0.6390	4353.23145	113.53429	94.8866

Table 4.1, entry 2



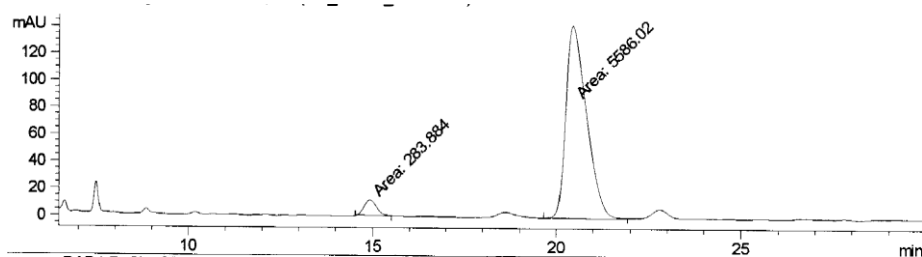
HPLC Conditions: Column: Chiralpak IC (Column No. IC00CE-MJ032), Daicel Chemical Industries, Ltd. **Eluent:** Hexanes/IPA (70/30); **Flow rate:** 1.0 mL/min; **Detection:** UV210

Racemic



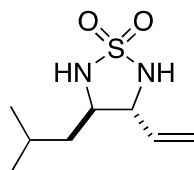
Peak #	RetTime [min]	Type	Width [min]	Area [mAU*s]	Height [mAU]	Area %
1	14.231	MM	0.5422	1.12320e4	345.23639	49.5652
2	19.955	MM	0.7421	1.14290e4	256.66498	50.4348

Chiral



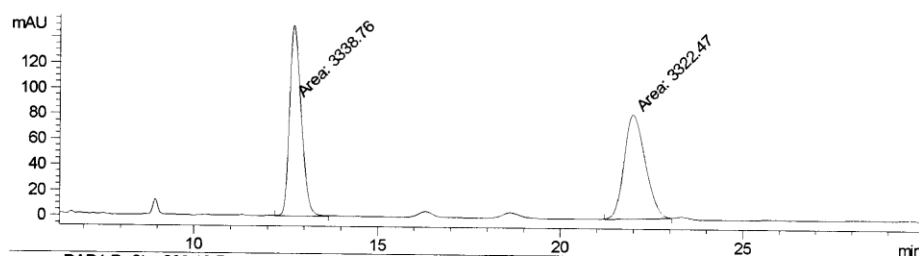
Peak #	RetTime [min]	Type	Width [min]	Area [mAU*s]	Height [mAU]	Area %
1	14.919	MM	0.4087	283.88440	11.57713	4.8363
2	20.430	MV	0.6551	5586.01807	142.11674	95.1637

Table 4.1, entry 3



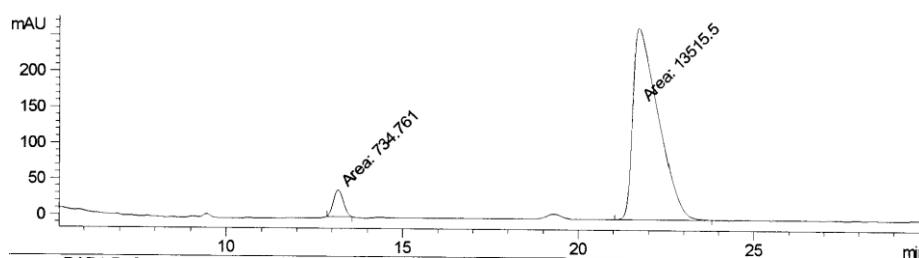
HPLC Conditions: Column: Chiralpak IC (Column No. IC00CE-MJ032), Daicel Chemical Industries, Ltd. **Eluent:** Hexanes/IPA (70/30); **Flow rate:** 1.0 mL/min; **Detection:** UV210

Racemic



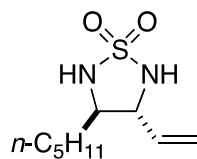
Peak #	RetTime [min]	Type	Width [min]	Area [mAU*s]	Height [mAU]	Area %
1	12.695	MV	0.3721	3338.75513	149.54039	50.1223
2	21.972	MM	0.6782	3322.46582	81.65154	49.8777

Chiral



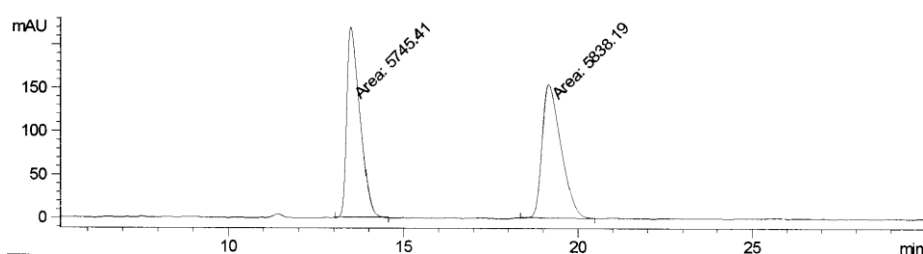
Peak #	RetTime [min]	Type	Width [min]	Area [mAU*s]	Height [mAU]	Area %
1	13.159	MM	0.3310	734.76068	36.99473	5.1561
2	21.711	MM	0.8444	1.35155e4	266.78217	94.8439

Table 4.1, entry 4



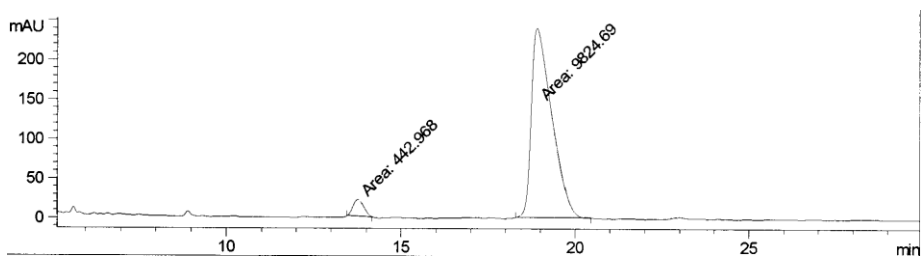
HPLC Conditions: Column: Chiralpak IC (Column No. IC00CE-MJ032), Daicel Chemical Industries, Ltd. Eluent: Hexanes/IPA (70/30); Flow rate: 1.0 mL/min; Detection: UV210

Racemic



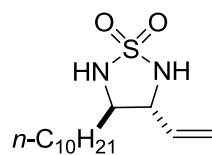
Peak #	RetTime [min]	Type	Width [min]	Area [mAU*s]	Height [mAU]	Area %
1	13.483	VM	0.4363	5745.41406	219.47356	49.5995
2	19.151	MM	0.6325	5838.19385	153.83551	50.4005

Chiral



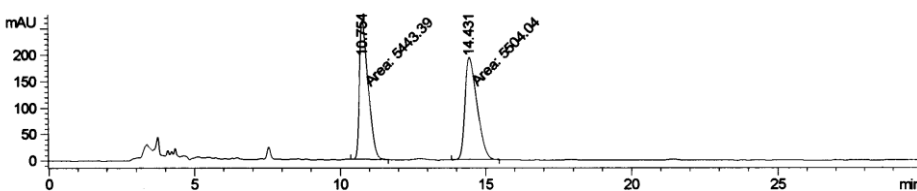
Peak #	RetTime [min]	Type	Width [min]	Area [mAU*s]	Height [mAU]	Area %
1	13.760	MM	0.3485	442.96762	21.18212	4.3142
2	18.903	MM	0.6847	9824.68945	239.13670	95.6858

Table 4.1, entry 5



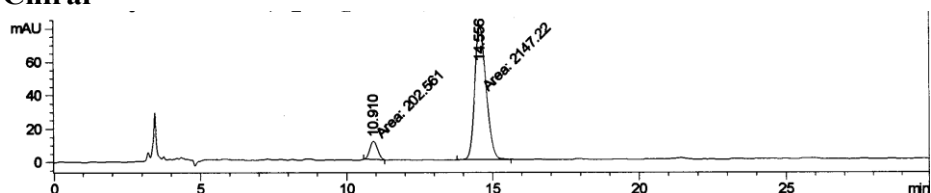
HPLC Conditions: Column: Chiralpak IC (Column No. IC00CE-MJ032), Daicel Chemical Industries, Ltd. Eluent: Hexanes/IPA (70/30); Flow rate: 1.0 mL/min; Detection: UV210

Racemic



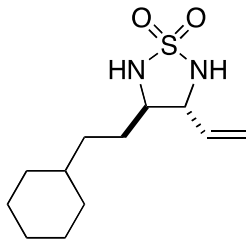
Peak #	RetTime [min]	Type	Width [min]	Area [mAU*s]	Height [mAU]	Area %
1	10.754	MM	0.3471	5443.39209	261.38745	49.7230
2	14.431	MM	0.4757	5504.04102	192.85849	50.2770

Chiral



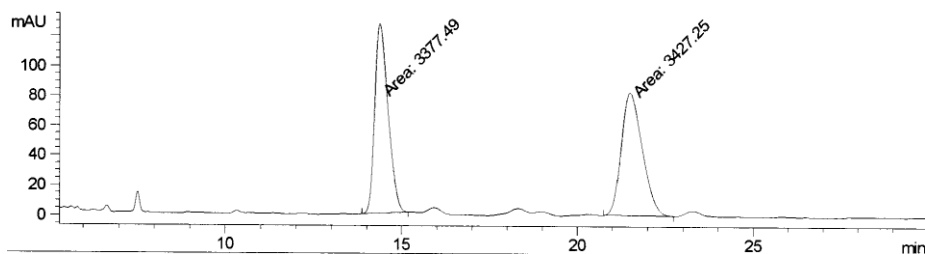
Peak #	RetTime [min]	Type	Width [min]	Area [mAU*s]	Height [mAU]	Area %
1	10.910	MM	0.3086	202.56142	10.94083	8.6204
2	14.556	MM	0.4487	2147.21973	79.75562	91.3796

Table 4.1, entry 6



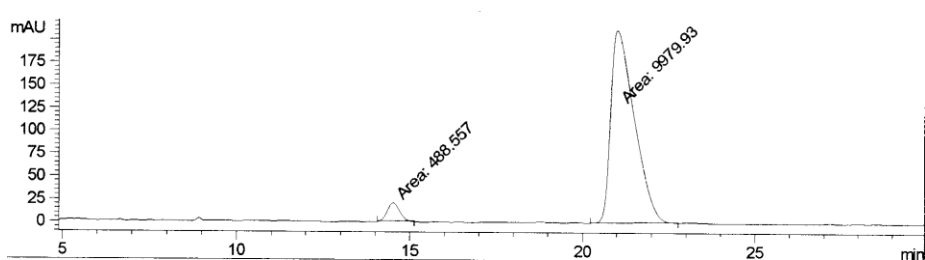
HPLC Conditions: Column: Chiralpak IC (Column No. IC00CE-MJ032), Daicel Chemical Industries, Ltd. **Eluent:** Hexanes/IPA (70/30); **Flow rate:** 1.0 mL/min; **Detection:** UV210

Racemic



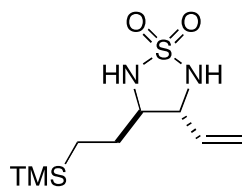
Peak #	RetTime [min]	Type	Width [min]	Area [mAU*s]	Height [mAU]	Area %
1	14.360	MM	0.4438	3377.49414	126.82595	49.6344
2	21.479	MM	0.6945	3427.24829	82.24599	50.3656

Chiral



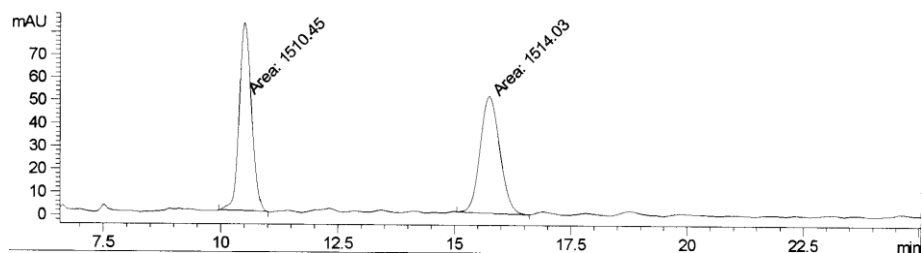
Peak #	RetTime [min]	Type	Width [min]	Area [mAU*s]	Height [mAU]	Area %
1	14.508	MM	0.4061	488.55731	20.04921	4.6669
2	21.005	MV	0.7876	9979.92969	211.19110	95.3331

Table 4.1, entry 7



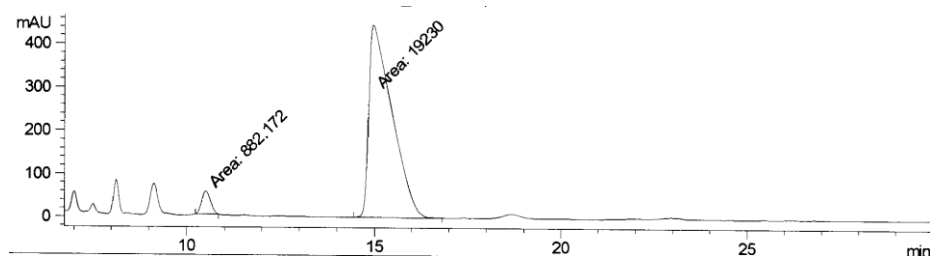
HPLC Conditions: Column: Chiralpak IC (Column No. IC00CE-MJ032), Daicel Chemical Industries, Ltd. **Eluent:** Hexanes/IPA (70/30); **Flow rate:** 1.0 mL/min; **Detection:** UV210

Racemic



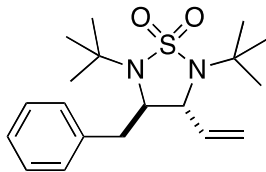
Peak #	RetTime [min]	Type	Width [min]	Area [mAU*s]	Height [mAU]	Area %
1	10.502	MM	0.3063	1510.44727	82.18114	49.9408
2	15.742	MM	0.4963	1514.02917	50.84820	50.0592

Chiral



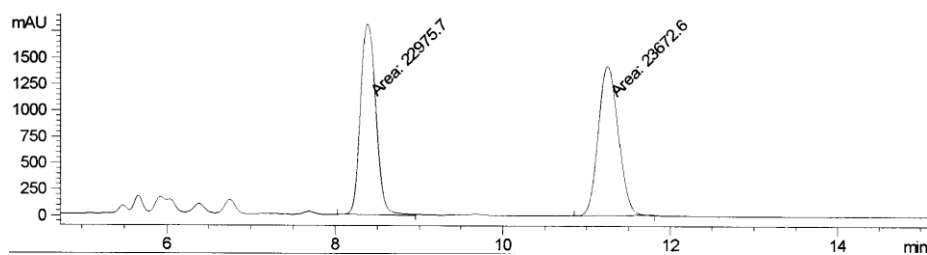
Peak #	RetTime [min]	Type	Width [min]	Area [mAU*s]	Height [mAU]	Area %
1	10.501	MM	0.2748	882.17200	53.49947	4.3863
2	14.952	VM	0.7204	1.92300e4	444.92090	95.6137

Table 4.1, entry 8



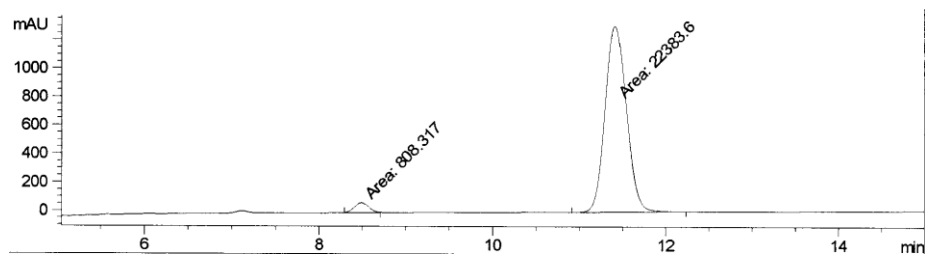
HPLC Conditions: Column: Chiralpak IC (Column No. IC00CE-MJ032), Daicel Chemical Industries, Ltd. **Eluent:** Hexanes/IPA (80/20); **Flow rate:** 1.0 mL/min; **Detection:** UV210

Racemic



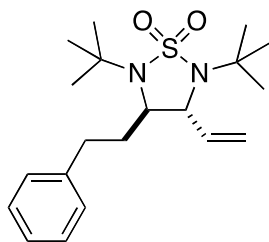
Peak #	RetTime [min]	Type	Width [min]	Area [mAU*s]	Height [mAU]	Area %
1	8.379	MM	0.2112	2.29757e4	1812.76794	49.2531
2	11.248	MM	0.2778	2.36726e4	1420.46838	50.7469

Chiral



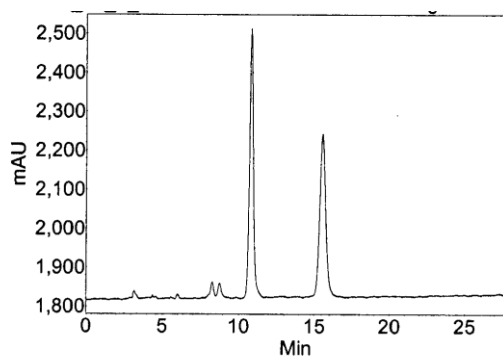
Peak #	RetTime [min]	Type	Width [min]	Area [mAU*s]	Height [mAU]	Area %
1	8.486	MM	0.1910	808.31714	70.55151	3.4853
2	11.410	MM	0.2849	2.23836e4	1309.51123	96.5147

Table 4.1, entry 9



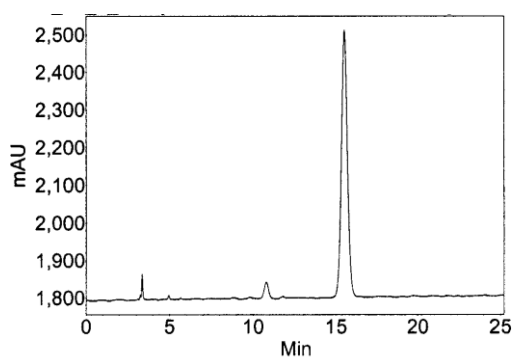
HPLC Conditions: Column: Chiralpak IC (Column No. IC00CE-NJ016), Daicel Chemical Industries, Ltd. **Eluent:** Hexanes/IPA (80/20); **Flow rate:** 1.0 mL/min; **Detection:** UV200

Racemic



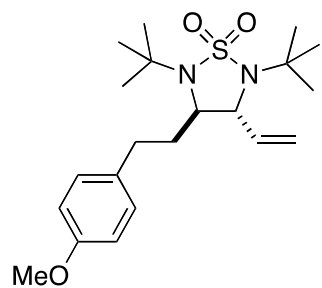
Index	Time [Min]	Area % [%]
2	10.81	50.909
1	15.55	49.091
Total		100.000

Chiral



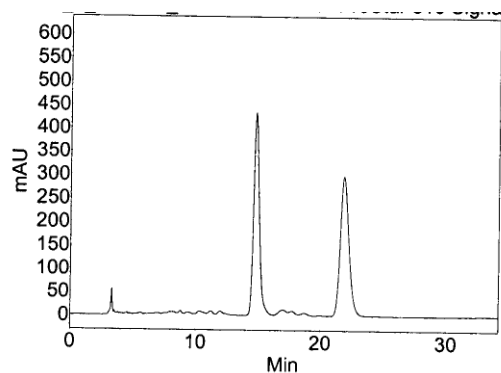
Index	Time [Min]	Area % [%]
2	10.78	3.771
1	15.51	96.229
Total		100.000

Table 4.1, entry 10



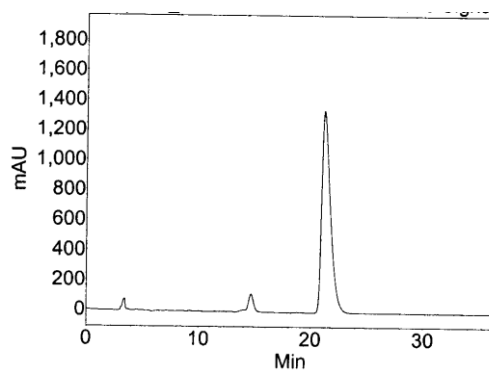
HPLC Conditions: Column: Chiralpak IC (Column No. IC00CE-NJ016), Daicel Chemical Industries, Ltd. **Eluent:** Hexanes/IPA (80/20); **Flow rate:** 1.0 mL/min; **Detection:** UV230

Racemic



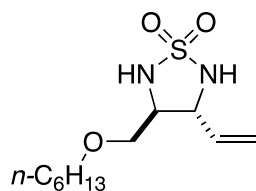
Index	Time [Min]	Area %
1	14.77	49.691
2	21.84	50.309
Total		100.000

Chiral



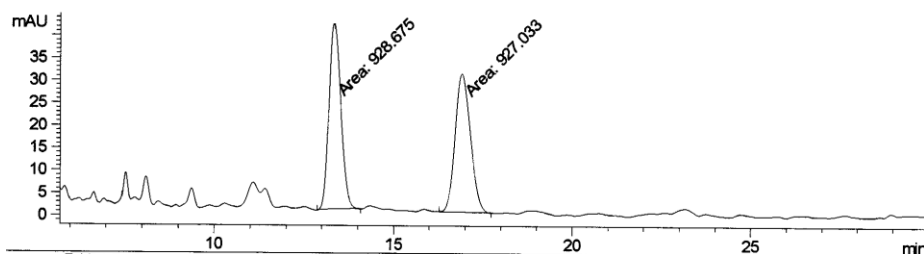
Index	Time [Min]	Area %
2	14.68	4.931
1	21.18	95.069
Total		100.000

Table 4.1, entry 11



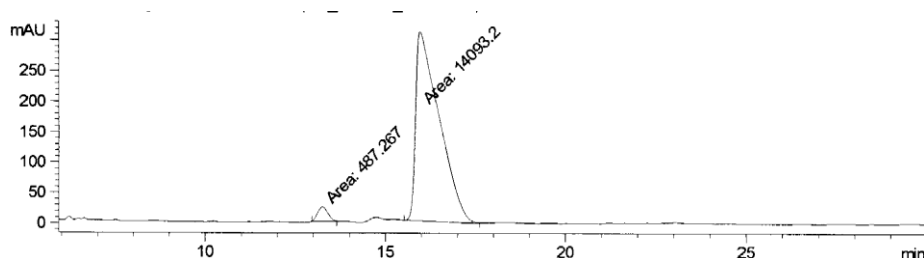
HPLC Conditions: Column: Chiralpak IC (Column No. IC00CE-MJ032), Daicel Chemical Industries, Ltd. Eluent: Hexanes/IPA (70/30); Flow rate: 1.0 mL/min; Detection: UV210

Racemic



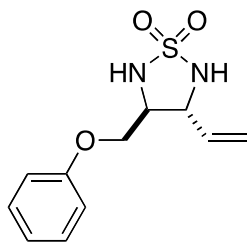
Peak #	RetTime [min]	Type	Width [min]	Area [mAU*s]	Height [mAU]	Area %
1	13.321	MM	0.3759	928.67542	41.18030	50.0442
2	16.891	MM	0.5038	927.03345	30.66966	49.9558

Chiral



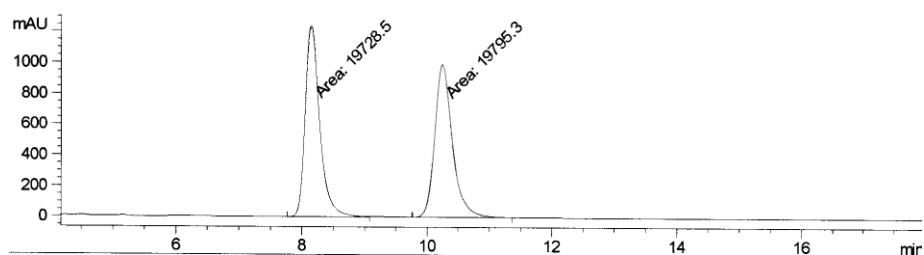
Peak #	RetTime [min]	Type	Width [min]	Area [mAU*s]	Height [mAU]	Area %
1	13.247	MM	0.3392	487.26651	23.94153	3.3419
2	15.952	MM	0.7573	1.40932e4	310.18173	96.6581

Table 4.1, entry 12



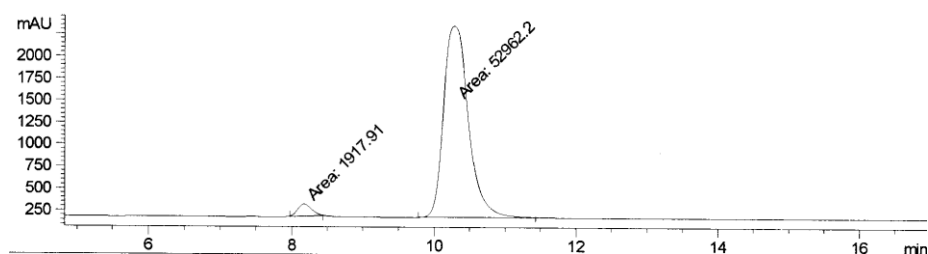
HPLC Conditions: Column: Chiralpak IA (Column No. IA00CE-ML034), Daicel Chemical Industries, Ltd. **Eluent:** Hexanes/IPA (80/20); **Flow rate:** 1.0 mL/min; **Detection:** UV210

Racemic



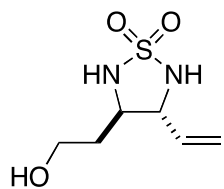
Peak #	RetTime [min]	Type	Width [min]	Area [mAU*s]	Height [mAU]	Area %
1	8.144	MM	0.2649	1.97285e4	1241.44409	49.9154
2	10.241	MM	0.3328	1.97953e4	991.23071	50.0846

Chiral



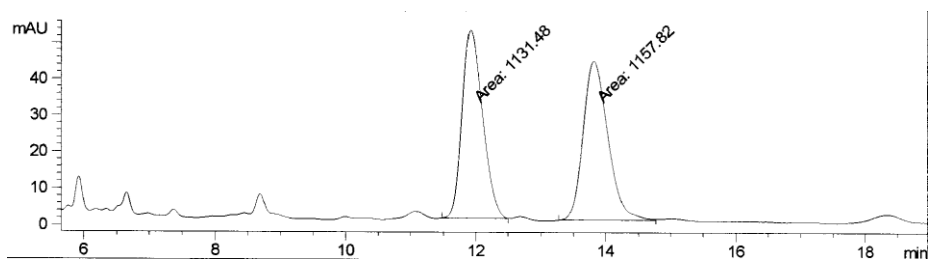
Peak #	RetTime [min]	Type	Width [min]	Area [mAU*s]	Height [mAU]	Area %
1	8.173	MM	0.2313	1917.90613	138.20412	3.4947
2	10.282	MM	0.4083	5.29622e4	2161.80103	96.5053

Table 4.1, entry 13



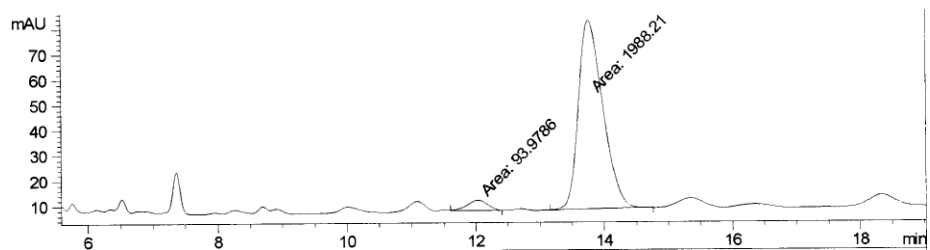
HPLC Conditions: Column: Chiralpak IC (Column No. IC00CE-MJ032), Daicel Chemical Industries, Ltd. Eluent: Hexanes/IPA (70/30); Flow rate: 1.0 mL/min; Detection: UV210

Racemic



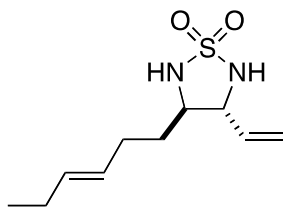
Peak #	RetTime [min]	Type	Width [min]	Area [mAU*s]	Height [mAU]	Area %
1	11.916	MM	0.3648	1131.47742	51.68816	49.4246
2	13.811	MV	0.4436	1157.82422	43.50105	50.5754

Chiral



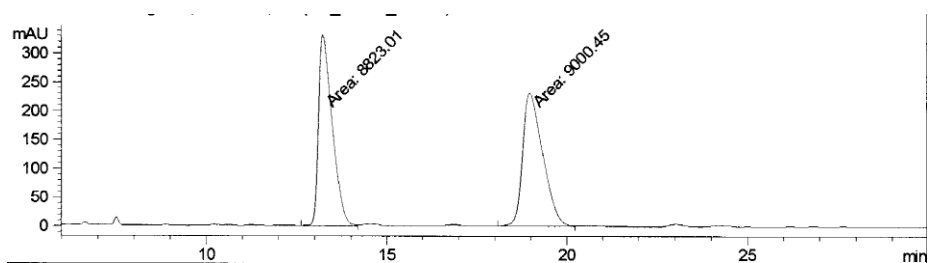
Peak #	RetTime [min]	Type	Width [min]	Area [mAU*s]	Height [mAU]	Area %
1	12.027	MM	0.3753	93.97863	4.17313	4.5135
2	13.763	MM	0.4439	1988.20605	74.64914	95.4865

Table 4.1, entry 14



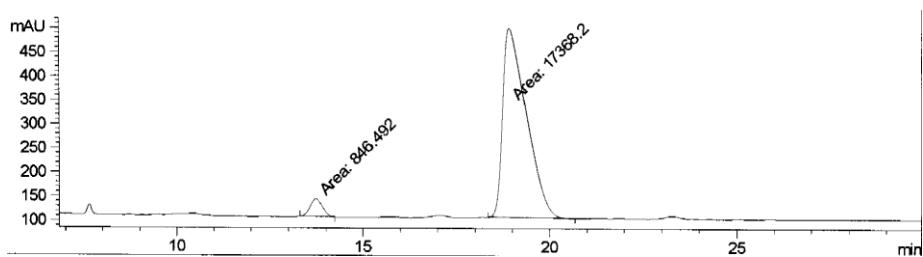
HPLC Conditions: Column: Chiralpak IC (Column No. IC00CE-MJ032), Daicel Chemical Industries, Ltd. **Eluent:** Hexanes/IPA (70/30); **Flow rate:** 1.0 mL/min; **Detection:** UV210

Racemic



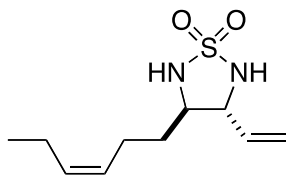
Peak #	RetTime [min]	Type	Width [min]	Area [mAU*s]	Height [mAU]	Area %
1	13.224	MV	0.4430	8823.01270	331.94012	49.5022
2	18.969	MV	0.6483	9000.44922	231.39961	50.4978

Chiral



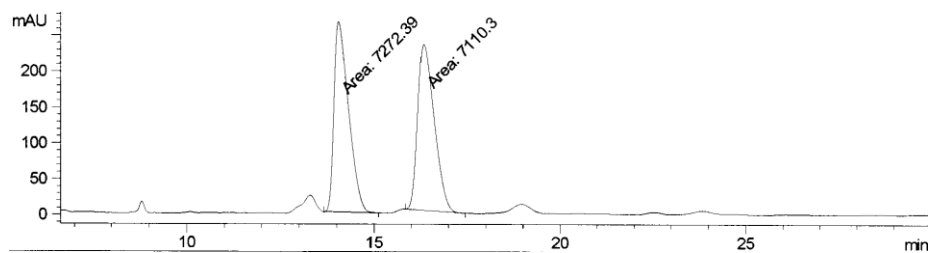
Peak #	RetTime [min]	Type	Width [min]	Area [mAU*s]	Height [mAU]	Area %
1	13.731	MM	0.3802	846.49249	37.10445	4.6473
2	18.903	MM	0.7354	1.73682e4	393.63812	95.3527

Table 4.1, entry 15



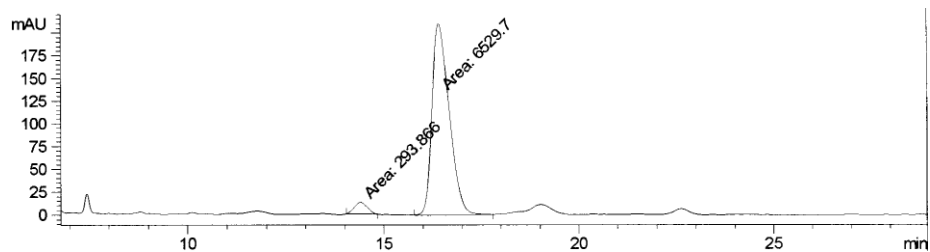
HPLC Conditions: Column: Chiralpak IC (Column No. IC00CE-MJ032), Daicel Chemical Industries, Ltd. **Eluent:** Hexanes/IPA (70/30); **Flow rate:** 1.0 mL/min; **Detection:** UV210

Racemic



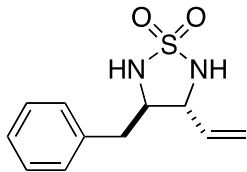
Peak #	RetTime [min]	Type	Width [min]	Area [mAU*s]	Height [mAU]	Area %
1	14.043	VM	0.4565	7272.38525	265.50165	50.5635
2	16.332	MM	0.5127	7110.29785	231.15279	49.4365

Chiral



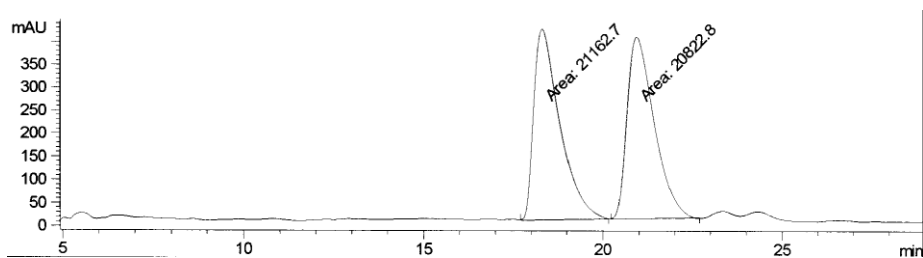
Peak #	RetTime [min]	Type	Width [min]	Area [mAU*s]	Height [mAU]	Area %
1	14.401	MM	0.3835	293.86566	12.77134	4.3066
2	16.406	MM	0.5180	6529.70215	210.09157	95.6934

Scheme 4.8



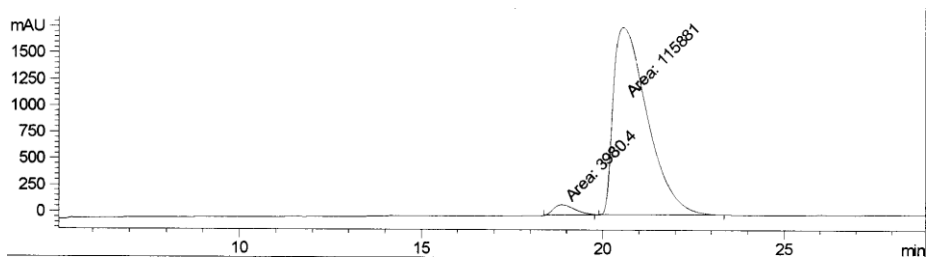
HPLC Conditions: Column: Chiralpak OD-H (Column No. ODHOCE-FB013), Daicel Chemical Industries, Ltd. **Eluent:** Hexanes/IPA (90/10); **Flow rate:** 1.0 mL/min; **Detection:** UV210

Racemic



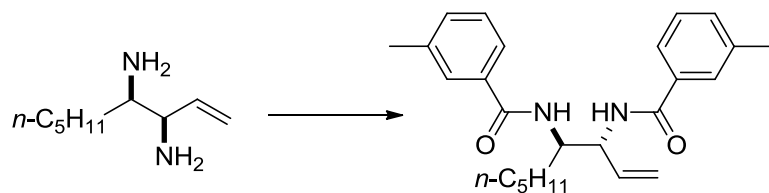
Peak #	RetTime [min]	Type	Width [min]	Area [mAU*s]	Height [mAU]	Area %
1	18.295	MM	0.8512	2.11627e4	414.35797	50.4048
2	20.932	MM	0.8811	2.08228e4	393.89938	49.5952

Chiral



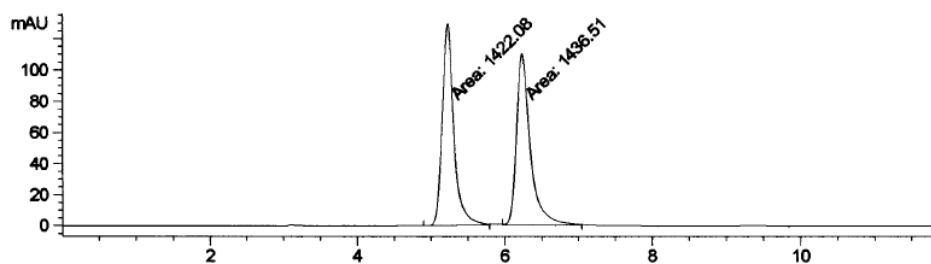
Peak #	RetTime [min]	Type	Width [min]	Area [mAU*s]	Height [mAU]	Area %
1	18.863	MM	0.6797	3980.39795	97.59868	3.3208
2	20.550	VM	1.0912	1.15881e5	1769.96094	96.6792

Scheme 4.8



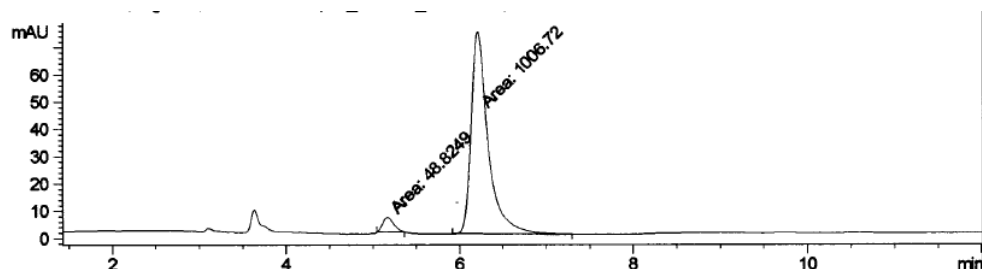
HPLC Conditions: Column: Chiralpak IA (Column No. IC00CE-NJ016), Daicel Chemical Industries, Ltd. **Eluent:** Hexanes/IPA (90/10); **Flow rate:** 1.0 mL/min; **Detection:** UV254

Racemic



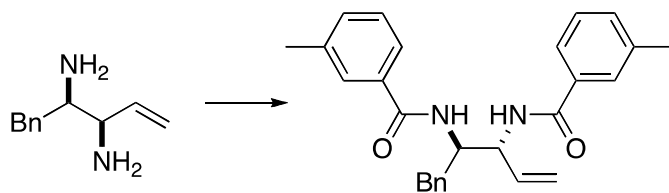
Peak #	RetTime [min]	Type	Width [min]	Area [mAU*s]	Height [mAU]	Area %
1	5.225	MM	0.1822	1422.08386	130.10666	49.7476
2	6.233	MM	0.2166	1436.51440	110.54897	50.2524

Chiral



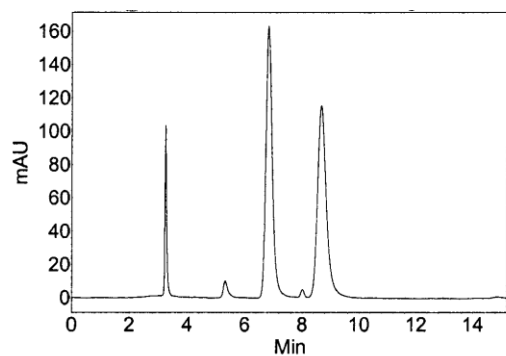
Peak #	RetTime [min]	Type	Width [min]	Area [mAU*s]	Height [mAU]	Area %
1	5.164	MM	0.1484	48.82494	5.48486	4.6256
2	6.215	MM	0.2257	1006.72247	74.35581	95.3744

Scheme 4.8



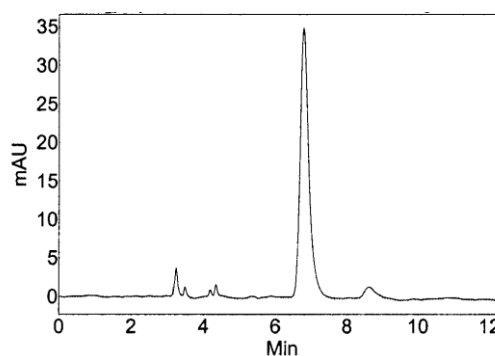
HPLC Conditions: **Column:** Chiralpak IC (Column No. IC00CE-NJ016), Daicel Chemical Industries, Ltd. **Eluent:** Hexanes/IPA (95/5); **Flow rate:** 1.0 mL/min; **Detection:** UV220

Racemic

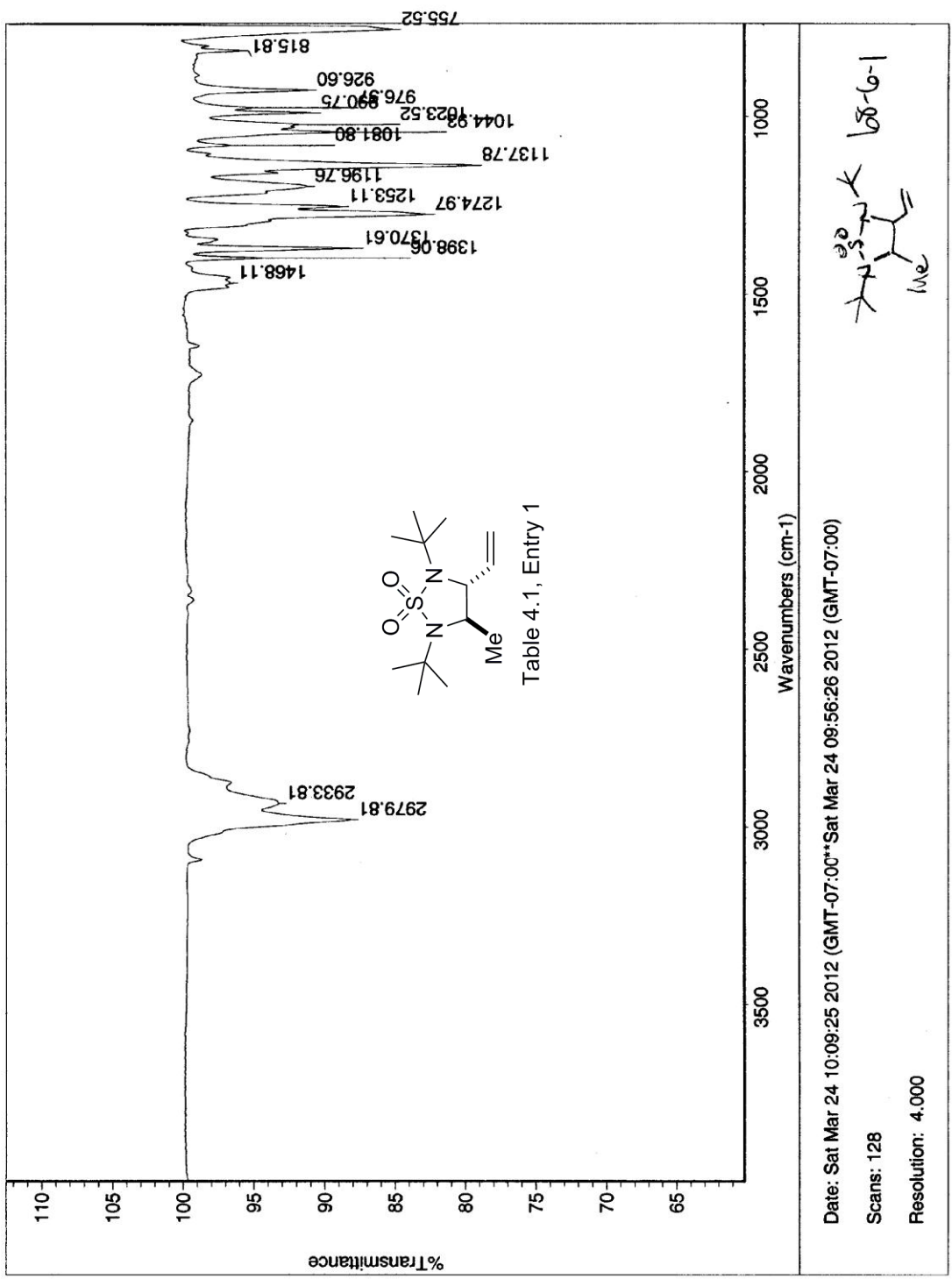


Index	Time [Min]	Area %
1	6.83	49.933
2	8.68	50.067
Total		100.000

Chiral



Index	Time [Min]	Area %
1	6.78	96.604
2	8.63	3.396
Total		100.000



STANDARD 1H OBSERVE

Pulse Sequence: s2pu1
 Solvent: CDCl3
 Ambient Temperature
 CDCl3
 INOVA-500 "ppm 100"
 Relax. delay 0.000 sec
 Pulse 26.0 degrees
 Acq. time 2.668 sec
 Width 5995.2 Hz
 8 repetitions
 OBSERVE H1, 300.1592164 MHz
 DATA PROCESSING
 Relaxation 0.896 sec
 FT size 32768
 Total time 0 min, 26 sec

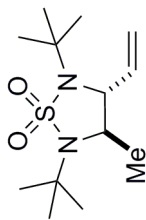
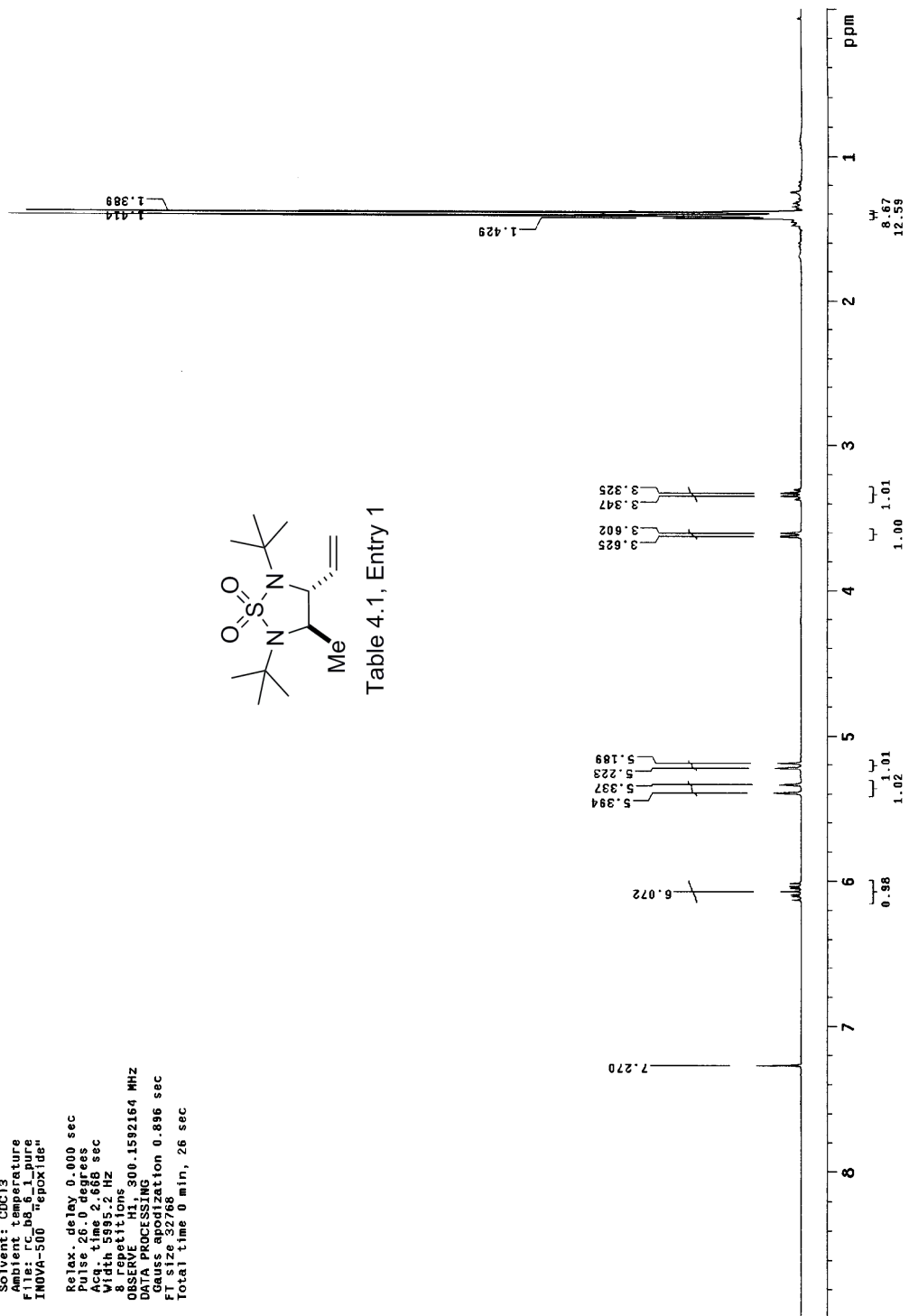


Table 4.1, Entry 1



b8-6-1
 Archive directory: /home/DATA/walkup/cornwall
 Sample directory: b8-6-1_20120316_01
 Pulse Sequence: s2pu1
 Solvent: cdcl3
 Acq. temperature: 300.2 K
 Sample #46: Operator: cornwall
 File: rc_b8_6_1_13C
 INOVA-500 "epoxide"
 Relax. delay 1.000 sec
 Pulse 45.0 degrees
 Acq. time 1.285 sec
 Width 25510.2 Hz
 Observed: 13C, 100.5058907 MHz
 DECOUPLE: H1, 399.7070404 MHz
 Power 38 dB
 continuously on
 WALTZ-16 modulated
 DATA PROCESSING
 FT. time beginning 0.5 Hz
 FT. time ending 19.5 Hz
 Total time 19 min, 34 sec

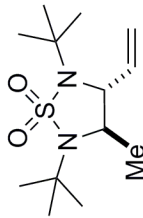
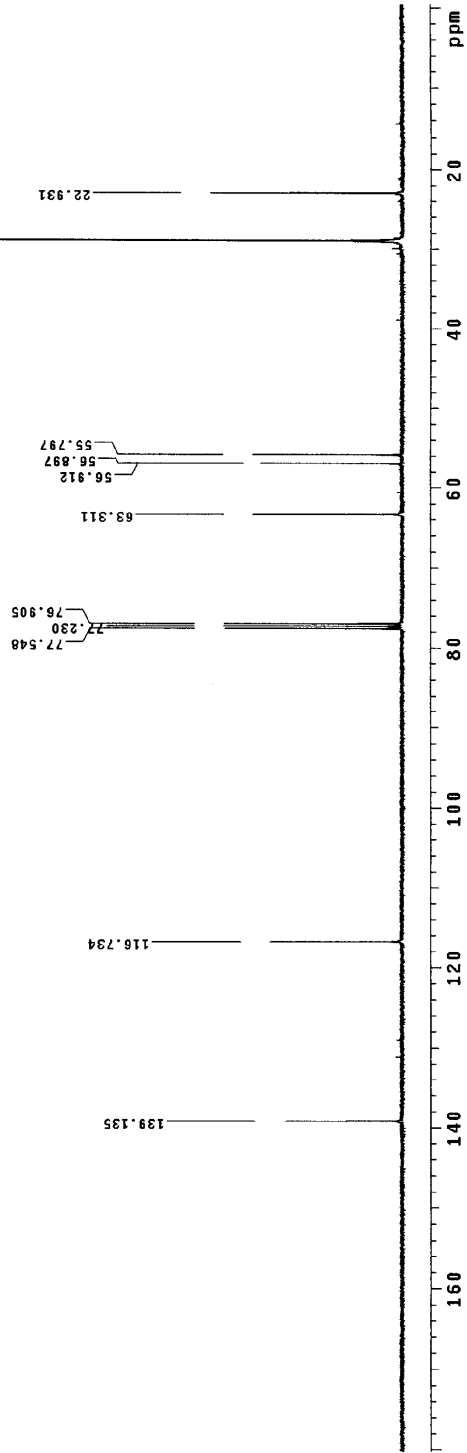
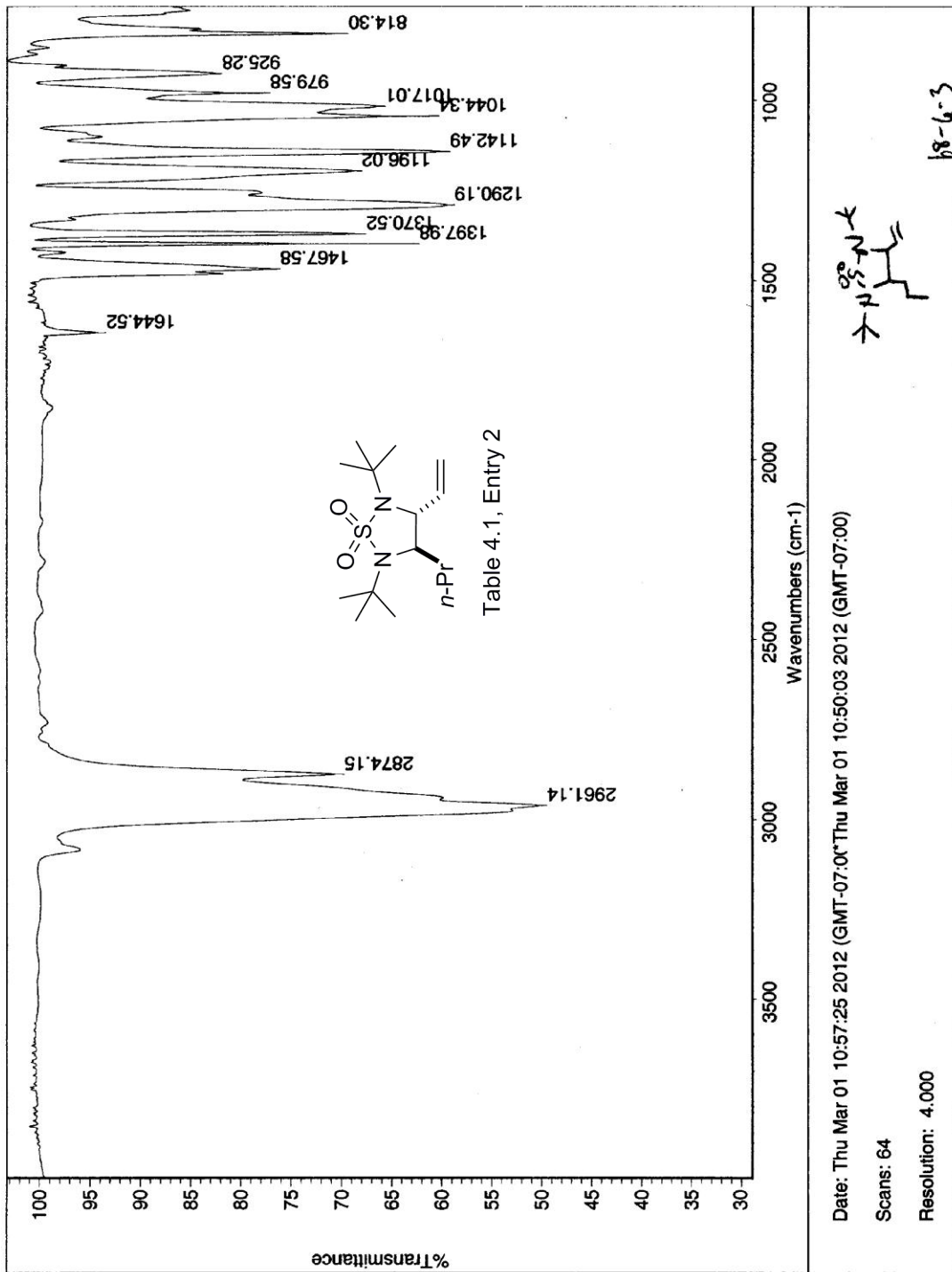


Table 4.1, Entry 1





STANDARD 1H OBSERVE

Pulse Sequence: s2pu1
 Solvent: CDCl3
 Temperature: 300.1592160 MHz
 File: rc_b8_3_pure
 INOVA-500 "repx1de"
 Relax. delay 0.000 sec
 Pulse 26.0 degrees
 Acq. time 2.668 sec
 Width 5995.2 Hz
 Spectrometer
 OBSERVE: 300.1592160 MHz
 DATA PROCESSING
 Gauss apodization 0.496 sec
 FT size 32768
 Total time 0 min, 16 sec

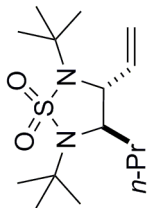
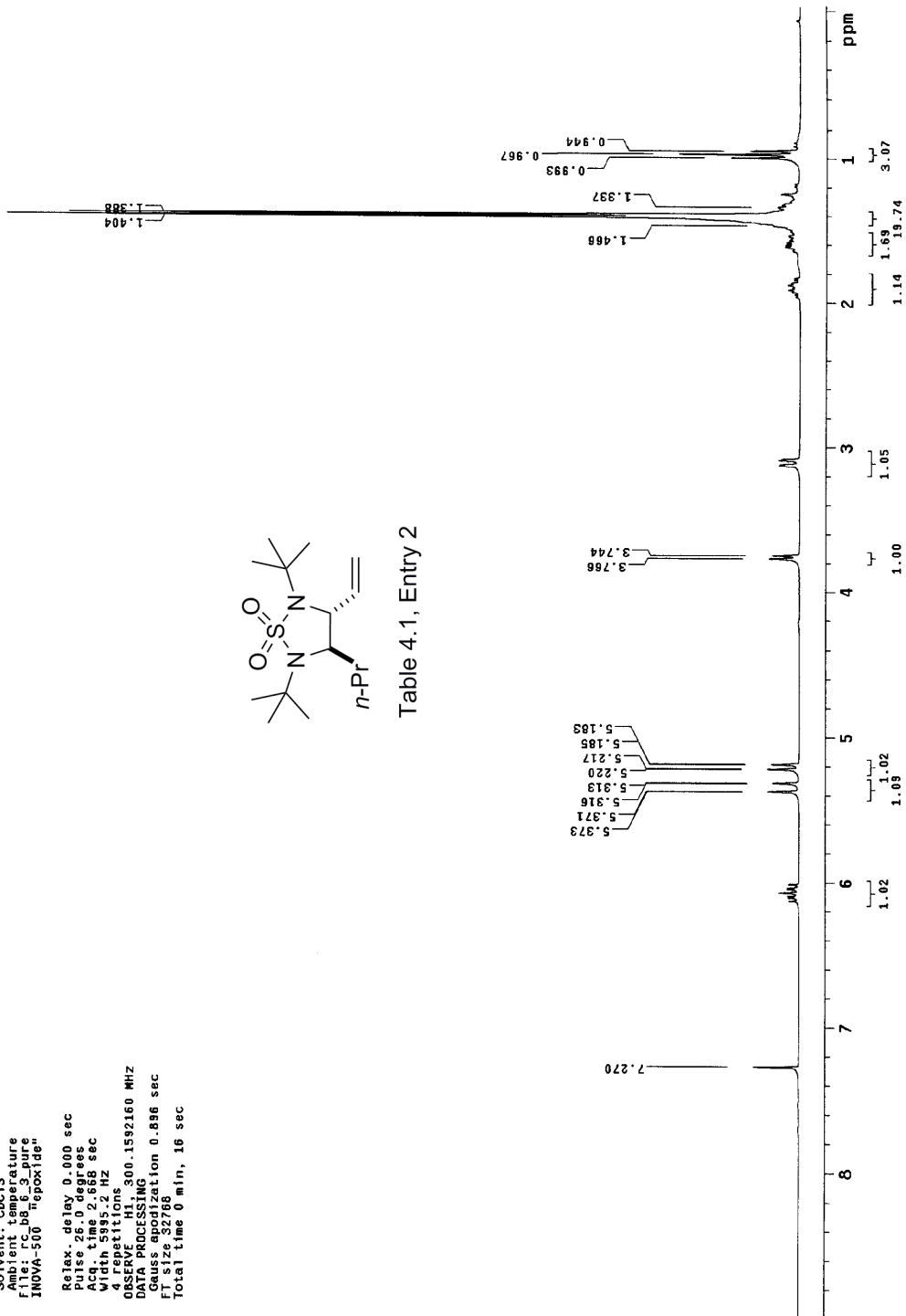


Table 4.1, Entry 2



13C OBSERVE

Pulse Sequence: s2pul
Solvent: CDCl3
Ambient Temperature
F1 size: 32766
INOVA-500 "epoxide"
Relax. delay 1.000 sec
Pulse 46.3 degrees
Acq. time 0.697 sec
Width 22935.8 Hz
48 repetitions
OBSERVE C13, 75.4750818 MHz
PULSE P1, 300.1686799 MHz
power 40 dB,
continuously on
WALTZ-16 modulated
DATA PROCESSING
Line broadening 2.0 Hz
F1 size: 32766
Total time 4 hr, 44 min, 20 sec

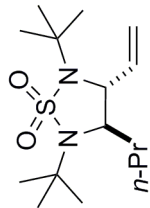
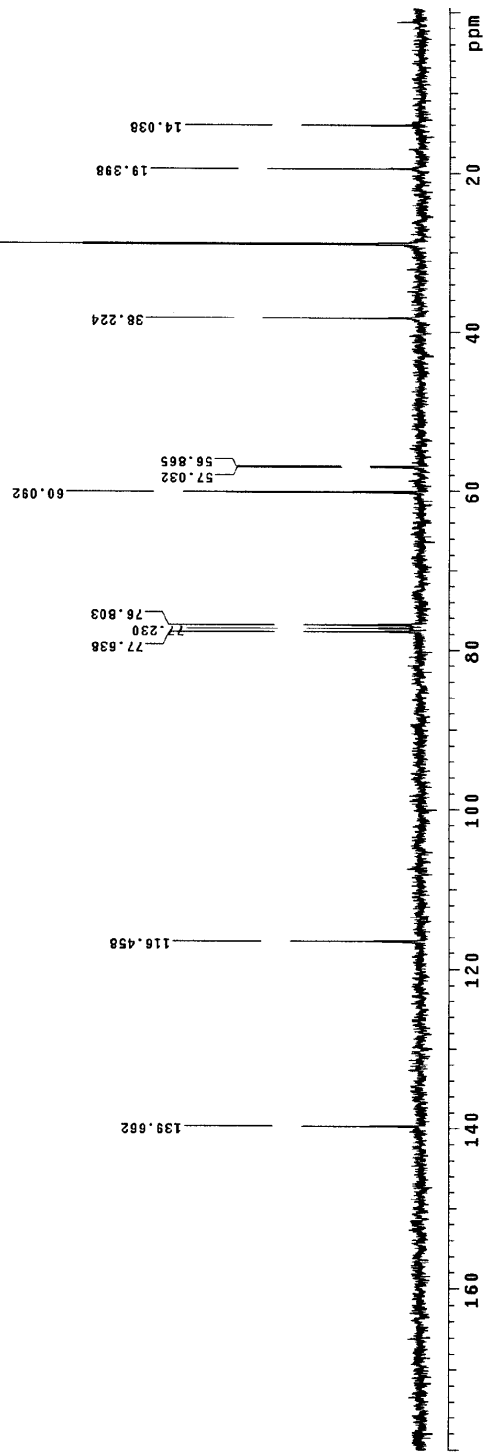
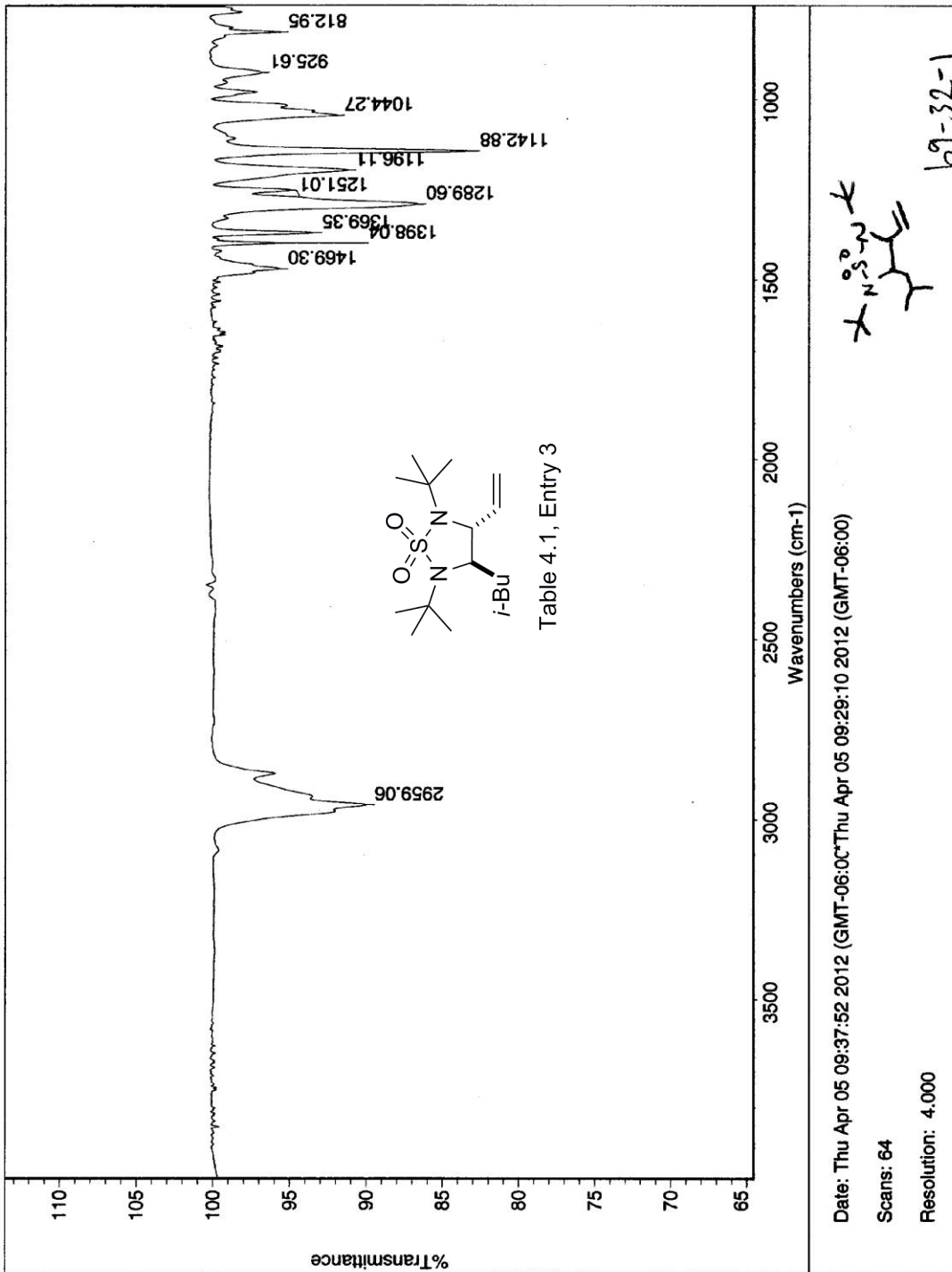


Table 4.1, Entry 2





STANDARD 1H OBSERVE

Pulse Sequence: s2pul
Solvent: CDCl3
Ambient temperature
F1: 101.254 MHz
INOVA-500 "repsol100"
Relax. delay 1.000 sec
Pulse 45.0 degrees
Acq. time 1.998 sec
Width 4500.5 Hz
4 repetitions 300.1592164 MHz
OBSERVE H1
P1: 12.000000000000000
P2: 12.000000000000000
P3: 12.000000000000000
P4: 12.000000000000000
P5: 12.000000000000000
P6: 12.000000000000000
P7: 12.000000000000000
P8: 12.000000000000000
P9: 12.000000000000000
P10: 12.000000000000000
P11: 12.000000000000000
P12: 12.000000000000000
P13: 12.000000000000000
P14: 12.000000000000000
P15: 12.000000000000000
P16: 12.000000000000000
P17: 12.000000000000000
P18: 12.000000000000000
P19: 12.000000000000000
P20: 12.000000000000000
P21: 12.000000000000000
P22: 12.000000000000000
P23: 12.000000000000000
P24: 12.000000000000000
P25: 12.000000000000000
P26: 12.000000000000000
P27: 12.000000000000000
P28: 12.000000000000000
P29: 12.000000000000000
P30: 12.000000000000000
P31: 12.000000000000000
P32: 12.000000000000000
P33: 12.000000000000000
P34: 12.000000000000000
P35: 12.000000000000000
P36: 12.000000000000000
P37: 12.000000000000000
P38: 12.000000000000000
P39: 12.000000000000000
P40: 12.000000000000000
P41: 12.000000000000000
P42: 12.000000000000000
P43: 12.000000000000000
P44: 12.000000000000000
P45: 12.000000000000000
P46: 12.000000000000000
P47: 12.000000000000000
P48: 12.000000000000000
P49: 12.000000000000000
P50: 12.000000000000000
P51: 12.000000000000000
P52: 12.000000000000000
P53: 12.000000000000000
P54: 12.000000000000000
P55: 12.000000000000000
P56: 12.000000000000000
P57: 12.000000000000000
P58: 12.000000000000000
P59: 12.000000000000000
P60: 12.000000000000000
P61: 12.000000000000000
P62: 12.000000000000000
P63: 12.000000000000000
P64: 12.000000000000000
P65: 12.000000000000000
P66: 12.000000000000000
P67: 12.000000000000000
P68: 12.000000000000000
P69: 12.000000000000000
P70: 12.000000000000000
P71: 12.000000000000000
P72: 12.000000000000000
P73: 12.000000000000000
P74: 12.000000000000000
P75: 12.000000000000000
P76: 12.000000000000000
P77: 12.000000000000000
P78: 12.000000000000000
P79: 12.000000000000000
P80: 12.000000000000000
P81: 12.000000000000000
P82: 12.000000000000000
P83: 12.000000000000000
P84: 12.000000000000000
P85: 12.000000000000000
P86: 12.000000000000000
P87: 12.000000000000000
P88: 12.000000000000000
P89: 12.000000000000000
P90: 12.000000000000000
P91: 12.000000000000000
P92: 12.000000000000000
P93: 12.000000000000000
P94: 12.000000000000000
P95: 12.000000000000000
P96: 12.000000000000000
P97: 12.000000000000000
P98: 12.000000000000000
P99: 12.000000000000000
P100: 12.000000000000000
Total time 0 min, 12 sec

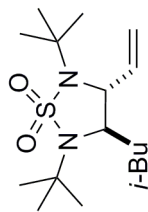
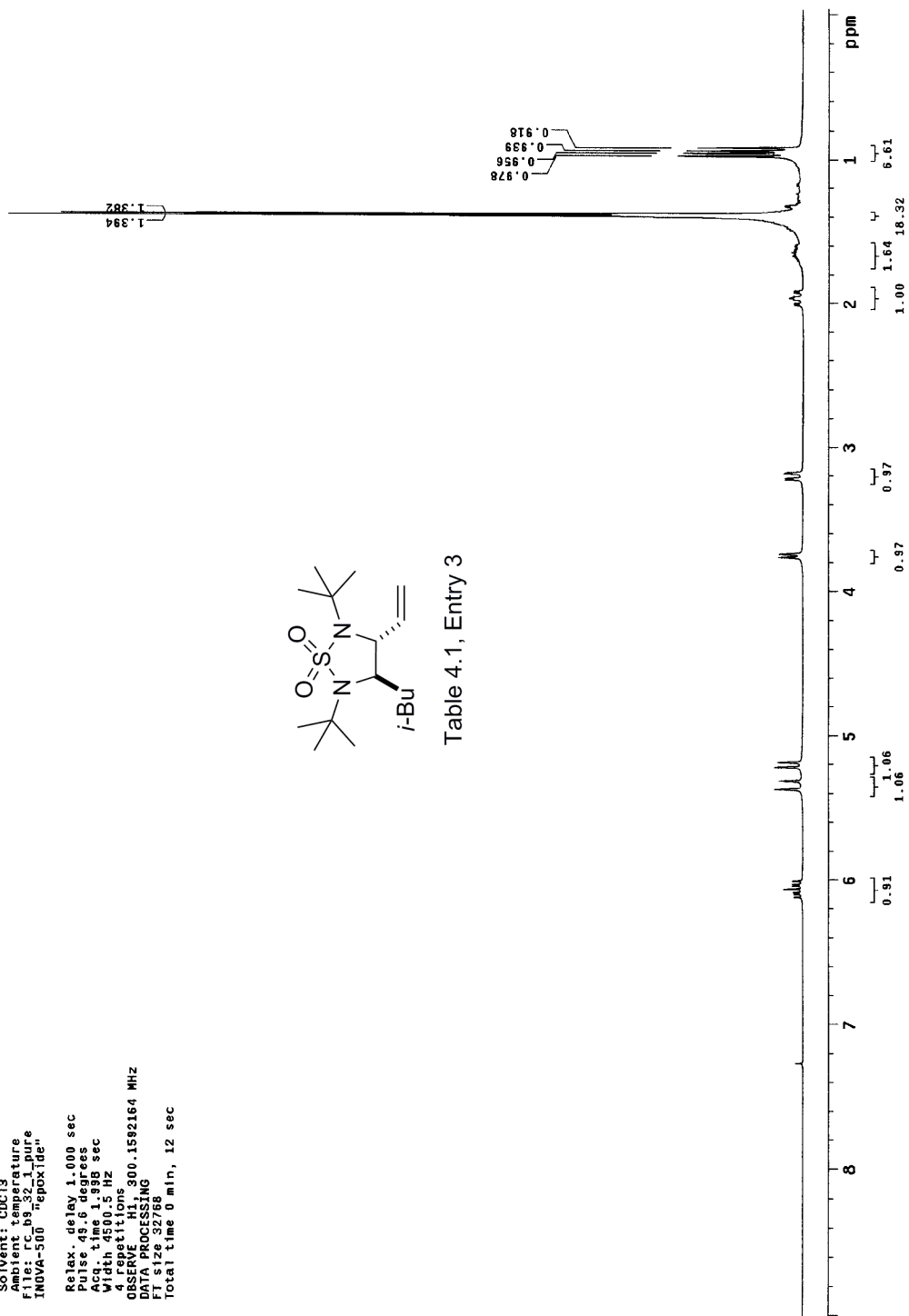


Table 4.1, Entry 3



13C OBSERVE

Pulse Sequence: s2pul
Solvent: CDCl3
Ambient temperature
F1: 101.625 MHz
INVA-500 80X160
Pulse 55.7 degrees
Acq time 1.815 sec
Width 18761.7 Hz
48 repetitions
OBSERVE C13, 75.4750814 MHz
DECOUPLE H1, 300.1606800 MHz
Power 40 dB
Modulation ON
WALTZ-16 modulated
DATA PROCESSING
Line broadening 1.0 Hz
FT size 131072
Total time 3 min, 2 sec

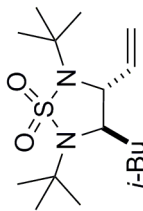
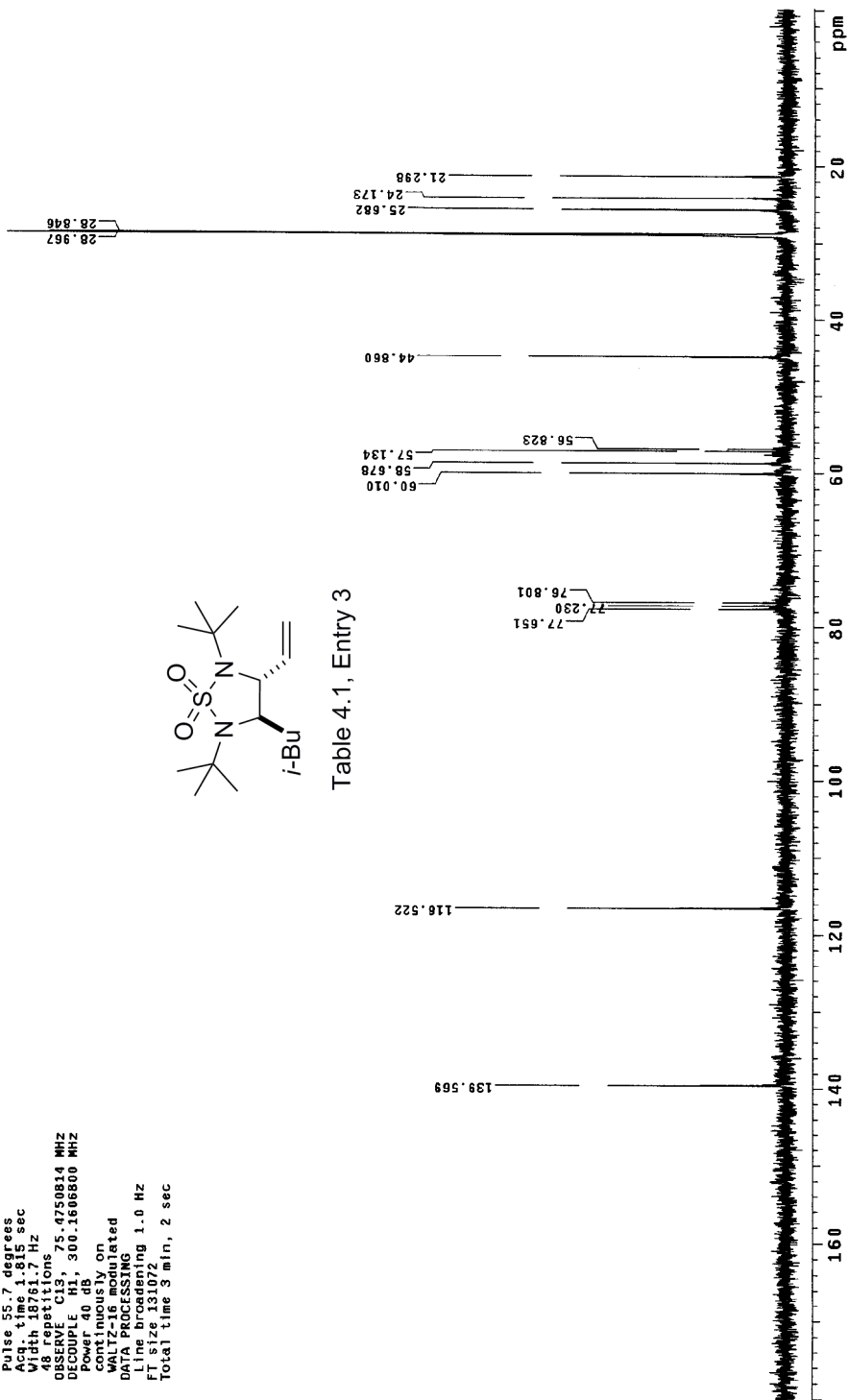
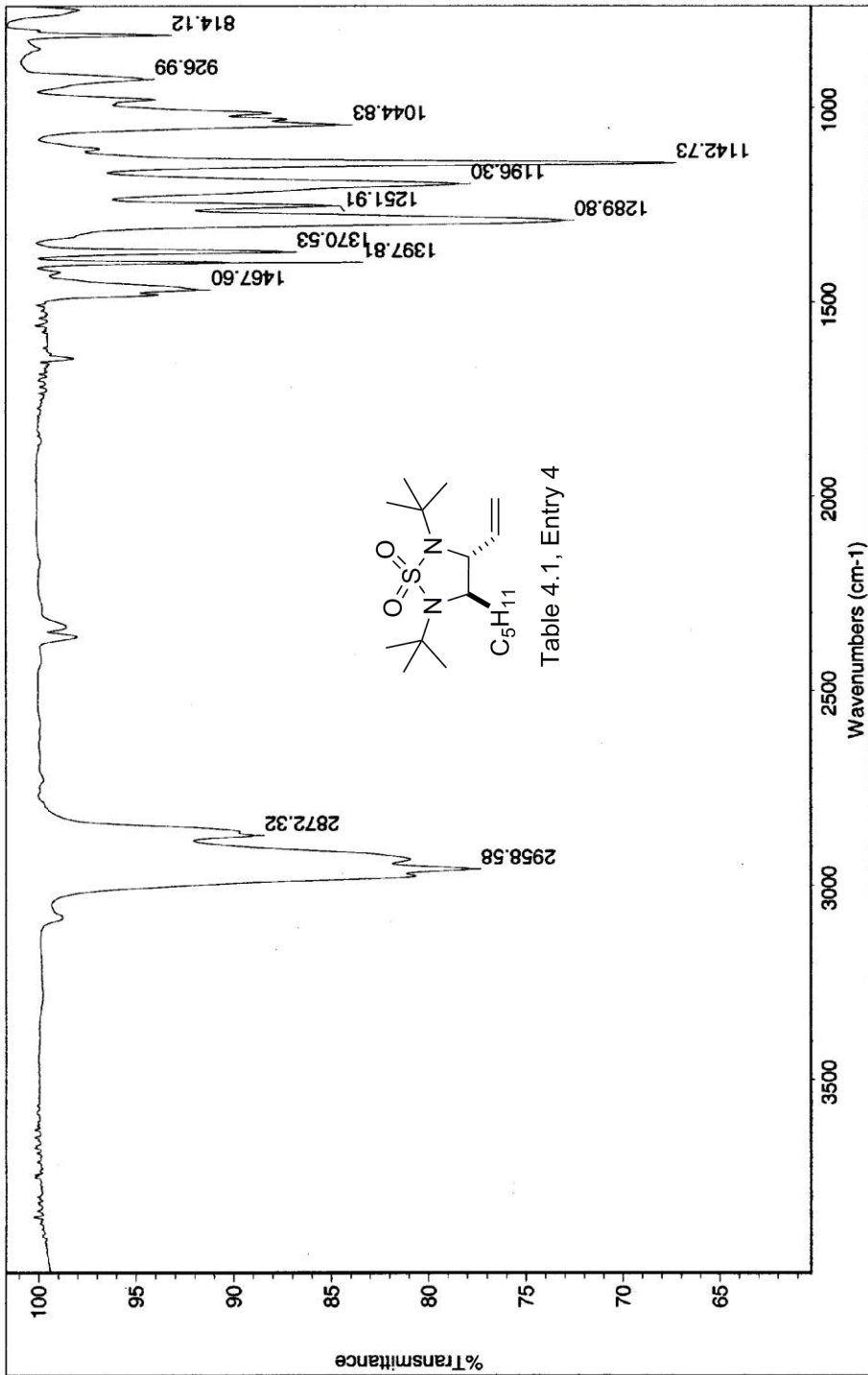


Table 4.1, Entry 3

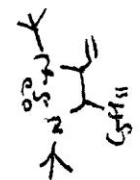




Date: Thu Mar 01 11:31:53 2012 (GMT-07:00) Thu Mar 01 11:27:04 2012 (GMT-07:00)

Scans: 64

Resolution: 4.000



68-G-10

STANDARD 1H OBSERVE

Pulse Sequence: s2pu1
Solvent: CDCl3
Ambient Temperature
F1: 500.136098 MHz
INOVA-500 "gprx1de"

Relax. delay 1.000 sec
Pulse 49.5 degrees
Acq. time 1.998 sec
Width 4500.5 Hz
4 repetitions

OBSERVE H1, 300.1592161 MHz
DATA PROCESSING
F1: 27.000000 MHz
Total time 0 min, 12 sec

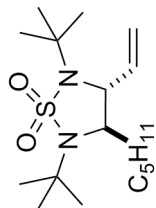
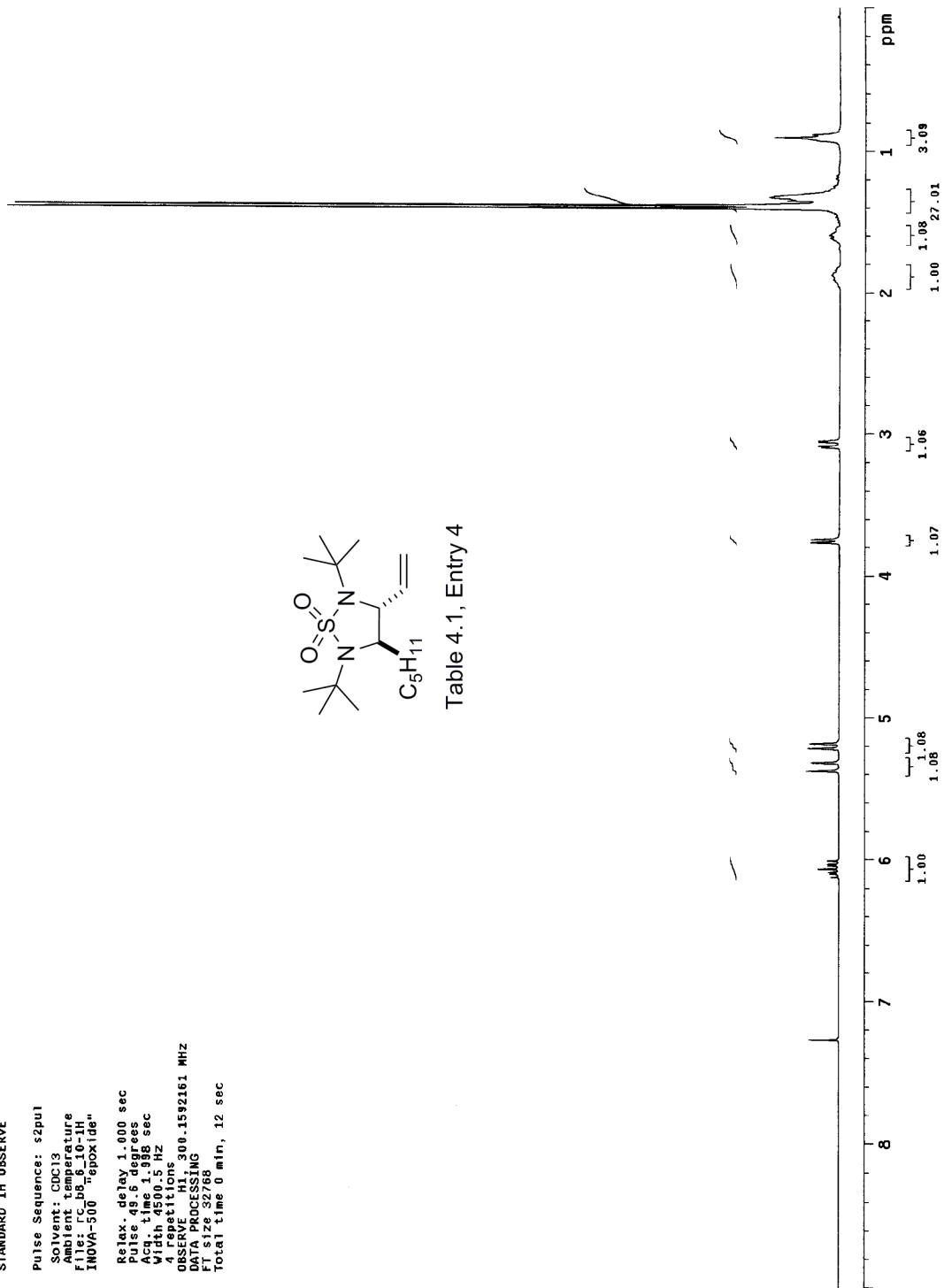


Table 4.1, Entry 4



13C OBSERVE

Pulse Sequence: s2pu1

Solvent: CDCl3

Ambient Temperature

INNOVA-500

epoxide"

Pulse: 55.7 degrees

Acq. time: 1.815 sec

Width: 18761.7 Hz

48 repetitions

OBSERVE: C13, 75.4750800 MHz

DECOUPLE: H1, 300.1606800 MHz

Power: 100% on

WALTZ-16 modulated

DATA PROCESSING

Line broadening: 1.0 Hz

FT size: 131072

Total time: 3 min, 2 sec

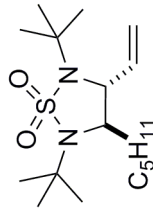
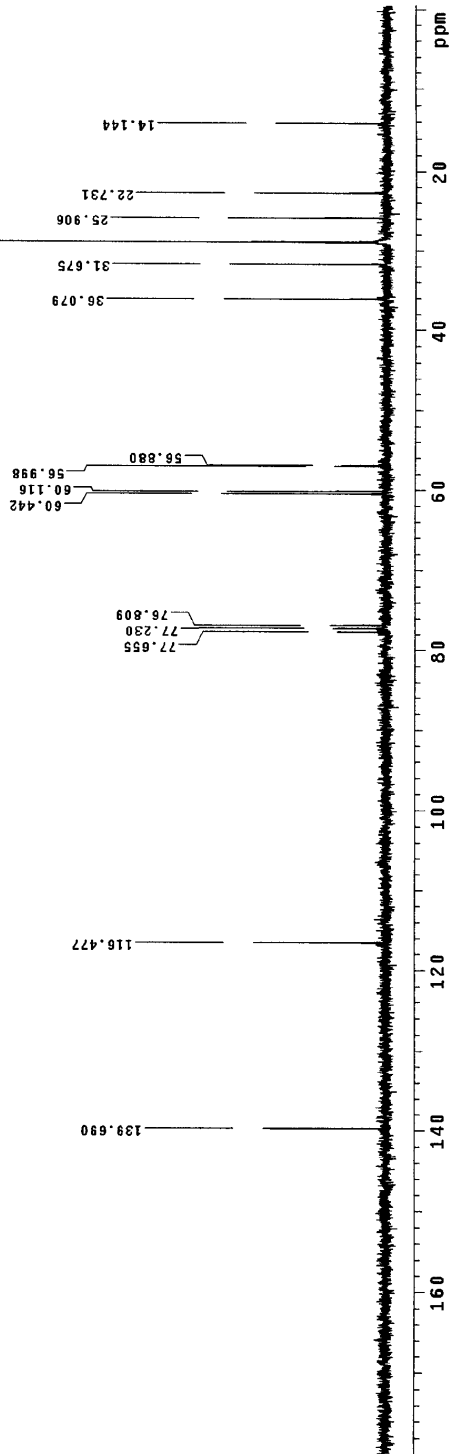
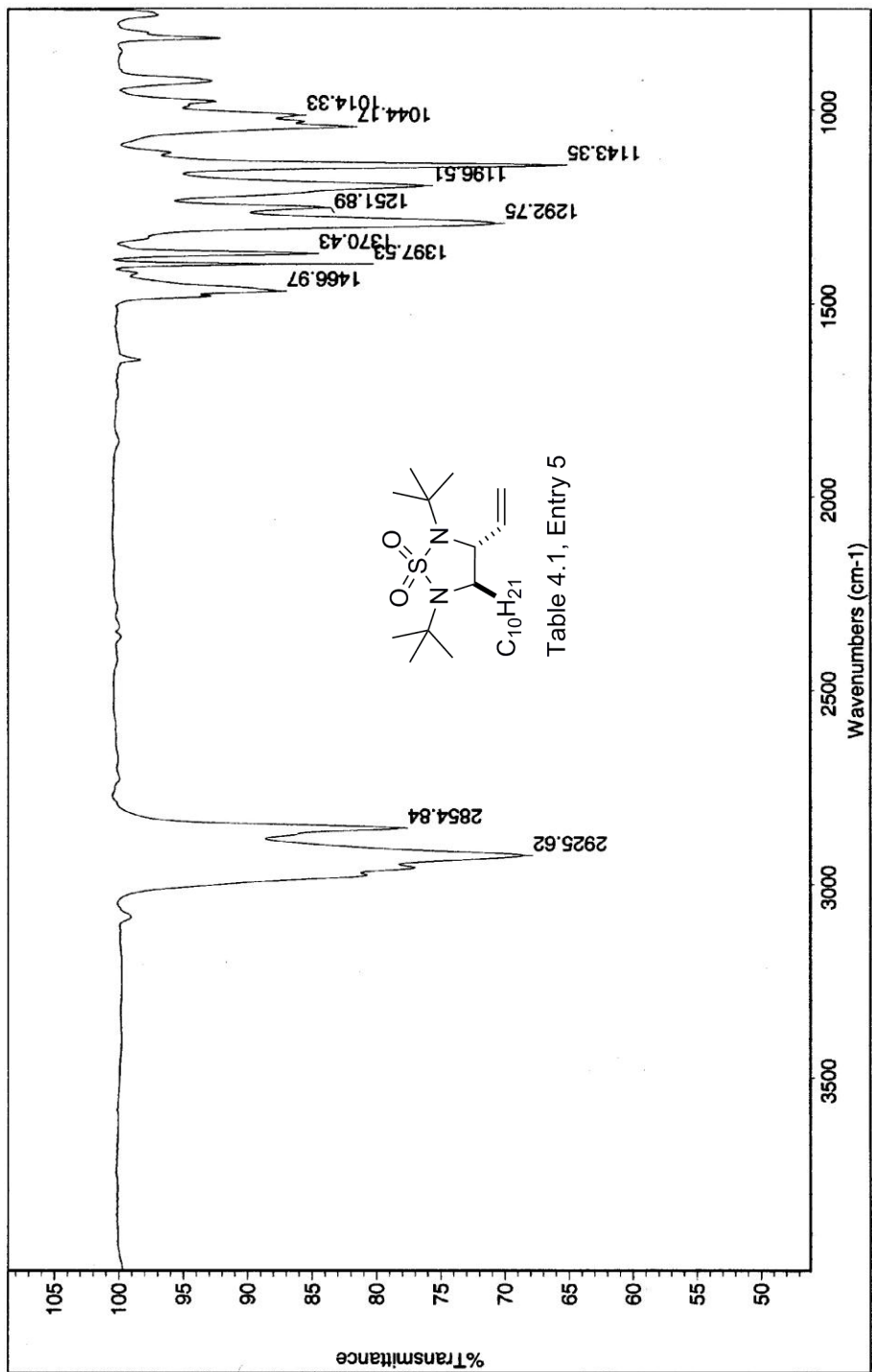


Table 4.1, Entry 4

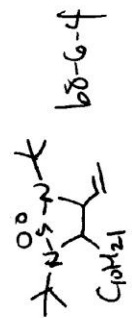




Date: Sat Mar 24 10:22:35 2012 (GMT-07:00)*Sat Mar 24 10:20:46 2012 (GMT-07:00)

Scans: 64

Resolution: 4.000



STANDARD 1H OBSERVE

Pulse Sequence: s2pul

Solvent: CDCl3

File: FC_b8_6_4_pure

INOVA-500 "epox11de"

Relax. delay 0.000 sec

Pulse 26.0 degrees

Acq. time 2.668 sec

Width 5335.2 Hz

Observe 110mhz

OBSERVE_H1 300.1582164 MHZ

DATA PROCESSING

Gauss apodization 0.886 sec

FT size 32768

Total time 0 min, 16 sec

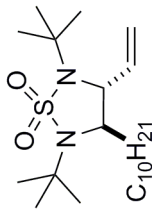
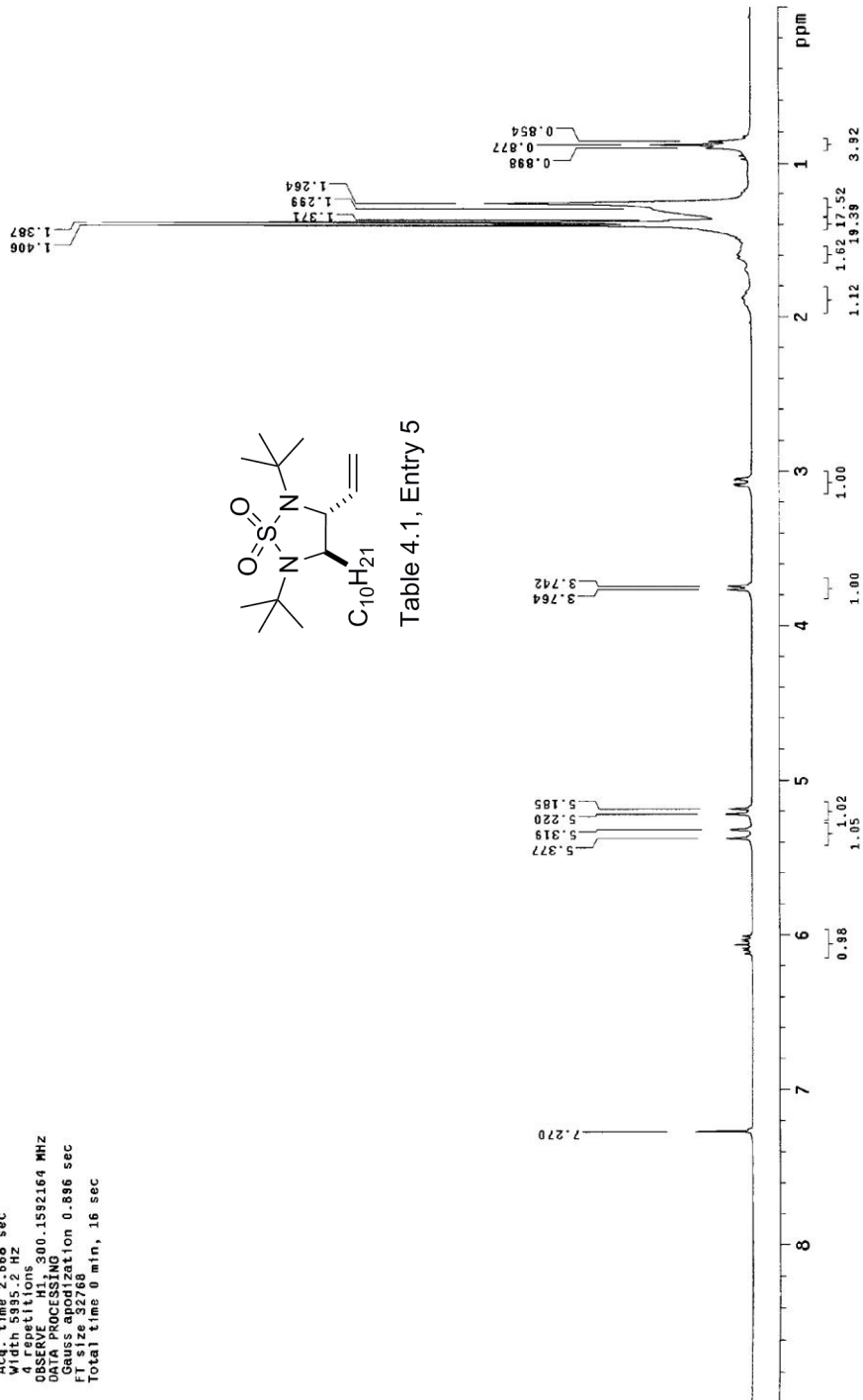


Table 4.1, Entry 5



Archive directory: /home/DATA/wakup/cornwall
Sample directory: rc_b8_6_4_13C_20120112_01

Pulse sequence: s2pul

Solvent: cdcl3
Ambient temperature
Sample #40, Operator: cornwall
IN: FC08_6_4_13C
INVA-500 "epoxide"

Relax. delay 1.000 sec
Pulse 45.0 degrees
Acq. time 1.285 sec
Width 25510.2 Hz
512 repetitions
OBSERVE C13, 100.5058883 MHz
PULPROG zgpg30
PCouple 38 dB
continuous on
WALTZ-16 modulated
DATA PROCESSING
Line broadening 0.5 Hz
FT size 65536
Total time 19 min, 34 sec

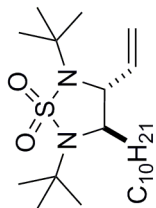
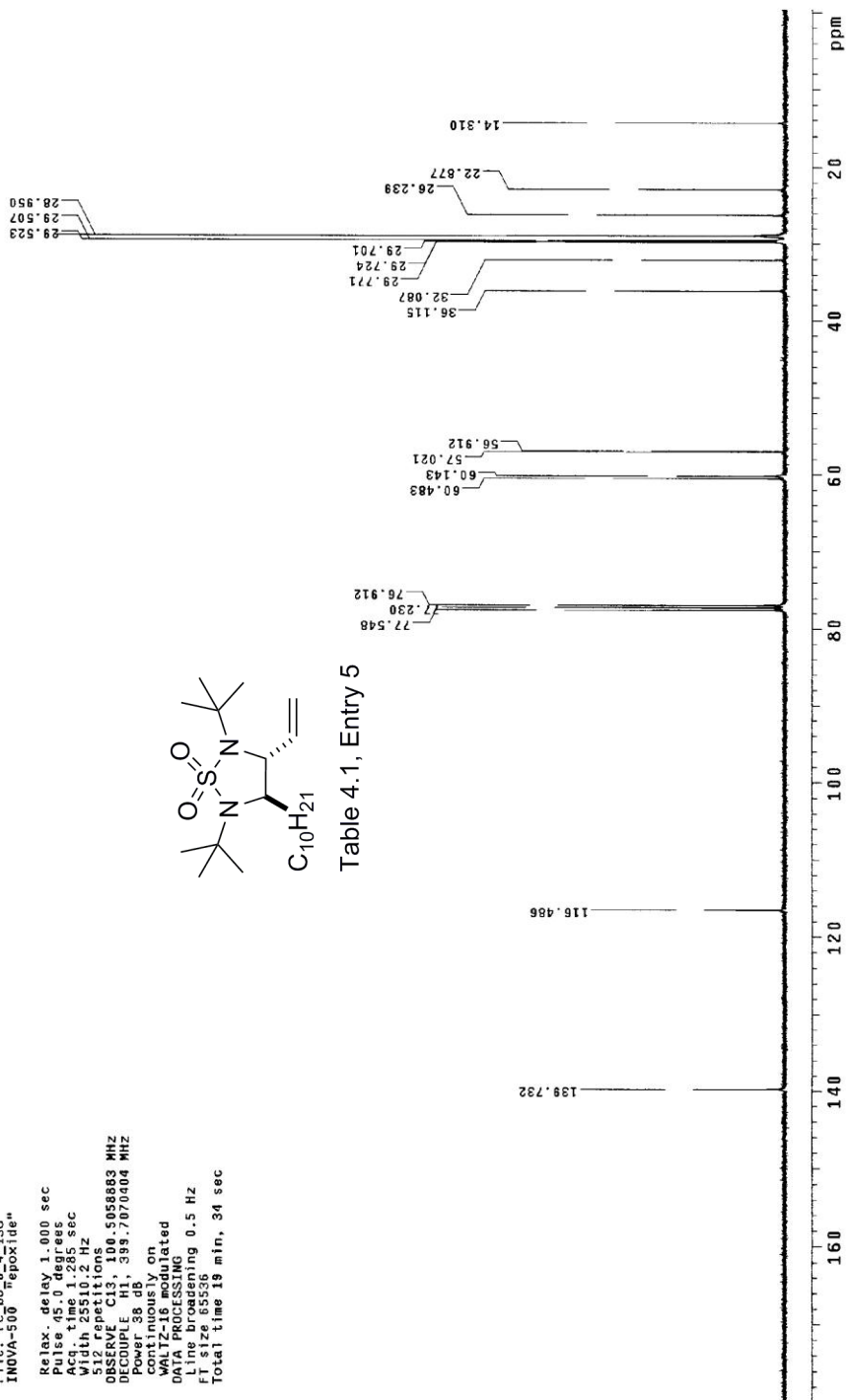
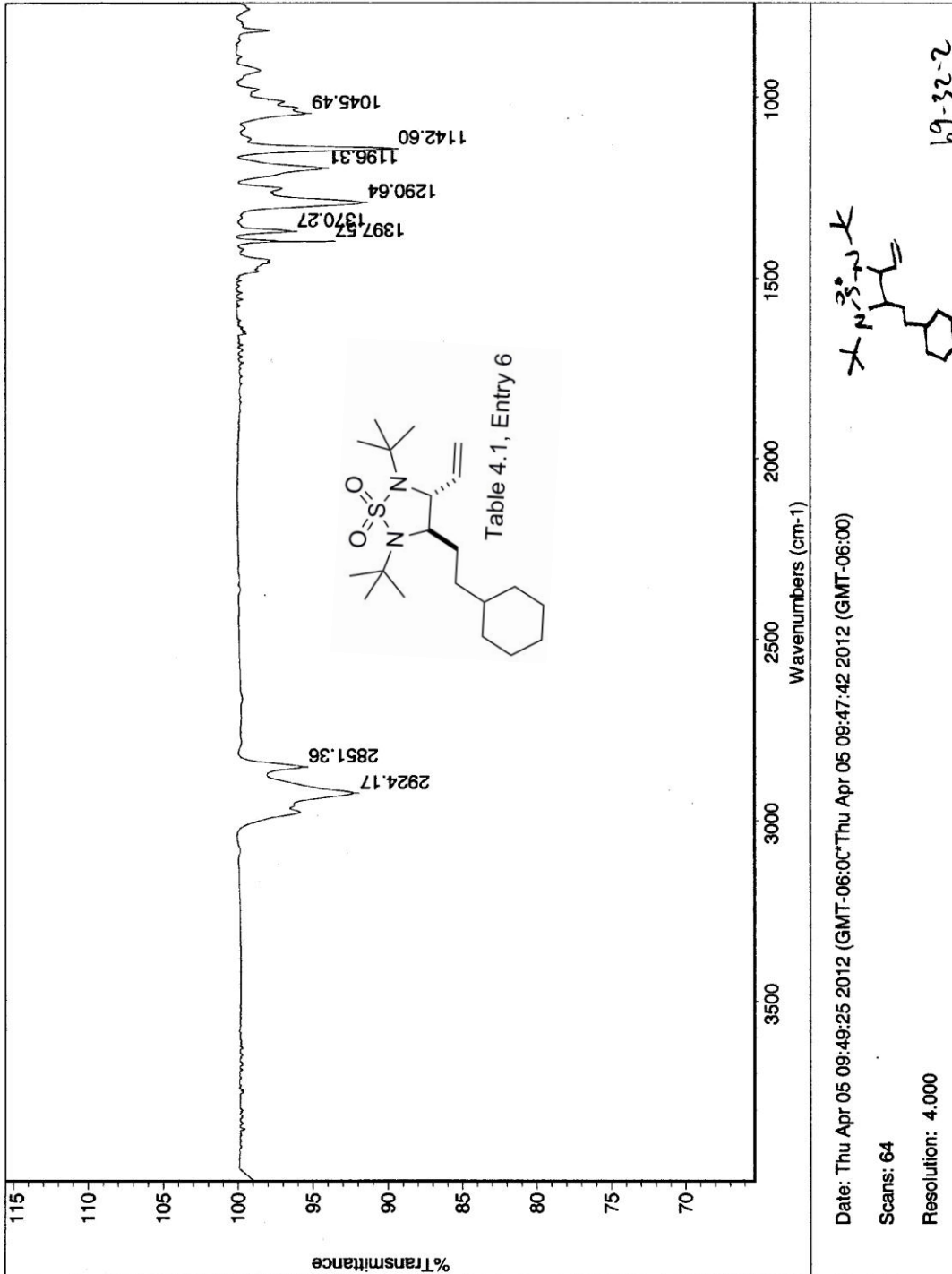


Table 4.1, Entry 5





13C OBSERVE

Pulse Sequence: s2pul

Solvent: CDCl3

Ambient temperature

File: 53371313

INOVA-500 "proxi"de"

Pulse 55.7 degrees

Acq. time 1.835 sec

Width 18761.7 Hz

100 repetitions

OBSERVE C13, 75.4750814 MHz

DECOUPLE H1, 300.1606800 MHz

continuously on

WALTZ-16 modulated

DATA PROCESSING

Line broadening 1.0 Hz

FT size 131072

Total time 3 min, 2 sec

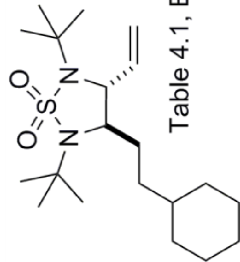
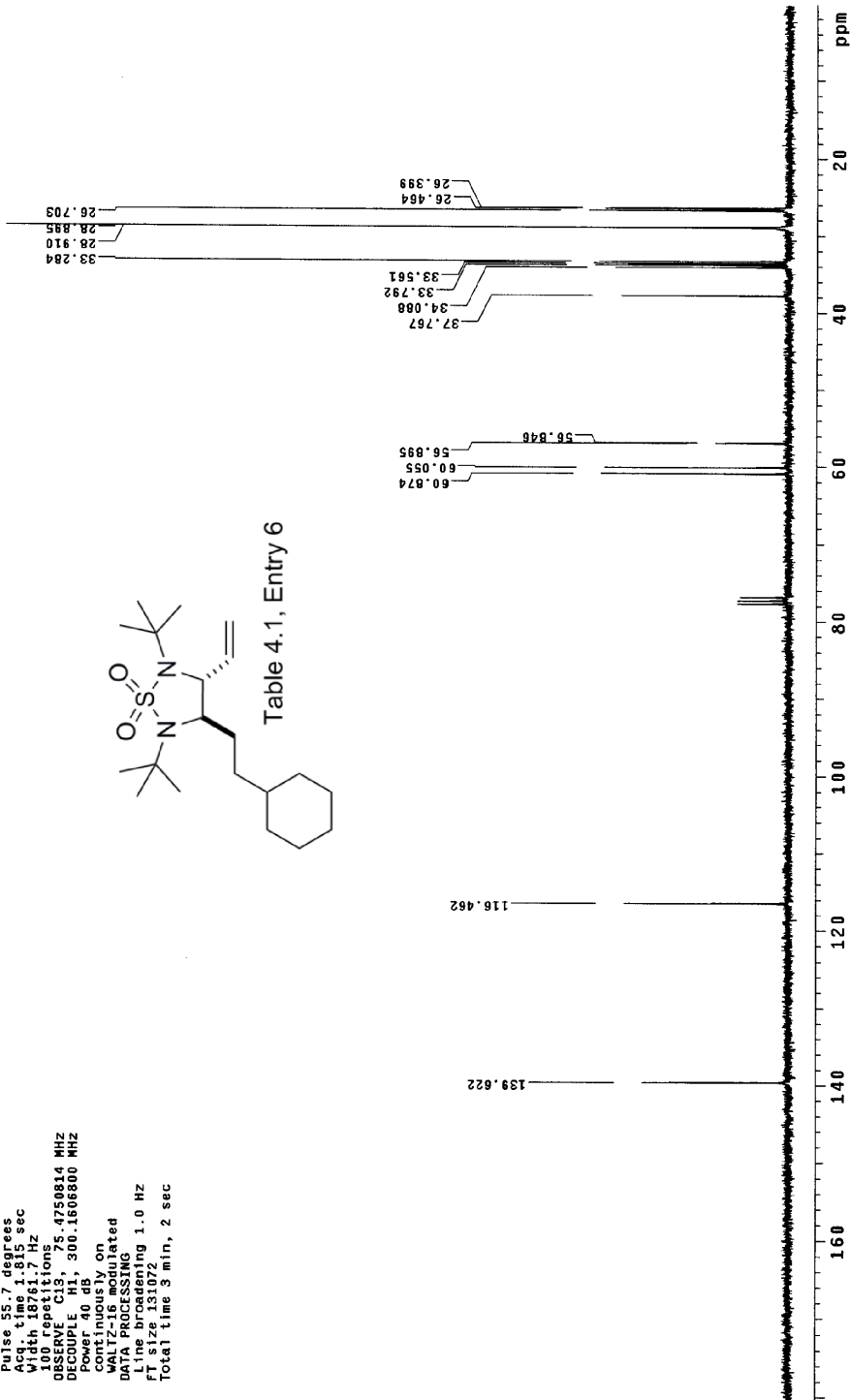
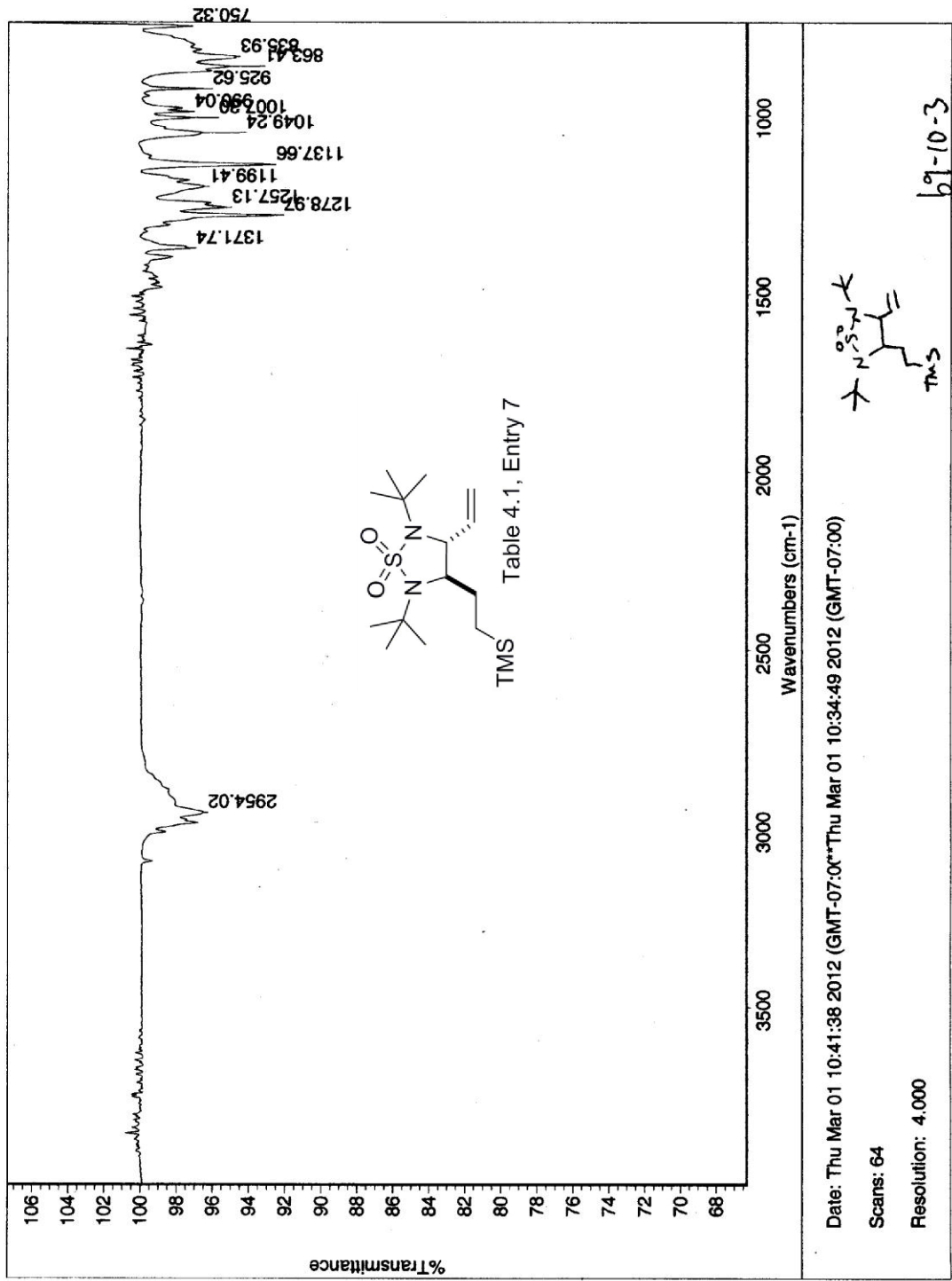


Table 4.1, Entry 6





STANDARD 1H OBSERVE

Pulse Sequence: s2pul
 Solvent: CDCl3
 Ambient temperature
 File name: 1592184
 INOVA-500 "gpcr18e"
 Relax. delay 1.000 sec
 Pulse 49.6 degrees
 Acq. time 1.998 sec
 Width 4500.5 Hz
 4 repetitions
 OBSERVE H1, 300.1592184 MHz
 PROCNO 1
 F1 51232788
 Total time 0 min, 12 sec

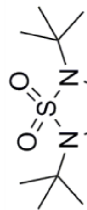
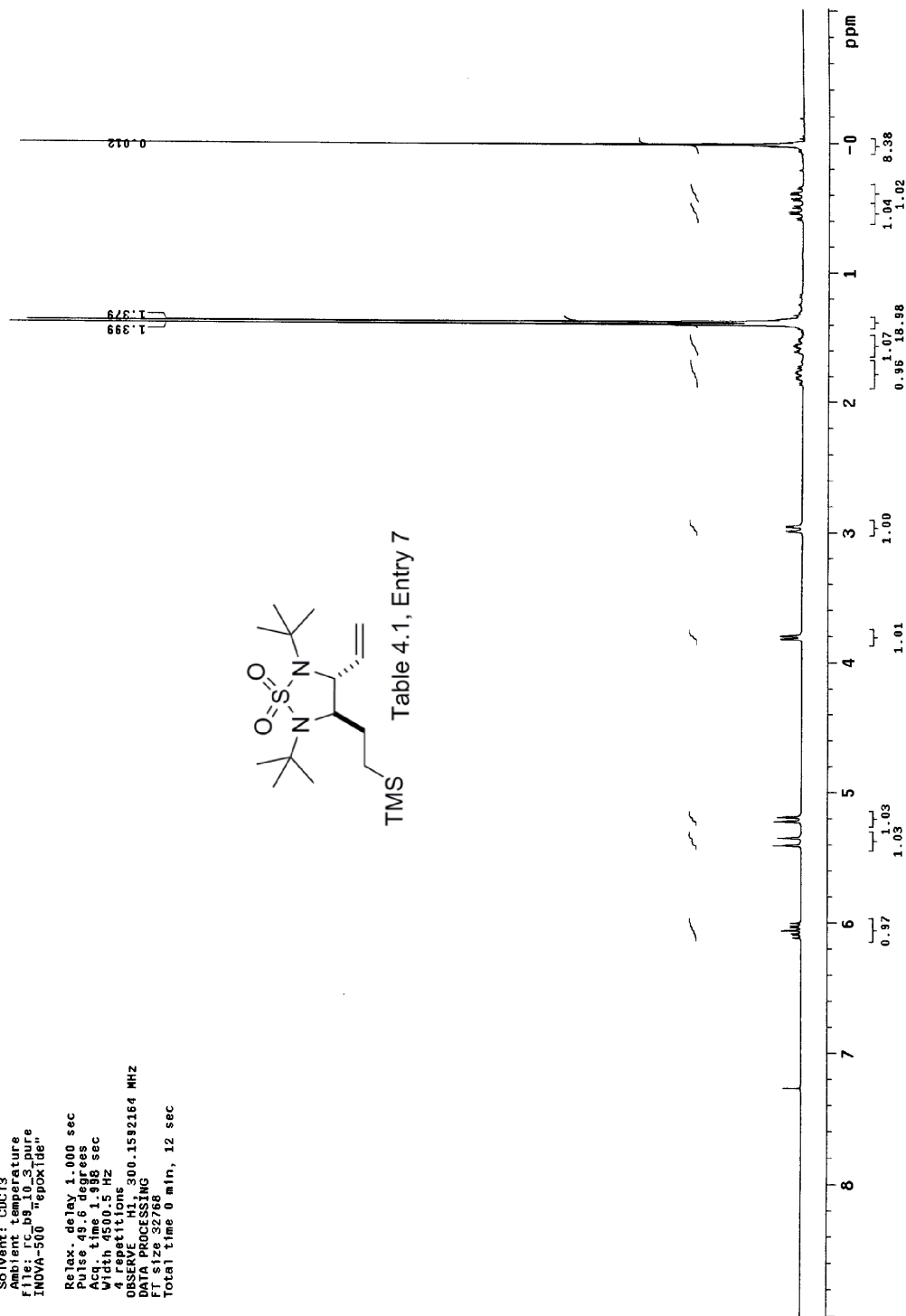


Table 4.1, Entry 7

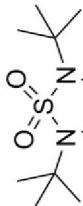


Archive directory: /home/DATA/walkup/cornwall
Sample directory: rc_b8_12_carbon_20120414_01

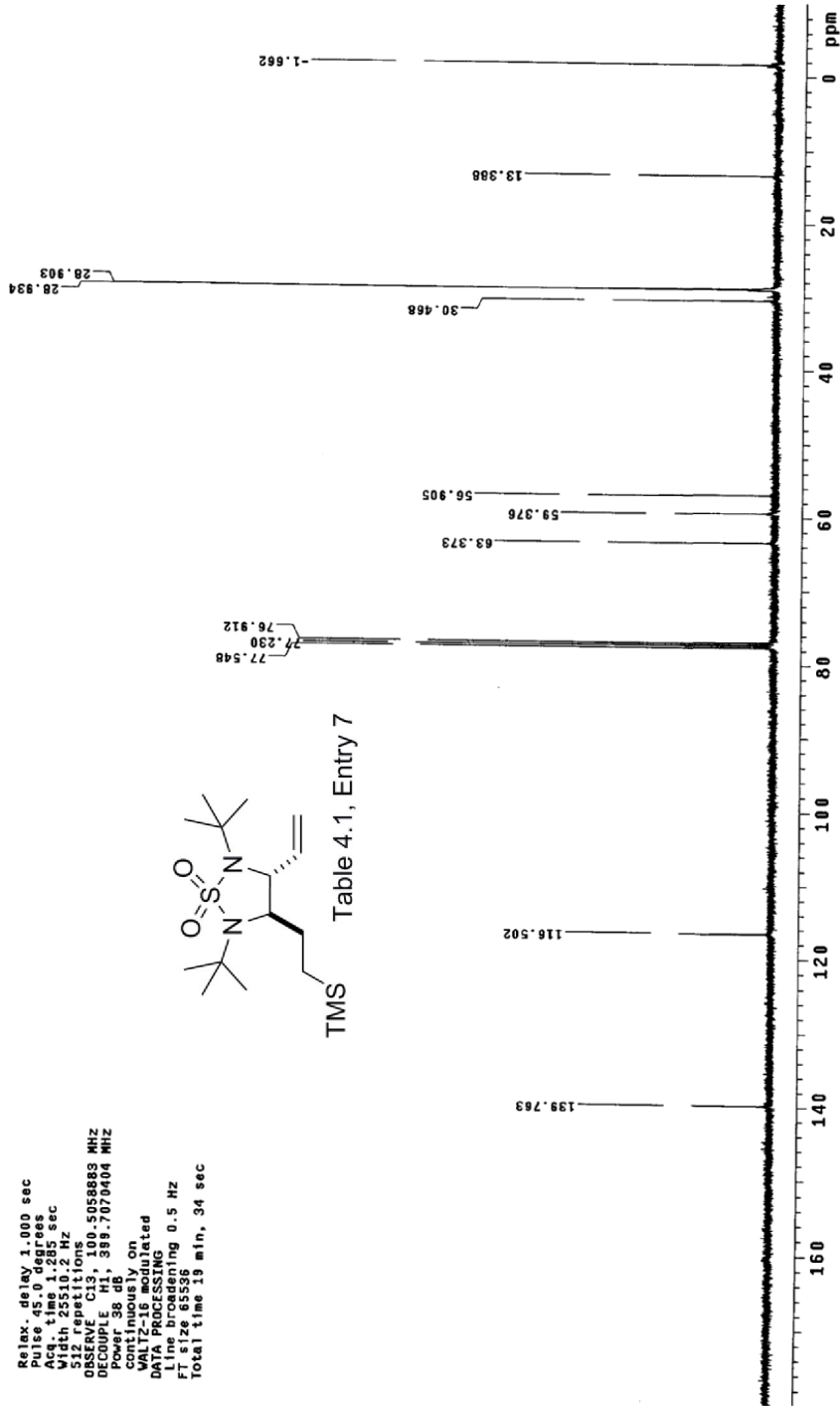
Pulse Sequence: s2pul

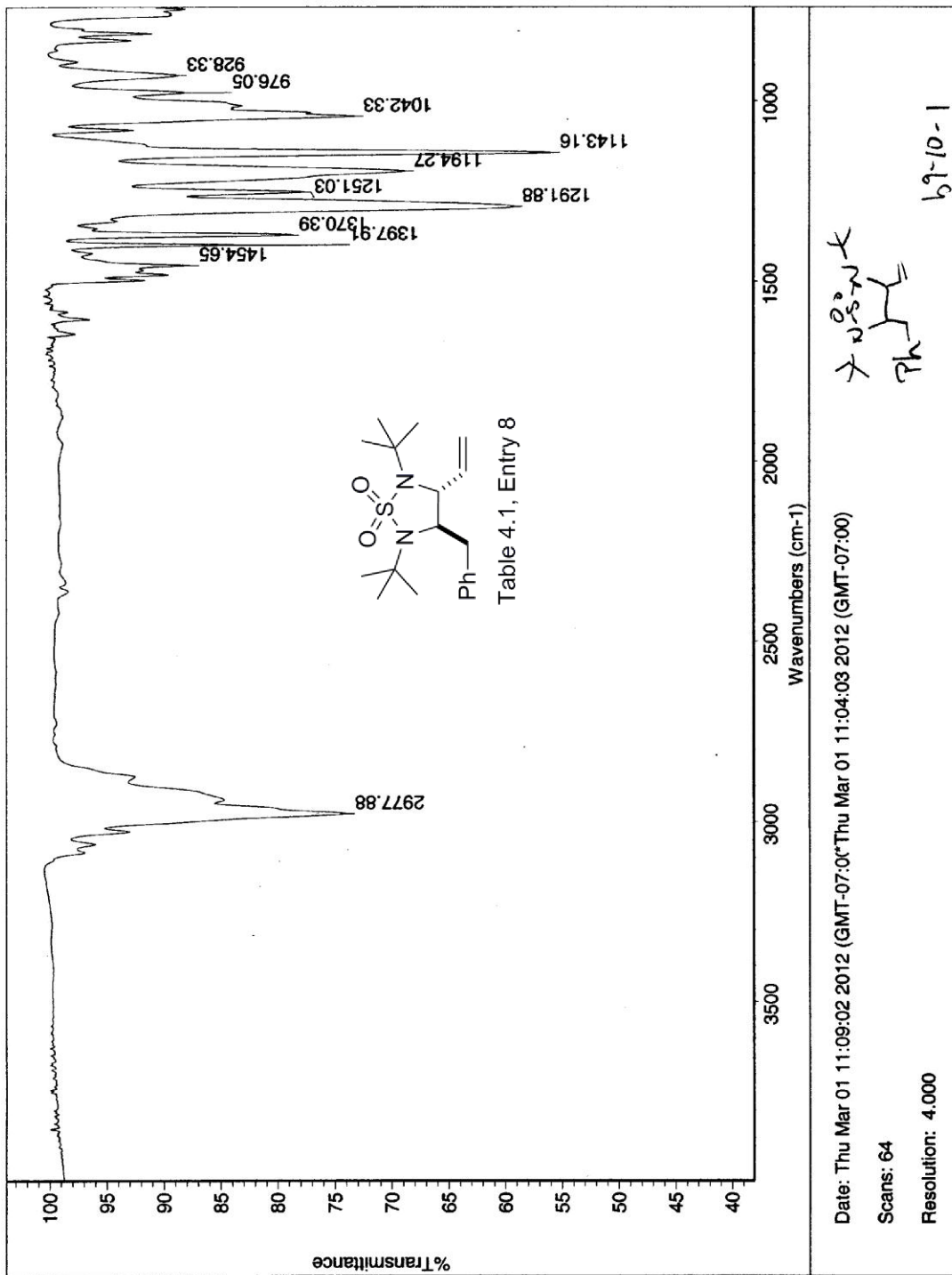
Solvent: cdcl3
Sample temperature: 40
File: rc_b8_10_313c_reun
INOVA-500 "epoxide"

Relax. delay 1.000 sec
Pulse 45.0 degrees
Acq. time 1.285 sec
Sbth 25510.2 Hz
S15
OBSERVE F1 100.5058883 MHz
DECOUPLE H1 399.7070404 MHz
Power 38 dB
Continuously on
WALTZ16 accumulated
DANTE
Line broadening 0.5 Hz
FT size 65536
Total time 19 min, 34 sec



TMS Table 4.1, Entry 7





b9_10_1
 Archive directory: /home/DATA/walkup/cornwall
 Sample directory: b9_10_1_20120305_01
 Pulse Sequence: s2pul
 Solvent: cdcl3
 Ambient temperature
 Sample name: cornwall
 File: b9_10_1_pure
 INOVA-500 "epoxide"
 Relax. delay 1.000 sec
 Pulse 45.0 degrees
 Acq. time 2.556 sec
 Width 6410.3 Hz
 8 repetitions
 Frequency 99.7050307 MHz
 DATA PROCESSING
 FT size 32768
 Total time 0 min, 28 sec

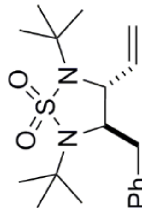
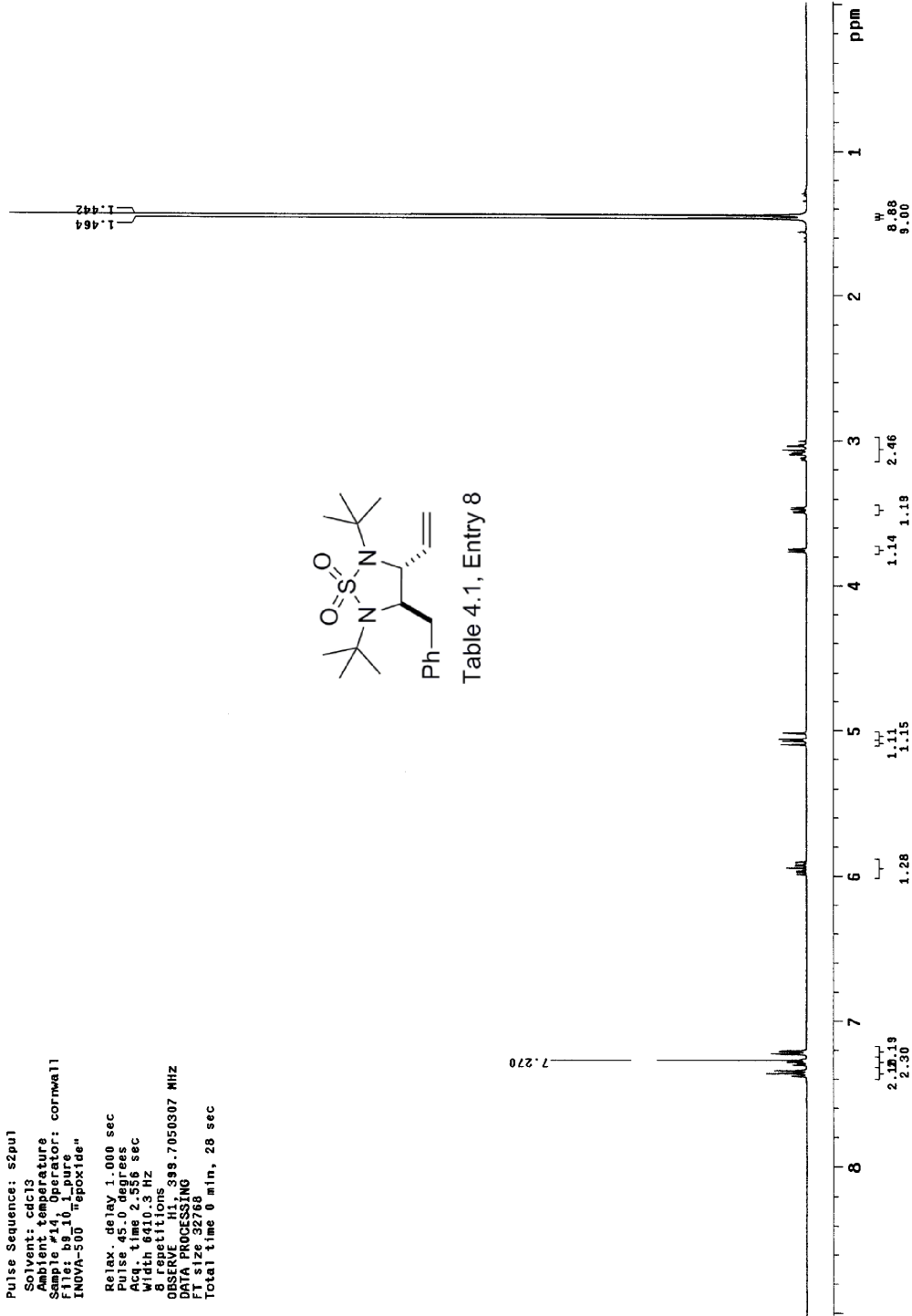


Table 4.1, Entry 8



bs_10_1
 Archive directory: /home/DATA/walkup/cornwall
 Sample directory: bs_10_1_20120305_01
 Pulse Sequence: s2pul
 Solvent: cdcl3
 Sample Name:
 Sample #14:
 Operator: cornwall
 File: bs_10_1_13C
 INOVA-500 "epoxide"
 Relax. delay 1.000 sec
 Pulse 45.0 degrees
 Acq. time 1.285 sec
 Width 25510.2 Hz
 Frequency 125.760 MHz
 OBSERVE C13, 100.5058875 MHz
 DECOUPLE H1, 399.7078404 MHz
 Power 38 dB
 continuously on
 WALTZ-16 modulated
 DATA PROCESSING
 F1 acq. processing 0.5 Hz
 FT acq. processing
 Total time 19 min, 34 sec

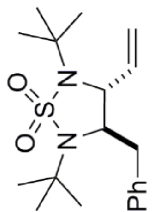
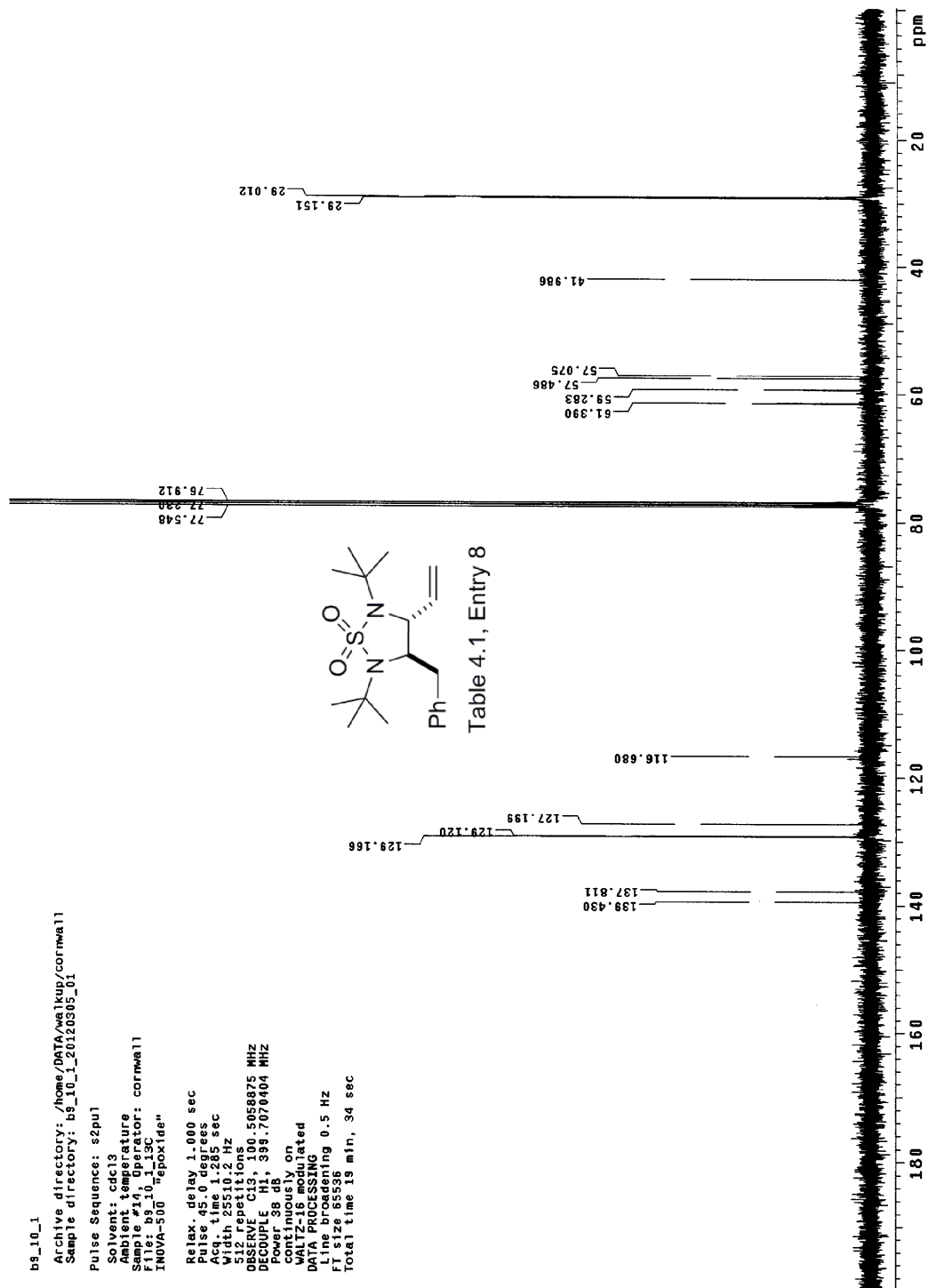
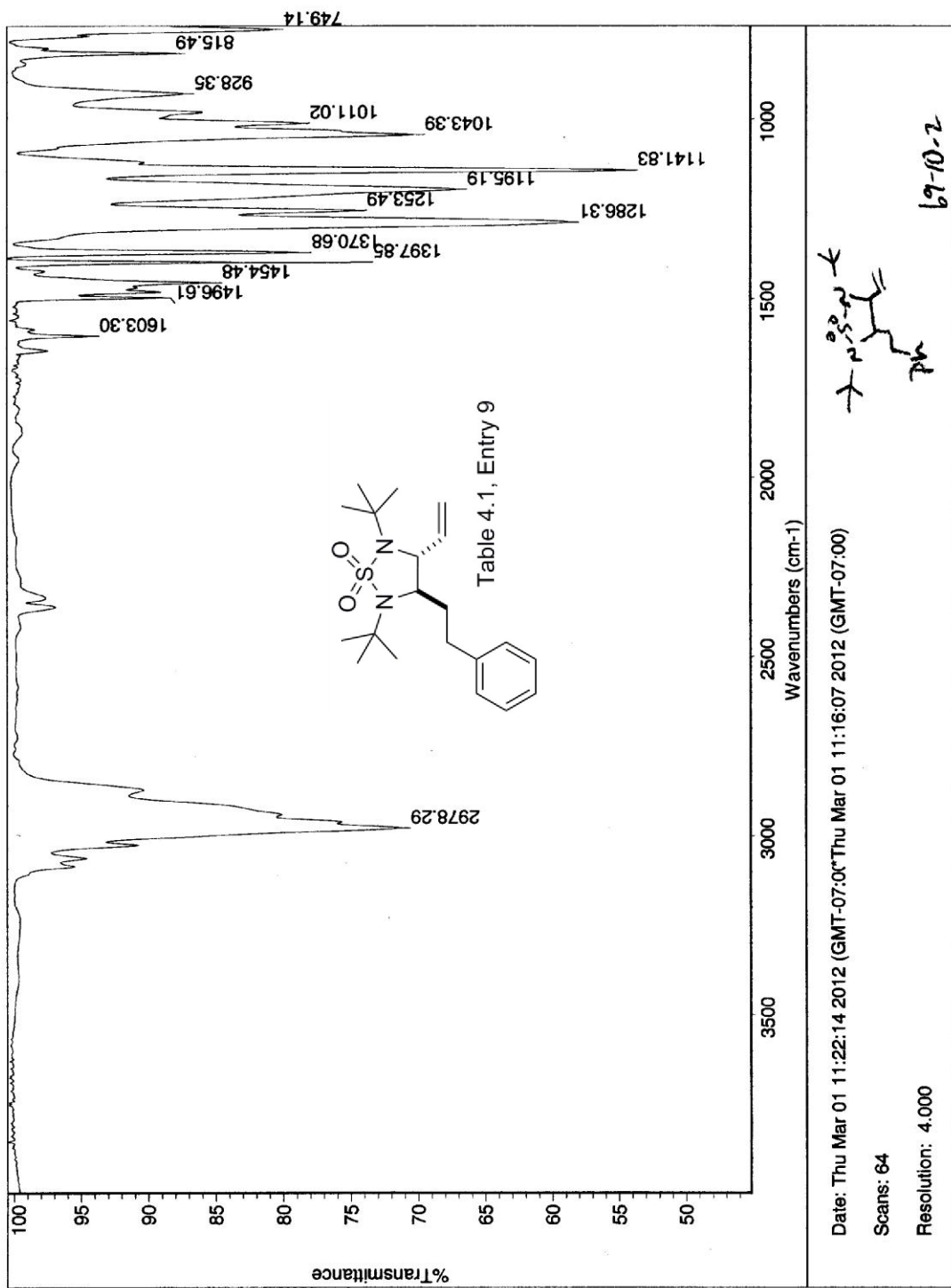


Table 4.1, Entry 8





STANDARD 1H OBSERVE

Pulse Sequence: s2pul
 Solvent: CDCl3
 Ambient Temperature: 25.00 C
 File Name: INDVA-500_180X1061
 Relax. delay: 1.000 sec
 Pulse: 45.0 degrees
 Acq. time: 1.998 sec
 Width: 4500.5 Hz
 4 repetitions
 OBSERVE F1: 300.1592196 MHz
 F1 File: 327861
 F2 File: 327861
 Total time: 0 min, 12 sec

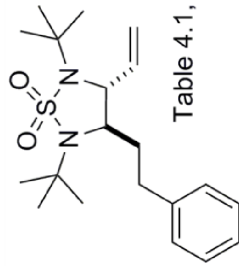
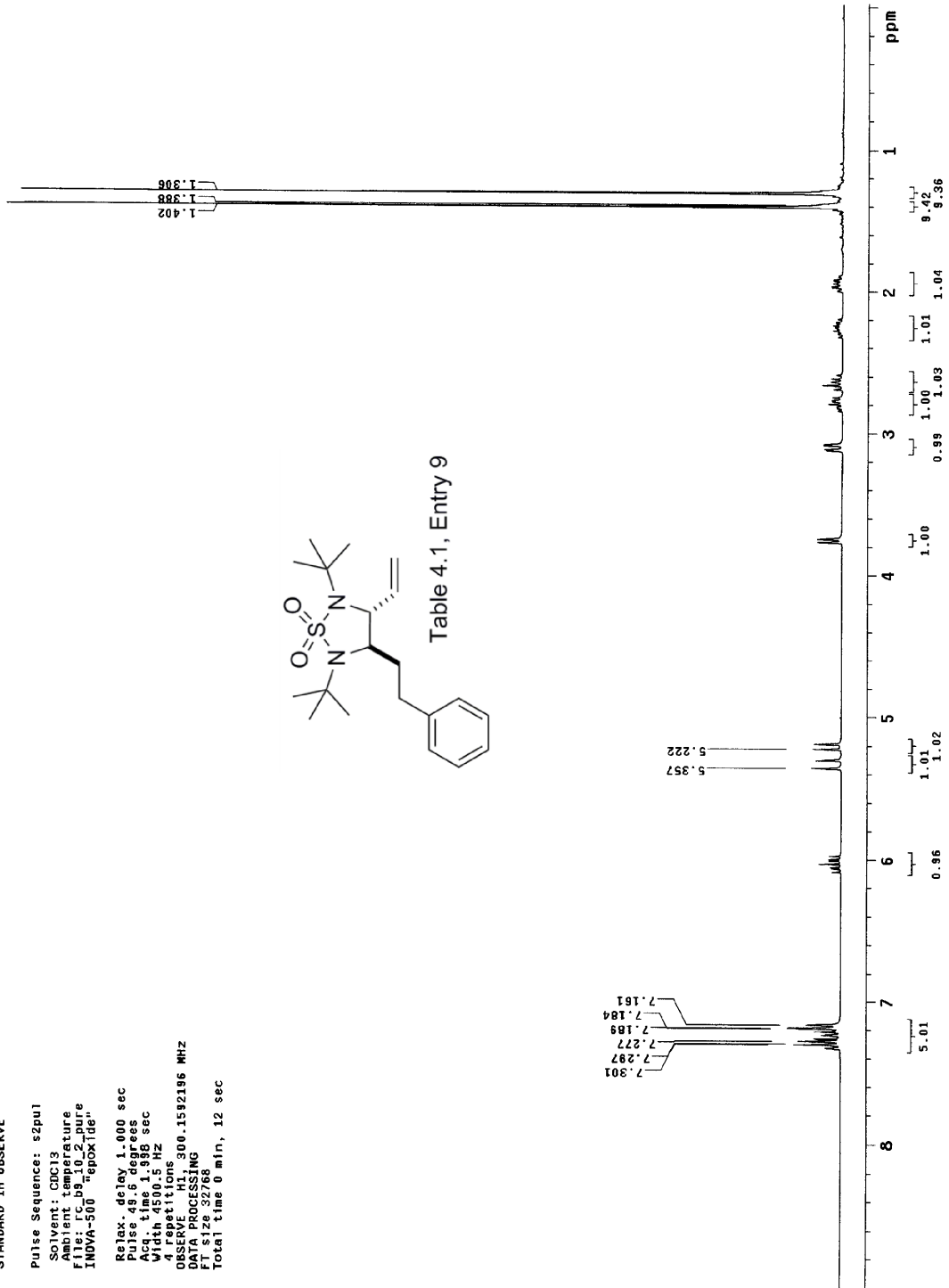


Table 4.1, Entry 9



rc_b9_10_2
Archive directory: /home/DATA/anal/kup/cornwall
Sample directory: rc_b9_10_2/20120306_01

Pulse Sequence: s2pu1
Solvent: cdcl3
Ambient temperature
Sample #13, Operator: cornwall
File: rc_b9_10_2_13C
INDVA=500 "epoxide"

Relax. delay 1.000 sec
Pulse 45.0 degrees
Pulse width 12.500 sec
Width 25510.2 Hz
512 repetitions
OBSERVE C13, 100.5058922 MHz
DECOUPLE H1, 399.7070404 MHz
Power 38 dB
continuously on
Waltz16 PRERUN
DATA PROCESSING
Line broadening 0.5 Hz
FT size 65536
Total time 19 min, 34 sec

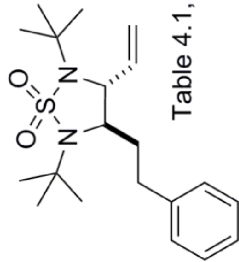
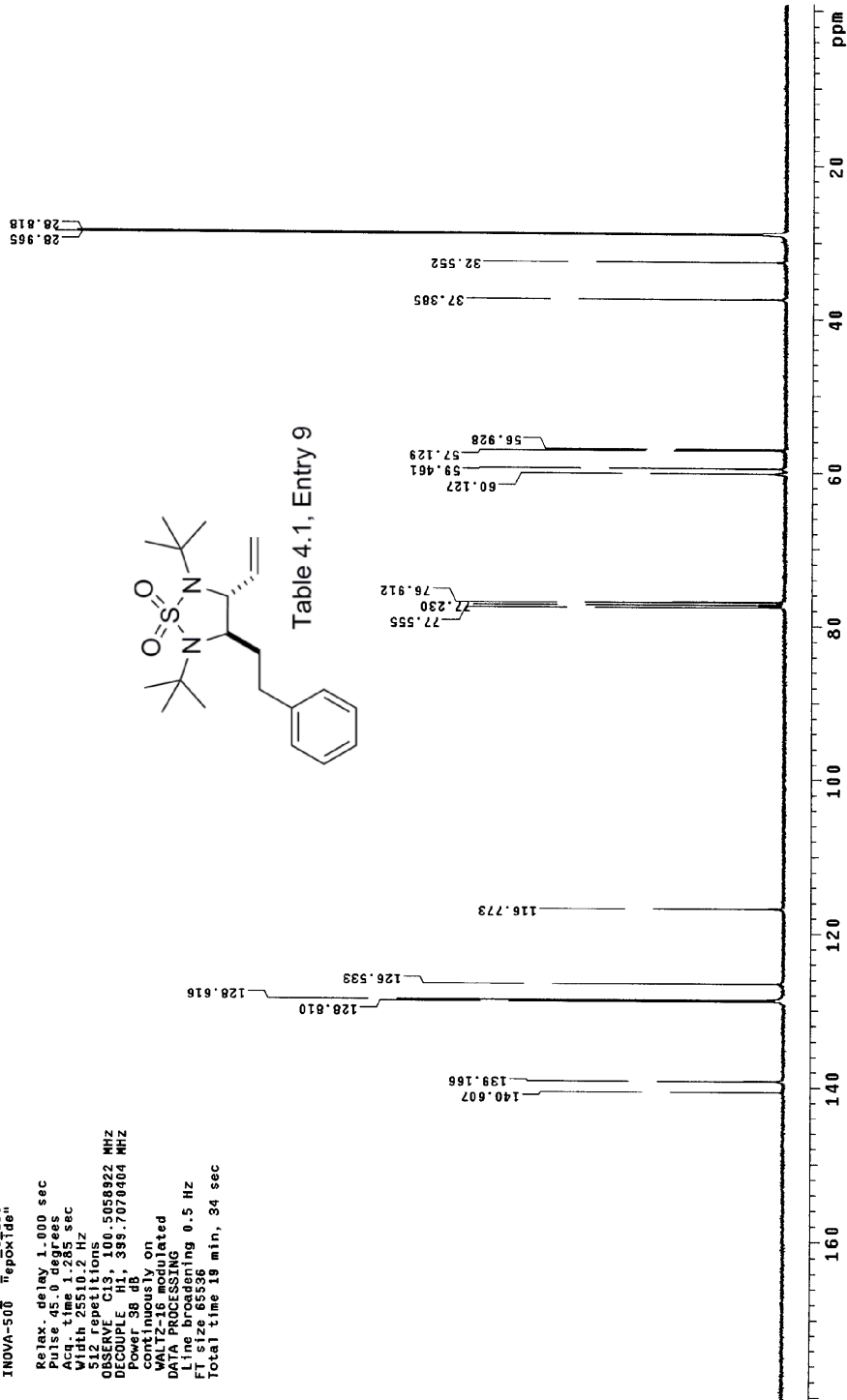
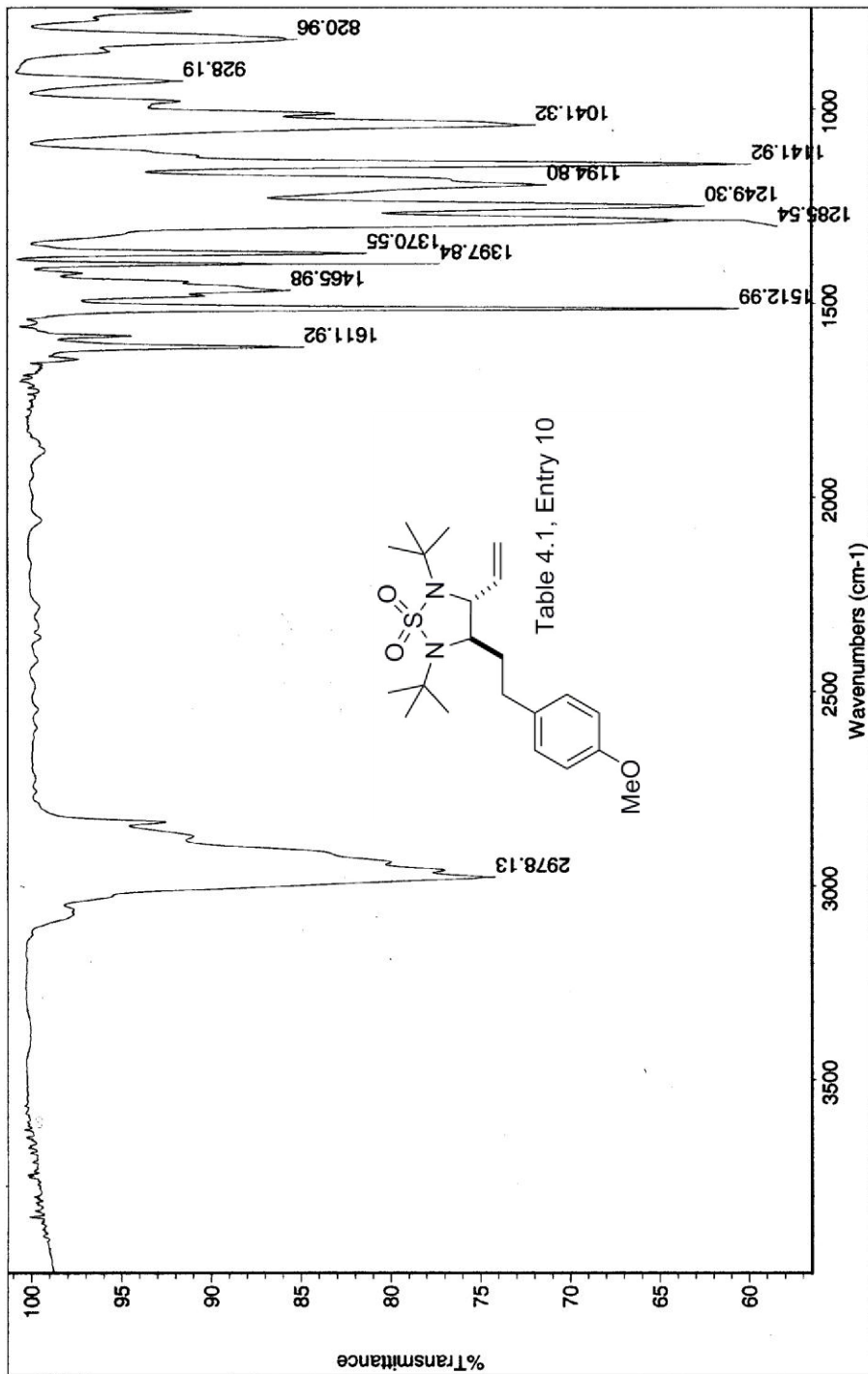


Table 4.1, Entry 9





Date: Thu Mar 01 10:15:56 2012 (GMT-07:00) Thu Mar 01 10:07:18 2012 (GMT-07:00)

Scans: 64

Resolution: 4.000

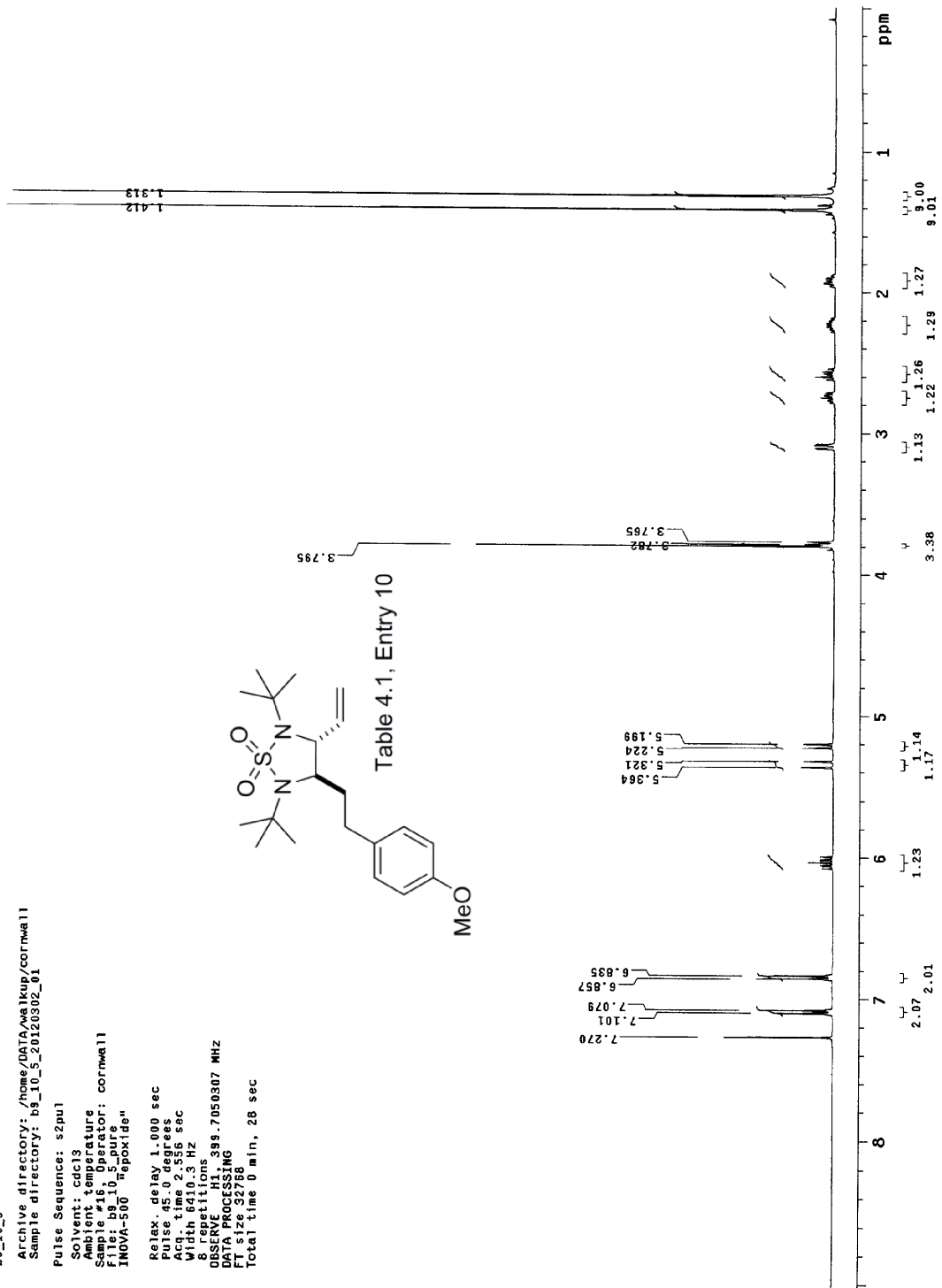
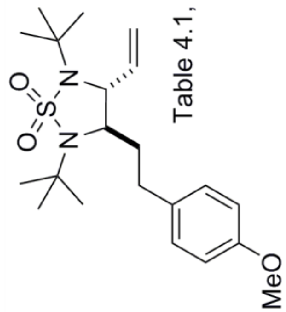


5-10-5

bs_10_5
 Archive directory: /home/DATA/wsl/kup/cornwall
 Sample directory: bs_10_5_20120302_01

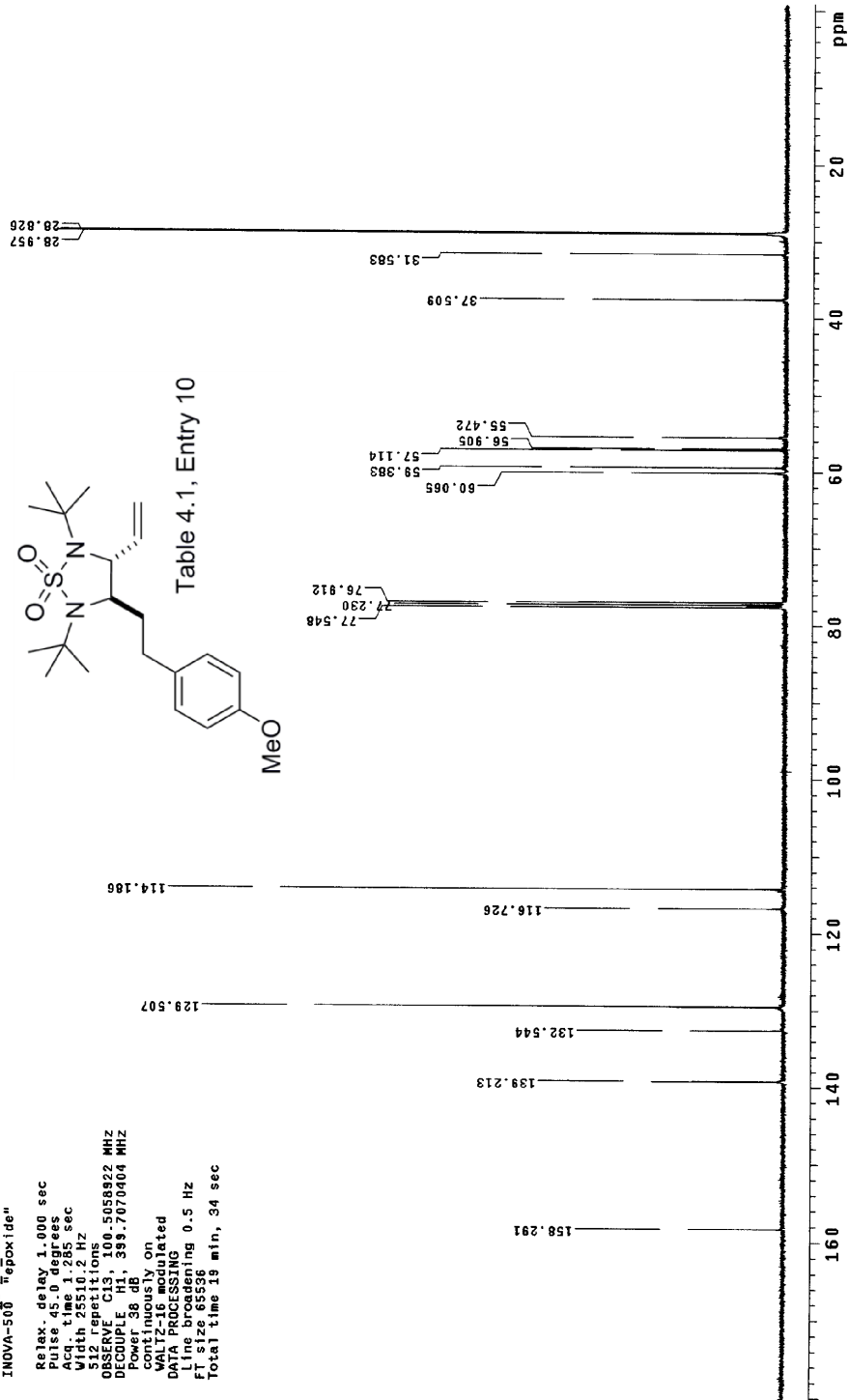
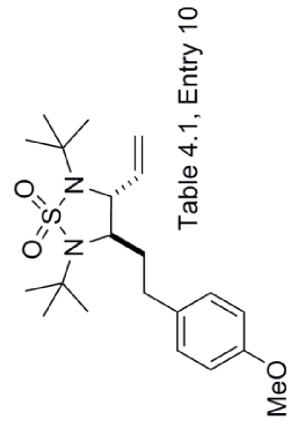
Pulse Sequence: s2pul
 Solvent: cdcl3
 Ambient temperature
 Sample #16, Operator: cornwall
 File: bs_10_5_pure
 INOVA-500 "epoxide"

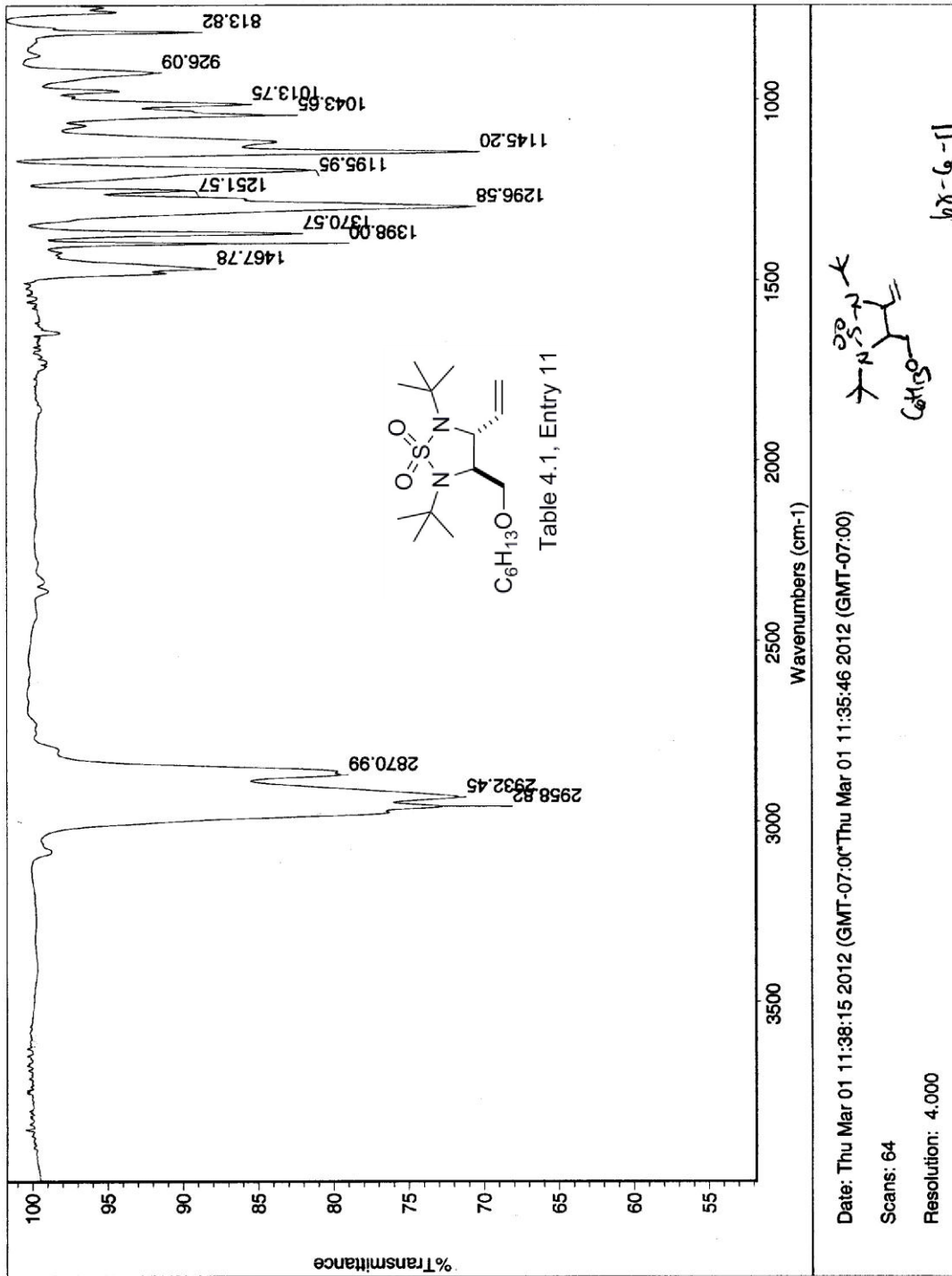
Relax. delay 1.000 sec
 Pulse 45.0 degrees
 Acq. time 2.356 sec
 Mhz 500.135
 8 repetitions
 OBSERVE H1, 399.7050307 MHz
 DATA PROCESSING
 FT size 32768
 Total time 0 min, 28 sec



b9_10_5
 Archive directory: /home/DATA/walkup/cornwall
 Sample directory: b9_10_5_0120302_01
 Pulse Sequence: s2pul
 Solvent: cdcl3
 Ambient temperature
 Sample #16, Operator: cornwall
 File: b9_10_5_13C
 INOVA-500 "epoxide"

Relax. delay 1.000 sec
 Pulse 45.0 degrees
 Width 1.265 sec
 Wdth 1.265 sec
 512 repetitions
 OBSERVE C13, 100.5058922 MHz
 DECOUPLE H1, 399.7070404 MHz
 Power 38 dB
 continuously on
 MULTICAN decoupled
 DATA ACQUISITION
 Line broadening 0.5 Hz
 FT size 65536
 Total time 18 min, 34 sec





b8_6_11
 Archive directory: /home/DATA/walkup/cornwall
 Sample directory: b8_6_11_20120305_01
 Pulse Sequence: s2pul
 Solvent: cdcl3
 Ambient temperature
 Sample #13, Operator: cornwall
 File: b8_6_11_pure
 INOVA-500 "epoxide"
 Relax. delay 1.000 sec
 Pulse 45.0 degrees
 Acq. time 2.556 sec
 F1 F2
 8410.3 MHz
 8 Juhn
 OBSERVE H1, 399.7050307 MHz
 DATA PROCESSING
 FT size 32788
 Total time 0 min, 20 sec

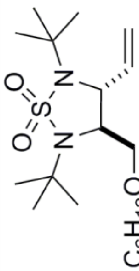
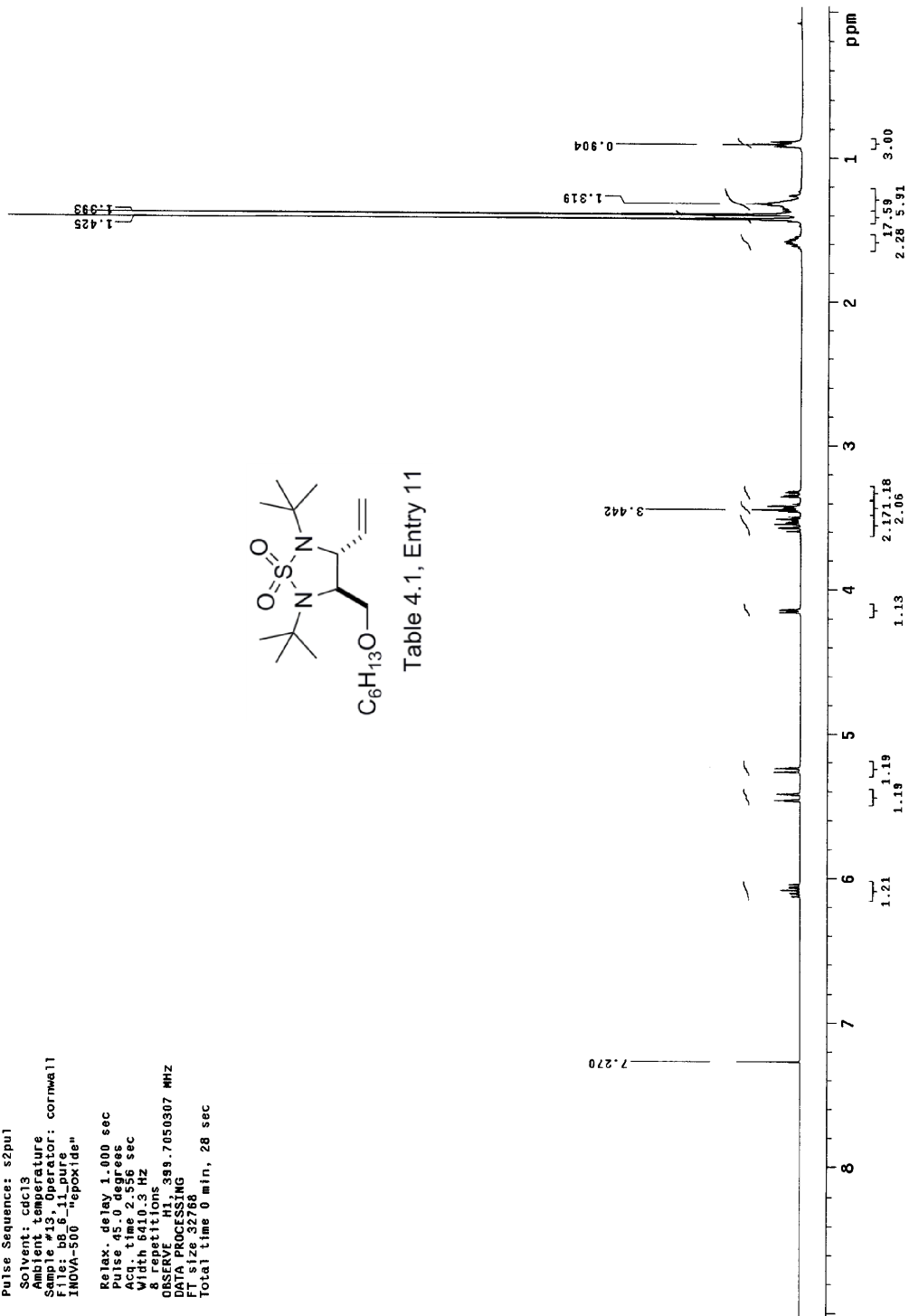


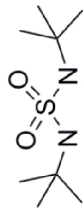
Table 4.1, Entry 11



13C OBSERVE

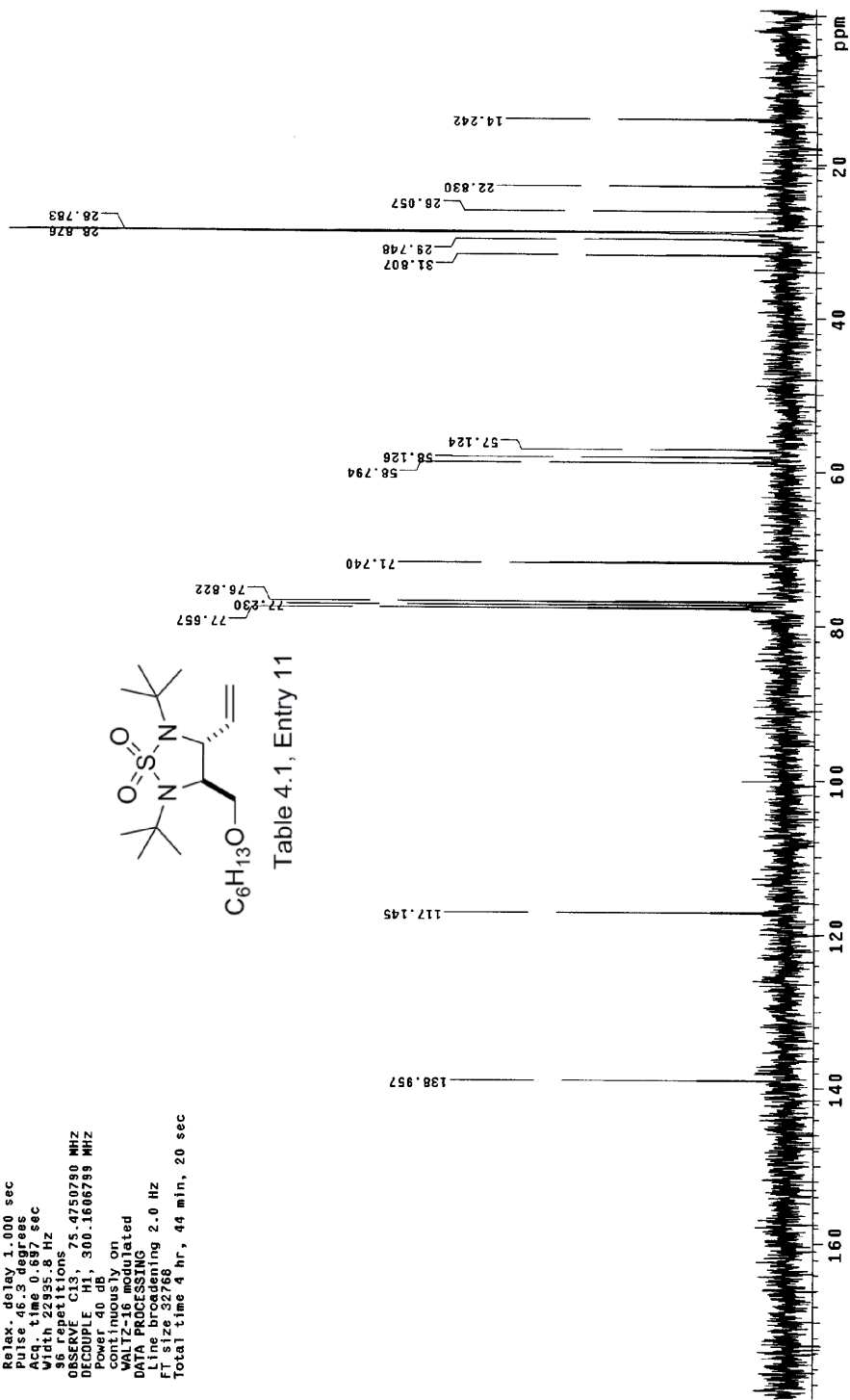
Pulse Sequence: s2pul
Solvent: CDCl3
Magnetic Temperature
File: r15611.cd3bon
INOVA-500 "spoxide"

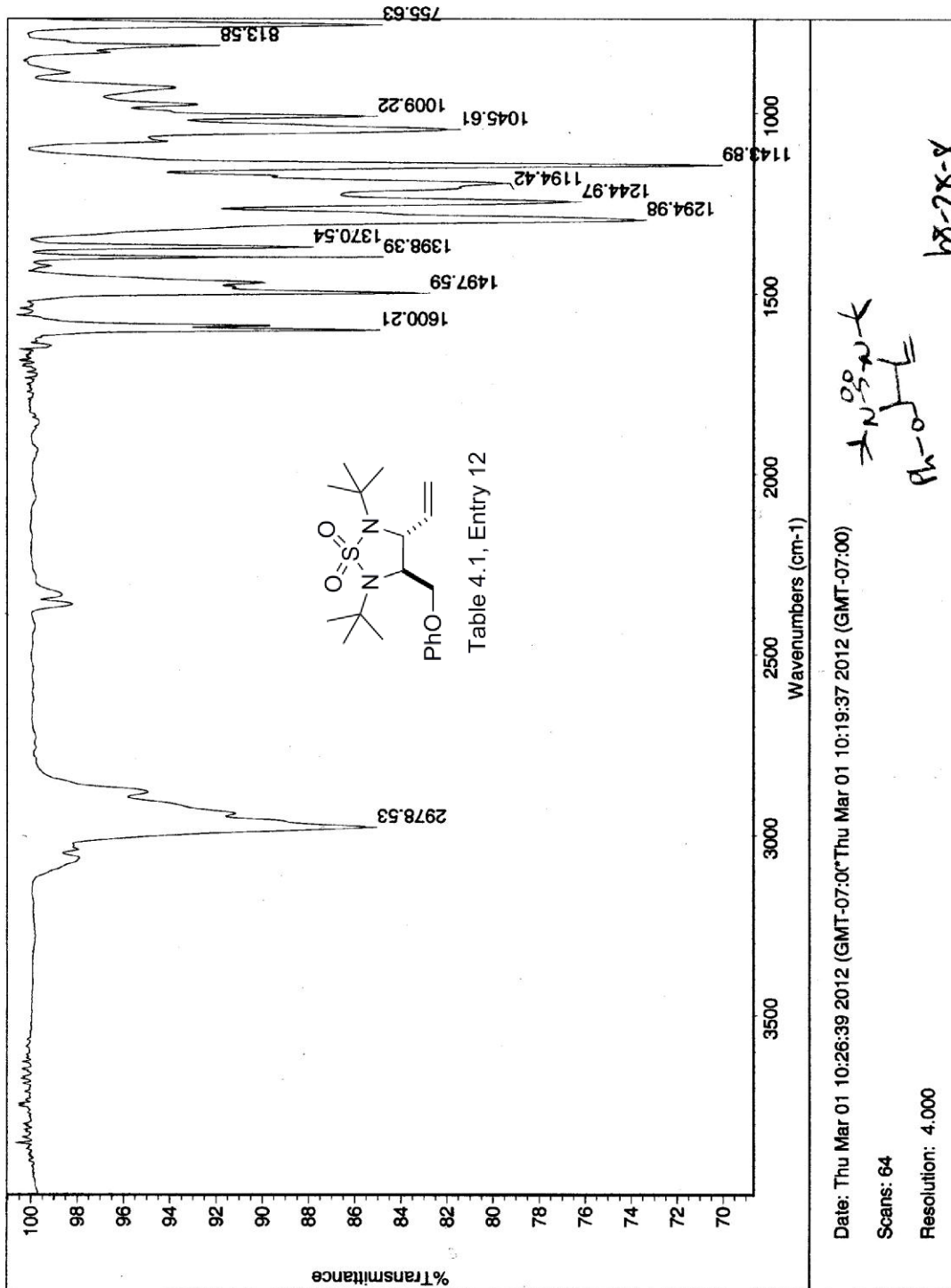
Relax. delay 1.000 sec
Pulse 45.3 degrees
Acq. time 0.697 sec
Width 22935.8 Hz
36 repetitions
SPECT. CH, 75.4750760 MHZ
DECOUPLE H3, 300.1688799 MHZ
Power 40 dB, continuously on
WALTZ-16 modulated
DATA PROCESSING
Line broadening 2.0 Hz
F1 size 52766
Total time 4 hr, 44 min, 20 sec



C₆H₁₃O

Table 4.1, Entry 11





STANDARD 1H OBSERVE

Pulse Sequence: s2pul
Solvent: CDCl3
Ambient temperature
File: r5_b8_28_8_11162012
INOVA-500 "epoxide"
Relax. delay 1.000 sec
Pulse 49.6 degrees
Acq. time 1.989 sec
Width 4500.5 Hz
SFO 300.1582186 MHz
OBSERVE H1
DATA PROCESSING
FT size 32768
Total time 0 min, 24 sec

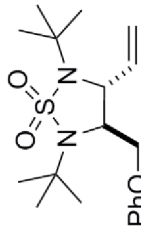
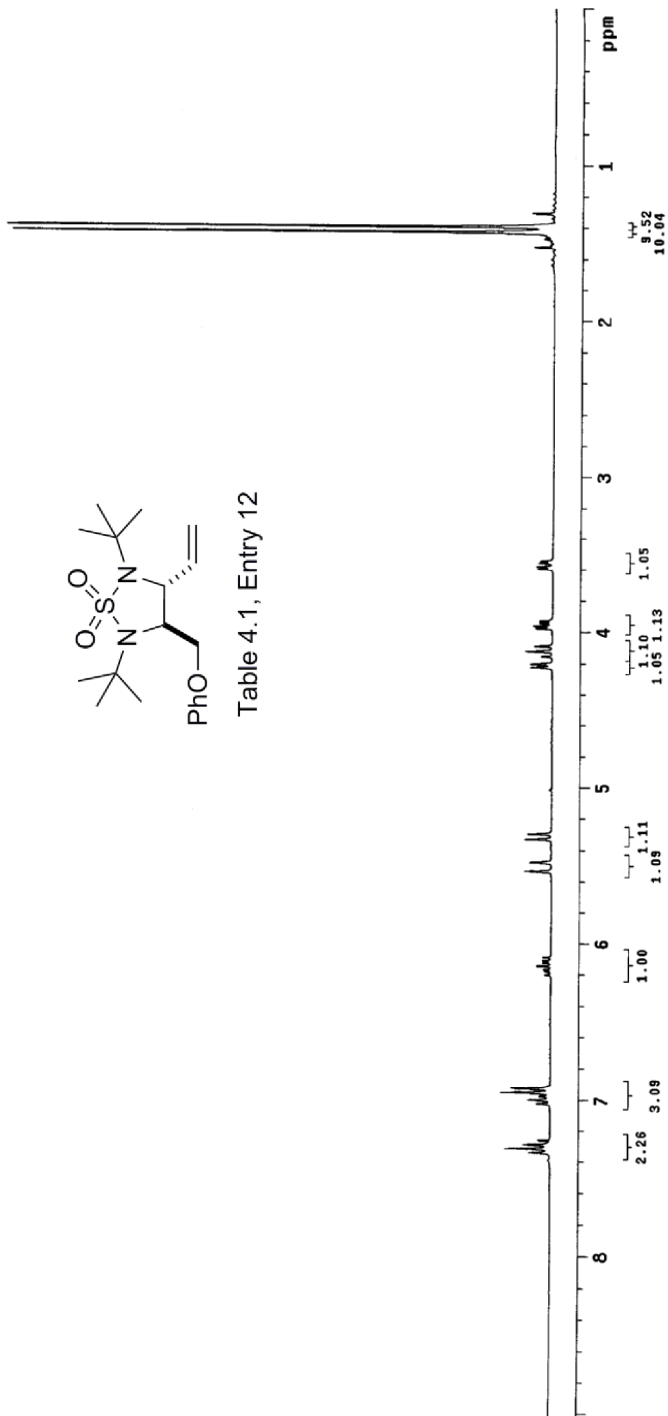


Table 4.1, Entry 12



13C OBSERVE

Pulse Sequence: szpul
Solvent: CDCl3
Ambient temperature
F1: 100.6263 Carbon
INOVA-500 "epox100"
Relax. delay 1.000 sec
Pulse 46.3 degrees
Acq. time 0.697 sec
Width 22935.8 Hz
48 repetitions
OBSERVE C13, 75.4750818 MHZ
DECOUPLE H1, 300.1606799 MHZ
Contingency on
WALTZ-16 modulated
DATA PROCESSING
Line broadening 2.0 Hz
FT size 32768
Total time 4 hr., 44 min., 20 sec

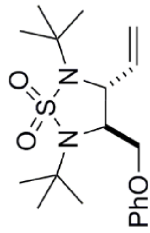
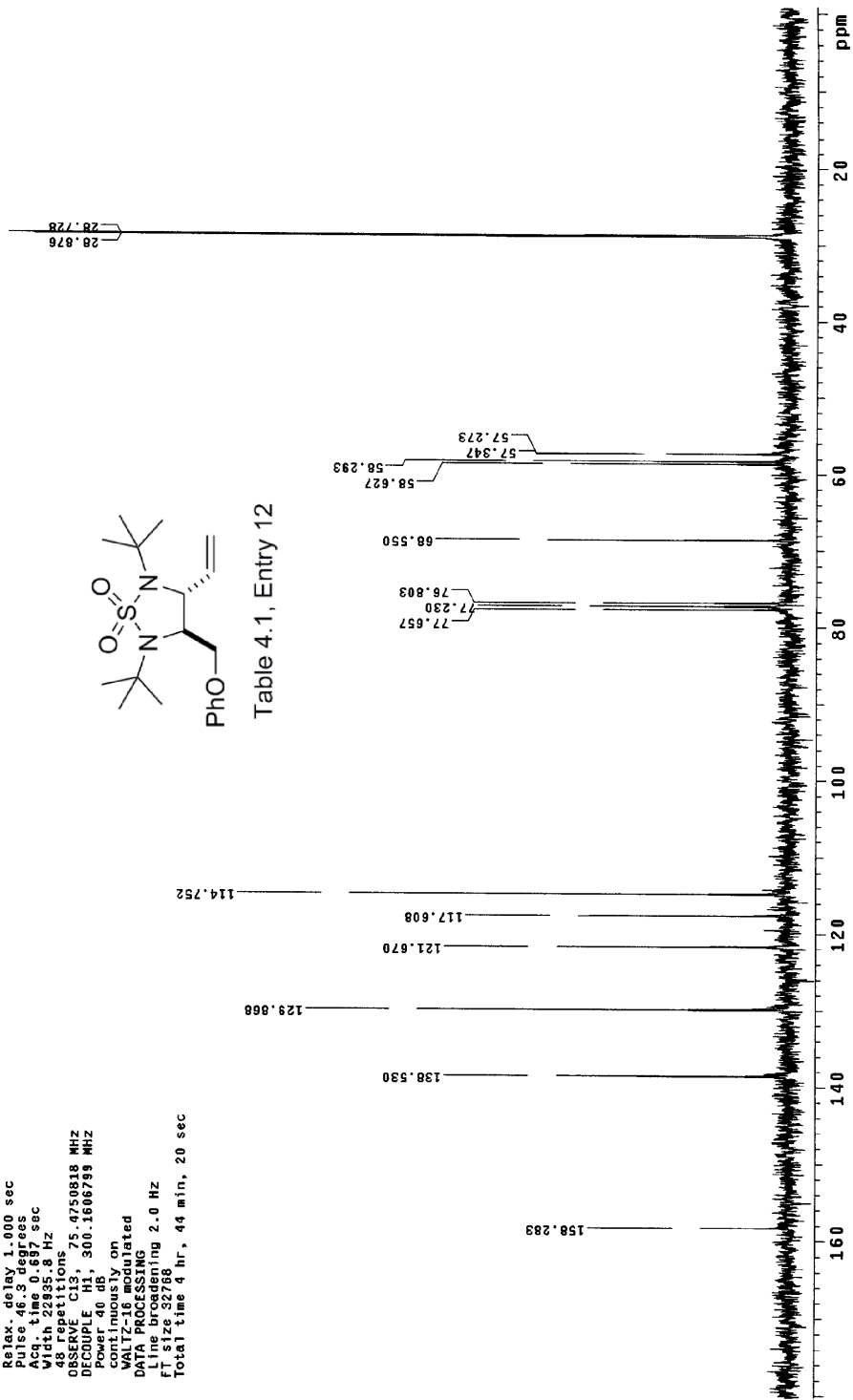
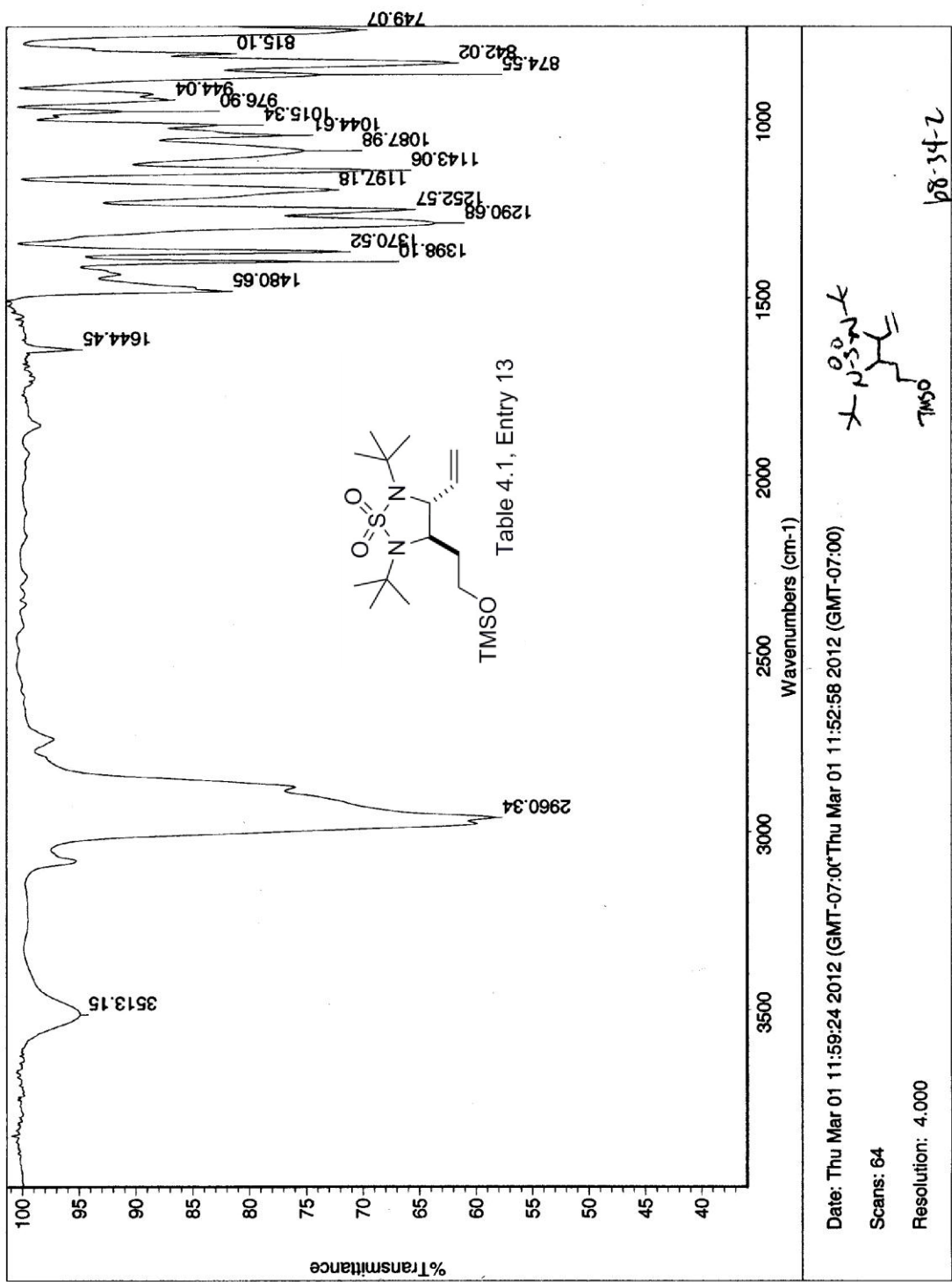


Table 4.1, Entry 12





STANDARD 1H OBSERVE

Pulse Sequence: s2pu1
Solvent: CDCl3
Ambient temperature
File: FC_ba_34_2_1H
INOVA-500 "epoxide"

Relax. delay 1.000 sec
Pulse 45.6 degrees
Acq. time 0.392 sec
Width 4500.5 Hz
8 repetitions
OBSERVE H1, 300.1592279 MHZ
DATA PROCESSING
FT size 32768
Total time 0 min, 24 sec

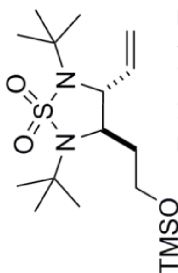
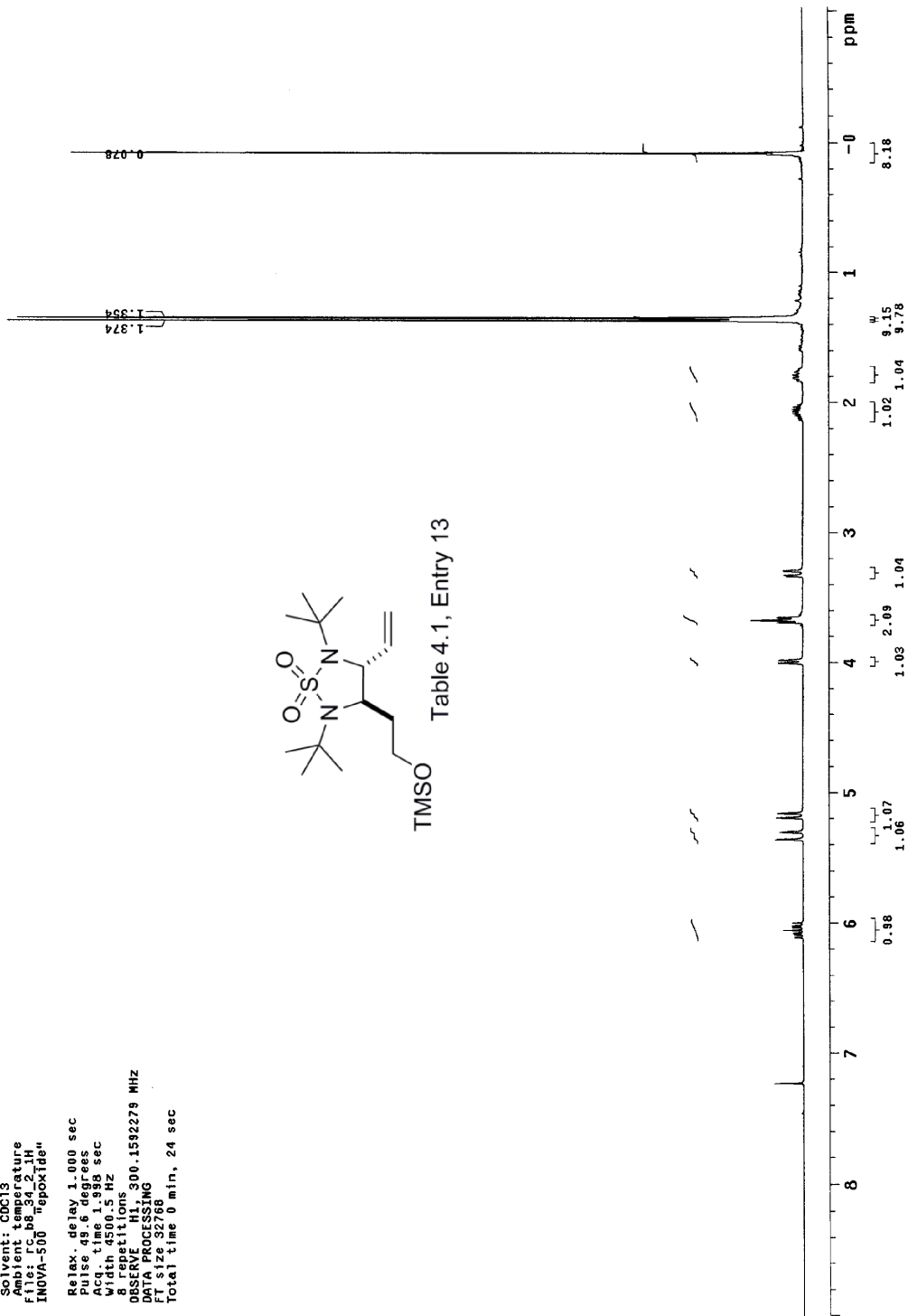
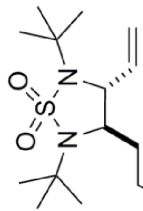


Table 4.1, Entry 13

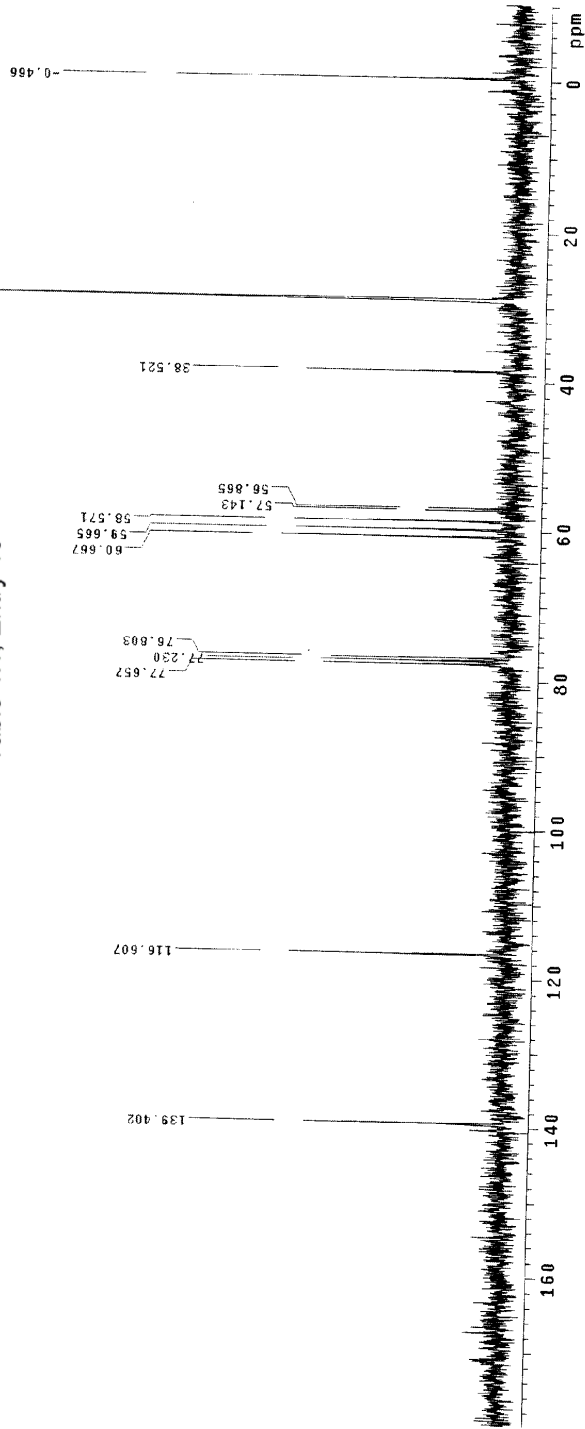


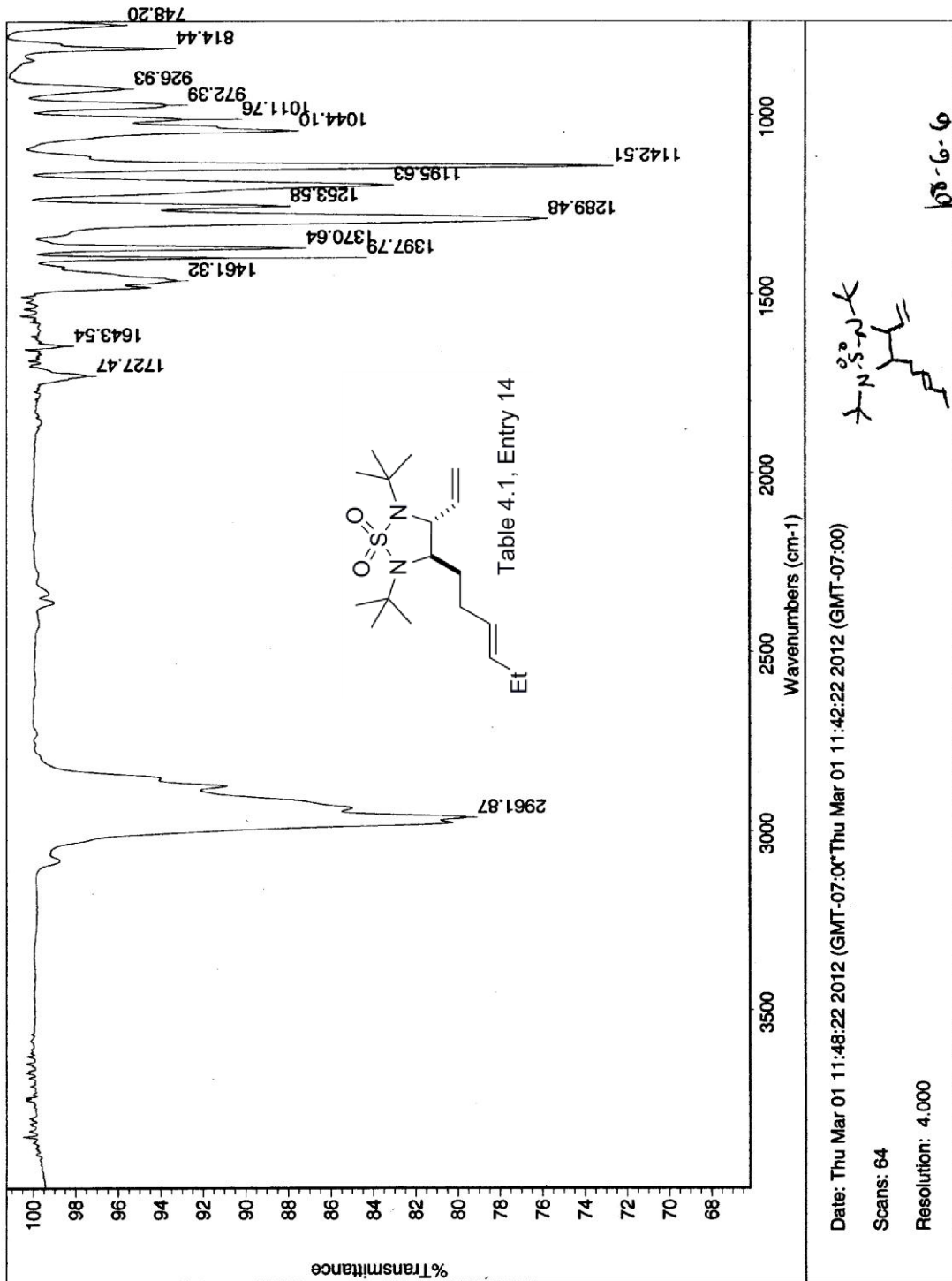
13C OBSERVE

Pulse Sequence: s2pu1
Solvent: CDCl3
Pulsed Temperature: 77.00000000
INOVA-500
Relax. delay 1.000 sec
Pulse 46.3 degrees
Acq. time 0.897 sec
Width 22935.8 Hz
Repetitions 1
OBSERVE CH1 75.4750504 MHZ
DECOUPLE H1 300.1606793 MHZ
Power 40 dB
Continuously on
WALTZ-16 modulated
DATA PROCESSING
FT 13C
Total time 4 hr, 44 min, 20 sec



TMSO Table 4.1, Entry 13





STANDARD 1H OBSERVE

Pulse Sequence: s2pul
Solvent: CDCl3
Ambient temperature
File name: 14
INDVA-500 In Epoxi1de
Relax. delay 0.000 sec
Pulse 26.0 degrees
Acq. time 2.668 sec
Width 5995.2 Hz
4 Repetitions
OBSERVE H1, 300.1592160 MHz
DATA PROCESSING
Spectral resolution 0.896 sec
FT size 32768
Total time 0 min, 16 sec

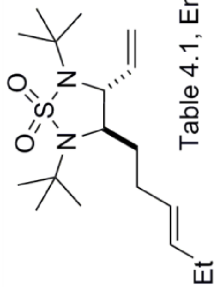
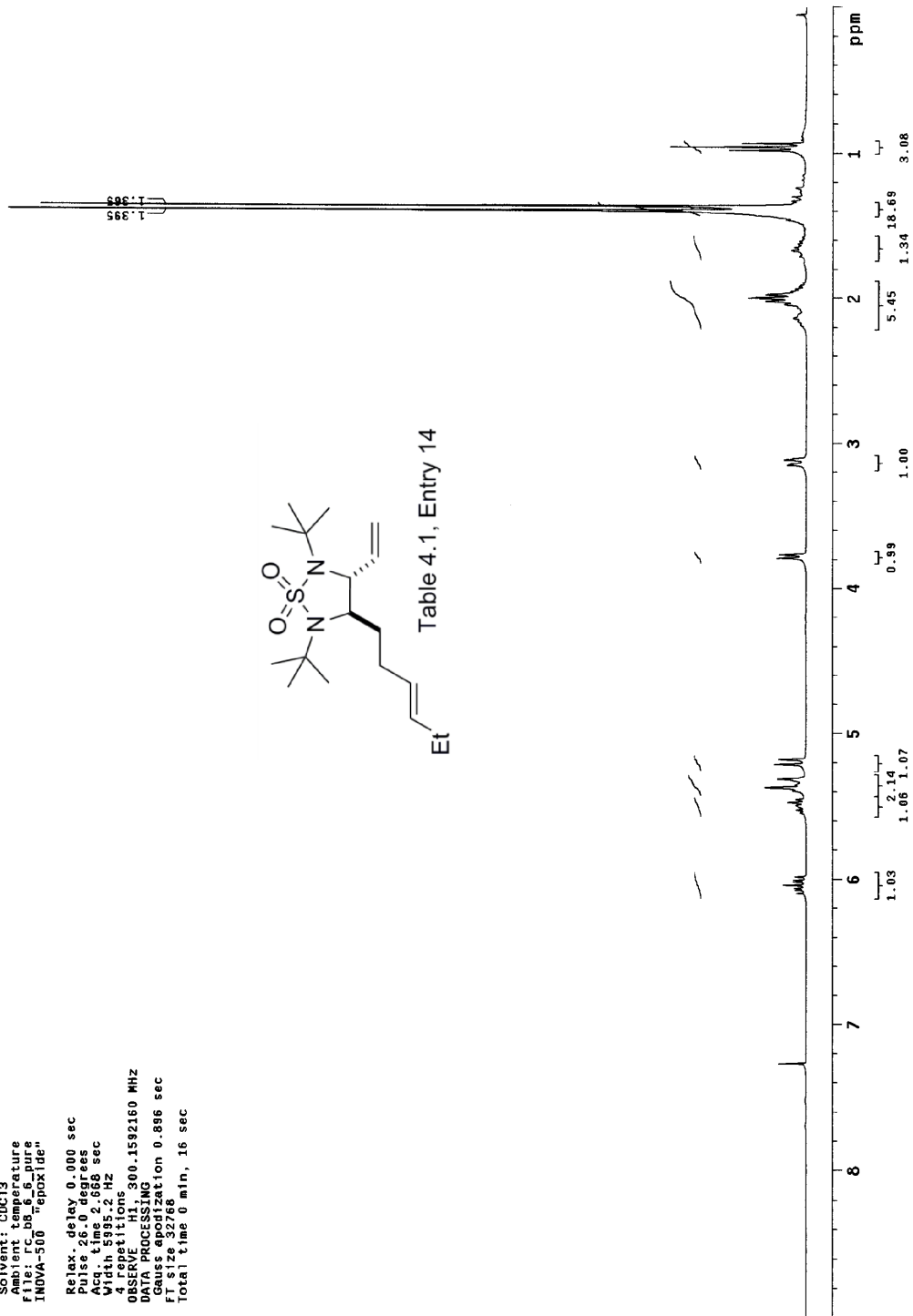


Table 4.1, Entry 14



13C OBSERVE

Pulse Sequence: s2pu1
Solvent: CDCl3
Ambient temperature
File: r5_bb_6_pure_13C_11142012
INOVA-500 "epoxide"

Pulse 55.7 degrees
Acq. time 1.315 sec
Waltz: 1.0 Hz
80 repetitions
OBSERVE C13, 75.4750767 MHz
DECOUPLE H1, 300.1606800 MHz
Power 40 dB
continuously on
Waltz: 1.0 Hz
DATA PROCESSING
Line broadening 1.0 Hz
FT size 131072
Total time 3 min, 2 sec

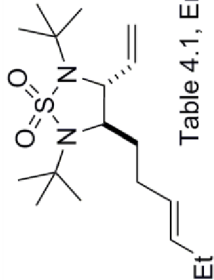
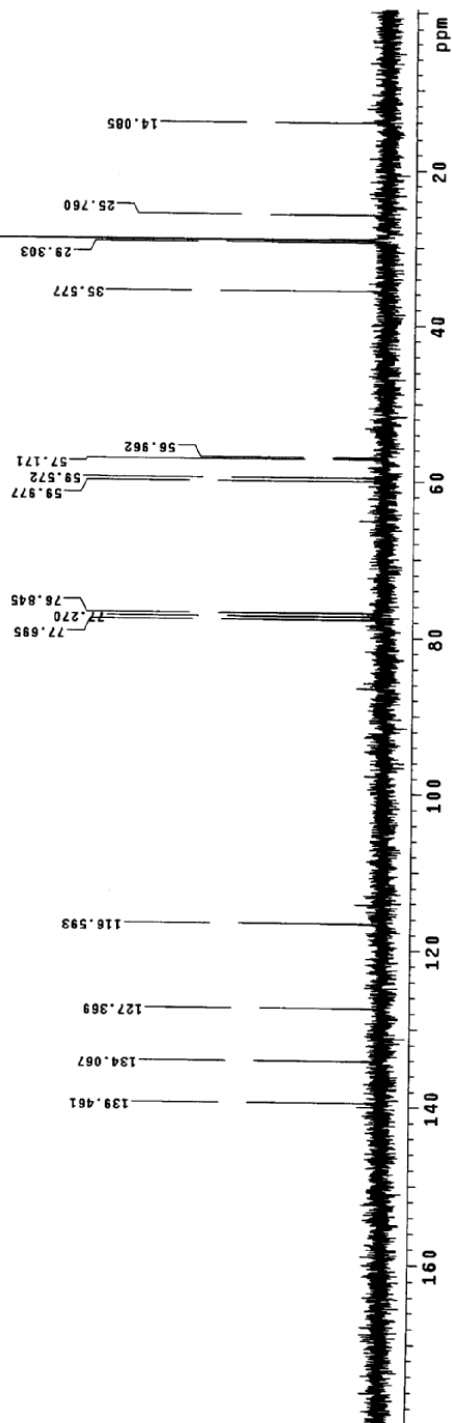
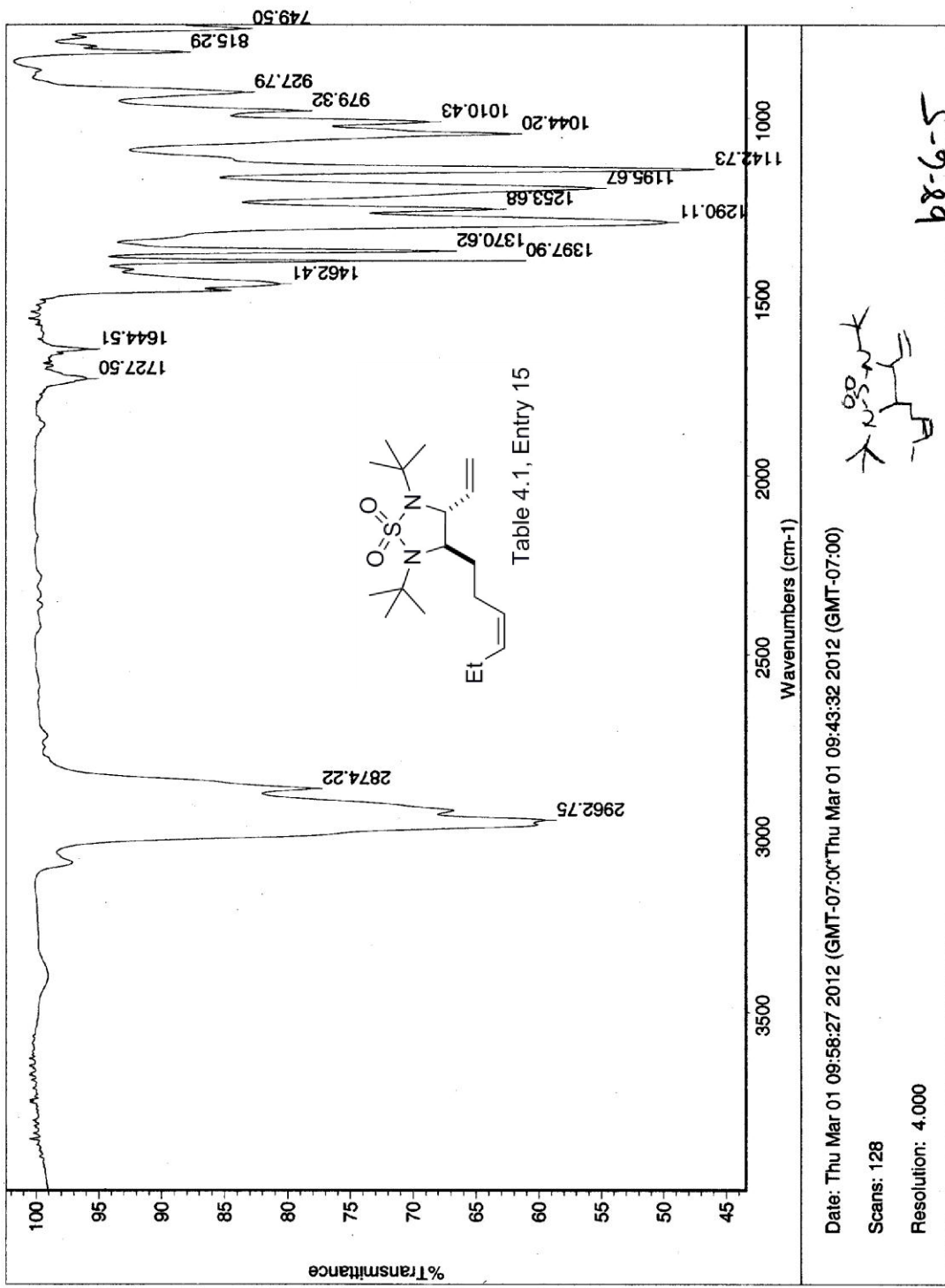


Table 4.1, Entry 14





Date: Thu Mar 01 09:58:27 2012 (GMT-07:00)*Thu Mar 01 09:43:32 2012 (GMT-07:00)

Scans: 128

Resolution: 4.000



b8-6-5

STANDARD 1H OBSERVE

Pulse Sequence: s2pul
 Solvent: CDCl3
 Ambient temperature
 File: FC88_5_pure
 INOVA-500 "epoxide"
 Relax... delay 0.000 sec
 Pulse... delay 0.000 sec
 Acq... time 2.656 sec
 Width 5995.2 Hz
 4 repetitions
 OBSERVE H1, 300.1592164 MHz
 DATA PROCESSING
 Phase... rotation 0.896 sec
 F2... 0.2762
 Total time 0 min, 16 sec

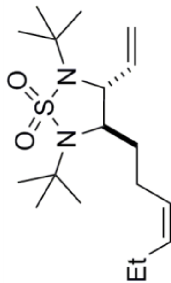
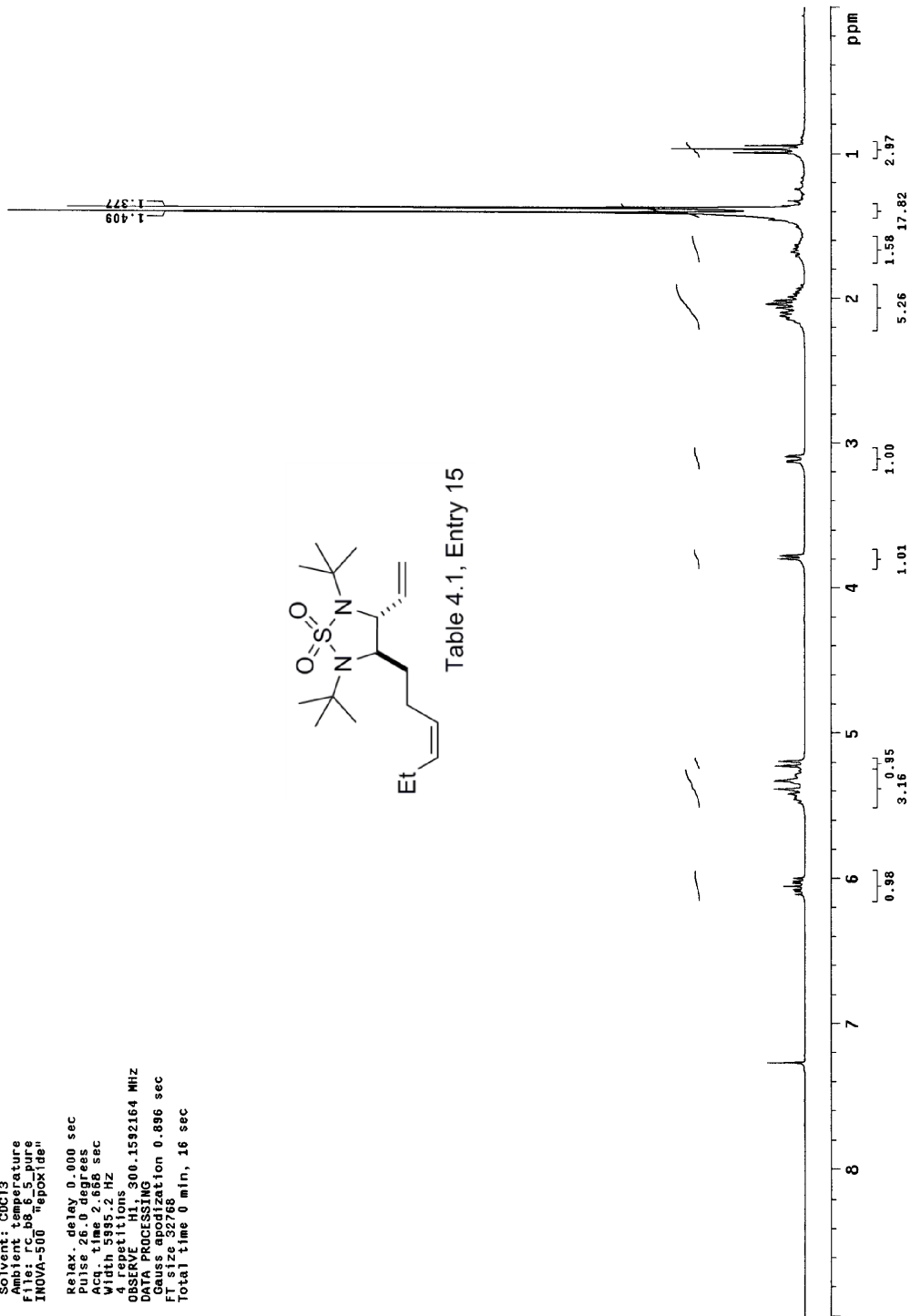


Table 4.1, Entry 15



13C OBSERVE

Pulse Sequence: zgpg30

Solvent: CDCl3
Acquisition Date: 11/11/04
File: 15_08_6_5_carbon
INDVA-500 "epoxide"

Relax. delay 1.000 sec

Pulse 46.3 degrees

Acq. time 0.687 sec

Width 22935.8 Hz

Observed F1 75.4750804 MHz

Decouple F1 300.1666798 MHz

Power 40 dB

continuously on

WALTZ-16 modulated

DATA PROCESSING

FT size 32768

Total time 4 hr, 44 min, 20 sec

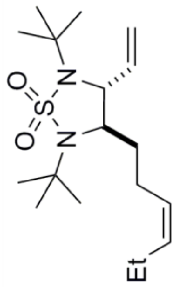
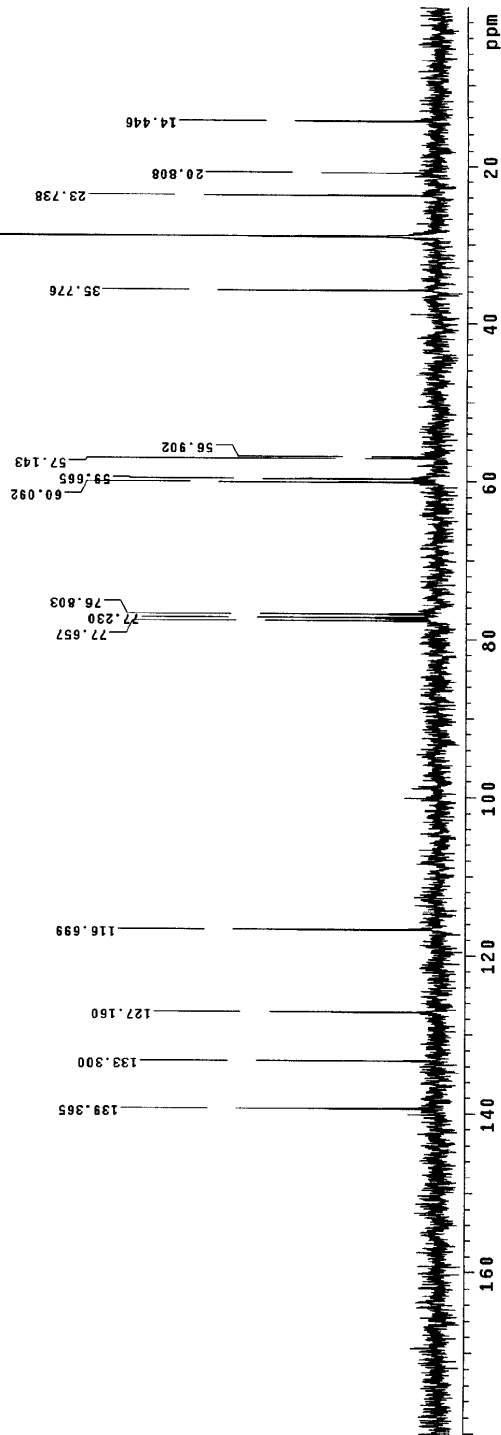
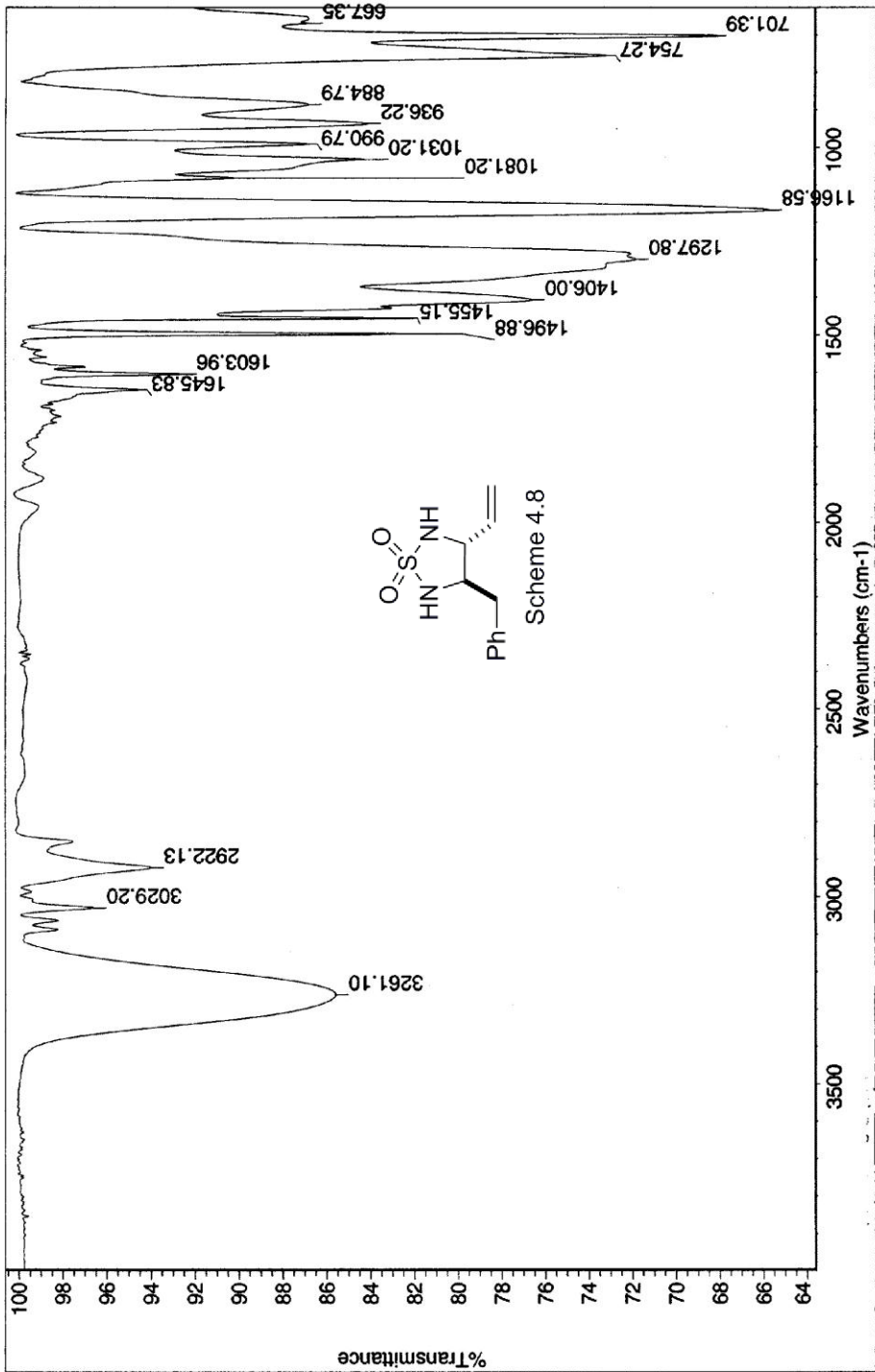


Table 4.1, Entry 15

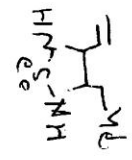




Date: Tue May 01 13:38:35 2012 (GMT-06:00) Tue May 01 13:35:54 2012 (GMT-06:00)

Scans: 64

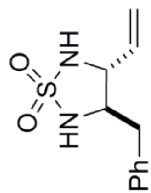
Resolution: 4.000



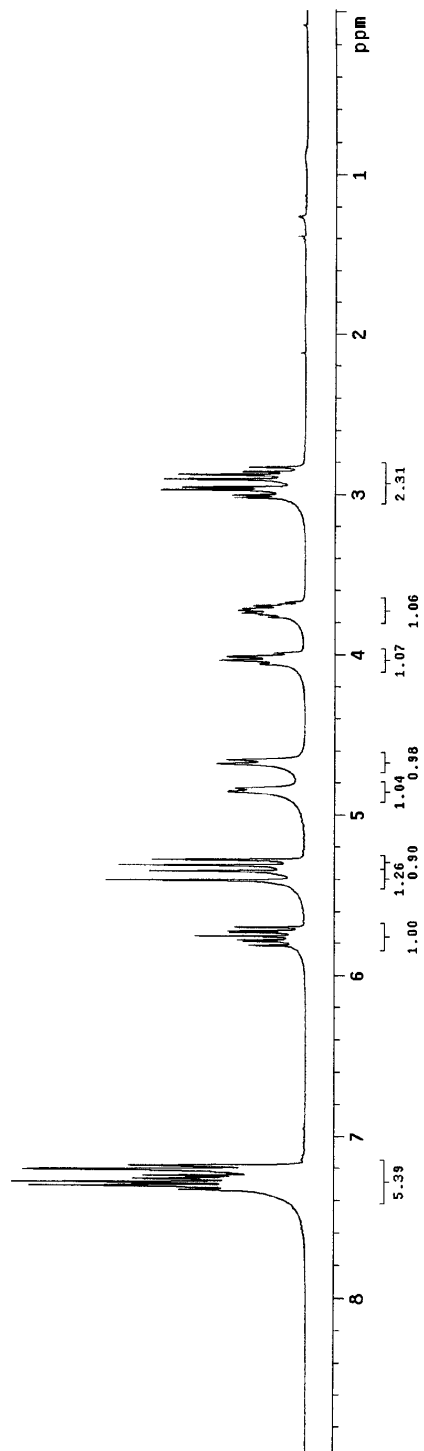
69-38-2

STANDARD 1H OBSERVE

Pulse Sequence: s2pul
Solvent: CDCl3
Acq. temperature: 300.15 K
File: FC_88_38_2_1H
INOVA-500 "epoxide"
Relax. delay: 1.000 sec
Pulse: 49.6 degrees
Acq. time: 1.988 sec
Width: 4500.5 Hz
of scans: 1024
of repetitions: 1
OBSERVE: 300.1592196 MHz
P1: 12.000000
P2: 12.000000
DATA PROCESSING
FT size: 32768
Total time: 0 min, 12 sec

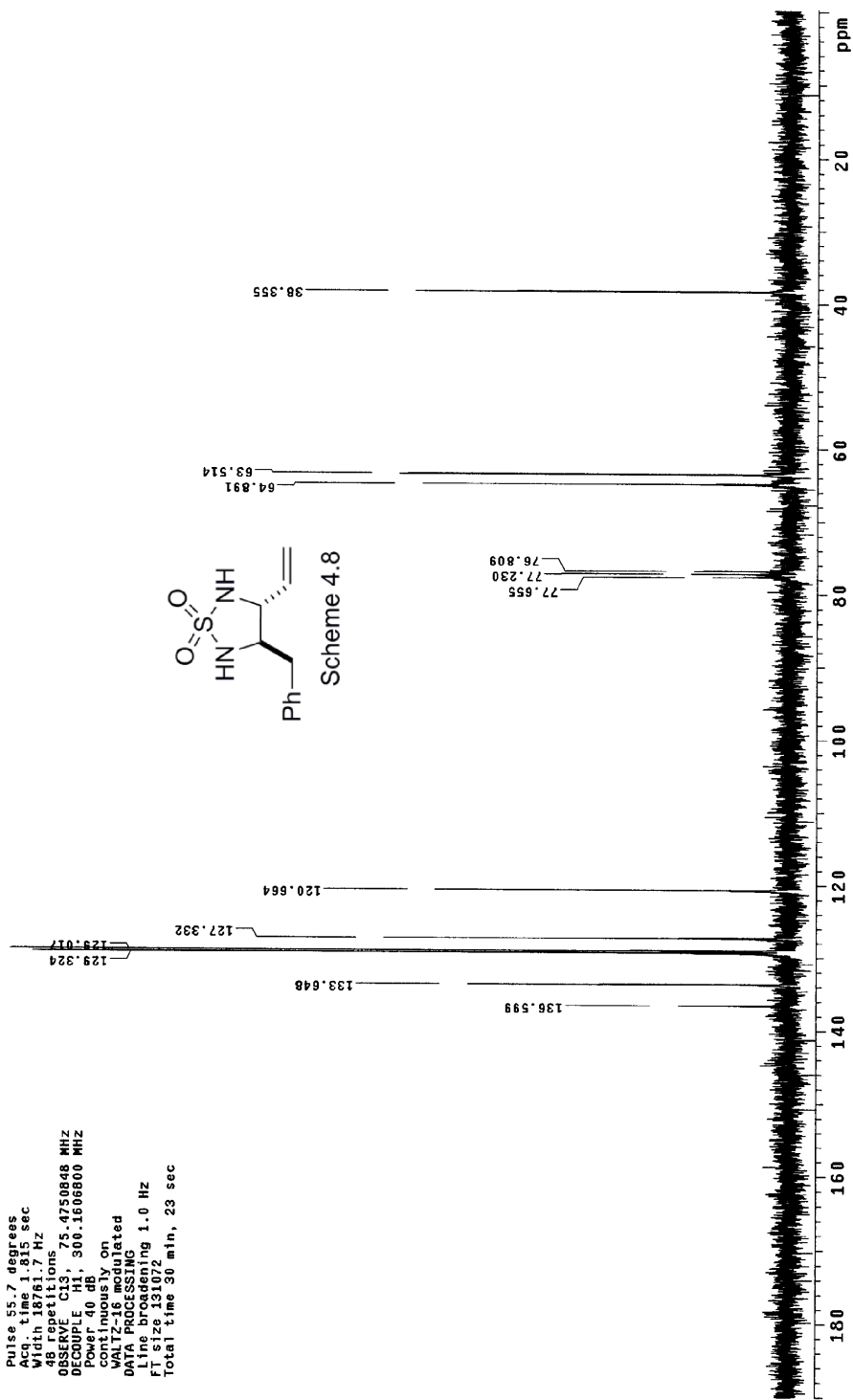


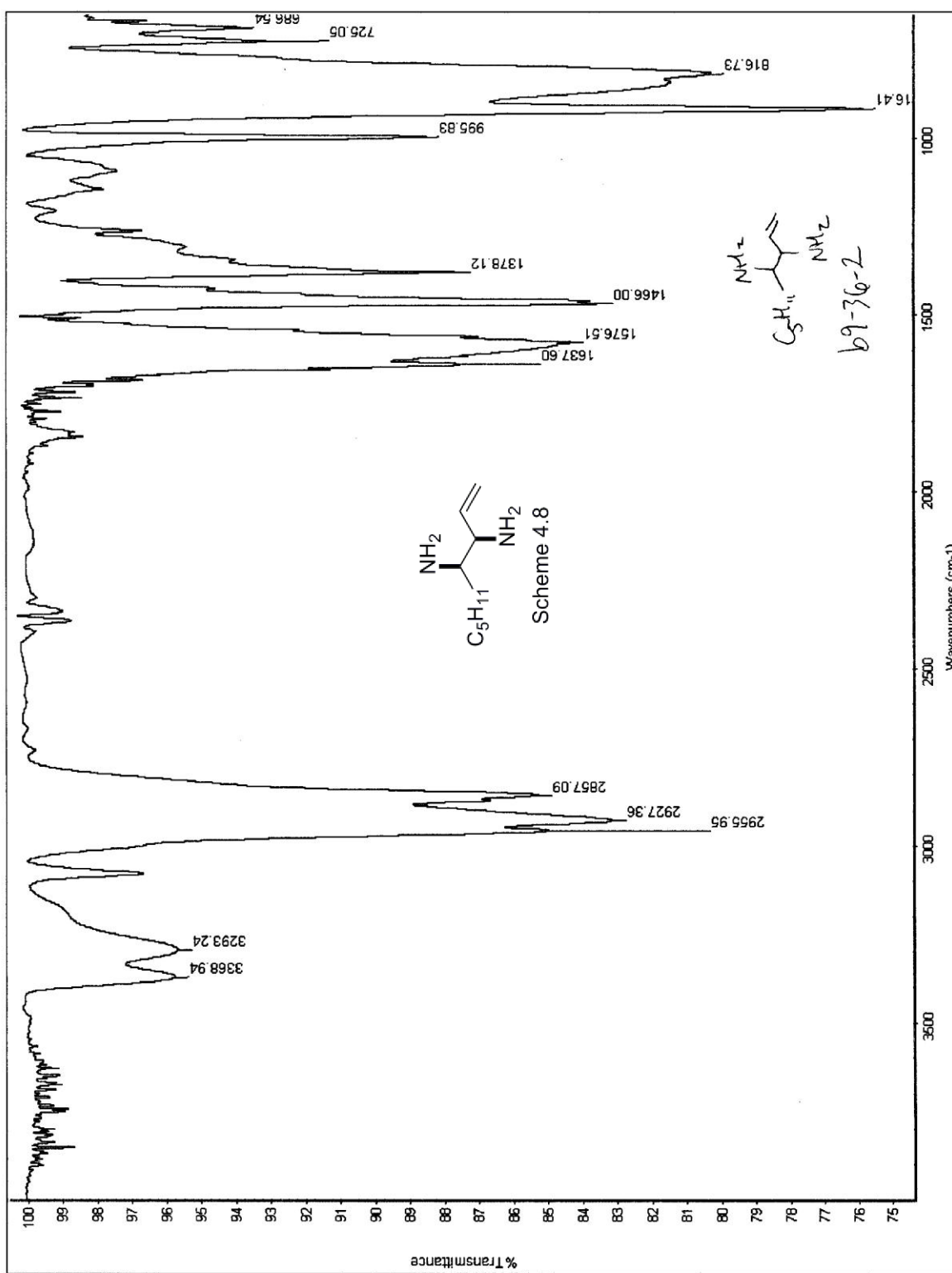
Scheme 4.8



13C OBSERVE

Pulse Sequence: s2pul
Solvent: CDCl3
Acq. temperature
File: rc_b9_38_2_13C
INOVA-500_Hepoxide"
Pulse 55.7 degrees
Acq. time 1.815 sec
Width 18761.7 Hz
48 repetitions
OBSERVE C13, 75.4750848 MHz
DECODE P1, 300.1606800 MHz
Power 60 dB
continuously on
WALTZ-16 modulated
DATA PROCESSING
Line broadening 1.0 Hz
F1 size 131072
Total time 30 min, 23 sec



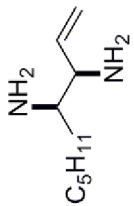


Archive directory: /home/DATA/walkup/cornwall
Sample directory: rc_lg_36_2_20120425_01

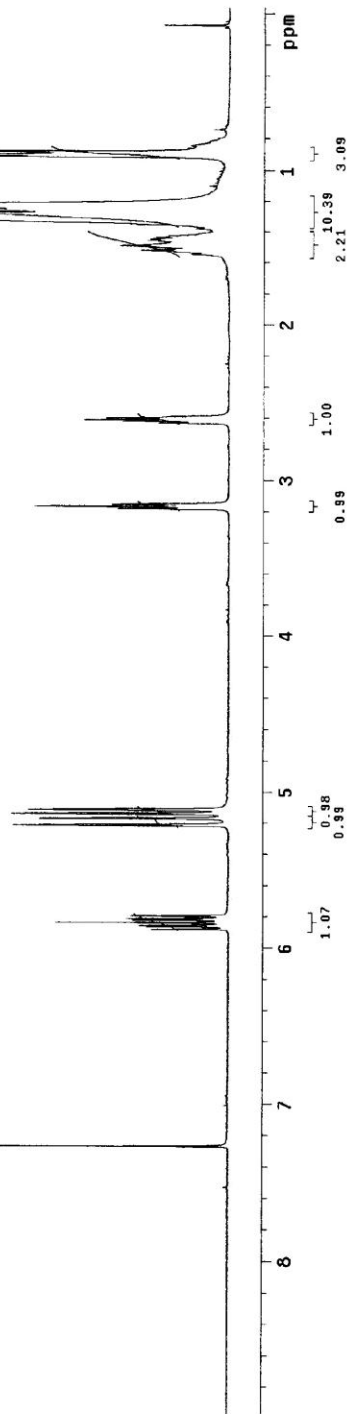
Pulse Sequence: s2pu1

Solvent: cdcl3
Ambient temperature
Sample #49, Operator: cornwall
INSTRUM: spect
INSTRUM: spect

Relax. delay: 1.000 sec
Pulse: 45.0 degrees
Acq. time: 2.556 sec
Width: 6410.3 Hz
18 repetitions
SOLVENT: CDCL3
DATA PROCESSING
FT size: 32788
Total time: 0 min, 57 sec



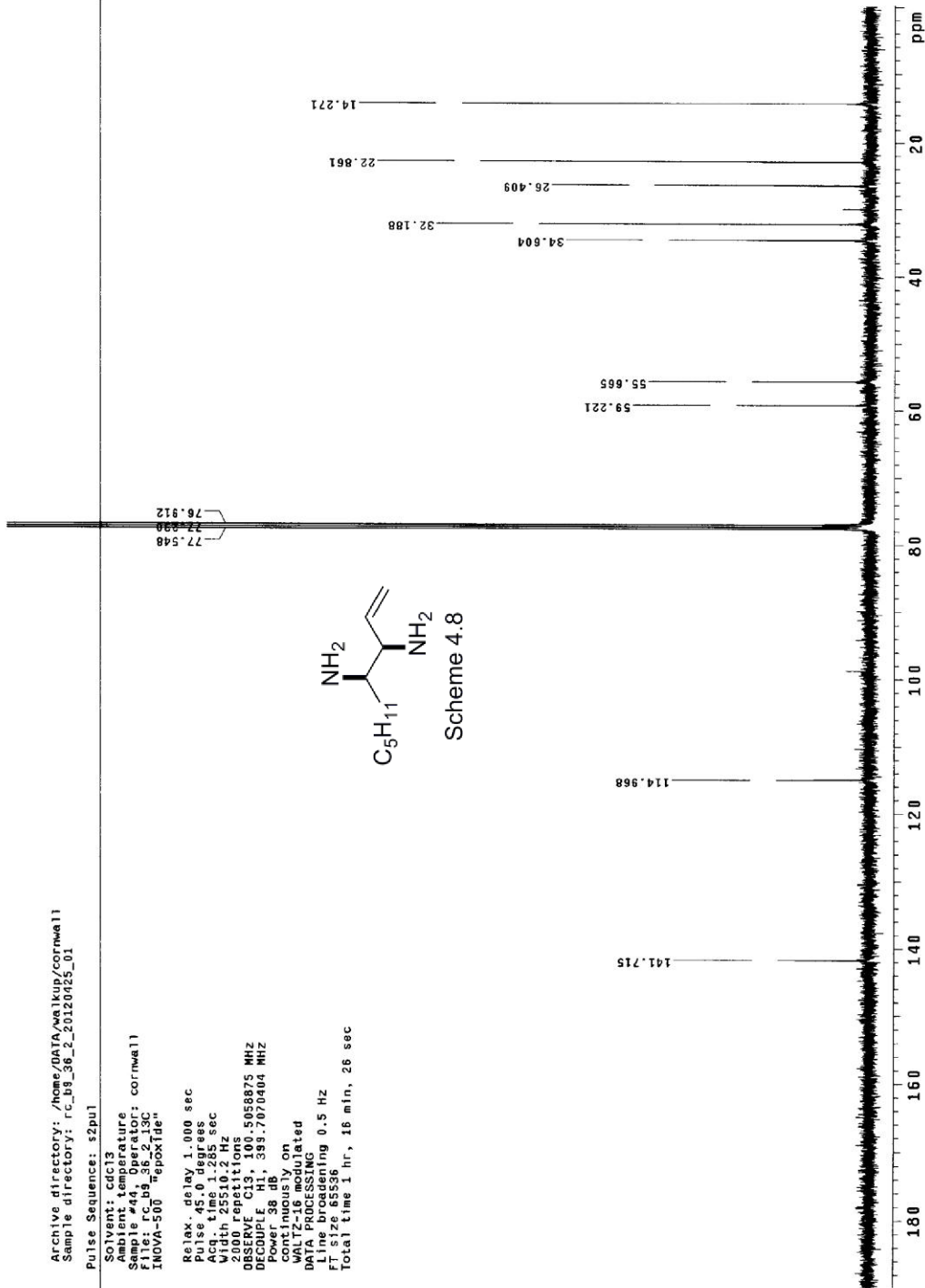
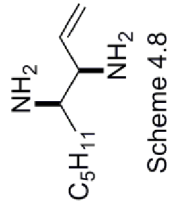
Scheme 4.8

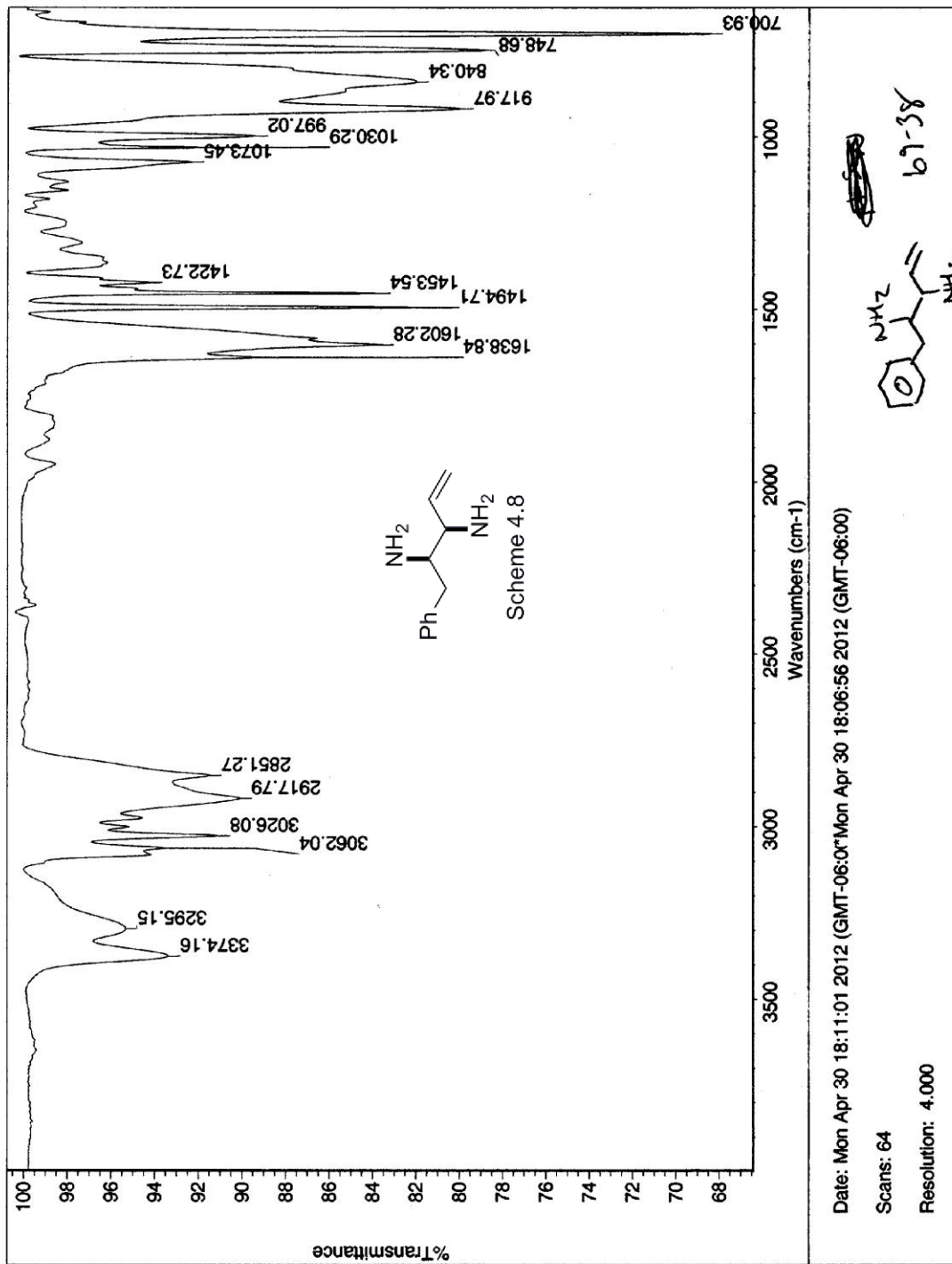


Archive directory: /home/data/walkup/cornwall
Sample directory: r_c_b9_36_2_20120425_01

Pulse Sequence: s2pul

Solvent: cdCl3
Ambient temperature
Sample #4, Operator: cornwall
File # 109, Date: 2/2/12
INOVA-500 "epoxide"
Relax. delay: 1.000 sec
Pulse: 45.0 degrees
Acq. time: 1.285 sec
Width: 25510.2 Hz
2000 Repetitions
OBSERVE C13, 300.5058875 MHz
PULSE PRG: zgpg30
Power: 58 db,
continuously on
WALTZ-16 modulated
DATA PROCESSING
F1 line broadening 0.5 Hz
SFO: 125.761350 MHz
Total time 1 hr, 18 min, 26 sec

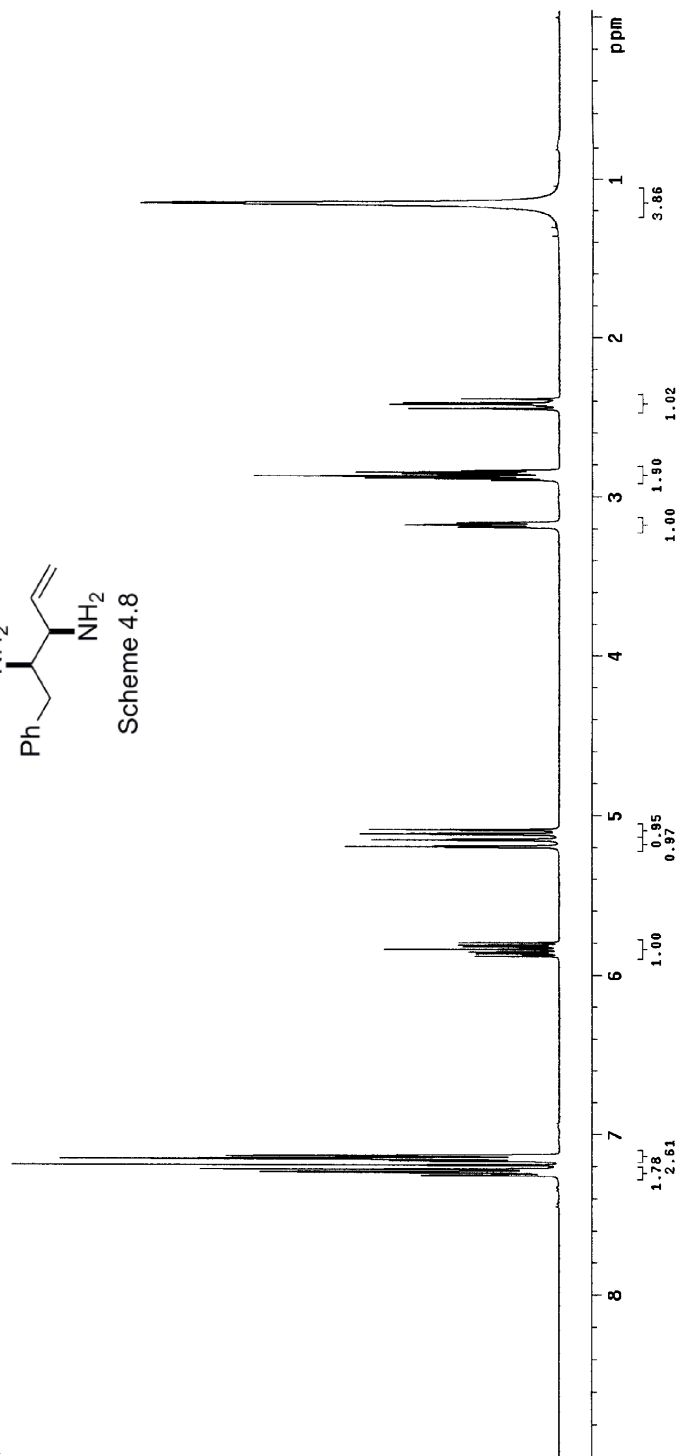
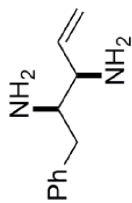


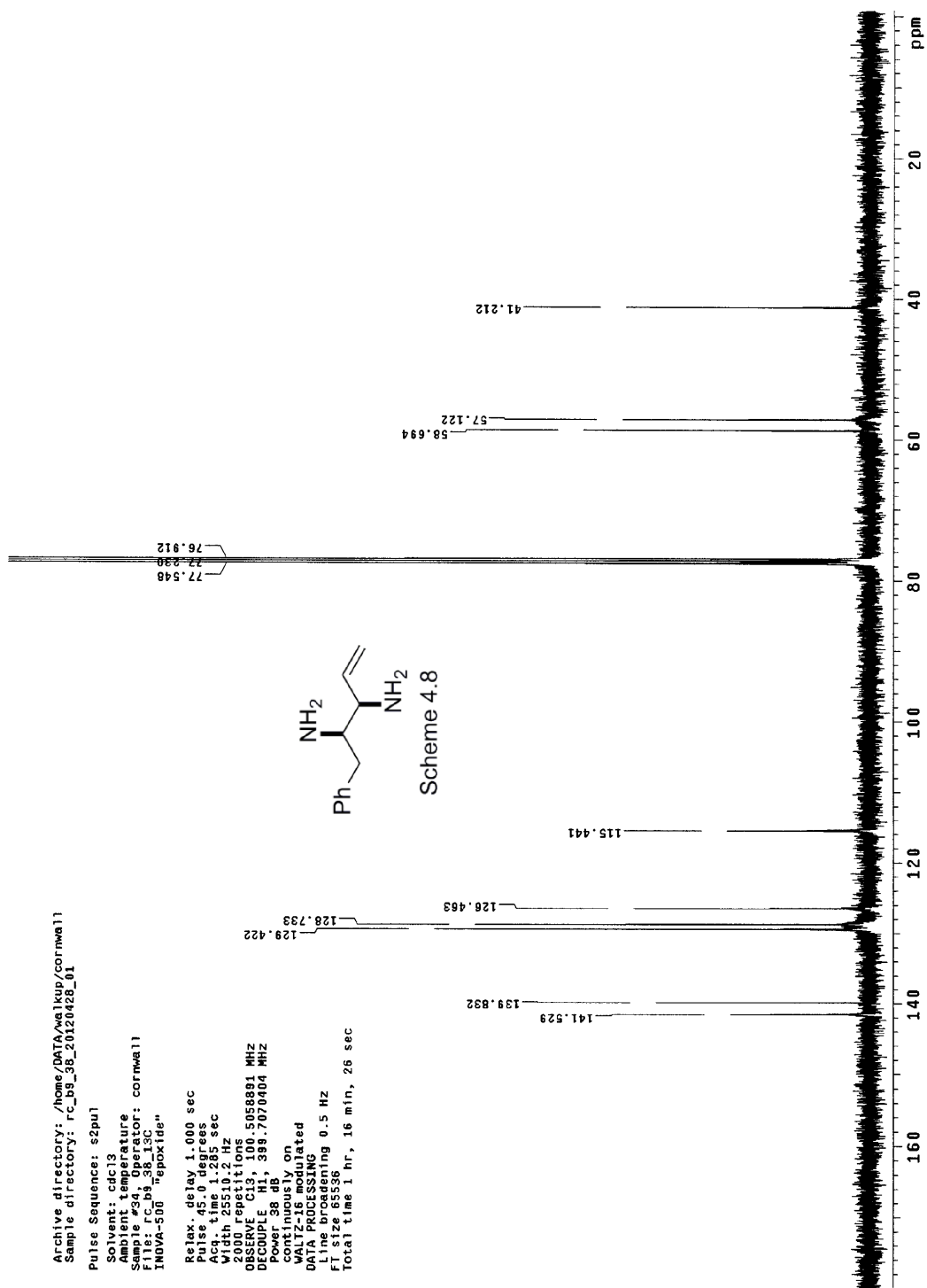


Archive directory: /home/DATA/walkup/cornwall
Sample directory: rc_b9_38_20120428_01

Pulse Sequence: s2pul
Solvent: cdcl3
Sample temperature: 300.2 K
Sample #34 Operator: cornwall
File: rc_b9_38_1h
INOVA-500 "epoxide"

Relax. delay 1.000 sec
Pulse 45.0 degrees
Acq. time 2.556 sec
Width 6410.3 Hz
Observer: HJ
OBSERVED F1 399.7050625 MHz
DATA PROCESSING
FT size 32788
Total time 0 min, 57 sec





X-ray Structure of 4-22g.

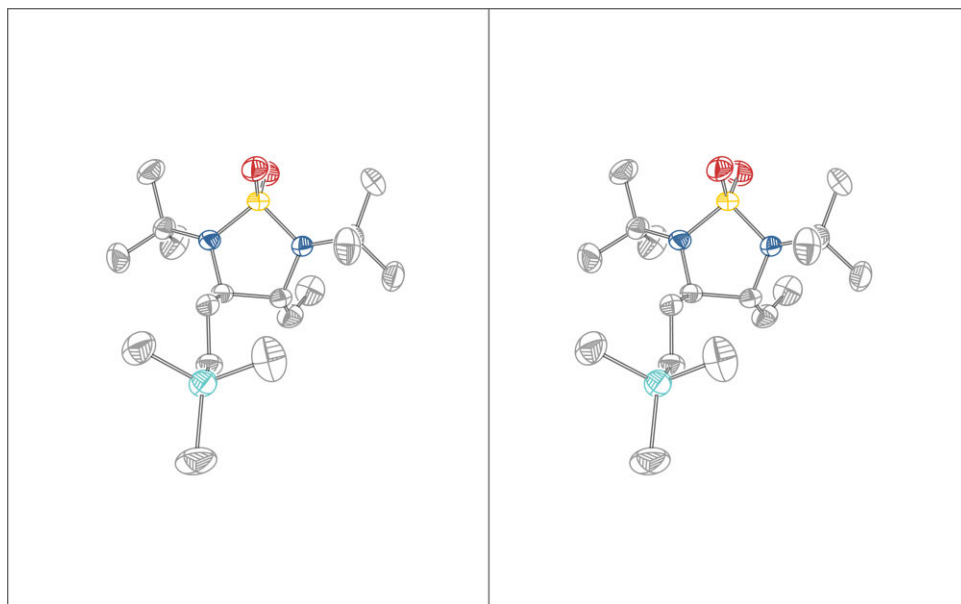
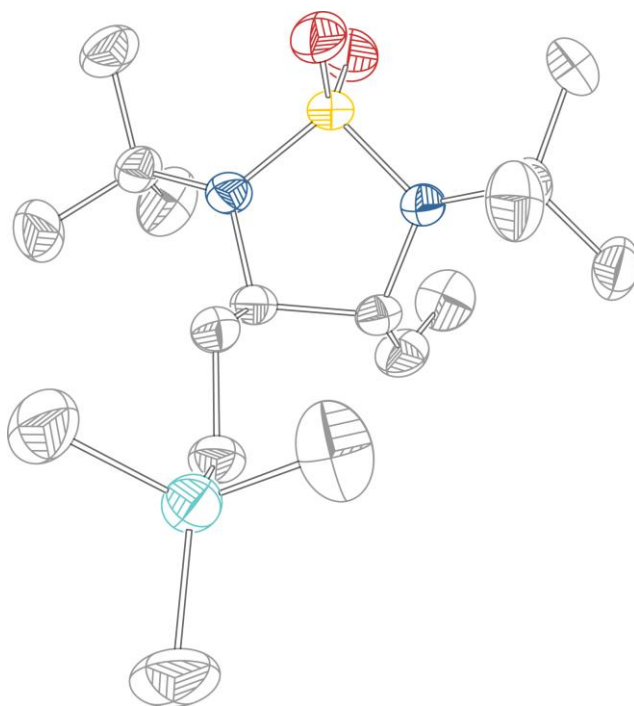


Table 1. Crystal data and structure refinement for **4-22g**

Identification code

ys200

Empirical formula	C17 H36 N2 O2 S Si	
Formula weight	360.63	
Temperature	100(2) K	
Wavelength	0.71073 Å	
Crystal system	Orthorhombic	
Space group	P21 21 21	
Unit cell dimensions	a = 10.963(3) Å	$\alpha = 90^\circ$.
	b = 11.569(4) Å	$\beta = 90^\circ$.
	c = 17.410(5) Å	$\gamma = 90^\circ$.
Volume	2208.0(12) Å ³	
Z	4	
Density (calculated)	1.085 Mg/m ³	
Absorption coefficient	0.211 mm ⁻¹	
F(000)	792	
Crystal size	0.43 x 0.39 x 0.35 mm ³	
Theta range for data collection	2.11 to 28.43°.	
Index ranges	-14 ≤ h ≤ 14, -14 ≤ k ≤ 15, -23 ≤ l ≤ 23	
Reflections collected	44743	
Independent reflections	5432 [R(int) = 0.0255]	
Completeness to theta = 28.43°	99.2 %	
Absorption correction	Semi-empirical from equivalents	
Max. and min. transmission	0.9291 and 0.9150	
Refinement method	Full-matrix least-squares on F ²	

Data / restraints / parameters	5432 / 0 / 217
Goodness-of-fit on F ²	1.034
Final R indices [I>2sigma(I)]	R1 = 0.0312, wR2 = 0.0857
R indices (all data)	R1 = 0.0360, wR2 = 0.0892
Absolute structure parameter	0.00(6)
Largest diff. peak and hole	0.171 and -0.150 e.Å ⁻³

Table 2. Atomic coordinates ($\times 10^4$) and equivalent isotropic displacement parameters ($\approx^2 \times 10^3$)

for ys200. $U(\text{eq})$ is defined as one third of the trace of the orthogonalized U^{ij} tensor.

	x	y	z	$U(\text{eq})$
C(1)	7214(2)	9233(3)	4160(1)	98(1)
C(2)	5652(3)	10531(2)	5341(1)	93(1)
C(3)	6118(3)	7950(2)	5527(1)	99(1)
C(4)	4486(2)	8816(1)	4226(1)	51(1)
C(5)	4085(1)	9800(1)	3692(1)	44(1)
C(6)	3100(1)	9448(1)	3110(1)	40(1)
C(7)	3615(1)	8701(1)	2446(1)	39(1)
C(8)	2693(2)	7827(1)	2155(1)	56(1)
C(9)	2176(2)	7823(2)	1478(1)	72(1)
C(10)	1318(1)	10926(1)	2939(1)	49(1)
C(11)	321(2)	10167(2)	2616(2)	85(1)
C(12)	1194(2)	12179(2)	2658(1)	74(1)
C(13)	1246(2)	10965(2)	3822(1)	81(1)
C(14)	5182(1)	9436(1)	1435(1)	49(1)
C(15)	6234(2)	9777(2)	1969(1)	74(1)
C(16)	5339(2)	8175(2)	1184(1)	69(1)
C(17)	5154(2)	10195(2)	717(1)	81(1)
N(1)	3981(1)	9538(1)	1851(1)	40(1)

N(2)	2553(1)	10459(1)	2725(1)	44(1)
O(1)	4087(1)	11705(1)	2007(1)	63(1)
O(2)	2375(1)	10915(1)	1309(1)	68(1)
S(1)	3239(1)	10763(1)	1920(1)	42(1)
Si(1)	5871(1)	9140(1)	4819(1)	57(1)

Table 3. Bond lengths [\AA] and angles [$^\circ$] for ys200.

C(1)-Si(1)	1.870(2)
C(2)-Si(1)	1.865(2)
C(3)-Si(1)	1.866(2)
C(4)-C(5)	1.534(2)
C(4)-Si(1)	1.8744(17)
C(5)-C(6)	1.5360(19)
C(6)-N(2)	1.4760(16)
C(6)-C(7)	1.5500(19)
C(7)-N(1)	1.4733(17)
C(7)-C(8)	1.516(2)
C(8)-C(9)	1.307(3)
C(10)-N(2)	1.5042(18)
C(10)-C(11)	1.510(3)
C(10)-C(12)	1.536(2)
C(10)-C(13)	1.541(3)
C(14)-N(1)	1.5078(18)
C(14)-C(17)	1.527(2)
C(14)-C(15)	1.532(3)
C(14)-C(16)	1.533(2)
N(1)-S(1)	1.6381(12)
N(2)-S(1)	1.6287(12)

O(1)-S(1)	1.4407(12)
O(2)-S(1)	1.4349(12)
C(5)-C(4)-Si(1)	114.70(11)
C(4)-C(5)-C(6)	113.86(12)
N(2)-C(6)-C(5)	112.02(11)
N(2)-C(6)-C(7)	104.56(11)
C(5)-C(6)-C(7)	112.53(10)
N(1)-C(7)-C(8)	112.69(12)
N(1)-C(7)-C(6)	104.89(10)
C(8)-C(7)-C(6)	112.17(12)
C(9)-C(8)-C(7)	126.30(16)
N(2)-C(10)-C(11)	110.52(13)
N(2)-C(10)-C(12)	109.86(13)
C(11)-C(10)-C(12)	111.51(17)
N(2)-C(10)-C(13)	107.64(13)
C(11)-C(10)-C(13)	110.56(18)
C(12)-C(10)-C(13)	106.61(16)
N(1)-C(14)-C(17)	109.30(14)
N(1)-C(14)-C(15)	110.19(12)
C(17)-C(14)-C(15)	111.37(16)
N(1)-C(14)-C(16)	107.99(13)
C(17)-C(14)-C(16)	108.45(16)

C(15)-C(14)-C(16)	109.46(16)
C(7)-N(1)-C(14)	121.66(11)
C(7)-N(1)-S(1)	112.44(9)
C(14)-N(1)-S(1)	122.43(9)
C(6)-N(2)-C(10)	122.56(11)
C(6)-N(2)-S(1)	111.94(9)
C(10)-N(2)-S(1)	123.45(10)
O(2)-S(1)-O(1)	114.22(8)
O(2)-S(1)-N(2)	111.05(8)
O(1)-S(1)-N(2)	111.78(7)
O(2)-S(1)-N(1)	112.33(7)
O(1)-S(1)-N(1)	109.99(7)
N(2)-S(1)-N(1)	96.10(6)
C(2)-Si(1)-C(3)	109.48(11)
C(2)-Si(1)-C(1)	110.56(15)
C(3)-Si(1)-C(1)	109.48(15)
C(2)-Si(1)-C(4)	109.65(10)
C(3)-Si(1)-C(4)	109.50(10)
C(1)-Si(1)-C(4)	108.15(9)

Symmetry transformations used to generate equivalent atoms:

Table 4. Anisotropic displacement parameters ($\approx 2 \times 10^3$) for ys200. The anisotropic displacement factor exponent takes the form: $-2\pi^2 [h^2 a^{*2} U^{11} + \dots + 2 h k a^* b^* U^{12}]$

	U ¹¹	U ²²	U ³³	U ²³	U ¹³	U ¹²
C(1)	64(1)	150(3)	79(1)	-24(2)	-13(1)	-11(2)
C(2)	139(2)	72(1)	68(1)	-20(1)	-30(1)	23(1)
C(3)	133(2)	79(2)	85(2)	13(1)	-48(2)	24(2)
C(4)	56(1)	50(1)	48(1)	8(1)	-6(1)	5(1)
C(5)	48(1)	41(1)	42(1)	3(1)	-1(1)	6(1)
C(6)	37(1)	38(1)	43(1)	9(1)	2(1)	2(1)
C(7)	38(1)	33(1)	45(1)	4(1)	-1(1)	0(1)
C(8)	56(1)	37(1)	76(1)	0(1)	6(1)	-11(1)
C(9)	62(1)	66(1)	88(1)	-15(1)	-10(1)	-21(1)
C(10)	41(1)	48(1)	59(1)	5(1)	5(1)	11(1)
C(11)	46(1)	84(1)	127(2)	-18(1)	5(1)	-2(1)
C(12)	67(1)	54(1)	102(2)	11(1)	14(1)	24(1)
C(13)	77(1)	100(2)	66(1)	8(1)	23(1)	37(1)
C(14)	51(1)	50(1)	47(1)	-5(1)	14(1)	-2(1)
C(15)	42(1)	94(1)	85(1)	-20(1)	11(1)	-10(1)
C(16)	74(1)	57(1)	77(1)	-16(1)	22(1)	6(1)
C(17)	108(2)	80(1)	56(1)	13(1)	35(1)	9(1)
N(1)	42(1)	35(1)	42(1)	2(1)	4(1)	0(1)
N(2)	42(1)	44(1)	46(1)	11(1)	6(1)	11(1)
O(1)	71(1)	38(1)	79(1)	-2(1)	20(1)	-10(1)

O(2)	79(1)	76(1)	49(1)	12(1)	-11(1)	22(1)
S(1)	49(1)	34(1)	41(1)	6(1)	2(1)	2(1)
Si(1)	68(1)	58(1)	45(1)	-4(1)	-17(1)	12(1)

Table 5. Hydrogen coordinates ($\times 10^4$) and isotropic displacement parameters ($\approx^2 \times 10^{-3}$) for ys200.

	x	y	z	U(eq)
H(1A)	7202	9961	3896	146
H(1B)	7177	8616	3792	146
H(1C)	7953	9169	4453	146
H(2A)	4841	10560	5550	139
H(2B)	5765	11165	4992	139
H(2C)	6235	10587	5751	139
H(3A)	6861	8087	5804	149
H(3B)	6173	7226	5260	149
H(3C)	5446	7926	5880	149
H(4A)	4648	8135	3917	62
H(4B)	3815	8632	4569	62
H(5A)	4793	10080	3414	52

H(5B)	3777	10432	4002	52
H(6)	2458	9014	3376	47
H(7)	4341	8289	2628	47
H(8)	2473	7238	2491	67
H(9A)	2367	8395	1123	87
H(9B)	1619	7247	1352	87
H(11A)	386	10144	2067	128
H(11B)	-460	10476	2758	128
H(11C)	404	9400	2819	128
H(12A)	1250	12198	2108	111
H(12B)	1836	12639	2875	111
H(12C)	419	12484	2815	111
H(13A)	455	11237	3976	122
H(13B)	1861	11479	4016	122
H(13C)	1378	10204	4025	122
H(15A)	6264	9252	2396	111
H(15B)	6107	10549	2154	111
H(15C)	6990	9742	1692	111
H(16A)	4681	7962	848	104
H(16B)	5333	7683	1628	104
H(16C)	6101	8089	918	104
H(17A)	5902	10102	437	122
H(17B)	5062	10990	865	122

H(17C)

4480

9971

399

122
